EORGIA INSTITUTE OF TECHNOLOGY — OFFICE OF CONTRACT ADMINISTRATION

[X] ORIGINAL

[ ] REVISION NO. ____

PROJECT ADMINISTRATION DATA SHEET

roject No. G33-603 — DATE: ____

roject Director: Gole — School/~~Lab~~ Chemistry

ponsor: U.S. Department of Energy, Morgantown Energy Technology Center, ATTN: R.R. Hill, PO Box 880, Morgantown, WV 26505

ype Agreement: Contract No. DE-AC21-81MC16537

ward Period: From 8-14-81 To ~~8-13-83~~ 10-30-84 (Performance) 10-13-83 (Reports)

ponsor Amount: $96,532. (Partially funded at $49,205) Contracted through:

ost Sharing: $4729 (G33-373), $12427 for first year GTRI/~~GIT~~

itle: The Characterization of High-Temperature Vapor Phase Species and Vapor-solid Interactions of Import to Combustion and Gasification Processes in the Energy Technologies

DMINISTRATIVE DATA — OCA CONTACT Don Hasty

) Sponsor Technical Contact: Kent H. Carleton, TPO, Morgantown Energy Technology Center, PO Box 880, Morgantown, WV 26505

) Sponsor Admin./Contractual Contact: ONR-RR Campus

eports: See Deliverable Schedule — Security Classification: N/A

efense Priority Rating: None

ESTRICTIONS

ee Attached DOE Supplemental Information Sheet for Additional Requirements

ravel: Foreign travel must have prior approval - Contact OCA in each case. Domestic travel requires sponsor approval where total will exceed greater of $500 or 125% of approved proposal budget category.

quipment: Title vests with Sponsor; however items costing less than 1000 vests with GIT, if prior approval is obtained from the Contracting Officer.

OMMENTS: Partially funded for first 12 months. No work is to be done on second year until written notification received from Sponsor.

RECEIVED
OCT 1981
Research Reports

OPIES TO:

dministrative Coordinator
esearch Property Management
ccounting Office
)curement/EES Supply Services
Research Security Services
~~Reports Coordinator (OCA)~~
Legal Services (OCA)
Library, Technical Reports
EES Research Public Relations
Project File (OCA)
Other: ____

GEORGIA INSTITUTE OF TECHNOLOGY OFFICE OF CONTRACT ADMINISTRATION

SPONSORED PROJECT TERMINATION/CLOSEOUT SHEET

Date 10/30/86

Project No. G-33-603 School/~~Lab~~ Chem

Includes Subproject No.(s) N/A

Project Director(s) Jim Gole GTRC / ~~GTI~~

Sponsor U.S. Dept., of Energy, Morgantown, W.VA

Title The Characterization of High-Temperature Vapor Phase Species and Vapor - solid Interactions of Import to Combustion and Gasification Processed in the Energy Technologies

Effective Completion Date: 4/30/84 (Performance) _____ (Reports)

Grant/Contract Closeout Actions Remaining:

- [X] None
- [ ] Final Invoice or Final Fiscal Report
- [ ] Closing Documents
- [ ] Final Report of Inventions
- [ ] Govt. Property Inventory & Related Certificate
- [ ] Classified Material Certificate
- [ ] Other _____

Continues Project No. _____ Continued by Project No. _____

COPIES TO:

Project Director
Research Administrative Network
Research Property Management
Accounting
Procurement/GTRI Supply Services
Research Security Services
Reports Coordinator (OCA)
Legal Services
Library
GTRC
Research Communications (2)
Project File
Other I. Newton
A. Jones
R. Embry

FORM OCA 69.285

Progress
August 14, 1981-November 14, 1981

Title of Contract: The Characterization of High Temperature Vapor Phase Species and Vapor-Solid Interactions of Import to Combustion and Gasification Processes in the Energy Techniques

Place of Work: Georgia Institute of Technology
Department of Chemistry
Atlanta, Georgia 30332

Principal Investigator: James L. Gole

Scope of Current Efforts:

We have been concerned with the application of chemiluminescent and laser fluorescent techniques to the determination of bond energies and spectroscopic constants for the monohydroxides, monoxides, and monosulfides of sodium and potassium. We have investigated and are continuing to investigate non-equilibrium routes for the formation of these compounds and have carried out some kinetic parameterization. The sodium systems have been extended to the region in which sodium cluster, M_n ($n \geq 3$), oxidation is now under study using optical techniques. This effort is soon to be supplemented with product analysis using a newly constructed mass spectrometric system. Efforts have been initiated toward the construction of a device for sodium surface oxidation.

Our research effort has been divided into five areas:

1. The production and characterization of single and multiple collision KOH emission spectra.

2. The investigation of alkali-oxide production in hydroxide environments.

3. The study of sodium atom and dimer oxidation to produce the metal oxides.

4. The initiation of sodium cluster, M_n ($n \geq 3$), oxidation studies.

5. The construction of a mass spectrometric system to allow simultaneous optical and mass spectrometric probing of the products of sodium oxidation.

We summarize in more detail the current status of research efforts 1-4.

Under tasks 1 and 2:

Both "single and multiple" collision chemiluminescent spectra have been observed and further characterized. Sample spectra are indicated in Figures (1) and (2). Note that the multiple collision diffusion flame spectrum onsets at ~3200Å whereas the single collision spectrum onsets at ~3900Å. As the enclosed reprint indicates, this difference in onset is of fundamental importance to the evaluation of the K-OH dissociation energy. One should also compare the significantly increased quality of the diffusion flame spectrum in Figure 2 with that depicted in Figure 4 of the enclosed reprint. As should be apparent from Figures 1 and 2, both the "single and multiple" collision KOH emission spectra are characterized by significant structure which we believe is attributable to emission to vibronic levels in the ground electronic state of potassium hydroxide, more specifically to primarily a progression in the K-OH stretch. There appears to be a reasonable if not one-to-one correlation between the "multiple" and "single" collision spectra for $\lambda > 3900$Å; however, there are some differences which may be attributable to (1) significant rotational relaxation in the multiple collision "diffusion flame" environment versus the high rotational excitation expected under single collision conditions or (2) the onset of rapid energy transfer and hence collisional depopulation of KOH excited state levels from which emission is observed under single collision conditions. The latter phenomena, collisional depopulation, should include collision induced dissociation of KOH molecules formed in the very weakly bound excited state from which emission is observed in the present study.

Unfortunately, the further investigation of the phenomena we have described here has been hampered by considerable experimental difficulties primarily associated with the difficulty entailed in handling 90+% hydrogen peroxide. Thus, a great deal of our recent research effort has entailed the replacement and reconstruction of both the single and multiple collision chemiluminescent systems. While this effort has slowed the continuation and completion of our work on KOH, it has led to significant discoveries concerning the formation of the alkali oxides in reactive hydroxide environments. In Figures (3) and (4) we depict chemiluminescent spectra which dominate emission observed in the Na-H_2O_2 and K-H_2O_2 systems under conditions where we have partial decomposition of the hydrogen peroxide either through heating to temperatures in excess of 320K or reaction with the container walls, both of which create a hydroxide rich environment. The observed spectra are believed to result from emission from either MO or MO_2 excited states. Based on a comparison with spectra observed in the Na-N_2O system, we favor formation of the latter MO_2 compounds.

Under task 3:

We have studied the single collision oxidation of equilibrium sodium (atom + 2% dimer) vapors with SO_2 and N_2O. The SO_2 system yields a weak, if nonexistent, chemiluminescent emission. The weak nature of the emission is such as to preclude an unequivocal correlation with SO_2 oxidation. The sodium oxidation with N_2O is characterized by an intense red flame, the spectrum of which is shown in Figure 5. Although the structure associated with this emission is, as yet, unresolved, it must be associated with NaO*. It should also be noted that the onset of the emission in Figure 5 is some 900Å to the red of that in Figure 3. If both spectra resulted from NaO or NaO_2 emission, it would be difficult to explain this difference in onset. Therefore, we

suspect that the spectrum which results from sodium oxidation in a hydroxide environment does not result from the same emitter as that characterizing the sodium-N_2O system. Based upon the available literature which deals with the alkali monoxides (see enclosed reprint) and the bonding characteristics of the series of molecules AO_2 where A=F,Cl,H,Na, and K, we tentatively correlate the emission, associated with sodium and potassium oxidation in a hydroxide environment, with NaO_2 and KO_2.

Under task 4:

We have constructed an apparatus for the study of sodium cluster oxidation. The ultimate goal for this apparatus will be the study of sodium cluster oxidation with SO_2 viz. $Na_x + SO_2 \rightarrow$ products; however, the initial experiments now being conducted involve sodium cluster oxidation with halogens. These experiments not only allow us to test the metal cluster oxidation system but also facilitate the characterization of a potentially important factor in energy generating systems. It has currently been suggested that chlorine interacts with the alkali impurities in a combustion stream, resulting in the formation of alkali chloride complexes which then repartition with O,S,H,C,Al, or Si ash particulates. Thus, the influence of chlorine on the formation of alkali clusters and the subsequent reaction of these clusters with SO_2 must be evaluated in the intermediate region between the gas and surface phases. A schematic of the cluster oxidation device is shown in Figure (6) and a sample of the chemiluminescent spectra observed thusfar is shown in Figure (7). This cluster oxidation device will soon be coupled with our newly acquired mass spectrometric capability so as to provide simultaneous optical and mass spectrometric probing of the system.

Associated Periferal Devices and Preliminary Studies

We should note that the mass spectrometric system which we will use in conjunction with our optical studies is in the final stages of construction. We have also initiated construction of a device for the study of sodium surface oxidation at pressures in the range 10^{-6}-10^{-9} torr. This effort will involve considerable collaboration with Professor R. A. Pierotti, a surface chemist in the Georgia Tech Chemistry Department.

Figure Captions

Figure 1: KOH* emission spectrum from the reaction $K_2 + H_2O_2 \rightarrow KOH^* + KOH$ under single collision conditions.

Figure 2: KOH* emission spectrum from the reaction $K_2 + H_2O_2 \rightarrow KOH^* + KOH$ taken under multiple collision conditions in a diffusion flame device

Figure 3: Emission spectrum tentatively attributed to NaO_2 formed in a multiple collision diffusion flame "hydroxide rich" environment characterized by sodium-oxidant interactions.

Figure 4: Emission spectrum tentatively attributed to KO_2 formed in a multiple collision diffusion flame "hydroxide rich" environment characterized by potassium-oxidant interactions.

Figure 5: Emission spectrum associated with the reaction $Na + N_2O \rightarrow NaO^* + N_2$ under single collision conditions.

Figure 6: Schematic of apparatus used for sodium cluster oxidation.

Figure 7: Chemiluminescent spectra associated with the reaction (a) $Na_2 + Cl_2 \rightarrow NaCl^* + NaCl$ and (b) $Na_3 + Cl \rightarrow Na_2^* + NaCl$ taken under single collision conditions. The spectrum (b) represents the first example of chemiluminescent spectra associated with metal cluster oxidation.

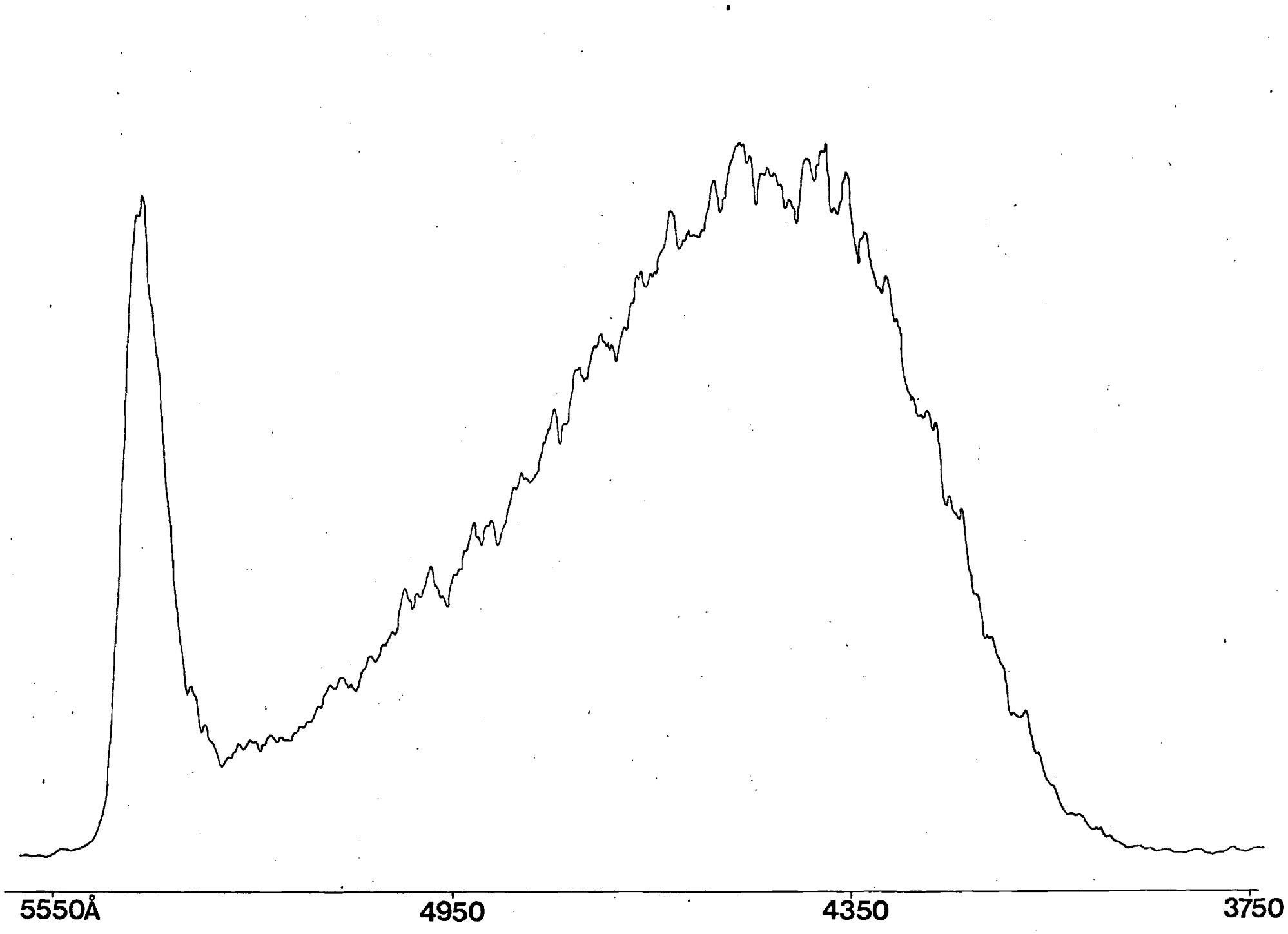

Figure 1

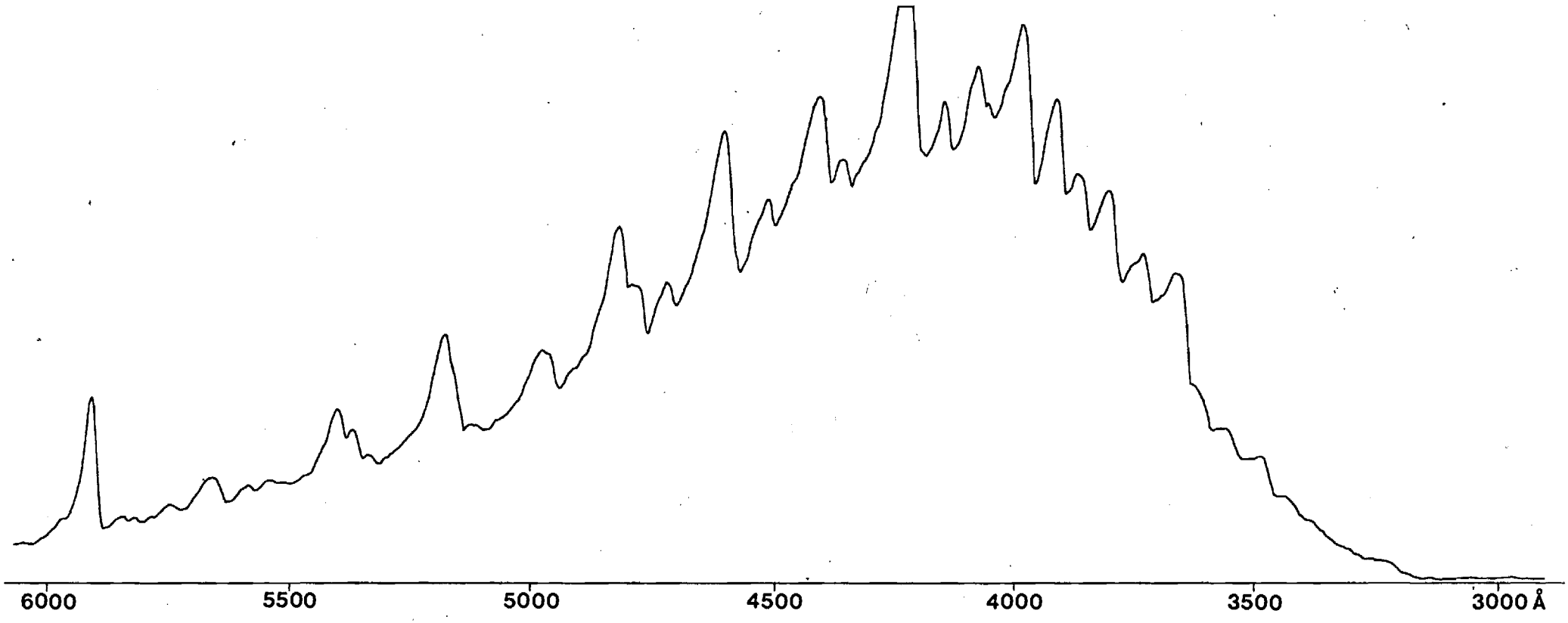

Figure 2

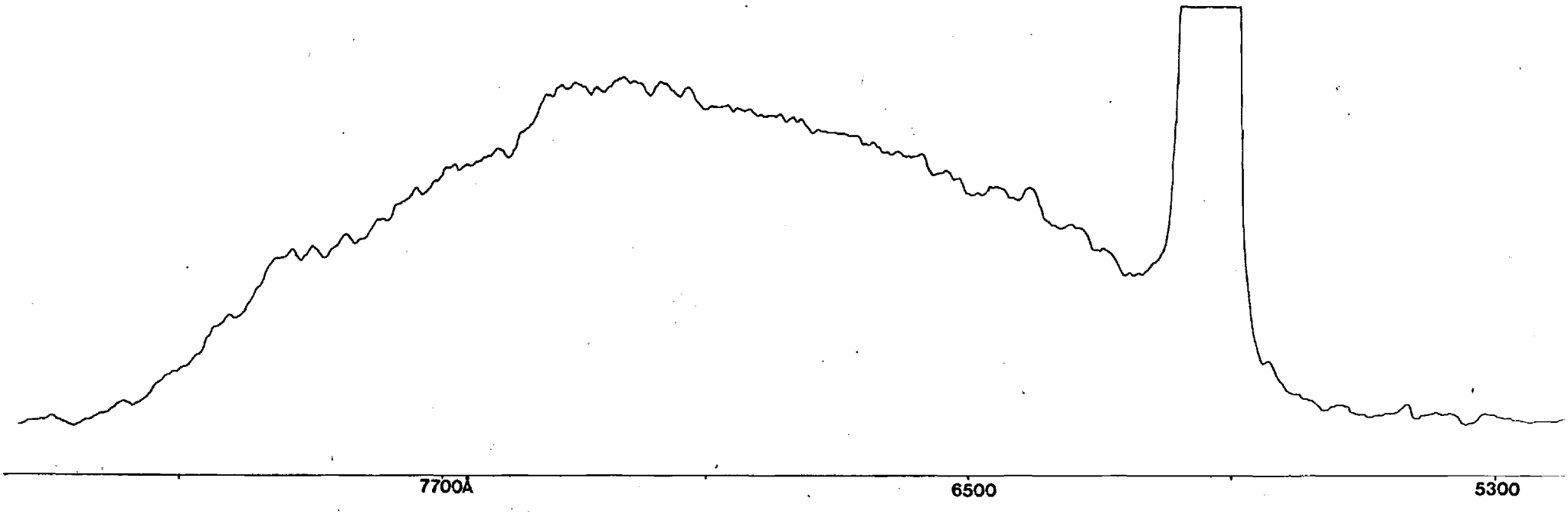

Figure 3

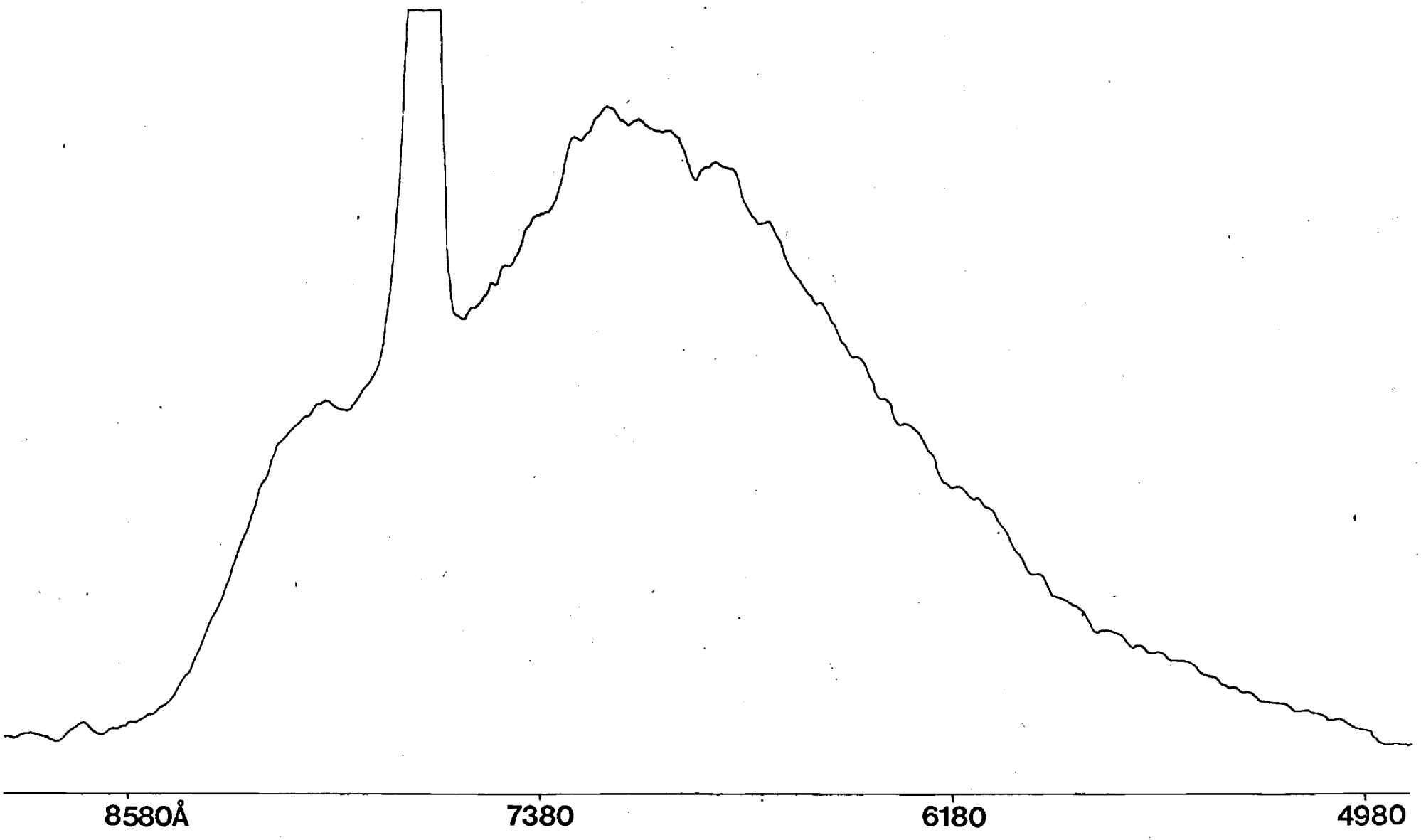

Figure 4

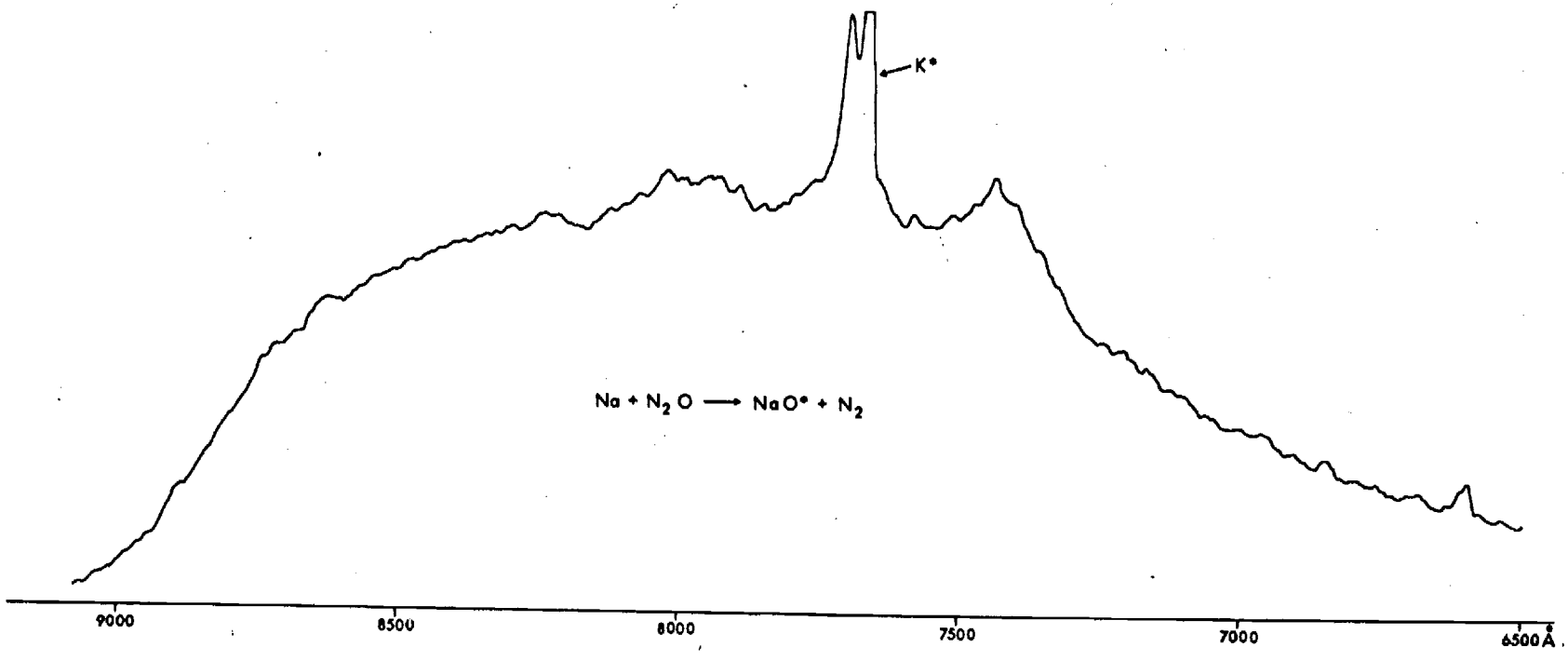

Chemiluminescent spectrum tentatively attributed to NaO* formed in the reaction $Na + N_2O \rightarrow NaO^* + N_2$

Figure 5

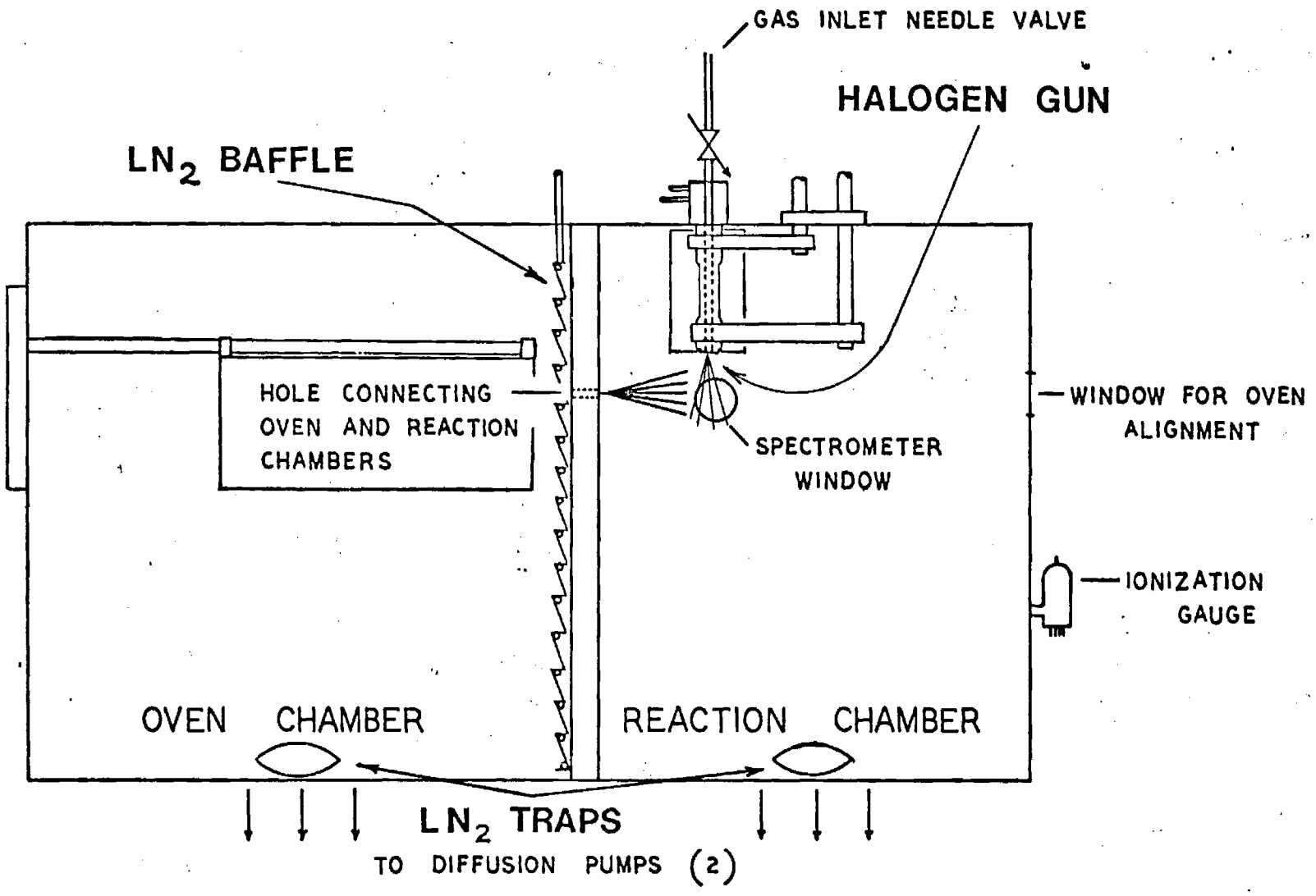
GAS INLET NEEDLE VALVE
HALOGEN GUN
LN2 BAFFLE
HOLE CONNECTING OVEN AND REACTION CHAMBERS
SPECTROMETER WINDOW
WINDOW FOR OVEN ALIGNMENT
IONIZATION GAUGE
OVEN CHAMBER
REACTION CHAMBER
LN2 TRAPS
TO DIFFUSION PUMPS (2)

Figure 6

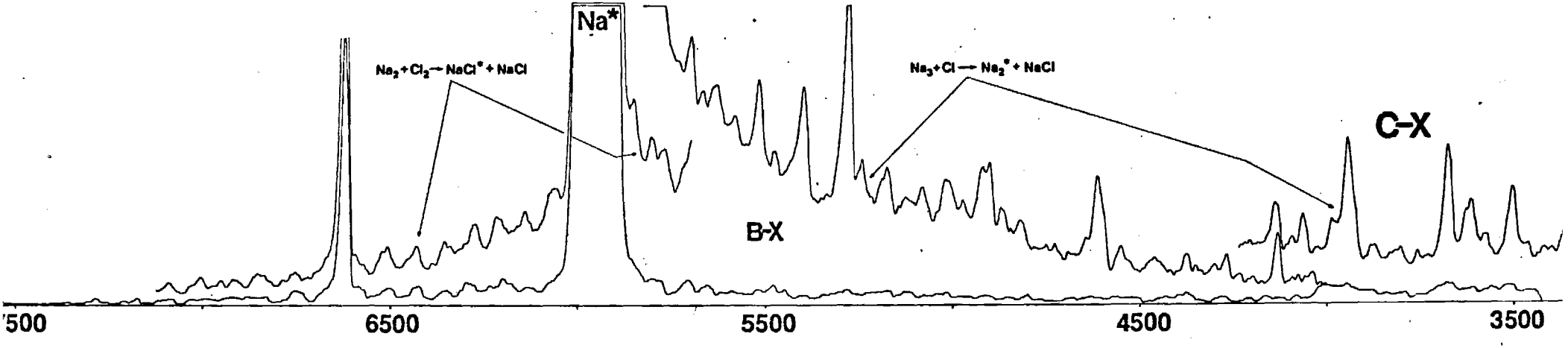
Na*
$Na_2 + Cl_2 \rightarrow NaCl^* + NaCl$
$Na_3 + Cl \rightarrow Na_2^* + NaCl$
B-X
C-X
'500
6500
5500
4500
3500

Figure 7

Aspects of sparsely studied gas phase chemistry of import to the energy technologies

James L. Gole
Georgia Institute of Technology
Department of Chemistry
Atlanta, Georgia 30332

Abstract. There is considerable interest in the need to improve the operation of systems which can potentially serve as alternate energy sources. Entailed in this effort is the desire to understand the vapor phase chemistry and compounds which may enter as by-products of the system under consideration. These compounds may have deleterious effects on the gas phase chemistry or play an important role through high temperature gas-solid corrosion kinetics. Here we outline the nature of the problem and focus on a subset of these molecules, the metal hydroxides and the alkali oxides and sulfides. A critical analysis of the data base is presented and new experiments are outlined which encompass the investigation of thermochemistry and the evaluation of molecular parameters through the study of visible, infrared, microwave and electron spin resonance (ESR) spectroscopy. Recent chemiluminescent experiments which lead to the evaluation of a new stringent lower bound for the K-OH band energy are summarized. This stringent lower bound (88.2 kcal/mole) correlates within the quoted error bounds with the absolute upper bound of previous experimental determinations. Preliminary laser fluorescence studies on Na_2O are reported and the possible influence of "ultrafast" energy transfer (E-E and V-E transfer among the excited states of high temperature molecules) on the behavior of energy generating systems is noted.

Keywords: combustion and analysis; gas phase chemistry; thermal/chemical processes.

Optical Engineering 20(4), 546-555 (July/August 1981).

ONTENTS

ted Paper EP-108 received March 4, 1981; accepted for publication March 11, 1981;
ived by Managing Editor March 19, 1981.

1. INTRODUCTION

Recently, substantial interest has focused on the development of systems and technologies which can serve to avert projected energy shortages through the use of alternate fuel sources. This need has heightened the necessity for improving and optimizing the efficient use of energy systems which are, at present, typically no more than 40% efficient.

For practically all viable energy conversion systems, the common optimization parameter is the temperature. Generally the higher the temperature, the greater the efficiency for converting a source of energy to useful work. This, of course, is a direct consequence of the Carnot efficiency relation, usually expressed as

$$E_{max} = (T_{source} - T_{sink})/T_{source}$$

where E_{max} is the maximum efficiency attainable for a given source and sink temperature. Based strictly on the efficiency criterion, it is apparent that a high source temperature is desirable for energy conversion systems.

Suitable high source temperatures are definitely attainable. In coal or oil combustors or in nuclear fission fuel elements, where temperatures in excess of 2000 C are readily achieved, basic system operation problems lie in the containment of these high temperature reactive fuel systems and of the working fluid used to transfer the heat to an energy conversion unit. While this is essentially a materials problem involving, in large part, mechanical or solid state chemical phenomena, some of the materials problems arise from high temperature gas-solid corrosion reactions and vapor phase phenomena

which may enter as by-products of the system under consideration (impurities such as the alkali metals, sulfur, water vapor, etc.) or because of the introduction of seed materials (K_2SO_4 or K_2CO_3 in magneto-hydrodynamic (MHD) applications) into the flow.

In this discussion, we will be concerned with a subset of those molecules which play an important role in high temperature vapor processes in the present technology or may be important in anticipated future developments. Unfortunately, data on these species are sparse and much work needs to be done. It is quite apparent that very stringent tolerance levels for certain species in process streams impose stronger requirements for reliable thermodynamic and kinetic data in order to predict the effects due to low level species concentrations. In addition, there must be serious concern focused on whether or not these systems are best represented via equilibrium or non-equilibrium models. The characterization of molecules in these systems requires the determination of bond energies and spectroscopic constants and may well require the elucidation of ultrafast intra- and intermolecular energy transfer.[1] The evaluation of spectroscopic data leads to the determination of important molecular constants which can be used for the statistical mechanical evaluation of heat capacities, entropies and free energies, all of which are important to the understanding of energy related combustion and gasification environments. In addition, the determination of the optical signature of those molecules of interest provides information useful for the characterization of non-equilibrium combustion phenomena and for the evaluation of kinetically dominated product formation routes. In order to focus on those areas where limited data need considerable augmentation, we will first outline the nature of certain specific systems.

NATURE OF THE PROBLEM

Considerable effort will be required to attain basic parameters for molecules playing an important role in energy generating devices whose goal is the utilization of fossil fuel gasification and liquification. An important subset of these systems includes combustion powered magneto-hydrodynamics (MHD). Because MHD attempts to make a more varied use of the combustion environment, we focus on the nature of MHD power generation; however, excluding the use of seed materials, all high temperature combustion systems (coal gasification, vapor phase processes associated with gas turbines, etc.) appear to be plagued by a similar group of deleterious high temperature vapor phase constituents.

2.1. MHD

The generation of electrical energy using combustion powered magneto-hydrodynamic (MHD) systems has been the subject of considerable research effort in the past decade. In an MHD system one creates an electrically conducting "fluid" which, when passed through a magnetic field, develops an induced electric field across the fluid, along which a current can flow.[2] A direct electric current will pass along the induced field to electrodes which may be connected to an external load. The typical MHD generator is usually comprised of a sequentially connected combustion chamber, a supersonic expansion nozzle, and a gas flow channel commonly referred to as a diffuser. Because the hot post-combustion materials normally have an insufficient free electron concentration to be good current carriers, thermally ionizable seed materials such as K_2CO_3 and KO_4 are generally added to the flow.[3]

Recent evaluations[4] of the status of MHD devices as viable and competitive power systems indicate that the problems of maintaining *conductivity*, seed recovery (98% recovery rate for economical operation) and of inhibiting channel materials degradation (prevention of corrosion of channel walls through coal slag-electrode and insulator interactions) remain largely unsolved.

In order to successfully model, and hence optimize, the design and operation of an MHD unit, it is essential to provide a rigorous accounting of the gas chemistry, particularly within the diffuser. Despite considerable effort in this direction, it does not appear that satisfactory predictions of the electrical conductivity associated with a seeded coal combustion gas are currently within the grasp of the technology. It is extremely difficult to determine species concentrations in these complex high temperature systems even if it is assumed that the gases are in thermodynamic equilibrium.

If equilibrium is assumed in the MHD channel, one can, from a knowledge of all the species present and their thermodynamic functions, calculate steady-state free electron concentrations for a variety of composition, temperature, and pressure conditions. Unfortunately, these calculations are based on primary thermochemical input data which are very uncertain for some of the species (see below). In addition, these thermochemical evaluations rely heavily on a correct choice of species, a factor which is again uncertain.

2.2. Approximate species concentrations

Based upon currently available thermochemical data, it can be calculated (determination of species concentrations) that approximately half the potassium seed is present in the form of essentially unionizable KOH and is therefore unavailable as an electron source. At temperatures in excess of 2600 K in a slightly lean coal/air combustion system at 3 atm pressure, the major potassium-containing species are calculated to be KOH, K, KO and K^+.[5] Other significant vapor species include SiO_2, FeO, OH, SO_2 and NO in addition to the major combustion gas components N_2, H_2O, CO_2 and CO. The primary slag or fly ash components include SiO_2, Al_2O_3, Fe_3O_4, TiO_2, MgO, CaO, Na_2O and K_2O; however, evidence now exists that the negative ions of PO_2, FeO_2, and AlO_2 are potentially important since all of these species have high electron affinities. The presence of these impurities has important implications for cation formation and electron behavior in the MHD channel. Typical slag concentrations in a coal-fired system, while only on the order of 0.1%, can result in as much as 19% loss in electrical conductivity.[6]

The species we have mentioned and their possible precursors are *not* well characterized. The combined uncertainties in the *heats of formation* and *molecular constants* used in computing partition functions for KOH (JANAF)[7] cause the concentration ratio of K to KOH to be uncertain by at least an order of magnitude. Because of this uncertainty, it is not possible to make a reasonable judgment as to whether the concentration of KOH is sufficiently high to require restrictions on the amount of hydrogen present in the fuel. Clearly, the successful thermodynamic modeling of MHD gas chemistry requires better basic data than are presently available.

2.3. Electron transfer cross sections

Given that the equilibrium assumption is valid, we can define a steady state electron concentration in the MHD channel. Electron mobility is then determined from momentum transfer cross sections between electrons and other species. The momentum cross sections can be obtained from electron-molecule collision cross sections. These cross section data are not known and can only be estimated very approximately. What can be said definitely is that the most polar species such as H_2O and KOH should have the highest cross sections. Indeed, the dipole moment of KOH is estimated to be 8 Debye.[8] In systems where calcium and magnesium impurities are found, it would seem that CaOH and MgOH should be carefully considered. KOH, CaOH and MgOH are, at present, sparsely characterized.

2.4. Metal hydroxides and the hydrogen fuel economy

Because of its close tie to those materials used to seed the MHD generator, KOH may well represent the most important hydroxide species in the MHD channel; however, the specific effect of the water vapor component of combustion gases on the channel components of any system (fossil fuel only or MHD) has not been considered carefully. It appears that volatile hydroxides of a number of species could be formed under typical operating conditions.[9]

The importance of metal hydroxide characterization increases markedly when one considers that many of the existing materials and seed recovery problems are derived from the presence of combustion impurities, particularly coal slag. Because future prospects for a hydro-

gen fuel economy may provide a source of clean fuel for MHD and other combustion systems, experimental and theoretical evaluations of an H_2-O_2 MHD generator have been underway.[10] A cost analysis indicates the H_2 fuel system to be comparable with other fuels since the reduced materials problems and low pollution produced make this an attractive alternative. There is one possible major drawback. The presence of a large H_2O concentration may prove to be detrimental if the high temperature materials are susceptible to the formation of hydroxide vapor species. In this light, it would seem that current and future possibilities for energy conversion will require a good hydroxide data base. At the very least this data base should include thermodynamic heats of formation and molecular constants on the hydroxides of sodium, iron, silicon, vanadium, calcium, and magnesium.

2.5. The alkali problem and sulfur chemistry

The nature of coal-fired systems in general and the MHD channel in particular is such that "alkali cleanup"[11] represents the most significant problem which must be addressed. While thermodynamic calculations indicate the importance of the alkali oxides (especially KO in the MHD channel), sulfur is also a significant impurity in coal-fired systems. Therefore, it is necessary to consider the nature of sulfur compounds and their relation to the only partially solved fuel corrosion problem. In focusing on turbine blade corrosion, the alkali sulfur salts are among the most important compounds which must be characterized. For example, in a combustion powered turbine system operating over a sea or ocean, sulfur may come in contact with sodium or potassium and one must assess the nature of alkali-sulfur compounds which are formed.

Such data are also of importance for the characterization of most coal and heavy fuel fired turbine generators.[12] Indeed, a great deal of effort is now focusing on fireside corrosion where one must consider the interactions of those alkali salts which plate out on boiler tubes.[12] With this strong interest it is amazing to note that the data on sodium and potassium sulfur compounds (NaS, KS, Na_2S, K_2S and higher sulfides) are minuscule. Information on molecular stabilities (heats of formation) and molecular constants must be obtained.

2.6. The equilibrium assumption

Our discussion thus far has been closely tied to the validity of the equilibrium assumption, and the problems of obtaining thermochemical and collision cross section data if this assumption is valid. However, one of the troublesome factors in the modeling of coal and heavy fuel fired systems appears to be a complex gas mixture which may not correspond to an equilibrium composition. The correct modeling may require the use of kinetic parameterization and the rates for product formation. Similarly, electron producing ionization kinetics may also be an important factor in determining MHD conductivity.

In this connection one need only note the complex ion chemistry that results between metal additives and electrons in atmospheric laboratory flames. Indeed, the presence of excess concentrations of charged species in the reaction zone of hydrocarbon-containing flames has led to the suggestion of a non-equilibrium low pressure (~0.1 atm) MHD generator.[13] It is anticipated that the use of low gas pressures should allow the excess radical and ion concentrations generated by the combustion process to be maintained in the diffuser itself. Calculations show that, under these conditions, a 1500 K flame could give an ion yield equivalent to that of an equilibrium system at 2000 K.[13]

The possibilities noted here point strongly to the importance of considering controlled non-equilibrium environments and species formation in the modeling of the behavior of energy generating systems. It may be inappropriate to model these systems using only the energy minimization schemes. Product formation rates and rafast energy transfer may play a much more significant role than thermodynamics. In any case, the parameterization of those gas phase molecules known to be present in these systems is of paramount importance to the successful application of any reliable approach to modeling.

3. THE NATURE OF THE DATA BASE

In the following sections, we will outline and assess the nature of available data on several of the molecules whose importance has been considered in the previous section. Our emphasis will be on the metal hydroxides and the alkali oxides and sulfides. Our purpose will be to evaluate critically the data base and to suggest where further experimentation is needed.

4. METAL HYDROXIDES

4.1. Water vapor-solid reactions with hydroxide vapor products

While there have been several recent reviews[14] outlining evidence for vapor phase hydroxide formation, much of the evidence for hydroxide species is of an indirect and sometimes ambiguous nature. In a gas-solid system, the enhanced rate of transport for a given oxide in the presence of water vapor is usually taken to indicate formation of a volatile hydroxide species. Through systematic variation of gas composition and temperature one attempts to infer a formula for the transport species. In order to determine and extrapolate the pressure dependence of transport and deposition processes, it is important to clarify the exact identity of the hydroxides involved.[15] Thus far very few verifications of species identity have been made. Here thermodynamic and spectroscopic data can be of great importance. Only the hydroxides of the alkali metals, barium and aluminum, appear to have been characterized by both mass and optical spectroscopy, and, in many cases, this optical spectroscopy is of an indirect nature (Table I). Our discussion will focus on the monohydroxides. Here compounds of the alkalis, BeOH, CaOH, BaOH, and AlOH are thought to be important in water vapor-solid interactions.[14]

4.2. Thermochemistry

It appears that the major thermodynamic characterization of the metal hydroxides has been through flame studies. Table I summarizes those monohydroxides identified in flames while Table II indicates currently accepted bond dissociation energies for the monohydroxides. For the most part, molecular emission has been excited in post flame gases and in many of the studies noted in Tables I and II, only *indirect* evidence is obtained for the hydroxide. Only recently (see below) has molecular emission from NaOH and KOH been excited in a "chemiluminescent" reaction.[16] Molecular emission tentatively attributed to CaOH* has also been observed in calcium oxidation flames[17] and some laser fluorescence studies of this alkaline earth hydroxide have also appeared.[18]

From Table II, it is clear that *only two compounds* have been characterized mass spectrometrically. Studies of the Group IIA hydroxides at elevated temperature are precluded for all but the barium compounds[19] because of a very high propensity for disproportionation to the oxides and resulting loss of water. Difficulties encountered in studying the alkali hydroxides may well stem from the tendency to form dimeric species upon vaporization. We should also note that lithium tends to form a very stable binary oxide. The bond energies determined for KOH[20-21] and BaOH[19,22] via flame and mass spectrometric studies are in reasonable but not spectacular agreement.

4.3. Molecular parameterization—the alkali hydroxides

With the exception of the alkali metal compounds, molecular parameterization is virtually nonexistent for the hydroxides. Abramowitz and coworkers[23,24] have obtained infrared spectra for matrix isolated NaOH, RbOH, and CsOH and their deuterated analogs. Belyaeva et al.[25] have studied the infrared spectra of matrix isolated KOH. The data from these groups are summarized in Table III and correspond to the assignment of ν_1, the M-O stretching mode and ν_2, the bending mode. Extensive microwave and millimeter wave studies have now yielded significant parameterization for the ground states of NaOH, KOH, RbOH, and CsOH,[26-31] and rotational con-

TABLE I. Observations of the Metal Monohydroxides

Species	Nature of the Detection Method and Comments	Species	Nature of the Detection Method and Comments
AlOH	Mass spectrometric analysis of lean H_2-O_2 flames containing aluminum.[a] Controversial results.	SrOH	Molecular emission observed in acetylene-air flames.[d,f] Presence also inferred from optical spectroscopic study of free atom depletion-dissociation energy from depletion studies.[e]
Alkali Hydroxides			
LiOH	Inferred from optical spectroscopic study of free atom depletion in H_2-O_2-N_2 [b] and H_2-O_2-CO_2 [c] flames.	BaOH	Emission in post-flame gases of H_2-O_2-N_2 flames.[d,e] Presence also inferred from spectroscopic study of free atom depletion-dissociation energy from depletion studies[e] and mass spectrometry.[g]
NaOH	Inferred from optical spectroscopic study of free atom depletion in H_2-O_2-N_2 [b] and H_2-O_2-CO_2 [c] flames.	CuOH	Some emission band spectra observed in acetylene-air flame.[f,h]
KOH	Inferred from optical spectroscopic study of free atom depletion in H_2-O_2-N_2 [b] and H_2-O_2-CO_2 [c] flames.	FeOH	Emisson band spectra observed in acetylene-air, H_2-O_2-N_2 and low pressure lean flames.[i] Presence also inferred from optical spectroscopic study of free atom depletion[j]
RbOH	Inferred from optical spectroscopic study of free atom depletion in H_2-O_2-N_2 [b] and H_2-O_2-CO_2 [c] flames.	MnOH	Emission band spectra observed in acetylene-air post-flame gases.[d,k]
CsOH	Inferred from optical spectroscopic study of free atom depletion in H_2-O_2-N_2 [b] and H_2-O_2-CO_2 [c] flames.	InOH	Presence inferred from optical spectroscopic study of free atom depletion.[e,l]
Alkaline Earth Hydroxides		GaOH	Presence inferred from optical spectroscopic study of free atom depletion.[e,l,m]
CaOH	Molecular emission observed in post-flame gases of H_2-O_2-N_2 flames. [d] Presence also inferred from optical spectroscopic study of free atom depletion[e]-dissociation energy from depletion studies.[e] Also observed in acetylene-air or O_2 flames.[f]		

[a] M. Farber, R. D. Srivastava, M. A. Frisch and S. P. Harris, Faraday Symposium 8, High Temperature Studies in Chemistry, London, 1973.

[b] D. E. Jensen and P. J. Padley, Trans. Faraday Society 62, 2132 (1966).

[c] R. Kelly and P. J. Padley, Trans. Faraday Society 67, 740 (1971).

[d] R. W. Reid and T. M. Sugden, Disc. Faraday Soc. 33, 213 (1962); L. V. Gurvich, V. G. Ryabova and A. N. Khitrov, in High Temperature Studies in Chemistry, Faraday Symp. No. 8, Paper 8, Chem. Soc. London (1973); J. Van der Hurk, J. Hollander and C. T. J. Alkemade, J. Quant. Spectrosc. Radiat. Transf. 13, 273 (1973).

[e] D. H. Cotton and D. R. Jenkins, Trans. Faraday Society 64, 2988 (1968).

[f] Cited in *Flame Spectroscopy* by R. Maurodiveanu and H. Boiteux, Wiley, New York (1965).

[g] F. E. Stafford and J. Berkowitz, J. Chem. Phys. 40, 2963 (1964).

[h] L. M. Bulewicz and T. M. Sugden, Trans. Faraday Society 52, 1481 (1956).

[i] M. J. Linevsky, Metal Oxide Studies; Iron Oxidation. Tech. Rep. RADC-TR-71-259.

[j] D. E. Jensen and G. A. Jones, J. Chem. Soc. Faraday Trans. I 69, 1448 (1973).

[k] P. J. Padley and T. M. Sugden, Trans. Faraday Society 55, 2054 (1959).

[l] E. M. Bulewicz and T. M. Sugden, Trans. Faraday Society 54, 830 (1958); 54, 1855 (1958).

[m] L. V. Gurvich and V. G. Ryabova, High Temp. USSR 2, 486 (1964).

stants have been obtained for several excited vibrational levels.

As we have noted, KOH is one of the most important constituents n the high stress environments characterizing energy generating ystems. While ground state rotational parameters have been deter-nined for KOH and KOD, vibrational frequencies are still estimated or higher vibrational levels.[32] Although matrix data are available on he fundamental vibrations, no gas phase measurements have been nade and no anharmonicities are known for any of the alkali hy-roxides. There is hope, however, that recent chemiluminescent tudies[16] can be correlated with the millimeter wave data to provide n extensive mapping of the vibrational structure of the ground lectronic state. These studies have already provided a stringent ower bound for the KOH dissociation energy (88.2 kcal/mole) gnificantly higher than that indicated in the JANAF tables (85.4). ecause of its potential for the parameterization of KOH and the kali hydroxides in general, we feel that a summary of the present atus of this work is appropriate. In this regard, it is instructive to mpare the alkali halides and hydroxides.

In Table IV, we present thermochemical data on the fluorides, lorides, and hydroxides of potassium, sodium and rubidium. Comparisons will be made between these species because (1) they are valence isoelectronic and (2) their observed emission spectra are expected to be similar.

It is generally felt that the nature of the bonding in the alkali hydroxides should be intermediate to that in the fluorides and chlorides. With this in mind, the trends in Table IV would seem to indicate the possibility of a KOH bond strength higher than the mass spectrometric value. This is significant since the flame studies do indicate a higher value for the bond energy. JANAF now recommends 85.4 kcal/mole in close agreement with the flame studies.

Cardelino et al.[16] have obtained a KOH* chemiluminescent spectrum under a variety of conditions. The observed emission for KOH correlates closely with expectations based on the known chemiluminescent emission for KCl. In order to understand the nature of the KOH emission spectrum, it is instructive to consider spectra for the alkali halides.

Alkali halide spectra have been obtained in three distinct experimental environments.[33] They have been observed under "single collision" conditions where alkali dimers and halogen molecules react in a four-center process

ıBLE II. Dissociation Energies of Metal Monohydroxides*

ecies	D_o(M-OH) kcals/mole	Comments
)H	103 ± 2[a]	H_2-O_2-CO_2 flames 2nd law determination
OH	79 ± 2[a]	H_2-O_2-CO_2 flames 2nd law determination
ıH	84 ± 2.5[a]	H_2-O_2-CO_2 flames 2nd law determination
ıH	80 ± 3[b]	Mass spectrometry
)H	86 ± 3[a]	H_2-O_2-CO_2 flames 2nd law determination
)H	96[c]	Rich hydrogen-air flames
	94 ± 3[d]	Rich hydrogen-air flames
	103.7[e]	
	103[f]	Quoted uncertainty ≤ 2.5 kcals/mole
)H	95[e]	
	103[e]	
	102[f]	Quoted uncertainty ≤ 2.5 kcals/mole
)H	111[c]	
	114.3[e]	
	113[f]	Quoted uncertainty ≤ 2.5 kcals/mole
	107[g]	Mass spectroscopy
	109 ± 3[d]	
-ł	90 ± 2[a]	H_2-O_2-CO_2 flames 2nd law determination
	86 ± 7[h]	H_2-O_2-N_2 flames 2nd and 3rd law determination
)H	102 ± 5[h]	H_2-O_2-N_2 flames 2nd and 3rd law determination
ł	<72[a]	H_2-O_2-CO_2 flames 2nd law determination
H	100 ± 3[i]	Low pressure H_2-O_2-N_2 flames
H	$<85 \pm 9$[j]	Low pressure H_2-O_2-N_2 flames
ł	130[k]	Thermochemistry and reactions in hydrogen oxygen flames

elly and P. J. Padley, Trans. Faraday Society 67, 740 (1971).

Gorokhov, A. V. Gusarov and I. G. Panchenkov, Russ. J. Phys. Chem. 44, 150 ı).

Gurvich, V. G. Ryabova and A. N. Khitrov, in High Temperature Studies in istry, Faraday Symposium No. 8, Paper 8, Chem. Soc. London (1973).

. Ryabova, A. N. Khitrov, and L. V. Gurvich, High Temperature 10, 669 (1973).

. Cotton and D. R. Jenkins, Trans. Faraday Society 64, 2988 (1968); also K. ield and T. M. Sugden, Symp. (Int.) Combust. 10th, p. 589, Combust. Inst., urgh, PA.

Kalff and C. T. J. Alkemade, Combust. Flame 19, 257 (1972).

Stafford and J. Berkowitz, J. Chem. Phys. 40, 2963 (1964).

. Bulewicz and T. M. Sugden, Trans. Faraday Society 54, 830, 1855 (1958).

Linevsky, Metal Oxide Studies; Iron Oxidation. Tech. Rep. RADC-TR-71-259.

Bulewicz and P. J. Padley, Trans. Faraday Soc. 67, 2337 (1971).

. Jackson, Thermodynamics of Gaseous Hydroxides, UCRL 51137, urvich and I. V. Veits, Dokl. Akad. Nauk. SSSR 108, 659 (1956). Note also M. and R. D. Srivastava, Thermochemical Reactions of aluminum and fluorine in ·en-oxygen flames, Combust. Flame 27, 99 (1976).

$$X_2 + MX^* + MX, \qquad (1)$$

sulting MX* product emitting a photon before undergoing quent collision.[34] These studies have been extended to "mul-ollision" conditions by entraining the alkali dimers in argon and quently oxidizing this mixture.[35] A much more effective colli- environment consists of a "diffusion flame" device where at is passed through a nozzle into a bulb containing several torr ali vapor and one to twenty torr of argon.

Fig. 1, we depict emission spectra obtained for KCl, RbCl, and nder single collision conditions. The nature of the potential which give rise to the spectra in Fig. 1 is depicted in Fig. 2. gh drawn for KBr, the general features are similar for all the

ADDED IN PROOF: The dissociation energy of cesium hydroxide has been ed. This data was not included in Table II. Using mass spectrometry, Gorokhov, , and Panchenkov (Table II Ref. b) determined D_0(Cs-OH) = 86 ± 3 kcal mole. nd Padley (Table I Ref. b) have used a third law analysis of an $H_2 + O_2 + N_2$ flame ce D_0(Cs-OH) = 91 ± 3 kcal mole. These determined bond energies are in fair nt.

TABLE III. Infrared Data for the Alkali Hydroxides

Molecules	ν_1 (cm^{-1})	ν_2 (cm^{-1})
CsOH[a]	335.6	309.8
		302.4
CsOD[a]	330.5	226
RbOH[b]	354.4	309.0
RbOD[b]	345 ± 3	229 ± 3
KOH[c]	408	300
KOD[c]	399	264
NaOH[b]	431	337
NaOD[b]	422 ± 3	250

a. Ref. 23
b. Ref. 24
c. Ref. 25

TABLE IV. Comparison of Thermochemical Data for the Alkali Fluorides, Chlorides, and Hydroxides

Molecules	D_o^o(M-X)	Comments
KF	117[a]	Thermochemical
KCl	102.6 ± 2[b]	Thermochemical and photofragment
KOH	84 ± 2.5[c]	H_2-O_2-CO_2 flames 2nd law determination
	80 ± 3[d]	Mass spectrometry
	85.4 ± 3	(JANAF tables estimate)
NaF	123	NaOH 79 ± 2 (flame—2nd law—JANAF)
NaCl	97.6 ± 2[b]	
RbF	115[e]	RbOH 86 ± 3 (flame—2nd law—JANAF)
RbCl	101.3 ± 2[b]	

[a] E. M. Bulewicz, C. G. James, T. M. Sugden, Trans. Faraday Soc. 37, 921 (1961); A. G. Gaydon, *Dissociation Energies and Spectra of Diatomic Molecules,* 3rd Edition, Chapman and Hall (1968).

[b] T-M. R. Su and S. J. Riley, J. Chem. Phys. 72, 6632 (1980).

[c] R. Kelly and P. J. Padley, Trans. Faraday Society, 67, 740 (1971); also the average of three other flame studies by Smith and Sugden Proc. Roy. Soc. A219, 304 (1953) [86 ± 1]; Jensen and Padley, Trans. Fara. Soc. 62, 2132 (1966) [82 ± 2]; Cotton and Jenkins, Trans. Fara. Soc. 65, 1537 (1969) [86 ± 2].

[d] L. N. Gorokhov, A. V. Gusarov and I. G. Panchenkov, Russ. J. Phys. Chem. 44, 150 (1970).

[e] See footnote a and A. D. Caunt and R. F. Barrow, Nature 164, 753 (1949).

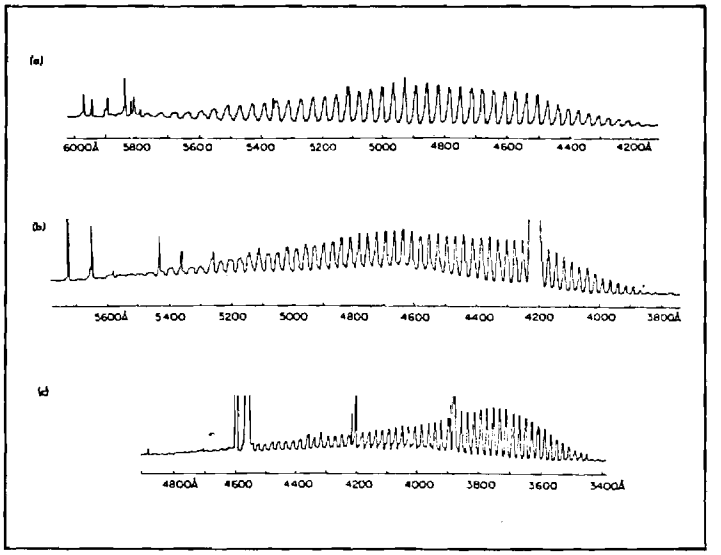

Fig. 1. Chemiluminescent spectra of (a) KCl, (b) RbCl, (c) CsCl, with a resolution of 5 Å or better. Also present in each trace are atomic (alkali) lines, some of which are off scale. (Taken from Ref. 34.) See text for discussion.

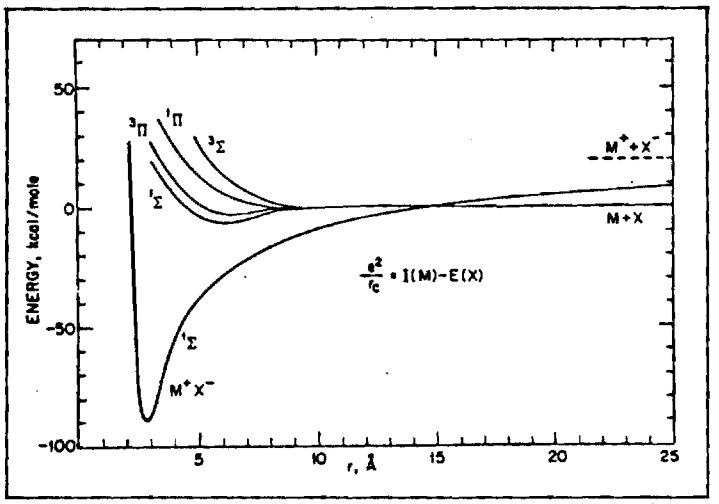

Fig. 2. Potential energy curves for an alkali halide molecule (drawn for KBr) showing the "zeroth order crossing" of the ionic and covalent states. Note the shallow excited electronic states close to the ground state dissociation asymptote.

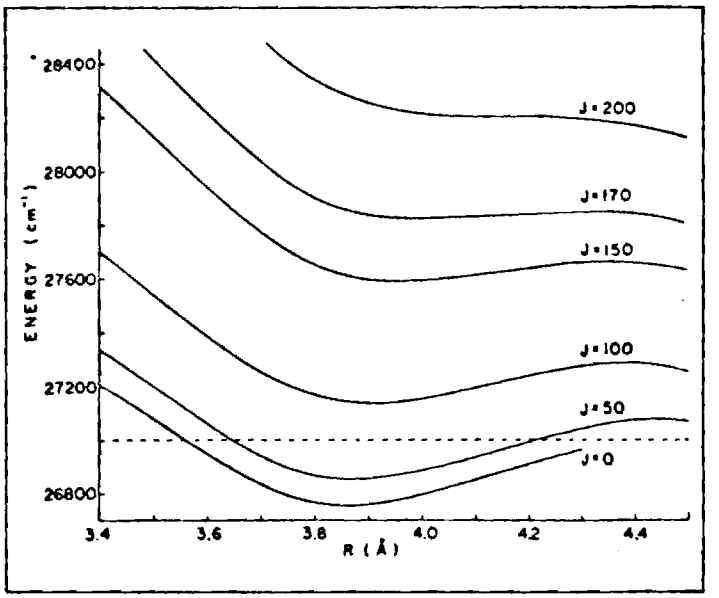

Fig. 3. Effective excited state potential curves for KI constructed from the rotationless potential of Kauffman, Kinsey, Palmer, and Tewarson (Ref. 37) assuming a dissociation asymptote of 2700 cm^{-1} (see Ref. 34).

alkali halides. The alkali halides are characterized by a relatively stable ionic ground state and a grouping of several very shallow or repulsive excited states. The emission which one observes corresponds to a transition from one of the shallow or repulsive states to levels of the ground electronic state, the spectrum corresponding to a long progression in the vibrational levels of the ground electronic (ionic) state. The very shallow nature of the excited state potential has important consequences. One finds that the KCl spectrum changes drastically with the form of excitation and the experimental technique used to produce the emission system. The "single collision" spectrum in Fig. 1 *onsets* at 4180 Å (68.4 kcal/mole). A very similar spectrum is obtained when potassium dimers are entrained in argon and this mixture oxidized in a multiple collision device. A drastic change occurs when the reaction (1) is studied in a diffusion flame environment. Here the onset of the KCl spectrum is at 2866 Å[36] some 300 Å to blue of the single and multiple collision spectrum. This large change signals an important characteristic of the alkali halide excited state potential. Whereas emission spectra involving strongly bound excited states are not drastically altered by the nature of a changing effective potential due to rotation, the shape and nature of shallow or repulsive states can be drastically altered by rotational excitation. This is exemplified for KI in Fig. 3.[37] Here effective potential curves are constructed as a function of the rotational quantum number J and the relation

$$V_{\text{effective}}(J) = V_{\text{rotationless}} + \hbar^2\left(\frac{J(J+1)}{2\mu R^2}\right) . \qquad (2)$$

It should be noted that there is a substantial change in the minima of the effective potentials as a function of increasing rotational excitation and hence the quantum number J. The high J potentials correspond to the single and multiple collision spectra onsetting at 80 Å;[36] the low J potentials correspond to the diffusion flame emission system onsetting at 2866 Å.[36] As a result of this shift in the excited state potential one observes emission to differing sets of bound state levels. In the diffusion flame experiments emission is observed to much lower regions of the ground state potential and hence the spectra onsets much further to the blue.[36]

The spectrum for potassium hydroxide has been obtained by Cardelino et al.[16] upon reacting potassium with hydrogen peroxide (O+%). The process which yields chemiluminescence is believed to correspond to the four center reaction

$$+ \text{HO-OH} \rightarrow \text{KOH}^* + \text{KOH} \qquad (3)$$

where KOH* denotes electronically excited KOH. The close analogy which the potassium hydroxide spectrum bears to that of KCl leads to comparisons between the two molecules which, in the final analysis, involve a direct determination of the K-OH bond energy.

The change in the emission spectra for the alkali halides as a function of experimental conditions may also be manifest in the alkali hydroxides. One anticipates that the potential function describing the K-OH stretch will be similar to that for KCl. If the potential curves for the excited states of K-OH are similar to those for KCl, they should be shallow and the KOH emission spectrum which results from reaction (3) should change significantly with excitation technique. This is observed, although the effect is not as pronounced as that in KCl. Single and multiple collision spectra for KOH onset at 3840 Å whereas the spectrum obtained in a diffusion flame (Fig. 4) onsets at 3240 Å. This significant change signals the observation of a shallow "effective" potential for the K-OH normal mode.[38]

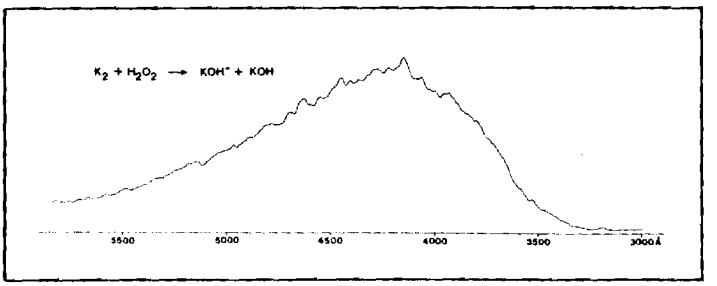

Fig. 4. Chemiluminescent spectrum obtained for KOH* formed in a diffusion flame environment. See text for discussion.

The KCl and KOH spectra correspond to emission from shallow effective potentials close to the dissociation asymptote (Figs. 2 and 3) of the ground electronic state. Given that we have strong evidence for these shallow effective potentials, we can use the onset of spectral emission to estimate the dissociation energy for the K-Cl and K-OH bonds. Because the diffusion-flame results must correspond to emission to lower levels of the ground state potential, this onset is chosen to give the best estimate of the bond dissociation energy. For K-Cl, the onset at 2866 Å corresponds to 99.8 kcal/mole. This should be compared to the value in Table IV: D_0^0(K-Cl) = 102.6 ± 2 kcal/mole.

uld be apparent that we are able to estimate a good lower to the K-Cl dissociation energy from the energy correspond- the onset of the K-Cl diffusion flame spectrum. The onset of)H diffusion flame spectrum at 3240 Å yields a lower bound of :al/mole for the K-OH bond energy.[39]

: result obtained by Cardelino et al.[16] is significant for several s. It represents the first direct measurement of the bond energy is species. The lower bound deduced for the K-OH bond th indicates that the correct dissociation energy is on the order :2 kcal/mole. This value considerably exceeds that obtained in ly mass spectrometric study of the monomer quoted in Table ıe much higher value for the KOH bond energy is more :ent with the bounds estimated from metal atom flame deple- udies, but does indicate a slightly higher value.[39] A several orie increase in the KOH bond strength has significant impli- ; for the stability and effect of this compound in energy generat- tems.[40]

anticipated that further studies of the K_2-H_2O_2 diffusion flame will improve the lower bound currently quoted for the K-OH nergy. It should be noted that the present result is not incon- with the recent findings of Wormhoudt and Kolb.[41] These s observe unusually high KOH concentrations in their studies -fired MHD plasmas. Also, recent theoretical calculations by d[42] indicate the possibility of a higher K-OH bond energy.

ıddition to a refinement of the K-OH bond energy, higher ion spectra of the K_2-H_2O_2 diffusion flame should provide ;eful information on the vibrational structure of the ground ormal mode "hot" bands. With reasonable luck, it should be e to correlate these studies with the millimeter wave results ned earlier. The structural parameters (molecular constants) :d will be of use in the calculation of thermodynamic proper- KOH.

e alkaline earth hydroxides

:, there is very little molecular parameterization on the alka- th hydroxides. Brom and Weltner have obtained ESR spectra)H[43] and MgOH.[44] Weeks et al.[45] have studied laser excited lar fluorescence from CaOH and SrOH in an air-acetylene proposing a preliminary energy level diagram for CaOH. ıuthors also comment on apparent earlier observations of and SrOH in both absorption[46] and fluorescence.[47] More / Haraguchi et al.[48] have excited laser fluorescence from again indicating the nature of previous absorption[49] and n[50] studies and presenting a preliminary energy level diagram. g the chemiluminescent emission from the Ca-H_2O_2 reac- anner et al.[51] have succeeded in obtaining "single collision" n from CaOH, determining a preliminary CaOH bond energy ; kcals/mole. This result is in good agreement with the flame of Cotton and Jenkins[52] and Kalff and Alkemade.[53] These will be extended to consider strontium and barium reactions g the determination of lower bounds for the alkaline earth de bond energies. It should be noted that the calcium and m compounds do not appear to be accessible to mass netry.

sparse nature of the data on the alkaline earth hydroxides y leaves a very fruitful and potentially significant area for study.

ıer metal hydroxides

; no doubt that experimental techniques developed for the ıd alkaline earth hydroxides will soon be extended to other nt metal hydroxides. Of particular note should be the hydrox- anadium, silicon, and iron. These species will weigh heavily : technological developments.

'DING AND SPECTRA OF THE ALKALI)XIDES AND MONOSULFIDES

ıding in the diatomic metal oxides and sulfides

ave been relatively few spectroscopic or thermodynamic studies of the alkali oxides. Based on the results of molecular beam experiments (alkali metals + NO_2), Herm and Herschbach[54] have estimated the MO bond dissociation energies as follows: LiO (82 ± 4), NaO (67 ± 3), KO (71 ± 3), RbO (68 ± 3), and CsO (70 ± 3 kcal/mole). The value for NaO is in fair but not spectacular agreement with the value of 60.3 ± 4 kcal/mole deduced by Murad and Hildenbrand[55] using mass spectroscopy. Fundamental frequencies for LiO (750 cm^{-1}),[56] KO (384),[57] and CsO (314)[57] have been measured using matrix isolation spectroscopy; however, the corresponding infrared absorptions in NaO and RbO have not yet been observed.

Evidence has been obtained for a change in the orbital makeup and symmetry of the ground electronic state upon traversing the series LiO...CsO. The electronic ground state of LiO is $^2\Pi$. Freund et al.[58] have obtained very detailed spectra which demonstrate that this molecule is well represented by a crystal field model based on $Li^{\oplus}$ $O^{\ominus}$. This model is in accord with *ab initio* calculations.[59]

Reactive scattering experiments[54] have indicated that NaO also has a $^2\Pi$ ground state whereas the ground state of CsO is of $^2\Sigma$ symmetry. Most recently ESR-matrix experiments[60] have also demonstrated that RbO and CsO have $^2\Sigma$ ground states whereas the ground states of LiO, NaO and KO are probably $^2\Pi$. A recent theoretical calculation[61] is in slight conflict with this conclusion indicating that the ground state of KO is $^2\Sigma^+$.

The observation of a $^2\Sigma^+$ ground state conflicts with the simple ionic model in which the electron donated by the alkali atom enters the $2p\sigma$ oxygen orbital along the internuclear axis, leaving a hole in the 2π orbital and resulting in a $^2\Pi$ state ($\sigma^2\pi^3$ molecular orbital configuration). An explanation for the observed trends can be obtained by evoking the concept of "inner shell bonding" in which one considers the mixing of filled (n − 1)p alkali orbitals with the 2p oxygen orbitals. Figure 5 contrasts the molecular orbital scheme for NaO based on the alkali valence orbitals with the adjusted intershell orbital scheme for CsO.[60,61] The alkali monoxides are highly ionic

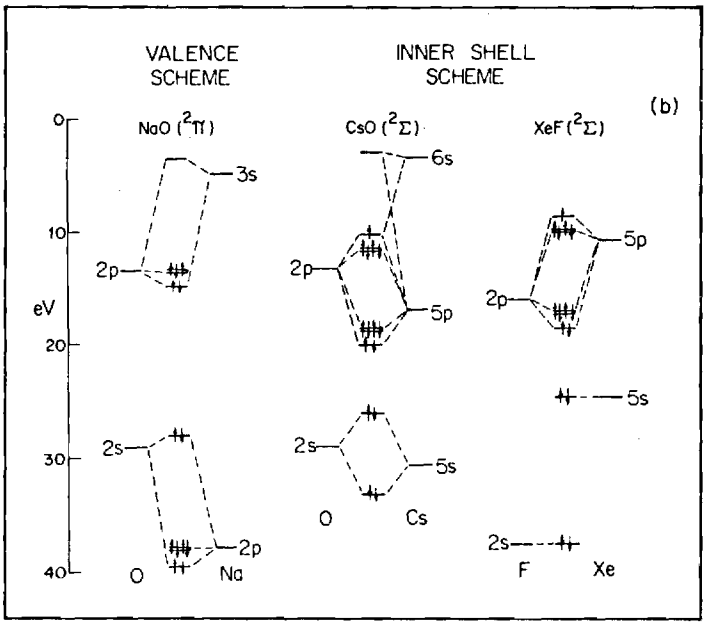

Fig. 5. Molecular orbital scheme for the alkali monoxides (taken from the work of Lindsay, Kwiram and Herschbach, Ref. 60). See text for discussion.

molecules, $M^{\oplus}$ $O^{\ominus}$, in both schemes but the latter gives a $^2\Sigma$ ground state (... $\pi^4\sigma$). The change from the valence to the inner shell scheme is governed by the location of the (n−1)p orbitals of M^+. These orbitals lie far below the 2p orbitals of O^- for Li or Na but become comparable in energy for Rb or Cs.

The significance of the orbital scheme discussed above can best be understood if we focus on the calculated *ab initio* curves for LiO (Fig.

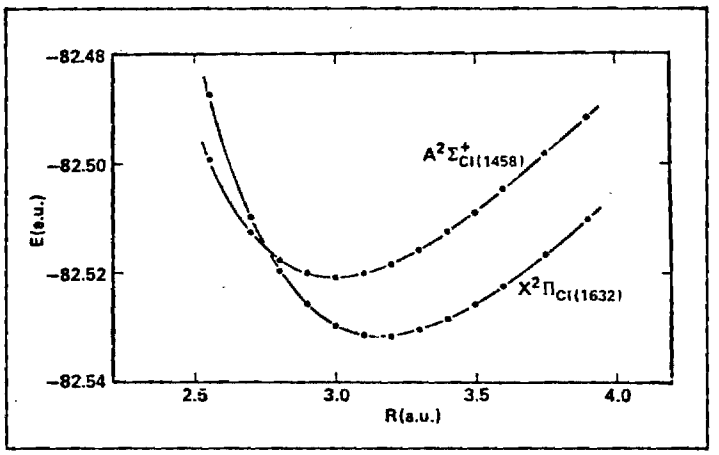

Fig. 6. Potential curves based on extensive configuration interaction calculations on the $X^2\Pi$ and $A^2\Sigma^+$ states of LiO.

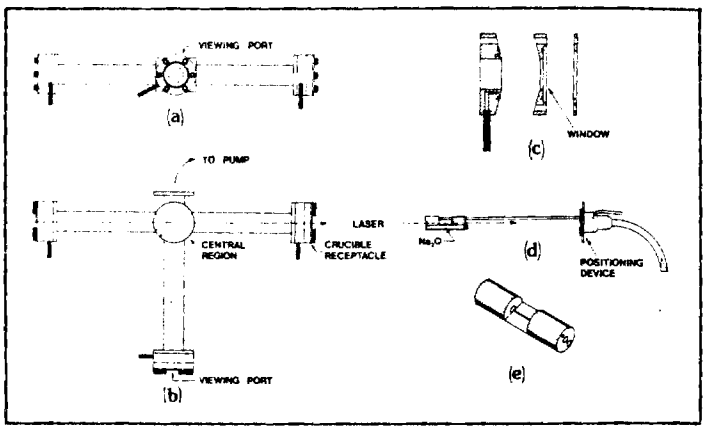

Fig. 7. Schematic diagram of apparatus for laser fluorescence studies of Na_2O. See text for discussion.

6). It is apparent that the ground $X^2\Pi$ and low lying $A^2\Sigma^+$ states are separated by less than 2300 cm^{-1}. This energy increment will decrease for the sodium and potassium oxides. For RbO, the $A^2\Pi_i$ state is separated by less than 3800 cm^{-1} from the ground $X^2\Sigma^+$ state.[60]

While the sulfides are expected to display similar bonding trends, it may well be that the possibility of "inner shell bonding" decreases because of the small binding energy for the 3p electron on sulfur. Therefore, the ground states of LiS, NaS and KS are expected to be $^2\Pi$ and the ground state of RbS may be $^2\Pi$ with a very low lying $^2\Sigma$ state. To date, no information is available on the alkali sulfides; however, the metal sulfide bond energies are expected to be somewhat lower than the corresponding oxides.

As should be apparent from the previous discussion, data which will prove of use for the future assessment of metal oxide and sulfide interactions is virtually unavailable. The characterization of these species will not represent a trivial problem. Experimental difficulties which are already substantial are further complicated by the presence of the very low-lying $^2\Sigma$ (LiO, NaO, etc.) or $^2\Pi$ (RbO, CsO, etc.) state. In order to characterize the $^2\Sigma$ and $^2\Pi$ states, it may be appropriate to search for higher-lying electronic states; however, predissociative effects will soon plague this search. There is indication that the chemiluminescent reactions $M + N_2O$, $M + O_3 - MO^* + \ldots$ may lead to some elucidation of the molecular parameters for the alkali oxides; however, these data are only in a preliminary state.[62]

5.2. Bonding in the triatomic alkali oxides and sulfides M_2O and M_2S

Yet another interesting group of compounds whose characterization will represent a significant contribution are the alkali oxides, M_2O. There have been several quantum chemical calculations performed on Li_2O[63] and infrared fundamentals (ν_3) have been reported for Li_2O,[56] K_2O,[57] Rb_2O,[57] and Cs_2O;[57] however, thus far, there appear to be no definitive gas phase data on these compounds and no data whatsoever on Na_2O.

5.3. Laser spectroscopy on Na_2O—a preliminary study

In order to efficiently excite fluorescence from Na_2O, Crumley et al.[64] have constructed the device depicted in Fig. 7. Figures 7(a) and 7(b) indicate the overall layout of the cell used in these experiments. Figure 7(c) indicates the window design which is frequently necessary when working with refractory species, the gas flow system being designed to provide a uniform circulation of gas over the windows. In order to carefully control the vaporization of Na_2O in a very localized region, the device depicted in Figs. 7(d) and 7(e) is used. It consists of a crucible which is suspended on a 1/8" stainless steel tube such that once the overall device is connected to the cell sidearm, the crucible is centrally located to the viewing port. The positioning control whose diameter is the same as the window shown in Fig. 7(c) is held in place in precisely the same fashion as the window. When connected to the overall cell, the crucible holder is rotated 90° with respect to its depiction in the figure. When the cell is in operation, a laser beam traverses the path indicated in Figs. 7(b) and 7(d). Na_2O is directly vaporized through a thin slit into the path of the laser beam. The slit and the laser beam are parallel and the laser induced fluorescence is viewed at 90°.[65]

Using the cell described above and various pumping schemes, Crumley et al.[64] have carried out experiments at both 100 μ (primarily background argon) and 10^{-6} torr. This range of background pressure allows one not only to do spectroscopy but also to observe quenching effects which appear to be quite significant for Na_2O. Thus far, experiments have been conducted primarily with an argon ion laser; however, some excitation has been accomplished with a rhodamine dye laser. Examples of the spectra *tentatively* assigned to Na_2O are shown in Fig. 8.[66] They correspond to excitation at 5145

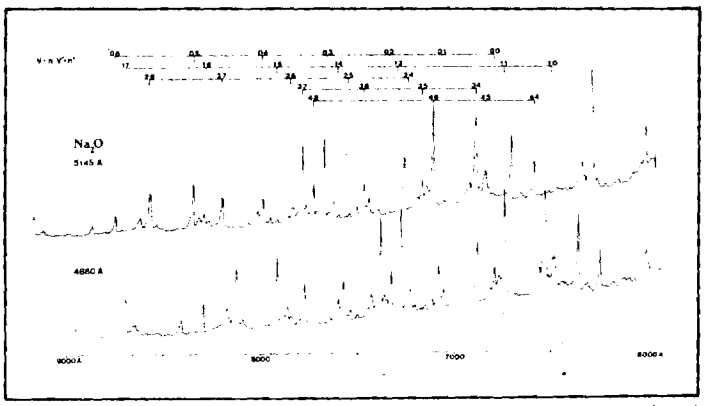

Fig. 8. Laser induced photoluminescence spectra tentatively correlated with Na_2O taken at a resolution of 1 Å and using the 5145 and 4880 Å argon ion laser lines for excitation. See text for discussion.

and 4880 Å. It appears that one can excite laser-induced fluorescence with several of the available argon ion laser lines (4579, 4880, 4965, 5017, 5145 Å) and that the fluorescence spectra can be interconnected (significant overlap) in a rather substantial Deslandres Table. Much of the analysis of the observed spectra has depended on relating the Na_2O studies to available information on Li_2O. These data come primarily from matrix isolation spectroscopy[56] and recent quantum chemical calculations.[63] Briefly, the data have been used to (1) attempt to estimate the normal frequencies of vibration for Na_2O based on a reasonable extrapolation from Li_2O, and (2) determine the most likely electronic transition which should be excited in the visible using an argon ion laser.

Using a notation common to several quantum chemical descrip-
ons of linear $D_{\infty h}$ Li_2O, the valence orbital configuration for the
ound state is

$$.(3\sigma_g)^2(2\sigma_u)^2(1\pi_u)^4 \qquad {}^1\Sigma_g^+ \qquad (4)$$

iere the valence orbitals are constructed primarily from 2s and 2p
:ctrons on lithium and oxygen. The lowest Li_2O excited states
rrespond to the promoted configurations

$$.(3\sigma_g)^2(2\sigma_u)^2(1\pi_u)^3(4\sigma_g)^1 \qquad {}^{1,3}\Pi_u \qquad (5)$$

$$.(3\sigma_g)^2(2\sigma_u)^2(1\pi_u)^3(3\sigma_u)^1 \qquad {}^{1,3}\Pi_g \qquad (6)$$

d Grow and Pitzer[63b] have shown that these states are very low
ng ($\Delta E_{excitation} \leqslant 1.3$ eV); therefore it is unlikely that even the
ongly allowed

$$_1 \rightarrow {}^1\Sigma_g^+$$

nsition corresponds to the fluorescence observed upon single
)ton pumping with an argon ion laser. A further promotion which
l result in a strongly allowed transition, most likely in the visible
ion, leads to the configuration

$$(3\sigma_g)^2(2\sigma_u)^1(1\pi_u)^4(4\sigma_g)^1 \qquad {}^{1,3}\Sigma_u^+ . \qquad (7)$$

: anticipates that the visible transition in Na_2O which is pumped
the argon ion laser corresponds to a ${}^1\Sigma_u^+ \leftarrow {}^1\Sigma_g^+$ excitation
)lving the analog of configurations (4) and (7). In pumping this
sition, one removes an electron from an orbital which is Na-O
bonding and Na-Na antibonding and promotes this electron to
)rbital which is both Na-O and Na-Na bonding. Hence, one
:cts that both the excited state stretching and bending frequen-
should exceed that of the ground electronic state of Na_2O.
'he ground state frequencies for Li_2O are (matrix isolation spec-
:opy) $\nu_1 \approx 760\ cm^{-1}$, $\nu_2 \approx 112\ cm^{-1}$, and $\nu_3 \approx 990\ cm^{-1}$. Formu-
g a normal coordinate analysis based on the Li_2O measure-
ts, one estimates a vibrational frequency of between 540 and 585
' for the symmetric stretch (ν_1) and 74 cm^{-1} for the bending
e of Na_2O. This is not unreasonable when comparisons are made
NaO where the vibrational frequency appears to be ~519
[61] (recall that Na_2O is thought to be a linear molecule).
lthough absolute quantum level numberings have not been
ned, extensive Deslandres Tables for the pumped transitions
ate an upper state vibrational frequency of ~650 cm^{-1} and a
r state (ground state) frequency of ~550 cm^{-1} consistent with
redictions outlined above. In addition, a closer view (Fig. 9) of a
n of the 5145 Å spectrum in Fig. 8 reveals what appear to be
cm^{-1} separations expected for the ground state bending mode
a_2O. *Tentatively*, it appears that the spectra correspond to
'essions in the symmetric stretching and bending modes of the
id and excited state in a ${}^1\Sigma_u^+ \rightarrow {}^1\Sigma_g^+$ transition.
iese studies hold the promise of providing information which is
iely useful for the understanding of fundamental dynamic pro-
; such as the reaction of sodium dimers and oxygen atoms and
lso establish a foothold for analyzing kinetic processes in which
) plays a significant role. Because Na_2O represents an important
ituent in energy generating systems, one desires a means to
ılly monitor its behavior. It should also be noted that in addi-
o their use for the characterization of reaction kinetics, such
s, while still in their early phases, may well allow the determina-
f parameters useful in thermodynamic evaluations. Before the
t of the laser, the study of these elevated temperature free
ls rested primarily within the province of the matrix isolation
oscopist. The versatility introduced by the laser should allow
ure comparison of molecular behavior in gas-phase and matrix
nments.

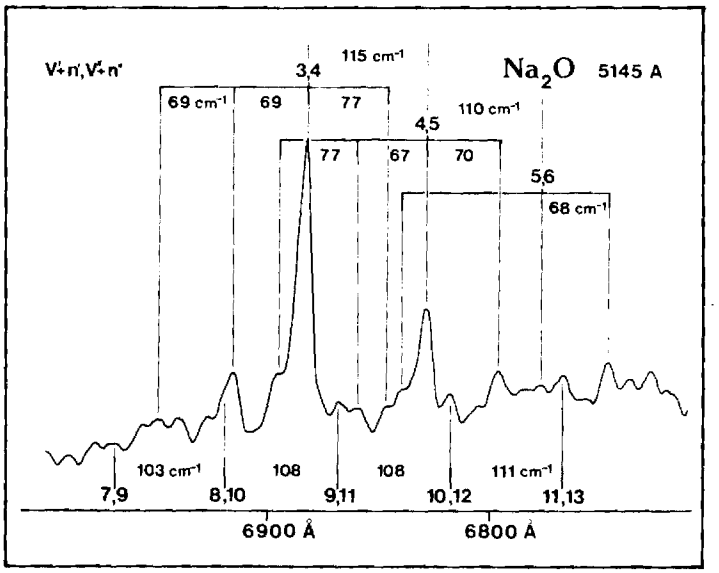

Fig. 9. Close-up of laser induced photoluminescence spectrum tentatively correlated with Na_2O taken at a resolution of 0.5 Å and using the 5145 Å argon ion laser line for excitation. See text for discussion.

6. FURTHER CONSIDERATIONS

We have attempted to indicate the nature of several important and yet sparsely characterized systems whose study will greatly aid the understanding of the gas phase chemistry associated with energy generating systems. While our discussion has focused primarily on bond energies and molecular parameterization, kinetics and energy transfer must also play an important role in the realistic description of a system. The correct modeling of energy generating systems is the subject of some controversy. Strong evidence is emerging which indicates that the modeling of an energy system assuming thermodynamic equilibrium and applying "free energy minimization" may not be entirely or even partially appropriate. In the vast majority of the systems where thermodynamics and kinetics both play a role, observed phenomena are in large part controlled by the rates of various processes. Hence current modeling efforts are incorporating kinetic parameters.[40] In carrying out chemiluminescent studies across a wide pressure range ($10^{-6} - 10^2$ torr), we have observed and characterized ultrafast intramolecular energy transfer routes among the electronically and vibrationally excited states of several high temperature molecules. Thus far, these studies have indicated that energy transfer can occur at rates which may approach 500 times the calculated gas kinetic rates. These surprising results demonstrate that vibrationally and/or electronically excited high temperature molecules act as if they were "large" or "diffuse" entities capable of strong interaction at very long range. This rapid energy transfer is a general phenomenon and effects have been observed in several molecules including SiO and KOH. The observation of such rapid energy transfer may have significant implications for the modeling of energy generating systems and the characterization of heat flow in these systems.

7. ACKNOWLEDGMENTS

It is a pleasure to acknowledge partial support of some of the work described here by the U. S. Department of Energy. Professor W. H. Eberhardt read the first draft of this manuscript and provided many helpful suggestions.

8. REFERENCES

1. D. M. Lindsay and J. L. Gole, J. Chem. Phys. 66, 3886 (1977); M. J. Sayers and J. L. Gole, J. Chem. Phys. 67, 5442 (1977); J. L. Gole and S. A. Pace, J. Chem. Phys. 73, 836 (1980); A. W. Hanner and J. L. Gole, J. Chem. Phys. 73, 5025 (1980).
2. R. J. Ross, *Magnetohydrodynamic Energy Conversion*, McGraw-Hil, New York (1968).

3. S. A Medin, V. A. Ovcharenko and E. E. Shpil'rain, High Temp. U.S.S.R. 10, 390 (1972).
4. H. C. Hottel and J. B. Howard, *New Energy Technology—Some Facts and Assessments,* M.I.T. Press, Cambridge, MA (1971); L. P. Harris and G. E. Moore, IEEE Trans. Power App. Syst. 90, 2030 (1972).
5. *Open Cycle Magnetohydrodynamic Power Generation,* J. B. Heywood and G. J. Womack, eds., Pergamon, Oxford (1969).
6. F. E. Spencer, Jr., J. C. Hendrie and D. Bienstock, Symp. Eng. Aspects Magnetohydrodynam., 13th, Stanford Univ., p. VII.4.1; VII.4.6.
7. *Joint Army Navy Air Force Thermochemical Tables.* 2nd ed., NSRDS-NBS37. U.S. Govt. Printing Office, Washington, D.C.
8. W. B. England, J. Chem. Phys. 68, 4896 (1978).
9. Sulfur impurities are also important. See for example, R. K. Sinha and P. L. Walker, Jr., Fuel 51, 329 (1972); F. S. Karn, R. A. Friedel and A. G. Sharkey, Jr., Fuel 51, 113 (1972).
10. J. Marlin Smith, L. D. Nichols and G. R. Seikel, NASA Lewis H_2-O_2 MHD Program, Int. Symp. Eng. Aspects of Magnetohydrodynamics, 14th April, 1974, Tullahoma, TN, p. III.7.1.
11. G. W. Stewart, A. Chakrabasti, C. Stinespring and K. Casleton, Western States Symposium/Combustion Institute, October, 1980.
12. Session on High Pressure Sampling, 10th Materials Research Symposium on Characterization of High Temperature Vapors and Gases, National Bureau of Standards, Gaithersburg, MD. September 18-22, 1978.
13. I. Fells, in *Combustion and Propulsion,* AGARD Colloq. 6th, Energy Sources and Energy Conversion, H.M. DeGroff, R. F. Hogland, J. Fabri, T. F. Nagey and M. E. Rumbaugh, Jr., eds., Gordon and Breach, New York (1967), p. 477.
14. See, for example, J. W. Hastie, *High Temperature Vapors, Science and Technology,* Academic Press, New York (1975); see also, O. Glemser and H. G. Wendlandt, Advan. Inorg. Chem. Radiochem. 5, 215 (1963); F. T. Greene, S. P. Randall and J. L. Margrave, in *Thermodynamic and Transport Properties of Gases, Liquids and Solids,* Am. Soc. Mech. Eng., New York (1959), p. 222; D. D. Jackson, *Thermodynamics of Gaseous Hydroxides,* UCRL—51137 (1959).
15. Laboratory data on the hydroxides when extrapolated may well be related to practical problems such as the nature of solid deposition in steam turbines.
16. B. Cardelino, W. Crumley and J. L. Gole, work in progress.
17. A. W. Hanner and J. L. Gole, unpublished data.
18. W. D. Winefordner et al. to be published; see also Refs. 45 and 47.
19. F. E. Stafford and J. Berkowitz, J. Chem. Phys. 40, 2963 (1964).
20. R. Kelly and P. J. Padley, Trans. Faraday Soc. 67, 740 (1971); H. Smith and T. M. Sugden, Proc. R. Soc. A 219, 304 (1953); D. H. Cotton and D. R. Jenkins, Trans. Faraday Soc. 65, 1537 (1970); D. E. Jensen and P. J. Padley, Trans. Faraday Soc. 62, 2132 (1966).
21. L. N. Gorokhov, A. V. Gausarov and I. G. Panchenkov, Russ. J. Phys. Chem. 44, 150 (1970).
22. See Table II references c, d, e.
23. N. Acquista, S. Abramowitz and D. R. Lide, J. Chem. Phys. 49, 780 (1968).
24. N. Acquista and S. Abramowitz, J. Chem. Phys. 51, 2911 (1969).
25. A. A. Belyaeva, M. I. Dvorkin, and L. D. Sheherba, Opt. and Spectrosc. 31, 210 (1971).
26. D. R. Lide and R. L. Kuczkowski, J. Chem. Phys. 46, 4768 (1967).
27. C. Matsumura and D. R. Lide, J. Chem. Phys. 50, 71 (1969); D. R. Lide and C. Matsumura, J. Chem. Phys. 50, 3080 (1969).
28. E. F. Pearson and M. B. Trueblood; J. Chem. Phys. 58, 826 (1973); Astrophys. Journal 174, L145 (1973).
29. E. F. Pearson, B. P. Winnewisser and M. B. Trueblood, Z. Naturforsch 31a, 1259 (1976).
30. P. Kuijpers, T. Törring and A. Dymanus, Chem. Phys. 15, 457 (1976); Z. Naturforsch 31a, 1256 (1975).
31. P. Kuijpers, T. Törring and A. Dymanus, Z. Naturforsch 32a, 930 (1977).
32. D. E. Jensen, J. Phys. Chem. 74, 207 (1970).
33. J. L. Gole, The Characterization of High Temperature Vapors of Import to Combustion and Gasification Processes in the Energy Technologies, Proceedings of the Morgantown Energy Technology Center Meeting on High Temperature, High Pressure Particulate and Alkali Control in Coal Combustion Process Streams, Morgantown, West Virginia, 1981.
34. For a discussion of single collision conditions, see J. L. Gole, Ann. Rev. Phys. Chem. 27, 525 (1976); for the alkali halides, see R. C. Oldenborg, J. L. Gole and R. N. Zare, J. Chem. Phys. 60, 4032 (1974).
35. See Ref. 1 and G. J. Green and J. L. Gole, Chem. Phys. 46, 67 (1980).
36. A. Tewarson, Studies of Chemiluminescent Emission in Selected Low-Pressure Diffusion Flames, Ph.D. Thesis, Penn State University, 1969. The long wavelength limit of the diffusion flame spectrum is 4654 Å versus 5708 Å for the single collision spectrum. Hence the entire KCl spectrum is shifted to the blue ~1200 Å when experimental conditions are changed from the single collision to the diffusion flame environment.
37. Taken from Oldenborg et al. Ref. 34. Based on the study by K. J. Kaufmann, J. L. Kinsey, H. B. Palmer and A. Tewarson, J. Chem. Phys. 60, 4023 (1974).
38. Of course it is not completely correct to speak of an isolated K-O stretch in the KOH molecule. In reality there will be some coupling with the O-H stretch and the bending mode of the triatomic.
39. This is a stringent lower bound and more refined diffusion flame studies should yield an even higher value. Based upon the probable dissociation products for the ground and excited states of KOH, it is likely that the upper excited state potential may be significantly bound with respect to the dissociation asymptote of the ground electronic state. The much smaller change in the diffusion flame vs single collision spectrum for KOH vs that for KCl indicates that this is probably the case. We anticipate that the emitting excited state of KOH may be bound by as much as 10 kcal/mole relative to the dissociation asymptote of the ground state.
40. J. Wormhoudt, V. Yousefian, M. H. Weinberg, C. E. Kolb and M. M. Slugter, A Review of Plasma Chemical Considerations in MHD Generator Design, Seventh International Conference on MHD Electrical Power Generation, Cambridge Mass. 1980, p.530.
41. J. Wormhoudt and C. E. Kolb, Mass Spectrometric Determination of Negative and Positive Ion Concentrations in Coal-Fired MHD Plasmas, 10th Materials Research Symposium, NBS Special Publication 561, Volume 2.
42. W. B. England, J. Chem. Phys. 68, 4896 (1978).
43. J. Brom and W. Weltner, J. Chem. Phys. 64, 3894 (1976).
44. J. Brom and W. Weltner, J. Chem. Phys. 58, 5322 (1973).
45. S. J. Weeks, H. Haraguchi and J. D. Winefordner, J. Quant. Spectrosc. Radiat. Trans. 19, 633 (1978).
46. S. R. Koirtyohann and E. E. Pickett, Anal. Chem. 38, 585 (1966); M. Yoshimura et al. unpublished.
47. H. G. C. Human and P. J. Th. Zeegers, Spectrochim. Acta 30B, 203 (1975); M. B. Blackburn, J. M. Mermet and J. D. Winefordner, Spectrochim. Acta, 34A, 847 (1977).
48. H. Haraguchi, S. J. Weeks and J. D. Winefordner, Spectrochim. Acta, 35A, 391 (1979).
49. See Refs. 46-48.
50. See Refs. 46-48.
51. A. W. Hanner and J. L. Gole, unpublished.
52. D. H. Cotton and D. R. Jenkins, Trans. Faraday Soc. 64, 2988 (1968).
53. P. J. Kalff and C. T. J. Alkemade, Combust. Flame 19, 257 (1972).
54. R. R. Herm and D. R. Herschbach, J. Chem. Phys. 52, 5783 (1970).
55. D. L. Hildenbrand and E. Murad, J. Chem. Phys. 53, 3403 (1970).
56. (a) R. C. Spiker, Jr. and Lester Andrews, J. Chem. Phys. 58, 702 (1973); (b) D. White, K. S. Seshardri, D. F. Dever, D. E. Mann and M. J. Linevsky, J. Chem. Phys. 39, 2463 (1963); (c) K. S. Seshardri, D. White and D. E. Mann, J. Chem. Phys. 45, 4697 (1966).
57. R. C. Spiker and L. Andrews, J. Chem. Phys. 58, 713 (1973).
58. S. M. Freund, E. Herbst, R. P. Mariella, Jr. and W. Klemperer, J. Chem. Phys. 56, 1467 (1972).
59. M. Yoshimine, J. Chem. Phys. 57, 1108 (1972); B. Liu and M. Yoshimine, J. Chem. Phys. 60, 1427 (1974). For further work see also M. J. Clugston and R. G. Gordon, J. Chem. Phys. 66, 244 (1977).
60. D. M. Lindsay, D. R. Herschbach and A. L. Kwiram, Mol. Phys. 32, 1199 (1976).
61. For a discussion of the "inner shell valence scheme" see: J. R. Morton and W. E. Falconer, J. Chem. Phys. 39, 427 (1963); W. E. Falconer, J. R. Morton and A. G. Streng, ibid 41, 902 (1964); R. C. Eachus and M. C. R. Symons, J. Chem. Soc. A304 (1971). For a further comment on alkali oxide bonding considering a ground $^2\Sigma^+$ state for KO, see S. P. So. and W. G. Richards, Chem. Phys. Lett. 32, 227 (1975).
62. W. Crumley, B. Cardelino and J. L. Gole, work in progress.
63. (a) R. J. Buenker and S. D. Peyerimhoff, J. Chem. Phys. 45, 3682 (1966); (b) D. T. Grow and R. M. Pitzer, J. Chem. Phys. 67, 4019 (1977); (c) E. L. Wagner, Theoret. Chim. Acta 32, 310 (1974); (d) T. K. Lin and D. D. Ebbing, Int. J. Quant. Chem. 6, 297 (1972).
64. W. Crumley, J. Appling and J. L. Gole, work in progress.
65. It should be noted that extensive baffling is used in the system to avoid problems with scattered laser light.
66. The notation in Fig. 8 is designed to give a relative numbering. Because v' and v", the absolute quantum numbers for the upper and lower states are not known, we use the notation v' + n', v" + n" where the indices in the figure denote the values of n' and n". In this case it is likely that the value of v" will exceed that for the level from which laser pumping occurs.

Progress
November 14, 1981-February 14, 1982

Title of Contract:	The Characterization of High Temperature Vapor Phase Species and Vapor-Solid Interactions of Import to Combustion and Gasification Processes in the Energy Techniques
Place of Work:	Georgia Institute of Technology Department of Chemistry Atlanta, Georgia 30332
Principal Investigator:	James L. Gole

Scope of Current Efforts:

We have been concerned with the application of chemiluminescent and laser fluorescent techniques to the characterization of alkali oxidation. Our focus has included the combination of several facets of these techniques for the determination of bond energies and spectroscopic constants for the monohydroxides, monoxides, and monosulfides of sodium and potassium and the assessment of alkali oxide formation in various reactive environments. We have investigated and are continuing to investigate nonequilibrium routes for the formation of these compounds and have carried out some kinetic parameterization. The sodium systems have been extended to the region in which sodium cluster, M_n ($n \geq 3$), oxidation is now under study using optical techniques. This effort is soon to be supplemented with product analysis using a newly constructed mass spectrometric system.

Unfortunately the research effort for this quarter has been severely limited by a major laboratory fire which occurred on December 11, 1981. The laboratory and its equipment have required extensive repair, the completion of which should occur by the end of February.

The limited research effort in this period has been divided into three areas:

1. The study of sodium and potassium atom and dimer oxidation to produce the metal oxides.

The continued investigation of sodium cluster, M_n ($n \geq 3$) oxidation.

3. The continued investigation of alkali oxide production in hydroxide environments.

Under Task 1:

We have studied the single collision oxidation of equilibrium sodium (atom + 2% dimer) vapors with NO_2 finding this system produces only dark ground state products. Similar results have not also been obtained for the reaction of sodium (atom + dimer) with SO_2. The single collision oxidation of equilibrium potassium (atom + 1.5% dimer) vapors with NO_2 and SO_2 also produces only ground state products. Potassium oxidation with N_2O, like sodium, is characterized by an intense red flame, the spectrum of which is shown in Figure 1. Although the structure associated with this emission is, as yet, marginally resolved, the emission region[1] and the combination with the results previously discussed for Na-N_2O oxidation (Progress Report 1 - See Figure 5 and discussion under Task 3) lead us to associate the emission with KO*. A preliminary analysis of the spectrum yields a K-O bond energy of 75±5 kcal/mole whereas a similar analysis on the Na-N_2O system (NaO* emission) yields an Na-O bond energy of 70±5 kcal/mole. Both of these bond energies are uncorrected for the activation energies of the Na-N_2O and K-N_2O reactions which may be quite significant in view of the small negative electron affinity of N_2O. The value for the K-O bond energy should be compared to the "estimate" of Herm and Herschbach[2] (71±3 kcal/mole) whereas that for NaO should be compared to the thermochemical value of Murad and Hildenbrand[3] (60 ±3 kcal/mole). Our current results would indicate that the K-O and Na-O bond energies are quite comparable. These results represent the first direct experimental confirmation of the K-O and

Na-O bond energies. They indicate that the K-O bond energy is approximately that estimated by Herm and Herschbach whereas the Na-O bond energy may be somewhat higher than previously determined.

Under Task 2:

We have continued our studies of sodium cluster oxidation. As we have stated previously, the ultimate goal for the apparatus described previously (Progress Report 1 - Under Task 4 - See Figure 6) will be the study of sodium cluster oxidation with SO_2 viz. $Na_x + SO_2 \rightarrow$ products. Preliminary studies of sodium cluster oxidation with SO_2 have been carried out and the resultant emission spectrum is shown in Figure 2. There are two points of interest thusfar: (1) an emission spectrum is observed in contrast to the dark reactions of sodium atoms and dimers with SO_2 and (2) the emission spectrum is distinct from that obtained for sodium atom and dimer oxidation with N_2O. There have been some problems with the SO_2 source used in the preliminary studies and a modified design is now in the final stage of completion.

In order to better test the sodium cluster oxidation apparatus, our major research thrust has involved cluster oxidation with chlorine, bromine, or iodine atoms. Sample spectra for the chlorine and bromine system are shown in Figures 3, 4, and 5. The spectra shown in these figures are associated in large part with Na_2^* emission; however, experiments will soon be underway to test for ion formation and chemiluminescence via electric field deflection of the chemiluminescent product beam. Here we have constructed a small insulated plate which is positioned in the apparatus shown in Figure 6, in the reaction chamber, above the hole connecting the oven and reaction chambers. Those chemiluminescent product ions formed will be deflected out of the field of view of our spectrometer decreasing significantly their signal. Further, to improve resolution in the system, we have installed a device which is capable

of increasing the pressure in the reaction chamber though the introduction of a rare gas such as helium or argon. The device is designed to create a merged metal cluster-rare gas flow; the entrained clusters are then oxidized under controlled conditions at elevated pressure where collisions promote rotational relaxation. The introduction of the merged flow source also facilitates the introduction of two oxidant gases simultaneously into the system. We believe that this is significant for it has been suggested that chlorine interacts with the alkali impurities in a combustion stream, resulting in the formation of alkali chloride complexes which then repartition with O, S, H, C, Al, or Si ash particulates. Thus, the influence of chlorine on the formation of alkali clusters and the subsequent reaction of these clusters with SO_2 must be evaluated in the intermediate region between gas and surface phases. We believe that the modification described above will make the apparatus in Figure 6 at least partially amenable to this task. Finally, we should note that we have characterized the temperature dependence of several emission features associated with the sodium cluster-halogen oxidation processes (Figure 3, 4, 5). In addition, we have proceeded with modifications which allow us to couple our newly developed mass spectrometric capability with the clusters apparatus so as to provide simultaneous optical and mass spectrometric probing of the system.

Under Task 3:

We have continued our pursuit of single and multiple collision KOH emission spectra. Unfortunately, these experiments are now fraught with difficulties associated with a fluctuating reactant concentration. Several design modifications are being incorporated to alleviate this problem (see also page 3 - Progress Report 1). We have converted our gas handling system completely to stainless steel to alleviate any possible problems with hydrogen perioxide. Nevertheless, under multiple collision diffusion flame conditions, modest

hydroxide decomposition is the source of a quenched KOH* emission spectrum and a dominating metal oxide system. We are continuing our investigation of this metal oxide formation in an "hydroxide" environment.

References

1. J. L. Gole, Optical Engineering 20, 546 (1981).

2. R. R. Herm and D. R. Herschbach, J. Chem. Phys. 32, 5783 (1970).

3. E. Murad and D. L. Hildenbrand, J. Chem. Phys. 53, 3403 (1970).

Figure Captions

Figure 1: Emission spectrum associated with the reaction $K + N_2O \rightarrow KO^* + N_2$ under single collision conditions.

Figure 2: Chemiluminescent spectrum associated with the reaction of sodium clusters and SO_2 molecules.

Figure 3: Chemiluminescent spectra associated with the reaction (a) $Na_2 + Cl_2 \rightarrow NaCl^* + NaCl$ and (b) $Na_x + Cl \rightarrow (Na_2^*...) + NaCl$ taken under single collision conditions. The spectrum (b) represents the first example of chemiluminescent spectra associated with metal cluster oxidation.

Figure 4: Chemiluminescent spectra associated with the reaction Na_x ($x \geqslant 3$) + $Cl \rightarrow (Na_2^*...) + NaCl$ taken under single collision conditions (continuation of Fig. 3).

Figure 5: Chemiluminescent spectra associated with the reaction $Na_x (x \geqslant 3) + Br \rightarrow (Na_2^*...) + NaBr$ taken under single collision conditions.

Figure 6: Schematic of Apparatus for sodium cluster oxidation.

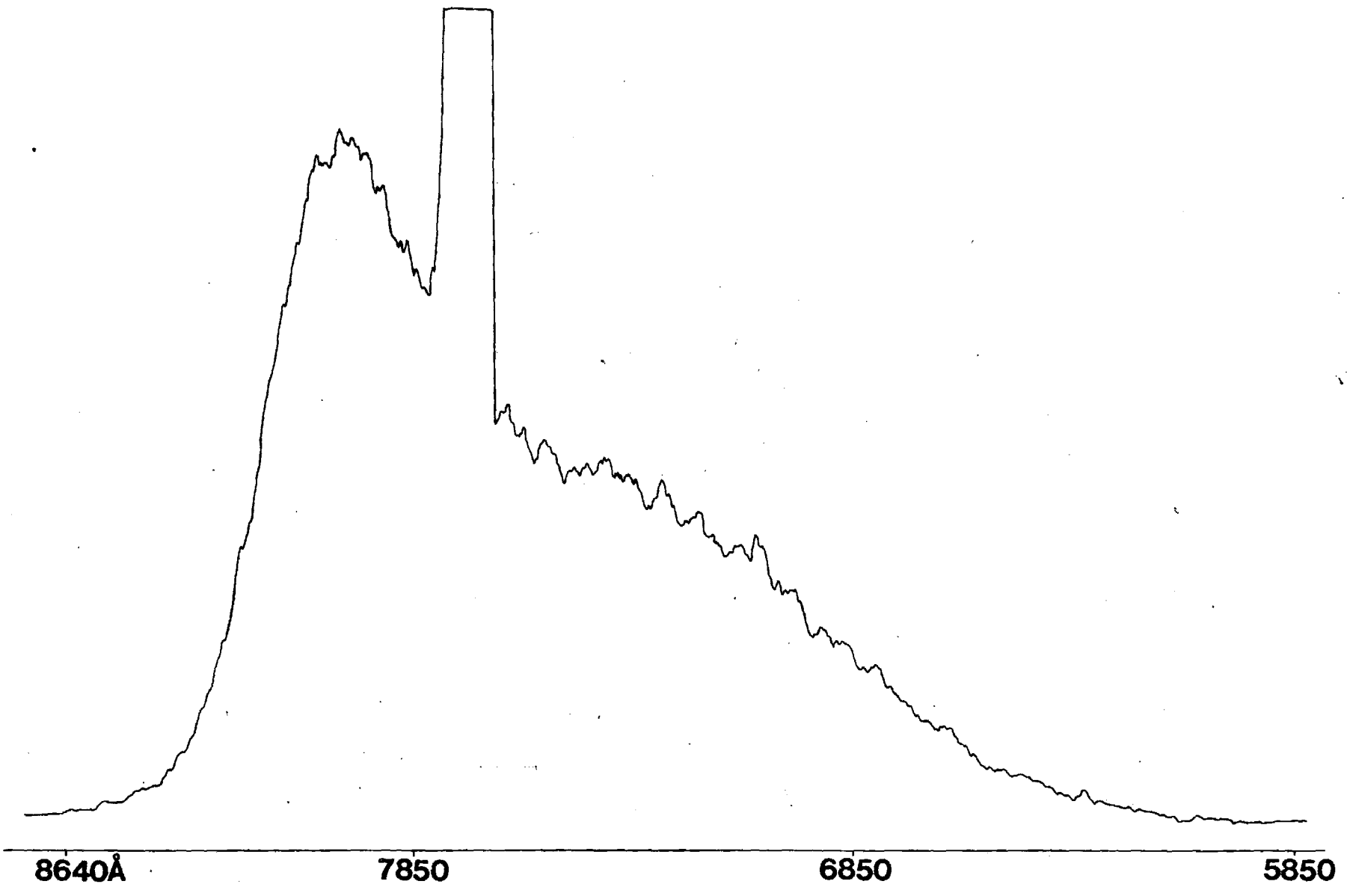

Figure 1

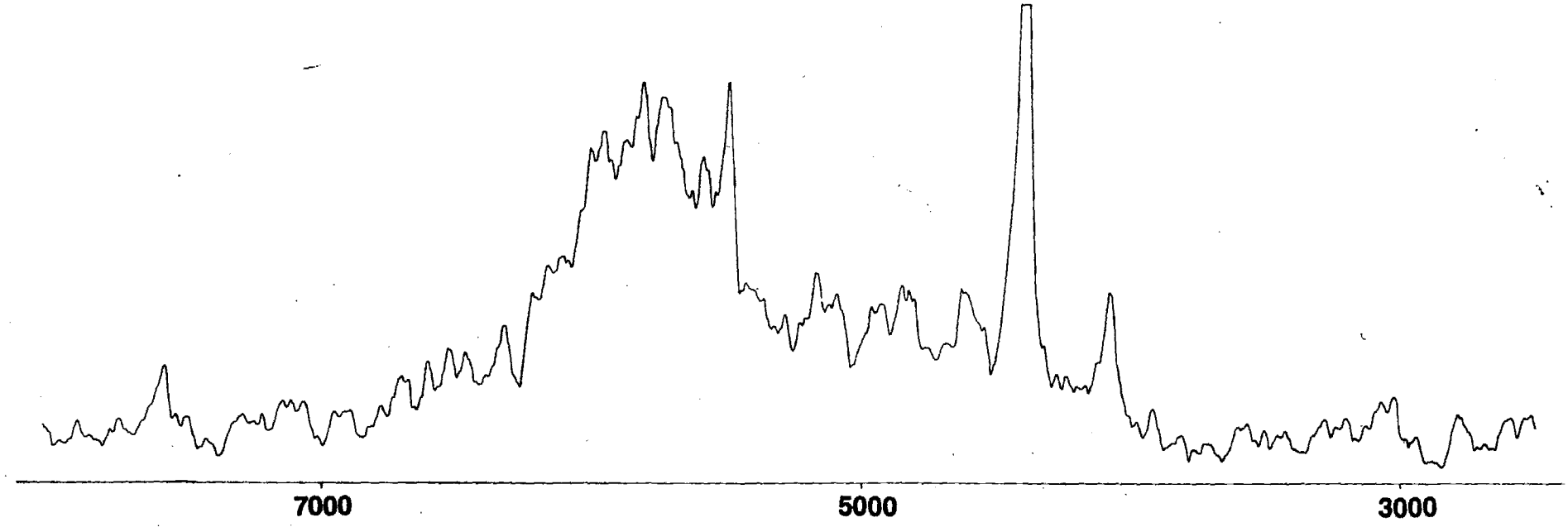

Figure 2

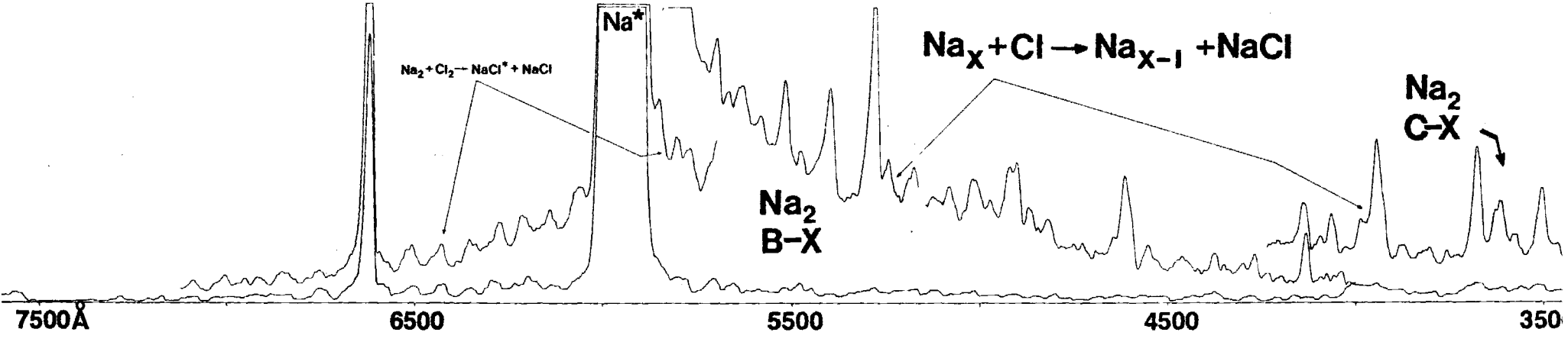
$Na_2 + Cl_2 \rightarrow NaCl^* + NaCl$
Na*
$Na_X + Cl \rightarrow Na_{X-1} + NaCl$
Na_2 C–X
Na_2 B–X
7500Å
6500
5500
4500
350

Figure 3

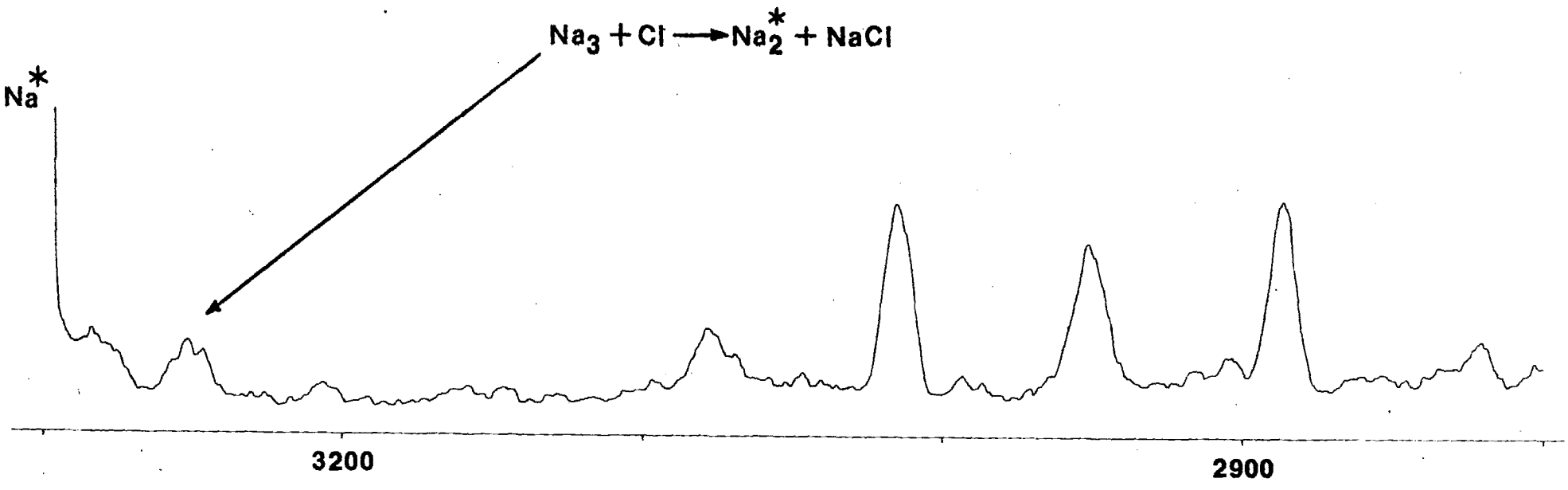

Figure 4

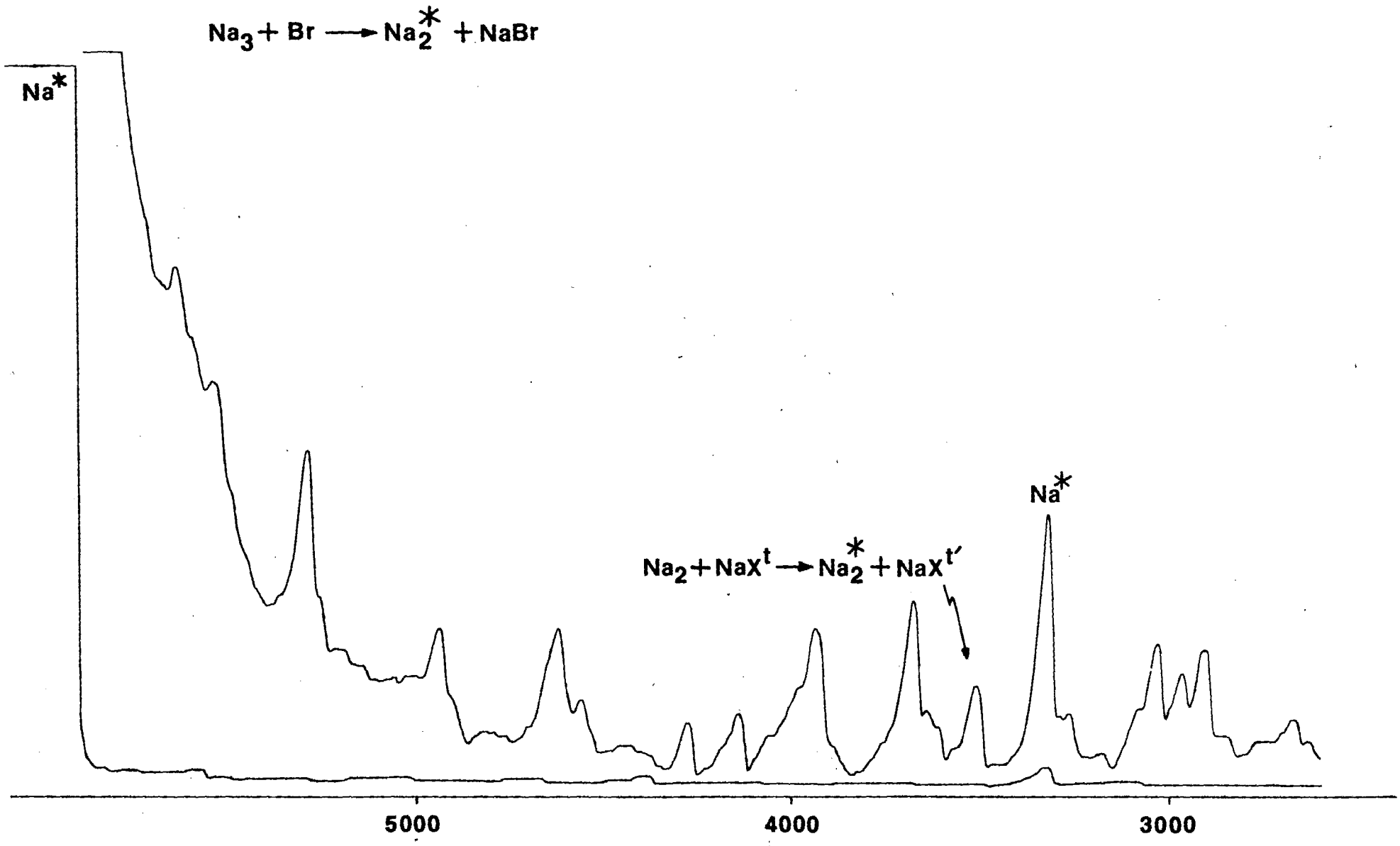
$Na_3 + Br \longrightarrow Na_2^* + NaBr$
Na^*
$Na_2 + NaX^t \longrightarrow Na_2^* + NaX^{t'}$
Na^*
5000
4000
3000

Figure 5

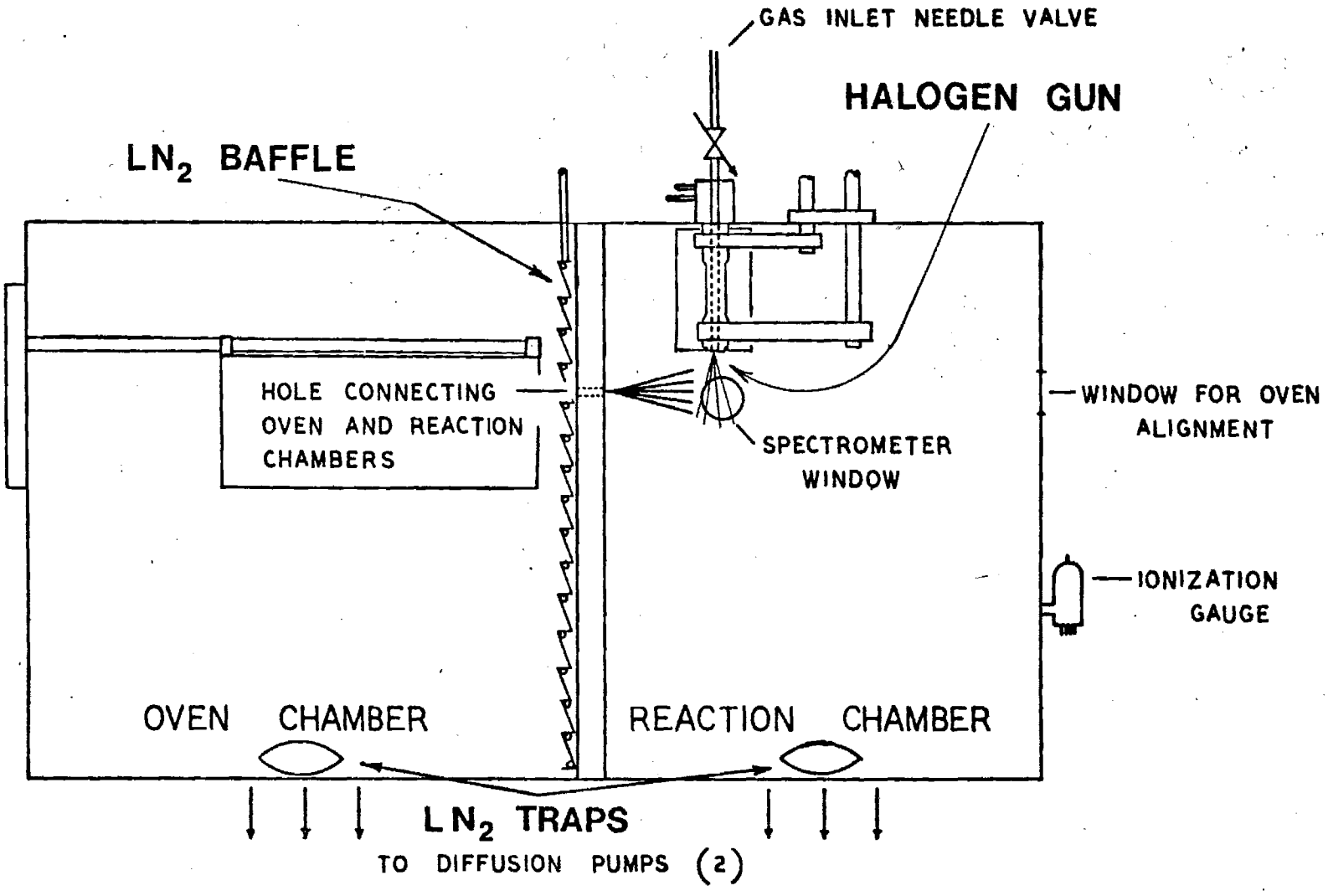
GAS INLET NEEDLE VALVE
HALOGEN GUN
LN_2 BAFFLE
HOLE CONNECTING OVEN AND REACTION CHAMBERS
SPECTROMETER WINDOW
WINDOW FOR OVEN ALIGNMENT
IONIZATION GAUGE
OVEN CHAMBER
REACTION CHAMBER
LN_2 TRAPS
TO DIFFUSION PUMPS (2)

Figure 6

LIBRARY DOES NOT HAVE

QPR no. 1-4

THE CHARACTERIZATION OF HIGH TEMPERATURE VAPOR PHASE SPECIES AND VAPOR-SOLID INTERACIONS OF IMPORT TO COMBUSTION AND GASIFICATION PROCESSES IN THE ENERGY TECHNOLOGIES

Quarterly Technical Progress Report No. 5
for the Period 1 October 1982 to 9 January 1983

James L. Gole

Chemistry Department
Georgia Institute of Technology
Atlanta, Georgia 30332

11 January 1983

PREPARED FOR THE UNITED STATES
DEPARTMENT OF ENERGY
Morgantown Energy Technology Center
Morgantown, West Virginia

Under Contract No. DE-AC21-81MC16537

NOTICE

FOREWORD

This report summarizes technical progress accomplished during the third quarterly reporting period of a two-year study being conducted for the U.S. Department of Energy (DOE). This work period was 1 October 1982 to 9 January 1983. Work was accomplished under the direction of James L. Gole. Graduate and undergraduate students who have contributed to the technical progress and to this document are Mr. W. H. Crumley, Mr. Thomas Mays, and Mr. David Semmes. Mr. Ken Williams, Supervisor of the Machine Shop has provided assistance in design and construction of oven components.

Abstract

This report summarizes work completed during the fifth quarter of a two-year study focused on the determination of bond energies and spectra for the alkali hydroxides and oxides, the study of pronounced particulate matter formed in alkali oxidation, and the characterization of sodium cluster and sodium surface oxidation with various oxidants.

We have developed and are continuing to improve experimental configurations for generating intense, stable, and long-lasting chemiluminescent emission from the alkali hydroxides NaOH and KOH and the alkali oxides NaO and KO. The first electronic emission spectra for these compounds have been generated and are being studied in our laboratory. Commensurate with this effort has been the study of extensive particulate formation which appears to be pathelogical to the alkali hydorxide and oxide systems. This particulate matter, formed in an extremely efficient manner in the oxidation process, is being studied employing mass spectrometry, EPR spectrometry, and, in the future, Raman Spectroscopy. The major emphasis in our sodium cluster oxidation studies over the past three month period has been the development of devices whereby the spectra obtained from the oxidation process can be relaxed to the point where ready analysis of spectral features is facilitated.

TABLE OF CONTENTS

LIST OF FIGURES

LIST OF TABLES

Introduction

Background

Low tolerance levels for certain species in process streams impose stronger requirements for reliable thermodynamic and kinetic data in order to predict low level species concentrations. In addition evidence now indicates that serious concern must be focused on whether or not these systems are best represented via equilibrium or non equilibrium models. Unfortunately, the necessary thermodynamic and kinetic data required to perform accurate calculations of species concentrations is not available for many such gas stream species. Of equal importance is the fact that little detailed information is available which will allow the ready direct monitoring of these species in the process stream. In addition, many of the details of the mechanisms for process stream product formation, including the formation and growth of particulates, are yet unknown while many postulated routes to product formation are yet only meagerly tested. This arises primarily because many of the molecular entities for which data are needed correspond to elusive and very reactive radicals or high temperature molecules. Our laboratory has been concerned with the characterization of several of the important molecules and possible processes thought to be present in the inherently high temperature environment of the process stream.

We have applied chemiluminescent and laser fluorescent techniques to the determination of bond energies, spectroscopic constants, and the evaluation of those spectral regions which will be most useful for the kinetic parameterization and monitoring of the species of interest. In addition, through the study of certain select processes, we are attempting to shed some light on the feasibility of postulated interactions in the process stream,

some of which include the surprisingly efficient gas phase formation of particulate matter. Finally, in the course of these studies, we are documenting the presence of ultrafast energy transfer, both intra- and intermolecular, as it pertains to the nature of heat flow in high temperature systems and, in particular, to those molecules of interest in process streams. It should be noted that the attainment and evaluation of reliable spectroscopic data leads to the determination of important molecular constants which can be used for the statistical mechanical evaluation of heat capacities, entropies and free energies, all of which are important to the understanding of energy related combustion and gasification environments.

Objectives

The general objectives of the present research effort which represents a continuation of previous efforts under DOE sponsorship are: (a) to characterize alkali monoxide chemiluminescent spectra, specifically spectra for NaO and KO which can be used in kinetic studies of the behavior of these species and for their direct monitoring in process streams and to determine lower bounds for the NaO and KO bond energies; (b) to characterize pronounced particular formation in gas phase alkali oxidation environments; (c) to further characterize the KOH chemiluminescent emission spectrum at a resolution and under conditions which will allow the determination of currently unavailable molecular constants for this molecule and an improved measure of the K-OH bond dissociation energy; (d) to carry out and characterize the oxidation of sodium clusters with various oxidants including SO_2; (e) to attempt to prepare clean sodium and sodium contaminated surfaces whose oxidation with various constituents including SO_2 will be characterized; (f) to further characterize the NaOH chemiluminescent emission spectrum in order to obtain an improved measure of the Na-OH bond energy. Specific tasks of interest

in the current report are indicated below.

Characterization of Alkali Oxide Emission Spectra and Gas Phase Particulate Formation in Alkali Oxidation Environments

The object of a portion of this task is to observe and characterize chemiluminescence from NaO and KO using the reactions of sodium or potassium atoms with primarily N_2O and O_3. These studies have yielded the first electronic emission spectra for NaO and KO resulting from the low pressure "single collision" reaction of sodium and potassium atoms with N_2O. Our current efforts focus primarily on the stepwise extension of these single collision studies to higher pressures where relaxation effects lead to an improvement in spectral resolution, facilitating the evaluation of molecular constants for NaO and KO and furnishing reliable spectral regions which can be used to probe for these elusive oxides. Further, preliminary values for the bond dissociation energies of NaO and KO(D_0^o(NaO) = 70±5, D_0^o(KO) = 75±5 kcal/mole) are corroborated through the combination of single and multiple collision studies.

These alkali oxidation systems, involving formation of the alkali oxides, are found to exhibit a pronounced virtually gas phase homogeneous particulate formation (see Annual Progress Report 1[1]) which is not observed in any other oxidation system. A major focus of our research effort involves the characterization of the polymeric alkali-oxygen-nitrogen species which constitute the framework of the observed particulate matter using mass spectroscopy, EPR spectroscopy, and, in the near future, Raman Spectroscopy. We believe that the extremely efficient formation of these polymers can provide a seed for particulate formation in process streams.

Sodium Cluster Oxidation

The object of this task is to evaluate the nature of sodium oxidation in the intermediate region between the gas and surface phase. The products

of sodium cluster oxdiation are being characterized through direct observation of the chemiluminescent emission for highly exothermic processes, through a newly developed electron impact excitation technique, and through mass spectrometric sampling of the oxidation region. Current efforts focus on the desire to obtain relaxed (rovibronic) chemiluminescent emission spectra for these systems in order to facilitate spectral resolution. Thusfar both the halogen and SO_2 oxidation of sodium clusters has been under study.

Alkali Hydroxide Emission Spectra

Electronic emission spectra for the alkali hydroxides have been obtained over a wide pressure range. The reactions of sodium and potassium dimers with hydrogen peroxide are being used to excite chemiluminescence from NaOH and KOH. The objective of this task is to determine stringent lower bounds for the K-OH and Na-OH bond energies and molecular constants for several levels of the ground electronic state of K-OH. KOH emission has been observed at low pressures under "single collision" conditions, at intermediate pressures where the effects of collisional relaxation are apparent ("multiple collision" conditions) and at higher pressures in a "diffusion flame" device, the combination of these studies leading to the first evaluation of a stringent lower bound for the K-OH bond energy[2] using a direct optical measurement. Continued improvements in the "diffusion flame" apparatus have now led to long term flame stability. Because flame instabilities tend to "washout" spectral features, stabilization was a major task before us. We are now attempting to solve a major aspect of this problem by recording the entire KOH emission spectrum on film and in 200Å sections using an optical multichannel analyzer. These efforts will be used to obtain a more stringent lower bound for the KOH bond energy and to obtain higher resolution spectra to evaluate molecular constants for several ground state levels.

Technical Progress-Plans for Future Study

Alkali Oxide Emission Spectra

Previously, we have noted the design of a system used with reasonable success to characterize the alkali oxide emission spectra for sodium and potassium oxide produced from Na,K + N_2O,O_3 reactions under multiple collision conditions (See Annual Topical Report 1[1]). With this system, we were able to produce resolved alkali oxide emission spectra for NaO[1]; however, there were still questions regarding long term alkali and, in the case of ozone, oxidant source stability. A further modification of the apparatus used for these multiple collision studies has now greatly improved long term stability in the intermediate multiple collision regime. This improvement is significant for it is not only important that we deduce the location of the alkali oxide emission bands but also their precise relative intensities. In correlation with theory, these relative intensities allow us to assess the best regions for in-situ laser excitation of the alkali oxides. Hence they provide a means of monitoring the kinetics of these species.

A schematic of the oven system now used to produce stable alkali beams is shown in Figure 1. There are two important features of this device. We now use a modified double oven design where alkali metal heated in a large reservoir region passes into an independently heated and more confined region and then through an effusive or near effusive orifice. As in our most recent previous design,[1] the oxidant is introduced via a nozzle offset and perpendicular to an entrained metal flow in order to prevent pronounced particulate formation. The present design involves the direct oxidation of the effusing alkali metal in a system containing, for example, 200μ of N_2O. The configuration is very similar to a high pressure beam-gas system. Thusfar we have not entrained

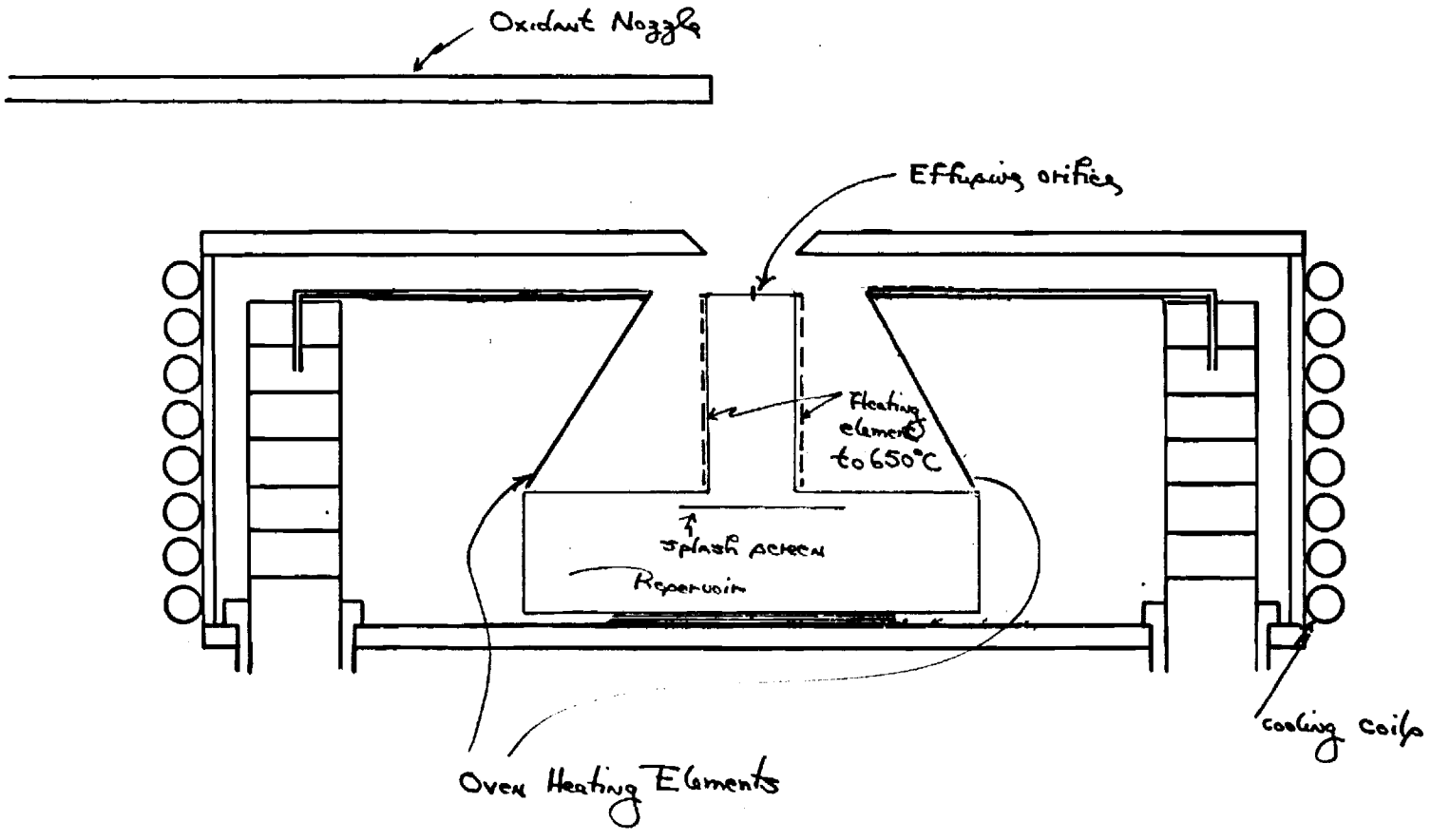
Oxidant Nozzle
Effusing orifice
Heating element to 650°C
Splash screen
Reservoir
Oven Heating Elements
cooling coils

Figure 1

the effusing alkali metal in argon; however, a device for this purpose is under construction which should allow us to operate a stable alkali flow at considerable higher pressures. Note that the design depicted in Figure 1 is in contrast to the normal multiple collision device where the entrained metal is oxidized using a concentric ring injector device.[2] The injector design quickly leads to pronounced particulate formation and hence is characterized by extremely short run times. Using the perpendicular entrained metal-oxidant flow scheme, one is able to run for several hours without encountering extensive particulate formation. Given long run times, there is yet another problem associated with the higher alkali metal reactant concentrations characteristic of the multiple collision system. The transition moments associated with alkali metal excited electronic states are among the largest known. Therefore the collisional excitation of alkali dimer electronic emission systems can provide a strong interference to the ready analysis of alkali oxide emission features. For this reason, the upper chamber from which the alkali metal effuses is heated to 650°C to induce dissociation of the exiting alkali metal dimers. With this precaution, the multiple collision spectra are characterized by alkali atomic and alkali oxide emissions.

Using the device described above, we have continued our study of the Na + N_2O and Na + O_3 reactions in the multiple collision region. Our focus has been on the 7400A system of NaO. This new oven system has high alkali source stability producing a stable, intense, red chemiluminescent flame in alkali metal metatheses with both N_2O and O_3. In order to carry out the ozone reactions, we have entrained the ozone in argon by flowing the rare gas through a previously constructed trap in which ozone is deposited on silica gel at dry ice temperatures. The effluent argon + ozone flow is then passed through the oxidant nozzle into the reaction chamber. This procedure

yields a significant ozone flow and allows us to produce an intense chemiluminescent flame.

The spectrum obtained for the Na-N_2O system is depicted in Figure 2. Note the three pronounced bands at 7160, 7400, and 7700Å. Their correlation with the NaO* single collision spectrum[1] is excellent. The relative intensity of these bands is much more reliably and reproducibly determined and the current spectral intensity is considerably in excess of that previously obtained. The spectrum in Figure 2 was taken at considerably higher resolution (0.4 vs 5Å) than those spectra previously obtained providing a clean separation of the Na D-line emission and that of the oxide. Similar spectra are obtained for the Na+O_3 system, however, the peaks are somewhat skewed relative to those for $Na + N_2O \rightarrow NaO^* + N_2$. The skewed nature of these peaks may be significant for the observed spectral peaks may result from the combination of both a short ground and excited state progression, each feature appearing in the spectrum (note the symmetric nature of the peaks) also corresponding to a sequence grouping. If a sequence grouping corresponds to each of the major peaks observed in the NaO spectrum (Figure 2), the slightly skewed nature of the peaks observed in the NaO emission spectrum which characterizes the $Na + O_3$ system relative to that for the $Na + N_2O$ system may result from a population distribution peaked at slightly different excited state quantum levels. We are proceeding further with our analysis of the 7400Å band system in order to elucidate several of these points of contention.

This work is now being supplemented through a collaborative effort with W. A. Goddard's research group at the California Institute of Technology. Professor Goddard's group is now extending their previous quantum chemical studies on the alkali oxides in order to aid in the evaluation of those

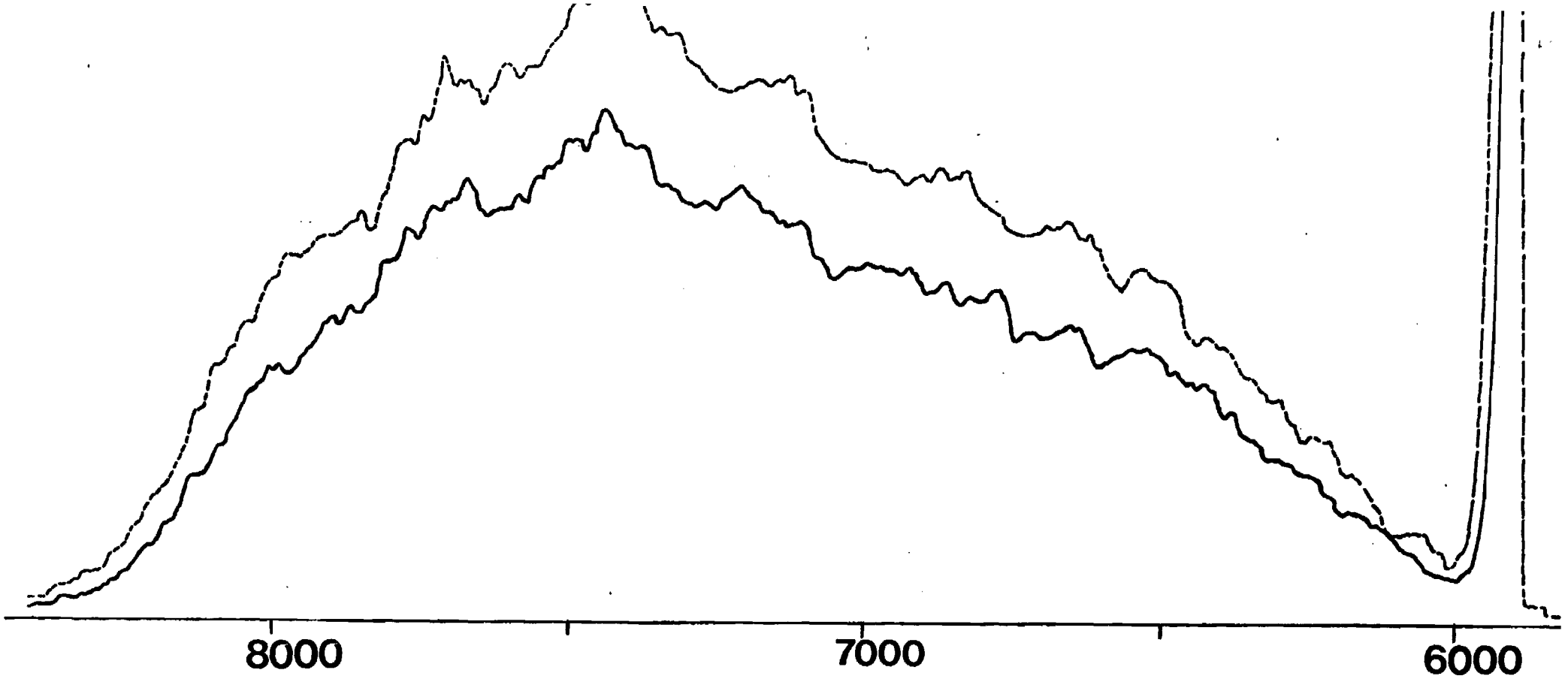

Figure 2

states in the 7400Å region. The evaluation of the NaO 7400Å system is quite significant for it provides the first straightforward in-situ route by which one can probe for sodium oxide in a combustion gas stream. Recently (see enclosed) systems have been demonstrated at the Morgantown Energy Technology Center which employ LIBS and CARS spectroscopies to detect the sodium and potassium content of coal gasification streams. The LIBS technique requires that a laser dissociate alkali species and then detect alkali metal formed in the dissociation process. With the discovery of the NaO 7400Å system, it will be possible to detect this gas stream constituent in a single step with a laser operating at close to this wavelength alleviating the need to carry out a dissociation process. Based on the information already obtained, it should be possible to probe sodium oxide using laser induced fluorescence by pumping a band system in the region around 7500Å. We suggest that NaO could be prepared by an appropriate in-situ synthesis passing entrained sodium metal over NaO_2 viz

$$Na + NaO_2 \longrightarrow 2NaO.$$

The subsequent products could then be excited by a krypton ion pumped dye laser.

Gas Phase Particulate Formation in Alkali Oxidative Environments

(1) We have used mass spectrometry as a means of analyzing the nature of the pronounced particulate matter formed via what appears to be the homogeneous gas phase oxidation of alkali metals. Specifically, we have been concerned with the nature of particulate matter characterizing the $K+N_2O$ system. Constructing an appropriate probe and vaporizing particulate material at temperatures between 50 and 300°C, we have found thus far a relatively simple spectrum with major mass peaks at 90, 118, 178, and 238 amu. The possible polymeric species which correspond to these mass peaks given

aureole

A CLEAN-UP JOB FOR LASERS

Coal gas, which is produced by reacting coal with steam, has a long if dirty history. It illuminated the original London Bridge in the days of George the Third. By the mid-19th century it had become the fuel of choice in big cities everywhere, reigning supreme until it was knocked out of the box by the advent of cheap oil.

Now that oil is no longer cheap, coal gas is well positioned to make a strong comeback as a leading fuel technology of the future — if it can clean up its act. Coal is abundant, and the gasification process is relatively inexpensive. But the environmental problems, which no one thought much about in the gaslight era, are a very big worry today. Coal gas won't win widespread public acceptance until it can be efficiently laundered.

That's where lasers come in. At the US Department of Energy's experimental coal gasifier in Morgantown, W. Va., researchers from the Los Alamos National Laboratory have been demonstrating a continuous-monitoring laser technique for determining process pollutants and increasing process efficiency. The success of their work to date strongly suggests that coal gasification plants of the future will come equipped with laser systems to keep real-time tabs on pollutant levels in the gas stream and make sure that scrubber systems are preventing noxious material from escaping into the air we breathe.

Two laser systems are being used in the Morgantown experiments, and like just about everything else these days, they're known by their acronyms. LIBS (for Laser-Induced Breakdown Spectroscopy) is used primarily for determining sodium and potassium contents of coal gasification streams, which is important in controlling costly corrosion of equipment exposed to hot combustion products. CARS (for Coherent Anti-Stokes Raman Scattering) is a more complex system for determining the presence and temperature of a variety of air-polluting molecules. Both use readily available lasers.

A tricky aspect of CARS is that it employs two lasers to produce a third laser beam. By mixing two beams of different frequencies, researchers can tune to the vibrational frequency of the molecule they want to examine. The intensity of the third beam, generated by the interaction of the two initial beams with the molecule, yields the molecule's concentration. This technique has enabled CARS to measure concentrations of nitrogen, carbon monoxide and hydrogen sulfide in the dirtiest parts of the gas stream where temperatures run to 1000°F and pressures are 200 pounds per square inch, with high particle and tar-vapor loadings.

LIBS and CARS are complementary systems. "Together," says Los Alamos scientist David Taylor, "they can tell you everything you ever wanted to know about what is happening in the gasification system and what is coming out of it." Armed with that kind of information, the producers of coal gas should be able to give us a fuel we can live with, while making a significant contribution to the nation's eventual energy self-sufficiency. ☐

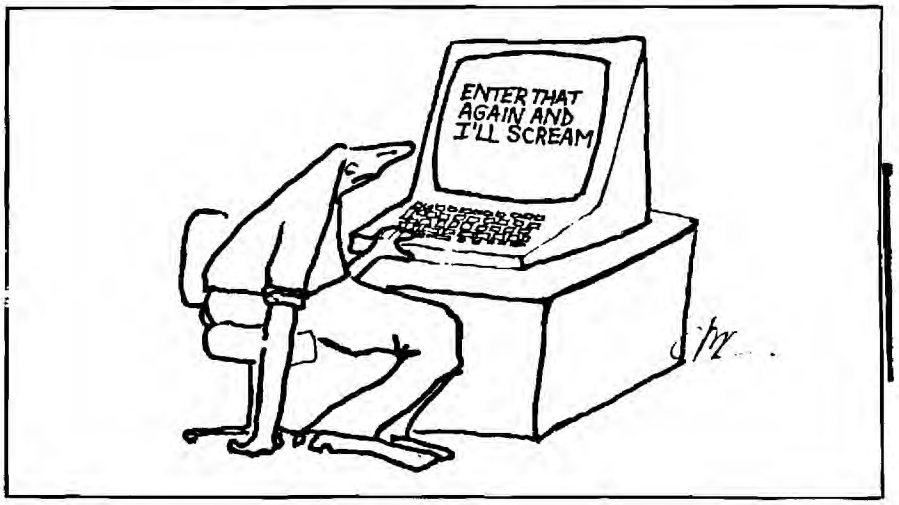

the presence of heated alkali (potassium with slight sodium impurity), nitrogen, and oxygen are given in Table 1. It should be apparent that polymeric alkali-oxygen-nitrogen compounds can account for the mass spectra which we observe. We have probed other regions of the particulate matter which is formed in oxidation. We find that certain samplings yield the four mass peaks (90,118,178, and 238 amu) discussed in Table 1 while others are characterized by a negligible vapor pressure in the temperature range 50-300°C. In other words, the particulate samples are characterized by regions of distinctly different vapor pressure. In order to further characterize the regions of lower vapor pressure, we have prepared samples which will be analyzed, at higher temperatures, in the High Temperature Laboratory of Professor John Margrave at Rice University.

(2) We have now been able to study the EPR spectrum of a powdered sample of the particulate matter formed in alkali oxidation. In order to carry out this effort, we have constructed a special liquid nitrogen cooled EPR probe. In an argon atmosphere (dry-box) the hydroscopic particulate powder was placed in a pyrex capillary which was then sealed. This capillary is placed in a quartz tube (probe) which is then liquid nitrogen cooled. The spectrum depicted in Figure 3 and centered at 3200 gauss, was obtained at liquid nitrogen temperature, 77K. It is now clear that a portion of the powdered sample contains what must be very reactive free radicals. During the course of our EPR studies, we have also noticed that the powdered sample changes color reversibly. In cooling from room to liquid nitrogen temperature, the color of the sample darkens from dull orange to red and back to dull orange. Upon warming to room temperature this process repeats. We will continue to probe other regions of the particulate matter formed in oxidation. We feel that these polmeric species which constitute the particulate can

Table 1

Possible Polymeric Species Formed in Alkali Oxidation[a]

Atomic Mass Peaks[b]	Possible Compounds[c]
90	$\underline{KNaN_2}$, Na_2N_2O
118	$\underline{KNaN_4}$, Na_2N_4O
178	$KNaN_6O_2$, KNa_3, N_5
	$Na_2N_6O_3$, Na_4N_5O,
	$\underline{K_2N_6O}$
238	$KNaN_8O_4$, $KNa_3N_7O_2$, KNa_5N_6
	$Na_2N_8O_5$, $Na_4N_7O_3$
	Na_6N_5O, $Na_4N_7O_3$, $Na_2N_8O_5$
	$K_2N_8O_3$, $\underline{K_2Na_2N_7O}$, $\underline{K_3NaN_7}$

a. Potassium, Nitrogen, Oxygen, and small Sodium impurity present.

b. Relative intensities ~3(90)/5(118)/1(178)/1.5(238).

c. Favored compound is underlined.

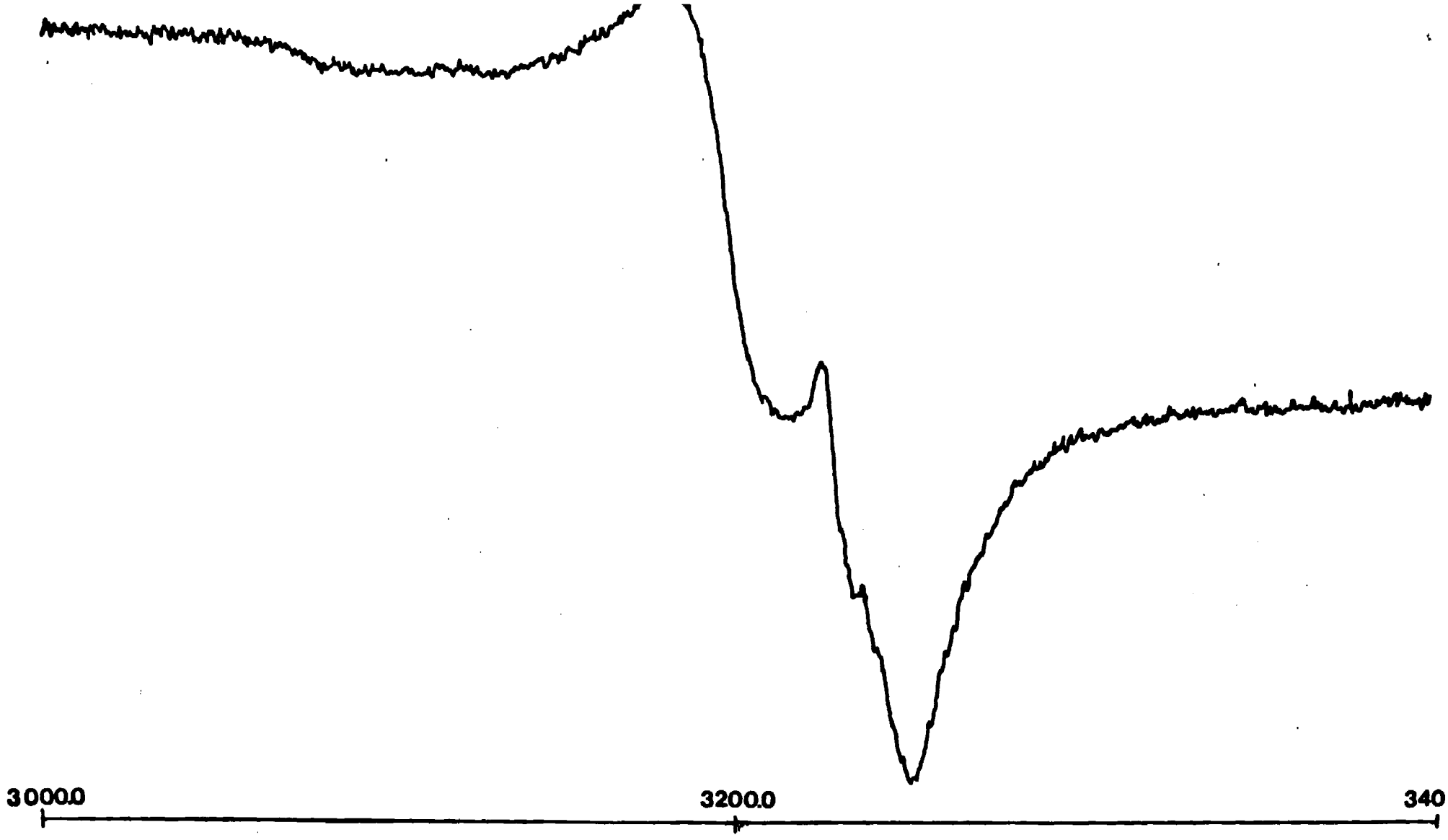

Figure 3

be formed with unusual efficiency in the gas phase and that they can represent the nuclei for large scale particulate formation in process streams.

Sodium Cluster Oxidation

In our previous discussions of sodium cluster oxidation[1] we noted that the chemiluminescent spectra which characterize the Na_x + Cl, Na_x + Br, and Na_x + SO_2 (chlorine impurity introduced) systems are characterized by a very high degree of internal excitation which renders ready resolution of spectral features difficult (Figure 4). To improve the resolution in the system, we constructed an entraining device placed at the point of entrance of the supersonic Na_x beam into the reaction chamber. The ring injector device was designed to increase the pressure in the reaction chamber through the introduction of a rare gas such as helium or argon. The device was designed to create a merged metal cluster-rare gas flow, in an attempt to oxidize entrained clusters under controlled conditions at elevated pressure where collisions promote rotational relaxation. In order to operate this device, the forepump system in the metal clusters apparatus was extensively modified to handle increased gas loads. The oven chamber is now pumped independently of the reaction chamber by a 17 CFM forepump and the reaction chamber is pumped by a 50 CFM forepump. (This should be contrasted to the previous pumping of the entire system by a 17 CFM pump.) Using this pumping configuration, we studied the Na_x + Br + Ar system and successfully introduced some internal relaxation thus increasing our ability to resolve those spectral features of interest. However, the carrier gas pressure and hence the reaction chamber pressure were somewhat oscillatory. Recently, we improved this situation with (1) a modification of the ring injector annulus so as to decrease the width of the ring orifice while increasing its convergence angle and (2) the introduction of a further needle valve into the rare gas

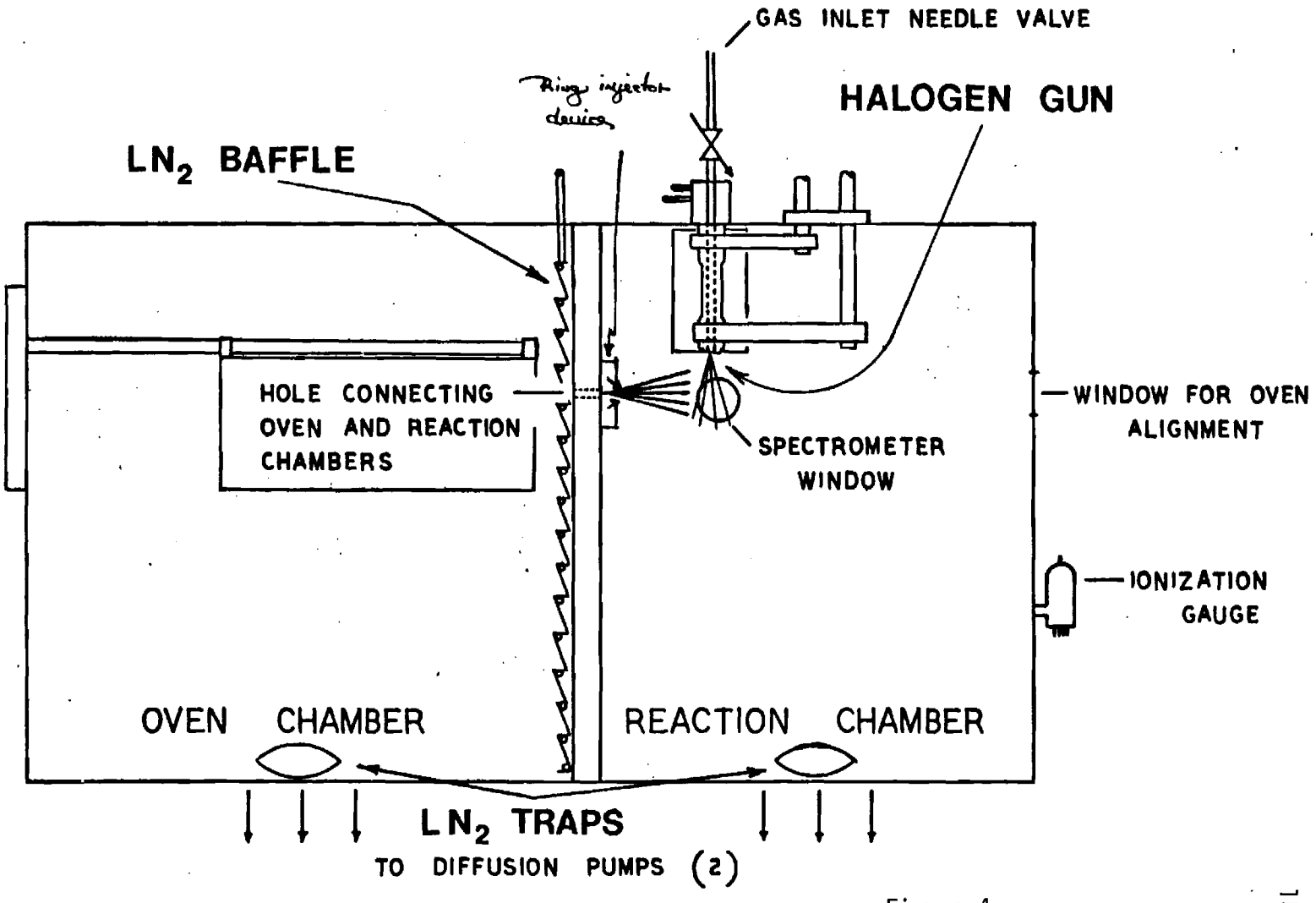
GAS INLET NEEDLE VALVE
Ring injector device
HALOGEN GUN
LN_2 BAFFLE
HOLE CONNECTING OVEN AND REACTION CHAMBERS
SPECTROMETER WINDOW
WINDOW FOR OVEN ALIGNMENT
IONIZATION GAUGE
OVEN CHAMBER
REACTION CHAMBER
LN_2 TRAPS
TO DIFFUSION PUMPS (2)

Figure 4

inlet in order to control the gas pressure. This device alleviated oscillatory behavior, produced spectra which showed some relaxation, and could be operated to reaction chamber pressures of 10^{-1} torr. However, as with previous studies, the chemiluminescent flame was considerably weakened due to the rarification of alkali-halogen encounters in the viewing zone region as the result of rare gas dilution. It is also likely that the observed spectral emission emanates from excited electronic states which are sufficiently short-lived so that they do not encounter a significant number of rare gas atoms before emission. To attempt to solve this problem, we will simultaneously supersonically expand a mixture of sodium and helium or argon creating alkali-rare gas complexes. The clusters can then be oxidized in an insured "local" environment of helium or argon atoms. The appropriate device is now under construction.

Alkali Hydroxide Emission Spectra

We have now constructed a new device to study the KOH emission spectrum. This device is based on a modification of the diffusion flame apparatus which we have discussed previously and is designed to facilitate the attainment of the KOH spectrum on film or using an optical multichannel analyzer. The device employs all of the improvements which we have previously incorporated and discussed in previous reports and considerably improves the optical system.

Technical Publications and Presentations

The following paper will soon be submitted for publication and is included in Appendix A.

J. L. Gole and G. J. Green, "On the Nature of the Energy Balance and Branching Ratios Associated with the Chemiluminescent Reaction $Si(^3P) + N_2O(^1\Sigma) \rightarrow SiO^*$ $(a^3\Sigma^+, b^3\Pi, A^1\Pi) + N_2$ $(v'' \geq 5)$ - Possible Formation of Vibrationally Excited N_2.

The following are presentations given in which DOE sponsored research was discussed

1. Oak Ridge National Laboratory "Metal Cluster Formation, Characterization and Oxidation" 11/30/82

2. Tulane University "Metal Cluster Formation and Characterization" 10/7/82

APPENDIX A

ON THE NATURE OF THE ENERGY BALANCE AND BRANCHING RATIOS ASSOCIATED WITH THE CHEMILUMINESCENT REACTION $Si(^3P) + N_2O(^1\Sigma) \rightarrow SiO^*(a^3\Sigma^+, b^3\Pi, A^1\Pi) + N_2(v'' \geq 5)$ - POSSIBLE FORMATION OF VIBRATIONALLY EXCITED N_2

James L. Gole and Gary J. Green

Department of Chemistry
Georgia Institute of Technology
Atlanta, Georgia 30332

Abstract

Silicon atoms react under single collision conditions with N_2O to yield chemiluminescent emission corresponding to the SiO $a^3\Sigma^+ - X^1\Sigma^+$ and $b^3\Pi - X^1\Sigma^+$ intercombination systems and the $A^1\Pi - X^1\Sigma^+$ band system. A most striking feature is the energy balance associated with the formation of SiO product molecules in the $A^1\Pi$ and $b^3\Pi$ states. The analysis of the emission from these states provides evidence for the formation of vibrationally excited N_2 in a fast Si-N_2O reactive encounter. The comparison of several M+N_2O reactions (M=Si,Al,Ti,Sc,Y,La,Ca,Sr,Ba) indicates an energy discrepancy between the available energy to populate the highest energetically accessible excited state quantum level and the highest quantum level from which emission is observed. This difference appears to be characteristic of a vibrational excitation in N_2, the average value of the internuclear distance for which corresponds to an N-N bond length comparable to that in linear N-NO. Emission from the SiO $a^3\Sigma^+$ ($A^1\Pi$) and $b^3\Pi$ ($A^1\Pi$,$E^1\Sigma_o^+$) triplet state manifold results primarily from intensity borrowing involving the indicated singlet states. Perturbation calculations indicate the magnitude of the mixing between the $b^3\Pi$, $A^1\Pi$, and $E\ ^1\Sigma_o^+$ states ranges between 0.5 and 2%. On the basis of these calculations, the branching ratio (excited triplet)/(excited singlet) is found to be well in excess of 500. An approximate vibrational population distribution is deduced for those molecules formed in the $b^3\Pi$ state. The present studies are correlated with those of previous workers in order to explain diverse relaxation effects as well as the change in the ratio of $a^3\Sigma^+$ to $b^3\Pi$ emission as a function of pressure and experimental environment. Some of these effects are attributable to a strong coupling between the $a^3\Sigma^+$ and $b^3\Pi$ state. Based on the current results, there appears to be little correlation between either (1) the branching ratio for

excited state formation or (2) the total absolute cross section for excited state formation and (3) the measured quantum yield for the Si-N_2O reaction. Implications for chemical laser development are considered.

Introduction

For several years, the nature of the structure, energetics, and formation of the SiO molecule has been the subject of a number of experimental and theoretical studies.[1] The low-lying states of SiO have recently been discussed in detail by Field et al.[2] An important contribution to our knowledge of the low-lying states of SiO has come from recent studies of the chemiluminescent reaction

$$SiO(^3P) + N_2O \longrightarrow SiO^*(a^3\Sigma^+, b^3\Pi \ldots) + N_2 \qquad (1)$$

by Hager et al.[3] and Linton and Capelle.[4] Much of the impetus for this effort has been the desire to exploit "spin conservation" in order to produce the low-lying "$a^3\Sigma^+$" and "$b^3\Pi$" states of SiO. These studies have offered the opportunity to characterize the "$a^3\Sigma^+$"-$X^1\Sigma^+$ and "$b^3\Pi$"-$X^1\Sigma^+$ intercombination band systems of SiO and investigate the possibility of using spin conservation to advantage in order to create a population inversion on the "$a^3\Sigma^+$"-$X^1\Sigma^+$ or "$b^3\Pi$"-$X^1\Sigma^+$ transitions and hence develop a medium for a visible chemical laser.

With the emphasis outlined above, previous studies have focused on the evaluation of the chemiluminescent emission from reaction (1) primarily as a means of determining spectroscopic constants for the $a^3\Sigma^+$ and $b^3\Pi$ states,[3,4] the relative population distributions in these states,[3] and the total quantum yield for fluorescence from those SiO excited states populated in reaction.

It is the purpose of the current effort to augment the information garnered in previous studies by characterizing the Si-N_2O reaction at considerably lower pressures (10^{-5}-10^{-1} torr) than those associated with the Hager et al. (2-4 torr)[3] and Linton and Capelle[4] (0.5-20 torr) studies. Based on our study of the "single collision ($P_{Tot.} \leq 10^{-4}$ torr) Si-N_2O reaction, we wish to suggest an explanation for the rather diverse $b^3\Pi$ excited state vibrational excitation which characterizes the spectral emissions observed by Hager et al. ($v' \leq 2$) and Linton and Capelle ($v' \leq 8$) in their "multiple collision" flame experiments. In addition, we have

determined that a component of the analysis of the chemiluminescence from the intercombination band systems is errant in the sense that these systems have been treated as allowed transitions when in fact the observed "$a^3\Sigma^+$" and "$b^3\Pi$" emission results primarily from intensity borrowing involving a low-lying $A^1\Pi$ state. The pursuit of the analysis of the intercombination band systems is necessary for two reasons: (1) It indicates that the chemiluminescence corresponding to the intercombination transitions ($Si + N_2O \rightarrow SiO^*(a^3\Sigma^+, b^3\Pi)$ is characterized by a much different population distribution than previously envisioned. The modified population distribution may have significant implications for the creation of a population inversion on the intercombination band transitions. (2) There is a question of the assessment of the quantum yield for these intercombination transitions in view of the fact that they are observed primarily as a result of intensity borrowing.

Previous researchers have focused primarily on SiO spectroscopy and excited state product distributions leaving apparently unnoticed an intriguing question concerning the dynamics of the $Si-N_2O$ reaction. One finds that there is a significant discrepancy between the available energy to populate SiO excited electronic states (reaction (1) exoergicity 53000 cm^{-1}) and the observed excitation which characterizes the $Si-N_2O$ system. We consider this differential and offer an explanation which appears to be consistent with observations of excited state metal oxide formation in several $M+N_2O$ reactions.

Experimental

Silicon atoms distributed thermally among the ground state $^3P_{0,1,2}$ components were reacted with N_2O in a highly exothermic process to produce an intense blue emission. The observed chemiluminescence was observed under both "single"[5-7]($\leq 10^{-3}$ torr) and multiple[8] (10^{-2}-1 torr) collision conditions in slightly modified versions of devices described elsewhere.[5,6]

In the single collision studies, silicon was vaporized from a cylindrical graphite crucible (c.s. grade-Micromechanisms). This crucible was heated by a graphite radiator substituted for the tantalum radiators (graphite inner sheath) previously used in our study of the Si-OCS reaction.[7,9] The graphite radiator was surrounded by two tantalum heat shields. Maximum temperatures ranging from 1900 to 2100°C were achieved with this construction, all temperatures being measured with a Leeds and Northrup optical pyrometer to $\pm$10°C. The graphite crucible/heat shield assembly was surrounded by a water cooled copper jacket attached to a newly designed "quick-load" bus bar/flange assembly.[10] The effusive silicon atom beam intersected a tenuous atmosphere (10^{-5} to 10^{-3} torr) of N_2O (Matheson, >98%) and the resulting diffuse chemiluminescence resulting from the Si-N_2O reaction was observed at right angles to the metal flow through a Suprasil quartz viewing port. Light baffles were placed in the reaction chamber to minimize the interference from blackbody radiation emanating from the oven chamber.

Multiple collision studies were carried out by vaporizing silicon at temperatures between 1600 and 1800°C from a c.s. grade graphite crucible.[11] The crucible was machined to fit inside a commercial tungsten basket heater (R. D. Mathis, Long Beach, CA) which was wrapped with several layers of zirconia ZrO_2 cloth (Zircar Products, Florida, NY). The silicon vapor was reacted directly with N_2O or entrained in an argon buffer gas (Airco, 99.998%) and transported to the reaction zone where the resulting mixture underwent oxidation. Typical operating pressures were on the order of 10-100μ of oxidant and, at higher pressures, one to two torr of argon.

Spectra were taken with a 1 meter Czerny-Turner scanning spectrometer operated in first order with a Bausch and Lomb 1200 groove/mm grating blazed at 5000Å. For the study of the wavelength regions below 2500Å, the spectrometer was purged with dry N_2. Both RCA 4840 and 1P28 photomultiplier tubes were used in these experiments. In order to insure high sensitivity at wavelengths less than 2500Å, the 1P28 photomultiplier tube was coated with sodium salicylate. The sensitivity of the optical system, quartz viewing port, quartz lens system, and purged spectrometer, to short wavelength radiation was tested by monitoring the 1850Å mercury resonance line. This emission was readily detected demonstrating our ability to easily monitor chemiluminescent emission below 2000Å. The photomultiplier signal was detected with a Keithley 417 fast picoammeter whose output signal (partially damped) drove a Leeds and Northrup stripchart recorder. All spectra were wavelength calibrated using a low pressure mercury pen lamp.

Chemiluminescent Spectra

The Si-N_2O reaction is characterized by an intense blue chemiluminescence. The emission spectrum, which extends from 2250 to 4400Å (Figures 1-4), consists of contributions from the $A^1\Pi - X^1\Sigma^+$, $b^3\Pi - X^1\Sigma^+$, and $a^3\Sigma^+ - X^1\Sigma^+$ band systems of SiO and is dominated by the $b^3\Pi - X^1\Sigma^+$ band system onsetting at 2800Å. The spectra were all taken under single collision conditions ($P_{Total} \leq 10^{-4}$ torr).

a. $a^3\Sigma^+ - X^1\Sigma^+$

Resolvable features for the $a^3\Sigma^+ - X^1\Sigma^+$ band system extend from 3500-4400Å Figure 2). As has been observed by previous workers[3,4] under multiple collision conditions, only a single progression arising from the v' = 0 level of the $a^3\Sigma^+$ state can definitely be identified. If emission features originating in v'=1 are present they are weak and hidden under the $b^3\Pi - X^1\Sigma^+$ features. Therefore there has yet been no confirmation of the spectroscopic constants for the $a^3\Sigma^+$ state predicted by Field et al.[2] and partially determined by Linton and Capelle.[4]

b. $b^3\Pi - X^1\Sigma^+$

Emission features corresponding to the $b^3\Pi - X^1\Sigma^+$ band system extend from 2800 to 3950Å (Figures 1,2, and 3). Under single collision or near single collision conditions several new additional bandheads corresponding to vibrational levels $9 \leq v' \leq 11$ have been observed in the b-X system. This observation should be contrasted to the multiple collision studies of Hager et al.[3] where only emission from $v' \leq 2$ is observed and the notably different vibrational excitation, $v' \leq 8$, found by Linton and Capelle.[4] Clearly vibrational deactivation has begun to onset in the Linton and Capelle study and is quite pronounced in the experiments of Hager et al. Observed bandheads and relative intensities corrected for phototube response are given in Table 1. Some twenty new bandheads have been observed.

c. $A^1\Pi - X^1\Sigma^+$

The $A^1\Pi - X^1\Sigma^+$ emission features observed in this study are depicted in Figures 3 and 4. As Figure 3 demonstrates, the A-X emission which is much weaker than that from the b-X system is dominated by a progression emanating from v'=0.

While Linton and Capelle[4] have observed some A-X emission in their multiple collision study, Hager et al.[3] observed no such emission. On the basis of these results, Linton and Capelle reasoned that the A-X emission observed in their study resulted from the collisional population of the A state. Because we observe the emission system under single collision conditions and find a first order dependence of the A-X emission feature on pressure we have evidence for the direct population of the A state and the significant quenching of emission from this state in the experiments of Hager et al. In other words, our results would seem to indicate minimal vibrational and electronic deactivation in the multiple collision studies of Linton and Capelle and complete quenching of the A-X band system, which can be populated directly, in the experiments of Hager et al. No emission from $A^1\Pi$ vibrational quantum levels greater than $v'=2$ (Figures 3 and 4) was found in this study. If we consider the energy available to populate excited electronic states, we might expect to observe emission from $A^1\Pi$ vibrational quantum levels $v' \leqslant 15$.

Kinetics and Emission Behavior with Increasing Pressure

We find that the observed chemiluminescent emission from the $a^3\Sigma^+$, $b^3\Pi$, and $A^1\Pi$ states of SiO increases linearly with oxidant pressure over the range 3×10^{-5} to 6×10^{-4} torr indicating that these states are formed in a process first order in N_2O. Although detailed temperature dependence studies to determine the activation energy for the Si-N_2O reaction were not performed, the chemiluminescent intensity as a function of the Si beam source temperature was followed with sufficient accuracy so as to determine that reaction with ground state Si ^3P atoms had occurred.

At elevated pressures the relative emission from the three excited states populated in the initial Si-N_2O reactive process was found to vary. Specifically the $b^3\Pi$ emission intensity was found to increase relative to the $a^3\Sigma^+$ emission such that the ratio $I(a^3\Sigma^+)/I(b^3\Pi)$ decreased to a minimum at $\sim 5 \times 10^{-2}$ torr, virtually leveling off up to a pressure on the order of 2 torr. At pressures in excess of 5×10^{-1} torr, the $A^1\Pi$ emission intensity increased relative to that from the $b^3\Pi$ and $a^3\Sigma^+$ states and some vibrational deactivation occurred in the $b^3\Pi$ state, both of these findings being in agreement with the observations of Linton and Capelle.[4]

Nature of the Intercombination Band Systems

In a strictly first order description $^3\Sigma^+ - {}^1\Sigma^+$ or $^3\Pi - {}^1\Sigma^+$ transitions are spin-forbidden and should have little or no intensity. However, in the presence of perturbations the SiO $a^3\Sigma^+$ or $b^3\Pi$ states may mix with nearby $^1\Pi(A^1\Pi)$ and $^1\Sigma_0^+(E^1\Sigma_0^+)$ states, leading to nonzero "$a^3\Sigma^+$" - $X^1\Sigma^+$ or "$b^3\Pi$" - $X^1\Sigma^+$ transition moments. If the population of the "$^3\Sigma^+$" or "$^3\Pi$" states is sufficient to balance the very small "$^3\Sigma^+$" - $X^1\Sigma^+$ or "$^3\Pi$" - $X^1\Sigma^+$ oscillator strengths induced by this mixing, one can observe the corresponding band systems in emission. We are dealing with branching ratios in chemical reaction and hence the probable magnitude of the spin conservation entailed in reaction (1) leads to the strong probability that the Si-N_2O reaction forms the metal oxide largely in the "$a^3\Sigma^+$" and "$b^3\Pi$" states. This, in turn, leads to the observation of emission from these states.

We have found that a perturbation description is appropriate for the prediction of (1) the relative intensities of vibronic transitions for the "$b^3\Pi$" - $X^1\Sigma^+$ band system, (2) the relative intensities of the a"$^3\Sigma^+$"- $X^1\Sigma^+$ and "$b^3\Pi$" - $X^1\Sigma^+$ intercombination emission systems, and (3) the relative emission intensity from the $^3\Pi_{0,1,2}$ components of the $b^3\Pi$ state. In order to approach the analysis of the observed SiO* emission from the Si-N_2O reaction, we have evaluated the mixing coefficients among several of the low-lying states of SiO resulting from the following electronic configurations:

(2)...$5\sigma^2 6\sigma^2 7\sigma^2 2\pi^4$	$X^1\Sigma^+$
(3)...$5\sigma^2 6\sigma^2 7\sigma 2\pi^4 3\pi$	$b^3\Pi$, $A^1\Pi$
(4)...$5\sigma^2 6\sigma^2 7\sigma^2 2\pi^3 3\pi$	$a^3\Sigma^+$, $d^3\Delta$, $e^3\Sigma^-$, $C^1\Sigma^-$, $D^1\Delta$,$(E^1\Sigma_0^+)$.

The determinantal wavefunctions applicable to several of these states are believed to be quite analogous to those presented by Field et al.[12] for CO and will not be given in detail here. Using the appropriate parity adapted wavefunctions we have determined the interaction matrix for several

of these states employing a simplified microscopic form of the spin-orbit operator, commonly used for semiempirical calculations

$$H_{so} = \sum_i \hat{a}_i \ell_i \cdot s_i \qquad \hat{a}_i = \sum_k z_k / r_{ki}^3$$

where ℓ_i is the orbital angular momentum of electron i, s_i is the spin angular momentum of electron i, z_k is the effective charge on nucleus k, and r_{ki} is the distance between electron i and nucleus k. Spin-other-orbit interactions have been neglected and we have assumed negligible effects due to the coriolis interaction which is expected to be at least two orders of magnitude smaller than spin-orbit coupling.

In Table 2, the matrix elements in units of cm^{-1} are represented as the product of a numerical electronic factor and a vibrational overlap. In order to obtain the results presented in Table 2, the appropriate basis functions were expressed in terms of antisymmetrized products of one electron molecular orbitals in a manner similar to that described in a previous study on AlO. We assume that the 7σ and 2π orbitals correspond to $p\sigma$ and $p\pi$ orbitals respectively centered on oxygen and that the 3π orbital is derived from a $3p\pi$ orbital centered on silicon. We also assume that the electronic states with which we are concerned are well represented by the charge distribution Si^+O^-. Hence to good approximation the 7σ and 2π orbitals can be represented by atomic p orbitals $P_-(O^-)$ and $P_0(O^-)$ centered on the oxygen ion (O^-) and

$$a = 2^{\frac{1}{2}} a_0 \langle v | v' \rangle \tag{5a}$$

where

$$a_0 = \langle P(O^-) | \varepsilon_0(r) | P(O^-) \rangle \sim 121 \text{ cm}^{-1} \tag{5b}$$

[13]

where this equality is not exact because (1) approximate representations were assumed for 7σ and 2π, and (2) the spin orbit coupling constant, $a_0 \sim 121$ cm^{-1}, is strictly appropriate to O^- and not Si^+O^-. The vibrational overlap factor (eq. 5a) is determined from RKR curves[14] which are obtained

using the molecular constants given by Field et al.[2] for the various states of interest. The parameter

$$a_z = \langle 3\pi|\hat{a}|3\pi\rangle \text{ cm}^{-1} \quad \sim 146\text{cm}^{-1} \tag{6}$$

is taken from Field et al.[2] In our calculations the $E\ ^1\Sigma_o^+$ state is assigned to configuration (4). In fact this state probably corresponds to a mixed configuration valence state with dominant contribution from configuration (4).[2] The matrix element connecting $E\ ^1\Sigma_o^+$ and $b^3\Pi_o$ will be overestimated.

In fitting the observed chemiluminescent spectra for the mixed "$b^3\Pi$" state, the wavefunctions for the components of interest may be written to reasonable approximation as

$$\psi(\text{"}b^3\Pi_1\text{"}) = c(b^3\Pi_1) + d(A^1\Pi_1) \tag{7a}$$

$$\psi(\text{"}b^3\Pi_o\text{"}) = c'(b^3\Pi_o) + d'(E^1\Sigma_o^+) \tag{7b}$$

where c>>d, c'>>d', and the $A^1\Pi$ and $E^1\Sigma_o^+$ states correspond to nearby excited states (configs. (3) and (4)) which mix significantly (Table 2) with the $^3\Pi_1$ and $^3\Pi_o$ components of the $b^3\Pi$ state and from which emission occurs in an allowed transition to the ground $^1\Sigma^+$ state. If the $^3\Pi$ components are described as in equation (7), the relative intensities $I_{v',v''}$ of vibronic transitions (v',v") in emission are related to the excited state populations $N_{v'}$ by

$$I_{em}^{v',v''} = N_{v'}\varepsilon(\nu)\nu_{v',v''}^4 \Sigma_v c^2_{v',v} q_{v,v''} \tag{8}$$

where $c_{v',v}$ is the mixing coefficient between $b^3\Pi_1$ and $A^1\Pi_1$ or $b^3\Pi_o$ and $E^1\Sigma_o^+$, $N_{v'}$ is the number of molecules in the $^3\Pi$ components, $\nu_{v',v''}$ is the frequency of the transition, and $q_{v,v''}$ is the Franck-Condon-Factor (FCF) between vibrational levels v of $A^1\Pi$ or $E^1\Sigma_o^+$ and v" of $X^1\Sigma^+$.

A similar expression can be written for the mixed "$^3\Sigma^+$" state

$$\psi(\text{"}a^3\Sigma^+\text{"}) = c''(a^3\Sigma_1^+) + d''(A^1\Pi) \qquad (9)$$

In fact, the description represented by expressions (7) and (9) is complicated further since the "$^3\Sigma^+$" and "$^3\Pi$" states can (Table 2) and apparently do couple so that the "$^3\Sigma^+$" state has some "$^3\Pi$" character and vice-versa. This point will be considered in a following section.

Upon evaluating the matrix elements in Table 2 using the molecular constants given by Field et al.[2] for the low-lying states of SiO, we find the largest mixing between $b^3\Pi_1$ and $A^1\Pi_1$. The interaction between $a^3\Sigma_1^+$ and $A^1\Pi_1$ is considerably smaller not only because of a smaller electronic factor but also because the Σ configured states (Eq. 4) are shifted relative to the Π states to considerably larger internuclear distance, thus decreasing the vibrational overlap factor. Both the $^3\Pi$ and $^1\Pi$ states derived from the same electronic configuration have similar internuclear distances and hence a significantly higher vibrational overlap. The $^3\Pi_0$ component derives its intensity from the mixed valence $E^1\Sigma_0^+$ state and therefore is characterized by a much smaller vibrational overlap than $^3\Pi_1$ - $^1\Pi_1$. Based upon these considerations and the fact that $E^1\Sigma_0^+$ is a mixed state, we anticipate that the intensity of emission from the $^3\Pi_1$ component should dominate that from the $^3\Pi_0$ component. In turn, the $^3\Pi_0$ component should dominate $^3\Pi_2$ which derives the major contribution to its intensity from a Coriolis interaction.

The predictions outlined above are born out in the spectra depicted in Figure 1(b) where the (0,0) and (0,1) bands of the "$^3\Pi$" - $X^1\Sigma^+$ band system are resolved. The "$^3\Pi_2$" emission feature should appear to the blue of the dominant "$^3\Pi_1$" feature and is barely discernable. Based on an evaluation of the matrix elements in Table 2, the intensity ratio $^3\Pi_0/^3\Pi_1$ is at a maximum for v' = 0 and tails off rapidly for levels v'>1. Therefore, the

relative intensities of the bands depicted in Figure 1(a), where the "$^3\Pi_1$" and "$^3\Pi_0$" components are unresolved, are determined primarily by the "$^3\Pi_1$" component emission, the dominance of $^3\Pi_1$ over $^3\Pi_0$ increasing with increasing v'. In addition, based on the matrix elements given in Table 2 and discussed above, we can determine that the emission corresponding to the "$b^3\Pi$" - $X^1\Sigma^+$ intercombination system should dominate that for the "$a^3\Sigma^+$" - $X^1\Sigma^+$ system. Indeed, this is observed.

Within the "$b^3\Pi$" - $X^1\Sigma^+$ band system, the relative intensity of emission from individual vibrational quantum levels v' appears to be well predicted by equation (8) where $c^2_{v',v}$ represents the mixing coefficient between the vibrational level v' of "$b^3\Pi$" and vibrational levels v of $A^1\Pi$. The population of individual vibrational levels in the "$b^3\Pi$" state rises from v' = 0 to v' = 2 tailing off for vibrational levels $v' \geqslant 3$.

Finally, we wish to estimate the branching ratio for population of the "$b^3\Pi$" vs. the $A^1\Pi$ state. In order to do so, we compare the intensity of certain "$b^3\Pi$" and $A^1\Pi$ emission features. This procedure is implemented by considering the "$b^3\Pi$" - $A^1\Pi$ mixing coefficients (Eq (8) and above) which are generally on the order of 0.01 or less, the largest mixing being with the v'=0 level of "$b^3\Pi$". If, correcting for phototube response, we compare the relative intensity of the (0,0) bands for the "$b^3\Pi$" - $X^1\Sigma^+$ and $A^1\Pi$ - $X^1\Sigma^+$ transitions, the relative populations of "$b^3\Pi$", v'=0, and $A^1\Pi$,v=0 are given by

$$\frac{N_o(\text{"}b^3\Pi\text{"})}{N_o(A^1\Pi)} = \frac{I(\text{"}b^3\Pi\text{"} - X^1\Sigma^+)(FCF=0.141)}{I(A^1\Pi - X^1\Sigma^+)\quad C} \left(\frac{\nu_{oo}(A^1\Pi - X^1\Sigma^+)}{\nu_{oo}(\text{"}b^3\Pi\text{"} - X^1\Sigma^+)}\right)^4 \qquad (10a)$$

$$C = (0.141c^2_{0,0} + 0.277\ c^2_{0,1} + 0.274\ c^2_{0,2}) \qquad (10b)$$

where 0.141, 0.279, and 0.274 correspond to Franck-Condon factors for the $A^1\Pi$ - $X^1\Sigma^+$ (0,0), (1,0), and (2,0) transitions, and $c^2_{0,0}$, $c^2_{0,1}$, and $c^2_{0,2}$

correspond to the mixing coefficients for the v=0,1,2 levels of $A^1\Pi$ with v'=0, "$b^3\Pi$". The C term derives from equation 8, the dominant mixing with v'=0 $b^3\Pi$ being with the v=0,1,2 levels of $A^1\Pi$. The intensity of the "$b^3\Pi$" (0,0) band may be compared to any of the (v,v") $A^1\Pi$ emission bands simply by modifying the numerator in Eq. 10a, replacing the Franck-Condon factor and frequency for the (0,0) band with the appropriate quantities for the $A^1\Pi$ - $X^1\Sigma^+$ band of interest.

The intensities for the "$b^3\Pi$"- $X^1\Sigma^+$ and $A^1\Pi$ - $X^1\Sigma^+$ (0,0) bands are taken to be 350 and 48 respectively. These relative band intensities were determined on the basis of a conservative estimate of the relative phototube response between 2300 and 3000Å, a region in which phototube sensitivities are such that precise calibration is tenuous. In order to aid our determination of the relative phototube response in the short wavelength region, we made use of the known Franck-Condon factors for the (0,v") and (1,v") progressions of the $A^1\Pi$ - $X^1\Sigma^+$ system (Fig. 3), determining a response consistent with expected relative emission intensities. The quoted relative intensities for the (0,0) bands correspond to an upper bound estimate of the corrected relative intensity for the $A^1\Pi$ - $X^1\Sigma^+$(0,0) band (underestimate of relative phototube response) obtained on the basis of the analysis of the $A^1\Pi$ - $X^1\Sigma^+$ progressions (Fig. 3). Substituting into Eq. 10a with $\nu_{00}(A^1\Pi)$ = 42640.9 cm^{-1}[2] and C = 0.00502 we estimate that the population of "$b^3\Pi$"(v'=0) is on the order of 500 times larger than $A^1\Pi$(v=0). Similar results are obtained if we choose to compare the"$b^3\Pi$"- $X^1\Sigma^+$(0,0) band with other $A^1\Pi$ - $X^1\Sigma^+$(0,v") bands.

The estimated branching ratio for formation of "$b^3\Pi$" vs. $A^1\Pi$ excited state species assumes that the radiative lifetimes of the two states are comparable and that the region viewed by the spectrometer is sufficiently

large so that the relative intensity of emission from the two states is an accurate measure of the relative rates of formation in these states. However, in the present study, it is certainly the case that the two states considered have drastically different radiative lifetimes and that their relative intensities are no longer simply related to the relative rates of formation. Since the radiative lifetime of the "$b^3\Pi$" state is considerably longer than that of the $A^1\Pi$ state (see following discussion), a larger fraction of molecules formed in the "$b^3\Pi$" state will leave the viewing region before radiating and therefore will not be detected. The consideration of this fact and the nature of the estimates in our perturbation calculations leads us to the conclusion that the ratio of population which we have calculated is certainly a lower bound to the actual branching ratio.

Energy Balance for the $Si + N_2O \rightarrow SiO^* + N_2$ Reaction

In this section, we focus on the large discrepancy between the available energy to populate SiO excited states, due primarily to the exoergicity of the $Si + N_2O$ reaction, and the energy for which we can account through determination of the highest excited state quantum levels populated in reaction.

From the single collision $Si-N_2O$ reaction it is potentially possible to set a lower bound on the dissociation energy of silicon monoxide. Using reaction (1) and a previously discussed energy balance[15-17] we arrive at the inequality

$$D_o^o(SiO) \geq D_o^o(N_2O) + E_{int}(SiO) - E_{int}(Si) - E_{int}(N_2O) - E_T^i - E_A(Si\text{-}N_2O) \quad (11)$$

where the silicon atom is in the ground ^3P state and E_{int} (Si), E_{int} (N_2O), and E_{int} (SiO) are the internal energies of the species noted in parenthesis.* E_T^i is the relative translational energy of the reactants and $E_A(Si\text{-}N_2O)$ is the measured activation energy for the metathesis considered. In considering the products of the $Si\text{-}N_2O$ reaction, SiO and N_2, neither $E_{int}(N_2)$ nor E_T^f, the final relative translational energy of product separation can be readily determined. Therefore these quantities are not included in Eq. (11) and the inequality applies.

If we neglect for the moment the activation energy for the $Si\text{-}N_2O$ reaction[18] and focus on the available energy to populate SiO excited states

$$E_{Available} = D_o^o(SiO) - D_o^o(N_2O) + E_{int}(N_2O) + E_{int}(Si) + E_T^i$$

The available energy is partitioned to

$$E_{int}(SiO) + E_{int}(N_2) + E_T^f \quad (13)$$

*For the silicon reaction, we select as our reference (zero) energy the reactants and products in eq. (11) at 0°K, that is $Si(^3P_o)$, $N_2O(^1\Sigma^+, v=J=0)$, $SiO(^1\Sigma^+, v=J=0)$ and $N_2(^1\Sigma^+, v=J=0)$.

The SiO molecule is among the most widely studied high temperature molecules. Its bond energy is not only well known but represents a standard for mass spectrometry. We adopt the recent determination by Hildenbrand et al.,[19] $D_o^o(SiO) = 8.16eV = 65827\ cm^{-1}$. The N_2-O bond energy[20] is 13400 cm^{-1}.

To calculate $E_{int}(N_2O)$, we adopt a procedure similar to that described previously[21] for the determination of $E_{int}(OCS)$ and find $E_{int}(N_2O) = 298\ cm^{-1}$. To calculate $E_{int}(Si)$ we need consider only the internal energy of the ground ^3P state since it is this state which reacts to produce the observed chemiluminescence. Using standard techniques[22] we find $E_{int}(Si) = 145\ cm^{-1}$ for a beam temperature of 2170°K.

Dagdigian et al. have shown that, to good approximation[23]

$$E_T^i = 3/2kT_{eff} \qquad T_{eff} = (m_G T_B + m_B T_G)/(m_G + m_B) \tag{14}$$

where T_G is the temperature of the oxidant gas (300K), T_B is the silicon beam temperature (2170 K) and m_B and m_G are the masses of the beam atoms and gas molecules respectively. For the Si-N_2O reaction, we find $E_T^i = 1501\ cm^{-1}$.

Summing the energies considered above, we find

$$E_{Available} = 54371\ cm^{-1} \tag{12a}$$

In order to evaluate $E_{int}(SiO)$, we seek the highest quantum level populated by the Si-N_2O reaction. Here, we exclude the use of the $a^3\Sigma^+$ state since, as we have noted, (1) the emission from this state is much weaker than and obscured by that from the $b^3\Pi$ state and (2) for levels v'>0 possible strong $a^3\Sigma^+ - b^3\Pi$ coupling may also play a role in obscuring the $a^3\Sigma^+$ emission features.

The highest vibrational quantum level populated in the SiO $A^1\Pi$ state is v = 2. Choosing the (2,7) band in the $A^1\Pi - X^1\Sigma^+$ system, we obtain

$$E_{int}(SiO) = \nu(2,7) + G''(7) - G''(0)$$
$$= 35951 \pm 30 \text{ cm}^{-1} + G''(7) - G''(0) \quad (15)$$
$$= 44314 \pm 35 \text{ cm}^{-1}$$

The highest vibrational quantum level populated in the SiO "$b^3\Pi$" state is v' = 11. Choosing the (11,16) band in the "$b^3\Pi$" - $X^1\Sigma^+$ system we obtain

$$E_{int}(SiO) = 43992 \pm 40 \text{ cm}^{-1} \quad (16)$$

The energy for which we can account using the SiO excited state emissions is some 10,000 cm^{-1} less than the potential available energy to the system! It implies that the SiO bond energy is over an electron volt less than the reliable value given in the literature, a highly unlikely possibility.

In general, single collision chemiluminescence studies yield dissociation energies that are in close agreement with careful mass spectrometric measurements. With few exceptions,[24] any discrepancies are encompassed if one takes into account the temperature dependence of the metathesis yielding chemiluminescence and the nature of the metal atom reactant. In all cases, discrepancies have resulted in the prediction of slightly higher bond energies. Therefore the result obtained here represents a significant deviation from expectation. In the present study, we have found that ground state ^3P silicon atoms react to yield the observed chemiluminescence. If, in order to provide a correction for the possible reaction of metal atoms in the high energy tail of their translational energy distribution, we determine the activation energy for the Si-N_2O reaction, this energy increment must be added to the available energy,[25] Eq. (12). Therefore the energy discrepancy is even larger than 10,000 cm^{-1}.

It is apparent that when the products SiO and N_2 are formed over an electron volt of energy must be accounted for by either the product N_2 internal

energy or the relative translational energy of product separation. In the following discussion, we document that the observed behavior in the Si-N_2O system appears to be characteristic of several M-N_2O reactions. We suggest that the most logical choice to account for the observed energy discrepancy corresponds to the internal excitation of product N_2 molecules.

Discussion

A. Energy Balance in M-N_2O Reactions

In spite of repeated efforts, we have been unable to use the Si-N_2O reaction to populate vibrational levels $v' \geq 3$ in the $A^1\Pi$ state of SiO. In addition, we have not observed fluorescence from the $E\ ^1\Sigma_o^+$ state although it should be possible to populate two vibrational levels in this state. The Si-N_2O reaction is of sufficient exothermicity to populate 15 vibrational quantum levels in the $A^1\Pi$ state. Emission from these levels can readily be observed and recently we have employed the spin conserving Si-O_3 reaction

$$Si(^3P) + O_3(^1A_1) \rightarrow SiO(A^1\Pi) + O_2(^2\Sigma_g^-) \qquad (17)$$

to populate a minimum of 12 vibrational quanta in the $A^1\Pi$ state. In short, there appears to be little reason to suspect that the lack of $A^1\Pi$ vibrational excitation which characterizes the Si-N_2O reaction can be attributed to factors associated with the intimate molecular electronic structure of the $A^1\Pi$ state. Rather it appears that the observed effects are to be associated with the dynamics of the Si-N_2O reaction. We would like to suggest a plausible explanation for the observed results based upon a comparison of the molecular N-N bond in the reactant N_2O and the product N_2 (Eq. 1).

The bond length of the N-N bond in the linear N-N-O molecule is 1.128Å.[26] The N-N bond length in molecular nitrogen is 1.0977Å.[27] We ask what vibrational excitation must be associated with the N_2 molecule in order that the corresponding bond length be 1.128Å. The vibrational excitation corresponds to $v''=5$. In other words, the average value of the internuclear distance for the fifth vibrational quantum level in the ground state of N_2 corresponds to the N-N bond distance in N_2O. The energy associated with $v''=5$ is 11350 cm^{-1}, in close agreement with the 10,000 cm^{-1} energy discrepancy which characterizes the Si-N_2O

reaction*. We suggest that this correlation may not be fortuitous and that the Si-N_2O reaction, which certainly does not proceed via an electron jump mechanism, may occur via a sufficiently fast stripping or rebound process such that the N-N bond does not have sufficient time to adjust to its equilibrium value in N_2 before the products SiO and N_2 separate. Thus, energy balance requires that the N_2 be produced in a vibrationally excited state.

The results obtained in the present study cause us to focus on the nature of the energy balance in several M + N_2O reactions where we find that the proposed explanation is consistent with observation. Consider, for example, the Ti-N_2O reaction, the chemiluminescent emission from which is depicted in Figure 5. Based on the energetics for this process, the available energy to populate excited electronic states is

$$\begin{aligned} D_o^o(TiO) &\geq D(N_2\text{-}O) + E_{int}(Ti) + E_{int}(N_2O) + E_T^i \\ &= 55440 - 13400 + 282 + 298 + 1384 \text{ cm}^{-1} \\ &= 44004 \text{ cm}^{-1} \end{aligned} \qquad (18)$$

where titanium atoms at 2400°K thermally distributed throughout the ground ^3F state react with N_2O to produce several TiO excited electronic states. Although the fluorescence from all of these states has not yet been analyzed, the emission corresponding to the D-$X^3\Delta$ band system of TiO (Table 3) has been analyzed and the population of vibrational levels in this state has been assessed using much higher resolution scans than that depicted in Figure 5.[28] The D state is the highest lying excited electronic state populated (and monitored) by the titanium-N_2O reaction. Based on the observed fluorescence the maximum energy associated with TiO internal excitation is

$$E_{int}(TiO) = 34840 \text{ cm}^{-1} \qquad (19)$$

---

*Note that the activation energy $E_A(Si\text{-}N_2O)$ for the silicon-N_2O reaction was not included in the evaluation of the energy discrepancy. Its inclusion would raise the calculated value by between 1000 and 2000 cm^{-1}.[18]

Here, we have an ~9000 cm^{-1} energy discrepancy between $E_{Available}$ (Eq. 18) and $E_{int}(TiO)$. We believe that this discrepancy may also be attributed to the formation of vibrationally excited N_2.

The production of vibrationally excited N_2 may also serve to explain a puzzling aspect of the chemiluminescent emission associated with highly exothermic aluminum oxidation.[29] The aluminum-ozone reaction produces extensive chemiluminescence from the $A^2\Pi$ and $B^2\Sigma^+$ states of AlO, the "single collision" process populating up to 18 vibrational quanta in the $B^2\Sigma^+$ state. Using independent measurements,[30] one finds that this is virtually the highest vibrational excitation which can be expected on the basis of the available energy ($D_o^o(AlO) - D(O-O_2) + E_{int}(Al) + E_{int}(O_3) + E_T^i$). Given the excitation which characterizes the $Al-O_3$ reaction and the relatively small energy difference, 0.63eV., between the N_2-O and O_2-O bond energies, we certainly expect to observe emission from the AlO $B^2\Sigma^+$ state if we react aluminum with N_2O. We would expect to populate 12 vibrational quanta (ω_e = 870.05 cm^{-1}, $\omega_e x_e$ = 3.5 cm^{-1}), however, no emission is observed. We feel that this result is again explained through an energy balance involving vibrationally excited N_2.

Similar and in some cases larger energy discrepancies are found to characterize several M + N_2O reactions involving the Group IIIB (Sc,Y,La) and Group IIA metals. The data is summarized in Table 4. In many of these cases further characterization of the product metal oxide chemiluminescence will be required in order to better assess the actual magnitude of the energy discrepancy.

The significant fact which emerges is that all the reactions considered display an energy balance which is consistent with the formation of a vibrationally excited N_2 product. While one might argue that the translational energy of product separation can account for a portion of these observations, it seems highly unlikely that the final relative translational energy of separation, E_T^f (Eq. 13), can account for the rather sharp energy cutoffs especially those

associated with the silicon, titanium, and aluminum reactions.

There are several experiments which might be pursued in order to obtain direct evidence for the formation of vibrationally excited N_2 produced in M = Al, Si, or Ti + N_2O reaction. The major problem confronting the experimenter is the detection of very low effective product N_2 concentrations ($\sim 10^{-7}$ torr). Promising detection techniques might involve the use of either electron bombardment excitation and ionization or multiphoton ionization. In the former studies one might attempt to use an electron gun to excite the Second Positive system of N_2 monitoring directly the N_2 $C^3\Pi_u$ - $B^3\Pi_g$ fluorescence and back extrapolating to the ground state N_2 population distribution.[31] Alternatively, we are attempting to produce N_2^+ $B^2\Sigma_u^+$, monitoring the $B^2\Sigma_u^+$ - $X^2\Sigma_g^+$ emission and again back-extrapolating to the N_2 population distribution.[31] Thusfar these studies have met with only marginal success (N_2 concentrations $\leq 10^{-5}$ torr have been detected), however the signal-to-noise in the system can be considerably improved if the reaction zone and electron gun are magnetically confined.[32] An alternate experiment might involve the elegant pulsed laser multiphoton technique which Dehmer[33], Kay[34] and coworkers have used to detect CO^+. The direct assessment of the vibrational excitation characterizing the product N_2 formed in highly exothermic M + N_2O reactions will contribute important new perspectives on the nature of reactive encounters. We encourage other workers to pursue the detection of vibrationally excited N_2 in low concentration.

B. Comparison and Correlation with Previous Studies

The present study augments and can be used to correlate the previous studies of Linton and Capelle[4] and Hager et al.[3] on the Si-N_2O reaction. Linton and Capelle studied the reaction of argon entrained silicon atoms with N_2O over the pressure range 1 to 30 torr (primarily argon >> N_2O), observing emission corresponding to the SiO $A^1\Pi - X^1\Sigma^+$, $a^3\Sigma^+ - X^1\Sigma^+$, and $b^3\Pi - X^1\Sigma^+$ band systems. The ratio of $a^3\Sigma^+$ to $b^3\Pi$ emission was unchanged with pressure and the chemiluminescence was dominated by the b-X band system. Hager et al. entrained the products of a discharge into a silane-helium mixture reacting the entrained species with N_2O at total pressures of 2 and 4 torr. These authors observed only emission from the "$a^3\Sigma^+$" (a-X) and "$b^3\Pi$" (b-X) states, finding that only levels $v' \geq 2$ were populated in the $b^3\Pi$ state in contrast to the much higher vibrational excitation ($v' \leq 8$) observed by Linton and Capelle. As the pressure was increased from 2 to 4 torr, the ratio of $a^3\Sigma^+$ to $b^3\Pi$ emission increased substantially (see also discussion of observed band systems and kinetics).

Our results obtained at low pressure ($\leq 10^{-3}$ torr) demonstrate that the "$a^3\Sigma^+$", "$b^3\Pi$", and $A^1\Pi$ states of SiO are populated directly in the Si-N_2O chemical reaction, although the branching ratio strongly favors triplet state formation in agreement with the spin conservation associated with reaction (1). Under multiple collision conditions (1-2 torr) the emission from the $A^1\Pi$ state does not increase significantly relative to that from the $b^3\Pi$ state. From these results we reach the following conclusions: (1) The population of the $A^1\Pi$ state in the Linton and Capelle study must result in large part from its direct formation in chemical reaction (in the low pressure range) and not from a collisional transfer[4] process. (2) The lack of $A^1\Pi$ emission in the Hager et al. study results from the efficient quenching of $A^1\Pi$ emitters under their experimental conditions. It is not surprising that their experimental conditions provide a

much more efficient medium for the collisional quenching of the $A^1\Pi$ state than does an argon + N_2O (argon >> N_2O) mixture at comparable pressures. (3) At higher pressures, from 4 to 30 torr, the Linton and Capelle study indicates that the $A^1\Pi$ state may also be populated by a collisional process in addition to direct $A^1\Pi$ formation. We speculate that direct $A^1\Pi$ formation, collisional population, and collisional quenching are all operative in their system, the former two processes dominating the latter.

The pressure dependent behavior of the "$a^3\Sigma^+$" and "$b^3\Pi$" emission features is distinctly different in the Linton and Capelle and Hager et al. studies. The behavior of the chemiluminescent emission in our system may serve to explain some of these differences. We believe that the present results indicate that at least 11 vibrational quanta in the "$b^3\Pi$" state are populated by the direct Si-N_2O reaction.[35] Linton and Capelle observe emission from only 8 vibrational quantum levels indicating that the argon + N_2O mixture present in their system acts as a mild vibrational quencher. In contrast, the mixture of helium, N_2O, and the discharge products of silane serves to promote significant vibrational relaxation in the experiments of Hager et al. where only emission from v'=0,1,2, "$b^3\Pi$" is observed.

Although Linton and Capelle observe no change in the relative intensities of the "$a^3\Sigma^+$" and "$b^3\Pi$" emission features as a function of pressure, Hager et al. observe a substantial increase in the $a^3\Sigma^+/b^3\Pi$ intensity ratio. This result at first appears difficult to explain in view of the location of the $a^3\Sigma^+$ and $b^3\Pi$ states (Figure 6), however, the results obtained in the present study, where the ratio of "$a^3\Sigma^+$" to "$b^3\Pi$" emission first decreases and then levels off, provide some indication of the processes involved. Consistent with observation in all three studies is the direct population of the "$a^3\Sigma^+$" state and subsequent transfer to "$b^3\Pi$". Because of its location at larger internuclear distance, the

"$a^3\Sigma^+$" state should represent the first state encountered during the SiO triplet forming process. At the very least the $a^3\Sigma^+$ and $b^3\Pi$ states should compete on equal ground for the final SiO triplet formed in reaction. Recall (Table 2) that the "$a^3\Sigma^+$" and "$b^3\Pi$" states are strongly coupled and therefore that the transfer from the mixed "$a^3\Sigma^+$" state to the mixed "$b^3\Pi$" state is readily facilitated Thus, while both the "$a^3\Sigma^+$" and "$b^3\Pi$" states may be formed in the initial stages of reaction, our results indicate that the strong coupling between these states promotes significant "$a^3\Sigma^+$" → "$b^3\Pi$" transfer with increasing pressure.

We believe that a significant coupling between the "$a^3\Sigma^+$" and "$b^3\Pi$" states also plays an important role in the pressure dependent behavior observed by Hager et al. Because vibrational deactivation is strongly manifest under their experimental conditions, one finds a substantial population buildup in the lowest vibrational levels of the "$a^3\Sigma^+$" and "$b^3\Pi$" states. That vibrational deactivation is significant in these systems is not surprising since the "$a^3\Sigma^+$" and "$b^3\Pi$" states are quite long-lived[36] (see also following discussion). An increase in the ratio of "$a^3\Sigma^+$" to "$b^3\Pi$" emission intensity results when vibrational relaxation dominates and is enhanced by all other processes in the system. Recall that we observe emission from only the v'=0 level of "$a^3\Sigma^+$." Although some emission from higher v'=1,2,... quantum levels of "$a^3\Sigma^+$" may occur, the dominance of $^3\Pi_1$ - $A^1\Pi_1$ verses $^3\Sigma_1^+$ - $A^1\Pi_1$ coupling (Table 2 and previous discussion) leads to an effective "$b^3\Pi$" - $X^1\Sigma^+$ transition moment which considerably exceeds that for "$a^3\Sigma^+$" - $X^1\Sigma^+$. Therefore the emission from vibrational levels $v' \geq 1$ in "$a^3\Sigma^+$" will underline the more dominant "$b^3\Pi$" emission system. Only the v'=0 level of "$a^3\Sigma^+$" is not overlapped by "$b^3\Pi$." As vibrational relaxation dominates to the extent that the population of the v'=0 level of "$a^3\Sigma^+$" increases significantly relative to "$b^3\Pi$," v'=0-2, the "$a^3\Sigma^+$" emission intensity can increase relative to and dominate "$b^3\Pi$." Relaxation to v'=0, "$a^3\Sigma^+$" is facilitated by the significant coupling between the a and b states. In a strong sense, one observes

relaxation to the lowest vibrational quantum level of the triplet manifold where one might envision the "$a^3\Sigma^+$" and "$b^3\Pi$" states in tandem forming a combined triplet state reservoir.

In summary, the pressure dependent effects associated with the "$a^3\Sigma^+$" and "$b^3\Pi$" states observed in the present study and in the study of Hager et al. can be attributed to a combination of (1) strong coupling between the "$a^3\Sigma^+$" and "$b^3\Pi$" states, (2) the nature of the effective transition moments for "$a^3\Sigma^+$" and "$b^3\Pi$" and (3) at higher pressures, in certain environments, pronounced vibrational relaxation. Based upon our results, the "$a^3\Sigma^+$"/"$b^3\Pi$" intensity ratio levels off when a steady-state $a^3\Sigma^+ - b^3\Pi$ transfer occurs. This is consistent with the negligible changes observed in the study of Linton and Capelle and is only modified when the extent of vibrational relaxation is such as to promote the significant population of the v'=0 level of "$a^3\Sigma^+$".

C. Branching Ratios and Quantum Yield Determinations

The results obtained in the present study in tandem with the lifetime determinations of other workers[36,37] cause us to focus on the meaning of the quantum yield determinations previously made on the Si-N_2O system. Linton and Capelle have measured a total quantum yield on the order of 0.05%. We believe that the measured quantum yield (1) does not reflect the relative populations of the $b^3\Pi$, $a^3\Sigma^+$ and $A^1\Pi$ states and (2) that the magnitude of the total quantum yield does not reflect the actual product yield in this system.

The radiative lifetime associated with the $A^1\Pi - X^1\Sigma^+$ system is 9.6 ± 1 microseconds[37] whereas the estimated radiative lifetime for the $b^3\Pi - X^1\Sigma^+$ system is 48 milliseconds.[36] The ratio of these radiative lifetimes indicates that the branching ratio calculated previously represents a definite lower bound (note previous discussion). Because the radiative lifetimes differ by a factor of 5000, and the $b^3\Pi$ state is quite long-lived, the viewing zone[38] used to assess the relative excited state quantum yields will clearly prejudice measurements of the yield of the $A^1\Pi$ over the $b^3\Pi$ state. The effect will be more pronounced for the "$a^3\Sigma^+$" state whose radiative lifetime is expected to exceed that for "$b^3\Pi$" because of its smaller coupling to the $A^1\Pi$ state.

The extremely long radiative lifetimes for the "$b^3\Pi$" and "$a^3\Sigma^+$" states require that we make use of a very large viewing zone in order to correctly assess the absolute total quantum yield for the Si-N_2O reaction. From the information given in the literature, it does not appear that this requirement has yet been satisfied.[38] Therefore, the measured total quantum yield must represent a lower bound measurement of direct excited triplet state formation. This may have significant implications for the possible use of the Si-N_2O reaction as a visible chemical laser medium.

D. A Possible Chemical Laser Candidate

Much attention has focused on the Sn-N_2O reaction and the production of the low-lying "$a^3\Sigma^+$" state of tin oxide in high quantum yield (~45%). It is[39] thought that lasing action might be initiated on the SnO $a^3\Sigma^+ - X^1\Sigma^+$ band system, specifically on the (0,2), (0,3), and (0,4) transitions at ~5307, ~5532, and ~5799Å. The results obtained in this study indicate, in correlation with the efforts of other workers, that the Si-N_2O system may also represent an equally interesting candidate.

Recently, Davis and other workers[40] have determined the absolute rate coefficients for total product formation in several Group IVA metal oxidations. Their results for N_2O indicate that the rate coefficients increase in the order C > Si > Ge > Sn. The rate coefficient for $Si(^3P)$ with N_2O is $(8.2\pm4) \times 10^{-11}$ cm^3/molecule-sec whereas those for $Sn(^3P_1)$ and $Sn(^3P_2)$ with N_2O are 1.1×10^{-12} and $3.5\pm0.7 \times 10^{-11}$ respectively. This is significant, especially because the Si-N_2O reaction is expected to conserve spin more readily than Sn-N_2O which must involve the heavier intermediate complex. If spin conservation holds (Eq. (1)) and the rate coefficient measured by Davis et al. is indicative of the magnitude of triplet state formation in the Si-N_2O system, this reaction may hold possibilities for the development of a visible chemical laser.

Our interest should focus not only on the possibility of producing copious quantities of triplet state emitters in order to create a population inversion on the intercombination band system but also on the possibility of using vibrational relaxation to produce molecules in the v'=0 level of the "$a^3\Sigma^+$" state (see previous discussion). Because coupling to the ground $^1\Sigma^+$ electronic state appears to be at a minimum for the "$a^3\Sigma^+$" and "$b^3\Pi$" states, the possibility of formulating a system very much analogous to the O_2 ($^1\Delta_g$) - iodine transfer laser may well exist. In other words, one would hope to carry out an efficient energy transfer process

$$SiO(\text{"}a^3\Sigma^+\text{"},v'=0) + X \longrightarrow SiO(X^1\Sigma^+,v''=2\text{-}7) + X^*$$

where X* preferably represents an atomic species and the energy transfer involves the formation of SiO ground state molecules in one of the vibrational levels v"=2,3,...,7.

Acknowledgement: It is a pleasure to acknowledge helpful discussions with Dr. C. D. Jonah and Professors Stewart Novick and Arthur Fontijn. This work was partly supported by the Scientific Services Program (A.R.O.) and by the Department of Energy, METC.

References

1. H. Bredohl, R. Cornet, I. Dubois, and F. Remy, J. Phys. B. 7, L66 (1974); T. G. Heil, H. F. Schaefer III, J. Chem. Phys. 56, 958 (1972); J. Drowart, A. Pattoret, and S. Smoes, Proc. Brit. Ceram. Soc. 8, 67 (1967); D. L. Hildenbrand, High Temp. Sci. 4, 244 (1972); K. F. Zmbov, L. L. Ames, and J. L. Margrave, High Temp. Sci. 5, 235 (1973); H. Kvande and P. G. Wahlbeck, High Temp.-High Press. 8, 45 (1976); D. L. Hildenbrand and E. Murad, J. Chem. Phys. 51, 807 (1969).

2. R. W. Field, A. Lagerqvist, and I. Renhorn, Phys. Scripta 14, 298 (1976).

3. G. Hager, R. Harris, and S. G. Hadley, J. Chem. Phys. 63, 2810 (1975). G. Hager, L. E. Wilson, and S. G. Hadley, Chem. Phys. Lett. 27, 439 (1974).

4. C. Linton and Gene A. Capelle, Jour. Molec. Spectros. 66, 62 (1977).

5. L. H. Dubois and J. L. Gole, J. Chem. Phys. 66, 779 (1977).

6. A. W. Hanner and J. L. Gole, J. Chem. Phys. 73, 5025 (1977). G. J. Green and J. L. Gole, Chem. Phys. Lett. 69, 45 (1980).

7. G. J. Green and J. L. Gole, Chem. Phys. 46, 67 (1980).

8. J. L. Gole and S. A. Pace, J. Chem. Phys. 73, 836 (1980).

9. J. L. Gole and G. J. Green, Chem. Phys. 69, 357 (1982).

10. S. A. Pace and J. L. Gole unpublished.

11. Silicon was also vaporized from a high purity (Union Carbide) boran nitride crucible.

12. R. W. Field, B. G. Wicke, J. D. Simmons, and S. G. Tilford, J. Molec. Spectros. 44, 383 (1972).

13. H. Hotop, T. A. Patterson, and W. C. Lineberger, Phys. Rev. A8, 762 (1973).

14. The programs used in these calculations were written by Dr. Brian Wicke. See also R. N. Zare, J. Chem. Phys. 40, 1934 (1964).

15. J. L. Gole and R. N. Zare, J. Chem. Phys. 57, 5331 (1972). R. N. Zare, Ber. Bunsenges Physik. Chem. 78, 153 (1974).

16. J. L. Gole and C. L. Chalek, J. Chem. Phys. 65, 4384 (1976).

17. C. L. Chalek and J. L. Gole, Chem. Phys. 19, 59 (1977).

18. D. R. Preuss and J. L. Gole, J. Chem. Phys. 66, 880 (1977).

19. D. L. Hildenbrand, High Temp. Sci. 4, 244 (1972).

20. D. B. Stull and H. Prophet, JANAF Thermochemical Tables, 2nd ed., Natl. Stand. Ref. Data Series, Natl. Bur. Stand. 37 (1971).

21. R. Jones and J. L. Gole, Chem. Phys. 20, 311 (1977).

22. We determine $E_{int}(Si)$ from a statistical average of the $^3P_o(0cm^{-1})$, $^3P_1$ $(77.15cm^{-1})$, and $^3P_2$ $(223.31cm^{-1})$ components of the ground ^3P state.

23. P. J. Dagdigian, H. W. Cruse, and R. N. Zare, J. Chem. Phys. 62, 1824 (1973).

24. C. R. Dickson and R. N. Zare, Chem. Phys. 7, 361 (1975).

25. See discussions in references 7 and 18.

26. K. P. Huber and G. Herzberg, Constants of Diatomic Molecules, Van Nostrand-Reinhold Company, 1979.

27. J. Pliva, J. Molec. Spectros. 12, 360 (1964).

28. L. H. Dubois and J. L. Gole unpublished.

29. Reference 15 and D. M. Lindsay and J. L. Gole, J. Chem. Phys. 66, 3886 (1977); R. C. Oldenborg and J. L. Gole unpublished data.

30. See reference 23 and E. Murad, AFGL-TR-77-0235 Environmental Research Papers. No. 610, October 1977.

31. The N_2 or N_2^+ emission spectrum obtained under reaction conditions is compared to that for room temperature N_2 at low concentrations.

32. The authors are indebted to Stewart Novick for helpful discussions on the subject of increasing the signal-to-noise from electron gun sources.

33. P. Dehmer private communication.

34. R. Kay private communication.

35. Because of the extremely long radiative lifetime of the "$b^3\Pi$" state, it is possible that a small component of "$b^3\Pi$" molecules undergo collision before entering or leaving the viewing zone. See J. L. Gole, D. R. Preuss, and C. L. Chalek, J. Chem. Phys. 66, 548 (1977).

36. B. Meyer, J. J. Smith, and K. Spitzer, J. Chem. Phys. 53, 3616 (1970).

37. W. H. Smith and H. S. Liszt, J. Quant. Spectrosc. Radiative Transfer 12, 505 (1972).

38. For an indication of the viewing zone see J. B. West, R. S. Bradford, J. D. Eversole, and C. R. Jones, Rev. Sci. Instruments 46, 164 (1975); C. R. Jones and H. P. Broida, J. Chem. Phys. 60, 4369 (1974).

39. See for example A. Fontijn, "Kinetic Spectroscopy of Metal Atom/Oxidizer Chemiluminescent Reactions for Laser Applications", Aerochem Report TP-388; W. Felder and A. Fontijn, J. Chem. Phys. 69, 1112 (1978). M. J. Linevsky and R. A. Carabetta, "Chemical Laser Potential of Selected Group IV-A Metal Oxides", AFWF-TR-77-121.

40. P. M. Swearengen, S. J. Davis, and T. M. Niemczyk, Chem. Phys. Letters 55, 274 (1978). See also references to previous work in Table 1 of this article.

Table 1

Measured SiO Bandhead Positions and Vibrational Assignments

$b^3\Pi - X^1\Sigma^+$

bandhead assignment (v',v")[a]	bandhead origin λ_{air} (Å)	bandhead origin ν_{vacuum} (cm^{-1})	relative intensity[g]
(2,0)	2791.2	35816	---
(3,1)	2811.6	35556	45.9
(4,2)	2832.6	35293	54.0
(5,3)	2853.7	35032	35.6
(1,0)[b,c]	2869.2	34843	55.2
(2,1)[b,c]	2889.8	34594	44.6
(3,2)[b]	2911.2	34340	25.0
(4,3)	2932.4	34092	12.6
(0,0)[b,c]	2953.7	33846	100
(1,1)	2973.8	33617	33.6
(2,2)	2995.2	33377	---
[(4,4)][d]	3038.9	32897	---
(0,1)[b,c]	3065.2	32615	90.1
(1,2)[b,c]	3085.8	32397	82.0
(2,3)[b,c]	3107.3	32172	59.8
(3,4)[b]	3129.2	31948	27.2
(4,5)	3151.3	31724	12.1
(0,2)[b,c]	3184.0	31398	18.8
(1,3)[b,c]	3205.2	31190	24.9
(2,4)[b,c]	3226.9	30981	34.4
(3,5)[b]	3249.2	30768	22.5
(4,6)[b]	3272.0	30554	25.1
(5,7)[b]	3295.8	30333	17.4
(0,3)[b]	3310.9	30195	12.6
(6,8)[b]	3320.2	30110	14.0
(1,4)[b,c]	3332.5	29999	11.5
(2,5)[b]	3354.8	29799	17.6
(3,6)[b]	3377.6	29598	11.4
(4,7)[b]	3401.0	29395	14.1
(5,8)[b]	3425.3	29186	16.3
(6,9)[b]	3450.5	28973	18.3

Measured SiO Bandhead Positions and Vibrational Assignments

$b^3\Pi - X^1\Sigma^+$ (continued)

bandhead assignment (v',v'') [a]	bandhead origin λ_{air} (Å)	bandhead origin ν_{vacuum} (cm^{-1})	relative intensity [g]
(7,10) [b]	3475.9	28761	13.4
(9,12) [e]	3530.6	28316	(6.4)
(4,8) [b]	3538.9	28249	6.4
(5,9) [b]	3564.1	28050	6.8
(6,10) [b]	3589.6	27850	9.5
(7,11) [b]	3616.1	27646	11.0
(8,12) [b]	3643.6	27438	(5.6)
(9,13)	3671.9	27226	5.2
(10,14)	3699.4	27024	2.9
(5,10)	3712.6	26928	2.9
(6,11)	3739.5	26734	3.4
(7,12)	3765.9	26547	4.1
(8,13) [f]	3792.2	26362	4.6
(10,15)	3849.7	25969	3.3
[(11,16)] [d]	3883.7	25741	2.0
[(7,13)] [d]	3926.8	25459	2.2
[(8,14)] [d]	3952.8	25291	2.7

a. Bandhead corresponding to $^3\Pi_1$ component

b. Previously observed by Linton and Capelle reference 4

c. Previously observed by Hager et al. reference 3

d. Weak feature - wavelength approximate

e. (8,11) band under (0,4) band of $a^3\Sigma^+ - X^1\Sigma^+$ band system

f. (9,14) band under (0,6) band of $a^3\Sigma^+ - X^1\Sigma^+$ band system

g. Corrected for phototube response

Table 2
Nonzero Matrix Elements of Spin-Orbit Operator Coupling
Low-Lying States of SiO (cm^{-1})

$\langle A^1\Pi_1, |H_{So}| a^3\Sigma_1^{+\pm}, v' \rangle = 1/4a^a \langle v|v' \rangle = 43 \langle v|v' \rangle$

$\langle A^1\Pi_1^{\pm}, v|H_{So}|b^3\Pi_1^{\pm}, v' \rangle = a_z^b \langle v|v' \rangle = 146 \langle v|v' \rangle$

$\langle E^1\Sigma_o^+, v|H_{So}|b^3\Pi_o^{\pm}, v' \rangle = -1/4(2)^{1/2}a \langle v|v' \rangle = -61\langle v|v' \rangle$

$\langle b^3\Pi_1^{\pm}, v|H_{So}|a^3\Sigma_1^{+\pm}, v' \rangle = 1/4a\langle v|v' \rangle = 43\langle v|v' \rangle$

$\langle e^3\Sigma_1^{-\pm}, v|H_{So}|b^3\Pi_1^{+\pm}, v' \rangle = -1/4a \langle v|v' \rangle = -43\langle v|v' \rangle$

$\langle e^3\Sigma_1^-, v|H_{So}|A^1\Pi_1, v' \rangle = -1/4a \langle v|v' \rangle = -43\langle v|v' \rangle$

$\langle {}^3\Pi_2^{\pm}, v|H_{So}|{}^3\Pi_2^{\pm}, v' \rangle = A({}^3\Pi) = 1/2a_z \delta_{v,v'} = 73\delta_{v,v'}$

$\langle {}^3\Pi_o^{\pm}, v|H_{So}|{}^3\Pi_o^{\pm}, v' \rangle = -A({}^3\Pi) = -1/2a_z \delta_{v,v'} = -73\delta_{v,v'}$

---

a. a defined in text.

b. a_z defined in text.

Table 3

Observed Bandheads for the

$D\text{-}X\,^3\Delta$ Bandsystem of TiO[a]

Observed Band Head (v',v")	Wavelength (Å)
(2,1)	2955
(1,0)[b]	3049
(0,0)[b]	3148
(0,1)[b]	3250
(0,2)	3359
(0,3)	3473
(0,4)	3595

a. L.H. Dubois and J.L. Gole, J. Chem. Phys. 66, 779 (1977).

b. C.M. Pathak and H.B. Palmer, J. Mol. Spectrosc. 33, 137 (1970).

Table 4

Energy Balance Discrepancies in $M+N_2O$ Reactions

Reaction	$E_{Available}$	Measured MO Excitation	$E_{int}(MO)$ (cm^{-1})	ΔE[a]
$Sc(^2D)+N_2O$[b]	45856 cm^{-1}[c]	Short Wavelength Limit ($C^2\Pi-X^2\Sigma^+$) (3000Å)	33324 cm^{-1}	12532 cm^{-1}
$Y(^2D)+N_2O$[b]	48154 cm^{-1}[c]	Short Wavelength Limit ($C^2\Pi-X^2\Sigma^+$) (3000Å)	33324 cm^{-1}	14830 cm^{-1}
$La(^2D)+N_2O$[d]	55862 cm^{-1}[c]	LaO*,$D^2\Sigma^+$,v'=17[e]	39400 cm^{-1}	16462 cm^{-1}
$Ba(^1S)+N_2O$[f]	33652 cm^{-1}	Short Wavelength Limit (4000Å)	24993 cm^{-1}	8659 cm^{-1}
$Ca(^3P)+N_2O$[g,h]	34792 cm^{-1}	Short Wavelength Limit (3850Å)	25967 cm^{-1}	9095 cm^{-1}
$Sr(^3P)+N_2O$[h]	37553 cm^{-1}	Short Wavelength Limit (3700Å)	27019 cm^{-1}	10534 cm^{-1}

a. $E_{Available} - E_{int}(MO)$

b. Reference 17.

c. $D_o^o(MO) + E_{int}(M) + E_{int}(N_2O) + E_T^i - D(N-NO)$. See text for definitions.

d. Reference 16.

e. J. L. Gole unpublished data.

f. Data from C. D. Jonah, R. N. Zare, and Ch. Ottinger, J. Chem. Phys. 56, 263(1972).

g. Data from J. A. Irwin and P. J. Dagdigian, J. Chem. Phys. 74, 6178(1981).

h. Data from B. E. Wilcomb and P. J. Dagdigian, J. Chem. Phys. 69, 1779(1978). See also P. J. Dagdigian, Chem. Phys. Lett. 55, 239(1978).

Figure Captions

Figure 1: (a) Chemiluminescent spectrum in the region 2850-3600Å resulting from the reaction $Si + N_2O \rightarrow SiO^* + N_2$ recorded under single collision conditions. The spectrum in this region corresponds to the SiO "$b^3\Pi$" - $X^1\Sigma^+$ band system. The bandheads are designated (v',v"). Spectral resolution is 10Å. (b) Higher resolution scan of (0,0) and (0,1) bands for SiO"$b^3\Pi$" - $X^1\Sigma^+$ system showing $^3\Pi_1$ and $^3\Pi_0$ component emission and dominant intensity associated with $^3\Pi_1$ component. Spectral resolution is 0.5Å. See text for discussion.

Figure 2: Chemiluminescent spectrum in the region 3550-4200Å resulting from the reaction $Si + N_2O \rightarrow SiO^* + N_2$ recorded under single collision conditions. Emission from high vibrational levels of SiO "$b^3\Pi$" and the v' = 0 level of SiO "$a^3\Sigma^+$" is monitored. The bandheads are designated (v',v"). Spectral resolution is 10Å. See text for discussion.

Figure 3: Chemiluminescent spectrum in the region 2350-2950Å resulting from the reaction $Si + N_2O \rightarrow SiO^* + N_2$ recorded under single collision conditions. The high energy end of the SiO "$b^3\Pi$ - $X^1\Sigma^+$ band system extends into the SiO $A^1\Pi$ - $X^1\Sigma^+$ emission system. The bandheads in both systems are designated (v',v"). Spectral resolution is 15Å. See text for discussion.

Figure 4: Chemiluminescent spectrum in the region ~2150-2550Å resulting from the reaction $Si + N_2O \rightarrow SiO^* + N_2$ recorded under single collision conditions. The observed spectrum corresponds to the SiO $A^1\Pi$ - $X^1\Sigma^+$ band system. Bandheads are designated (v',v"). Spectral resolution is 20Å. See text for discussion.

Figure 5: Chemiluminescent spectrum in the region 2500-7500Å for the reaction $Ti + N_2O \rightarrow TiO^* + N_2$ taken under single collision conditions. The unresolved features correspond in large part to emission from the $B^3\Pi$ and $C^3\Delta$ states of TiO. Emission from the TiO D state has been resolved in this and separate scans and bands identified (Table 2). Bandheads for the D - $X^3\Delta$ system are designated (v',v"). Spectral resolution is 10Å. See text for discussion.

Figure 6: Potential curves (RKR) for the ground and select low-lying states of SiO generated from spectral data given in reference 2.

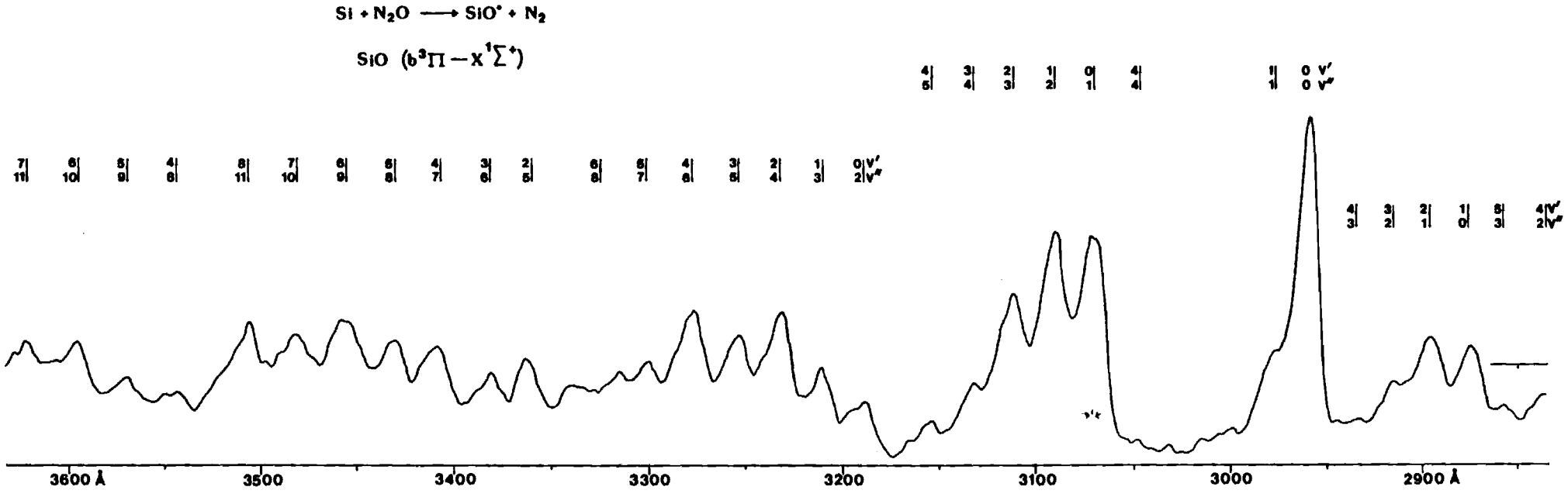
Si + N2O ⟶ SiO* + N2
SiO (b3Π − X1Σ+)
3600 Å
3500
3400
3300
3200
3100
3000
2900 Å

Figure 1(a)

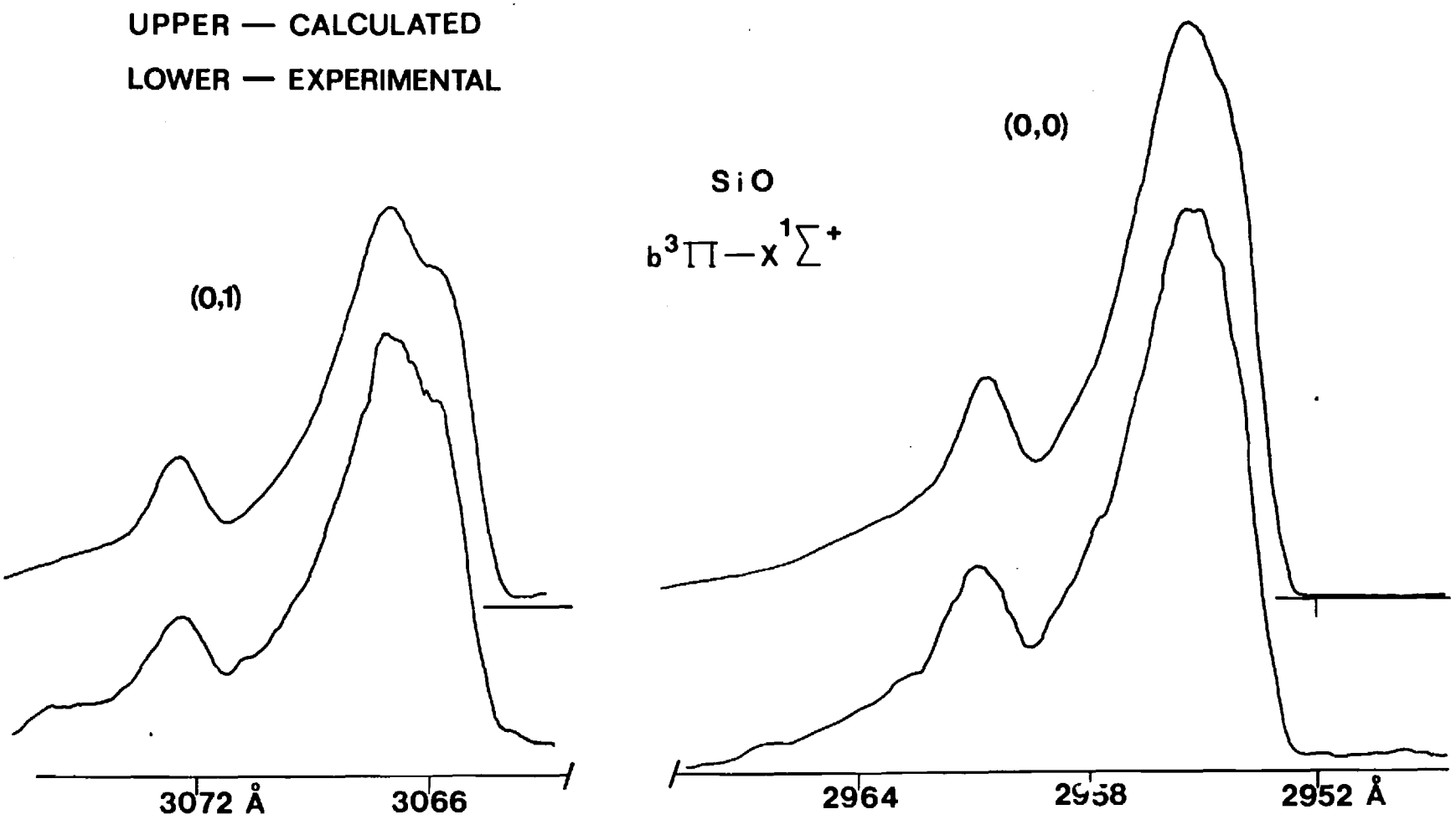
UPPER — CALCULATED
LOWER — EXPERIMENTAL
(0,1)
(0,0)
SiO
$b^3\Pi - X^1\Sigma^+$
3072 Å
3066
2964
2958
2952 Å

Figure 1(b)

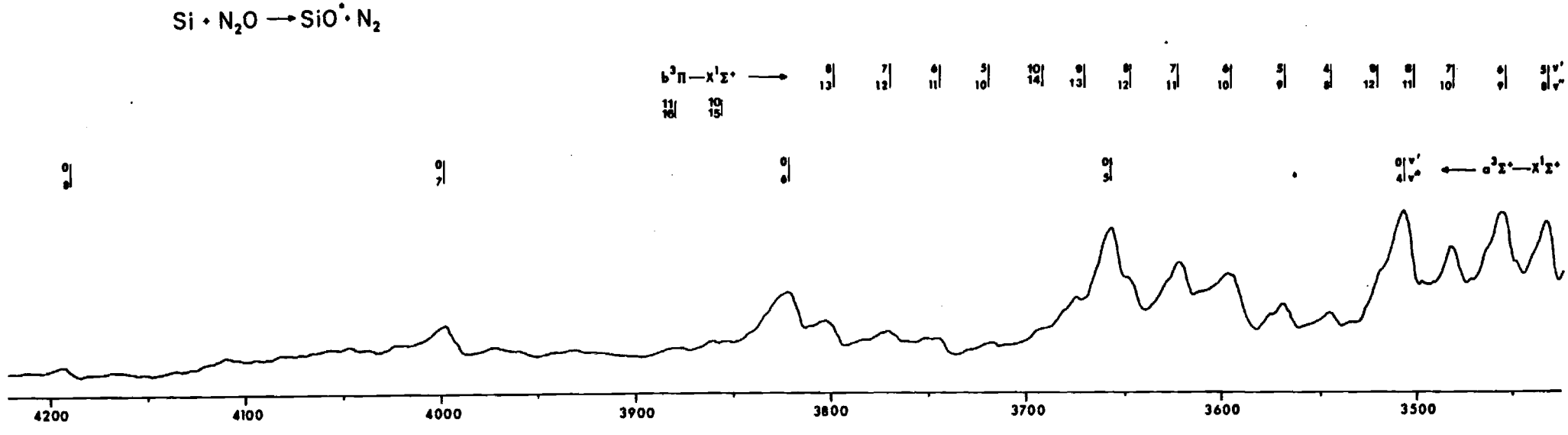
Si + N2O → SiO* + N2
b3Π—X1Σ+ →
a3Σ+—X1Σ+
4200
4100
4000
3900
3800
3700
3600
3500

Figure 2

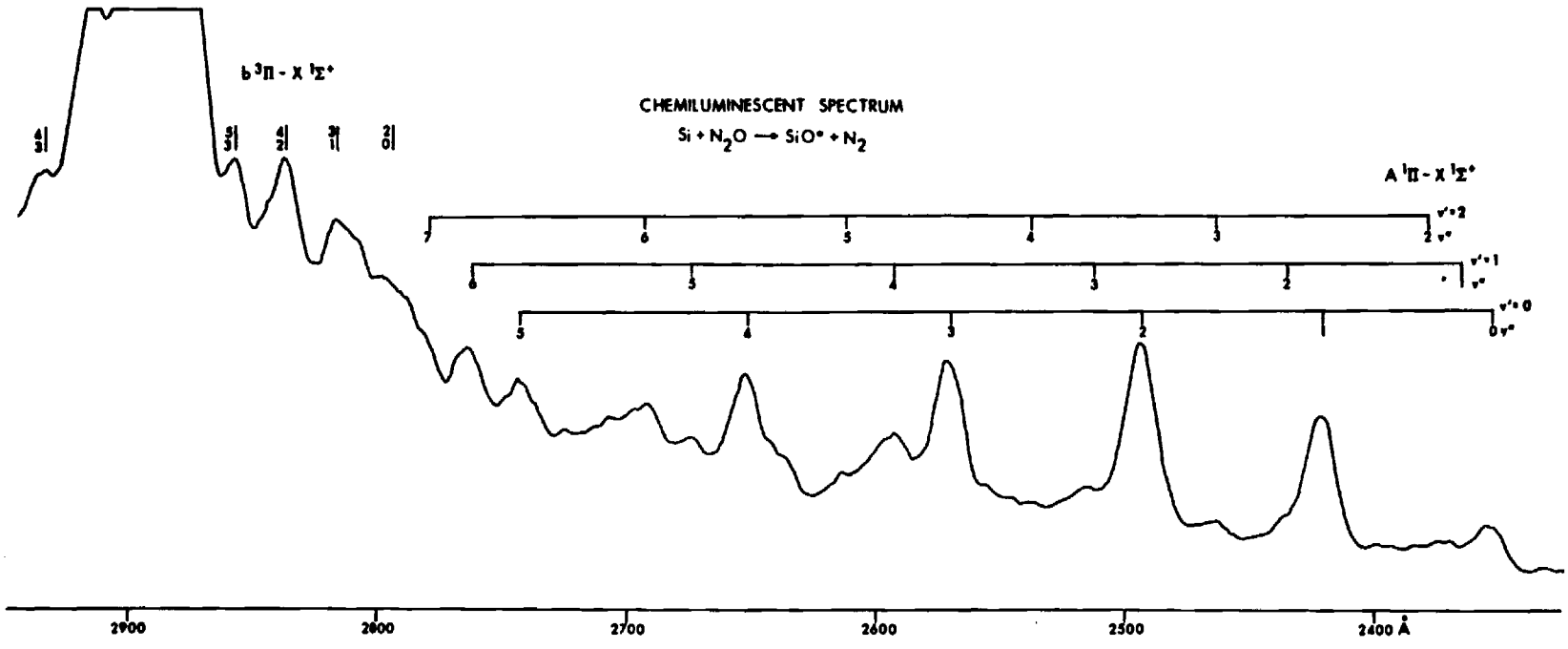
CHEMILUMINESCENT SPECTRUM
$Si + N_2O \rightarrow SiO^* + N_2$
$b\,^3\Pi - X\,^1\Sigma^+$
$A\,^1\Pi - X\,^1\Sigma^+$
v'=2
v'=1
v'=0
v"
2900
2800
2700
2600
2500
2400 Å

Figure 3

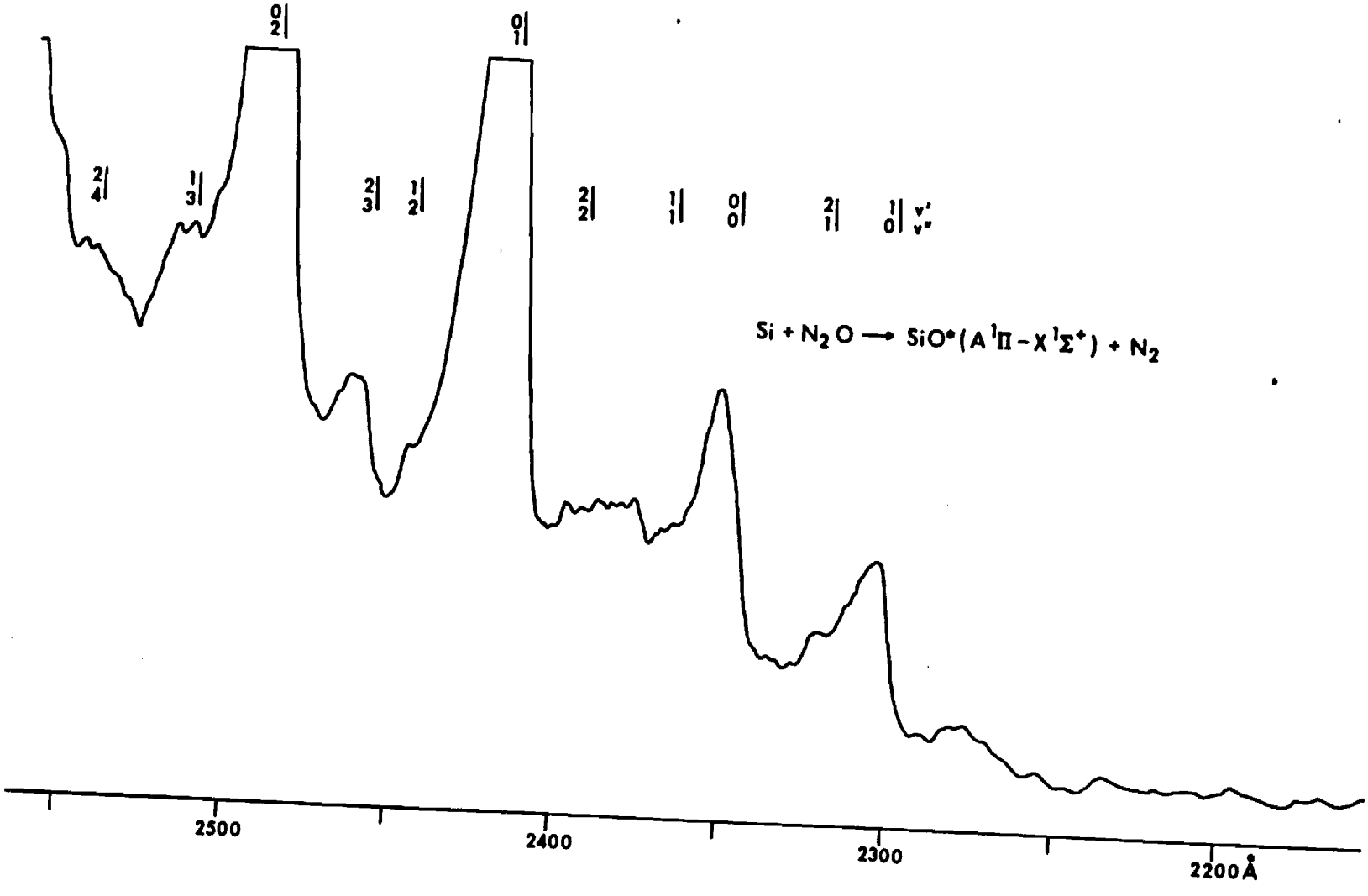
0 2
0 1
2 4
1 3
2 3
1 2
2 2
1 1
0 0
2 1
1 0
v'
v"
Si + N2O → SiO*(A 1Π - X 1Σ+) + N2
2500
2400
2300
2200Å

Figure 4

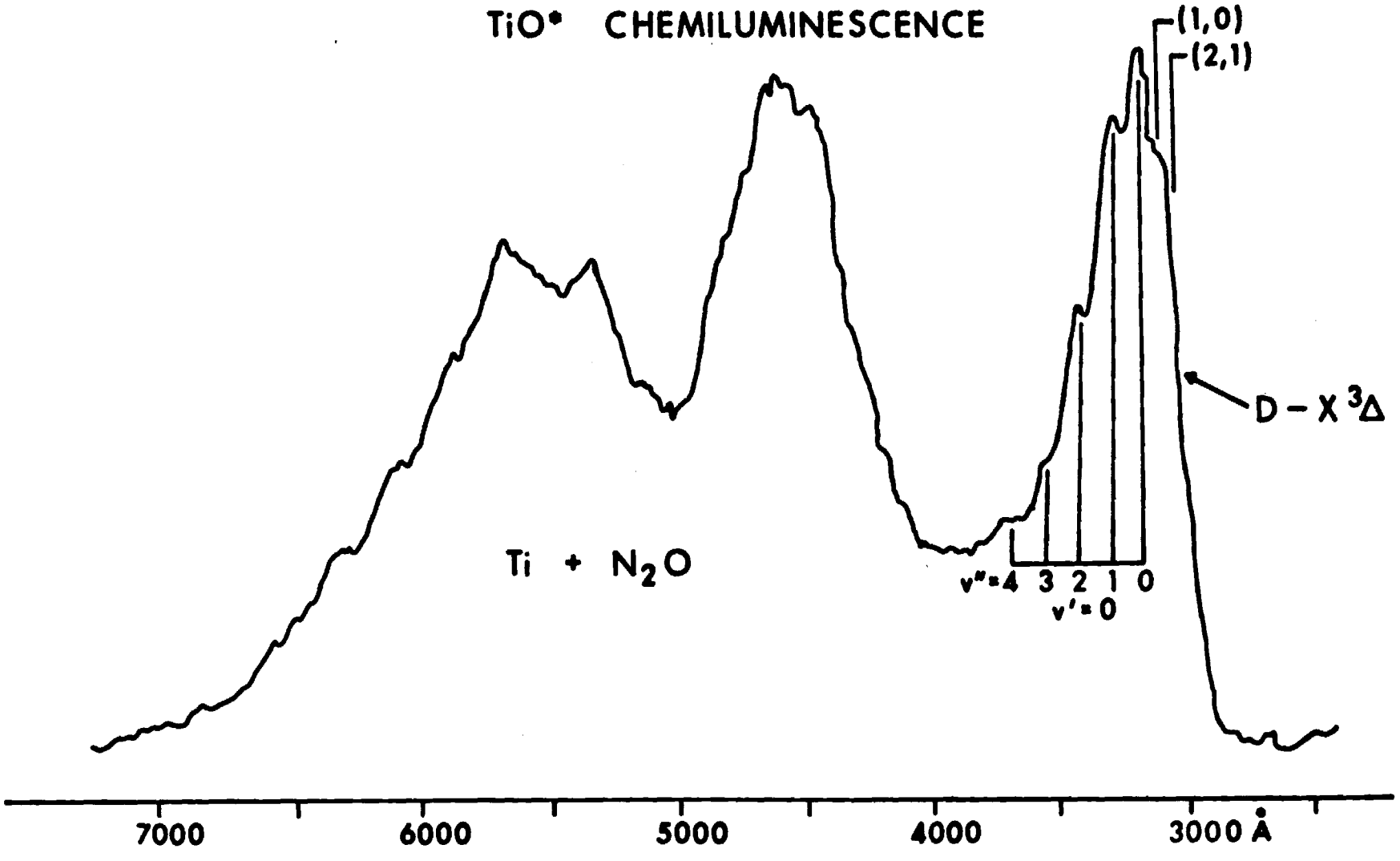
TiO* CHEMILUMINESCENCE
(1,0)
(2,1)
D – X ³Δ
Ti + N₂O
v"=4 3 2 1 0
v'=0
7000
6000
5000
4000
3000 Å

Figure 5

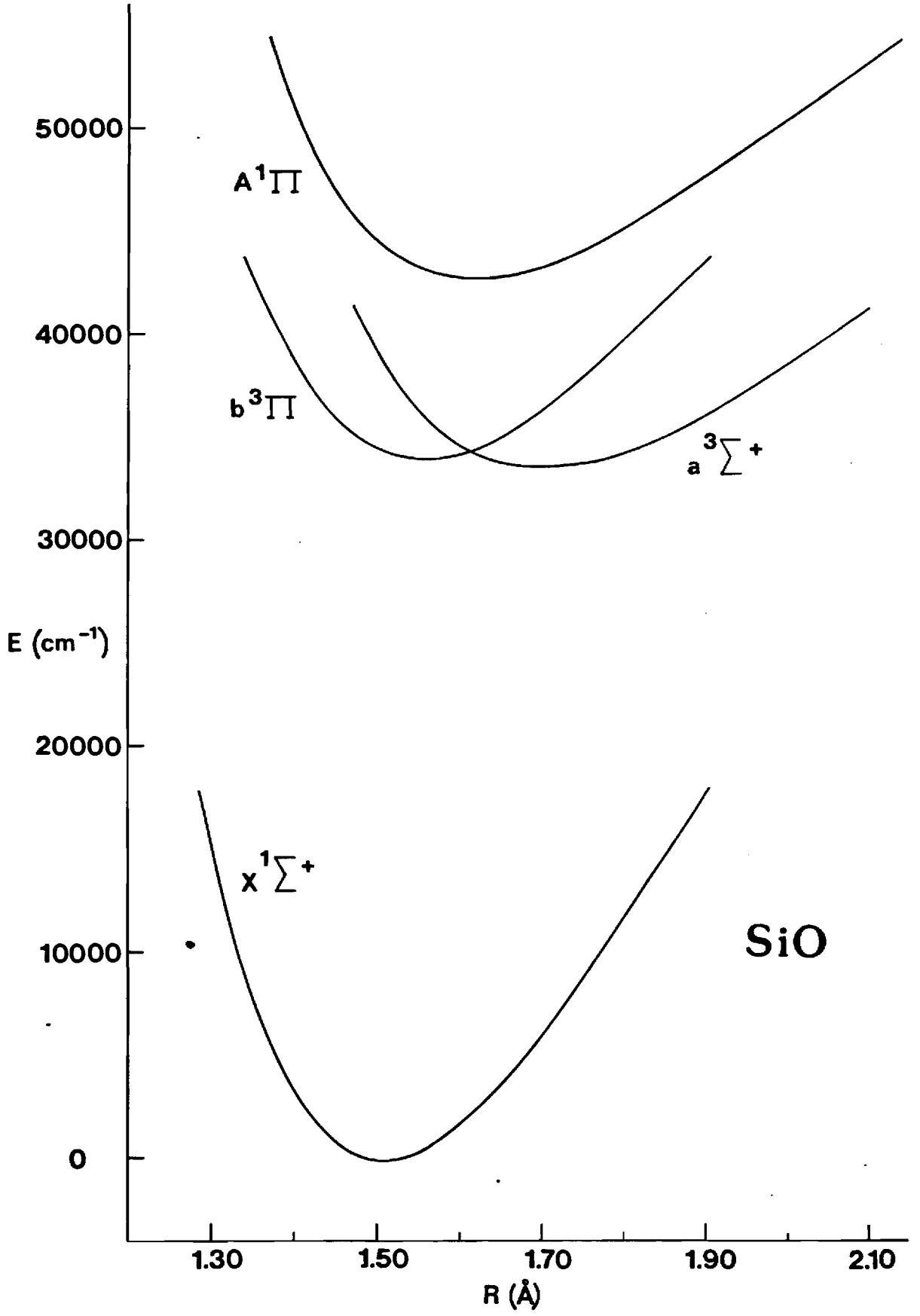
50000
40000
30000
20000
10000
0
E (cm⁻¹)
A¹Π
b³Π
a³Σ+
X¹Σ+
SiO
1.30
1.50
1.70
1.90
2.10
R (Å)

Figure 6

References

1. J. L. Gole, "The Characterization of High Temperature Vapor Phase Species and Vapor-Solid Interactions of Import to Combustion and Gasification Processes in the Energy Technologies" Annual Topical Report 1, October 1, 1981-October 1, 1982, Morgantown Energy Technology Center, DOE.

2. See for example J. L. Gole "The Characterization of High Temperature Vapors of Import to Combustion and Gasification Processes in the Energy Technologies," Proceedings of the Morgantown Energy Technology Center Meeting on High Temperature, High Pressure Particulate and Alkali Control in Coal Combustion Process Streams - Morgantown, West Virginia, 1981.

THE CHARACTERIZATION OF HIGH TEMPERATURE VAPOR PHASE SPECIES AND VAPOR-SOLID INTERACTIONS OF IMPORT TO COMBUSTION AND GASIFICATION PROCESSES IN THE ENERGY TECHNOLOGIES

Quarterly Technical Progress Report No. 6
for the Period 10 January 1983 to 14 April 1983

James L. Gole

School of Chemistry
Georgia Institute of Technology
Atlanta, Georgia 30332

14 April 1983

PREPARED FOR THE UNITED STATES
DEPARTMENT OF ENERGY
Morgantown Energy Technology Center
Morgantown, West Virginia

Under Contract No. DE-AC21-81MC16537

NOTICE

FOREWARD

This report summarizes technical progress accomplished during the sixth quarterly reporting period of a two-year study being conducted for the U. S. Department of Energy (DOE). This work period was 10 January 1983 to 14 April 1983. Work was accomplished under the direction of James L. Gole. Graduate and undergraduate students who have contributed to the technical progress and to this document are Mr. W. H. Crumley, Mr. Joerg Pfeifer and Mr. David Semmes. Mr. Ken Williams, Supervisor of the Machine Shop has provided assistance in design and construction of oven components.

Abstract

This report summarizes work completed during the sixth quarter of a two-year study focused primarily on the determination of bond energies and spectra for the alkali hydroxides and oxides, the study of pronounced particulate matter formed in alkali oxidation, and the characterization of sodium cluster and sodium surface oxidation with various oxidants.

We have developed and are continuing to improve experimental configurations for generating intense, stable, and long-lasting chemiluminescent emission from the alkali hydroxides NaOH and KOH and the alkali oxides NaO and KO. The first electronic emission spectra for these compounds have been generated and are being studied in our laboratory. Commensurate with this effort has been the study of extensive particulate formation which appears to be pathelogical to the alkali hydroxide and oxide systems. This particulate matter, formed in an extremely efficient manner in the oxidation process, has been studied using "low temperature" mass spectrometry, EPR spectrometry, and, attempts have been made to observe a Raman spectrum. The possibility of obtaining an X-ray powder pattern is under consideration. The major emphasis in our sodium cluster oxidation studies over the past three month period has been the development of devices whereby the spectra obtained from the oxidation process can be relaxed to the point where ready analysis of spectral features is facilitated. In addition studies of silicon monoxide formation which complement previous studies under DOE sponsorship were carried out during this period. From these studies the bond energy of SiO was confirmed from a purely spectroscopic measurement thus complementing and confirming the mass spectrometric determinations.

TABLE OF CONTENTS

LIST OF FIGURES

LIST OF TABLES

Introduction

Background

Low tolerance levels for certain species in process streams impose stronger requirements for reliable thermodynamic and kinetic data in order to predict low level species concentrations. In addition evidence now indicates that serious concern must be focused on whether or not these systems are best represented via equilibrium or non-equilibrium models. Unfortunately, the necessary thermodynamic and kinetic data required to perform accurate calculations of species concentrations is not available for many such gas stream species. Of equal importance is the fact that little detailed information is available which will allow the ready direct monitoring of these species in the process stream. In addition, many of the details of the mechanisms for process stream product formation, including the formation and growth of particulates, are yet unknown while many postulated routes to product formation are yet only meagerly tested. This arises primarily because many of the molecular entities for which data are needed correspond to elusive and very reactive radicals or high temperature molecules. Our laboratory has been concerned with the characterization of several of the important molecules and possible processes thought to be present in the inherently high temperature environment of the process stream.

We have applied chemiluminescent and laser fluorescent techniques to the determination of bond energies, spectroscopic constants, and the evaluation of those spectral regions which will be most useful for the kinetic parameterization and monitoring of the species of interest. In addition, through the study of certain selected processes, we are attempting to shed some light on the feasibility of postulated interactions in the process stream,

some of which include the surprisingly efficient gas phase formation of particulate matter. Finally, in the course of these studies, we are documenting the presence of ultrafast energy transfer, both intra- and intermolecular, as it pertains to the nature of heat flow in high temperature systems and, in particular, to those molecules of interest in process streams. It should be noted that the attainment and evaluation of reliable spectroscopic data leads to the determination of important molecular constants which can be used for the statistical mechanical evaluation of heat capacities, entropies and free energies, all of which are important to the understanding of energy related combustion and gasification environments.

Objectives

The general objectives of the present research effort which represents a continuation of previous efforts under DOE sponsorship are: (a) to characterize alkali monoxide chemiluminescent spectra, specifically spectra for NaO and KO which can be used in kinetic studies of the behavior of these species and for their direct monitoring in process streams and to determine lower bounds for the NaO and KO bond energies; (b) to characterize pronounced particular formation in gas phase alkali oxidation environments; (c) to further characterize the KOH chemiluminescent emission spectrum at a resolution and under conditions which will allow the determination of currently unavailable molecular constants for this molecule and an improved measure of the K-OH bond dissociation energy; (d) to carry out and characterize the oxidation of sodium clusters with various oxidants including SO_2; (e) to attempt to prepare clean sodium and sodium contaminated surfaces whose oxidation with various constituents including SO_2 will be characterized; (f) to further characterize the NaOH chemiluminescent emission spectrum in order to obtain an improved measure of the Na-OH bond energy; (g) to determine the SiO bond

energy from the chemiluminescent process Si + NO_2 → SiO* + NO. Specific tasks of interest in the current report are indicated below.

Characterization of Alkali Oxide Emission Spectra and Gas Phase Particulate Formation in Alkali Oxidation Environments

The object of a portion of this task is to observe and characterize chemiluminescence from NaO and KO using the reactions of sodium or potassium atoms with primarily N_2O and O_3. These studies have yielded the first electronic emission spectra for NaO and KO resulting from the low pressure "single collision" reaction of sodium and potassium atoms with N_2O. Our efforts in this quarter have focused primarily on the stepwise extension of these single collision studies to higher pressures where relaxation effects lead to an improvement in spectral resolution, facilitating the evaluation of molecular constants for NaO and KO and furnishing reliable spectral regions which can be used to probe for these elusive oxides. Several experimental devices (see also outline in Appendix A) have now been developed which, at least for sodium oxide, overcome numerous factors associated with the attainment of NaO chemiluminescence across a wide pressure range. Further, preliminary values for the bond dissociation energies of NaO and KO(D_0^o(NaO) = 70±5, D_0^o(KO) = 75±5 kcal/mole) are corroborated through the combination of single and multiple collision studies.

These alkali oxidation systems, involving formation of the alkali oxides, are found to exhibit a pronounced virtually gas phase homogeneous particulate formation (see Annual Progress Report 1[1]) which is not observed in any other oxidation system. A major focus of our research effort involves an attempt to characterize the polymeric alkali-oxygen-nitrogen species which constitute the framework of the observed particulate matter employing mass spectroscopy, EPR spectroscopy, Raman Spectroscopy, and X-ray powder spectra. We believe that the extremely efficient formation of these polymers can provide a seed

for particulate formation in process streams.

Sodium Cluster Oxidation

The object of this task is to evaluate the nature of sodium oxidation in the intermediate region between the gas and surface phase. The products of sodium cluster oxidation are being characterized through direct observation of the chemiluminescent emission for highly exothermic processes, through a newly developed electron impact excitation technique, and through mass spectrometric sampling of the oxidation region. Current efforts focus on the desire to obtain relaxed (rovibronic) chemiluminescent emission spectra for these systems in order to facilitate spectral resolution. Thusfar both the halogen and SO_2 oxidation of sodium clusters has been under study.

Alkali Hydroxide Emission Spectra

Electronic emission spectra for the alkali hydroxides have been obtained over a wide pressure range. The reactions of sodium and potassium dimers with hydrogen peroxide are being used to excite chemiluminescence from NaOH and KOH. The objective of this task is to determine stringent lower bounds for the K-OH and Na-OH bond energies and molecular constants for several levels of the ground electronic state of K-OH. KOH emission has been observed at low pressures under "single collision" conditions, at intermediate pressures where the effects of collisional relaxation are apparent ("multiple collision" conditions) and at higher pressures in a "diffusion flame" device, the combination of these studies leading to the first evaluation of a stringent lower bound for the K-OH bond energy[2] using a direct optical measurement. Continued improvements in the "diffusion flame" apparatus have now led to long term flame stability. Because flame instabilities tend to "washout" spectral features, stabilization was a major task before us. We are now attempting

to solve a major aspect of this problem by recording the entire KOH emission spectrum on film and in 200Å sections using an optical multichannel analyzer. These efforts will be used to obtain a more stringent lower bound for the KOH bond energy and to obtain higher resolution spectra to evaluate molecular constants for several ground state levels. The data obtained thusfar for NaOH and KOH when correlated with that of other workers (e.g. Hastie-N.B.S.) demonstrates that a massive revision of the data in the Janaf tables for the alkali hydroxides will be necessary.

Silicon Monoxide Emission Spectra

The focus of this research effort has been to supplement previous studies whose object has been to determine molecular constants for the SiO molecule and, more importantly, to determine the SiO bond energy using a direct spectroscopic approach. In studying the reaction of silicon atoms with NO_2, we have determined an SiO bond energy in excellent agreement with mass spectroscopy.

Technical Progress-Plans for Future Study

Alkali Oxide Emission Spectra

Previously, we have noted the design of a system used with reasonable success to characterize the alkali oxide emission spectra for sodium and potassium oxide produced from Na,K + N_2O,O_3 reactions under multiple collision conditions (see Annual Topical Report 1[1]). With this system, we were able to produce reasonably resolved alkali oxide emission spectra for NaO[1]; however, there were still questions regarding long term alkali and, in the case of ozone, oxidant source stability. A further modification of the apparatus used for multiple collision studies which greatly improved long-term stability in the intermediate multiple collision regime was reported in Quarterly Report 5. We have now further improved systems used for the studies of the alkali metal

metatheses overcoming numerous problems associated with the attainment of NaO chemiluminescence across a wide pressure range. We have focused primarily on the study of the chemiluminescent emission from the processes (see reprint in Appendix A)

$$Na + N_2O \rightarrow NaO^* + N_2 \qquad (1)$$

and

$$Na + N_2O + X \rightarrow NaO^* + N_2 + X \qquad (2)$$

where Eq (1) denotes that the Na-N_2O reaction has been studied under low pressure single collision conditions. Temperature dependence studies indicate that the Na-N_2O reaction is characterized by a substantial activation energy ($\geq$15 kcal/mole) whereas the Na-O_3 reaction proceeds more rapidly, having a much smaller barrier to product formation. Eq (2) represents the extension of the single collision studies to the multiple collision pressure regime where X = N_2O, Ar, CO, and N_2. The second group of experiments were carried out in order to relax the internal excitation characteristic of the electronic spectrum obtained under single collision conditions. Here, a stream of sodium atoms was reacted with N_2O at $P_{Total}(N_2O)$=50-150 μ, using the configuration described in Quarterly Progress Report 5, or sodium atoms entrained in argon (P_{Ar} ~850-1200μ), N_2(P_{N_2} ~950-1500μ), or CO(P_{CO} $\approx$650-850μ) were oxidized with a concentric flow of N_2O using the device depicted in Figure 1(a). Several problems discussed in part in the enclosed preprint were overcome to carry out these studies. Under multiple collision conditions, for a given sodium beam flux, the alkali oxide emission spectrum was obtained over a very narrow range of oxidant and carrier gas pressure. This, in concert with previous difficulties (Quarterly Report 5) encountered in studying these systems, probably accounts for the inability of previous workers to observe the NaO emission

spectrum. The enclosed preprint demonstrates that there appears to be an outstanding correlation between the results of the current studies and the detailed quantum chemical calculations on the alkali oxides carried out at Cal Tech by Goddard and coworkers, however, an alternate interpretation which we will discuss below is also possible.

A schematic of the apparatus used to produce stable operating conditions for the oxidation of sodium atoms with N_2O (Eq (2)) under multiple collision conditions is shown in Figure 1(a). This oven system incorporates many of the previous improvements made to study the Na-N_2O metathesis in the intermediate pressure range (Figure 1(b)). We again used a modified double oven design where alkali metal heated in a large reservoir region passes into an independently heated and more confined region and then through an effusive or near effusive orifice. In order to study the Na-N_2O system for P_{Total} (N_2O)~50-150μ we introduced oxidant via a nozzle offset and perpendicular to the metal flow. For the higher pressure studies, the effusing sodium metal was entrained in Ar, N_2, or CO as depicted in Figure 1(a) producing, under carefully adjusted conditions, a stable intense alkali (sodium) flux at notably higher pressures. The alkali-entrainment gas mixture is oxidized by a flow of N_2O introduced concentrically from a ring injector system of a considerably more open design than used previously. While particulate formation does ensue, the open design, operated with care, allows sufficient run times for the study of NaO* produced in the Na-N_2O metathesis.

Given long run times, there is yet another problem associated with the higher alkali metal reactant concentrations characteristic of the multiple collision system. The transition moments associated with alkali metal excited electronic states are among the largest known. Therefore the collisional excitation of alkali dimer electronic emission systems can provide a

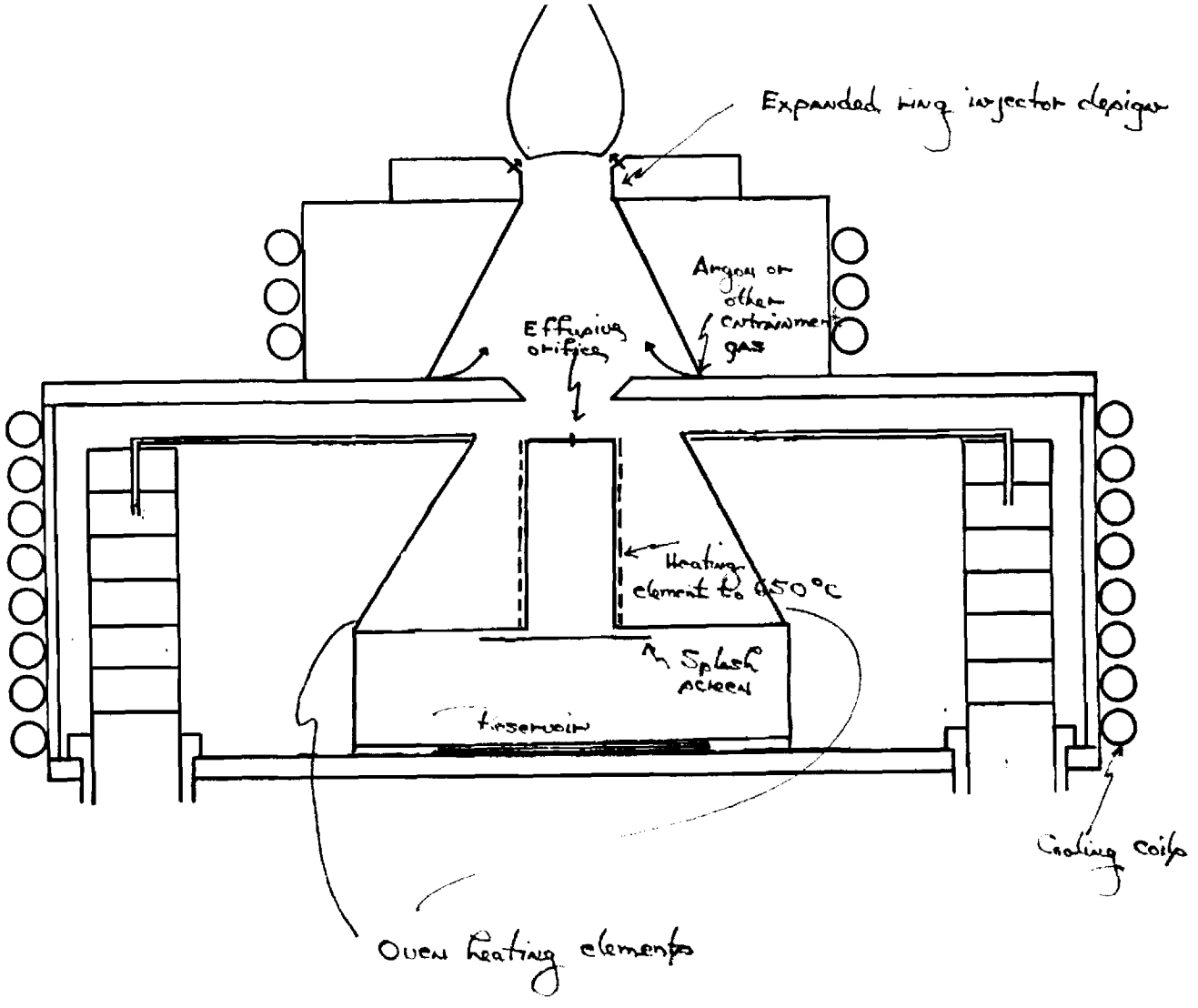
Expanded ring injector design
Argon or other containment gas
Effusive orifice
Heating element to 650°C
Splash screen
Reservoir
Cooling coils
Oven heating elements

Figure 1(a)

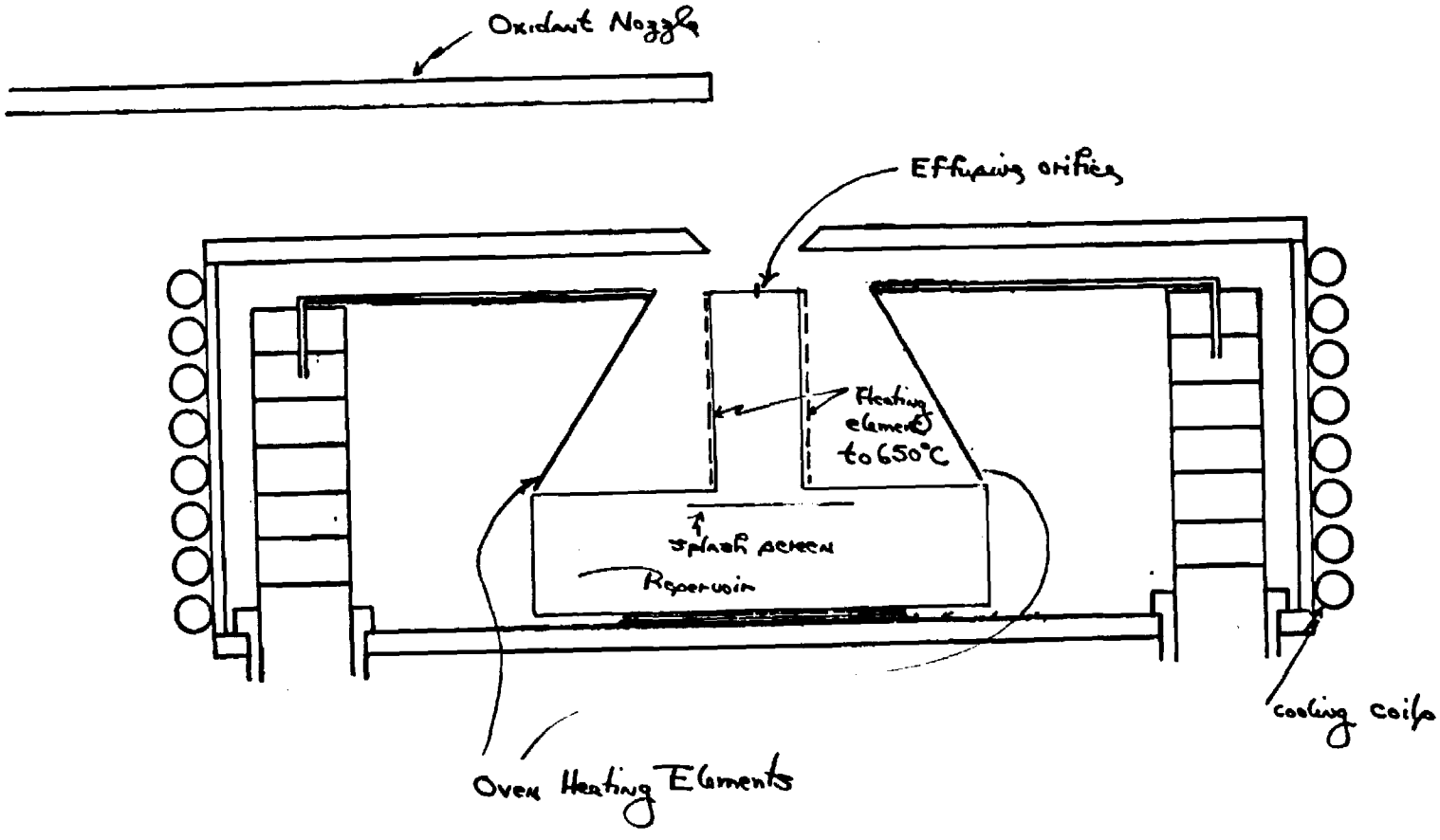
Oxidant Nozzle
Effusing orifice
Heating element to 650°C
splash screen
Reservoir
cooling coils
Oven Heating Elements

Figure 1(b)

Figure Caption:

NaO* $A^2\Sigma^+ \rightarrow X^2\pi$ Chemiluminescent Emission Spectra for the processes (a) Na + $N_2O(P_{N_2O} \simeq 125\mu)$ → NaO* + N_2, (b) Na + $N_2O(P_{N_2O} \simeq 75\mu)$ + $Ar(P_{Ar} \sim 950\mu)$ → NaO* + N_2 + Ar, (c) Na + $N_2O(P_{N_2O} \simeq 50\mu)$ + $CO(P_{CO} \simeq 850\mu)$ → NaO* + N_2 + CO, (d) Na + $N_2O(P_{N_2O} \simeq 75\mu)$ + $N_2(P_{N_2} \simeq 1100\mu)$ → NaO* + N_2, and (inset) single collision chemiluminescent spectrum for the metathesis Na + $N_2O(P_{N_2O} \simeq 5\times10^{-5}$ torr) → NaO* + N_2. Spectral resolution for (a) through (d) is 1Å while the single collision spectrum was obtained at 5Å resolution. The dashed region outlined at the longest wavelengths in the single collision spectrum indicates a component of blackbody radiation.

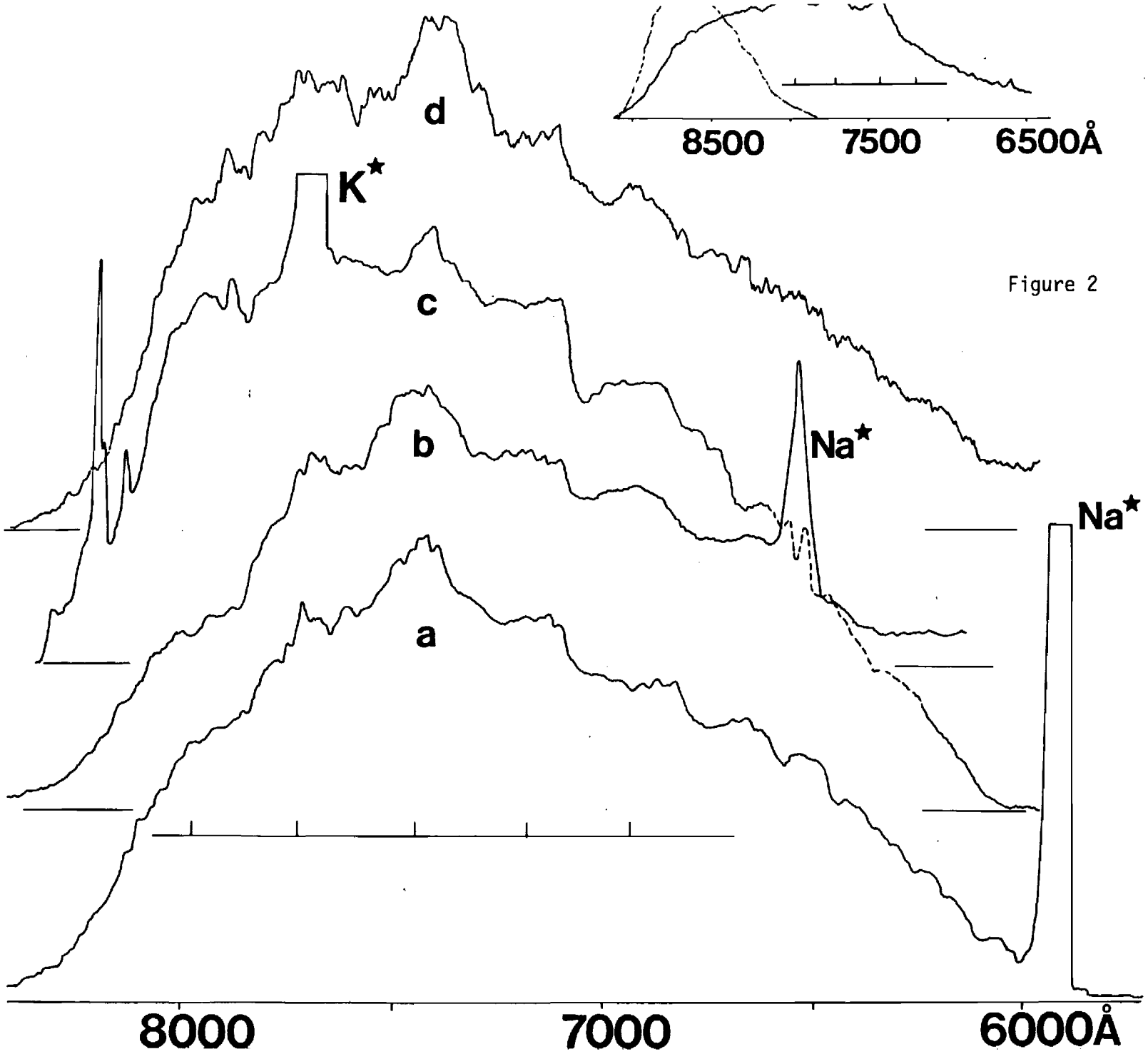

Figure 2

Table 1

Observed Bands for NaO* $A^2\Sigma^+ - X^2\Pi$

λ (Å)[a]	(cm^{-1} vacuum)	$\Delta\nu$ (cm^{-1})
6930	14426±20	
		502±20
7180	13924±20	
		487±20
7440	13437±20	
		487±20
7720	12950±20	
		406±20
7970	12544±20	

a. Measured at the center of the observed emission feature

strong interference to the ready analysis of alkali oxide emission features. For this reason, the upper chamber from which the alkali metal effuses is heated to 650°C to induce dissociation of the exiting alkali metal dimers. With this precaution, the multiple collision spectra are characterized by alkali atomic and alkali oxide emissions.

Spectra obtained for the Na-N_2O system under a wide variety of conditions are depicted in Figure 2. We identify five bands attributable to NaO whose wavelengths and intensities are listed in Table 1. The correlation of the multiple collision spectra with the NaO* single collision spectrum also shown in the Figure is excellent. An interpretation of the observed spectral features can be found in the reprint presented in Appendix A. Here we correlate the experimental results with the quantum chemical calculations of Allison, Cave, and Goddard which may indicate that the observed spectral features are to be assigned to emission from high vibrational levels of the $A^2\Sigma^+$ state terminating in the lowest vibrational quantum levels of the NaO $^2\Pi$ ground state. An alternate and considerably more exciting interpretation is possible. We may have observed emission from a higher-lying covalent state of the oxide which is bound by ~5000$^+$cm^{-1} relative to dissociation. Feasibility calculations indicate that this is indeed possible. We are now conducting experiments to establish the correct interpretation. There are two approaches. First, we are preparing to extend our studies further into the red (longer wavelengths) using a new phototube system and second, we are attempting to extend our successful Na + N_2O + X(Ar,N_2,CO) studies to the ozone system. We have had moderate success with the ozone experiments using the configuration described in Figure 1(b), however, further experimental modifications will be necessary in order to facilitate the higher pressure entrainment experiments. In order to carry out the ozone reactions, we have entrained the ozone in argon by flowing the rare gas through a previously constructed trap in which

ozone is deposited on silica gel at dry ice temperatures. The effluent argon + ozone flow is then passed through the oxidant nozzle into the reaction chamber. This procedure yields a significant ozone flow and allows us to produce an intense chemiluminescent flame. The peaks observed for the Na + O_3 system are somewhat skewed relative to those for Na + $N_2O \rightarrow NaO^* + N_2$. The skewed nature of these peaks may be significant for the observed spectral peaks may result from the combination of both a short ground and excited state progression, each feature appearing in the spectrum (note the symmetric nature of the peaks in Figure 2) also corresponding to a sequence grouping. If a sequence grouping corresponds to each of the major peaks observed in the NaO spectrum (Figure 2), the slightly skewed nature of the peaks observed in the NaO emission spectrum which characterizes the Na + O_3 system relative to that for the Na + N_2O system may result from a population distribution peaked at slightly different excited state quantum levels. We are proceeding further with our analysis of the "7400Å" band system in order to elucidate several of these points of contention.

The evaluation of the NaO 7400Å system is quite significant for it provides the first straightforward in-situ route by which one can probe for sodium oxide in a combustion gas stream. Recently systems have been demonstrated at the Morgantown Energy Technology Center which employ LIBS and CARS spectroscopies to detect the sodium and potassium content of coal gasification streams. The LIBS technique requires that a laser dissociate alkali species and then detect alkali metal formed in the dissociation process. With the discovery of the NaO 7400Å system, it will be possible to detect this gas stream constituent in a single step with a laser operating at close to this wavelength alleviating the need to carry out a dissociation process. Based on the present chemiluminescence studies and their extension to longer wavelengths, we anticipate that we will "pin-down" regions in which it will be

possible to probe sodium oxide using laser induced fluorescence. In order to carry out this effort we are in the process of constructing a hydrogen cell which will be used as a Raman shifter for a dye laser system so as to extend to wavelengths longer than 7000Å. Based on the information already obtained, it should be possible to probe sodium oxide using laser induced fluorescence by pumping a band system in the region between 7000 and 7500Å. We suggest that NaO be prepared by an appropriate in-situ synthesis passing entained sodium metal over NaO_2 viz

$$Na + NaO_2 \rightarrow 2NaO.$$

The subsequent products might also be excited by a krypton ion pumped dye laser. It should also be noted that these experiments must be carried out as a preliminary to the study of sodium surface oxidation.

Gas Phase Particulates Formed in Alkali Oxidative Environments

Previously, we reported our use of moderate temperature mass spectrometry as a means of analyzing the nature of the pronounced particulate matter formed via what appears to be the homogeneous gas phase oxidation of alkali metals, constructing an appropriate probe and vaporizing particulate material at temperatures between 50 and 300°C. Extensions of this temperature range to 400°C have produced no new information in addition to that reported in Quarterly Progress Report 5. In order to further characterize regions of lower vapor pressure associated with the particulate matter, we have prepared samples which will be analyzed, at higher temperature, in the high temperature laboratory of Professor John Margrave at Rice University. We are still waiting for the high temperature quadrupole mass spectrometers previously discussed to be brought on-line and hope that these will be available for particulate study in the next month. We have also attempted to study a sample of the

particulate matter using EPR and Laser Raman spectroscopies. We have obtained an EPR spectrum at low temperature (Quarterly Report 5) but have as yet, been unsuccessful in our attempts to interpret this spectrum. While attempts to obtain a Laser Raman spectrum have been unsuccessful thusfar, we are contemplating other means of attacking the problem. Finally we anticipate that an X-ray powder pattern will be obtained shortly. We are convinced that alkali-oxygen-nitrogen polymers can be formed with unusual efficiency in the gas phase and that they can represent the nuclei for large scale particulate formation in process streams.

Sodium Cluster Oxidation

In our previous discussions of sodium cluster oxidation[1] we noted that the chemiluminescent spectra which characterize the Na_x + Cl, Na_x + Br, and Na_x + SO_2 (chlorine impurity introduced) systems are characterized by a very high degree of internal excitation which renders ready resolution of spectral features difficult. We have considered and augmented several experimental approaches (Quarterly Progress Report 5) to deal with this problem, some of which have met with marginal success. We have concluded that it will be necessary to simultaneously supersonically expand a mixture of sodium and helium or argon creating alkali-rare gas complexes. The clusters can then be oxidized in an insured "local" environment of helium or argon atoms. The appropriate device is now under construction.

Alkali Hydroxide Emission Spectra

We have now constructed a new device to study the KOH emission spectrum. This device is based on a modification of the diffusion flame apparatus which we have discussed previously and is designed to facilitate the attainment of the KOH spectrum on film or using an optical multichannel analyzer. The device employs all of the improvements which we have previously incorporated

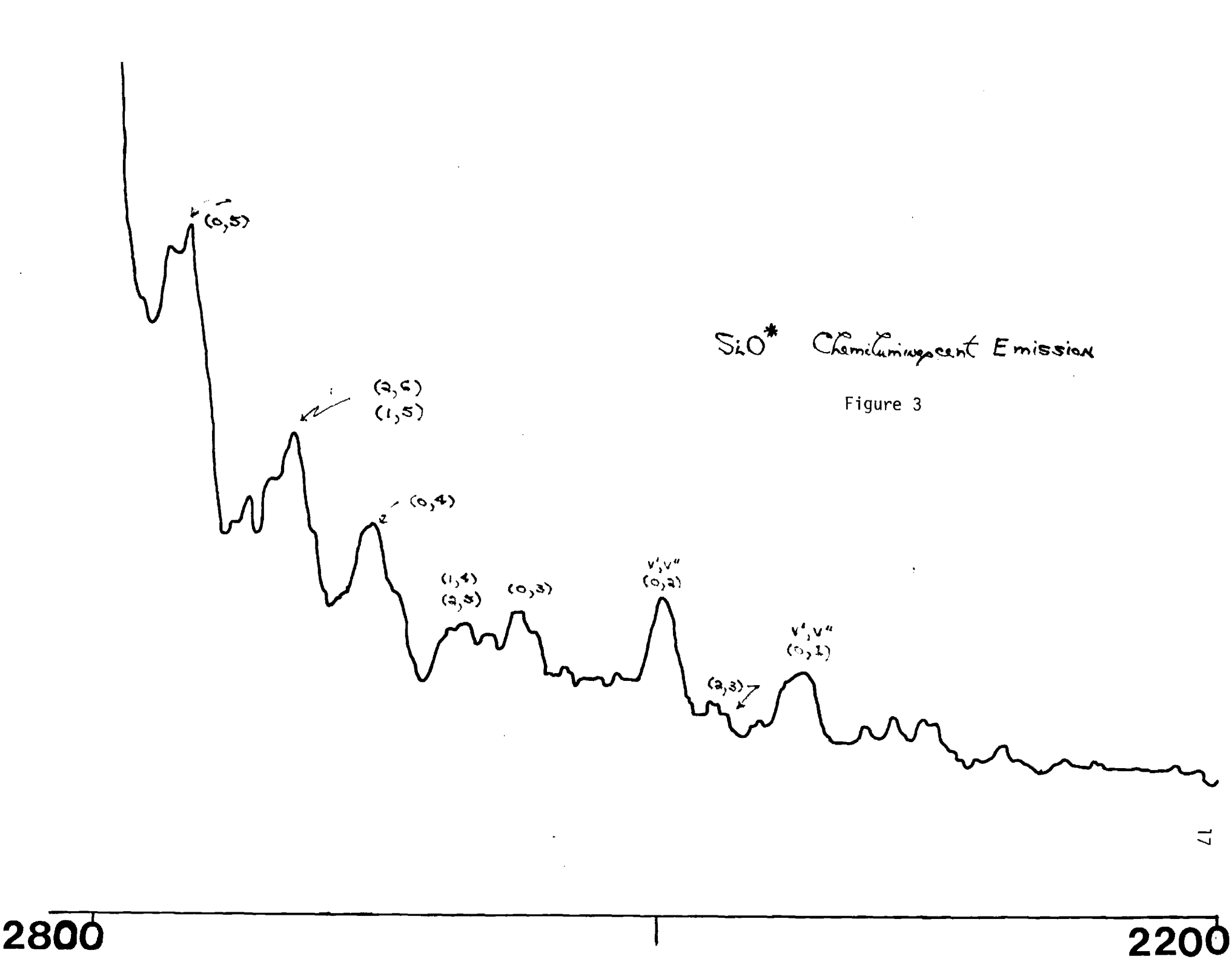

Si_2O^* Chemiluminescent Emission

Figure 3

and discussed in previous reports and considerably improves the optical system. Preliminary results while indicating the necessity for some improvements in the optical system are encouraging. In correlation with the efforts of other workers, the results obtained thusfar indicate that the Janaf tables on the alkali hydroxides will require massive revision.

The $Si-NO_2$ Reaction - Determination of $D_0^o(SiO)$

In Figure 3 we depict the SiO $A^1\Pi$ - $X^1\Sigma^+$ emission which characterize the $Si-NO_2$ reaction. We have found that the $Si-NO_2$ reaction populates the v' = 0, 1, 2 levels of the SiO $A^1\Pi$ state in a process whose activation energy is ~6-7 kcal/mole. When combined in an appropriate thermochemical cycle, this data yields an SiO bond energy of 187.9 kcal/mole in good agreement with the mass spectrometric determination of Hildenbrand et al.[3]

Publications

The following paper has been submitted and accepted for publication and is included with this report as Appendix A

"Observation of Alkali Oxide Electronic Emission Spectra: Analysis of the NaO $A^2\Sigma^+$ - $X^2\Pi$ '7600Å' Band System" by James L. Gole.

Presentations

The following are presentations given in which DOE sponsored research was discussed

1. University of Alabama, "Metal Cluster Formation and Oxidation"
2. Fenn Symposium, Yale University, "Formation, Characterization, and Oxidation of Metal Clusters"

APPENDIX A

Observation of Alkali Oxide Electronic Emission Spectra: Analysis of the NaO $A^2\Sigma^+ - X^2\Pi$ "7600 Å" Band System

James L. Gole

Department of Chemistry and High Temperature Laboratory
Georgia Institute of Technology
Atlanta, GA 30332

The alkali elements, their oxides and hydroxides, are commonly found in many high temperature systems,[1] their influence often being critical in determining proper operating conditions. In addition the sodium oxides are thought to play an important role in stratospheric sodium chemistry.[2] Unfortunately, spectroscopic data on these molecules which might well be used to probe the kinetics of their formation and interaction is extremely sparse, especially for the alkali oxides. Some gas phase rotational transitions have been determined for LiO;[3] matrix isolation infrared spectra[4] have been obtained for LiO, KO, and CsO while ESR transitions[5] have been observed for RbO and CsO and the alkali dioxides NaO_2-CsO_2.[6] Thusfar, infrared data has not been obtained for NaO and RbO and no electronic transitions have been reported. Electronic spectra, once obtained, offer not only the opportunity to understand various fundamental aspects of molecular electronic structure but also the potential to monitor the species of interest in a spectral region where detection sensitivity considerably exceeds that at longer wavelengths.

This report outlines a research effort which has led to the first observation of alkali monoxide electronic emission spectra. Out initial studies have focused primarily on the NaO and KO A-X emission systems because of (1) the importance which the analysis of these band systems may have for the ready detection of the oxides using modern laser techniques[7] and (2) the potential correlation of experiment with detailed theoretical calculations.[8] Here we focus on the "7600 Å" band system of NaO.

Several experimental devices, which will be described in more detail in a future report,[9] have been used to excite and observe electronic emission from the alkali oxides. Briefly, for sodium oxide, we have focused on the study of the chemiluminescent emission from the processes

$$Na + N_2O \rightarrow NaO^* + N_2 \qquad (1)$$

and

$$Na + N_2O + X \rightarrow NaO^* + N_2 + X \qquad (2)$$

where Eq. (1)[10] denotes that the Na-N_2O reaction was studied under single collision conditions ($P_{Total} \leq 5 \times 10^{-5}$ torr, Na flux ranging to a maximum of $10^{18}/cm^2sec.$) in a beam gas arrangement[10] and Eq. (2) represents the extension of the single collision studies to the multiple collision pressure regime where X = N_2O, Ar, CO, and N_2. The second group of experiments were carried out in order to relax the internal excitation characteristic of the electronic spectrum obtained under single collision conditions. Here, a stream of sodium atoms was crossed by an uncollimated oxidant flow under multiple collision conditions ($P_{N_2O} \simeq 50\text{-}150\mu$) or a mixture formed when sodium was entrained in argon ($P_{Ar} \simeq 850\text{-}1200\mu$), N_2($P_{N_2} \simeq 950\text{-}1500\mu$) or CO($P_{CO} \simeq 650\text{-}850\mu$) was oxidized by a concentric flow of N_2O($P_{N_2O} \simeq 50\text{-}95\mu$)[11] forming a flame which was adjusted to obtain the maximum alkali oxide emission.

Figure 1 depicts the NaO $A^2\Sigma^+ - X^2\Pi$ chemiluminescent emission obtained under a variety of experimental conditions. All of the observed spectra, both single and multiple collision, are characterized by a substantial internal excitation which hampers the precise evaluation of band locations, however, five features associated primarily with a short progression in the NaO ground state vibrational level spacing are discernable in the spectrum. These features are catalogued in Table 1.

The spectrum which results from the single collision Na-N_2O reaction is found to be first order in both the Na and N_2O concentrations. A small potassium impurity leads to the observation of K D-line emission[12] in the single collision spectrum. Initial temperature dependent studies[13] indicate that the Na-N_2O reaction is characterized by a substantial activation energy ($\geq$15 kcal/mole) whereas the Na-O_3 reaction proceeds more rapidly, having a much smaller barrier to product formation.

Under multiple collision conditions, for a given sodium beam flux, a maximized alkali oxide emission spectrum was obtained over a very narrow range of oxidant and carrier gas pressure. In addition, the multiple collision studies were further complicated by the collisional excitation of electronically excited sodium dimer (eq. $NaO^{\dagger} + Na_2 \rightarrow Na_2^* + NaO...$), the oscillator strength of whose transitions in overlapping spectral regions considerably exceeds that of the NaO $A^2\Sigma^+ - X^2\Pi$ band system. This problem was alleviated using a double oven system whereby the dimers vaporized from a first oven were thermally dissociated before entrainment in the appropriate carrier gas.[14] Hence, in order to observe the oxide, one requires a careful balance between internal deexcitation, energy transfer, and quenching. We believe that the stringent conditions required to obtain the alkali oxide emission spectrum account, in large part, for the inability of previous workers to observe the spectrum.

The data in Table 1 can be correlated with recent extensive quantum chemical calculations by Allison et al.[8] These authors find a 2177 cm^{-1} $^2\Pi - {}^2\Sigma$ excitation energy and estimate a ground state vibrational frequency, ω_e = 464 cm^{-1} ($A^2\Sigma^+$) $\simeq$ 493 cm^{-1}). Based on the results of their calculations on NaCl, LiO, KO, and CsO, where comparison with experiment can be made, the calculated frequency is expected to be 20-35 cm^{-1} lower than the experimental value. Energy conservation dictates that the spectrum which we observe in the present study must result from transitions among higher vibrational quantum levels of the $A^2\Sigma^+$ state and the lowest vibrational quantum levels of the ground $X^2\Pi$ state. The frequency separations which characterize the shorter wavelength bands catalogued in Table 1 (487$\pm$20 cm^{-1}) are to be associated with a progression in the lowest vibrational quantum levels of the ground electronic state although it is not clear that the 6930Å feature should be associated with v"=0, $X^2\Pi$. We associate the 406$\pm$20 cm^{-1} frequency increment with two adjacent vibrational quantum levels in the $A^2\Sigma^+$ state.

If we take T_{oo} for the NaO $A^2\Sigma^+ - X^2\Pi$ transition to be 2177 cm^{-1} and assume that the 6930Å feature corresponds to v" = 0, we estimate the upper state vibrational quantum level as v' = 26 or 27 corresponding to an anharmonicity $\omega_e x_e$ = 2 cm^{-1}. This result corresponds to $\omega_e(A^2\Sigma^+) \simeq 525$ cm^{-1} and an expected frequency separation $\Delta\nu$ = 417 cm^{-1} for the two long wavelength bands listed in Table 1, both values being consistent with the theoretically determined vibrational frequency, ω_e, and the error bound in the observed frequency separation, $\Delta\nu$. If the 6930Å feature corresponds to v" > 0, the v' numbering should be increased by the corresponding increase in the v" quantum level numbering, however, based on energy conservation[15] it is highly unlikely that this band is associated with v" > 2. Thus the upper state quantum levels from which we observe emission are in the range v' = 26-29.

We have summarized the results of initial efforts in our continuing study of alkali oxide electronic emission spectra. We are attempting to improve our knowledge of the NaO emission spectrum by extending this study to longer wavelength.[9] In addition we have obtained preliminary spectra for the $A^2\Sigma^+ - X^2\Pi$ emission system in LiO and KO[9] and the $A^2\Pi - X^2\Sigma^+$ band system of RbO.[9] We anticipate that future detailed temperature dependent studies[13] of both the M + N_2O and M + O_3 metatheses analogous to Eq(1) will also lead to an independent determination of the alkali oxide bond energies.

Acknowledgement: It is a pleasure to acknowledge the assistance of Mr. David Semmes and Mr. Joerg Pfeifer in these experiments.

References

1. See for example J. L. Gole, Optical Engineering 20, 546 (1981); D. E. Jensen and G. A. Jones, Comb. and Flame 41, 71-85 (1981); Y. Yousefian, I. W. May, and J. A. Heimerl, "An Algebraic Criterion for the Prediction of Secondary Muzzle Flash - A Progress Report" Presented at the 18th JANAF Combustion Meeting, Pasadena, California, 1982; S. A. Medin, V. A. Ovcharenko, and E. E. Shpil'rain, High Temp. U.S.S.R. 10, 390 (1972).

2. See for example C. E. Kolb and J. B. Elgin, Nature, 263, 488 (1976) also E. Murad private communication.

3. S. M. Freund, E. Herbst, R. P. Mariella Jr., and W. Klemperer, J. Chem. Phys. 56, 1467 (1972).

4. a. R. C. Spiker, Jr. and Lester Andrews, J. Chem. Phys. 58, 702 (1973).
   b. D. White, K. S. Seshardri, D. F. Dever, D. E. Mann and M. J. Linevsky, J. Chem. Phys. 39, 2463 (1963).
   c. K. S. Seshardri, D. White and D. E. Mann, J. Chem. Phys. 45, 4697 (1966).
   d. R. C. Spiker and L. Andrews, J. Chem. Phys. 58, 713 (1973).

5. D. M. Lindsay, D. R. Herschbach, and A. L. Kwiram, Mol. Phys. 32, 1199 (1976), D. M. Lindsay and D. R. Herschbach, J. Chem. Phys. 60, 315 (1973).

6. D. M. Lindsay, D. R. Herschbach, and A. L. Kwiram, Chem. Phys. Lett. 25, 175 (1974).

7. C. Kolb, private communication.

8. J. N. Allison, R. J. Cave, and W. A. Goddard III, J. Chem. Phys. 77, 4259 (1982) also "The Alkali Oxides. Analysis of Bonding and Explanation of the Reversal in Ordering of the $^2\Pi$ and $^2\Sigma^+$ States" - preprint.

9. J. Pfeifer, D. Semmes, and J. L. Gole, to be published.

10. See for example
    C. L. Chalek and J. L. Gole, J. Chem. Phys. 65, 2845 (1976);
    J. L. Gole and S. A. Pace, J. Phys. Chem. 85, 2651 (1981);
    J. L. Gole, Ann. Rev. Phys. Chem. 27, 525 (1976).

11. See for example
    D. M. Lindsay and J. L. Gole, J. Chem. Phys. 66, 3886 (1977);
    M. J. Sayers and J. L. Gole, J. Chem. Phys. 67, 5442 (1977);
    J. L. Gole and S. A. Pace, J. Chem. Phys. 73, 836 (1980).

12. This spectrum was obtained using 99.5% purity sodium. A similar spectrum with a slightly diminished K D-line was obtained using 99.99% sodium.

13. D. R. Preuss and J. L. Gole, J. Chem. Phys. 66, 2994 (1977); J. L. Gole and D. R. Preuss, J. Chem. Phys. 66, 3000 (1977); L. H. Dubois and J. L. Gole, J. Chem. Phys. 66, 779 (1977).

14. The Na D-line emission which results from primarily V-E transfer also represents a problem especially in the CO_2 entrainment experiments where the process $NaCO + NaO^{\dagger} \rightarrow Na^* + CO + NaO^{\dagger}$ can dominate the process $NaO^* + CO \rightarrow NaO^* + CO$ corresponding to internal deexcitation of the NaO^*.

15. Energy conservation considerations are based on the data from R. R. Herm and D. R. Herschbach, J. Chem. Phys. 52, 5783 (1970), D. L. Hildenbrand and E. Murad, J. Chem. Phys. 53, 3403 (1970).

Table 1

Observed Bands for NaO* $A^2\Sigma^+ - X^2\Pi$

λ (Å)[a]	(cm^{-1} vacuum)	$\Delta\nu$ (cm^{-1})
6930	14426±20	
		502±20
7180	13924±20	
		487±20
7440	13437±20	
		487±20
7720	12950±20	
		406±20
7970	12544±20	

a. Measured at the center of the observed emission feature

Figure Caption:

NaO* $A^2\Sigma^+ \rightarrow X^2\pi$ Chemiluminescent Emission Spectra for the processes (a) Na + $N_2O(P_{N_2O} \simeq 125\mu)$ → NaO* + N_2, (b) Na + $N_2O(P_{N_2O} \simeq 75\mu)$ + $Ar(P_{Ar} \sim 950\mu)$ → NaO* + N_2 + Ar, (c) Na + $N_2O(P_{N_2O} \simeq 50\mu)$ + $CO(P_{CO} \simeq 850\mu)$ → NaO* + N_2 + CO, (d) Na + $N_2O(P_{N_2O} \simeq 75\mu)$ + $N_2(P_{N_2} \simeq 1100\mu)$ → NaO* + N_2, and (inset) single collision chemiluminescent spectrum for the metathesis Na + $N_2O(P_{N_2O} \simeq 5\times10^{-5}$ torr) → NaO* + N_2. Spectral resolution for (a) through (d) is 1Å while the single collision spectrum was obtained at 5Å resolution. The dashed region outlined at the longest wavelengths in the single collision spectrum indicates a component of blackbody radiation.

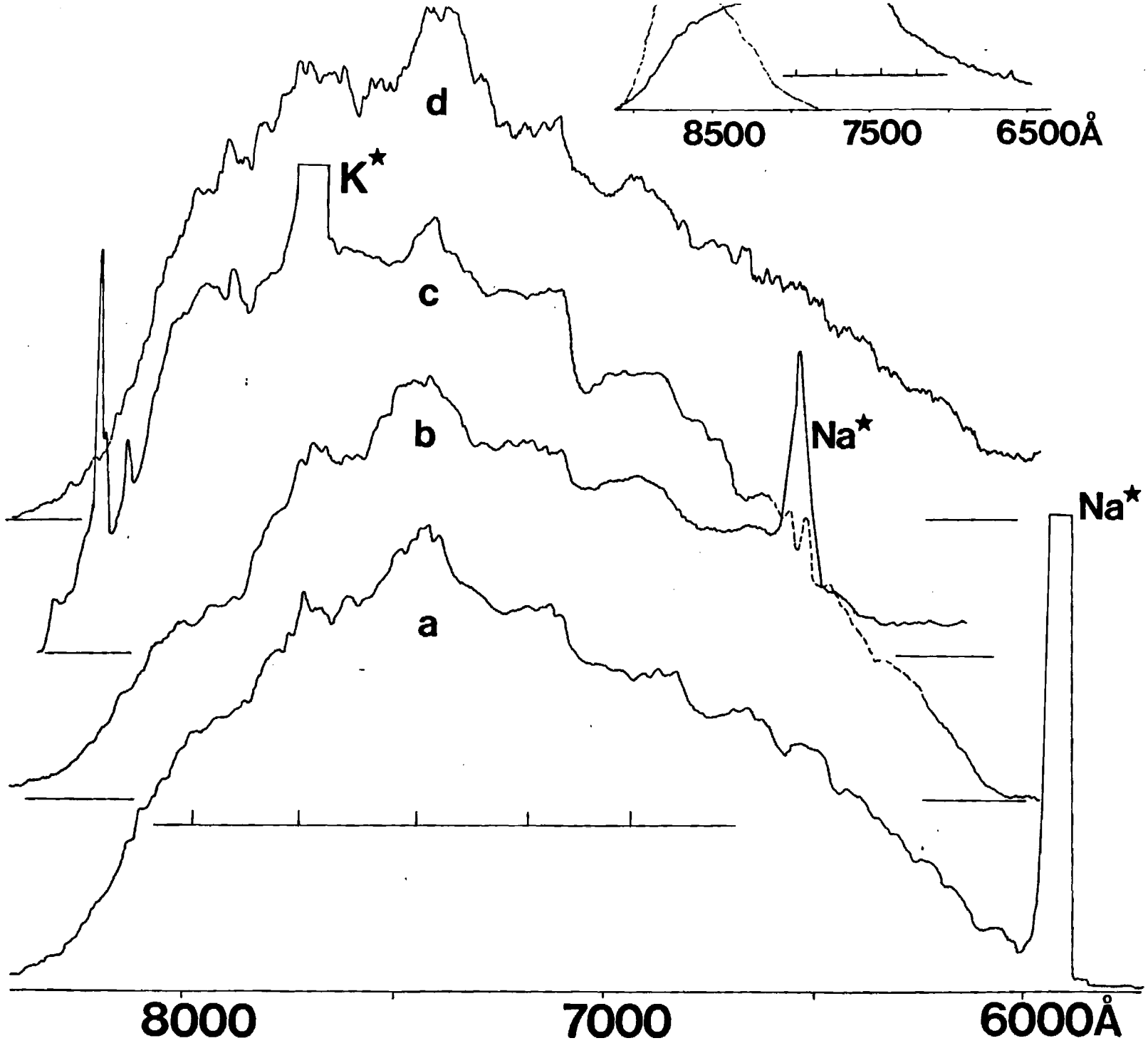
d
K*
c
b
Na*
Na*
a
8500
7500
6500Å
8000
7000
6000Å

References

1. J. L. Gole, "The Characterization of High Temperature Vapor Phase Species and Vapor-Solid Interactions of Import to Combustion and Gasification Processes in the Energy Technologies" Annual Topical Report 1, October 1, 1981-October 1, 1982, Morgantown Energy Technology Center, DOE.

2. See for example J. L. Gole "The Characterization of High Temperature Vapors of Import to Combustion and Gasification Processes in the Energy Technologies," Proceedings of the Morgantown Energy Technology Center Meeting on High Temperature, High Pressure Particulate and Alkali Control in Coal Combustion Process Streams - Morgantown, West Virginia, 1981.

3. D. L. Hildenbrand, High Temp. Sci. 4, 244 (1972).

THE CHARACTERIZATION OF HIGH TEMPERATURE VAPOR PHASE SPECIES AND VAPOR-SOLID INTERACTIONS OF IMPORT TO COMBUSTION AND GASIFICATION PROCESSES IN THE ENERGY TECHNOLOGIES

Quarterly Technical Progress Report No. 7
for the Period 14 April,1983 to 15 July, 1983

James L. Gole

School of Chemistry
Georgia Institute of Technology
Atlanta, Georgia 30332

15 July 1983

PREPARED FOR THE UNITED STATES
DEPARTMENT OF ENERGY
Morgantown Energy Technology Center
Morgantown, West Virginia

Under Contract No. DE-AC21-81MC16537

NOTICE

FOREWARD

This report summarizes technical progress accomplished during the seventh quarterly reporting period of a two-year study being conducted for the U.S. Department of Energy (DOE). This work period was 14 April 1983 to 15 July 1983. Work was accomplished under the direction of James L. Gole. Graduate and undergraduate students who have contributed to the technical progress and to this document are Mr. W. H. Crumley, Mr. Joerg Pfeifer and Mr. David Semmes. Mr. Ken Williams, Supervisor of the Machine Shop has provided assistance in design and construction of oven components.

Abstract

This report summarizes work completed during the seventh quarter of a two-year study focused primarily on the determination of bond energies and spectra for the alkali hydroxides and oxides, the study of pronounced particulate matter formed in alkali oxidation, and the characterization of sodium cluster and sodium surface oxidation with various oxidants.

We have developed and are continuing to improve experimental configurations for generating intense, stable, and long-lasting chemiluminescent emission from the alkali hydroxides NaOH and KOH and the alkali oxides NaO and KO. The first electronic emission spectra for these compounds have been generated and are being studied in our laboratory. Commensurate with this effort has been the study of extensive particulate formation which appears to be pathelogical to the alkali hydroxide and oxide systems. This particulate matter, formed in an extremely efficient manner in the oxidation process, has been studied using a number of techniques ("low temperature mass spectrometry, EPR spectrometry, and Raman spectroscopy). Initial efforts to obtain an X-ray powder pattern and a high temperature quadrupole mass spectrum have been instituted. Sodium cluster oxidation studies over the past three month period have focused on the desire to observe emission from highly exothermic processes which characterize the Na_x-SO_2-Cl_2 system. In addition, refinements of studies of silicon monoxide formation which complement previous studies under DOE sponsorship were carried out during this period. From these studies the bond energy of SiO was confirmed from a purely spectroscopic measurement thus complementing and confirming the mass spectrometric determinations.

TABLE OF CONTENTS

LIST OF FIGURES

Introduction

Background

Low tolerance levels for certain species in process streams impose stronger requirements for reliable thermodynamic and kinetic data in order to predict low level species concentrations. In addition evidence now indicates that serious concern must be focused on whether or not these systems are best represented via equilibrium or non-equilibrium models. Unfortunately, the necessary thermodynamic and kinetic data required to perform accurate calculations of species concentrations is not available for many such gas stream species. Of equal importance is the fact that little detailed information is available which will allow the ready direct monitoring of these species in the process stream. In addition, many of the details of the mechanisms for process stream product formation, including the formation and growth of particulates, are yet unknown while many postulated routes to product formation are yet only meagerly tested. This arises primarily because many of the molecular entities for which data are needed correspond to elusive and very reactive radicals or high temperature molecules. Our laboratory has been concerned with the characterization of several of the important molecules and possible processes thought to be present in the inherently high temperature environment of the process stream.

We have applied chemiluminescent and laser fluorescent techniques to the determination of bond energies, spectroscopic constants, and the evaluation of those spectral regions which will be most useful for the kinetic parameterization and monitoring of the species of interest. In addition, through the study of certain selected processes, we are attempting to shed some light on the feasibility of postulated interactions in the process stream,

some of which include the surprisingly efficient gas phase formation of particulate matter. Finally, in the course of these studies, we are documenting the presence of ultrafast energy transfer, both intra- and intermolecular, as it pertains to the nature of heat flow in high temperature systems and, in particular, to those molecules of interest in process streams. It should be noted that the attainment and evaluation of reliable spectroscopic data leads to the determination of important molecular constants which can be used for the statistical mechanical evaluation of heat capacities, entropies and free energies, all of which are important to the understanding of energy related combustion and gasification environments.

Objectives

The general objectives of the present research effort which represents a continuation of previous efforts under DOE sponsorship are: (a) to characterize alkali monoxide chemiluminescent spectra, specifically spectra for NaO and KO which can be used in kinetic studies of the behavior of these species and for their direct monitoring in process streams and to determine lower bounds for the NaO and KO bond energies; (b) to characterize pronounced particular formation in gas phase alkali oxidation environments; (c) to further characterize the KOH chemiluminescent emission spectrum at a resolution and under conditions which will allow the determination of currently unavailable molecular constants for this molecule and an improved measure of the K-OH bond dissociation energy; (d) to carry out and characterize the oxidation of sodium clusters with various oxidants including SO_2; (e) to attempt to prepare clean sodium and sodium contaminated surfaces whose oxidation with various constituents including SO_2 will be characterized; (f) to further characterize the NaOH chemiluminescent emission spectrum in order to obtain an improved measure of the Na-OH bond energy; (g) to determine the SiO bond

energy from the chemiluminescent process $Si + NO_2 \rightarrow SiO^* + NO$. Specific tasks of interest in the current report are indicated below.

Characterization of Alkali Oxide Emission Spectra and Gas Phase Particulate Formation in Alkali Oxidation Environments

The object of a portion of this task is to observe and characterize chemiluminescence from NaO and KO using the reactions of sodium or potassium atoms with primarily N_2O and O_3. These studies have yielded the first electronic emission spectra for NaO and KO resulting from the low pressure "single collision" reaction of sodium and potassium atoms with N_2O. Our efforts in this quarter have focused primarily on (1) the stepwise extension of these single collision studies to higher pressures where relaxation efforts lead to an improvement in spectral resolution, facilitating the evaluation of molecular constants for NaO and KO and furnishing reliable spectral regions which can be used to probe for these elusive oxides and (2) the extension of the spectral range over which the NaO and KO emission spectra are probed from a previous long wavelength limit of 8200Å to a current limit of 10,500Å. Several experimental devices have now been developed which, at least for sodium oxide, overcome numerous factors associated with the attainment of NaO chemiluminescence across a wide pressure range. Further, preliminary values for the bond dissociation energies of NaO and KO(D_0^o(NaO) = 70±5, D_0^o(KO) = 75±5 kcal/mole) are corroborated through the combination of single and multiple collision studies.

These alkali oxidation systems, involving formation of the alkali oxides, are found to exhibit a pronounced virtually gas phase homogeneous particulate formation (see Annual Progress Report 1[1]) which is not observed in any other oxidation system. A major focus of our research effort has involved an attempt to characterize the polymeric alkali-oxygen-

nitrogen species which constitute the framework of the observed particulate matter employing mass spectroscopy, EPR spectroscopy, Raman Spectroscopy, and X-ray powder spectra. We believe that the extremely efficient formation of these polymers can provide a seed for particulate formation in process streams.

Sodium Cluster Oxidation

The objective of this task is to evaluate the nature of sodium oxidation in the intermediate region between the gas and surface phase. The products of sodium cluster oxidation are being characterized through direct observation of the chemiluminescent emission for highly exothermic processes, through a newly developed electron impact excitation technique, and through mass spectrometric sampling of the oxidation region. Current efforts focus on the desire to obtain emission spectra corresponding to very exothermic processes associated with the combined halogen and SO_2 oxidation of sodium clusters.

Alkali Hydroxide Emission Spectra

Electronic emission spectra for the alkali hydroxides have been obtained over a wide pressure range. The reactions of sodium and potassium dimers with hydrogen peroxide are being used to excite chemiluminescence from NaOH and KOH. The objective of this task is to determine stringent lower bounds for the K-OH and Na-OH bond energies and molecular constants for several levels of the ground electronic state of K-OH. KOH emission has been observed at low pressures under "single collision" conditions, at intermediate pressures where the effects of collisional relaxation are apparent ("multiple collision" conditions) and at higher pressures in a "diffusion flame" device, the combination of these studies leading to the first evaluation of a stringent lower bound for the K-OH bond energy[2] using a direct optical measurement. Continued

improvements in the "diffusion flame" apparatus have now led to long term flame stability. Because flame instabilities tend to "washout" spectral features, stabilization was a major task before us. We are now attempting to solve a major aspect of this problem by recording the entire KOH emission spectrum on film and in 200Å sections using an optical multichannel analyzer. These efforts will be used to obtain a more stringent lower bound for the KOH bond energy and to obtain higher resolution spectra to evaluate molecular constants for several ground state levels. The data obtained thusfar for NaOH and KOH when correlated with that of other workers (e.g. Hastie-N.B.S.) demonstrates that a massive revision of the data in the Janaf tables for the alkali hydroxides will be necessary.

Silicon Monoxide Emission Spectra

The focus of this research effort has been to supplement previous studies whose object has been to determine molecular constants for the SiO molecule and, more importantly, to determine the SiO bond energy using a direct spectroscopic approach. In studying the reaction of silicon atoms with NO_2, we have determined an SiO bond energy in excellent agreement with mass spectroscopy and are currently refining the data obtained for publication.

Technical Progress-Plans for Future Study

Alkali Oxide Emission Spectra

In Quarterly Report 6 (QPR-6), we noted the need to study the sodium oxide emission spectrum resulting from the metathesis $Na + N_2O \rightarrow NaO^* + N_2$ at wavelengths longer than the limit of an 8200Å capability. In the last quarter, we have developed the appropriate system to carry out these studies and have extended our spectral scans to 10,500 Å (Figure 1). The optical system has also been improved to the extent that we have increased spectral

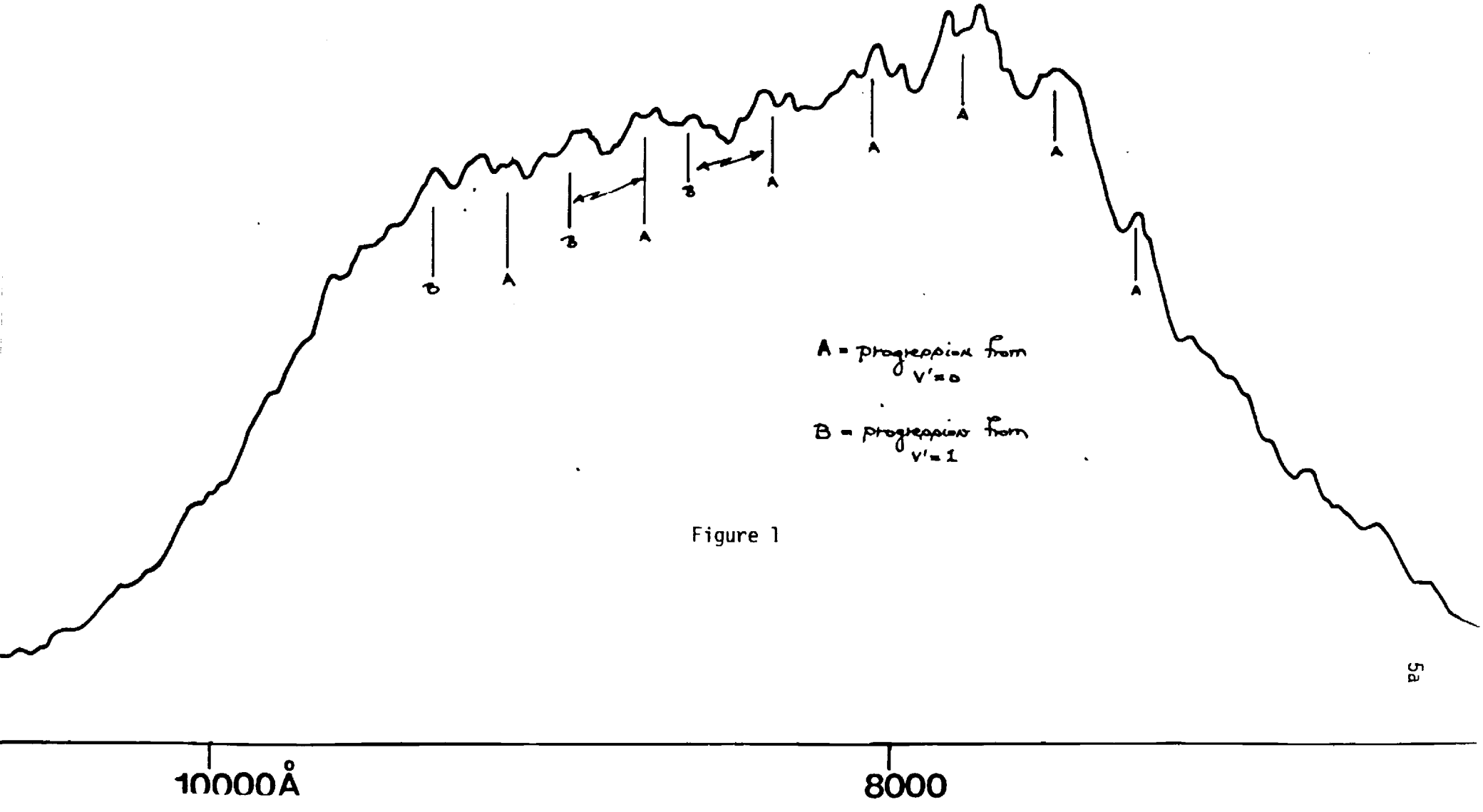
B
A
B
A
B
A
A
A
A
A = progression from v'=0
B = progression from v'=1
10000Å
8000

Figure 1

sensitivity by almost three orders of magnitude. Although the spectra obtained thusfar are not yet totally definitive, we observe spectral features which appear to be correlated in large part with a long progression in the ground state sodium oxide vibronic levels. We have found that the observed spectral features at wavelengths longer than 8200Å appear very sensitive to a variety of conditions local to the flame region although those spectral features extending from 8200 to 6000Å are not nearly so strongly affected. We hope to cast more light on this puzzling result using a variety of alkali atom entrainment gases. In the present experiments, we have used the system developed and discussed in QPR-6 to study the $Na + N_2O \rightarrow NaO^* + N_2$ metathesis at elevated pressures ($P_{total} \geq 1$ torr). The elevated pressure has been obtained thusfar by introducing N_2 as a sodium atom entrainment gas, however, it is apparent that further experiments with carriers such as Argon, CO, and possibly O_2 will be needed to definitively correlate and definitively identify the observed spectral features. At present, our preliminary analysis indicates that we have monitored emission from low vibrational quantum levels of a low-lying and previously unobserved covalent state of NaO. The features marked in Figure 1 appear to be dominated by a long progression in the ground state vibrational quantum levels of NaO. At the shortest wavelengths only one progression is apparent tentatively assigned to the lowest vibrational quantum level of an upper covalent state; however, at wavelengths longer than 8500Å, additional features are observed which are shifted by $\sim$265 cm^{-1} from the initial progression. This frequency separation is consistent with the anticipated vibrational level spacing ($\omega_e \sim 283$ cm^{-1}) of a Morse Potential modeled covalent state dissociating to ground state sodium and ground state oxygen atoms. Further studies are now underway to obtain more definitive information.

After some modification and improvement of the knife edges used to seal our stainless steel oven system, we are again in the process of studying the $K + N_2O \rightarrow KO^* + N_2$ reaction under conditions similar to those employed in our previously reported and present studies on the analog sodium system (see also QPR-6). We have now extended out studies of the potassium oxide emission spectrum resulting from the metathesis $K + N_2O \rightarrow KO^* + N_2$ to the wavelength range extending to 10,500Å. Here, the extension to longer wavelengths reveals that the emission feature peaked at 7800Å in the previously reported emission spectrum for the potassium-N_2O system actually extends from 7500 to 9800Å (Figure 2). Again, the behavior of this system is quite sensitive to flame conditions, the observed emission corresponding to either a continuous or structured feature dependent upon the nature of the flame region. The experiments carried out thusfar employ a system in virtually exact analog of that used for sodium, elevated pressures being obtained by introducing N_2 as the postassium atom entrainment gas. Here, it is again apparent that further experiments with carriers such as Ar, CO, and possibly O_2 may prove useful in analyzing the observed spectral features. We are currently attempting to obtain some foothold in the analysis of the structured emission features apparent in Figure 2. As a final point we should note that particulate formation is notable in both the sodium and potassium systems being much more pronounced in the potassium system.

The evaluation of the NaO covalent to ionic (ground state) emission system is quite significant for it provides the first straightforward in-situ route by which one can probe for sodium oxide in a combustion gas stream. Recently systems have been demonstrated at the Morgantown Energy Technology Center which employ LIBS and CARS spectroscopies to detect the sodium and

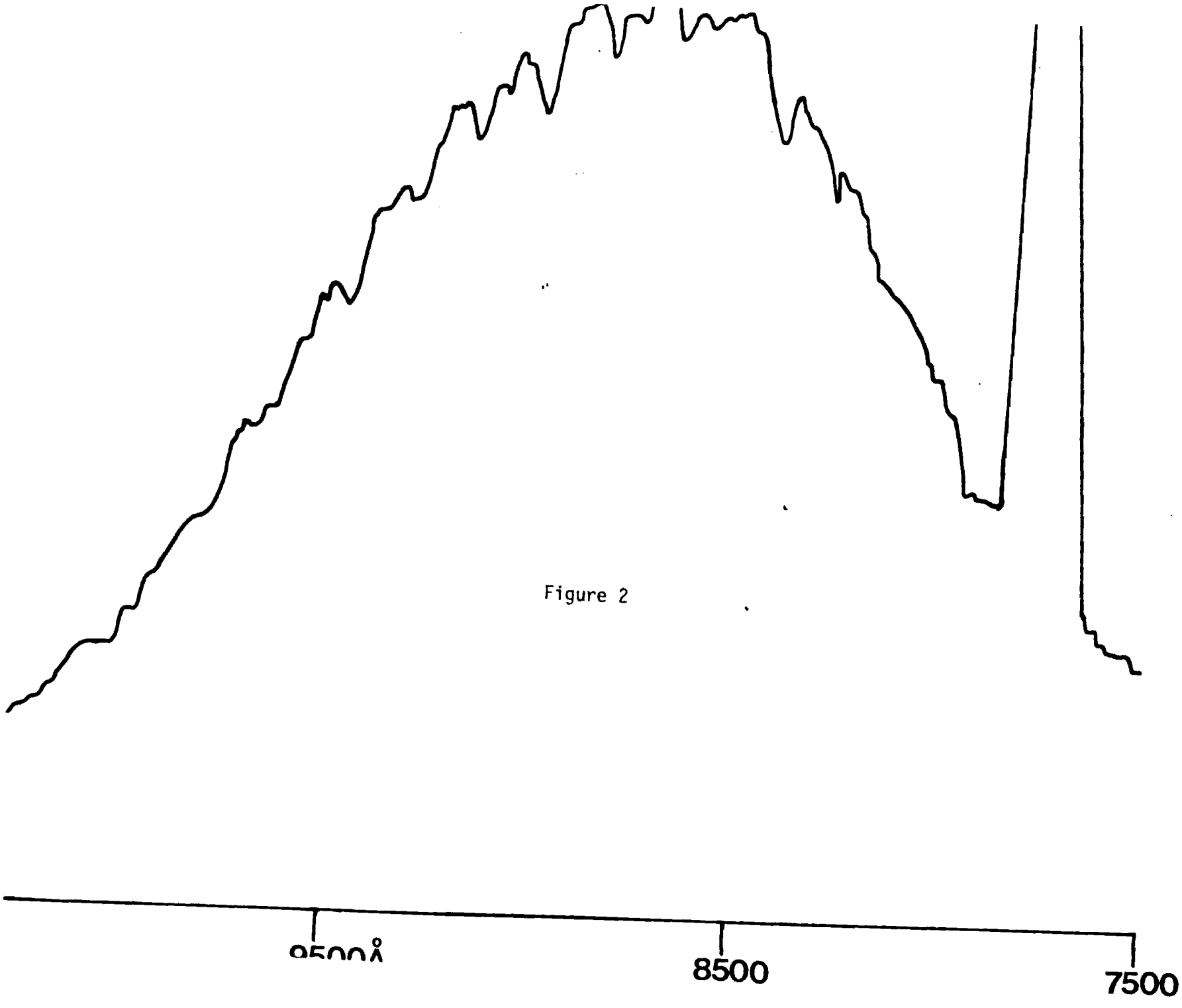

Figure 2

potassium content of coal gasification streams. The LIBS technique requires that a laser dissociate alkali species and then detect alkali metal formed in the dissociation process. With the discovery of the NaO 6500Å system, it will be possible to detect this gas stream constituent in a single step with a laser operating at close to this wavelength alleviating the need to carry out a dissociation process. Based on the present chemiluminescence studies, we anticipate that we will "pin-down" regions in which it will be possible to probe sodium oxide using laser induced fluorescence. In order to carry out this effort we have constructed a hydrogen cell which will be used as a Raman shifter for a Neodymium-YAG pumped dye laser system which we hope to make use of in order to extend to wavelengths longer than 7000Å. Based on the information already obtained, it should be possible to probe sodium oxide using laser induced fluorescence by pumping the presently identified band system in the region between 6000 and 7500Å. We suggest that NaO be prepared by an appropriate in-situ synthesis passing entrained sodium metal over NaO_2 viz

$$Na + NaO_2 \rightarrow 2NaO.$$

The subsequent products might also be excited by a krypton ion pumped dye laser. It should also be noted that these experiments must be carried out as a preliminary to the study of sodium surface oxidation.

Gas Phase Particulates Formed in Alkali Oxidative Environments

Previously, we reported our use of moderate temperature mass spectrometry as a means of analyzing the nature of the pronounced particulate matter formed via what appears to be the homogeneous gas phase oxidation of alkali metals,

constructing an appropriate probe and vaporizing particulate material at temperatures between 50 and 400°C. In order to further characterize regions of lower vapor pressure associated with the particulate matter, we have prepared samples which will be analyzed, at higher temperature, in the high temperature laboratory of Professor John Margrave at Rice University. We are still waiting for the high temperature quadrupole mass spectrometers previously discussed to be brought on-line and completely tested and hope that these will be available for definitive particulate study in the next few months. Our previously reported efforts to study a sample of the particulate matter using Laser Raman spectroscopy have been unsuccessful. Although we have obtained an EPR spectrum at low temperature, we have as yet, been unsuccessful in our attempts to interpret this spectrum. In addition, we are still awaiting the results of X-ray crystal structure analysis. Previous attempts at analysis had been hampered by machine breakdown. We are convinced that alkali-oxygen-nitrogen polymers can be formed with unusual efficiency in the gas phase and that they can represent the nuclei for large scale particulate formation in process streams.

Sodium Cluster Oxidation

Several experiments to study the $Na_x + SO_2 + Cl_2$ system were initiated during this period. Here we are attempting to test the catalytic activity of a slight chlorine impurity to produce a highly exothermic metathesis involving alkali clusters and SO_2 (see Annual Topical Report 1[1]). In the present approach, a device has been constructed which allows for the flow of SO_2 over a channel contaminated with chlorine prior to its (SO_2) introduction. In a second approach, SO_2 can be mixed with slight amounts of chlorine, this mixture interacting with the sodium cluster beam. Both the $Na_x + Cl_2$ and $Na_x + SO_2$ systems within themselves do not produce the

the chemiluminescent emission which has been found to characterize the mixed system (the $Na_x + Cl_2$ system does produce Na D-line and NaCl* emission (see Annual Topical Report 1), however, this emission is almost completely at wavelengths longer than that characterizing the mixed system). In all of the experimental runs conducted this period, initial visual observations of the anticipated weak chemiluminescence (blue-green) were encouraging, however, before a spectrum could be taken the oven system lost necessary power (short and oven burn out) resulting in a rapidly decreasing flame intensity. The oven system is now being reworked, modified and rewired.

In our previous discussions of sodium cluster oxidation[1] we noted that the chemiluminescent spectra which characterize the $Na_x + Cl$, $Na_x + Br$, and $Na_x + SO_2$ (chlorine impurity introduced) systems are characterized by a very high degree of internal excitation which renders ready resolution of spectral features difficult. We have considered and augmented several experimental approaches to deal with this problem concluding that it will be necessary to simultaneously supersonically expand a mixture of sodium and helium or argon creating alkali-rare gas complexes. The clusters can then be oxidized in an insured "local" environment of helium or argon atoms. The appropriate device is currently under construction.

Alkali Hydroxide Emission Spectra

A new student is now engaged in improving our apparatus ("student eater") for the study of the KOH emission spectrum. Two new system configurations were tried during this period and neither provided a significant improvement in the magnitude of the KOH emission previously observed. Correlating the information available from previous studies, we have returned to a slight modification of a previous design. Attempts to obtain the KOH emission spectrum on standard films have been unsuccessful, although a notable

thruput can be obtained at the exit slits of our spectrometer. Therefore, we have obtained several special films with much stronger ultraviolet response which we anticipate testing shortly.

The Si-NO_2 Reaction

We have attempted to refine the data previously reported for SiO (QPR-6). Several attempts to run these experiments were thwarted by an unusual skeen of oven burn-outs and by the disintegration of the carbon used for crucible materials. New carbon, new ovens, and new insulation material were ordered. New crucibles have now been constructed and the first refined spectrum shown in Figure 3 has been obtained.

Presentations

The following are presentations given in which DOE sponsored research was discussed

1. A.C.S. Colloid and Surface Science Symposium, Toronto, Canada "Formation, Characterization, and Oxidation of Metal Clusters".

Figure 3

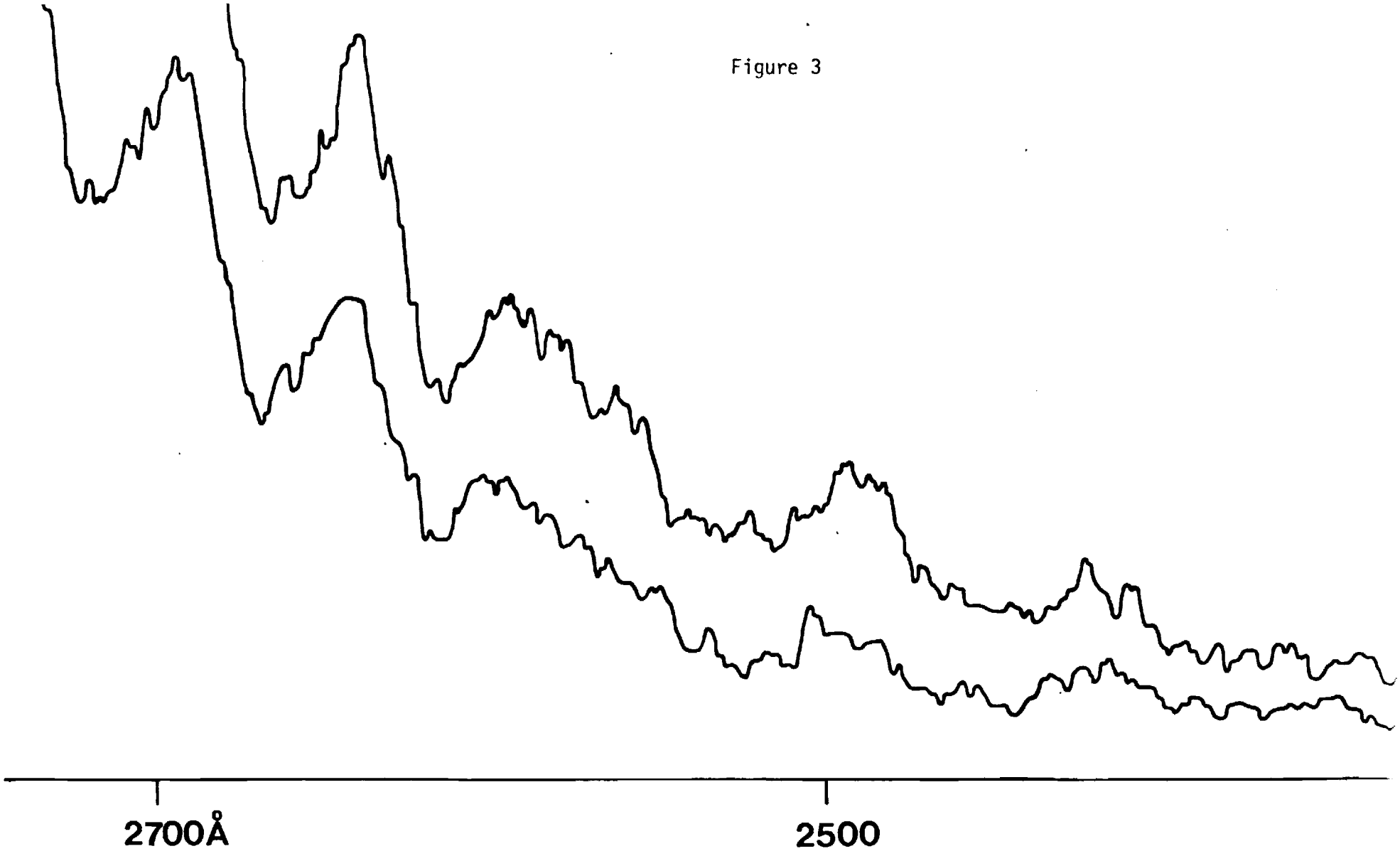

References

1. J. L. Gole, "The Characterization of High Temperature Vapor Phase Species and Vapor-Solid Interactions of Import to Combustion and Gasification Processes in the Energy Technologies" Annual Topical Report 1, October 1, 1981-October 1, 1982, Morgantown Energy Technology Center, DOE.

THE CHARACTERIZATION OF HIGH TEMPERATURE VAPOR PHASE SPECIES AND VAPOR-SOLID INTERACTIONS OF IMPORT TO COMBUSTION AND GASIFICATION PROCESSES IN THE ENERGY TECHNOLOGIES

Annual Topical Report No. 1

for the period October 1, 1981-October 1, 1982

James L. Gole

Chemistry Department
Georgia Institute of Technology
Atlanta, Georgia 30332

July 1982

PREPARED FOR THE UNITED STATES
DEPARTMENT OF ENERGY
Morgantown Energy Technology Center
Morgantown, West Virginia

Under Contract No. DE-AC21-81MC16537

NOTICE

FOREWORD

This report details the results of a research program carried out over the period October 1, 1981 - October 1, 1982 for the Morgantown Energy Technology Center under Contract No. DE-AC21-81MC16537. Work was accomplished under the direction of James L. Gole. Graduate and undergraduate students who have contributed to the technical progress are Mr. W. H. Crumley, Ms. Beatriz Cardelino, Mr. Gary Green, and Mr. Edward Green. Mr. Ken Williams, Supervisor of the machine shop has provided assistance in the design and construction of oven components. It should be noted that although the period covered here represents a 12 month effort, this project was severely interrupted by a major laboratory fire on December 11, 1981 necessitating extensive equipment repair which was completed by February 15, 1982.

ABSTRACT

The alkali hydroxides, NaOH and KOH, and the alkali oxides, NaO and KO, have been studied. Emphasis has been on the determination of bond energies and spectra for these species. Sodium "cluster" oxidation with several oxidants including the halogens and SO_2 has been characterized.

Several experimental configurations have been tested as a means for generating intense, stable, and long-lasting chemiluminescent emission from the alkali hydroxides NaOH and KOH and the alkali oxides NaO and KO. Studies have been carried out over a wide pressure range from a very low pressure (10^{-4} torr) single collision environment through stages of pressure increase which promote desired changes in the observed chemiluminescent emission spectra as an aid to the evaluation of molecular constants. At the highest pressures, chemiluminescence has been obtained in a diffusion flame environment. Thusfar, from the chemiluminescent studies we have determined stringent lower bounds for the K-OH (88.6 kcal/mole) and NaOH (82.5 kcal/mole) bond energies, notably higher than those values given in the Janaf Tables. The NaO and KO bond energies have been determined to be 70 ± 5 and 75 ± 5 kcal/mole respectively. Preliminary molecular constants have been determined for K-OH and NaO. A major impetus of the present studies has been the attempt to develop oven systems which circumvent problems in flame formation and stability common to the alkali hydroxides and oxides but not present in typical chemiluminescent metal oxidation systems. Most pronounced among these is the extremely efficient formation of extensive particulate matter which appears to result from the formation of alkali hydroxide and alkali oxide polymers.

The major emphasis in sodium cluster oxidation studies as they represent potential models for sodium surface oxidation has been (1) the definition

of the system through the characterization of highly exothermic chemiluminescent channels associated with sodium cluster - halogen atom oxidation and through mass spectrometry, (2) the characterization of highly exothermic channels for the oxidation of sodium clusters with SO_2, (3) the development of diagnostics for the detection of product ion formation in sodium cluster oxidation, and (4) the development of electron impact excitation techniques as a means of probing the dark products of chemical reaction.

PURPOSE AND SCOPE

This research program focuses on the study of alkali metals and the interactions which they undergo, the stability and molecular constants for several elusive and sparsely studied alkali compounds, and the evaluation of alkali polymer formation and interaction in oxidative environments. The interactions of the alkali metals and their compounds represent very deleterious elements in process streams; therefore the tolerance levels for these species are low necessitating the attainment of reliable thermodynamic and kinetic data in order to predict low level species concentrations and the probable mechanisms for compound formation.

Our objectives have been to (a) characterize the KOH chemiluminescent emission spectrum at a resolution and under conditions which will allow the determination of currently unavailable molecular constants for this molecule and an improved measure of the K-OH bond dissociation energy: (b) to characterize the NaOH chemiluminescent emission spectrum in order to obtain an improved measure of the Na-OH bond energy; (c) to characterize alkali monoxide chemiluminescent spectra specifically spectra for NaO and KO and to determine lower bounds for the NaO and KO bond energies; (d) to carry out and characterize the oxidation of sodium clusters with various oxidants including the halogens and SO_2; (e) to attempt to prepare clean sodium and sodium contaminated surfaces whose oxidation with various constituents including SO_2 will be characterized; (f) if feasible, to institute laser induced fluorescence studies on the alkali monoxides and continue studies on Na_2O.

This Topical Report is concerned with progress on program elements (a) through (d). Described are the design of devices used to generate low pressure chemiluminescent flames in highly exothermic dynamic processes,

the design and modification of devices used to extend these low pressure studies in a "controlled manner" to elevated pressures in order to better obtain and interpret spectroscopic constants and evaluate ultrafast energy transfer routes, and the design and modifications to insure the stability of a diffusion flame device used to study the alkali hydroxides. Further the design of a device which has been used to generate sodium clusters and study their oxidation will be detailed.

Table of Contents

INTRODUCTION

General Impetus for Study

Because of our increasing demand for energy, the significant increase in the cost of fuels and the decrease of domestic supplies of clean fuels including natural gas, increased emphasis has now been placed on coal as a source of electrical power generation and industrial heating. While coal is an abundant and inexpensive source of energy compared to the cost of petroleum and natural gas, it is a dirty fuel especially when compared to natural gas. Many deleterious compounds are present in the gas stream and their formation and interactions must be understood as thoroughly as possible.

Background

Low tolerance levels for certain species in process streams impose stronger requirements for reliable thermodynamic and kinetic data in order to predict low level species concentrations. In addition evidence now indicates that serious concern must be focused on whether or not these systems are best represented via equilibtium or non equilibrium models. Unfortunately, the necessary thermodynamic and kinetic data required to perform accurate calculations of species concentrations is not available for many such gas stream species. Of equal importance is the fact that little detailed information is available which will allow the ready direct monitoring of these species in the process stream. In addition, many of the details of the mechanisms for process stream product formation, including the formation and growth of particulates, are yet unknown while many postulated routes to product formation are yet only meagerly tested. This arises primarily because many of the molecular entities for which data are needed correspond to elusive and

very reactive radicals or high temperature molecules. Our laboratory has been concerned with the characterization of several of the important molecules and possible processes thought to be present in the inherently high temperature environment of the process stream.

We have applied chemiluminescent and laser fluorescent techniques to the determination of bond energies, spectroscopic constants, and the evaluation of those spectral regions which will be most useful for the kinetic parameterization and monitoring of the species of interest. In addition, through the study of certain select processes, we are attempting to shed some light on the feasibility of postulated interactions in the process stream, some of which include the surprisingly efficient gas phase formation of particulate matter. Finally, in the course of these studies, we are documenting the presence of ultrafast energy transfer, both intra- and intermolecular, as it pertains to the nature of heat flow in high temperature systems and, in particular, to those molecules of interest in process streams.

Specific Considerations - Alkali Metal and Compound Characterization - The Data Base

For a fixed bed gasifier, the exiting gas at approximately 550°C contains particulates, tar vapor, and vaporized alkali. The particulates consist of coal fines and ash, the ash being of particular concern because of its high alkali content. The alkali metals in a variety of forms are known to represent deleterious and corrosive constituents in process streams. The nature of coal-fired systems, in general, is such that "alkali cleanup"[1] represents one of the most significant problems which must be addressed. It has been well established[2] that the primary slag or flyash components include the alkali compounds Na_2O and K_2O. Significant vapor phase species (impurities) especially in a water rich environment are known to include the potassium and sodium hydroxides. Thermodynamic calculations[3] also indicate the probable importance of the alkali monoxides NaO and KO (KO is of special interest

n a potassium seeded MHD channel), however, sulfur is also a significant impurity n a coal-fired system.[1-4] Therefore, it is necessary to consider sulfur compounds nd their relation to the only partially solved fuel corrosion problem. In con-;idering the problem of turbine blade corrosion, researchers have established that ılkali-sulfur and alkali oxide salts may be of great importance.[5,1,6] Therefore the properties of these species, which establish the nature of their formation in the combustion environment proceeding the turbine, and their behavior upon deposition, must be characterized to the greatest extent possible. In order to obtain this information, means must be found to (1) determine the kinetics of both formation and reaction of the alkali oxides and hydroxides and their corresponding sulfur analogs both in model systems which allow for a detailed determination of reaction rates which can be used in the kinetic modeling of the process stream and in the process stream itself, (2) monitor the species of interest directly in the process stream, and (3) deduce any aspects of the internal energy level structure or molecular electronic structure of these compounds which can lead to unexpected behavior in the process stream including ultrafast energy transfer.

The data base to which we wish to contribute is also of importance for the characterization of most coal and heavy fuel fired turbine generators.[7] Indeed, a great deal of interest is also now focusing on fireside corrosion where one must consider the interaction of the alkali salts and the boiler tubes onto which they plate. With this interest, it is noteworthy that the data on sodium and potassium-oxygen and sulfur compounds is miniscule. Information on molecular stabilities (heats of formation) and molecular constants must be obtained.

As a contribution to the necessary data base, our research effort has focused on the characterization of alkali hydroxides and oxides, both important compound groups in process streams, coupled with an effort to provide information which can be used to elucidate the nature of alkali metal interactions which lead to the formation of alkali sulfates in process streams.

Our efforts to study the alkali hydroxides NaOH and KOH have led to the first direct observation of electronic emission spectra for these species, furnishing what is potentially a much easier means of following these species in the gas phase. Prior to this effort, the major thermodynamic characterization of these metal hydroxides had been through indirect flame studies.[5] That is, the presence of the hydroxide had been inferred from the study of metal atom depletion. A second law analysis of this metal atom depletion had been used to deduce bond energies for primarily the alkali and alkaline earth hydroxides. Only two of the alkali and alkaline earth hydroxides have been characterized mass spectrometrically. Studies of the Group IIA hydroxides are precluded for all but the barium compounds[8] because of a very high propensity for disproportionation to the oxides and resulting loss of water. Difficulties encountered in studying the alkali hydroxides may well stem from the tendency to form dimeric species on vaporization. The bond energies determined for KOH[5] and BaOH[5,8] via flame and mass spectrometric studies are in reasonable but not spectacular agreement. For KOH, flame studies indicate 84 ± 2.5[9] and mass spectrometry yields 80 ± 3[10] for the M-O bond dissociation energy.

Direct chemiluminescent studies as employed in our laboratory provide a cleaner means of determining the K-OH bond energy than either the flame or mass spectrometric techniques. These studies have already provided a lower bound for the KOH dissociation energy, 88.2 kcal/mole,[5] and recent efforts described in the following discussion have provided a more stringent determination, 88.6 kcal/mole. This value is significantly higher than that recommended in the JANAF tables (85.4 kcal/mole) and is in good agreement with the recent mass spectrometric studies of Hastie et al.[11] The JANAF number is based primarily on the results from flame studies. The nature of the bond energy determination from chemiluminescent processes is summarized in detail in Appendix A and in the following discussion. As we will consider in following discussion, a lower bound for the Na-OH bond energy has also

now been determined using the chemiluminescent technique and the value obtained, 82.5 kcal/mole is in good agreement with recent photodissociation studies, being notably higher than that recommended by JANAF.

Gas phase molecular parameterization is meager if nonexistent for the alkali hydroxides, however, Abramowitz and coworkers[5,12,13] have obtained infrared spectra for NaOH, RbOH, and CsOH and their deuterated analogs trapped in rare gas matrices. Belyaeua et al.[5,14] have studied the matrix infrared spectrum of matrix isolated KOH. Extensive microwave and millimeter wave studies have now yielded significant parameterization for the ground states of NaOH, KOH, RbOH, and CsOH, and rotational constants have been obtained for several excited vibrational levels.[15] All of these studies are very impressive yet microwave spectroscopy does not furnish a means of readily detecting NaOH and KOH for the study of their reaction kinetics or as a means of following these species in process streams, nor is there a guarantee that the vibrational frequencies recorded in the matrix are sufficiently close to those in the gas phase so as to allow straightforward detection of these molecules using forms of infrared spectroscopy. The most useful current techniques for detecting molecules in the infrared involve diode lasers; their use represents a very expensive proposition when frequencies are not precisely known. Thus, if the alkali hydroxide electronic emission spectrum can be used to pinpoint appropriate monitoring regions in the infrared, they greatly cut the cost of needed experiments. Finally, based on the studies currently underway, it should be feasible to assess whether the current hydroxide spectra demonstrate that electronic spectroscopy can be used as a means of detecting and monitoring NaOH and KOH. If the electronic spectrum can be employed as a detector, sensitivity can be greatly increased.

Because K-OH is one of the more important constituents in the high stress environments characterizing energy generating systems, the higher K-OH bond energy now determined in our studies has significant implications for the

understanding of KOH chemistry in the combustion gas stream. Of course, because of this larger K-OH bond energy, the degree of dissociation which is proportional to $e^{-D_o/kT}$ decreases. Hence the K-OH concentration must be somewhat higher than previously believed and its influence on the gas stream kinetics may be slightly modified relative to previous expectations. While ground state rotational parameters have been determined for KOH and KOD, vibrational frequencies are still estimated for higher vibrational levels. Although matrix data is available on the fundamental vibrations, no gas phase measurements have been made and no anharmonicities are available for any of the alkali hydroxides. As following discussion will demonstrate, there is reason to believe that the present chemiluminescent studies on KOH will yield extensive vibrational parameterization for the ground electronic state.[5,16] Using standard statistical mechanical techniques, this vibrational data can be used to evaluate the vibrational contribution to the heat capacity, enthalpy, entropy, and hence the free energy of the KOH molecule. This data is, of course, useful for the thermodynamic modeling of these systems.

In very close analog to the alkali hydroxides, few gas phase emission spectra or molecular constants have been obtained for the oxides and sulfides of sodium and potassium. In addition there have been very few bond energy determinations for these compounds. For this reason, it is appropriate to study the alkali oxides employing a variety of chemiluminescent processes. These efforts have been undertaken in our laboratory leading, at present, to the determination of bounds for the Na-O and K-O bond energies and to the preliminary assessment of molecular constants for NaO. The success of this study indicates that it may be possible to excite laser fluorescence from these compounds in order to obtain further molecular parameterization. The usefulness of this effort can be exemplified by our current studies (see

following) of an NaO band system in the spectral region near 7400Å. The evaluation of the NaO 7400Å system is quite significant for it provides the first straightforward in-situ route by which one can probe for sodium oxide in a combustion gas stream. Recently (see Appendix D) systems have been demonstrated at the Morgantown Energy Technology Center which employ LIBS and CARS spectroscopies to detect the sodium and potassium content of coal gasification streams. The LIBS technique requires that a laser dissociate alkali species and then detect alkali metal formed in the dissociation process. With the discovery of the NaO 7400Å system, it will be possible to detect this gas stream constituent in a single step with a laser operating at close to this wavelength alleviating the need to carry out a dissociation process.

The above studies are also useful as a precursor to efforts whose objective is to assess possible routes for alkali sulfate formation in process streams.

It is known that alkali sulfates represent a portion of the deleterious material formed in process streams. It is necessary that we gain some understanding of how the alkali present in the stream leads to this alkali sulfate formation. Several workers have attempted to understand the important role played by alkali metals in the process stream. Recently, Stewart et al.[1] have been concerned with the nature of alkali metal interactions. These workers have proposed a model which involves the migration of alkali metal through the slag component of the process stream, creating an alkali enriched surface where heterogeneous gas phase reactions may take place. SO_2 is known to be an important gas stream species and it is thought that alkali enriched surface-SO_2 interactions lead eventually to formation of the sulfate.

It is apparent that one need ascertain the nature of the alkali-SO_2 interaction. With this impetus, we are attempting to observe the products of oxidation of various sized sodium clusters. Although the Na-SO_2 and probably the Na_2-SO_2 reactions are endothermic, it is not obvious that this

thermodynamic behavior will hold for multicenter processes involving $n \geqslant 3$ sodium atoms. Here it is possible that NaO, NaS, and Na_2O may represent the products of cluster oxidation. In a strong sense the study of cluster oxidation represents a forerunner to the study of sodium surface oxidation. In addition, the formulation of cluster generating devices affords the opportunity to develop appropriate sources for the efficient preparation of sodium surfaces whose oxidation can be characterized. It is also noteworthy that other workers have suggested that chlorine interacts with the alkali impurities in a combustion stream, resulting in the formation of alkali chloride complexes which then repartition with O, S, H, C, Al, or Si ash particulates. Thus, the influence of chlorine on the formation of alkali clusters and the subsequent reaction of these clusters with sulfur oxides should be evaluated in the intermediate region between gas and surface phases. In following discussion, we outline progress toward these goals.

RESULTS AND DISCUSSION

The general objective of the studies detailed in this report is the characterization via optical and mass spectrometric techniques of several alkali vapor phase species and vapor-solid interactions which are thought to be of import to the understanding of phenomena associated with the combustion and gasification of coal. Major activities during this period can be grouped into three categories; the generation and characterization of alkali hydroxide emission spectra to determine bond dissociation energies and molecular constants, the generation and characterization of alkali oxide emission spectra to determine bond dissociation energies and molecular constants and assess the feasibility of laser fluorescence probes of these species and the characterization of sodium cluster oxidation with the halogens and SO_2.

Alkali Hydroxide Emission Spectra

Short Summary

Electronic emission spectra for the alkali hydroxides are being obtained over a wide pressure range. The reactions of sodium and potassium dimers with hydrogen peroxide are being used to excite chemiluminescence from NaOH and KOH. The objective of this task is to determine stringent lower bounds for the K-OH and Na-OH bond energies and molecular constants for several levels of the ground electronic state of K-OH. KOH emission has been observed at low pressures under "single collision" conditions, at intermediate pressures where the effects of collisional relaxation are apparent ("multiple collision" conditions) and at higher pressures in a "diffusion flame" device, the combination of these studies leading to the evaluation of a stringent lower bound for the K-OH bond energy using a direct optical measurement. Similarly, a strong NaOH diffusion flame spectrum has now led to the determination of a

stringent lower bound for the Na-OH bond energy by direct optical measurement. While constants have been determined for the lowest vibrational quantum levels of the ground electronic state of KOH (the KOH fundamental frequency in the gas phase is determined to be 423 cm^{-1}), continued improvements in the diffusion flame apparatus promise the ability to obtain higher resolution spectra in order to evaluate molecular constants for several ground state levels. Further, using a combination of single and multiple collision studies it may be possible to extend further the evaluation of ground state molecular constants. The major challenge which confronts us in these efforts is the generation of a long term, intense, stable flame. Flame instabilities and the possibility of multiple processes leading to KOH excited states tend to "wash out" spectral features, a factor which plagues electrooptical scans. Therefore, a spectrum must be obtained either on film or through use of an optical multichannel analyzer. Because the KOH emission spectrum extends across a rather wide range (3000Å), the limited range (200Å) of a given OMA scan is not conducive to a ready analysis. Thus the task confronting the efficient analysis of the KOH emission spectrum is the generation of this spectrum on film requiring a long term, intense flame. This is not a straightforward task due primarily to the extremely efficient gas phase formation of particulate matter in these systems.

Generation of Emission Spectra - Analysis and Experimental Considerations

Depicted in Figures (1) and (2) are "single"[17] and "multiple"[17] collision chemluminescent spectra for KOH generated via electrooptical scans of a very low pressure ($\leq 10^{-4}$ torr) system and a diffusion flame environment. At very low pressures, energetics dictates that the observed emission must result from the process

$$K_2 + H_2O_2 \longrightarrow KOH^* + KOH \qquad (1)$$

Figure 1: KOH* emission spectrum from the reaction $K_2 + H_2O_2 \rightarrow KOH^* + KOH$ under single collision conditions.

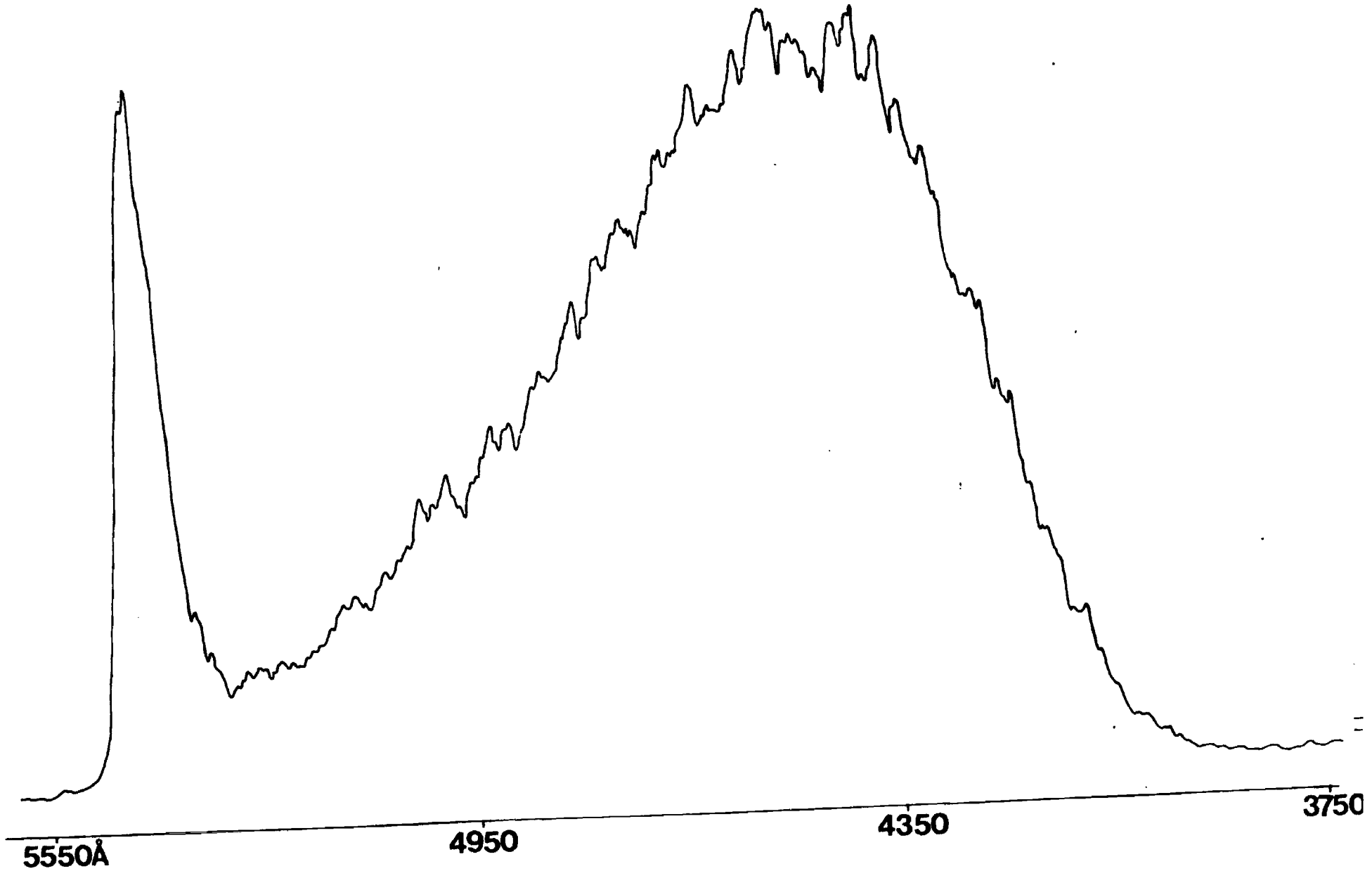
5550Å
4950
4350
3750

Figure 2: KOH* emission spectrum taken under multiple collision conditions in a diffusion flame device. The spectrum results predominantly from the reaction $K_2 + H_2O_2 \rightarrow KOH^* + KOH$ although some contribution also results from the process $K + OH + M \rightarrow KOH^* + M$.

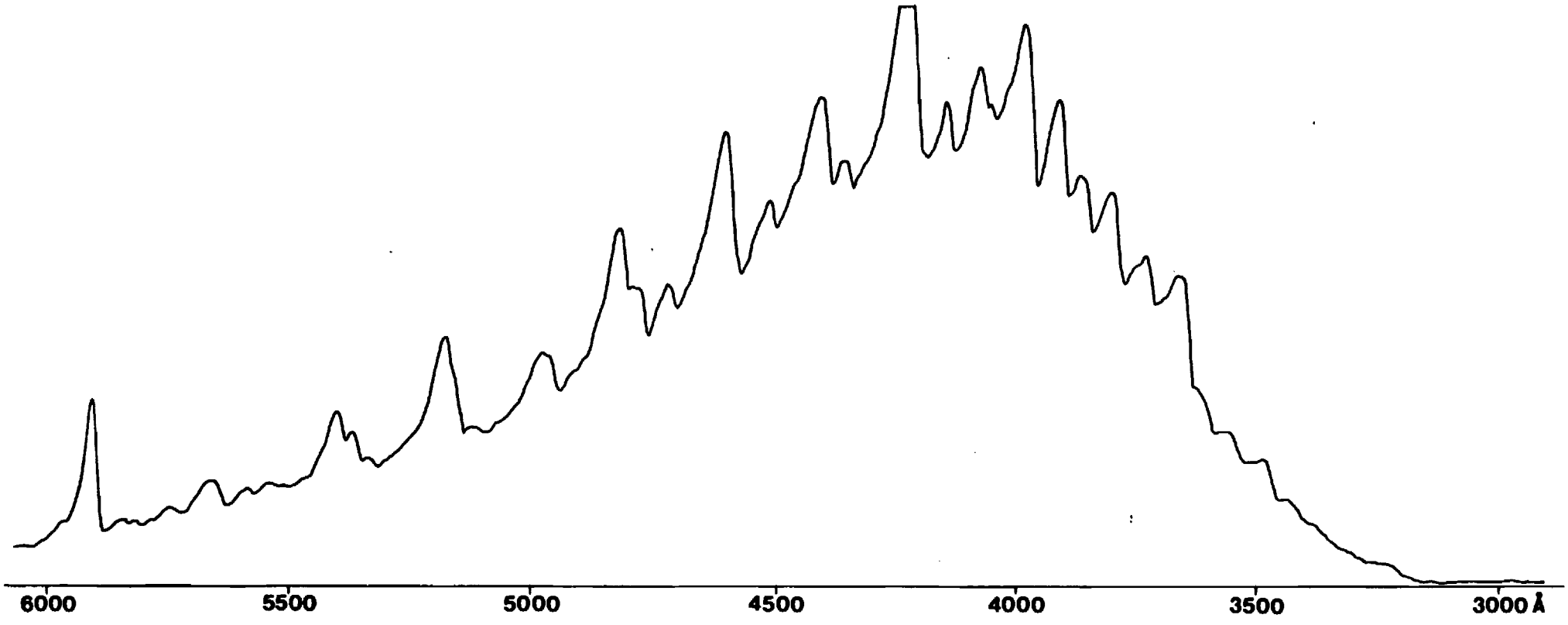
6000
5500
5000
4500
4000
3500
3000 Å

whereas, in the "diffusion flame" environment, the three body encounter

$$K + OH + M \longrightarrow KOH^* + M \qquad (2)$$

may also contribute to the observed emission. Note that the multiple collision diffusion flame spectrum onsets at ~3200Å whereas the single collision spectrum onsets at 3900Å. As we discuss in detail in Appendix A, this difference in onset which results from a change in rotational excitation is of fundamental importance to the evaluation of the K-OH dissociation energy. The difference in onset is characteristic of the nature of emission from a very weakly bound excited state. One should compare the significantly increased quality of the diffusion flame spectrum in Figure 2 with that depicted in Figure 4, Appendix A.

As should be apparent from Figures 1 and 2, both the "single and multiple" collision KOH emission spectra are characterized by significant structure which we believe is attributable to emission to vibronic levels in the ground electronic state of potassium hydroxide, more specifically to what is primarily a progression in the K-OH stretch. There appears to be a reasonable if not one-to-one correlation between several of the features in the "multiple" and "single" collision spectra for $\lambda > 3900$Å; however, there are some differences which may be attributable to (1) significant rotational relaxation in the multiple collision "diffusion flame" environment versus the high rotational excitation expected under single collision conditions or (2) the onset of rapid energy transfer and hence collisional depopulation of KOH excited state levels from which emission is observed under single collision conditions. The latter phenomena, collisional depopulation, should include collision induced dissociation of KOH molecules formed in the very weakly bound excited state from which emission is observed in the present study.

At present, we can obtain an estimate of the K-OH stretch ground state vibrational frequency, ω_0 ~423 cm^{-1}, from the short wavelength peak separations measured in Figure 2. Also, from the directly measured short wavelength limit of the diffusion flame spectrum, 3225Å, we obtain a stringent lower bound to the K-OH bond energy, 88.6 kcal/mole (3225Å = 30996 cm^{-1}/349.76 cm^{-1}/kcal = 88.6 kcal/mole), slightly higher than that reported in reference 5 (see Appendix A). In order to improve the results presented in Figures 1 and 2 thus obtaining higher resolution KOH emission spectra, one requires an increase in spectral intensity and hence it is necessary to increase reactant concentrations. Unfortunately, in contrast to all previously encountered metal oxidation systems, for several significant reasons, we have found that it is substantially more difficult to formulate and maintain stable and intense alkali hydroxide or oxide chemiluminescent sources. In the case of the alkali hydroxides, our efforts have been hampered by the experimental difficulties entailed in handling 90+% hydrogen peroxide and the nature of extensive particulate formation in the reaction zone.

There have been a number of modifications to the single collision and diffusion flame systems used to generate the spectra presented in Figures 1 and 2. Of course these modifications have been made in order to maintain higher reactant concentration levels. If not carefully approached, the increase of reactant concentrations may lead to the quenching of the desired chemiluminescence as opposed to its linear increase with reactant concentration.

The major experimental device which has been used thusfar to generate the KOH emission spectrum is shown in Figure 3. The nipple of the diffusion flame bulb is filled with potassium metal. After the system has been evacuated, the entire bulb is heated to a temperature producing approximately a 1 torr vapor pressure of potassium which can be maintained while exposing the system

Figure 3: Schematic of diffusion flame apparatus.

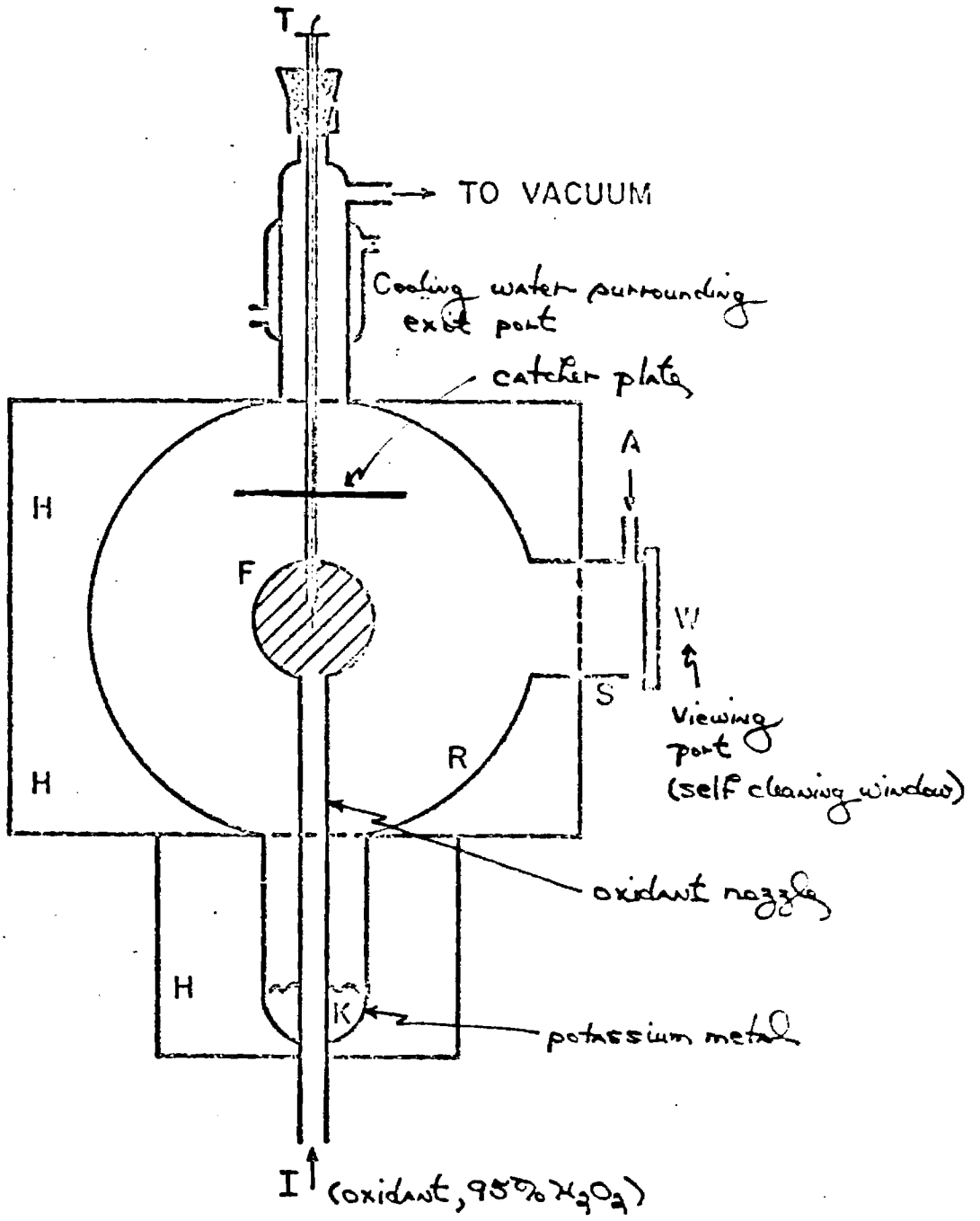
T
TO VACUUM
Cooling water surrounding exit port
catcher plate
A
H
F
W
S
Viewing port (self cleaning window)
R
H
oxidant nozzle
H
K
potassium metal
I
(oxidant, 95% X_2O_2)

to vacuum. Attached to the viewing port is a self-cleaning window over which argon flows constantly to prevent potassium or potassium hydroxide condensation. 90+% hydrogen peroxide is introduced through the oxidant nozzle and a flame is created in the region F. The correct operation of this device entails that the hydrogen perioxide not be heated to temperatures in excess of 320K. If one attempts to increase the H_2O_2 vapor pressure and hence the oxidant flow rate by going to temperatures in excess of 320K, the hydrogen peroxide begins to decompose and severe pressure fluctuations are encountered followed by the quenching of KOH fluorescence and the apparent formation of a strongly emitting KO_2 species. In Figures (4) and (5) we depict chemiluminescent spectra which dominate the emission observed in the sodium-H_2O_2 and potassium-H_2O_2 systems under conditions where we have partial decomposition of the hydrogen peroxide either through its heating to temperatures in excess of 320K or reaction with the container walls, both of which create a hydroxide rich environment. The observed spectra are believed to result from emission from either MO or MO_2 excited states. Based on a comparison with the spectra associated with the Na-N_2O and K-N_2O systems, we favor formation of the latter MO_2 compounds.

Preliminary studies now indicate that the likely mechanism for KO_2 formation is

$$HO\text{-}OH \xrightarrow{\Delta} 2OH$$

$$OH + HO\text{-}OH \longrightarrow HO_2^* + H_2O$$

$$HO_2^* + K \longrightarrow KO_2^* + H$$

where the * denotes a highly vibrationally excited HO_2 or the lowest-lying excited electronic state of this peroxy radical. The problem of hydrogen peroxide decomposition is a serious one. We have converted our gas handling systems completely to stainless steel to alleviate any possible problems with

Figure 4: Emission spectrum tentatively attributed to NaO_2 formed in a multiple collision diffusion flame "hydroxide rich" environment characterized by sodium-oxidant interactions.

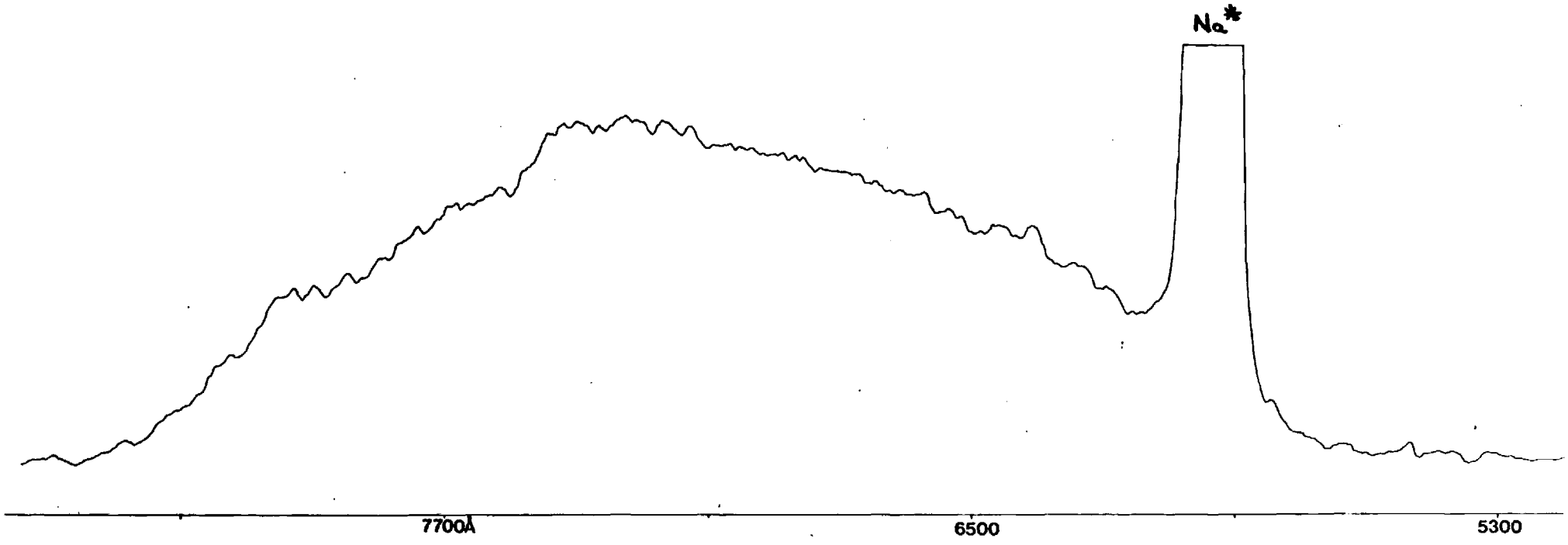
Na*
7700Å
6500
5300

Figure 5: Emission spectrum tentatively attributed to KO_2 formed in a multiple collision diffusion flame "hydroxide rich" environment characterized by potassium-oxidant interactions.

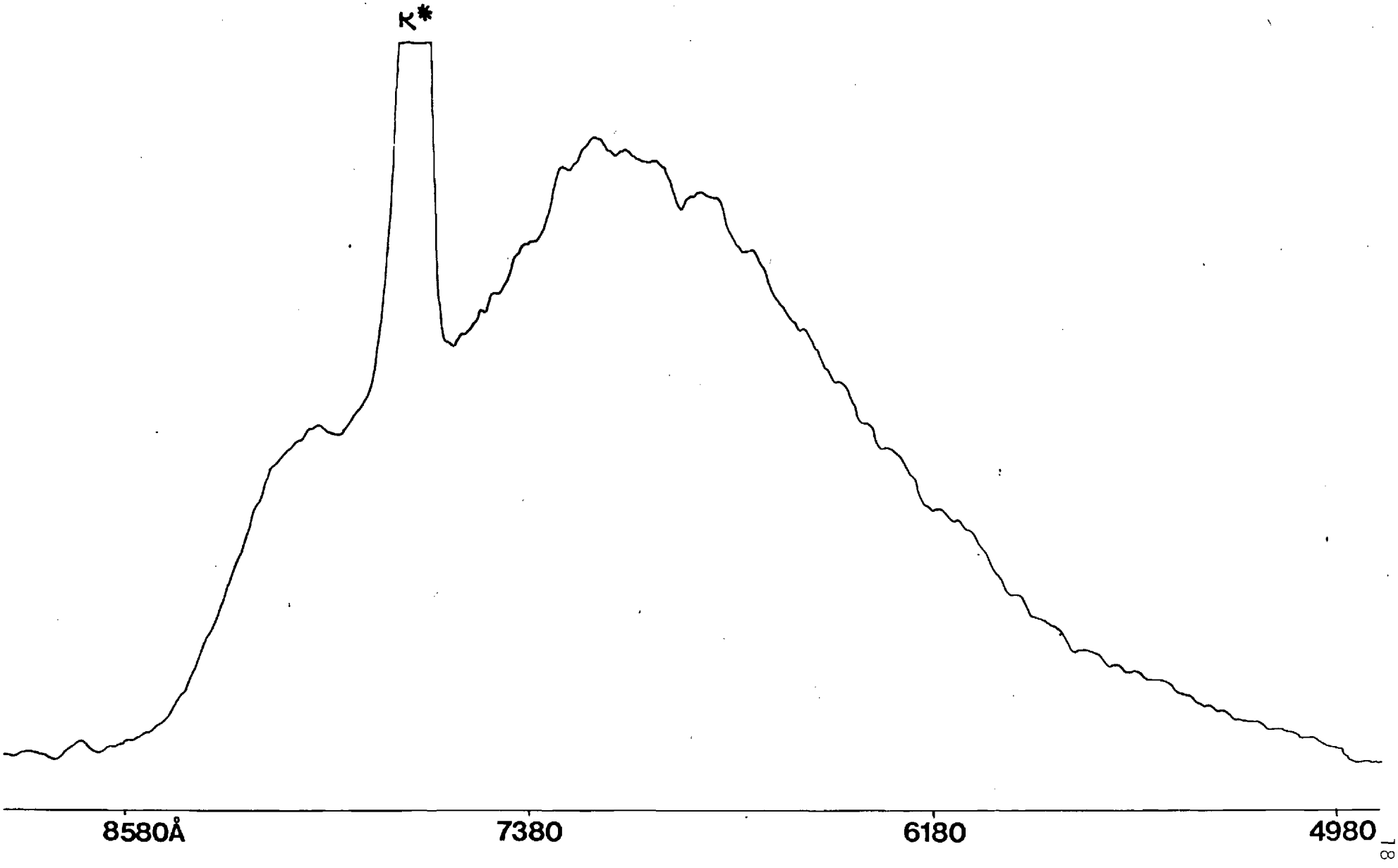
K*
8580Å
7380
6180
4980

the peroxide. Nevertheless, under multiple collision diffusion flame conditions, modest hydroxide decomposition is the source of a quenched KOH* emission spectrum and a dominating metal oxide emission spectrum (Figures 4 and 5).

At a temperature of 320K or less, the vapor pressure of H_2O_2 is not sufficient to produce a KOH emission spectrum of sufficient intensity. Hence methods to increase the H_2O_2 flux into the reaction zone must be devised in order to promote the necessary four-center $K_2 + H_2O_2$ reaction. Thus we have chosen to entrain the hydrogen peroxide in argon so as to increase the relative flux of H_2O_2 into our diffusion flame reaction bulb. Several entrainment configurations were tried in order to develop a stable, readily controllable flow, maintaining a virtually constant H_2O_2 concentration. This effort was also instituted to alleviate problems with blockage of the oxidant nozzle leading to the potassium atmosphere in the diffusion flame bulb. This effort has been successful in that an intense and relatively stable KOH flame has been obtained. In addition, several minor modifications have allowed us to increase the temperature of the diffusion flame bulb and hence the potassium vapor pressure. These modifications produce a considerable increase in the potassium monomers and dimers which are oxidized during reaction, leading to a substantial deposition of oxidized material. In combination with the strong flow patterns created by the entrained hydrogen peroxide (argon), the formation of condensible material was found to lead to a blockage in the exit port of the diffusion flame device, limiting run time to periods at a maximum of one hour. In order to alleviate this problem and allow extended run times and exposures, a catcher plate was incorporated into the diffusion flame bulb. As a given run progressed, a stalactite of what appears to be a potassium hydroxide oxidation product is formed on the catcher plate. This formation was found to have little effect on the KOH flame for periods extending to

2½ hours. During this time, a stalagmite of what also appears to be a material similar to that deposited on the catcher plate fans out and grows up from the oxidant entrance port. The rate of growth of this stalagmite was found to determine the duration of an intense, relatively stable, and reasonably long-lasting diffusion flame.

It appears that additional improvements can be made in the diffusion flame device. Indeed, a configuration has been devised which appears to almost completely alleviate severe particulate formation. This design has been tested for the sodium-hydrogen peroxide system. The intense emission generated from the $Na_2 + H_2O_2$ reaction was maintained for 4½ hours virtually better than doubling all previous run times. The end of the run was signaled by the almost complete oxidation of almost all sodium in the system. During the course of this run several electrooptical scans were taken of the chemiluminescent flame. The resultant NaOH emission spectrum is shown in Figure (6) as it extends at long wavelength to the intense sodium D-line. From the short-wavelength (3465Å) limit of the NaOH chemiluminescent spectrum which is much more intense than any previously obtained, we obtain a new and considerably higher stringent lower bound for the Na-OH bond dissociation energy. This value is now 82.5 kcal/mole (3465Å = 2885/cm^{-1}/349.76 cm^{-1}/kcal = 82.5 kcal/mole) in good agreement with the onset of NaOH photodissociation (82.6 kcal/mole estimated).[18] This new value should be compared to that reported in Appendix A. Indeed the improved diffusion flame device has led to a considerable improvement in our determination of a lower bound for the Na-OH bond energy. The current value is considerably higher than that recommended by the JANAF Tables.

The modification of the diffusion flame device, which in conjunction with other modifications, leads to the substantial improvement just outlined, involves the transfer of the oxidant inlet tube from an entrance through the

Figure 6: NaOH* emission spectrum taken under multiple collision conditions in a diffusion flame device. The spectrum results predominantly from the reaction $Na_2 + H_2O_2 \rightarrow NaOH^* + NaOH$ although some contribution also results from the process $Na + OH + M \rightarrow NaOH^* + M$.


4900
3900
2900
1900

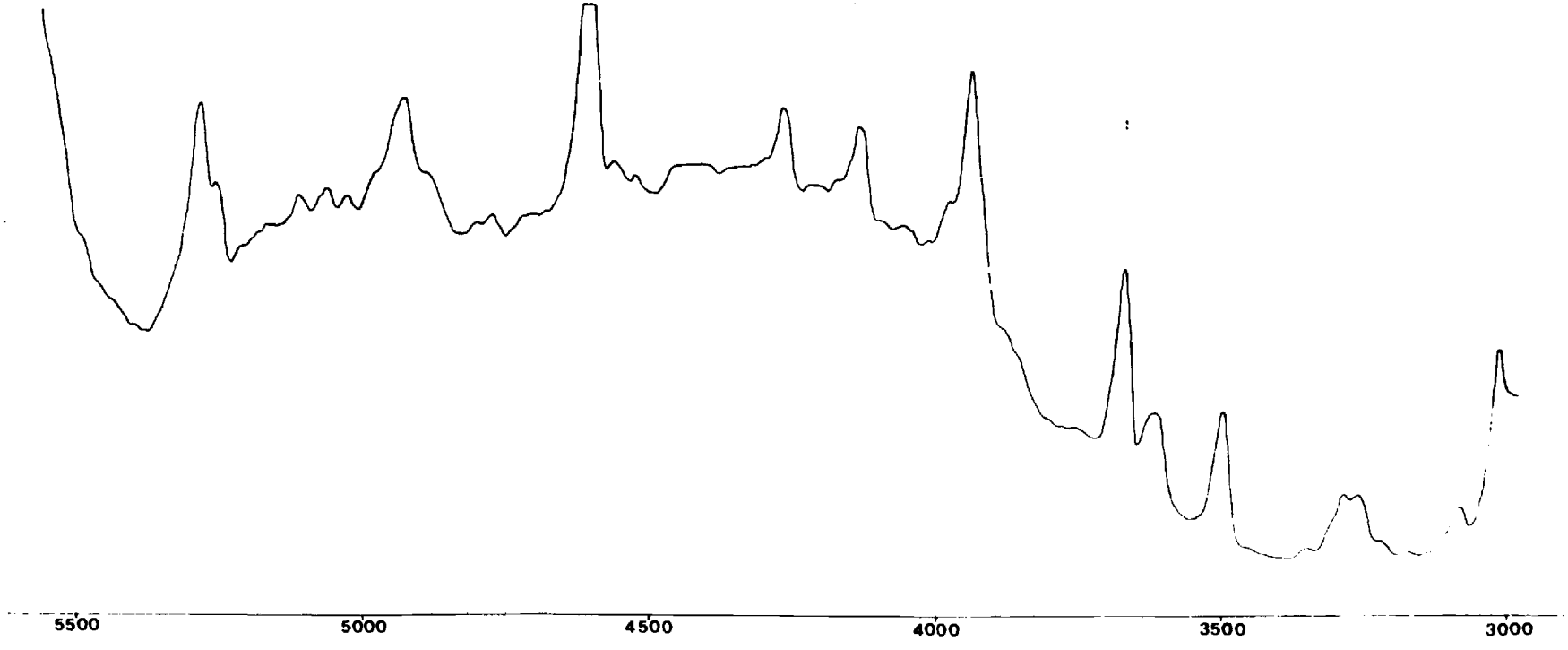
5500
5000
4500
4000
3500
3000

bottom of the diffusion flame device to an entrance at the point R in Figure (3). Hence the oxidant inlet tube no longer passes through the potassium nipple and is oriented at a 45° angle relative to the vertical. This new diffusion flame design has now been tested with potassium and we find that particulate formation can again be minimized with run times remaining on the order of 4+ hours.

The impetus for improving the diffusion flame apparatus is our desire to record the entire KOH emission spectrum on film. We have chosen this approach since we believe, based on a comparison with previous studies of the $K_2 + Cl_2$ reaction,[19] that for this system even slight pressure fluctuations can lead to a masking of important spectral features when running an electro-optical scan. Thus far we have not been successful in our attempts to record the emission spectrum on film, however, several improvements in the optical system should facilitate success. Most important among these is the attainment of a recording film whose reciprocity is commensurate with a 3 to 4 hour run time. This film has been ordered. If we are not successful in recording the entire spectrum on film, we will attempt to record the spectrum in 200Å sections using our optical multichannel analyzer system. The intensity of the KOH flame is now sufficient so as to make experiments with this device feasible.

As we have noted previously (see also Appendix A), the "single collision" KOH emission spectrum (Figure 1) can be used to monitor a set of vibrational quantum levels corresponding to high vibrational excitation in the ground electronic state of KOH. While efforts to improve the quality of the spectrum have taken a "back burner" to our diffusion flame studies, modifications of the single collision system have been undertaken which include the development of a larger and more versatile alkali source. These studies are still in the preliminary stages and will be reported on in conjunction with sodium surface generation in a future topical report.

Alkali Oxide Emission Spectra

Short Summary

The object of this effort is to study the reactions of sodium and potassium with NO_2, N_2O, O_3, and SO_2 and to observe and characterize chemiluminescence from NaO and KO via the reaction of sodium and potassium with N_2O and O_3. We have observed the first electronic emission spectra for NaO and KO resulting from the low pressure "single collision"[17] reaction of sodium and potassium atoms with N_2O. From these studies, preliminary values for the dissociation energies ($D_0^o(NaO) = 70\pm5$, $D_0^o(KO) = 75\pm5$ kcal/mole) of NaO and KO have been obtained. This effort is being extended to the "multiple collision" pressure regime as an aid to the evaluation of molecular constants for NaO and KO and as a means of studying ultrafast energy transfer. Using the current results, the feasibility of laser fluorescence studies is being assessed. As we have alluded to earlier, a major problem in these alkali systems is the formation of extensive particulate matter. This problem is particularly acute for the alkali oxide systems. Termination of a given experiment results largely from particulate formation and the blockage of devices used to transport oxidant to the reaction zone.

The Generation of Alkali Oxide Emission Spectra - Analysis and Experimental Considerations

Two apparatuses have been used to obtain chemiluminescent emission from the alkali oxides under a variety of conditions which range from very low pressure ($<10^{-4}$ torr) single collision studies (bond energies for NaO, KO) through stages of pressure increase which promote changes in the chemiluminescent emission spectra resulting from relaxation and rapid energy transfer. Based on previous studies, the combination of techniques used here should be conducive to the determination of molecular constants and the assessment of rapid intra- and inter-molecular energy transfer.

"Single Collision Studies"

The sodium oxidation with N_2O is characterized by a rather intense red flame under single collision conditions. The corresponding spectrum is depicted in Figure 7 and identified features (bands), which correlate in part with a higher pressure multiple collision spectrum are listed in Table I. It appears that these bands are associated with states whose vibrational level spacings are approximately 520 and 460 cm^{-1} respectively; however further confirmations will be obtained upon studying the sodium-ozone reaction. A further improvement in the signal-to-noise of the NaO* emission spectrum should also be obtained upon operating at a higher sodium flux, a project in which we are currently involved.

The single collision potassium oxidation with N_2O, like sodium, is characterized by a rather intense red flame, the spectrum of which is shown in Figure 8. Although the structure associated with this emission is, as yet, marginally resolved, the emission region[5] and the combination with the results previously discussed for Na-N_2O oxidation lead us to associate the emission with KO*. Under single collision conditions the reactions leading to NaO* and KO* must be

$$Na,K + N_2O \longrightarrow NaO^*,KO^* + N_2 \qquad (3)$$

An analysis of the spectra in Figures 7 and 8, considering energy balance, yields a K-O bond energy of 75±5 kcal/mole and an Na-O bond energy of 70±5 kcal/mole. Both of these bond energies are uncorrected for the activation energies of the Na-N_2O and K-N_2O reactions which may be quite significant in view of the small negative electron affinity of N_2O. The value for the K-O bond energy should be compared to the "estimate" of Herm and Herschbach[20] (71+3 kcal/mole) whereas that for NaO should be compared to the thermochemical

Figure 7: Emission spectrum associated with the reaction $Na + N_2O \rightarrow NaO^* + N_2$ under single collision conditions.

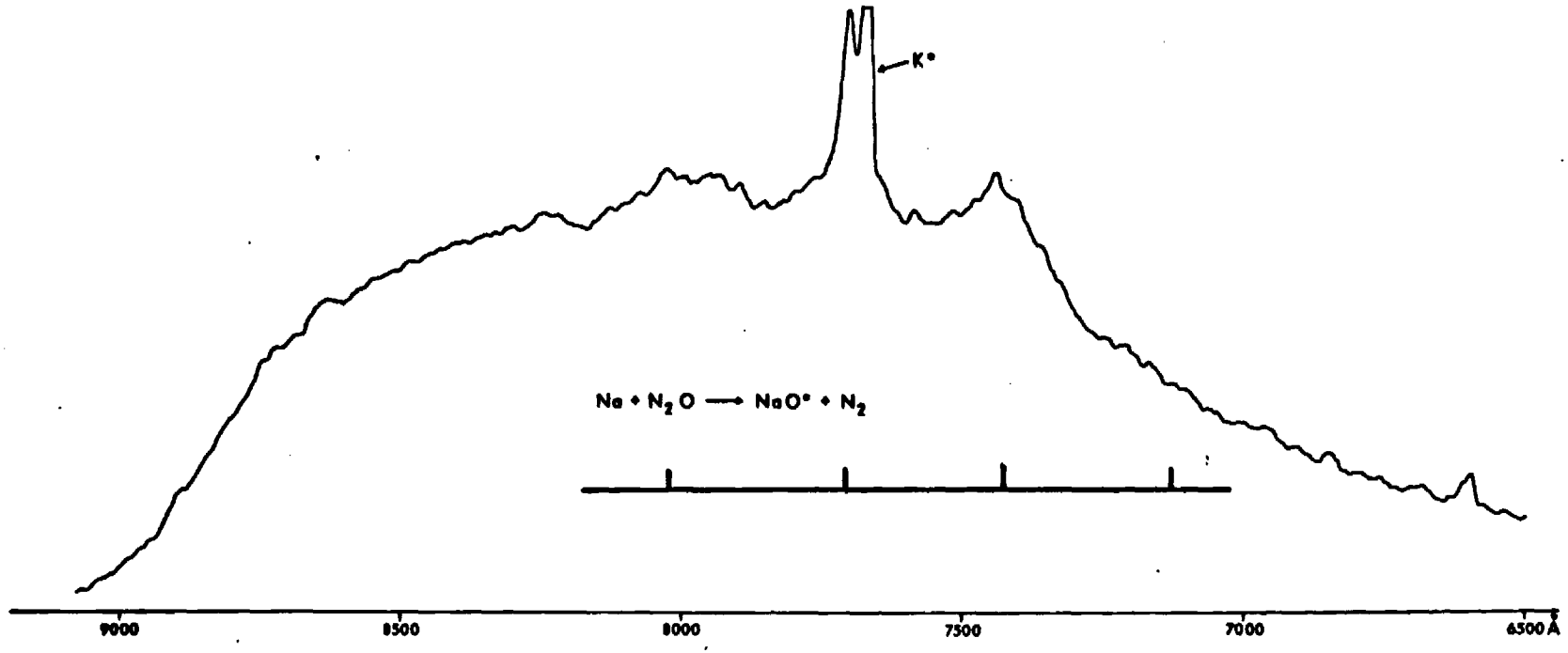
K*
Na + N2O ⟶ NaO* + N2
9000
8500
8000
7500
7000
6500 Å

Table I

Observed NaO* Emission Bands

$Na + N_2O \longrightarrow NaO^* + N_2$ [a]

λ(Å)	$\nu(cm^{-1})$	$\Delta\nu(cm^{-1})$
(6932Å)[b]	14422	
		460
7160Å	13962	
		456
7402Å	13506	
		517
7697Å	12989	
		527
8022Å	12462	

a. See chemiluminescent spectra - Figures 7 and 10

b. Observed in multiple collision chemiluminescent spectrum - Figure 10

Figure 8: Emission spectrum associated with the reaction $K + N_2O \rightarrow KO^* + N_2$ under single collision conditions.

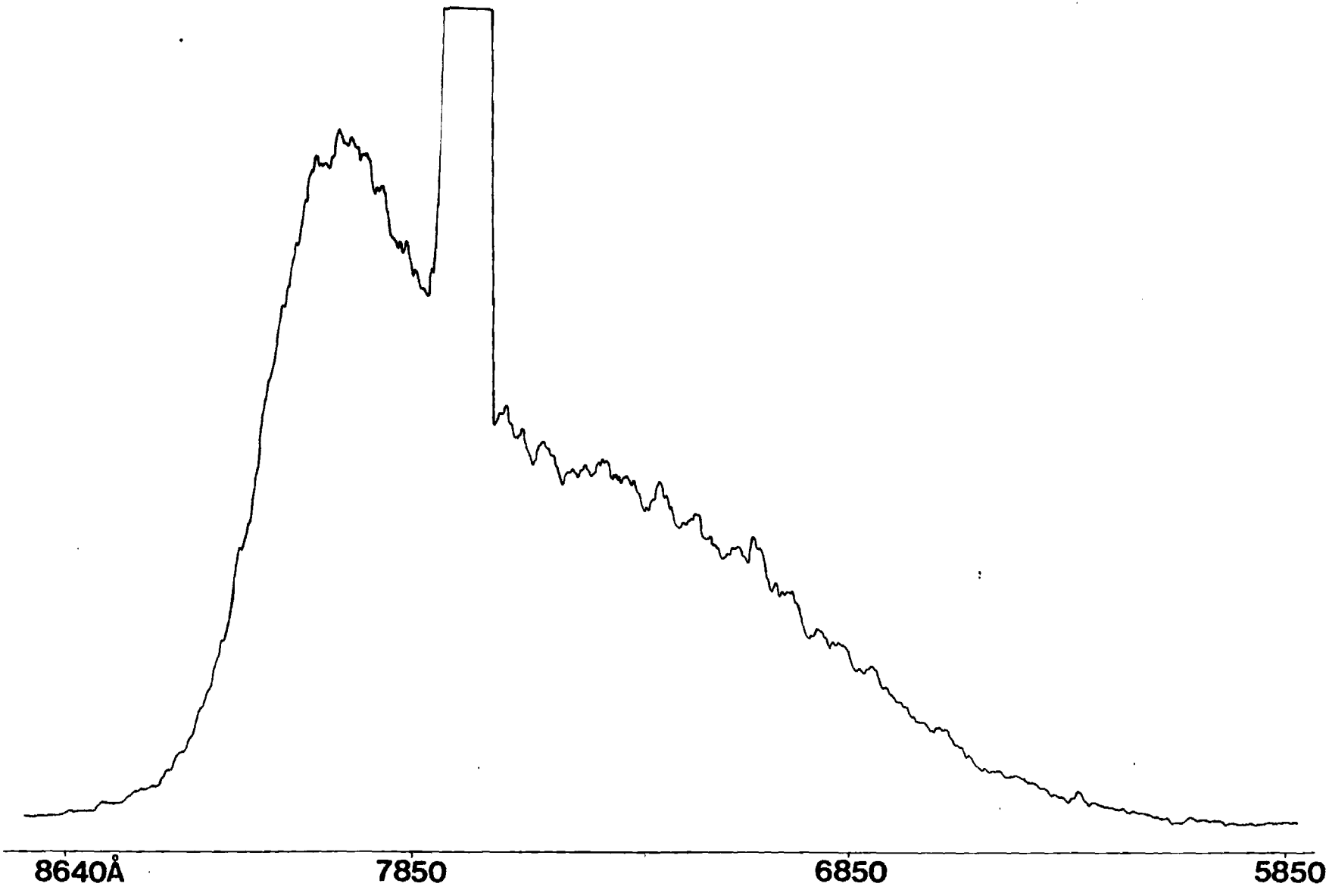
8640Å
7850
6850
5850

value of Murad and Hildenbrand[21] (60±3 kcal/mole). Our current results would indicate that the K-O and Na-O bond energies are quite comparable. These results represent the first direct experimental confirmation of the K-O and Na-O bond energies. They indicate that the K-O bond energy is approximately that estimated by Herm and Herschbach whereas the Na-O bond energy may be somewhat higher than previously determined. Further confirmation of the bond dissociation energies will also be obtained through use of the alkali atom-ozone metathesis and the measurement of the temperature dependence[22] of the N_2O- and O_3-alkali atom reactions.

It should also be noted that the onset of the emission in Figure 7 is some 900Å to the red of that in Figure 4. If both spectra resulted from NaO or NaO_2 emission, it would be difficult to explain this difference in onset. Therefore, we suspect that the spectrum which results from sodium oxidation in a hydroxide environment does not result from the same emitter as that characterizing the sodium-N_2O system. Similar comments can also be made with regard to Figures 8 and 5 and the K-N_2O system. Based upon the available literature which deals with the alkali monoxides (see enclosed reprint) and the bonding characteristics of the series of molecules AO_2 where A=F,Cl,H,Na, and K,[23] we tentatively correlate the emission, associated with sodium and potassium oxidation in a hydroxide environment, with NaO_2 and KO_2.

We have studied the single collision oxidation of equilibrium sodium (atom + 2% dimer) vapors with NO_2 finding this system produces only dark (no visible light emission) ground electronic state products. Similar results have not also been obtained for the reaction of sodium (atom + dimer) with SO_2. The single collision oxidation of equilibrium potassium (atom + 1.5% dimer) vapors with NO_2 and SO_2 also produces only ground electronic state products.

Recently we have constructed and are in the process of testing a new larger and more versatile oven design for the study of alkali oxide and hydroxide chemiluminescence under single collision conditions. Tests thusfar indicate that this device, which operates with a considerably larger alkali charge than the oven systems typically used in beam-gas chemiluminescent studies, produces a considerably higher and more stable alkali metal flux (monomer + dimer). This is the first step in obtaining a considerable increase in the intensity of alkali monoxide spectra generated under single collision conditions. The purpose of this effort is primarily to allow a finer determination of the NaO and KO dissociation energies and to facilitate the attainment of well resolved spectra for these species, considerably improving current signal to noise. Because of severe particulate formation, the diffusion flame device now employed to study the alkali hydroxides is not appropriate for the study of the alkali oxides in its present configuration. A dark brown polymeric material quickly condenses during reaction, blocking the oxidant entrance nozzle (Figure 3), preventing the oxidant flow, and hence extinguishing chemiluminescence.

"Multiple Collision Studies"

Although the study of the Na,K + N_2O reactions is not yet amenable to a diffusion flame device, we have been successful in devising a system to study these reactions under multiple collision conditions. A schematic of the oven system is presented in Figure 9. There are two important features. In order to prevent pronounced particulate formation, the oxidant is introduced via a nozzle offset and perpendicular to an entrained alkali metal flow. Although the alkali metal exits through a nozzle device above a containment crucible, it is still entrained by an argon flow concentric to the nozzle. Note that this design is in contrast to the normal multiple

Figure 9: Schematic of apparatus for the study of the multiple collision processes $Na,K + N_2O \rightarrow NaO^*,KO^* + N_2$.

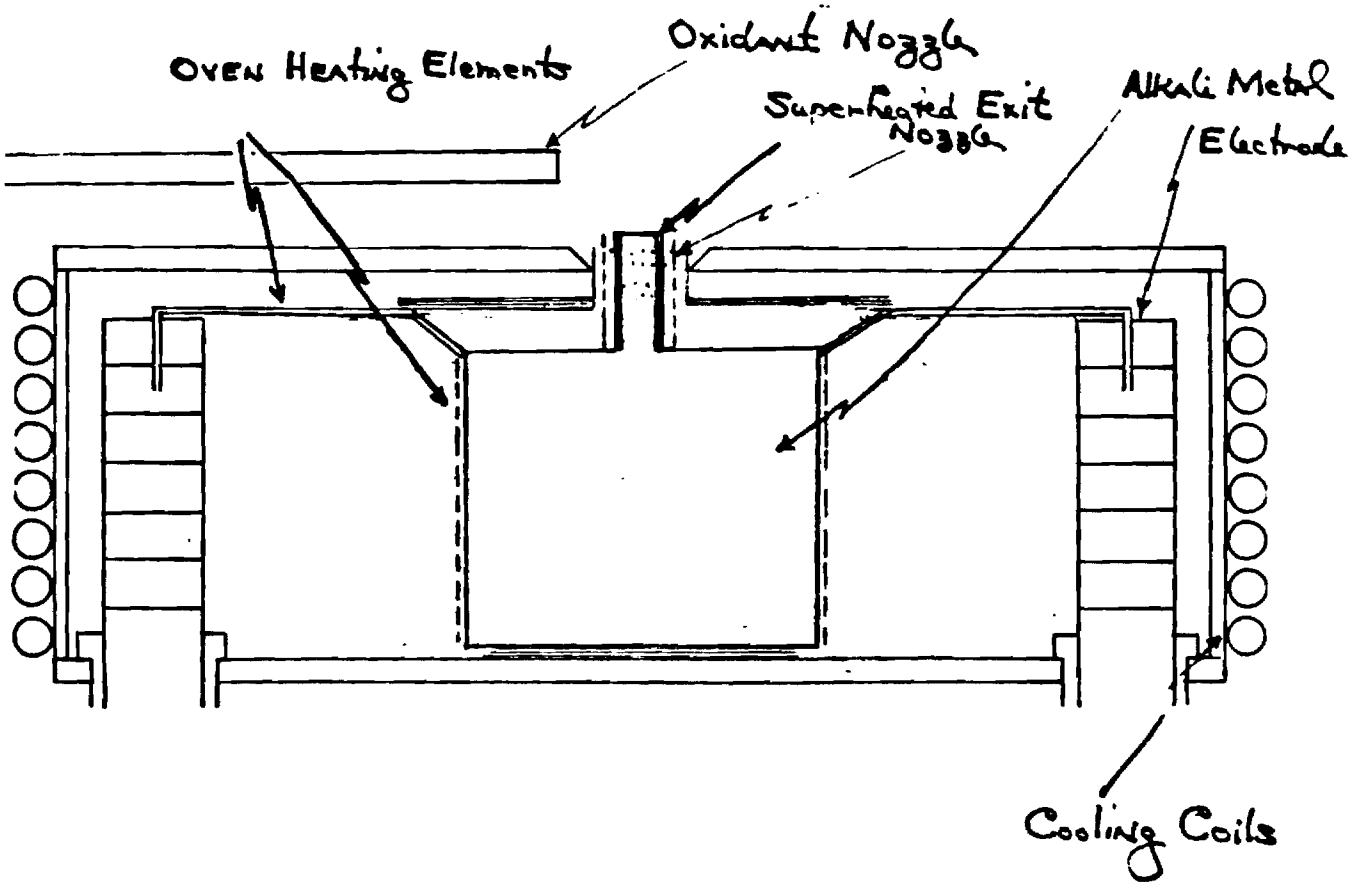
Oven Heating Elements
Oxidant Nozzle
Superheated Exit Nozzle
Alkali Metal Electrode
Cooling Coils

collision device[24] where the entrained metal is oxidized using a concentric ring injector. The injector design quickly leads to pronounced particulate formation and hence is characterized by extremely short run times. Using the perpendicular entrained metal-oxidant flow scheme, one is able to run for several hours without encountering extensive particulate formation. Given long run times, there is yet another problem associated with the higher alkali metal reactant concentrations characteristic of the multiple collision system. The transition moments associated with alkali metal excited electronic states are among the largest known. Therefore the collisional excitation of alkali dimer electronic emission systems can provide a strong interference to the ready analysis of alkali oxide emission features. For this reason, the nozzle through which the alkali metal exits is heated to 650°C to induce dissociation of the exiting alkali metal dimers. With this precaution, the multiple collision spectra are characterized by alkali atomic and alkali oxide emissions. The spectrum obtained for the Na-N_2O system is depicted in Figure 10. Note the three pronounced bands at 7160, 7400, and 7700Å and their correlation with the NaO* single collision spectrum (Figure 7 - Table I). Also note the relative intensity of these bands which indicates the occurance of rapid energy transfer involving the NaO excited electronic state.[25] This multiple collision NaO spectrum and the similar spectrum for KO will be the subject of further experiments and study.

Sodium Cluster Oxidation

Short Summary

The object of this task is to evaluate the nature of sodium oxidation in the intermediate region between the gas and surface phase. The products of sodium cluster oxidation are being characterized through direct observation of the chemiluminescent emission for highly exothermic processes,

Figure 10: Chemiluminescent spectrum resulting from the process $Na + N_2O + Ar \rightarrow NaO^* + N_2 + Ar$.

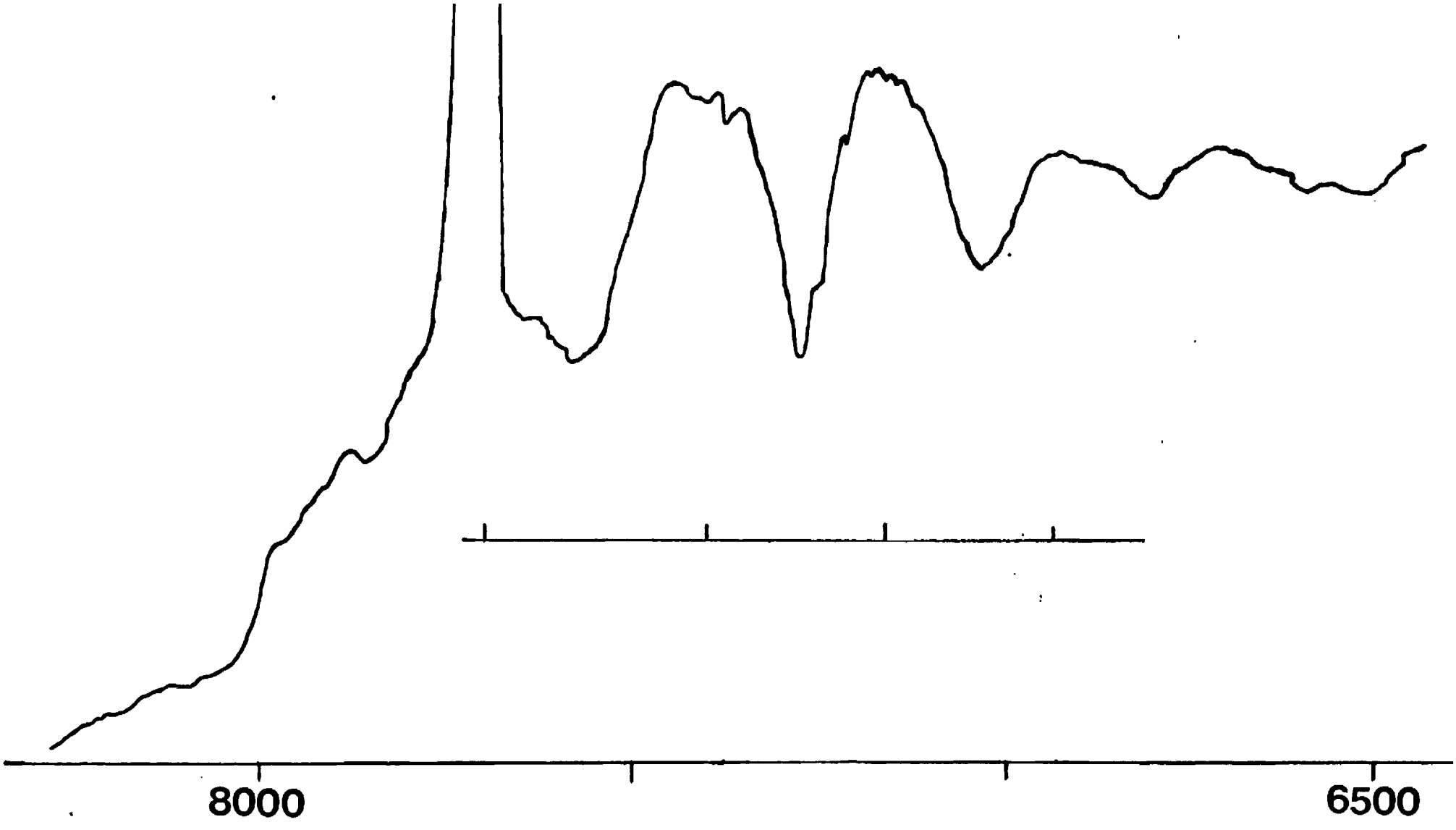
8000
6500

through a newly developed electron impact excitation technique, and through mass spectrometric sampling of the oxidation region. Thusfar, both the halogen and SO_2 oxidation of sodium clusters has been under study.

Sodium Cluster Oxidation - Analysis and Experimental Considerations

We have constructed an apparatus for the study of sodium cluster oxidation. The emphasis in our sodium cluster oxidation studies has been (1) the characterization of highly exothermic chemiluminescent processes associated with sodium cluster-halogen atom oxidation, (2) the characterization of highly exothermic channels for the oxidation of sodium clusters with SO_2, (3) the development of diagnostics for the detection of product ion formation in sodium cluster oxidation, (4) the development of electron impact excitation techniques as a means of probing the dark products of chemical reaction (species which do not chemiluminescence in the visible) and the development of appropriate mass spectrometric probes for the reaction zone.

"Design of Cluster Oxidation Apparatus"

The apparatus used for the study of sodium cluster oxidation is shown schematically in Figure 11. Briefly, the system consists of oven and reaction chambers connected by a variable sized channel 20 mm in length which, in the present experiments, is ~6 mm in diameter.

The oven depicted in Figure 11 is a stainless steel (316) double oven used for the supersonic expansion of alkali metals-sodium in the current study. It will be discussed in more detail shortly. It consists of a large backing oven and smaller frontal nozzle device. In general, the nozzle chamber is operated at a temperature 50 to 100 degrees hotter than the backing oven. The backing oven is typically operated at a temperature between 850 and 1000K corresponding to a sodium vapor pressure between 20

Figure 11: Schematic of apparatus used for sodium cluster oxidation.

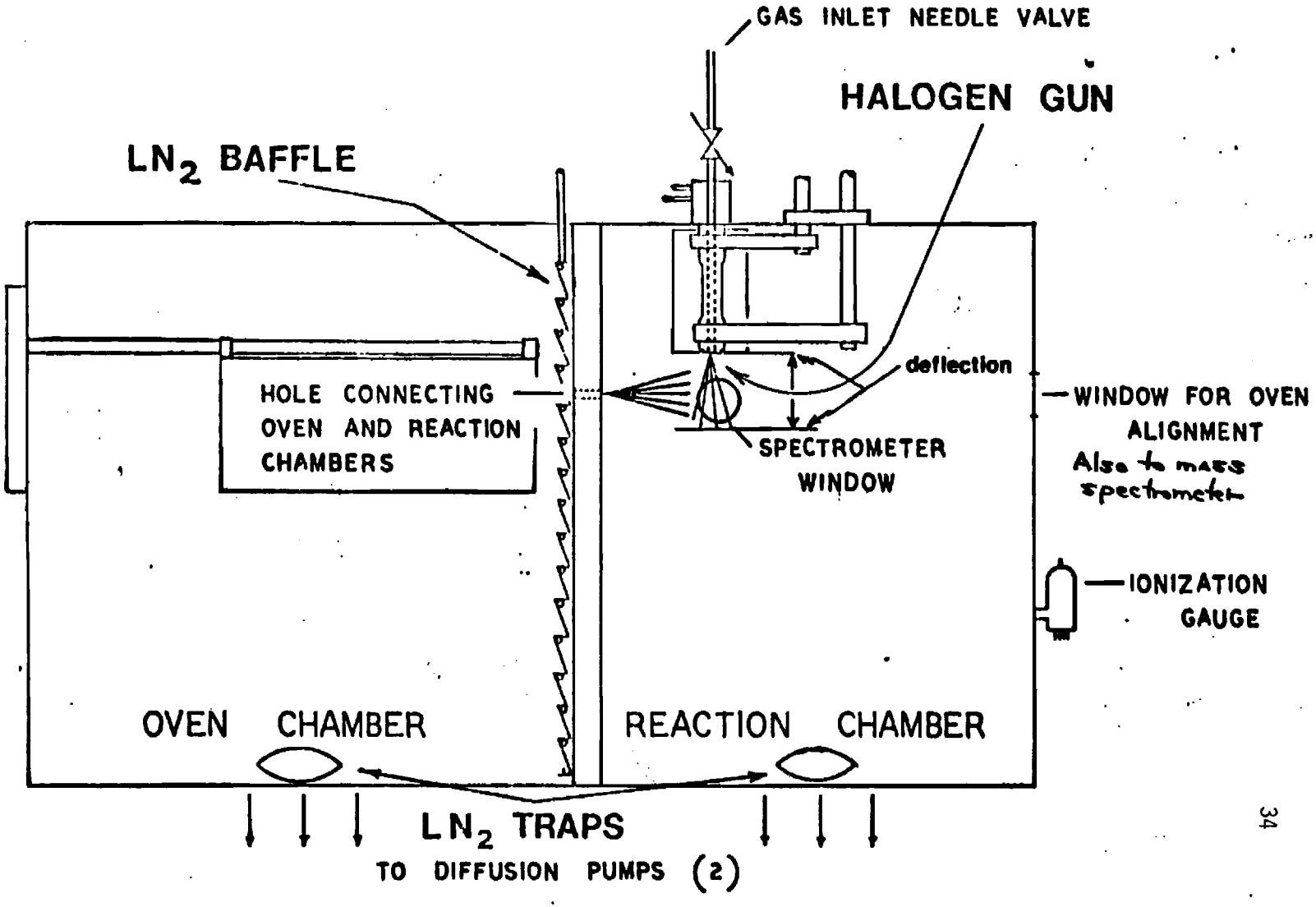
GAS INLET NEEDLE VALVE
HALOGEN GUN
LN2 BAFFLE
deflection
HOLE CONNECTING OVEN AND REACTION CHAMBERS
SPECTROMETER WINDOW
WINDOW FOR OVEN ALIGNMENT
Also to mass spectrometer
IONIZATION GAUGE
OVEN CHAMBER
REACTION CHAMBER
LN2 TRAPS
TO DIFFUSION PUMPS (2)

and 120 torr. Temperatures were measured with chromel alumel thermocouples. In order to facilitate smooth oven operation and to control aerosol formation, a "splash baffle" is inserted between the backing oven and nozzle chamber. This splash baffle is a small tantalum baffle perforated with several small pinholes. It controls the passage of sodium vapor from the large backing oven to the frontal nozzle chamber. To prepare for a given run, the oven was heated slowly to the melting point of sodium and then (2K/min) up to 550K. During this gradual heating, large quantities of hydrogen were released by the sample. Based on previous experience, when hydrogen evolution was complete as evidenced by the system pressure, the oven was quickly brought to the desired operating conditions. The nozzle diameter was typically 0.25 mm. The separation between the nozzle orifice and fluorescence zone is approximately 17 cm. The molecular beam density produced in the fluorescence zone is $\sim 10^{13}$ molecules/cm^3.

The halogen oxidation studies were carried out with the halogen gun depicted in Figure 11, typically operated at 1850K. It consists of an upper water cooled copper jacket surrounding a 6 mm stainless tube which extends 12.5 mm from the copper jacket; this assembly is connected to a carbon rod with 6 mm channel and small 1.5 mm end-on orifice. The "clamped" carbon rod is heated to and maintained at 1850K by passing a current of 500 amps at 2 volts. At these temperatures chlorine molecules passing through the gun should be 99% converted to chlorine atoms. The halogen gun required extensive outgassing before use and was typically brought to the operating temperature a minimum of six hours before a given run. In order to conduct experiments with SO_2, the halogen gun was replaced by a rather simple inlet device which could also be used to provide a route for SO_2 contamination with chlorine.

The system is operated in a beam-gas configuration. Pressures in the reaction chamber never exceeded 2×10^{-5} torr. In order to maintain these conditions and insure smooth oven operation, liquid nitrogen cooled baffles were operative above both the oven chamber and reaction chamber diffusion

pumps and a liquid nitrogen cooled shield was placed at the front wall of the oven chamber. The chemiluminescence is monitored from 2200 to 9000Å using a spex 1 meter spectrometer equipped with a Bausch and Lomb 1200 groove/mm grating blazed at 5000Å. An RCA 4840 photomultiplier cooled by the liquid nitrogen blow-off from the beam-gas system was used as the detector. The photomultiplier output was amplified by a partially damped Keithley 417 fast picoammeter which drove a Leads and Northrup Speedomax G recorder.

"Detail of Sodium Oven Design"

The oven used as the beam source for the sodium cluster experiments is shown in Figure 12. It is a basic two chamber design, cut from a single piece of 316 stainless steel (eliminating the need for welded joints). A constriction separates the nozzle chamber from the main body in order to facilitate individual temperature control of the two chambers. A replacable stainless steel nozzle is bolted onto the nozzle chamber. The vacuum seal is made with a 0.010" thick tantalum or copper gasket and a knife edge on the oven. The sodium sample, typically 100 grams of metal, is loaded into the main chamber through a large opening in the back. The opening is closed with a stainless steel flange. The vacuum seal is again made with a 0.010" thick tantalum or copper gasket and knife edge. The four screws which mount the nozzle and the six screws which mount the rear flange must maintain pressure on the tantalum gaskets throughout the run. They must be able to withstand high temperature without softening. Stainless steel (10-32) cap screws are used but these have a tendency to be welded into the oven by the combination of heat and pressure. To prevent this, a light coat of molybdenum sulfide based lubricant (Dow Corning, Molykote® Type L paste) is painted onto each screw before use. A small piece of tantalum sheet loosely covers the nozzle chamber where it connects to the main chamber. This serves as a splash baffle

Figure 12: Oven design for the supersonic expansion of sodium metal.

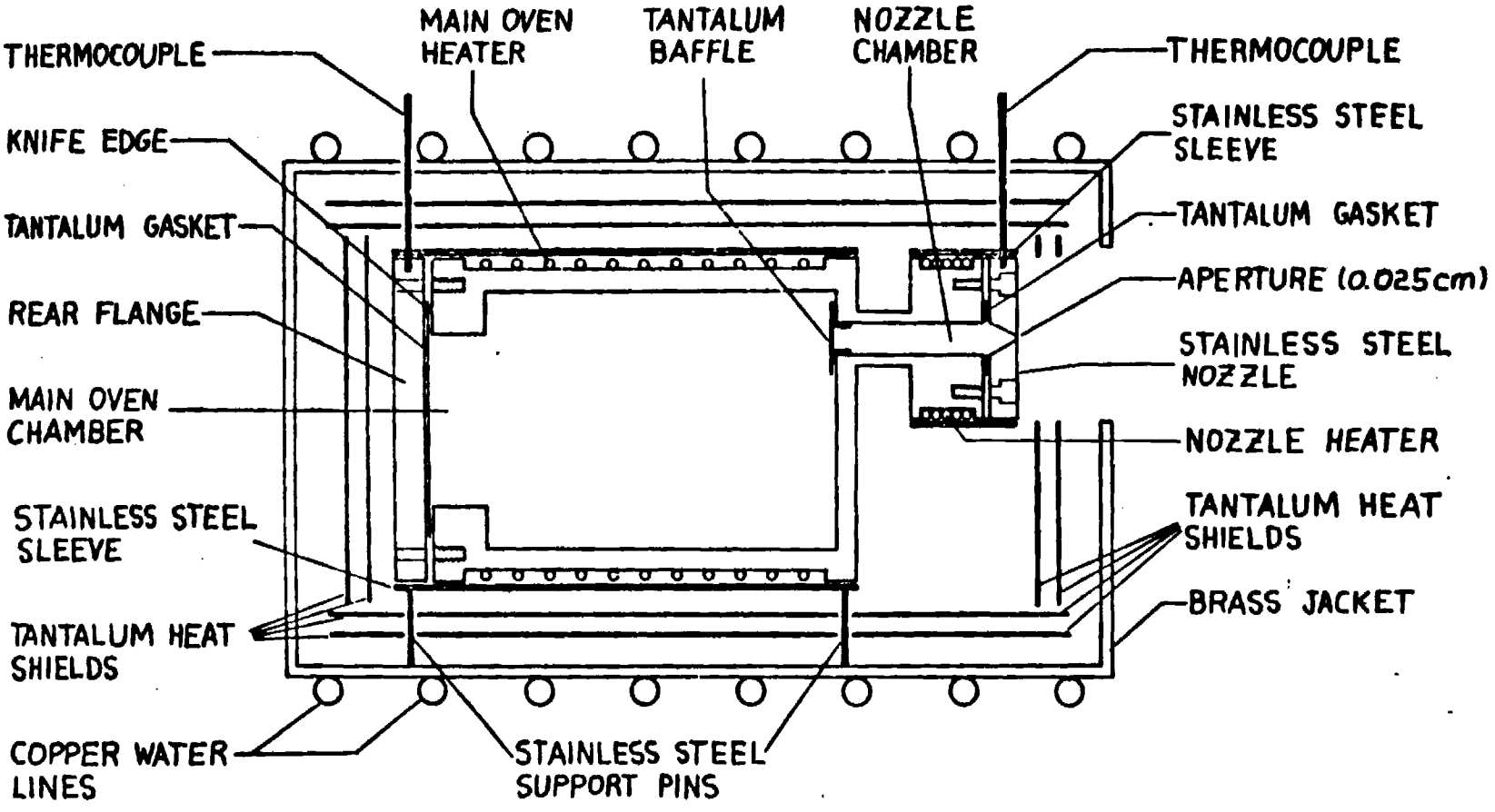
THERMOCOUPLE
MAIN OVEN HEATER
TANTALUM BAFFLE
NOZZLE CHAMBER
THERMOCOUPLE
KNIFE EDGE
STAINLESS STEEL SLEEVE
TANTALUM GASKET
TANTALUM GASKET
REAR FLANGE
APERTURE (0.025cm)
MAIN OVEN CHAMBER
STAINLESS STEEL NOZZLE
NOZZLE HEATER
STAINLESS STEEL SLEEVE
TANTALUM HEAT SHIELDS
BRASS JACKET
TANTALUM HEAT SHIELDS
COPPER WATER LINES
STAINLESS STEEL SUPPORT PINS

which prevents liquid metal from entering the nozzle as the oven is being heated.

The main chamber, which is operated at temperatures up to 1100K, is wrapped with 15 turns of thermocoax heating cable (Amprex Corp. IN20). The wrapped body is contained in a 1/16" wall stainless steel sleeve. The nozzle, which is operated at temperatures up to 1200K, is wrapped with a separate heating element consisting of a length of 0.025" diameter tantalum wire, sheathed with alumina beads for electrical insulation. The nozzle chamber and the tantalum wire heater are also housed in a 1/16" wall stainless steel sleeve. The temperatures of the main chamber and the nozzle chamber are monitored with chromel-alumel thermocouples (Omega Engineering model 4TJ36-CASS-316U-6") located as shown in Figure 12.

The oven and heaters are surrounded by two layers of tantalum shielding and then by a brass jacket which is wrapped with copper water lines for cooling. The oven is supported from the brass jacket by 6 stainless steel screws. The oven is mounted on a flange located directly to the rear (this would be to the left in Figure 11). Water, power and thermocouple connections are all made to this flange. The sodium oven is then mounted onto the vacuum system.

"Oxidation Studies"

Initial experiments conducted to study sodium cluster oxidation have involved cluster oxidation with the halogens. These experiments have not only allowed us to test the metal cluster oxidation system but also have facilitated the characterization of a potentially important factor in energy generating systems. It has currently been suggested that chlorine interacts with the alkali impurities in a combustion stream, resulting in the formation of alkali chloride complexes which then repartition with O,S,H,C,Al, or Si ash particulates. Thus, the influence of chlorine on the formation of alkali clusters and the subsequent reaction of these clusters with SO_2 should be

evaluated in the intermediate region between the gas and surface phases. Our initial research thrust has involved cluster oxidation with chlorine, bromine, or iodine atoms. Sample spectra for the chlorine and bromine system are shown in Figures 13, 14, and 15. The spectra shown in these figures are associated in large part with Na_2^* emission (a more detailed discussion can be found in Appendix B); however, recent experiments (see also following discussion) have tested positively for ion formation and chemiluminescence via electric field deflection of the chemiluminescent product beam.

We have now carried out preliminary studies of sodium cluster oxidation with SO_2. The results thusfar are quite intriguing as they apply to our previous discussion. Using an SO_2 inlet system slightly contaminated with halogen we generate the emission spectrum depicted in Figure 16. The observation of chemiluminescent emission is in contrast to the dark reactions of sodium atoms and dimers with SO_2 and, in addition, the emission spectrum shown in Figure 16 is distinct from that obtained for sodium atom and dimer oxidation with N_2O. Using a source exclusively limited to SO_2 oxidation, we find that the $Na_x + SO_2$ system is <u>dark</u>. The observed emission, if any, is depicted as the dashed background spectrum in Figure 16. The spectrum depicted in Figure 16 must result from a halogen catalyzed process. The emission bears little resemblance to that characterizing Na_x + halogen atom or dimer oxidation, thus it must result from the highly exothermic interaction of Na_x with a halogen-SO_2 complex. We feel that this result may be of significance in the assessment of the influence of chlorine on the formation of alkali chloride cluster intermediates and the subsequent reaction of these clusters with SO_2. In the near future (see following discussion) we anticipate further probes of this system in conjunction with our mass spectrometric and electron impact excitation capability.

Figure 13: Chemiluminescent spectra associated with the reactions (a) Na_2 + $Cl_2 \rightarrow NaCl^* + NaCl$ and (b) $Na_x + Cl \rightarrow (Na_2^* \ldots) + NaCl$ taken under single collision conditions. The spectrum (b) represents the first example of chemiluminescent spectra associated with metal cluster oxidation.

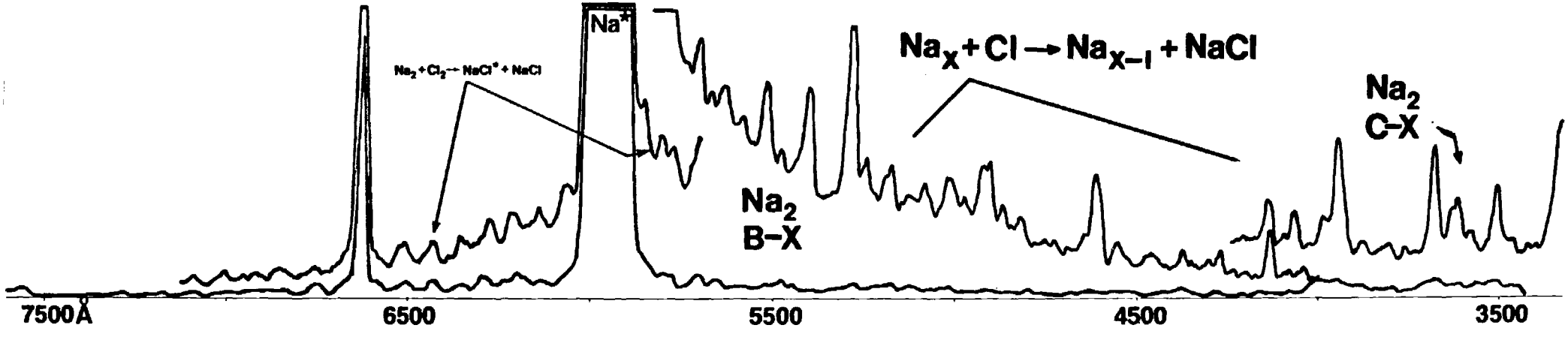
Na*
$Na_2 + Cl_2 \rightarrow NaCl^* + NaCl$
$Na_X + Cl \rightarrow Na_{X-1} + NaCl$
Na_2 B–X
Na_2 C–X
7500Å
6500
5500
4500
3500

Figure 14: Chemiluminescent spectra associated with the reactions $Na_x (x \geq 3)$ + Cl → $(Na_2^* ...)$ + NaCl taken under single collision conditions (continuation of Fig. 13).

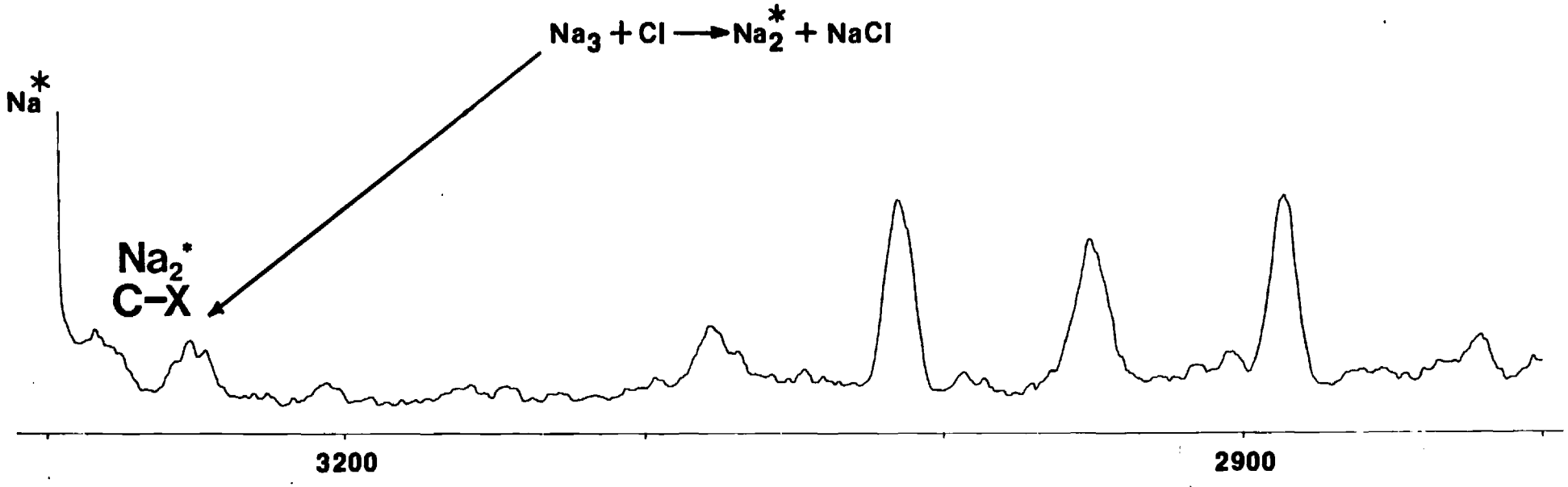
$Na_3 + Cl \rightarrow Na_2^* + NaCl$
Na^*
Na_2^*
C–X
3200
2900

Figure 15: Chemiluminescent spectra associated with the reactions $Na_x (x \geq 3)$ + Br → (Na_2*...) + NaBr taken under single collision conditions.

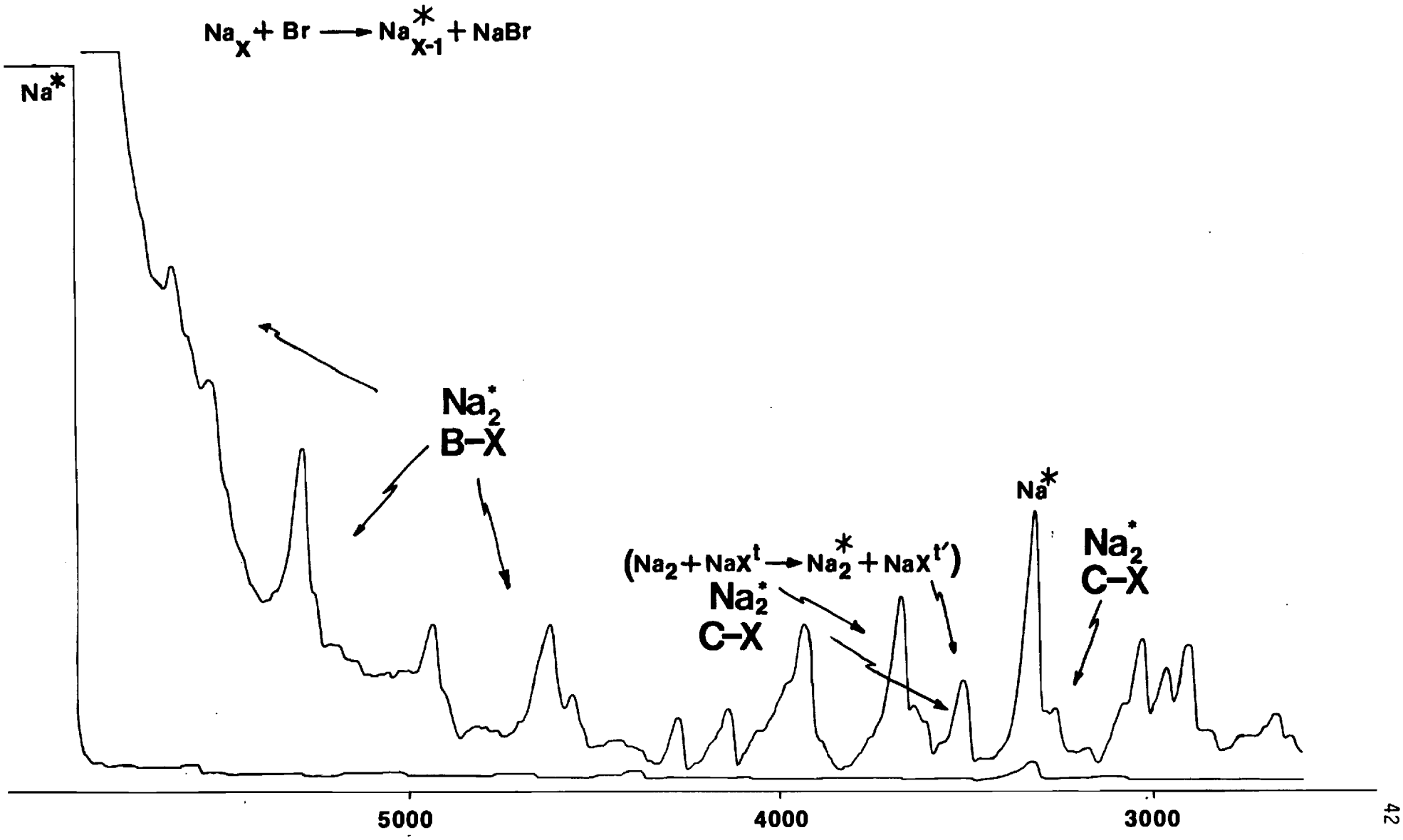
$Na_X + Br \longrightarrow Na^*_{X-1} + NaBr$
Na*
Na_2^*
B–X
$(Na_2 + NaX^t \longrightarrow Na_2^* + NaX^{t'})$
Na_2^*
C–X
Na*
Na_2^*
C–X
5000
4000
3000

Figure 16: Chemiluminescent emission from Na_x-SO_2 and Na_x-SO_2 (+ chlorine impurity)

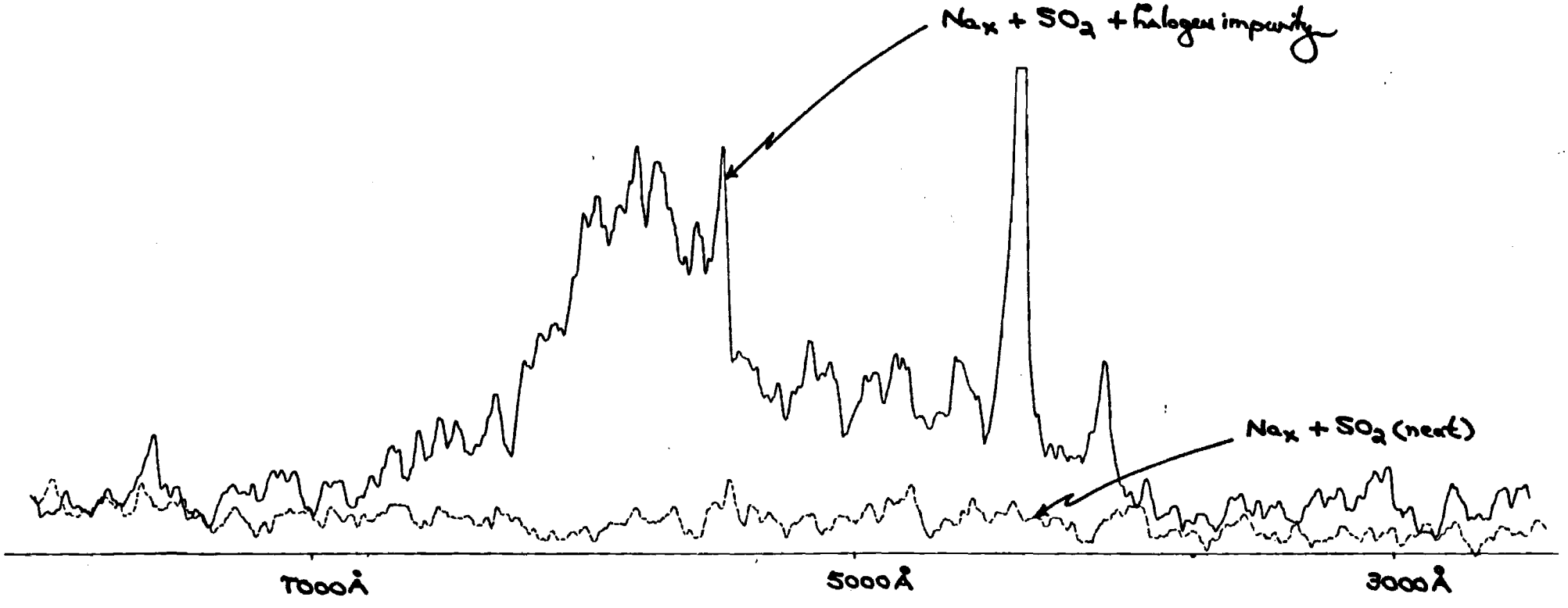
$Na_x + SO_2$ + halogen impurity
$Na_x + SO_2$ (neat)
7000Å
5000Å
3000Å

Notable in the apparatus depicted in Figure 11 are two deflection plates. The purpose of these plates is the inhomogeneous electric field deflection of positive or negative ions formed in reaction. This deflection device has now indicated that ions are formed in the sodium cluster-halogen atom reaction system. The position of the deflection plates is such as to surround the reaction zone. Fields of up to 14,000 volts have now been applied between the two plates. We intend to use this deflection capability in conjunction with our mass spectrometric detection capability to facilitate the direct and ready identification of the ionic products formed in reaction (see also following discussion).

There is an important further aspect of the newly installed deflection device. In conjunction with the halogen gun, which not only dissociates halogen molecules but also produces copious quantities of electrons, the potential exists for electron impact induced excitation. The potential between the upper (below halogen gun) and lower deflection plates is readily varied and either can be set to a positive voltage of up to 14,000 volts with respect to the other at ground. Based on the plate separation, the field induced is approximately 7000 volts/cm. The spectra shown in Figure 17 indicate the results of this exercise when the lower plate is at a given positive voltage with respect to a grounded upper plate. The lower-most spectrum corresponds to the observed chemiluminescent emission when sodium clusters are oxidized with bromine atoms. The intermediate spectrum corresponds to that observed when a 10,000 volt field is applied and the upper spectrum corresponds to the application of a 14000 volt field. Note that a significant field dependent increase in spectral intensity is observed over the region 3600 ± 200Å. This increase in spectral emission intensity is due to electron impact excitation. The effect is more pronounced if the upper plate

Figure 17: Chemiluminescence from Na_x + Br as a function of deflection fields showing electron impact excitation.

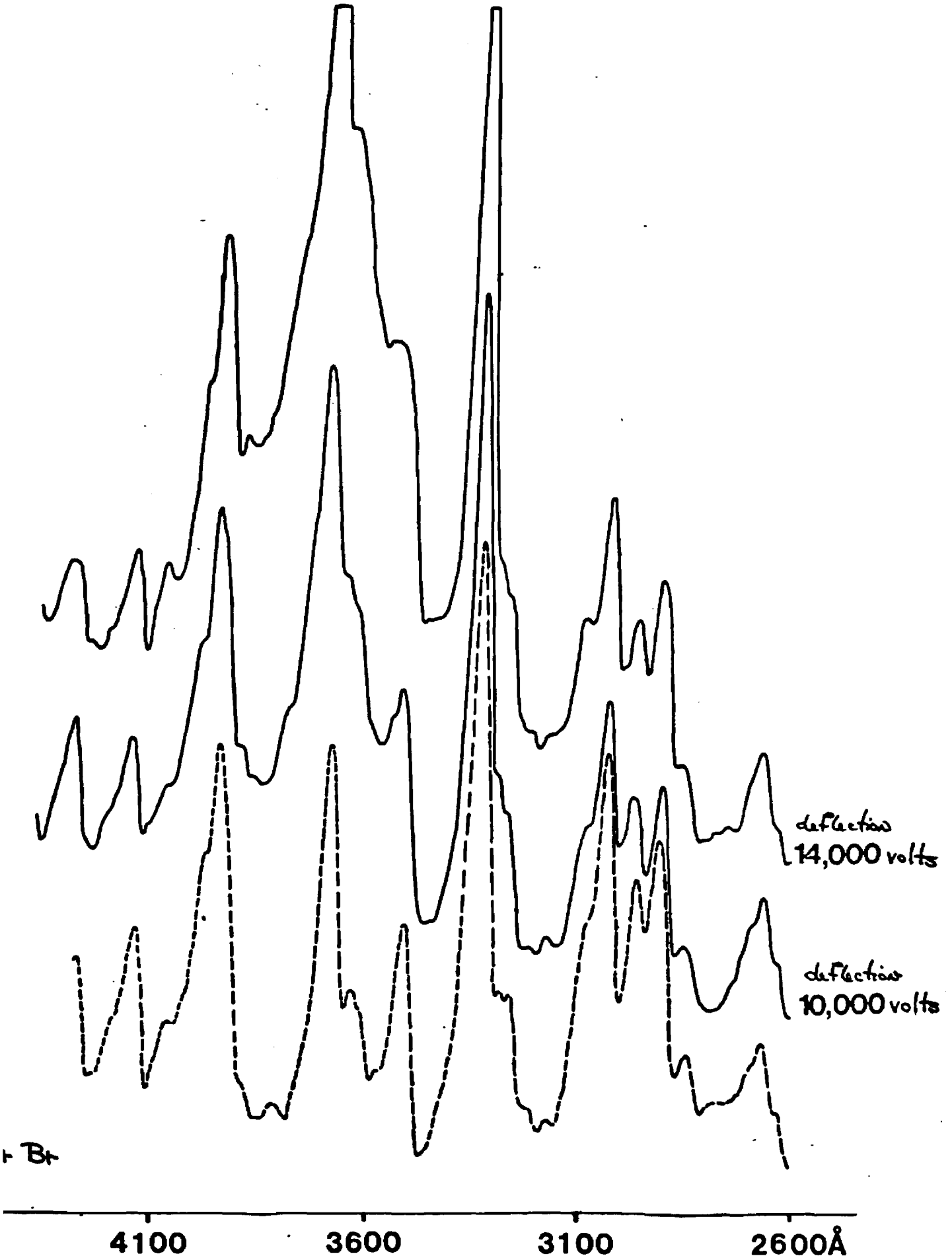
deflection
14,000 volts
deflection
10,000 volts
Bt
4100
3600
3100
2600Å

is at positive voltage relative to a lower grounded plate. This occurs because the electrons formed in the gun are more readily accelerated into the reaction zone because they feel a higher effective positive potential. We feel that there is great potential in this electron impact excitation of reaction products. The signal observed in the experiments conducted thusfar is found to be first order with respect to oxidant concentration, indicating that we have excited the dark products of sodium cluster oxidation. We feel that this technique has potential for the electron impact excitation and fluorescence monitoring of the dark products of other reaction systems, more specifically, we hope to probe the Na_x-SO_2 system using this technique in conjunction with mass spectrometry.

Two further experiments and a recently constructed device for spectral relaxation should also be noted. We have characterized the temperature dependence of several emission features associated with the sodium cluster-halogen atom oxidation processes (Figures 13, 14, 15) finding that we can distinguish whether product formation occurs via ground or low-lying metastable state reactions. More importantly, we have successfully probed the neutral products formed in the Na_x + Br system using mass spectrometry. Evidence has been obtained for the formation of $NaBr_2$ and NaBr and much smaller concentrations of Na_2Br, Na_3Br, and Na_3Br_2.[26] After some modification, the clusters apparatus will be adopted to probe the Na_x-SO_2 system and to study changes in product formation upon introduction of a small chlorine impurity (see also following discussion).

Quite recently we have embarked on efforts to improve the resolution of the spectra in Figures 13 through 17. The lack of resolution in these systems is due to the high internal excitation characteristic of single collision chemiluminescent studies. To improve the resolution in the system, an entraining device has been constructed which can be placed at the point of entrance of the

supersonic beam into the reaction chamber (Figure 11). This ring injector device is designed to increase the pressure in the reaction chamber through the introduction of a rare gas such as helium or argon. The device is designed to create a merged metal cluster-rare gas flow; the entrained clusters are then oxidized under controlled conditions at elevated pressure where collisions promote rotational relaxation.[25] Of further importance is the fact that the introduction of the merged flow source also facilitates the introduction of two oxidant gases simultaneously into the system. This may prove useful in studies where it is desireable to introduce SO_2 and chlorine into a sodium cluster environment.

In order to operate the metal entrainment-relaxation device, the forepump system in the metal clusters apparatus (Figure 11) has been extensively modified to handle increased gas loads. The oven chamber is now pumped independently of the reaction chamber by a 17 CFM forepump and the reaction chamber is pumped by a 50 CFM forepump. (This should be contrasted to the previous pumping of the entire system by a 17 CFM pump). Using this present pumping configuration, we have now studied the Na_x + Br + Ar system and have successfully introduced some internal relaxation thus increasing our ability to resolve those spectral features of interest. In these initial studies, we found that the carrier gas pressure and hence the reaction chamber pressure was somewhat oscillatory. We are attempting to improve this situation with (1) a modification of the ring injector annulus so as to decrease the width of the ring orifice while increasing its convergence angle and (2) the introduction of a further needle valve into the rare gas inlet line in order to control the gas pressure. These modifications are currently in process.

CONCLUSIONS AND RECOMMENDATIONS

From the previous discussion, it should be clear that extensive data has not previously been obtained on the alkali hydroxides and oxides. Although the alkali metals are more readily produced in the gas phase than the more refractory metals with which we have had considerable experience, their oxidations to produce the oxides and hydroxides are characterized by a very different gas phase chemistry than that accompanying virtually all other highly exothermic metal oxidations.

Several of the experiments conducted thusfar indicate important problems which should be pursued at length. The most important of these results are the discerned reaction of sodium clusters with SO_2 in an apparently highly exothermic step via a chlorine catalyzed process and the surprising efficiency of gas phase particulate formation especially in systems where the alkali oxides are formed.

Studies of the Na_x + SO_2(neat) reaction system should be pursued using our newly developed electron impact technique as a probe of possible ground state product formation. This method of excitation applied individually to SO_2, Na_x, and Na_x + SO_2 may demonstrate the formation of a sulfite complex. Similar experiments should be carried out on the system Na_x + SO_2 where a slight chlorine impurity is introduced. Lastly, we believe that a set of experiments studying the Na_x + SO_2Cl_2 (sulfonyl chloride) system is also appropriate. In view of our recent mass spectrometric studies of the Na_x + Br system we believe that mass spectrometry should be added as a probe of the three systems considered. A problem may exist. There is some question about the stability of those complexes whose reaction may lead to the highly exothermic process whose chemiluminescence has been observed. If these complexes are sufficiently weakly bound electron impact excitation may

represent a very harsh means of excitation and we may observe a negligible effect verses that evidenced in Figure 17 or obtain an invalid mass spectrometric probe of the systems. For this reason, we are incorporating the facility for direct photoionization in our mass spectrometer system. Here ions are produced via a much milder excitation technique and the probability for the dissociative ionization of the complexes of interest diminishes considerably. As we have mentioned previously a device which should allow the controlled relaxation of chemiluminescing product excited electronic states in the Na_x + oxidant system has been constructed. We wish to use this device to improve the resolution for those spectra obtained in the Na_x + Halogen and Na_x + SO_2 + halogen systems thus improving product characterization. This work should of course complement the previously considered studies.

Recent efforts thusfar involving the new low pressure beam-gas oven system to which we have alluded in our previous discussions have demonstrated that gas phase particulate formation is extremely efficient especially in the alkali oxide systems. Although mass spectrometry indicates that NaO and KO are formed as the products of the Na, K + N_2O systems, no probe of the particulate formation has yet been made. We have not, as yet, made a diligent effort to collect that particulate which forms in the gas phase; however, we feel that the extremely high efficiency of the particulate forming process and its possible influence as a seed for the formation of larger particles in the gas phase may warrant further investigation. This observed phenomena does not characterize any other metal oxidation system including systems which involve the oxidation of silicon, aluminum, titanium or vanadium. Thusfar, we have determined that the complex which is formed is hydroscopic; we have also collected a small sample for possible future assay.

We are now investigating several means of analyzing the nature of the pronounced particulate matter formed via what appears to be a homogeneous gas phase alkali oxidation. Three approaches appear possible. First, it should be possible to determine the laser Raman spectrum for a powdered sample of the particulate matter. Second, it should be possible to study the EPR spectrum of the powdered sample. Finally, we will attempt to observe the mass spectrum of the sample provided it can be vaporized at temperatures less than or equal to 350°C. Techniques for sample preparation are now being considered.

Clearly, sodium cluster oxidation studies should be followed by the study of both contaminated and clean sodium surfaces. The cluster studies represent a middle ground between the gas phase oxidation of sodium atoms and dimers and the metallic surface phase. We anticipate that at least the study of contaminated sodium surface oxidation can be carried out in the near future. We believe that there will be important correlations between these studies and the necessity to assess the nature of gas phase particulate formation. While we will sample these surface oxdiation phenomena in situ using optical and mass spectrometric techniques, it will probably be necessary to carry out further studies of a substantial surface residue left after oxidation. Here, it may be possible to carry out surface desorption studies, heating the sodium surfaces to remove the alkali oxidation products.

There are several other areas which will warrant continued study

(1) With the development of an intense, stable, and long-lasting alkali hydroxide diffusion flame, efforts should continue to obtain the KOH emission spectrum entirely on film (3000Å) or in 200Å sections using an optical multichannel analyzer system. The study will allow the evaluation of further molecular constants for the ground electronic state of KOH.

(2) Further studies of gas phase oxidations producing the alkali oxides NaO and KO should be pursued. More specifically there should be a focus on the improvement of the spectra in Figures 7, 8, and 10. The $Na + O_3$ and $K + O_3$

reactions should be studied in order to obtain further information on the chemiluminescence already observed for the Na + N_2O and K + N_2O reactions. The temperature dependence of the Na, K + N_2O and Na, K + O_3 reactions should be determined in order to obtain a stringent lower bound on the NaO and KO bond energies. Based on the information already obtained, it should be possible to probe sodium oxide using laser induced fluorescence by pumping a band system in the region around 7500Å. We suggest that NaO could be prepared by an appropriate in-situ synthesis passing entrained sodium metal over NaO_2 viz

$$Na + NaO_2 \longrightarrow 2NaO.$$

The subsequent products could then be excited by a krypton ion pumped dye laser.

We have begun studies of the Na + O_3 reaction. In order to carry out these studies, we have constructed a larger and more versatile sodium oven system a portion of whose design is based on the principal of the supersonic sodium oven which we have discussed previously. In other respects this oven is very similar to that used to study the Na + N_2O reaction. An ozone trap has been constructed and used to trap large quantities of ozone on silica gel. Preliminary results have been obtained indicating a rich spectrum in the region around 7500Å, however, flame stability is less than desirable due to instabilities in the ozone flow and some instability in the new sodium oven. This should be significantly improved by entraining both the sodium atom beam and the ozone in argon and reacting this mixture.

References

1. G. W. Stewart, A. Chakrabasti, C. Stinespring, and K. Castleton, Western States Symposium/Combustion Institute, October, 1980.

2. a) See, for example, J. W. Hastie, "High Temperature Vapors, Science and Technology," Academic Press, New York, 1975.

   b) See also "High Temperature, High Pressure Particulate and Alkali Control in Coal Combustion Process Streams" - Proceeding of the U.S. Department of Energy Contractor's Meeting, West Virginia, 1981.

3. "Open Cycle Magnetohydrodynamic Power Generation," J. B. Heywood and G. J. Womack, eds., Pergamon, Oxford, 1969.

4. H. C. Hottel and J. B. Howard, "New Energy Technology - Some Facts and Assessments," M.I.T. Press, Cambridge, MA (1971).

5. J. L. Gole, Optical Engineering 20, 546 (1981).

6. See for example, R. K. Sinha and P. L. Walker, Jr., Fuel 51, 329 (1972); F. S. Karn, R. A. Friedel and A. G. Sharkey, Jr., Fuel 51, 113 (1972). Note also references 2 and 3(b) also G. W. Stewart private discussions.

7. Session on High Pressure Sampling, 10th Materials Research Symposium on Characterization of High Temperature Vapors and Gases, National Bureau of Standards, Gaithersburg, MD. September 18-22, 1978.

8. F. E. Stafford and J. Berkowitz, J. Chem. Phys. 40, 2963 (1964).

9. R. Kelly and P. J. Padley, Trans. Faraday Society 67, 740 (1971).

10. L. N. Gorokhov, A. V. Gusarov and I. G. Panchenkov, Russ. J. Phys. Chem. 44, 150 (1970).

11. J. W. Hastie, E. R. Plante, D. W. Bonnell - private communication.

12. N. Acquista, S. Abramowitz and D. R. Lide, J. Chem. Phys. 49, 780 (1968).

13. N. Acquista and S. Abramowitz, J. Chem. Phys. 51, 2911 (1969).

14. A. A. Belyaeva, M. I. Dvorkin, and L. D. Sheherba, Opt. and Spectrosc. 31, 210 (1971).

15. D. R. Lide and R. L. Kuczkowski, J. Chem. Phys. 46, 4768 (1967).
C. Matsumura and D. R. Lide, J. Chem. Phys. 50, 71 (1969).
D. R. Lide and C. Matsumura, J. Chem. Phys. 50, 3080 (1969).
E. F. Pearson and M. B. Trueblood; J. Chem. Phys. 58, 826 (1973), Astrophys. Journal 174, L145 (1973).
E. F. Pearson, B. P. Winnewisser and M. B. Trueblood, Z. Naturforsch 31a, 1259 (1976).
P. Kuijpers, T. Törring and A. Dynamus, Chem. Phys. 15, 457 (1976); Z. Naturforsch 31a, 1256 (1975).
P. Kuijpers, T. Törring and A. Dynamus, Z. Naturforsch 32a, 930 (1977).

16. Of course this information will be useful for the statistical mechnical evaluation of thermodynamic properties such as the heat capacity, entropy, and free energy.

17. Under single collision conditions a KOH excited state product molecule is formed and emits a photon long before undergoing subsequent collisons. Under diffusion flame conditions a molecule formed in a given excited state undergoes several deactivating collisions before the emission of a photon or it may be involved in an ultrafast energy transfer process among the electronic manifold of states which characterize the species of interest (see for example G. J. Green and K. L. Gole, Chem. Phys. 46, 67 (1980)).

18. F. S. Rowland and Y. Makide, Geophys. Res. Letters 9, 473 (1982).

19. A. Tewarson, Studies of Chemiluminescent Emission in Selected Low Pressure Diffusion Flames, Ph.D. Thesis, Penn State University, 1969.

20. R. R. Herm and D. R. Herschbach, J. Chem. Phys. 32, 5783 (1970).

21. E. Murad and D. L. Hildenbrand, J. Chem. Phys. 53, 3403 (1970).

22. D. R. Pruess and J. L. Gole, J. Chem. Phys. 66, 880 (1977); 66, 2994 (1977). J. L. Gole and D. R. Preuss, J. Chem. Phys. 66, 3000 (1977).

23. J. L. Gole, Ph.D. Thesis, Rice University (1971).

24. See for example J. L. Gole "The Characterization of High Temperature Vapors of Import to Combustion and Gasification Processes in the Energy Technologies," Proceedings of the Morgantown Energy Technology Center Meeting on High Temperature, High Pressure Particulate and Alkali Control in Coal Combustion Process Streams - Morgantown, West Virginia, 1981.

25. J. L. Gole and S. A. Pace, J. Chem. Phys. 73, 836 (1980); A. W. Hanner and J. L. Gole, J. Chem. Phys. 73, 5025 (1980); J. L. Gole and S. A. Pace, J. Phys. Chem. 85, 2651 (1981).

26. Of course mass peaks readily attributable to Br, Br_2 and Na_x(x=1,2,3,4) are also observed.

Technical Publications and Presentations

The following two papers have been accepted for publication and are included in Appendices B and C

"Metal Cluster Oxidation: Chemiluminescence from the Reaction of Sodium Polymers (Na_n, $n \geq 3$) with Halogen Atoms (X=Cl,Br,I)" W. H. Crumley, J. L. Gole, and D. A. Dixon, J. Chem. Phys. 76, 6439 (1982).

"Dynamic Constraints Associated with the Formation of SiS ($a^3\Sigma^+$) from the Si-OCS Chemiluminescent Reaction" J. L. Gole and G. J. Green, Chem. Phys. 69, 357 (1982).

APPENDIX A

pects of sparsely studied gas phase chemistry of port to the energy technologies

; L. Gole
a Institute of Technology
ment of Chemistry
a, Georgia 30332

Abstract. There is considerable interest in the need to improve the operation of systems which can potentially serve as alternate energy sources. Entailed in this effort is the desire to understand the vapor phase chemistry and compounds which may enter as by-products of the system under consideration. These compounds may have deleterious effects on the gas phase chemistry or play an important role through high temperature gas-solid corrosion kinetics. Here we outline the nature of the problem and focus on a subset of these molecules, the metal hydroxides and the alkali oxides and sulfides. A critical analysis of the data base is presented and new experiments are outlined which encompass the investigation of thermochemistry and the evaluation of molecular parameters through the study of visible, infrared, microwave and electron spin resonance (ESR) spectroscopy. Recent chemiluminescent experiments which lead to the evaluation of a new stringent lower bound for the K-OH band energy are summarized. This stringent lower bound (88.2 kcal/mole) correlates within the quoted error bounds with the absolute upper bound of previous experimental determinations. Preliminary laser fluorescence studies on Na_2O are reported and the possible influence of "ultrafast" energy transfer (E-E and V-E transfer among the excited states of high temperature molecules) on the behavior of energy generating systems is noted.

Keywords: combustion and analysis; gas phase chemistry; thermal/chemical processes.

Optical Engineering 20(4), 546-555 (July/August 1981).

ENTS

per EP-108 received March 4, 1981; accepted for publication March 11, 1981; y Managing Editor March 19, 1981.
ciety of Photo-Optical Instrumentation Engineers.

1. INTRODUCTION

Recently, substantial interest has focused on the development of systems and technologies which can serve to avert projected energy shortages through the use of alternate fuel sources. This need has heightened the necessity for improving and optimizing the efficient use of energy systems which are, at present, typically no more than 40% efficient.

For practically all viable energy conversion systems, the common optimization parameter is the temperature. Generally the higher the temperature, the greater the efficiency for converting a source of energy to useful work. This, of course, is a direct consequence of the Carnot efficiency relation, usually expressed as

$$E_{max} = (T_{source} - T_{sink})/T_{source}$$

where E_{max} is the maximum efficiency attainable for a given source and sink temperature. Based strictly on the efficiency criterion, it is apparent that a high source temperature is desirable for energy conversion systems.

Suitable high source temperatures are definitely attainable. In coal or oil combustors or in nuclear fission fuel elements, where temperatures in excess of 2000 C are readily achieved, basic system operation problems lie in the containment of these high temperature reactive fuel systems and of the working fluid used to transfer the heat to an energy conversion unit. While this is essentially a materials problem involving, in large part, mechanical or solid state chemical phenomena, some of the materials problems arise from high temperature gas-solid corrosion reactions and vapor phase phenomena

ay enter as by-products of the system under consideration
ies such as the alkali metals, sulfur, water vapor, etc.) or
of the introduction of seed materials (K_2SO_4 or K_2CO_3 in
-hydrodynamic (MHD) applications) into the flow.
is discussion, we will be concerned with a subset of those
:s which play an important role in high temperature vapor
s in the present technology or may be important in antici-
ture developments. Unfortunately, data on these species are
id much work needs to be done. It is quite apparent that very
: tolerance levels for certain species in process streams im-
)nger requirements for reliable thermodynamic and kinetic
rder to predict the effects due to low level species concentra-
addition, there must be serious concern focused on whether
nese systems are best represented via equilibrium or non-
um models. The characterization of molecules in these sys-
uires the determination of bond energies and spectroscopic
s and may well require the elucidation of ultrafast intra- and
ecular energy transfer.[1] The evaluation of spectroscopic
ds to the determination of important molecular constants
in be used for the statistical mechanical evaluation of heat
:s, entropies and free energies, all of which are important to
:rstanding of energy related combustion and gasification
nents. In addition, the determination of the optical signature
: molecules of interest provides information useful for the
rization of non-equilibrium combustion phenomena and for
iation of kinetically dominated product formation routes. In
focus on those areas where limited data need considerable
ation, we will first outline the nature of certain specific

URE OF THE PROBLEM

rable effort will be required to attain basic parameters for
:s playing an important role in energy generating devices
)al is the utilization of fossil fuel gasification and liquifica-
: important subset of these systems includes combustion
magneto-hydrodynamics (MHD). Because MHD attempts
a more varied use of the combustion environment, we focus
iture of MHD power generation; however, excluding the use
materials, all high temperature combustion systems (coal
ion, vapor phase processes associated with gas turbines, etc.)
o be plagued by a similar group of deleterious high tempera-
or phase constituents.

D

ieration of electrical energy using combustion powered
-hydrodynamic (MHD) systems has been the subject of
able research effort in the past decade. In an MHD system
.tes an electrically conducting "fluid" which, when passed
a magnetic field, develops an induced electric field across
l, along which a current can flow.[2] A direct electric current
along the induced field to electrodes which may be con-
) an external load. The typical MHD generator is usually
:d of a sequentially connected combustion chamber, a super-
pansion nozzle, and a gas flow channel commonly referred
ffuser. Because the hot post-combustion materials normally
insufficient free electron concentration to be good current
thermally ionizable seed materials such as K_2CO_3 and
.re generally added to the flow.[3]
nt evaluations[4] of the status of MHD devices as viable and
tive power systems indicate that the problems of maintaining
luctivity, seed recovery (98% recovery rate for economical
n) and of inhibiting channel materials degradation (preven-
:orrosion of channel walls through coal slag-electrode and
ılator interactions) remain largely unsolved.
der to successfully model, and hence optimize, the design and
n of an MHD unit, it is essential to provide a rigorous
ing of the gas chemistry, particularly within the diffuser.
considerable effort in this direction, it does not appear that
ory predictions of the electrical conductivity associated with

a seeded coal combustion gas are currently within the grasp of the technology. It is extremely difficult to determine species concentrations in these complex high temperature systems even if it is assumed that the gases are in thermodynamic equilibrium.

If equilibrium is assumed in the MHD channel, one can, from a knowledge of all the species present and their thermodynamic functions, calculate steady-state free electron concentrations for a variety of composition, temperature, and pressure conditions. Unfortunately, these calculations are based on primary thermochemical input data which are very uncertain for some of the species (see below). In addition, these thermochemical evaluations rely heavily on a correct choice of species, a factor which is again uncertain.

2.2. Approximate species concentrations

Based upon currently available thermochemical data, it can be calculated (determination of species concentrations) that approximately half the potassium seed is present in the form of essentially unionizable KOH and is therefore unavailable as an electron source. At temperatures in excess of 2600 K in a slightly lean coal/air combustion system at 3 atm pressure, the major potassium-containing species are calculated to be KOH, K, KO and K^+.[5] Other significant vapor species include SiO_2, FeO, OH, SO_2 and NO in addition to the major combustion gas components N_2, H_2O, CO_2 and CO. The primary slag or fly ash components include SiO_2, Al_2O_3, Fe_3O_4, TiO_2, MgO, CaO, Na_2O and K_2O; however, evidence now exists that the negative ions of PO_2, FeO_2, and AlO_2 are potentially important since all of these species have high electron affinities. The presence of these impurities has important implications for cation formation and electron behavior in the MHD channel. Typical slag concentrations in a coal-fired system, while only on the order of 0.1%, can result in as much as 19% loss in electrical conductivity.[6]

The species we have mentioned and their possible precursors are *not* well characterized. The combined uncertainties in the *heats of formation* and *molecular constants* used in computing partition functions for KOH (JANAF)[7] cause the concentration ratio of K to KOH to be uncertain by at least an order of magnitude. Because of this uncertainty, it is not possible to make a reasonable judgment as to whether the concentration of KOH is sufficiently high to require restrictions on the amount of hydrogen present in the fuel. Clearly, the successful thermodynamic modeling of MHD gas chemistry requires better basic data than are presently available.

2.3. Electron transfer cross sections

Given that the equilibrium assumption is valid, we can define a steady state electron concentration in the MHD channel. Electron mobility is then determined from momentum transfer cross sections between electrons and other species. The momentum cross sections can be obtained from electron-molecule collision cross sections. These cross section data are not known and can only be estimated very approximately. What can be said definitely is that the most polar species such as H_2O and KOH should have the highest cross sections. Indeed, the dipole moment of KOH is estimated to be 8 Debye.[8] In systems where calcium and magnesium impurities are found, it would seem that CaOH and MgOH should be carefully considered. KOH, CaOH and MgOH are, at present, sparsely characterized.

2.4. Metal hydroxides and the hydrogen fuel economy

Because of its close tie to those materials used to seed the MHD generator, KOH may well represent the most important hydroxide species in the MHD channel; however, the specific effect of the water vapor component of combustion gases on the channel components of any system (fossil fuel only or MHD) has not been considered carefully. It appears that volatile hydroxides of a number of species could be formed under typical operating conditions.[9]

The importance of metal hydroxide characterization increases markedly when one considers that many of the existing materials and seed recovery problems are derived from the presence of combustion impurities, particularly coal slag. Because future prospects for a hydro-

:l economy may provide a source of clean fuel for MHD and ombustion systems, experimental and theoretical evaluations I_2-O_2 MHD generator have been underway.[10] A cost analysis es the H_2 fuel system to be comparable with other fuels since luced materials problems and low pollution produced make attractive alternative. There is one possible major drawback. esence of a large H_2O concentration may prove to be detri- if the high temperature materials are susceptible to the forma- hydroxide vapor species. In this light, it would seem that t and future possibilities for energy conversion will require a ıydroxide data base. At the very least this data base should : thermodynamic heats of formation and molecular constants hydroxides of sodium, iron, silicon, vanadium, calcium, and sium.

ıe alkali problem and sulfur chemistry

ıture of coal-fired systems in general and the MHD channel in ılar is such that "alkali cleanup"[11] represents the most signifi- roblem which must be addressed. While thermodynamic cal- ›ns indicate the importance of the alkali oxides (especially KO MHD channel), sulfur is also a significant impurity in coal- ystems. Therefore, it is necessary to consider the nature of compounds and their relation to the only partially solved fuel ion problem. In focusing on turbine blade corrosion, the alkali salts are among the most important compounds which must be terized. For example, in a combustion powered turbine sys- ›erating over a sea or ocean, sulfur may come in contact with n or potassium and one must assess the nature of alkali-sulfur ›unds which are formed.

:h data are also of importance for the characterization of most ıd heavy fuel fired turbine generators.[12] Indeed, a great deal of is now focusing on fireside corrosion where one must consider eractions of those alkali salts which plate out on boiler tubes.[12] his strong interest it is amazing to note that the data on sodium ›tassium sulfur compounds (NaS, KS, Na_2S, K_2S and higher :s) are minuscule. Information on molecular stabilities (heats nation) and molecular constants must be obtained.

ıe equilibrium assumption

iscussion thus far has been closely tied to the validity of the ›rium assumption, and the problems of obtaining thermo- :al and collision cross section data if this assumption is valid. ver, one of the troublesome factors in the modeling of coal and fuel fired systems appears to be a complex gas mixture which ot correspond to an equilibrium composition. The correct ing may require the use of kinetic parameterization and the or product formation. Similarly, electron producing ioniza- ıetics may also be an important factor in determining MHD ctivity.

his connection one need only note the complex ion chemistry :sults between metal additives and electrons in atmospheric tory flames. Indeed, the presence of excess concentrations of :d species in the reaction zone of hydrocarbon-containing ; has led to the suggestion of a non-equilibrium low pressure atm) MHD generator.[13] It is anticipated that the use of low gas res should allow the excess radical and ion concentrations ıted by the combustion process to be maintained in the diffuser Calculations show that, under these conditions, a 1500 K flame give an ion yield equivalent to that of an equilibrium system at [13]

: possibilities noted here point strongly to the importance of lering controlled non-equilibrium environments and species tion in the modeling of the behavior of energy generating ıs. It may be inappropriate to model these systems using only nergy minimization schemes. Product formation rates and ıst energy transfer may play a much more significant role than odynamics. In any case, the parameterization of those gas phase ules known to be present in these systems is of paramount importance to the successful application of any reliable approach to modeling.

3. THE NATURE OF THE DATA BASE

In the following sections, we will outline and assess the nature of available data on several of the molecules whose importance has been considered in the previous section. Our emphasis will be on the metal hydroxides and the alkali oxides and sulfides. Our purpose will be to evaluate critically the data base and to suggest where further experimentation is needed.

4. METAL HYDROXIDES

4.1. Water vapor-solid reactions with hydroxide vapor products

While there have been several recent reviews[14] outlining evidence for vapor phase hydroxide formation, much of the evidence for hydroxide species is of an indirect and sometimes ambiguous nature. In a gas-solid system, the enhanced rate of transport for a given oxide in the presence of water vapor is usually taken to indicate formation of a volatile hydroxide species. Through systematic variation of gas composition and temperature one attempts to infer a formula for the transport species. In order to determine and extrapolate the pressure dependence of transport and deposition processes, it is important to clarify the exact identity of the hydroxides involved.[15] Thus far very few verifications of species identity have been made. Here thermodynamic and spectroscopic data can be of great importance. Only the hydroxides of the alkali metals, barium and aluminum, appear to have been characterized by both mass and optical spectroscopy, and, in many cases, this optical spectroscopy is of an indirect nature (Table I). Our discussion will focus on the monohydroxides. Here compounds of the alkalis, BeOH, CaOH, BaOH, and AlOH are thought to be important in water vapor-solid interactions.[14]

4.2. Thermochemistry

It appears that the major thermodynamic characterization of the metal hydroxides has been through flame studies. Table I summarizes those monohydroxides identified in flames while Table II indicates currently accepted bond dissociation energies for the monohydroxides. For the most part, molecular emission has been excited in post flame gases and in many of the studies noted in Tables I and II, only *indirect* evidence is obtained for the hydroxide. Only recently (see below) has molecular emission from NaOH and KOH been excited in a "chemiluminescent" reaction.[16] Molecular emission tentatively attributed to CaOH* has also been observed in calcium oxidation flames[17] and some laser fluorescence studies of this alkaline earth hydroxide have also appeared.[18]

From Table II, it is clear that *only two compounds* have been characterized mass spectrometrically. Studies of the Group IIA hydroxides at elevated temperature are precluded for all but the barium compounds[19] because of a very high propensity for disproportionation to the oxides and resulting loss of water. Difficulties encountered in studying the alkali hydroxides may well stem from the tendency to form dimeric species upon vaporization. We should also note that lithium tends to form a very stable binary oxide. The bond energies determined for KOH[20-21] and BaOH[19,22] via flame and mass spectrometric studies are in reasonable but not spectacular agreement.

4.3. Molecular parameterization—the alkali hydroxides

With the exception of the alkali metal compounds, molecular parameterization is virtually nonexistent for the hydroxides. Abramowitz and coworkers[23,24] have obtained infrared spectra for matrix isolated NaOH, RbOH, and CsOH and their deuterated analogs. Belyaeva et al.[25] have studied the infrared spectra of matrix isolated KOH. The data from these groups are summarized in Table III and correspond to the assignment of ν_1, the M-O stretching mode and ν_2, the bending mode. Extensive microwave and millimeter wave studies have now yielded significant parameterization for the ground states of NaOH, KOH, RbOH, and CsOH,[26-31] and rotational con-

E I. Observations of the Metal Monohydroxides

as	Nature of the Detection Method and Comments	Species	Nature of the Detection Method and Comments
	Mass spectrometric analysis of lean H_2-O_2 flames containing aluminum.[a] Controversial results.	SrOH	Molecular emission observed in acetylene-air flames.[d,f] Presence also inferred from optical spectroscopic study of free atom depletion-dissociation energy from depletion studies.[e]
Hydroxides			
	Inferred from optical spectroscopic study of free atom depletion in H_2-O_2-N_2 [b] and H_2-O_2-CO_2 [c] flames.	BaOH	Emission in post-flame gases of H_2-O_2-N_2 flames.[d,e] Presence also inferred from spectroscopic study of free atom depletion-dissociation energy from depletion studies[e] and mass spectrometry.[g]
l	Inferred from optical spectroscopic study of free atom depletion in H_2-O_2-N_2 [b] and H_2-O_2-CO_2 [c] flames.	CuOH	Some emission band spectra observed in acetylene-air flame.[f,h]
	Inferred from optical spectroscopic study of free atom depletion in H_2-O_2-N_2 [b] and H_2-O_2-CO_2 [c] flames.	FeOH	Emisson band spectra observed in acetylene-air, H_2-O_2-N_2 and low pressure lean flames.[i] Presence also inferred from optical spectroscopic study of free atom depletion[j]
l	Inferred from optical spectroscopic study of free atom depletion in H_2-O_2-N_2 [b] and H_2-O_2-CO_2 [c] flames.	MnOH	Emission band spectra observed in acetylene-air post-flame gases.[d,k]
l	Inferred from optical spectroscopic study of free atom depletion in H_2-O_2-N_2 [b] and H_2-O_2-CO_2 [c] flames.	InOH	Presence inferred from optical spectroscopic study of free atom depletion.[c,l]
ne Earth Hydroxides		GaOH	Presence inferred from optical spectroscopic study of free atom depletion.[c,l,m]
l	Molecular emission observed in post-flame gases of H_2-O_2-N_2 flames.[d] Presence also inferred from optical spectroscopic study of free atom depletion[e]-dissociation energy from depletion studies.[e] Also observed in acetylene-air or O_2 flames.[f]		

arber, R. D. Srivastava, M. A. Frisch and S. P. Harris, Faraday Symposium h Temperature Studies in Chemistry, London, 1973.

Jensen and P. J. Padley, Trans. Faraday Society 62, 2132 (1966).

ılly and P. J. Padley, Trans. Faraday Society 67, 740 (1971).

. Reid and T. M. Sugden, Disc. Faraday Soc. 33, 213 (1962); L. V. Gurvich, V. ıbova and A. N. Khitrov, in High Temperature Studies in Chemistry, Faraday No. 8, Paper 8, Chem. Soc. London (1973); J. Van der Hurk, J. Hollander and . Alkemade, J. Quant. Spectrosc. Radiat. Transf. 13, 273 (1973).

Cotton and D. R. Jenkins, Trans. Faraday Society 64, 2988 (1968).

in *Flame Spectroscopy* by R. Maurodiveanu and H. Boiteux, Wiley, New York).

[g] F. E. Stafford and J. Berkowitz, J. Chem. Phys. 40, 2963 (1964).

[h] L. M. Bulewicz and T. M. Sugden, Trans. Faraday Society 52, 1481 (1956).

[i] M. J. Linevsky, Metal Oxide Studies; Iron Oxidation. Tech. Rep. RADC-TR-71-259.

[j] D. E. Jensen and G. A. Jones, J. Chem. Soc. Faraday Trans. I 69, 1448 (1973).

[k] P. J. Padley and T. M. Sugden, Trans. Faraday Society 55, 2054 (1959).

[l] E. M. Bulewicz and T. M. Sugden, Trans. Faraday Society 54, 830 (1958); 54, 1855 (1958).

[m] L. V. Gurvich and V. G. Ryabova, High Temp. USSR 2, 486 (1964).

s have been obtained for several excited vibrational levels.
s we have noted, KOH is one of the most important constituents e high stress environments characterizing energy generating ms. While ground state rotational parameters have been deter- d for KOH and KOD, vibrational frequencies are still estimated gher vibrational levels.[32] Although matrix data are available on ındamental vibrations, no gas phase measurements have been : and no anharmonicities are known for any of the alkali hy- ides. There is hope, however, that recent chemiluminescent es[16] can be correlated with the millimeter wave data to provide ctensive mapping of the vibrational structure of the ground onic state. These studies have already provided a stringent r bound for the KOH dissociation energy (88.2 kcal/mole) ficantly higher than that indicated in the JANAF tables (85.4). use of its potential for the parameterization of KOH and the i hydroxides in general, we feel that a summary of the present s of this work is appropriate. In this regard, it is instructive to ›are the alkali halides and hydroxides.

ı Table IV, we present thermochemical data on the fluorides, ·ides, and hydroxides of potassium, sodium and rubidium. Comparisons will be made between these species because (1) they are valence isoelectronic and (2) their observed emission spectra are expected to be similar.

It is generally felt that the nature of the bonding in the alkali hydroxides should be intermediate to that in the fluorides and chlorides. With this in mind, the trends in Table IV would seem to indicate the possibility of a KOH bond strength higher than the mass spectrometric value. This is significant since the flame studies do indicate a higher value for the bond energy. JANAF now recommends 85.4 kcal/mole in close agreement with the flame studies.

Cardelino et al.[16] have obtained a KOH* chemiluminescent spectrum under a variety of conditions. The observed emission for KOH correlates closely with expectations based on the known chemiluminescent emission for KCl. In order to understand the nature of the KOH emission spectrum, it is instructive to consider spectra for the alkali halides.

Alkali halide spectra have been obtained in three distinct experimental environments.[33] They have been observed under "single collision" conditions where alkali dimers and halogen molecules react in a four-center process

I. Dissociation Energies of Metal Monohydroxides*

D_0(M-OH) kcals/mole	Comments
103 ± 2[a]	H_2-O_2-CO_2 flames 2nd law determination
79 ± 2[a]	H_2-O_2-CO_2 flames 2nd law determination
84 ± 2.5[a]	H_2-O_2-CO_2 flames 2nd law determination
80 ± 3[b]	Mass spectrometry
86 ± 3[a]	H_2-O_2-CO_2 flames 2nd law determination
96[c]	Rich hydrogen-air flames
94 ± 3[d]	Rich hydrogen-air flames
103.7[e]	
103[f]	Quoted uncertainty ≤2.5 kcals/mole
95[e]	
103[e]	
102[f]	Quoted uncertainty ≤2.5 kcals/mole
111[c]	
114.3[e]	
113[f]	Quoted uncertainty ≤2.5 kcals/mole
107[g]	Mass spectroscopy
109 ± 3[d]	
90 ± 2[a]	H_2-O_2-CO_2 flames 2nd law determination
86 ± 7[h]	H_2-O_2-N_2 flames 2nd and 3rd law determination
102 ± 5[h]	H_2-O_2-N_2 flames 2nd and 3rd law determination
<72[a]	H_2-O_2-CO_2 flames 2nd law determination
100 ± 3[i]	Low pressure H_2-O_2-N_2 flames
$<85 \pm 9$[j]	Low pressure H_2-O_2-N_2 flames
130[k]	Thermochemistry and reactions in hydrogen oxygen flames

ınd P. J. Padley, Trans. Faraday Society 67, 740 (1971).

okhov, A. V. Gusarov and I. G. Panchenkov, Russ. J. Phys. Chem. 44, 150

rvich, V. G. Ryabova and A. N. Khitrov, in High Temperature Studies in ', Faraday Symposium No. 8, Paper 8, Chem. Soc. London (1973).

ıbova, A. N. Khitrov, and L. V. Gurvich, High Temperature 10, 669 (1973).

tton and D. R. Jenkins, Trans. Faraday Society 64, 2988 (1968); also K. and T. M. Sugden, Symp. (Int.) Combust. 10th, p. 589, Combust. Inst., ı, PA.

f and C. T. J. Alkemade, Combust. Flame 19, 257 (1972).

fford and J. Berkowitz, J. Chem. Phys. 40, 2963 (1964).

lewicz and T. M. Sugden, Trans. Faraday Society 54, 830, 1855 (1958).

evsky, Metal Oxide Studies; Iron Oxidation. Tech. Rep. RADC-TR-71-259.

ewicz and P. J. Padley, Trans. Faraday Soc. 67, 2337 (1971).

ackson, Thermodynamics of Gaseous Hydroxides, UCRL 51137, ich and I. V. Veits, Dokl. Akad. Nauk. SSSR 108, 659 (1956). Note also M. dR. D. Srivastava, Thermochemical Reactions of aluminum and fluorine in oxygen flames, Combust. Flame 27, 99 (1976).

$$\zeta_2 \rightarrow MX^* + MX, \qquad (1)$$

lting MX* product emitting a photon before undergoing ent collision.[34] These studies have been extended to "mul-lision" conditions by entraining the alkali dimers in argon and ently oxidizing this mixture.[35] A much more effective colli-nvironment consists of a "diffusion flame" device where is passed through a nozzle into a bulb containing several torr i vapor and one to twenty torr of argon.

g. 1, we depict emission spectra obtained for KCl, RbCl, and ıder single collision conditions. The nature of the potential vhich give rise to the spectra in Fig. 1 is depicted in Fig. 2. gh drawn for KBr, the general features are similar for all the

ADDED IN PROOF: The dissociation energy of cesium hydroxide has been d. This data was not included in Table II. Using mass spectrometry, Gorokhov, and Panchenkov (Table II Ref. b) determined D_0(Cs-OH) = 86 ± 3 kcal/mole. d Padley (Table I Ref. b) have used a third law analysis of an $H_2 + O_2 + N_2$ flame : D_0(Cs-OH) = 91 ± 3 kcal/mole. These determined bond energies are in fair t.

TABLE III. Infrared Data for the Alkali Hydroxides

Molecules	ν_1 (cm^{-1})	ν_2 (cm^{-1})
CsOH[a]	335.6	309.8
		302.4
CsOD[a]	330.5	226
RbOH[b]	354.4	309.0
RbOD[b]	345 ± 3	229 ± 3
KOH[c]	408	300
KOD[c]	399	264
NaOH[b]	431	337
NaOD[b]	422 ± 3	250

a. Ref. 23
b. Ref. 24
c. Ref. 25

TABLE IV. Comparison of Thermochemical Data for the Alkali Fluorides, Chlorides, and Hydroxides

Molecules	D_0^o(M-X)	Comments
KF	117[a]	Thermochemical
KCl	102.6 ± 2[b]	Thermochemical and photofragment
KOH	84 ± 2.5[c]	H_2-O_2-CO_2 flames 2nd law determination
	80 ± 3[d]	Mass spectrometry
	85.4 ± 3	(JANAF tables estimate)
NaF	123	NaOH 79 ± 2 (flame—2nd law—JANAF)
NaCl	97.6 ± 2[b]	
RbF	115[e]	RbOH 86 ± 3 (flame—2nd law—JANAF)
RbCl	101.3 ± 2[b]	

[a] E. M. Bulewicz, C. G. James, T. M. Sugden, Trans. Faraday Soc. 37, 921 (1961); A. G. Gaydon, *Dissociation Energies and Spectra of Diatomic Molecules*, 3rd Edition, Chapman and Hall (1968).

[b] T-M. R. Su and S. J. Riley, J. Chem. Phys. 72, 6632 (1980).

[c] R. Kelly and P. J. Padley, Trans. Faraday Society, 67, 740 (1971); also the average of three other flame studies by Smith and Sugden Proc. Roy. Soc. A219, 304 (1953) [86 ± 1]; Jensen and Padley, Trans. Fara. Soc. 62, 2132 (1966) [82 ± 2]; Cotton and Jenkins, Trans. Fara. Soc. 65, 1537 (1969) [86 ± 2].

[d] L. N. Gorokhov, A. V. Gusarov and I. G. Panchenkov, Russ. J. Phys. Chem. 44, 150 (1970).

[e] See footnote a and A. D. Caunt and R. F. Barrow, Nature 164, 753 (1949).

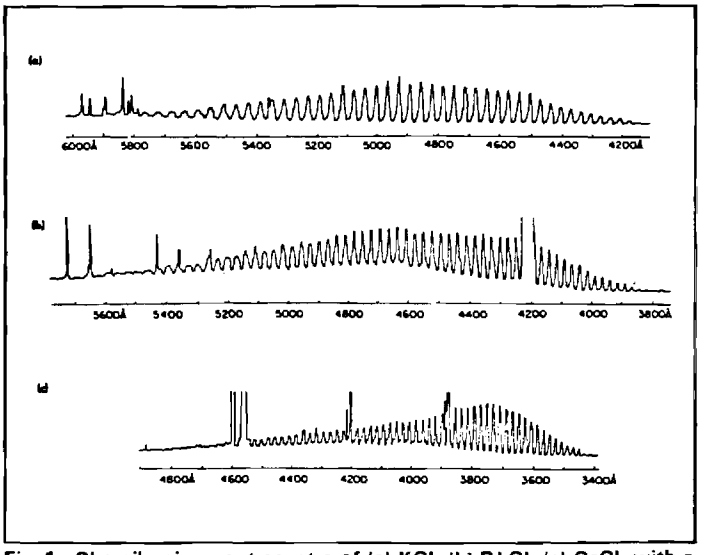

Fig. 1. Chemiluminescent spectra of (a) KCl, (b) RbCl, (c) CsCl, with a resolution of 5 Å or better. Also present in each trace are atomic (alkali) lines, some of which are off scale. (Taken from Ref. 34.) See text for discussion.

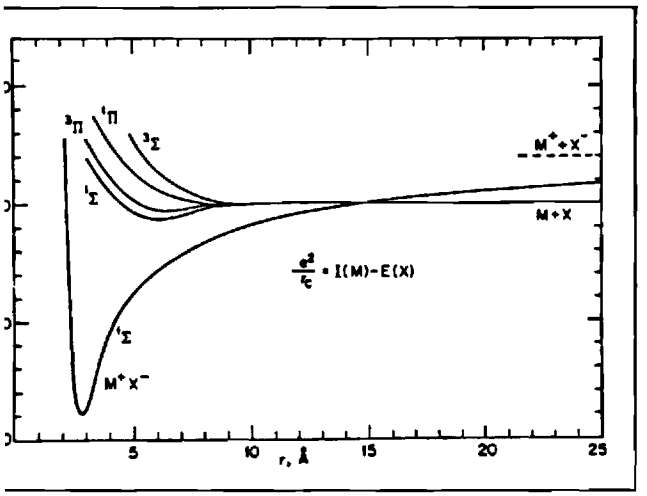

Potential energy curves for an alkali halide molecule (drawn for showing the "zeroth order crossing" of the ionic and covalent Note the shallow excited electronic states close to the ground lissociation asymptote.

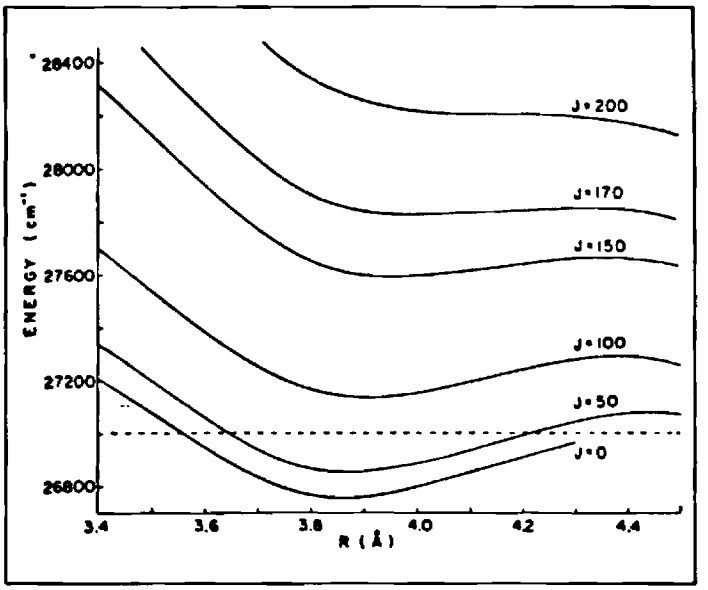

Fig. 3. Effective excited state potential curves for KI constructed from the rotationless potential of Kauffman, Kinsey, Palmer, and Tewarson (Ref. 37) assuming a dissociation asymptote of 2700 cm^{-1} (see Ref. 34).

halides. The alkali halides are characterized by a relatively ionic ground state and a grouping of several very shallow or ive excited states. The emission which one observes corres- to a transition from one of the shallow or repulsive states to of the ground electronic state, the spectrum corresponding to a rogression in the vibrational levels of the ground electronic state. The very shallow nature of the excited state potential portant consequences. One finds that the KCl spectrum es drastically with the form of excitation and the experimental que used to produce the emission system. The "single collision" um in Fig. 1 *onsets* at 4180 Å (68.4 kcal/mole). A very similar um is obtained when potassium dimers are entrained in argon is mixture oxidized in a multiple collision device. A drastic e occurs when the reaction (1) is studied in a diffusion flame nment. Here the onset of the KCl spectrum is at 2866 Å[36] some Å to blue of the single and multiple collision spectrum. This hange signals an important characteristic of the alkali halide state potential. Whereas emission spectra involving strongly excited states are not drastically altered by the nature of a ing effective potential due to rotation, the shape and nature of w or repulsive states can be drastically altered by rotational tion. This is exemplified for KI in Fig. 3.[37] Here effective ial curves are constructed as a function of the rotational um number J and the relation

$$V_{\text{ive}}(J) = V_{\text{rotationless}} + \hbar^2\left(\frac{J(J+1)}{2\mu R^2}\right) . \qquad (2)$$

hould be noted that there is a substantial change in the minima e effective potentials as a function of increasing rotational tion and hence the quantum number J. The high J potentials pond to the single and multiple collision spectra onsetting at Å;[36] the low J potentials correspond to the diffusion flame on system onsetting at 2866 Å.[36] As a result of this shift in the state potential one observes emission to differing sets of state levels. In the diffusion flame experiments emission is ed to much lower regions of the ground state potential and the spectra onsets much further to the blue.[36]

e spectrum for potassium hydroxide has been obtained by lino et al.[16] upon reacting potassium with hydrogen peroxide e). The process which yields chemiluminescence is believed to pond to the four center reaction

$$HO\text{-}OH + KOH^* + KOH \qquad (3)$$

where KOH* denotes electronically excited KOH. The close analogy which the potassium hydroxide spectrum bears to that of KCl leads to comparisons between the two molecules which, in the final analysis, involve a direct determination of the K-OH bond energy.

The change in the emission spectra for the alkali halides as a function of experimental conditions may also be manifest in the alkali hydroxides. One anticipates that the potential function describing the K-OH stretch will be similar to that for KCl. If the potential curves for the excited states of K-OH are similar to those for KCl, they should be shallow and the KOH emission spectrum which results from reaction (3) should change significantly with excitation technique. This is observed, although the effect is not as pronounced as that in KCl. Single and multiple collision spectra for KOH onset at 3840 Å whereas the spectrum obtained in a diffusion flame (Fig. 4) onsets at 3240 Å. This significant change signals the observation of a shallow "effective" potential for the K-OH normal mode.[38]

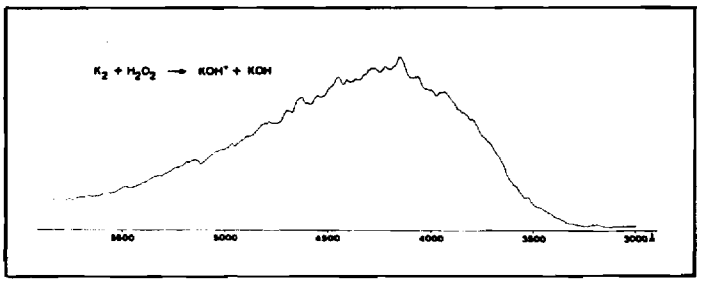

Fig. 4. Chemiluminescent spectrum obtained for KOH* formed in a diffusion flame environment. See text for discussion.

The KCl and KOH spectra correspond to emission from shallow effective potentials close to the dissociation asymptote (Figs. 2 and 3) of the ground electronic state. Given that we have strong evidence for these shallow effective potentials, we can use the onset of spectral emission to estimate the dissociation energy for the K-Cl and K-OH bonds. Because the diffusion-flame results must correspond to emission to lower levels of the ground state potential, this onset is chosen to give the best estimate of the bond dissociation energy. For K-Cl, the onset at 2866 Å corresponds to 99.8 kcal/mole. This should be compared to the value in Table IV: D_0°(K-Cl) = 102.6 ± 2 kcal/mole.

ıld be apparent that we are able to estimate a good lower to the K-Cl dissociation energy from the energy correspondhe onset of the K-Cl diffusion flame spectrum. The onset of H diffusion flame spectrum at 3240 Å yields a lower bound of al/mole for the K-OH bond energy.[39]

result obtained by Cardelino et al.[16] is significant for several :. It represents the first direct measurement of the bond energy ; species. The lower bound deduced for the K-OH bond h indicates that the correct dissociation energy is on the order 2 kcal/mole. This value considerably exceeds that obtained in y mass spectrometric study of the monomer quoted in Table e much higher value for the KOH bond energy is more ent with the bounds estimated from metal atom flame depleıdies, but does indicate a slightly higher value.[39] A several ›rie increase in the KOH bond strength has significant impli- for the stability and effect of this compound in energy generatems.[40]

anticipated that further studies of the K_2-H_2O_2 diffusion flame will improve the lower bound currently quoted for the K-OH ıergy. It should be noted that the present result is not incon- with the recent findings of Wormhoudt and Kolb.[41] These observe unusually high KOH concentrations in their studies fired MHD plasmas. Also, recent theoretical calculations by 1[42] indicate the possibility of a higher K-OH bond energy. ddition to a refinement of the K-OH bond energy, higher on spectra of the K_2-H_2O_2 diffusion flame should provide :ful information on the vibrational structure of the ground rmal mode "hot" bands. With reasonable luck, it should be to correlate these studies with the millimeter wave results ıed earlier. The structural parameters (molecular constants) d will be of use in the calculation of thermodynamic proper- KOH.

alkaline earth hydroxides

, there is very little molecular parameterization on the alkah hydroxides. Brom and Weltner have obtained ESR spectra H[43] and MgOH.[44] Weeks et al.[45] have studied laser excited ar fluorescence from CaOH and SrOH in an air-acetylene ›roposing a preliminary energy level diagram for CaOH. uthors also comment on apparent earlier observations of ınd SrOH in both absorption[46] and fluorescence.[47] More Haraguchi et al.[48] have excited laser fluorescence from again indicating the nature of previous absorption[49] and ı[50] studies and presenting a preliminary energy level diagram. ; the chemiluminescent emission from the Ca-H_2O_2 reacnner et al.[51] have succeeded in obtaining "single collision" from CaOH, determining a preliminary CaOH bond energy kcals/mole. This result is in good agreement with the flame ›f Cotton and Jenkins[52] and Kalff and Alkemade.[53] These ›ill be extended to consider strontium and barium reactions the determination of lower bounds for the alkaline earth le bond energies. It should be noted that the calcium and n compounds do not appear to be accessible to mass ıetry.

parse nature of the data on the alkaline earth hydroxides leaves a very fruitful and potentially significant area for study.

›r metal hydroxides

no doubt that experimental techniques developed for the d alkaline earth hydroxides will soon be extended to other ıt metal hydroxides. Of particular note should be the hydroxınadium, silicon, and iron. These species will weigh heavily technological developments.

DING AND SPECTRA OF THE ALKALI XIDES AND MONOSULFIDES

ling in the diatomic metal oxides and sulfides

ıve been relatively few spectroscopic or thermodynamic studies of the alkali oxides. Based on the results of molecular beam experiments (alkali metals + NO_2), Herm and Herschbach[54] have estimated the MO bond dissociation energies as follows: LiO (82 ± 4), NaO (67 ± 3), KO (71 ± 3), RbO (68 ± 3), and CsO (70 ± 3 kcal/mole). The value for NaO is in fair but not spectacular agreement with the value of 60.3 ± 4 kcal/mole deduced by Murad and Hildenbrand[55] using mass spectroscopy. Fundamental frequencies for LiO (750 cm^{-1}),[56] KO (384),[57] and CsO (314)[57] have been measured using matrix isolation spectroscopy; however, the corresponding infrared absorptions in NaO and RbO have not yet been observed.

Evidence has been obtained for a change in the orbital makeup and symmetry of the ground electronic state upon traversing the series LiO...CsO. The electronic ground state of LiO is $^2\Pi$. Freund et al.[58] have obtained very detailed spectra which demonstrate that this molecule is well represented by a crystal field model based on $Li^{\oplus}$ $O^{\ominus}$. This model is in accord with *ab initio* calculations.[59]

Reactive scattering experiments[54] have indicated that NaO also has a $^2\Pi$ ground state whereas the ground state of CsO is of $^2\Sigma$ symmetry. Most recently ESR-matrix experiments[60] have also demonstrated that RbO and CsO have $^2\Sigma$ ground states whereas the ground states of LiO, NaO and KO are probably $^2\Pi$. A recent theoretical calculation[61] is in slight conflict with this conclusion indicating that the ground state of KO is $^2\Sigma^+$.

The observation of a $^2\Sigma^+$ ground state conflicts with the simple ionic model in which the electron donated by the alkali atom enters the $2p\sigma$ oxygen orbital along the internuclear axis, leaving a hole in the 2π orbital and resulting in a $^2\Pi$ state ($\sigma^2\pi^3$ molecular orbital configuration). An explanation for the observed trends can be obtained by evoking the concept of "inner shell bonding" in which one considers the mixing of filled (n − 1)p alkali orbitals with the 2p oxygen orbitals. Figure 5 contrasts the molecular orbital scheme for NaO based on the alkali valence orbitals with the adjusted intershell orbital scheme for CsO.[60,61] The alkali monoxides are highly ionic

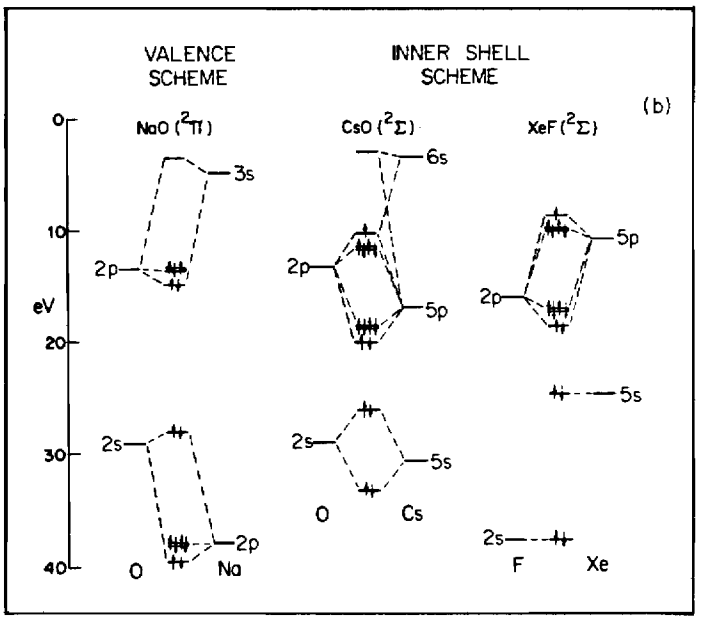

Fig. 5. Molecular orbital scheme for the alkali monoxides (taken from the work of Lindsay, Kwiram and Herschbach, Ref. 60). See text for discussion.

molecules, $M^{\oplus}$ $O^{\ominus}$, in both schemes but the latter gives a $^2\Sigma$ ground state (... $\pi^4\sigma$). The change from the valence to the inner shell scheme is governed by the location of the (n−1)p orbitals of M^+. These orbitals lie far below the 2p orbitals of O^- for Li or Na but become comparable in energy for Rb or Cs.

The significance of the orbital scheme discussed above can best be understood if we focus on the calculated *ab initio* curves for LiO (Fig.

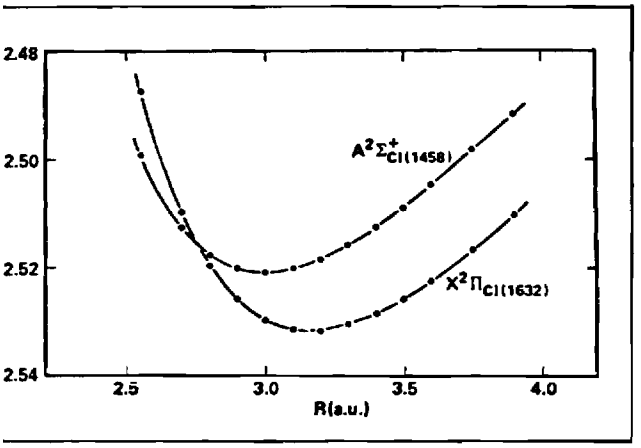

Potential curves based on extensive configuration interaction calns on the $X^2\Pi$ and $A^2\Sigma^+$ states of LiO.

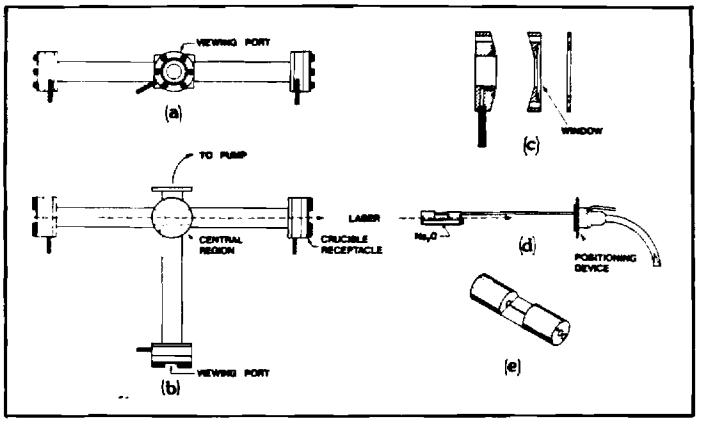

Fig. 7. Schematic diagram of apparatus for laser fluorescence studies of Na_2O. See text for discussion.

; apparent that the ground $X^2\Pi$ and low lying $A^2\Sigma^+$ states are ted by less than 2300 cm^{-1}. This energy increment will decrease : sodium and potassium oxides. For RbO, the $A^2\Pi_i$ state is ted by less than 3800 cm^{-1} from the ground $X^2\Sigma^+$ state.[60]

ile the sulfides are expected to display similar bonding trends, well be that the possibility of "inner shell bonding" decreases e of the small binding energy for the 3p electron on sulfur. ore, the ground states of LiS, NaS and KS are expected to be l the ground state of RbS may be $^2\Pi$ with a very low lying $^2\Sigma$ To date, no information is available on the alkali sulfides; er, the metal sulfide bond energies are expected to be somewer than the corresponding oxides.

should be apparent from the previous discussion, data which ove of use for the future assessment of metal oxide and sulfide tions is virtually unavailable. The characterization of these ; will not represent a trivial problem. Experimental difficulties are already substantial are further complicated by the presence very low-lying $^2\Sigma$ (LiO, NaO, etc.) or $^2\Pi$ (RbO, CsO, etc.) state. er to characterize the $^2\Sigma$ and $^2\Pi$ states, it may be appropriate to for higher-lying electronic states; however, predissociative will soon plague this search. There is indication that the uminescent reactions $M + N_2O$, $M + O_3 - MO^* + \ldots$ may lead e elucidation of the molecular parameters for the alkali oxides; er, these data are only in a preliminary state.[62]

nding in the triatomic alkali oxides and sulfides nd M_2S

other interesting group of compounds whose characterization present a significant contribution are the alkali oxides, M_2O. have been several quantum chemical calculations performed O[63] and infrared fundamentals (ν_3) have been reported for K_2O,[57] Rb_2O,[57] and Cs_2O;[57] however, thus far, there appear o definitive gas phase data on these compounds and no data ever on Na_2O.

ser spectroscopy on Na_2O—a preliminary study

er to efficiently excite fluorescence from Na_2O, Crumley et ve constructed the device depicted in Fig. 7. Figures 7(a) and dicate the overall layout of the cell used in these experiments. 7(c) indicates the window design which is frequently necessary working with refractory species, the gas flow system being ed to provide a uniform circulation of gas over the windows. In o carefully control the vaporization of Na_2O in a very localized , the device depicted in Figs. 7(d) and 7(e) is used. It consists of ble which is suspended on a 1/8" stainless steel tube such that ie overall device is connected to the cell sidearm, the crucible is lly located to the viewing port. The positioning control whose er is the same as the window shown in Fig. 7(c) is held in place in precisely the same fashion as the window. When connected to the overall cell, the crucible holder is rotated 90° with respect to its depiction in the figure. When the cell is in operation, a laser beam traverses the path indicated in Figs. 7(b) and 7(d). Na_2O is directly vaporized through a thin slit into the path of the laser beam. The slit and the laser beam are parallel and the laser induced fluorescence is viewed at 90°.[65]

Using the cell described above and various pumping schemes, Crumley et al.[64] have carried out experiments at both 100 μ (primarily background argon) and 10^{-6} torr. This range of background pressure allows one not only to do spectroscopy but also to observe quenching effects which appear to be quite significant for Na_2O. Thus far, experiments have been conducted primarily with an argon ion laser; however, some excitation has been accomplished with a rhodamine dye laser. Examples of the spectra *tentatively* assigned to Na_2O are shown in Fig. 8.[66] They correspond to excitation at 5145

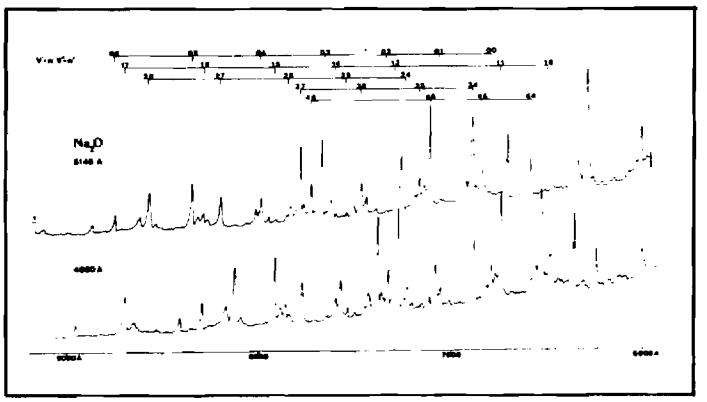

Fig. 8. Laser induced photoluminescence spectra tentatively correlated with Na_2O taken at a resolution of 1 Å and using the 5145 and 4880 Å argon ion laser lines for excitation. See text for discussion.

and 4880 Å. It appears that one can excite laser-induced fluorescence with several of the available argon ion laser lines (4579, 4880, 4965, 5017, 5145 Å) and that the fluorescence spectra can be interconnected (significant overlap) in a rather substantial Deslandres Table. Much of the analysis of the observed spectra has depended on relating the Na_2O studies to available information on Li_2O. These data come primarily from matrix isolation spectroscopy[56] and recent quantum chemical calculations.[63] Briefly, the data have been used to (1) attempt to estimate the normal frequencies of vibration for Na_2O based on a reasonable extrapolation from Li_2O, and (2) determine the most likely electronic transition which should be excited in the visible using an argon ion laser.

ıg a notation common to several quantum chemical descrip-
f linear $D_{\infty h}$ Li_2O, the valence orbital configuration for the
state is

$$_g)^2(2\sigma_u)^2(1\pi_u)^4 \qquad {}^1\Sigma_g^+ \qquad (4)$$

he valence orbitals are constructed primarily from 2s and 2p
ns on lithium and oxygen. The lowest Li_2O excited states
ond to the promoted configurations

$$_g)^2(2\sigma_u)^2(1\pi_u)^3(4\sigma_g)^1 \qquad {}^{1,3}\Pi_u \qquad (5)$$

$$_g)^2(2\sigma_u)^2(1\pi_u)^3(3\sigma_u)^1 \qquad {}^{1,3}\Pi_g \qquad (6)$$

ow and Pitzer[63b] have shown that these states are very low
$\Delta E_{excitation} \leq 1.3$ eV); therefore it is unlikely that even the
y allowed

$$\Sigma_g^+$$

on corresponds to the fluorescence observed upon single
pumping with an argon ion laser. A further promotion which
ult in a strongly allowed transition, most likely in the visible
leads to the configuration

$$_g)^2(2\sigma_u)^1(1\pi_u)^4(4\sigma_g)^1 \qquad {}^{1,3}\Sigma_u^+ . \qquad (7)$$

ticipates that the visible transition in Na_2O which is pumped
argon ion laser corresponds to a $^1\Sigma_u^+ - {}^1\Sigma_g^+$ excitation
ng the analog of configurations (4) and (7). In pumping this
on, one removes an electron from an orbital which is Na-O
ıding and Na-Na antibonding and promotes this electron to
ital which is both Na-O and Na-Na bonding. Hence, one
that both the excited state stretching and bending frequen-
ıuld exceed that of the ground electronic state of Na_2O.
ground state frequencies for Li_2O are (matrix isolation spec-
y) $\nu_1 \approx 760\ cm^{-1}$, $\nu_2 \approx 112\ cm^{-1}$, and $\nu_3 \approx 990\ cm^{-1}$. Formu-
a normal coordinate analysis based on the Li_2O measure-
one estimates a vibrational frequency of between 540 and 585
or the symmetric stretch (ν_1) and 74 cm^{-1} for the bending
f Na_2O. This is not unreasonable when comparisons are made
aO where the vibrational frequency appears to be ~519
(recall that Na_2O is thought to be a linear molecule).
ıough absolute quantum level numberings have not been
d, extensive Deslandres Tables for the pumped transitions
: an upper state vibrational frequency of ~650 cm^{-1} and a
tate (ground state) frequency of ~550 cm^{-1} consistent with
lictions outlined above. In addition, a closer view (Fig. 9) of a
of the 5145 Å spectrum in Fig. 8 reveals what appear to be
$^{-1}$ separations expected for the ground state bending mode
O. *Tentatively*, it appears that the spectra correspond to
ısions in the symmetric stretching and bending modes of the
and excited state in a $^1\Sigma_u^+ \rightarrow {}^1\Sigma_g^+$ transition.
se studies hold the promise of providing information which is
ly useful for the understanding of fundamental dynamic pro-
uch as the reaction of sodium dimers and oxygen atoms and
o establish a foothold for analyzing kinetic processes in which
lays a significant role. Because Na_2O represents an important
ıent in energy generating systems, one desires a means to
ly monitor its behavior. It should also be noted that in addi-
their use for the characterization of reaction kinetics, such
while still in their early phases, may well allow the determina-
parameters useful in thermodynamic evaluations. Before the
of the laser, the study of these elevated temperature free
s rested primarily within the province of the matrix isolation
scopist. The versatility introduced by the laser should allow
ıre comparison of molecular behavior in gas phase and matrix
ıments.

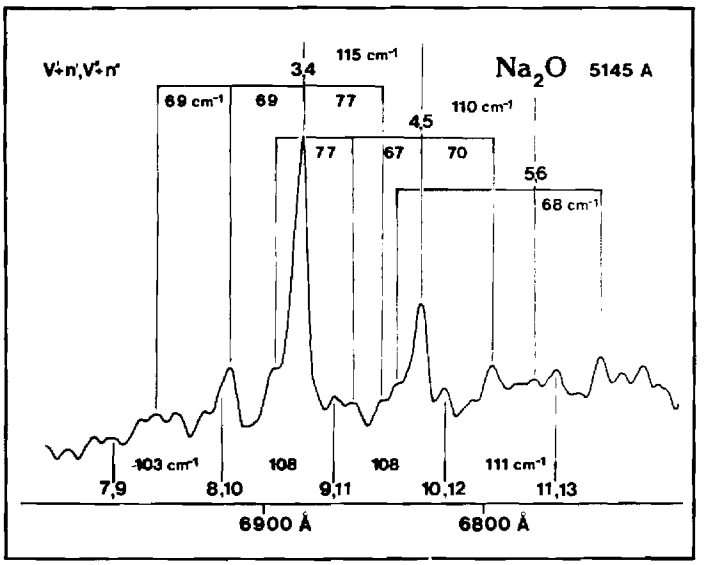

Fig. 9. Close-up of laser induced photoluminescence spectrum tentatively correlated with Na_2O taken at a resolution of 0.5 Å and using the 5145 Å argon ion laser line for excitation. See text for discussion.

6. FURTHER CONSIDERATIONS

We have attempted to indicate the nature of several important and yet sparsely characterized systems whose study will greatly aid the understanding of the gas phase chemistry associated with energy generating systems. While our discussion has focused primarily on bond energies and molecular parameterization, kinetics and energy transfer must also play an important role in the realistic description of a system. The correct modeling of energy generating systems is the subject of some controversy. Strong evidence is emerging which indicates that the modeling of an energy system assuming thermodynamic equilibrium and applying "free energy minimization" may not be entirely or even partially appropriate. In the vast majority of the systems where thermodynamics and kinetics both play a role, observed phenomena are in large part controlled by the rates of various processes. Hence current modeling efforts are incorporating kinetic parameters.[40] In carrying out chemiluminescent studies across a wide pressure range ($10^{-6} - 10^2$ torr), we have observed and characterized ultrafast intramolecular energy transfer routes among the electronically and vibrationally excited states of several high temperature molecules. Thus far, these studies have indicated that energy transfer can occur at rates which may approach 500 times the calculated gas kinetic rates. These surprising results demonstrate that vibrationally and/or electronically excited high temperature molecules act as if they were "large" or "diffuse" entities capable of strong interaction at very long range. This rapid energy transfer is a general phenomenon and effects have been observed in several molecules including SiO and KOH. The observation of such rapid energy transfer may have significant implications for the modeling of energy generating systems and the characterization of heat flow in these systems.

7. ACKNOWLEDGMENTS

It is a pleasure to acknowledge partial support of some of the work described here by the U. S. Department of Energy. Professor W. H. Eberhardt read the first draft of this manuscript and provided many helpful suggestions.

8. REFERENCES

1. D. M. Lindsay and J. L. Gole, J. Chem. Phys. 66, 3886 (1977); M. J. Sayers and J. L. Gole, J. Chem. Phys. 67, 5442 (1977); J. L. Gole and S. A. Pace, J. Chem. Phys. 73, 836 (1980); A. W. Hanner and J. L. Gole, J. Chem. Phys. 73, 5025 (1980).
2. R. J. Ross, *Magnetohydrodynamic Energy Conversion*, McGraw-Hil, New York (1968).

S. A Medin, V. A. Ovcharenko and E. E. Shpil'rain, High Temp. U.S.S.R. 10, 390 (1972).
H. C. Hottel and J. B. Howard, *New Energy Technology—Some Facts and Assessments*, M.I.T. Press, Cambridge, MA (1971); L. P. Harris and G. E. Moore, IEEE Trans. Power App. Syst. 90, 2030 (1972).
Open Cycle Magnetohydrodynamic Power Generation, J. B. Heywood and G. J. Womack, eds., Pergamon, Oxford (1969).
F. E. Spencer, Jr., J. C. Hendrie and D. Bienstock, Symp. Eng. Aspects Magnetohydrodynam., 13th, Stanford Univ., p. VII.4.1; VII.4.6.
Joint Army Navy Air Force Thermochemical Tables, 2nd ed., NSRDS-NBS37. U.S. Govt. Printing Office, Washington, D.C.
W. B. England, J. Chem. Phys. 68, 4896 (1978).
Sulfur impurities are also important. See for example, R. K. Sinha and P. L. Walker, Jr., Fuel 51, 329 (1972); F. S. Karn, R. A. Friedel and A. G. Sharkey, Jr., Fuel 51, 113 (1972).
J. Marlin Smith, L. D. Nichols and G. R. Seikel, NASA Lewis H_2-O_2 MHD Program, Int. Symp. Eng. Aspects of Magnetohydrodynamics, 14th April, 1974, Tullahoma, TN, p. III.7.1.
G. W. Stewart, A. Chakrabasti, C. Stinespring and K. Casleton, Western States Symposium/Combustion Institute, October, 1980.
Session on High Pressure Sampling, 10th Materials Research Symposium on Characterization of High Temperature Vapors and Gases, National Bureau of Standards, Gaithersburg, MD. September 18-22, 1978.
I. Fells, in *Combustion and Propulsion*, AGARD Colloq. 6th, Energy Sources and Energy Conversion, H.M. DeGroff, R. F. Hogland, J. Fabri, T. F. Nagey and M. E. Rumbaugh, Jr., eds., Gordon and Breach, New York (1967), p. 477.
See, for example, J. W. Hastie, *High Temperature Vapors, Science and Technology*, Academic Press, New York (1975); see also, O. Glemser and H. G. Wendlandt, Advan. Inorg. Chem. Radiochem. 5, 215 (1963); F. T. Greene, S. P. Randall and J. L. Margrave, in *Thermodynamic and Transport Properties of Gases, Liquids and Solids*, Am. Soc. Mech. Eng., New York (1959), p. 222; D. D. Jackson, *Thermodynamics of Gaseous Hydroxides*, UCRL—51137 (1959).
Laboratory data on the hydroxides when extrapolated may well be related to practical problems such as the nature of solid deposition in steam turbines.
B. Cardelino, W. Crumley and J. L. Gole, work in progress.
A. W. Hanner and J. L. Gole, unpublished data.
W. D. Winefordner et al. to be published; see also Refs. 45 and 47.
F. E. Stafford and J. Berkowitz, J. Chem. Phys. 40, 2963 (1964).
R. Kelly and P. J. Padley, Trans. Faraday Soc. 67, 740 (1971); H. Smith and T. M. Sugden, Proc. R. Soc. A 219, 304 (1953); D. H. Cotton and D. R. Jenkins, Trans. Faraday Soc. 65, 1537 (1970); D. E. Jensen and P. J. Padley, Trans. Faraday Soc. 62, 2132 (1966).
L. N. Gorokhov, A. V. Gausarov and I. G. Panchenkov, Russ. J. Phys. Chem. 44, 150 (1970).
See Table II references c, d, e.
N. Acquista, S. Abramowitz and D. R. Lide, J. Chem. Phys. 49, 780 (1968).
N. Acquista and S. Abramowitz, J. Chem. Phys. 51, 2911 (1969).
A. A. Belyaeva, M. I. Dvorkin, and L. D. Sheherba, Opt. and Spectrosc. 31, 210 (1971).
D. R. Lide and R. L. Kuczkowski, J. Chem. Phys. 46, 4768 (1967).
C. Matsumura and D. R. Lide, J. Chem. Phys. 50, 71 (1969); D. R. Lide and C. Matsumura, J. Chem. Phys. 50, 3080 (1969).
E. F. Pearson and M. B. Trueblood; J. Chem. Phys. 58, 826 (1973); Astrophys. Journal 174, L145 (1973).
E. F. Pearson, B. P. Winnewisser and M. B. Trueblood, Z. Naturforsch 31a, 1259 (1976).
P. Kuijpers, T. Törring and A. Dymanus, Chem. Phys. 15, 457 (1976); Z. Naturforsch 31a, 1256 (1975).
P. Kuijpers, T. Törring and A. Dymanus, Z. Naturforsch 32a, 930 (1977).
D. E. Jensen, J. Phys. Chem. 74, 207 (1970).
J. L. Gole, The Characterization of High Temperature Vapors of Import to Combustion and Gasification Processes in the Energy Technologies, Proceedings of the Morgantown Energy Technology Center Meeting on High Temperature, High Pressure Particulate and Alkali Control in Coal Combustion Process Streams, Morgantown, West Virginia, 1981.
For a discussion of single collision conditions, see J. L. Gole, Ann. Rev. Phys. Chem. 27, 525 (1976); for the alkali halides, see R. C. Oldenborg, J. L. Gole and R. N. Zare, J. Chem. Phys. 60, 4032 (1974).
See Ref. 1 and G. J. Green and J. L. Gole, Chem. Phys. 46, 67 (1980).
A. Tewarson, Studies of Chemiluminescent Emission in Selected Low-Pressure Diffusion Flames, Ph.D. Thesis, Penn State University, 1969.
The long wavelength limit of the diffusion flame spectrum is 4654 Å versus 5708 Å for the single collision spectrum. Hence the entire KCl spectrum is shifted to the blue ~1200 Å when experimental conditions are changed from the single collision to the diffusion flame environment.
37. Taken from Oldenborg et al. Ref. 34. Based on the study by K. J. Kaufmann, J. L. Kinsey, H. B. Palmer and A. Tewarson, J. Chem. Phys. 60, 4023 (1974).
38. Of course it is not completely correct to speak of an isolated K-O stretch in the KOH molecule. In reality there will be some coupling with the O-H stretch and the bending mode of the triatomic.
39. This is a stringent lower bound and more refined diffusion flame studies should yield an even higher value. Based upon the probable dissociation products for the ground and excited states of KOH, it is likely that the upper excited state potential may be significantly bound with respect to the dissociation asymptote of the ground electronic state. The much smaller change in the diffusion flame vs single collision spectrum for KOH vs that for KCl indicates that this is probably the case. We anticipate that the emitting excited state of KOH may be bound by as much as 10 kcal/mole relative to the dissociation asymptote of the ground state.
40. J. Wormhoudt, V. Yousefian, M. H. Weinberg, C. E. Kolb and M. M. Slugter, A Review of Plasma Chemical Considerations in MHD Generator Design, Seventh International Conference on MHD Electrical Power Generation, Cambridge Mass. 1980, p.530.
41. J. Wormhoudt and C. E. Kolb, Mass Spectrometric Determination of Negative and Positive Ion Concentrations in Coal-Fired MHD Plasmas, 10th Materials Research Symposium, NBS Special Publication 561, Volume 2.
42. W. B. England, J. Chem. Phys. 68, 4896 (1978).
43. J. Brom and W. Weltner, J. Chem. Phys. 64, 3894 (1976).
44. J. Brom and W. Weltner, J. Chem. Phys. 58, 5322 (1973).
45. S. J. Weeks, H. Haraguchi and J. D. Winefordner, J. Quant. Spectrosc. Radiat. Trans. 19, 633 (1978).
46. S. R. Koirtyohann and E. E. Pickett, Anal. Chem. 38, 585 (1966); M. Yoshimura et al. unpublished.
47. H. G. C. Human and P. J. Th. Zeegers. Spectrochim. Acta 30B, 203 (1975); M. B. Blackburn, J. M. Mermet and J. D. Winefordner, Spectrochim. Acta, 34A, 847 (1977).
48. H. Haraguchi, S. J. Weeks and J. D. Winefordner, Spectrochim. Acta, 35A, 391 (1979).
49. See Refs. 46-48.
50. See Refs. 46-48.
51. A. W. Hanner and J. L. Gole, unpublished.
52. D. H. Cotton and D. R. Jenkins, Trans. Faraday Soc. 64, 2988 (1968).
53. P. J. Kalff and C. T. J. Alkemade, Combust. Flame 19, 257 (1972).
54. R. R. Herm and D. R. Herschbach, J. Chem. Phys. 52, 5783 (1970).
55. D. L. Hildenbrand and E. Murad, J. Chem. Phys. 53, 3403 (1970).
56. (a) R. C. Spiker, Jr. and Lester Andrews, J. Chem. Phys. 58, 702 (1973); (b) D. White, K. S. Seshardri, D. F. Dever, D. E. Mann and M. J. Linevsky, J. Chem. Phys. 39, 2463 (1963); (c) K. S. Seshardri, D. White and D. E. Mann, J. Chem. Phys. 45, 4697 (1966).
57. R. C. Spiker and L. Andrews, J. Chem. Phys. 58, 713 (1973).
58. S. M. Freund, E. Herbst, R. P. Mariella, Jr. and W. Klemperer, J. Chem. Phys. 56, 1467 (1972).
59. M. Yoshimine, J. Chem. Phys. 57, 1108 (1972); B. Liu and M. Yoshimine, J. Chem. Phys. 60, 1427 (1974). For further work see also M. J. Clugston and R. G. Gordon, J. Chem. Phys. 66, 244 (1977).
60. D. M. Lindsay, D. R. Herschbach and A. L. Kwiram, Mol. Phys. 32, 1199 (1976).
61. For a discussion of the "inner shell valence scheme" see: J. R. Morton and W. E. Falconer, J. Chem. Phys. 39, 427 (1963); W. E. Falconer, J. R. Morton and A. G. Streng, ibid 41, 902 (1964); R. C. Eachus and M. C. R. Symons, J. Chem. Soc. A304 (1971). For a further comment on alkali oxide bonding considering a ground $^2\Sigma^+$ state for KO, see S.P. So. and W. G. Richards, Chem. Phys. Lett. 32, 227 (1975).
62. W. Crumley, B. Cardelino and J. L. Gole, work in progress.
63. (a) R. J. Buenker and S. D. Peyerimhoff, J. Chem. Phys. 45, 3682 (1966); (b) D. T. Grow and R. M. Pitzer, J. Chem. Phys. 67, 4019 (1977); (c) E. L. Wagner, Theoret. Chim. Acta 32, 310 (1974); (d) T. K. Lin and D. D. Ebbing, Int. J. Quant. Chem. 6, 297 (1972).
64. W. Crumley, J. Appling and J. L. Gole, work in progress.
65. It should be noted that extensive baffling is used in the system to avoid problems with scattered laser light.
66. The notation in Fig. 8 is designed to give a relative numbering. Because v' and v'', the absolute quantum numbers for the upper and lower states are not known, we use the notation v' + n', v'' + n'' where the indices in the figure denote the values of n' and n''. In this case it is likely that the value of v'' will exceed that for the level from which laser pumping occurs. ⊙

APPENDIX B

Metal cluster oxidation: Chemiluminescence from the reaction of sodium polymers (Na_n, $n \geq 3$) with halogen atoms (X=Cl, Br, I)

W. H. Crumley and J. L. Gole

Department of Chemistry and High Temperature Laboratory, Georgia Institute of Technology, Atlanta, Georgia 30332

D. A. Dixon

Department of Chemistry, The University of Minnesota, Minneapolis, Minnesota 55455
(Received 17 February 1982; accepted 8 April 1982)

The structure and bonding of small metal clusters represents a young topic which has become the focus of both experiment and theory.[1] The emphasis now placed on the study of the basic properties of these clusters stems, in part, from their possible importance to the understanding of the fundamental mechanisms of catalysts and numerous chemical conversions. Ligand-free metallic clusters have been produced in the gas phase through "free jet" supersonic expansion of the pure element[1(a),1(b),2] and through select cluster deposition[3] or diffusion controlled clustering[1(a),1(b)] in rare gas matrices. Emphasis has been primarily on spectroscopic characterization of the produced cluster with little focus on the binding energies of these species or "cluster oxidation." In studying gas phase metal cluster oxidation, we are afforded the opportunity to characterize the intermediate region bordered on the one side by the gas phase oxidation of metallic atoms and dimers and on the other by the surface oxidation of the bulk metallic phase. It is thought[4] that these studies will provide information which may be useful for the assessment of short and long range factors affecting surface oxidation.

This report outlines the first study of phenomena associated with gas phase polymeric sodium cluster oxidation. Initial efforts focus on oxidation with the halogen atoms chlorine, bromine, and iodine. These systems were chosen (1) because of their analogy to the previously studied[5] alkali dimer–halogen atom reactions and (2) because of the higher electronic transition moments generally characteristic of compounds of the alkali metals.[6]

The apparatus used in these studies will be described in more detail in a future report.[7] Briefly, the system consists of oven and reaction chambers connected by a variable sized channel 20 mm in length which, in the present experiments is 6 mm in diameter. Sodium is expanded from a stainless steel double oven used for the supersonic expansion of alkali metals.[1(b)] The oven was run at stagnation pressures between 20 and 120 Torr and the expansion nozzle diameter was typically 0.25 mm. The separation between nozzle orifice and fluorescence zone is approximately 17 cm and the molecular beam density in the fluorescence zone ranges to a maximum of $\approx 10^{13}$ particles/cm^3. The halogen atom gun is operated at temperatures in excess of 1500 K whence halogen molecules passing through the gun channel should be 95+% converted to halogen atoms. The system is operated in a beam-gas configuration. Pressures in the reaction chamber never exceeded 5×10^{-5} Torr. In order to maintain these conditions and insure smooth oven operation, liquid nitrogen cooling was used throughout the oven and reaction chambers.[7]

Figure 1 depicts the chemiluminescent emission which characterizes the exemplary sodium–chlorine system under two distinct experimental conditions. If the halogen atom gun is operative and the sodium beam is generated supersonically [Fig. 1(a)], we observe a molecular spectrum characterized in large part by strong emission corresponding to the Na_2^* $B\,^1\Pi_u$–$X\,^1\Sigma_g^+$ band system[8] and moderate emission associated with the Na_2 $A\,^1\Sigma_u^+$–$X\,^1\Sigma_g^+$ and $C\,^1\Pi_u^+$–$X\,^1\Sigma_g^+$[9] band systems. In addition, weak emission is tentatively attributed to the Na_2 D and E states.[8,10] Although not indicated in Fig. 1(a), the molecular emission characterizing the supersonic sodium–chlorine atom reaction is dominated by intense emission corresponding to both the Na D-line and $4\,^2P$–$3\,^2S$ sodium atom transitions.[11] There are also other emission features not readily associated with Na_2 or Na which are currently the subject of continued investigation in our laboratory. Most notable among these is the 3900 Å feature in close proximity to a region of the Na_2 C–X emission system. Based upon a comparison of the spectra characterizing both the chlorine and bromine atom reactions, this feature is molecular in origin and associated with a homonuclear sodium compound.

Over the range of oven conditions considered, the Na_3

 0021-9606/82/126439-03$02.10

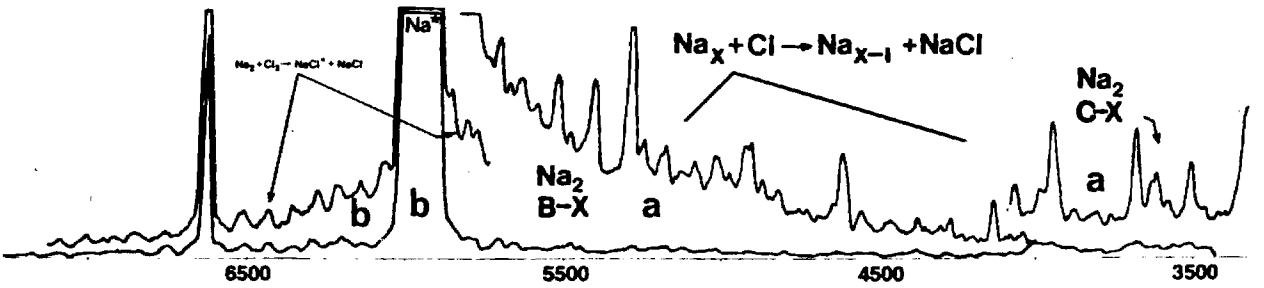

a) Chemiluminescent spectrum (3400–5800 Å) associated with the processes $Na_x + Cl \rightarrow Na_{x-1} + NaCl$, where the dominant spectrum corresponds to Na_2^* emission resulting primarily from the reaction of sodium trimer. The major features in nd C–X regions correspond to the overlap of several (v', v'') emission features (e.g., for the 5278 Å feature the inten- rived primarily from $\Delta v = v' - v'' = -9, -8$, transitions...). Below 4100 Å, the scale for the C–X region is multiplied by long wavelength limit, the emission rises sharply as the Na D-line is approached. The Na atomic emission features $-3\,^2S$, $4\,^2P-3\,^2S$), not depicted, are $\sim 10^2$ times the intensity of the molecular emission features. (b) Chemiluminescent r NaCl* and Na*. The NaCl emission is tentatively attributed to the reaction $Na_2 + Cl_2 \rightarrow NaCl^* + NaCl$. The observed * fluorescence is consistent with the process $NaCl^\dagger + Na \rightarrow Na^* + NaCl^{\dagger\prime}$. The feature at 6600 Å corresponds to second or- ion associated with the Na $4\,^2P-3\,^2S$ transition. In contrast the $Na_2 + Cl$ reaction leads only to atomic emission corre- o the Na D-line and $4\,^2P-3\,^2S$ transition. See the text for discussion.

nt of the supersonic sodium beam is expected from approximately 0.3%–2%[1(a),1(b),3] corre- ; to a concentration of 10^9 to $10^{11}/cm^3$. The in- f the Na_2 emission depicted in Fig. 1(a) appears lel closely the expected Na_3 concentration in the beam and, in addition, appears to vary linearly chlorine atom concentration. Hence, we as- the Na_2 chemiluminescence primarily with the [12]

$$+ Cl \rightarrow Na_2^* + NaCl\ .$$

ctra observed for the sodium–bromine system ilar to those observed for sodium–chlorine; :, there clearly is a decrease in excitation due easing reaction exoergicity and the emission ob- at shorter wavelengths is correspondingly di- d. A much more pronounced intensity dropoff erizes the sodium–iodine system.

e 1 is drawn to emphasize the significant changes re associated with the presence of sodium clus- d chlorine atoms. The Na_n–Cl emission spec- ould be compared with that obtained when the e gun is not operative, i.e., when only molecu- orine interacts with either the products of a su- ic or effusive sodium beam. An example of this m is indicated in Fig. 1(b) labeled as that which e associated with the $Na_2 + Cl_2$ metathesis. This m, which consists of a very strong Na D-line on, moderate Na $4\,^2P-3\,^2S$ emission, and weak s associated with an NaCl band system, can be as a "background" spectrum for the emission ated with the supersonically expanded sodium– e atom reaction. The two spectra depicted in differ only in that when the chlorine atom source rative, Na_2^* emission is observed over the wave- range 3200–5500 Å. This emission is conspicu- absent otherwise. We find, in agreement with workers,[13] that this background emission is vir- identical to that associated with the products of sive sodium (monomer + dimer) – chlorine mole- teraction. Therefore, based on reaction exoer- gicities,[14] we tentatively associate the NaCl emission in the region of the Na D-line with the four center process $Na_2 + Cl_2 \rightarrow NaCl^* + NaCl$ although a more compli- cated metathesis might be operative. In further ex- periments,[15] we have assessed the emission spectra which are associated with the reaction of chlorine atoms and sodium dimers. In agreement with the re- sults of Struve *et al.*[5] only sodium atomic emission cor- responding to the Na D-line and Na $4\,^2P-3\,^2S$ transitions is observed.

We have summarized the results of initial efforts in our continuing study of sodium cluster oxidation.[16] A more detailed analysis of the features associated with Reaction (1) indicates the population of minimum of 18 vibrational quantum levels in the $C\,^1\Pi_u$ state of Na_2. The association of the Na_2^* emission in Fig. 1 with sodium trimer oxidation provides a route for the estimation of the sodium trimer bond energy. This estimate will soon be obtained through use of our combined studies of chlorine, bromine, and iodine oxidation.

[1](a) A. Herrmann, M. Hofmann, S. Leutwyler, E. Schümacher, and L. Wöste, Chem. Phys. Lett. 62, 216 (1979); (b) J. L. Gole, G. J. Green, S. A. Pace, and D. R. Preuss, J. Chem. Phys. 76, 2247 (1982); (c) M. A. Duncan, R. E. Dietz, and R. E. Smalley, J. Am. Chem. Soc. 103, 5245 (1981); (d) V. E. Bondybey and J. H. English, J. Chem. Phys. 74, 6878 (1981) and references discussed in these articles.

[2]A. Herrmann, E. Schümacher, and L. Wöste, J. Chem. Phys. 74, 6511 (1978); A. Herrmann, S. Leutwyler, E. Schümacher, and L. Wöste, Helv. Chim. Acta 61, 453 (1978); A. Herrmann, S. Leutwyler, L. Wöste, and E. Schümacher, Chem. Phys. Lett. 62, 444 (1979); S. Leutwyler, A. Herrmann, L. Wöste, and E. Schümacher, Chem. Phys. 48, 253 (1980); D. R. Preuss, S. A. Pace, and J. L. Gole, J. Chem. Phys. 71, 3553 (1979).

[3]E. Schümacher, W. H. Gerber, H. P. Härri, M. Hofmann, and E. Scholl, in *Metal Bonding and Interactions in High Temperature Systems with Emphasis on Alkali Metals* A.C.S. Symposium Series 179, edited by J. L. Gole and W. C. Stwalley (Am. Chem. Soc., Washington, D.C.), p. 83.

[4]W. Ellis, T. Taylor, and C. Campbell, Los Alamos Scien-

tific Laboratory (private communication).
W. S. Struve, J. R. Krenos, D. L. McFadden, and D. R. Herschbach, J. Chem. Phys. 62, 404 (1975).
The electronic transition strengths for the alkali metals and their compounds are among the highest known, see, e.g., W. C. Stwalley and M. E. Koch, Opt. Eng. 19, 71 (1980).
W. H. Crumley, H. C. Lukefahr, and J. L. Gole (work in progress).
K. P. Huber and G. Herzberg, *Constants of Diatomic Molecules* (Van Nostrand Reinhold, New York, 1979).
A. K. Verma, T. H. Vu, and W. C. Stwalley, J. Mol. Spectrosc. (in press).
R. D. Hudson, J. Chem. Phys. 43, 1790 (1965).
Very weak emission corresponding to higher lying ^2P Rydberg states has also been tentatively observed.
The assignment of observed Na_2 fluorescence to Reaction (1) is also consistent with the apparent relatively high bond energies of the higher sodium clusters, Na_n, $n=4,5$ [J. Flad, H. Stoll, and H. Preuss, J. Chem. Phys. 71, 3042 (1979); M. C. Richtsmeier, D. A. Dixon, and J. L. Gole, J. Phys. Chem. (in press)] and their abundance relative to sodium dimer. It is unlikely that a reactive encounter between atomic chlorine and sodium tetramer or pentamer will produce a sodium dimer excited state.
[13]R. C. Oldenborg, J. L. Gole, and R. N. Zare, (unpublished data); D. O. Ham, Discuss. Faraday Soc. 55, 313 (1973).
[14]For Na_2, $D_0^0 = 6022\ cm^{-1}$, K. K. Verma, T. Vu, and W. C. Stwalley, J. Mol. Spectrosc. 74, 131 (1981); for Cl_2, $D_0^0 = 20001\ cm^{-1}$, A. G. Gaydon, *Dissociation Energies and Spectra of Diatomic Molecules* (Chapman and Hall, London, 1968); for NaCl, $D_0^0 = 34137\ cm^{-1}$, T-M. R. Su and S. J. Riley, J. Chem. Phys. 72, 6632 (1980).
[15]It has also been determined that the Na_2^* emission spectrum in Fig. 1(a) cannot be associated with the interaction of effusively or supersonically expanded sodium and CCl_x ($x=1-4$) compounds formed via reaction of chlorine atoms or molecules with the surface of the hot carbon gun.
[16]Current research efforts include deflection studies to characterize molecular ions formed in reaction and the extension of the present single collision studies in a controlled manner to the multiple collision pressure range [J. L. Gole and S. A. Pace, J. Chem. Phys. 73, 836 (1980); A. W. Hanner and J. L. Gole, *ibid.* 73, 5025 (1980); G. J. Green and J. L. Gole, Chem. Phys. 46, 67 (1980)].

APPENDIX C

Chemical Physics 69 (1982) 357–363
North-Holland Publishing Company

DYNAMIC CONSTRAINTS ASSOCIATED WITH THE FORMATION OF SiS($a\,^3\Sigma^+$) FROM THE Si–OCS CHEMILUMINESCENT REACTION

James L. GOLE and Gary J. GREEN
Department of Chemistry and High Temperature Laboratory, Georgia Institute of Technology, Atlanta, Georgia 30332, USA

Received 19 October 1981; in final form 31 March 1982

The Si–OCS reaction is characterized by chemiluminescent emission from the excited electronic $a\,^3\Sigma^+$ and $b\,^3\Pi$ states of SiS. The vibrational population distribution of the $a\,^3\Sigma^+$ state is found to be virtually Boltzmann at 645 K. In contrast, the vibrational distribution for the $b\,^3\Pi$ state appears to be far from Boltzmann. A surprisal analysis indicates that a dynamic constraint affects the population of vibrational quantum levels in the $a\,^3\Sigma^+$ state. This constraint appears to be the inability of the Si–OCS reaction to convert the internal energies of the silicon atoms and OCS molecules and the relative translational energy of these reactants into product SiS internal excitation.

1. Introduction

Recently, we presented a detailed report on the nature of SiS and GeS chemiluminescent emission from the Si–OCS and Ge–OCS reactions [1]. Here we present further analysis focusing on the dynamics of the Si–OCS reaction and the chemiluminescent emission from the SiS $a\,^3\Sigma^+$ and $b\,^3\Pi$ excited electronic states.

The Si–OCS reaction was studied across a wide pressure range from a single-collision beam–gas environment ($p \approx 2 \times 10^{-4}$ Torr) to "multiple-collision" conditions where typical operating pressures were on the order of 10–100 μ of oxidant plus 1–2 Torr argon [1]. Under single-collision conditions, we have observed emission from both the $a\,^3\Sigma^+$ and $b\,^3\Pi$ states of SiS whereas the $b\,^3\Pi$ emission is absent in the multiple-collision studies. Vibrational quantum levels $v' = 0$–3 are populated in both the $a\,^3\Sigma^+$ and $b\,^3\Pi$ states under single-collision conditions whereas emission from $v' = 0$–2, $a\,^3\Sigma^+$ is observed under multiple-collision conditions. The temperature dependence of the observed SiS $a\,^3\Sigma^+ – X\,^1\Sigma^+$ and $b\,^3\Pi – X\,^1\Sigma^+$ band systems has been analyzed to deduce that the reaction yielding chemiluminescence involves ground-state silicon atoms, viz.

$$\mathrm{Si}(^3\mathrm{P}) + \mathrm{OCS}(^1\Sigma^+) \rightarrow \mathrm{SiS}^*(a\,^3\Sigma^+, b\,^3\Pi, \ldots) + \mathrm{CO}(^1\Sigma^+). \quad (1)$$

The activation energies for formation of the $a\,^3\Sigma^+$ ($E_{act} \approx 5.5 \pm 1$ kcal/mole) and $b\,^3\Pi$ (5 ± 1.5 kcal/mole) states were found to be very similar. There appeared to be little measurable reaction selectivity with respect to a particular spin–orbit component of the ^{3}P state #, and the experimentally measured activation energy was readily associated with translational energy factors.

Previously, we had raised some questions about the population of various vibrational quantum levels in the $a\,^3\Sigma^+$ and $b\,^3\Pi$ states. If we consider the energy balance for the Si–OCS reaction, under single-collision conditions, the available energy to populate SiS excited electronic states is

For the reaction of silicon atoms at the average temperature of the studies reported in ref. [1], approximately 12% of the atoms is in $^3P_0$ (0.00 cm^{-1}), 35% in $^3P_1$ (77.15 cm^{-1}), and 53% in $^3P_2$ (223.31 cm^{-1}).

0301-0104/82/0000–0000/$ 02.75

$$E_{\text{available}} = [D_0^0(\text{SiS}) - D_0^0(\text{OCS})] + [E_{\text{int}}(\text{Si}) + E_{\text{int}}(\text{OCS}) + E_T^i] = 26352 + 2088 = 28440\ \text{cm}^{-1}, \quad (2)$$

where we have taken the mass-spectrometric value for $D_0^0(\text{SiS})$, $E_{\text{int}}(\text{Si})$ and $E_{\text{int}}(\text{OCS})$ are the internal energies for Si and OCS respectively, and E_T^i is the relative translational energy of the reactants. The total energy available is sufficient to populate both the $a\,^3\Sigma^+$ ($T_0 = 24450\ \text{cm}^{-1}$) and $b\,^3\Pi$ ($T_0(b\,^3\Pi_0) = 27249$, $T_0(b\,^3\Pi_1) = 27345\ \text{cm}^{-1}$) states whereas the reaction exoergicity alone $[D_0^0(\text{SiS}) - D_0^0(\text{OCS})]$ will allow the formation of molecules in a $^3\Sigma^+$ but not $b\,^3\Pi$. If the silicon atoms undergoing reaction are thermalized, the effective contributions of E_T^i and $E_{\text{int}}(\text{Si})$ to the available energy decrease to the extent that the population of $b\,^3\Pi$ levels no longer occurs in an exothermic process. Hence, it would appear that we should not observe this state under multiple-collision conditions.

Several attempts to observe the effects of electronic-to-electronic energy transfer from the $b\,^3\Pi$ state have indicated that, at most, energy transfer is marginal and therefore that the absence of $b\,^3\Pi$ emission under multiple-collision conditions stems primarily from reactant thermalization. We have also observed that a metathesis involving room-temperature reactants is sufficiently exothermic to populate six vibrational levels of the $a\,^3\Sigma^+$ state, noting that no defineable emission has been observed from the accessible $v' = 4$ and 5 levels under either single- or multiple-collision conditions. It was also deemed significant that only three vibrational levels of a $^3\Sigma^+$ are available to the reaction exoergicity.

We have now pursued some of the questions raised in our earlier study focusing primarily on the further characterization of the $a\,^3\Sigma^+$ state. We determine the vibrational population distribution for the $a\,^3\Sigma^+$ state finding, surprisingly, that it is virtually Boltzmann at 645 K. In contrast, the $b\,^3\Pi$ vibrational distribution appears far from Boltzmann. A surprisal analysis may provide some indication of why the $a\,^3\Sigma^+$ vibrational population terminates at $v' = 3$.

2. SiS* $a\,^3\Sigma^+$–$X\,^1\Sigma^+$ chemiluminescent spectrum. SiS $a\,^3\Sigma^+$ vibrational population distribution

In fig. 1, we depict a portion of the chemiluminescent spectrum resulting from the reaction of silicon atoms and carbonyl sulfide molecules under single-collision conditions ($p \approx 2 \times 10^{-4}$ Torr). The $a\,^3\Sigma^+$–$X\,^1\Sigma^+$ band system is characterized by a distinct progression which onsets at ≈4000 Å, peaks at ≈4800 Å and extends to 5650 Å. The spectrum is clearly dominated by emission from $v' = 0$, $a\,^3\Sigma^+$ although significant emission is observed from $v' = 1$, 2, and 3. In order to deduce the vibrational population distribution for the $a\,^3\Sigma^+$ state, the experimental spectrum for the SiS $a\,^3\Sigma^+$–$X\,^1\Sigma^+$ band system has been compared to a computer synthesized spectrum. There are several considerations associated with this computer synthesis.

In a strictly first-order description $a\,^3\Sigma^+(b)$–$^1\Sigma^+$ transition is spin forbidden and should have little or no intensity. In fact, this transition can become mildly allowed. The $^3\Sigma^+$ state may mix with nearby singlet states (usually through spin–orbit coupling) having a significant transition moment with respect to the ground electronic state and hence borrow intensity from these states. The selection rules governing a $^3\Sigma^+$–$^1\Sigma^+$ transition where the $^3\Sigma^+$ state follows Hund's case (b) coupling may break down slightly with increasing molecular weight whence the SiS molecule is described within an intermediate Hund's case (b)–Hund's case (c) coupling scheme (much closer to case (b)). In the former case, the wavefunction for the mixed $^3\Sigma^+$ state may be written

$$\psi(\text{“}a\,^3\Sigma^+\text{”}) = c(a\,^3\Sigma^+) + d(A\,^1\Pi), \quad (3)$$

where $c \gg d$ and the $A\,^1\Pi$ state corresponds to a nearby excited state of SiS which can mix significantly with SiS $a\,^3\Sigma^+$ and from which emission occurs in an allowed transition to the ground $^1\Sigma^+$ state. If the $^3\Sigma^+$ state is described as in eq. (3), the relative intensities $I_{v',v''}$ of vibronic transitions (v', v'') in emission are related to the excited-state populations $N_{v'}$ by

$$I_{\text{em}}^{v',v''} = N_{v'}\zeta(\nu)\nu_{v',v''}^4 \sum_v c_{v',v}^2 q_{v,v''}, \quad (4)$$

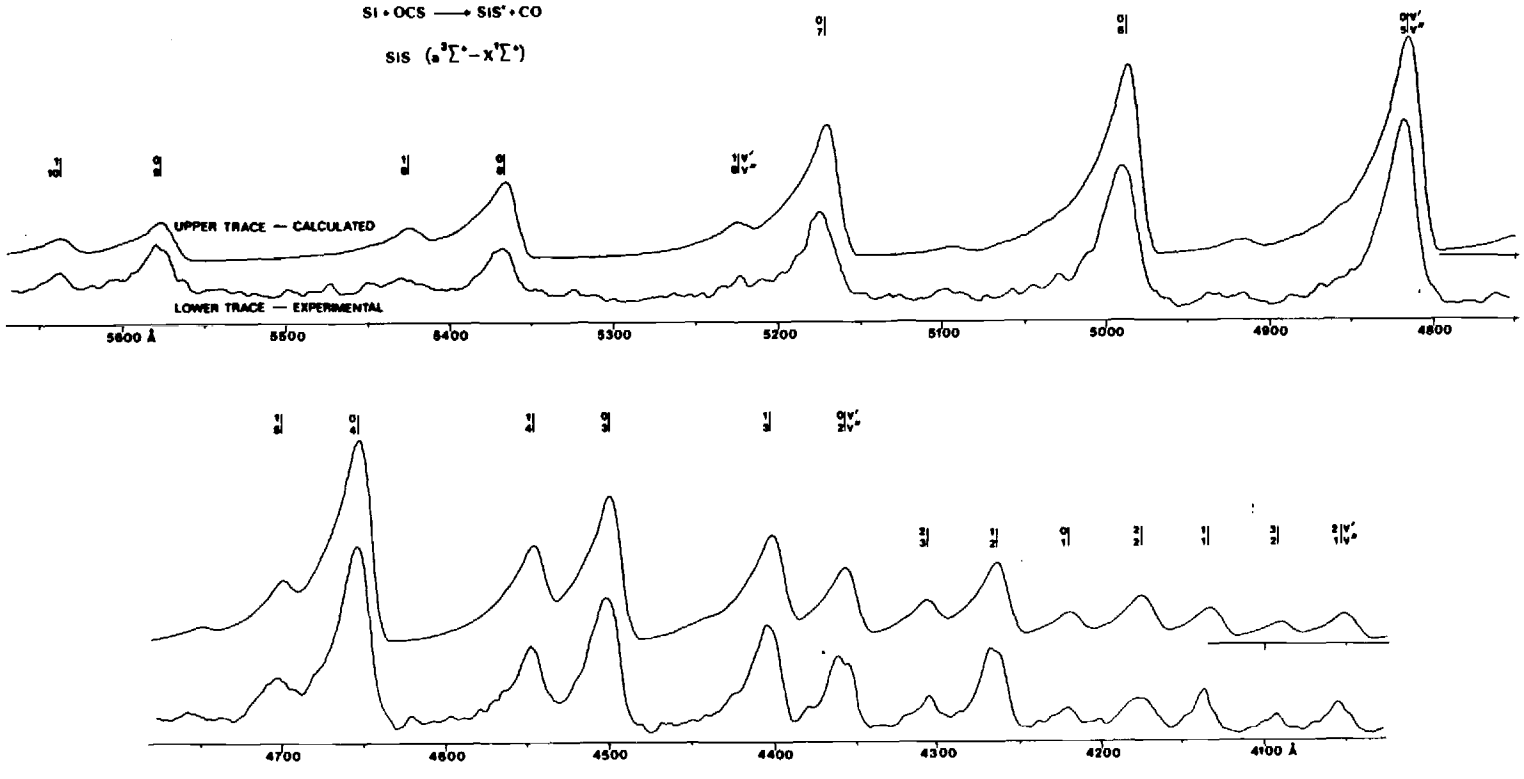

Fig. 1. Chemiluminescent spectrum obtained under single-collision conditions from the reaction $Si(^3P) + OCS(^1\Sigma^+) \rightarrow SiS^*(a\,^3\Sigma^+) + CO(^1\Sigma^+)$. Bandheads in the SiS $a\,^3\Sigma^+ - X\,^1\Sigma^+$ band system are denoted (υ', υ''). Spectra were taken at a scan speed of 0.5 Å/s at a resolution of 2 Å. The lower trace corresponds to the experimental spectrum while the upper trace is a computer simulation. See text for discussion.

where $c_{v',v}$ corresponds to the mixing coefficient between vibrational levels v' of $^3\Sigma^+$ and v of $^1\Pi$ and $q_{v,v''}$ is the appropriate Franck–Condon factor for the $A\,^1\Pi - X\,^1\Sigma^+$ transition of SiS; $\zeta(\nu)$ is a proportionality constant defined to include the variation of instrumental (spectrometer and photomultiplier tube) response with frequency and $\nu_{v',v''}$ is the measured frequency of the mixed $^3\Sigma^+ - X\,^1\Sigma^+$ transition.

In the Hund's case (c) limit a $^3\Sigma^+$ state splits into 1^+ and 0^- states, the emission to the ground $^1\Sigma^+(0^+)$ state corresponding to an allowed $\Delta\Omega = -1$ transition. The expressions appropriate for describing this transition are very similar to those for a strongly allowed $^1\Pi - ^1\Sigma^+$ transition. Here, for a given excited level, v', the relative intensity distribution to ground-state levels, v'', is given by

$$I_{v',v''} \propto \zeta(\nu)\nu^4_{v',v''}q_{v',v''}. \qquad (5)$$

The two possibilities outlined above can both lead to the observation of the emission spectrum in fig. 1, the question being which description, if either, is most appropriate and dominates. Clearly, expressions (4) and (5) will lead to distinctly different intensity distributions. Using the known ground-state constants for SiS, we have found [1] that the relative intensities for the observed (v', v'') transitions emanating from $v' = 0$ ("$a\,^3\Sigma^+$") and $v' = 1$ ("$a\,^3\Sigma^+$") are well fit by expression (5), determining B_e and α_e values in good agreement with a partial rotational analysis by Linton [2] ‡. This result indicates that the "$a\,^3\Sigma^+$" $-X\,^1\Sigma^+$ transition is not strictly forbidden in large part because of a tendency toward Hund's case (c) coupling which dominates the mixing exemplified by expression (3).

Recently this laboratory has been involved in studies of the Si–N_2O and Si–O_3 reactions. These reactions are characterized by emission from the $a\,^3\Sigma^+$, $b\,^3\Pi$, and $A\,^1\Pi$ states of SiO. By way of further comparison, we have attempted to fit the $a\,^3\Sigma^+ - X\,^1\Sigma^+$ and $b\,^3\Pi - X\,^1\Sigma^+$ emission systems of SiO with expression (5). This effort has been unsuccessful and further study demonstrates that the more complicated expression (4) is more appropriate to describe the relative populations of these intercombination band systems in the "lighter" SiO molecule.

Under the assumption that the SiS $a\,^3\Sigma^+ - X\,^1\Sigma^+$ emission system is observed primarily because of a tendency toward Hund's case (c), the relative intensities, $I_{v',v''}$, of vibronic transitions (v', v'') in emission are related to the excited-state populations $N_{v'}$ by

$$I_{v',v'} = N_{v''}\zeta(\nu)\nu^4_{v',v''}q_{v',v''}R^2_e(\bar{r}_{v',v''}), \qquad (6)$$

where $\zeta(\nu)$ is again a proportionality constant defined to include the variation of instrumental (spectrometer and photomultiplier tube) response with frequency $q_{v',v''}$ and $\bar{r}_{v',v''}$ are, respectively, the Franck–Condon factor [4] ‡ and r centroid for the (v', v'') transition. The electronic transition moment $R_e(\bar{r}_{v',v''})$ is written as an explicit function of the r centroid in accordance with the Fraser approximation [5]. This information is incorporated in a computer program to calculate the spectrum corresponding to the appropriate intermediate $^3\Sigma^+ - ^1\Sigma^+$ transition. The results of this analysis for the SiS $a\,^3\Sigma^+ - X\,^1\Sigma^+$ band system are indicated in fig. 1. The rotational temperature corresponding to the vibrational envelopes for all populated vibrational levels ($v' = 0$–3) is 600 ± 50 K. The vibrational populations are indicated in fig. 2. Strikingly, they correspond closely to a Boltzmann vibrational population distribution at 645 K. This is, by no means, typical of the vibrational populations characterizing the vast majority of chemiluminescent reactions. At first glance, it is tempting to surmise that SiS* $a\,^3\Sigma^+$ has been formed via a long-lived intermediate complex; however, further analysis does not support this conclusion.

One might also consider the population distribution associated with the $b\,^3\Pi$ state of SiS [1]. The spacings of the $b\,^3\Pi$ sublevels are irregular which indicates the possibility of irregular spin–orbit coupling effects. Each vibrational level can have a significantly different transition moment; therefore, we can only obtain a rough semiquantitative estimate of the relative populations for the lowest vibrational levels $v' = 0, 1$. Comparing the emission for the $^3\Pi_0$ and $^3\Pi_1$ components of the $b\,^3\Pi$ state, we estimate $N_{v'=0}/N_{v'=1} \approx 2$. In other words, the vibrational distribution for the $b\,^3\Pi$ state appears to be far from Boltzmann.

‡ Spectroscopic data for $a\,^3\Sigma^+$ are taken from refs. [1,2], and for $X\,^1\Sigma^+$ from ref. [3].

‡ The programs used to calculate the Franck–Condon factors were written by Dr. Brian G. Wicke.

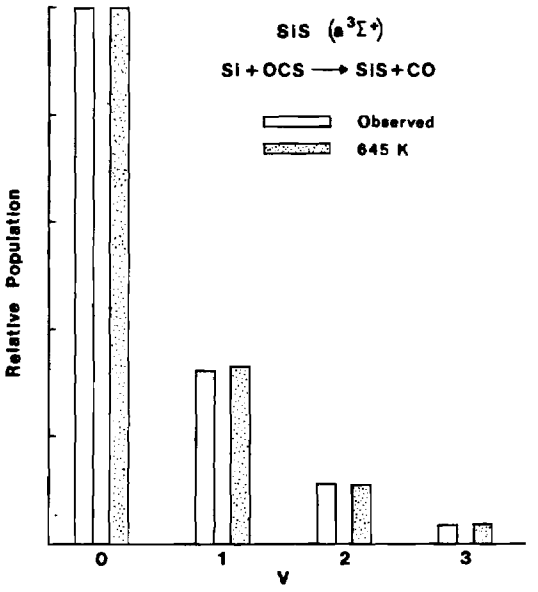

Fig. 2. SiS* $a^3\Sigma^+$ vibrational populations ($N_{v'}$) determined for the single-collision Si–OCS reaction. Relative populations are determined on the basis of the computer simulation in fig. 1.

3. Product-state distributions. The nature of dynamic constraints

In this section we will be concerned with an information theoretic analysis of the reaction type

$$M + ABS \rightarrow MS^* + AB, \tag{7}$$

in which AB (here CO) is formed in a manifold of rovibrational levels in its ground electronic state. Here we are concerned with the appropriate expressions from which one may calculate the density of states and hence the detailed prior relative rate constants for formation of product MS molecules assuming a statistical distribution of states with no dynamical constraints.

The appropriate conditional prior relative rate constant for formation of molecules in vibrational level v in electronic state n of the chemiluminescing product MS is given by [6,7]

$$P^0(v', n|E) = [\tfrac{8}{105}\, g_n A_1 A_T / B_v(\mathrm{MS})] \times [E - \Delta E_0 - E_v(\mathrm{MS})]^{7/2}, \tag{8}$$

where E is the total fixed energy, ΔE_0 is the zero-point to zero-point endoergicity for the formation of electronic state n $[D_0(\mathrm{ABS}) - D_0^0(\mathrm{MS}) + T_0(n)]$, E_v is the vibrational energy of the product molecule MS, $g(n)$ is an electronic degeneracy factor, and $B_v(\mathrm{MS})$ is the rotational constant for vibrational level v of MS. Here the AB molecule is treated within the rigid-rotor–harmonic-oscillator (RRHO) approximation. If $\rho_{I(\mathrm{AB})}(\epsilon)$ is the density of internal states of the AB molecule with internal energy ϵ,

$$\rho_{I(\mathrm{AB})}(\epsilon) = [\hbar\omega_e(\mathrm{AB})B_e(\mathrm{AB})]^{-1}\epsilon = A_I\epsilon, \tag{9}$$

where $\omega_e(\mathrm{AB})$ is the vibrational frequency and $B_e(\mathrm{AB})$ is the rotational constant for the ground electronic state of AB. Finally the factor A_T is related to the translational density of states. It is important to note that expression (8) is obtained under the assumption that the translational energy and internal energy in AB are treated as continuous variables. The vibrational energy in MS, however, is calculated for discrete vibrational quantum levels, MS being treated within the vibrating rotor approximation.

In order to carry out the appropriate analysis for the Si–OCS reaction, expression (8) can be simplified to

$$k^0_{v'} = C[E - \Delta E_0 - E_v(\mathrm{MS})]^{7/2}, \tag{10}$$

where $k^0_{v'}$ is again the prior relative rate constant.

We have taken three slightly different approaches to the calculation of the prior relative rate constants $k^0_{v'}$. In a first approach, the total fixed energy was taken to be 28440 cm^{-1} as evaluated from eq. (2) where $E_{\mathrm{int}}(\mathrm{Si})$, $E_{\mathrm{int}}(\mathrm{OCS})$, and $E_{\mathrm{trans}}(\mathrm{initial})$ are the average internal and most probable translational energies respectively. Using the vibrational constants given in ref. [1], we obtain the prior rates listed as $k^0_{v'}(\mathrm{a})$ in table 1.

There is some probability that the highest SiS excited-state vibrational quantum level populated in the Si–OCS reaction results from the reaction of Si atoms with translational energies in excess of the most probable value. In evaluating the SiS bond dissociation energy, we observed emission from $v' = 3$, $b\,^3\Pi_0$ (the $\Omega = 0$ component of the $b\,^3\Pi$ state) leading to the determination $E_{\mathrm{int}}(\mathrm{SiS}) = 29040$ cm^{-1}. Assuming that the reactant internal and translational energies are *completely converted* to internal SiS excitation, we take the total fixed energy to be 29040 cm^{-1}, obtaining the prior rates listed as $k^0_{v'}(\mathrm{b})$ in table 1.

Table 1
Relative experimental and statistical rate constants for formation of product electronic vibrational states and surprisals for Si + OCS → SiS* + CO

Electronic state	v'	$k_{v'}$ a)	$k^0_{v'}$(a) b)	$k^0_{v'}$(b) c)	$k^0_{v'}$(c) d)	$-\ln(k_{v'}/k^0_{v'})$		
						(a)	(b)	(c)
$a^3\Sigma^+$	0	0.679	0.459	0.427	0.704	−0.3911	−0.4634	0.0360
	1	0.223	0.287	0.285	0.241	+0.2523	+0.2453	0.0776
	2	0.075	0.167	0.180	0.052	+0.7952	+0.8701	0.3715
	3	0.022	0.088	0.108	(0.0032)	+1.3728	+1.5775	(−1.9414)

a) Experimental relative rate constant determined from vibrational population distribution.
b) Prior relative rate constant for total fixed energy = 28440 cm^{-1}.
c) Prior relative rate constant for total fixed energy = 29040 cm^{-1}.
d) Prior relative rate constant for total fixed energy = 26352 cm^{-1}, the reaction exoergicity.

In table 1, we have included the deviations of the observed experimental rates, $k_{v'}$, from the prior predictions in the form of surprisals, defined as $-\ln(k_{v'}/k^0_{v'})$. The experimental and prior rate constants, as well as the surprisals, plotted for the $a^3\Sigma^+$ state as a function of $f_{v'}$, the fraction of energy in vibration, are displayed in fig. 3. A slope of zero for a surprisal plot indicates exact agreement with statistical predictions. This is not the case and it is clear that for either method (a) or (b) of calculating the total fixed energy, we obtain a linear surprisal indicating a simple exponential gap behavior. Although the slopes of the two evaluated surprisals differ, their linearity is the significant result. The sign of the slopes of the surprisal plots is somewhat unusual [8,9] and reflects the pronounced lack of a vibrational population inversion in the $a^3\Sigma^+$ state. The formation of a long-lived complex usually leads to an essentially prior final-state distribution. The results obtained here do not indicate complex formation. They demonstrate that there is a clear dynamic constraint associated with the formation of SiS $a^3\Sigma^+$.

We feel that the dynamic constraint associated with the formation of SiS $a^3\Sigma^+$ may well be the inability to convert the energy increment associated

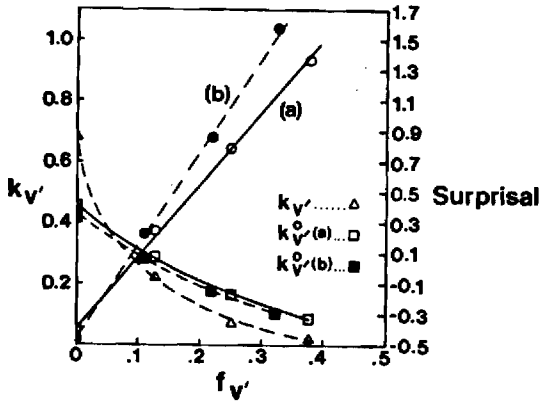

Fig. 3. Probabilities for formation of product vibrational states in SiS ($a^3\Sigma^+$) formed from the Si–OCS reaction as a function of $f_{v'}$, the fraction of energy in vibration for two fixed total energies. (△) Experimental probability, and (□ or ■) prior predictions for total fixed energies (a) or (b). (○, ●) Surprisals for total fixed energies (a) or (b) are plotted using the right-hand scale. See table 1 and text for discussion.

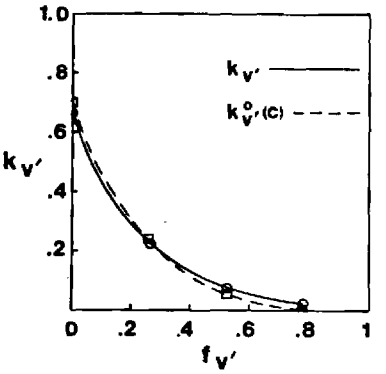

Fig. 4. Probabilities for formation of product vibrational states in SiS ($a^3\Sigma^+$) formed from the Si–OCS reaction as a function of the fraction of energy in vibration for a fixed total energy corresponding only to the reaction exoergicity $[D^0_0(SiS) - D_0(OCS)]$. (○) Experimental probability, and (□) prior prediction. See table 1 and text for discussion.

with the reactant internal energies and their relative translational energy to internal excitation of SiS $a\,^3\Sigma^+$. The results which lead to this conclusion are indicated in fig. 4 where we compare the experimental relative rate constants $k_{v'}$ with prior relative rate constants $k^0_{v'}(c)$ determined on the basis of a total fixed energy corresponding *exclusively* to the reaction exoergicity $[D^0_0(SiS) - D_0(OCS)]$. The close agreement between these rate constants indicates that the Si–OCS reaction may make little use of the excess energy increment associated with $E_{int}(Si) + E_{int}(OCS) + E^i_T$. A further calculation at a total fixed energy corresponding to $D^0_0(SiS) - D_0(OCS) + E_{int}(Si) + E_{int}(OCS)$ yields a prior relative rate constant which does not appear to be in as good agreement with experiment as $k^0_{v'}(c)$, however, the deviations are not of sufficient magnitude to completely rule out the contribution of $E_{int}(Si) + E_{int}(OCS)$ to $E_{int}(SiS)$.

4. Conclusion

The analysis presented in this study indicates that the observation of emission from only four vibrational levels in the SiS $a\,^3\Sigma^+$ state and the Boltzmann distribution characterizing these levels is the result of a dynamic constraint imposed on the Si–OCS reaction. It appears that this dynamic constraint may be the inability of the Si–OCS reaction to convert its initial relative translational energy into internal excitation of the SiS $a\,^3\Sigma^+$ state.

Acknowledgement

It is a pleasure to acknowledge helpful discussions with Dr. Kopin Liu. This work was partially supported by a grant from the U.S. Department of Energy.

References

[1] G.J. Green and J.L. Gole, Chem. Phys. 46 (1980) 67.
[2] C. Linton, J. Mol. Spectry. 79 (1980) 90.
[3] E. Tiemann, J. Hoeft and T. Torring, Z. Naturforsch. 27a (1972) 1566;
E. Tiemann, J. Phys. Chem. Ref. Data 5 (1976) 1147;
J. Hoeft, Z. Naturforsch. 20a (1965) 1327.
[4] R.N. Zare, J. Chem. Phys. 40 (1964) 1934, and references therein.
[5] P.A. Fraser, Can. J. Phys. 32 (1954) 515.
[6] C.L. Chalek, Ph.D. thesis, Massachusetts Institute of Technology, August 1977.
[7] R.D. Levine and J.L. Kinsey, in: Atom–molecule collision theory, ed. R.B. Bernstein (Plenum Press, New York, 1979).
[8] R.D. Levine, Ann. Rev. Phys. Chem. 29 (1978) 59.
[9] S. Green, Chem. Phys. 40 (1979) 1.

APPENDIX D

APPENDIX D

aureole

A CLEAN-UP JOB FOR LASERS

Coal gas, which is produced by reacting coal with steam, has a long if dirty history. It illuminated the original London Bridge in the days of George the Third. By the mid-19th century it had become the fuel of choice in big cities everywhere, reigning supreme until it was knocked out of the box by the advent of cheap oil.

Now that oil is no longer cheap, coal gas is well positioned to make a strong comeback as a leading fuel technology of the future — if it can clean up its act. Coal is abundant, and the gasification process is relatively inexpensive. But the environmental problems, which no one thought much about in the gaslight era, are a very big worry today. Coal gas won't win widespread public acceptance until it can be efficiently laundered.

That's where lasers come in. At the US Department of Energy's experimental coal gasifier in Morgantown, W. Va., researchers from the Los Alamos National Laboratory have been demonstrating a continuous-monitoring laser technique for determining process pollutants and increasing process efficiency. The success of their work to date strongly suggests that coal gasification plants of the future will come equipped with laser systems to keep real-time tabs on pollutant levels in the gas stream and make sure that scrubber systems are preventing noxious material from escaping into the air we breathe.

Two laser systems are being used in the Morgantown experiments, and like just about everything else these days, they're known by their acronyms. LIBS (for Laser-Induced Breakdown Spectroscopy) is used primarily for determining sodium and potassium contents of coal gasification streams, which is important in controlling costly corrosion of equipment exposed to hot combustion products. CARS (for Coherent Anti-Stokes Raman Scattering) is a more complex system for determining the presence and temperature of a variety of air-polluting molecules. Both use readily available lasers.

A tricky aspect of CARS is that it employs two lasers to produce a third laser beam. By mixing two beams of different frequencies, researchers can tune to the vibrational frequency of the molecule they want to examine. The intensity of the third beam, generated by the interaction of the two initial beams with the molecule, yields the molecule's concentration. This technique has enabled CARS to measure concentrations of nitrogen, carbon monoxide and hydrogen sulfide in the dirtiest parts of the gas stream where temperatures run to 1000°F and pressures are 200 pounds per square inch, with high particle and tar-vapor loadings.

LIBS and CARS are complementary systems. "Together," says Los Alamos scientist David Taylor, "they can tell you everything you ever wanted to know about what is happening in the gasification system and what is coming out of it." Armed with that kind of information, the producers of coal gas should be able to give us a fuel we can live with, while making a significant contribution to the nation's eventual energy self-sufficiency. □

From Laser Focus, August 1982

G-33-60-

FINAL REPORT
DOE/MC/16537-1499
(DE84000219)

THE CHARACTERIZATION OF HIGH TEMPERATURE VAPOR PHASE SPECIES AND VAPOR-SOLID INTERACTIONS OF IMPORT TO COMBUSTION AND GASIFICATION PROCESS IN THE ENERGY TECHNOLOGIES

James L. Gole

Prepared for

U.S. Department of Energy
Office of Fossil Energy
Morgantown Energy Technology Center
Morgantown, West Virginia

TECHNICAL INFORMATION CENTER
U.S. DEPARTMENT OF ENERGY

Under

Contract No. DE-AC21-81MC16537

February 1984

GEORGIA INSTITUTE OF TECHNOLOGY
SCHOOL OF CHEMISTRY
ATLANTA, GEORGIA 30332

THE CHARACTERIZATION OF HIGH TEMPERATURE VAPOR PHASE SPECIES AND VAPOR-SOLID INTERACTIONS OF IMPORT TO COMBUSTION AND GASIFICATION PROCESSES IN THE ENERGY TECHNOLOGIES

Final Report

James L. Gole

February 1984

PREPARED FOR THE UNITED STATES
DEPARTMENT OF ENERGY
Morgantown Energy Technology Center
Morgantown, West Virginia

Under Contract No.: DE-AC21-81MC16537

NOTICE

FOREWORD

This report details the results of a research program carried out for the Morgantown Energy Technology Center under Contract NO. DE-AC21-81MC16537. Work was accomplished under the direction of James L. Gole. Graduate and undergraduate students who have contributed to the technical progress are Ms. Beatriz Cardelino, Mr. W. H. Crumley, Mr. Robert Woodward, Mr. Joerg Pfeifer, Mr. David Semmes and Mr. T. Mays. Mr. Ken Williams, Supervisor of the Machine Shop has provided assistance in the design and construction of oven components.

ABSTRACT

The alkali oxides LiO, NaO, and KO and the alkali hydroxide NaOH and KOH have been studied. Emphasis has been on the determination of bond energies and the first electronic spectra for these species. In addition the oxidation of silicon to produce the metal monoxide has been characterized using chemiluminescent techniques in order to determine the SiO bond energy in an experiment independent of mass spectrometry. Attempts have been made to define the nature of sodium "cluster" oxidation with several oxidants including the halogens and SO_2.

Several experimental configurations have been tested as a means for generating intense, stable, and long lasting chemiluminescent emission from the alkali oxides NaO and KO and the alkali hydroxides NaOH and KOH. Studies have been carried out primarily at elevated pressures ($10^{-1} \rightarrow 10$ torr) as an aid to spectroscopic analysis and the determination of molecular constants. At the highest pressures, chemiluminescence has been obtained in a diffusion flame environment. Thusfar, from the chemiluminescent studies we have determined stringent lower bounds for the K-OH (88.6 kcal/mole) and Na-OH 82.5 kcal/mole) bond energies notably higher than those values given in the ANAF tables. The NaO and KO bond energies have been determined to be 65 ± 2 nd 73 ± 2 kcal/mole respectively. Preliminary molecular constants have been determined for KOH, NaO, and KO. This work has led to the discovery of a new low-lying "predominantly covalent" excited electronic state of the alkali oxides which appears to be ideally suited for the direct in-situ probing of these species.

Oven systems have been developed which circumvent problems in flame formation and stability common to the alkali hydroxides and oxides but not

present in typical chemiluminescent metal oxidation systems. Most pronounced among these is the difficulty caused by the extremely efficient formation of extensive particulate matter which appears to result from the synthesis of alkali hydroxide and alkali oxide polymers. Experiments have been initiated to characterize the particulate matter formed in the potassium-N_2O system. Here we have been successful in employing a combination of mass spectroscopy and EPR spectroscopy. Some, as yet unsuccessful attempts have been made to extend this work further using Laser Raman spectroscopy, High Temperature and mass spectroscopy, and X-ray crystallography.

We have been concerned with sodium cluster oxidation studies as they represent potential models for sodium surface oxidation. This research effort has included (1) the definition of the system through the characterization of highly exothermic chemiluminescent channels associated with sodium cluster - halogen atom oxidation and through mass spectroscopy, (2) the characterization of highly exothermic channels for the oxidation of sodium clusters with SO_2, and (3) the potential extension of initial studies in the low pressure "single collision" regime through stages of pressure increase which promote product relaxation and facilitate ready spectral analysis of those species formed in the oxidation process.

PURPOSE AND SCOPE

This research program focuses primarily on the study of alkali metals and the interactions which they undergo, the stability and molecular constants for several elusive and sparsely studied alkali compounds, and the evaluation of alkali polymer formation and interaction in oxidative environments. In addition some studies of silicon oxidation have also been undertaken. The interactions of the alkali and silicon metals and their compounds with their environments are such that they represent very deleterious elements in process streams; therefore the tolerance levels for these species are low and reliable thermodynamic and kinetic data must be obtained in order to predict low level species concentrations and the probable mechanisms for compound formation.

Our objectives have been to (a) characterize alkali monoxide chemiluminescent spectra, specifically spectra for NaO and KO and to determine lower bounds for the NaO and KO bond energies. In addition, as an aid to the analysis of the NaO and KO systems, some additional studies of lithium oxidation have been undertaken; (b) characterize pronounced particulate formation in gas phase alkali oxidation environments; (c) characterize the NaOH and KOH chemiluminescent emission spectra at a resolution and under conditions which will allow the determination of currently unavailable molecular constants for this molecule and an improved measure of the M-OH bond dissociation energy; (d) carry out a study of the silicon-NO_2 reaction in order to provide the first determination of the SiO bond energy independent of mass spectrometric determinations; (e) characterize the sodium cluster oxidation reactions with various oxidants including the halogens and SO_2; (f) attempt to prepare clean sodium and oxidant contaminated sodium surfaces whose oxidation with various constituents including SO_2 will be characterized; (g) if feasible, to insti-

tute laser induced fluorescence studies on the alkali monoxides and continue previous studies on the fluorescence spectrum of Na_2O.

This Report will outline progress on all the program elements outlined above. Described are the design of devices used to generate low pressure chemiluminescent flames in highly exothermic dynamic processes and the design and modification of devices used to extend these low pressure studies in a "controlled manner" to elevated pressures. This extension is undertaken in order to better obtain and interpret spectroscopic constants and elevate ultrafast energy transfer routes.

TABLE OF CONTENTS

INTRODUCTION

General Impetus for Study

Because of our increasing demand for energy, the significant increase in the cost of fuels and the decrease in the domestic supplies of clean fuels including natural gas, increased emphasis has now been placed on coal combustion as a source of electrical power generation and industrial heating. While coal is an abundant and inexpensive source of energy compared to the cost of petroleum and natural gas, it is a dirty fuel especially when compared to natural gas. Many deleterious compounds are present in the gas stream and their formation and interactions must be understood as thoroughly as possible.

Background

Low tolerance levels for certain species in process streams impose stronger requirements for reliable thermodynamic and kinetic data in order to predict low level species concentrations. In addition evidence now indicates that serious concern must be focused on whether or not these systems are best represented via equilibrium or non-equilibrium models. Unfortunately, the necessary thermodynamic and kinetic data required to perform accurate calculations of species concentrations is not available for many such gas stream species. Of equal importance is the fact that little detailed information is available which will allow the ready direct monitoring of these species in the process stream. In addition, many of the details of the mechanisms for process stream product formation, including the formation and growth of particulates, are yet unknown and many postulated routes to product formation are yet only meagerly tested. This arises primarily because many of the molecular entities for which data are needed correspond to elusive and very reactive radicals or high temperature molecules. Our laboratory has been concerned

with the characterization of several of the important molecules and possible processes thought to be present in the inherently high temperature environment of the process stream.

We have applied chemiluminescent and laser fluorescent techniques to the determination of bond energies, spectroscopic constants, and the evaluation of those spectral regions which will be most useful for the kinetic parameterization and monitoring of those species of interest. In addition, through the study of certain select processes, we are attempting to shed some light on the feasibility of postulated interactions in the process stream, some of which include the surprisingly efficient gas phase formation of particulate matter. In the course of these studies, we are documenting the presence of ultrafast energy transfer, both intra- and intermolecular, as it pertains to the nature of heat flow in high temperature systems and, in particular, to those molecules of interest in process streams. Finally it should be noted that the attainment and evaluation of reliable spectroscopic data leads to the determination of important molecular constants which can be used for the statistical mechanical[1] evaluation of heat capacities, entropies and free energies, all of which are important to the understanding of energy generation.

Specific Considerations - Alkali Metal and Compound Characterization - The Data Base

For a fixed bed gasifier, the exiting gas at approximately 550^{o}C contains particulates, tar vapor, and vaporized alkali. The particulates consist of coal fines and ash, the ash being of particular concern because of its high alkali content. The alkali metals in a variety of forms are known to represent deleterious and corrosive constituents in process streams. The nature of coal-fired systems, in general, is such that "alkali cleanup"[2] represents one of the most significant problems which must be addressed. It has been well

established[3] that the primary slag or fly ash components include the alkali compounds Na_2O and K_2O. Significant vapor phase species (impurities) especially in a water rich environment are known to include the potassium and sodium hydroxides. Thermodynamic calculations[4] also indicate the probable importance of the alkali monoxides NaO and KO (KO is of special interest in a potassium seeded MHD channel). However, sulfur is also a significant impurity in a coal-fired system.[2-5] Therefore, it is necessary to consider sulfur compounds and their relation to the only partially solved fuel corrosion problem. In considering the problem of turbine blade corrosion, researchers have established that alkali-sulfide and alkali oxide salts may be of great importance.[6,2,7] Therefore the properties of these species, which establish the nature of their formation in the combustion environment proceeding the turbine, and their behavior upon deposition, must be characterized to the greatest extent possible. In order to obtain this information, means must be found to (1) determine the kinetics of both formation and reaction of the alkali oxides and hydroxides and their corresponding sulfur analogs, both in model systems which allow for a detailed determination of reaction rates which can be used in the kinetic modeling of the process stream and in the process stream itself, (2) monitor the species of interest directly in the process stream, and (3) deduce any aspects of the internal energy level structure or molecular electronic structure of these compounds which can lead to unexpected behavior in the process stream including ultrafast energy transfer.

The research effort outlined in this report contributes primarily to the data base which must be associated with the monitoring of species in process streams; however, significant aspects of the kinetics and molecular electronic structure of these species are also probed. The data base to which we wish to contribute is also of importance for the characterization of most coal and

heavy fuel fired turbine generators.[8] Indeed, a great deal of interest is also focused on fireside corrosion where one must consider the interaction of the alkali salts and the boiler tubes onto which they plate. With this interest, it is noteworthy that the data on sodium and potassium-oxygen and sulfur compounds is miniscule. Information on molecular stabilities (heats of formation) and moleculalr constants must be obtained.

As a contribution to the necessary data base, our research effort has focused on the characterization of alkali hydroxides and oxides, both important compound groups in process streams. These studies are coupled with an effort to provide information which can be used to elucidata the nature of these alkali metal interactions which may lead eventually to the formation of alkali sulfates in process streams.

Our efforts to study the alkali hydroxides NaOH and KOH have led to the first direct observation of electronic emission spectra for these species, furnishing what is potentially a fruitful and much easier means of following these species in the gas phase. Prior to this effort, the major thermodynamic characterization of these metal hydroxides had been through indirect flame studies.[6] That is, the presence of the hydroxide had been inferred from the study of metal atom depletion. A second law analysis of this metal atom depletion has been used to deduce bond energies for primarily the alkali and alkaline earth hydroxides. Only two of the alkali and alkaline earth hydroxides have been characterized mass spectrometrically. Studies of the Group IIA hydroxides are precluded for all but the barium compounds[9] because of a very high propensity for disproportionation to the oxides and resulting loss of water. Difficulties encountered in studying the alkali hydroxides in large part result from the tendency to form dimeric species on vaporization. The bond energies determined for KOH[6] and BaOH[6,9] via flame and mass

spectrometric studies are in reasonable but not spectacular agreement. For KOH, flame studies indicate 84±2.5[10] and mass spectrometry yields 80±3[11] kcal/mole for the K-OH bond dissociation energy (see also Appendix A).

Direct chemiluminescent studies as employed in our laboratory provide a cleaner means of determining the K-OH bond energy than either the flame or mass spectrometric techniques. These studies have already provided a lower bound for the KOH dissociation energy, 88.6 kcal/mole.[11] This value is significantly higher than that recommended in the JANAF tables (85.5 kcal/mole) and is in good agreement with the recent mass spectrometric studies of Hastie et al.[12] The JANAF number is based primarily on the results from flame studies. The nature of the bond energy determination from chemiluminescent processes is summarized in detail elsewhere.[6]

A lower bound for the Na-OH bond energy has also now been determined using the chemiluminescent technique and the value obtained, 82.5 kcal/mole is in good agreement with recent photodissociation studies (see Appendix A), being notably higher than that recommended by JANAF.

Gas phase molecular parameterization is meager if nonexistent for the alkali hydroxides. Abramowitz and coworkers[6,13,14] have obtained infrared spectra for NaOH, RbOH, and CsOH and their deuterated analogs trapped in rare gas matrices. Belyaeua et al,[6,15] have studied the matrix infrared spectrum of matrix isolated KOH. Extensive microwave and millimeter wave studies have now yielded significant parameterization for the ground states of NaOH, KOH, RbOH, and CsOH, and rotational constants have been obtained for several excited vibrational levels.[16] All of these studies are very impressive yet microwave spectroscopy does not furnish a means of readily detecting NaOH and OH for the study of their reaction kinetics or as a means of following these species in process streams, nor is there a guarantee that the vibrational

frequencies recorded in the matrix are sufficiently close to those in the gas phase so as to allow straightforward detection of these molecules using state-of-the-art forms of infrared spectroscopy. For example, a very useful current technique for detecting molecules in the infrared involves diode lasers; their use represents a very expensive proposition when frequencies are not precisely known. Thus, if the alkali hydroxide electronic emission spectrum can be used to pinpoint appropriate monitoring regions in the infrared, their availability can greatly cut the cost of needed experiments. Finally, based on studies currently underway, it should be feasible to assess whether the current hydroxide spectra demonstrate that electronic spectroscopy can be used as a means of detecting and monitoring NaOH and KOH. If the electronic spectrum can be employed as a detector, sensitivity can be greatly increased.

Because KOH is one of the more important constituents in the high stress environments characterizing energy generating systems, the higher K-OH bond energy now determined in our studies has significant implications for the understanding of KOH chemistry in the combustion gas stream. Of course, because of this larger K-OH bond energy the degree of dissociation which is proportional to $e^{-D_o/kT}$ decreases. Hence the KOH concentration must be somewhat higher than previously believed and its influence on the gas stream kinetics may be slightly modified relative to previous expectations. While ground state rotational parameters have been determined for KOH and KOD, vibrational frequencies are still estimated for higher vibrational levels. Although matrix data is available on the fundamental vibrations, no gas phase measurements have been made and no anharmonicities are available for any of the alkali hydroxides. There is reason to believe, although this has not yet been brought to fruition, that chemiluminescent studies of the KOH electronic

emission spectrum will yield extensive vibrational parameterization for the ground electronic state.[6,17] Using standard statistical mechanical techniques, this vibrational data can be used to evaluate the vibrational contribution to the heat capacity, enthalpy, entropy, and hence the free energy of the KOH molecule. This data is, of course, useful for the thermodynamic modeling of these systems.

In very close analog to the alkali hydroxides, few gas phase emission spectra or molecular constants have been obtained for the oxides and sulfides of sodium and potassium. In addition there have been very few bond energy determinations for these compounds. For this reason, it is appropriate to study the alkali oxides employing a variety of chemiluminescent processes. These efforts have been undertaken in our laboratory leading, at present, to the determination of bounds for the Na-O and K-O bond energies and an assessment of molelcular constants for NaO. The success of this study indicates that it may be possible to excite laser fluorescence from these compounds in order to obtain further molecular parameterization. The usefulness of this effort can be exemplified by our current studies (see following) of an NaO and system in the spectral region extending from 6700-10,500Å. The evaluation of the NaO 6700Å system is quite significant for it provides the first straightforward in-situ route by which one can probe for sodium oxide in a combustion gas stream. Recently (see Appendix G) systems have been demonstrated at the Morgantown Energy Technology Center which employ LIBS and CARS spectroscopies to detect the sodium and potassium content of coal gasification streams. The LIBS technique involves the generation of a plasma arc, thermally dissociating all species within the arc by brute force, and producing emission from atomic alkali metal formed in the dissociation process. Of course, this is a multistep process which is not sensitive to the

specific dissociated alkali metal species whose plasma dissociation produces the observed atomic emission. With the discovery of the NaO 6700Å system, it should be possible to detect this gas stream constituent in a single step with a laser operating at or close to this wavelength alleviating the need to carry out a complex and precursor insensitive multistep dissociation process. If implemented, this later direct detection also more readily lends itself to calibration. These spectroscopy studies are also useful as a basis for efforts whose objective is to assess possible routes for alkali sulfate formation in process streams.

It is known that alkali sulfates represent a portion of the deleterious material formed in process streams and it is necessary that we gain some understanding of how the alkali present in the stream leads to this alkali sulfate formation. Recently, Stewart et al.[2] have been concerned with the nature of alkali metal interactions in process streams. These workers have proposed a model which involves the migration of alkali metal through the slag component of the process stream, creating an alkali enriched surface where heterogeneous gas phase reactions may take place. SO_2 is known to be an important gas stream species and it is thought that alkali enriched surface-SO_2 interactions lead eventually to formation of the sulfate.

It is apparent that one need ascertain the nature of the alkali-SO_2 interaction. With this final goal as an impetus, we are attempting to observe the products of oxidation of various sized sodium clusters. Although the Na-SO_2 and probably the Na_2-SO_2 reactions are endothermic, it is not obvious that this thermodynamic behavior will hold for multicenter processes involving $n \geq 3$ sodium atoms. Of further interest is the potential formation of oxidized alkali through very complex processes which, at first glance, might appear to be endothermic. For example, lithium metal when exposed to nitrogen reacts

rapidly to form a lithium nitride complex[18] although the N_2 bond energy is a substantial 225 kcal/mole. Hence, it may not be unreasonable to suspect that NaO, NaS, and Na_2O represent products of cluster oxidation. In a strong sense the study of cluster oxidation represents a forerunner to the study of sodium surface oxidation. In addition, the formulation of cluster generating devices affords the opportunity to develop appropriate sources for the efficient preparation of sodium surfaces whose oxidation can be characterized. It is also noteworthy that other workers have suggested that chlorine interacts with the alkali impurities in a combustion stream, resulting in the formation of alkali chloride complexes which then repartition with O, S, H, C, Al, or Si ash particulates. Thus, the influence of chlorine on the formation of alkali halide clusters and the subsequent reaction of these clusters with sulfur oxides should be evaluated in the intermediate region between gas and surface phases. In the following discussion, we outline additional progress toward these goals.[19]

Alkali Oxide Emission Spectra

Short Summary

The object of this effort has been to study the reactions of sodium and potassium with NO_2, N_2O, O_3 and SO_2 and to observe and characterize the chemiluminescent emission from NaO and KO via the reaction of sodium and potassium with N_2O and O_3. This work has now also been extended to the study of lithium oxidation (N_2O). We have observed the first electronic emission spectra for NaO, KO, and LiO resulting from the low pressure "single collision" reaction of sodium, potassium, and lithium atoms with N_2O and in the case of sodium, O_3. This work has now been extended to the "multiple collision" pressure regime as an aid to the evaluation of molecular constants for NaO, KO, and LiO and as a means of studying ultrafast energy transfer. From the combination of single and multiple collision studies we have deduced $D_0^o(KO) = 73\pm2$ kcal/mole and $D_0^o(NaO) = 65\pm2$ kcal/mole. Using the current results we have assessed the feasibility of laser fluorescence studies on the alkali oxides and have constructed a device to carry out such studies, specifically focusing on sodium oxide. Much of the impetus for this effort stems from the establishment that the alkali oxides are possessed of a low-lying predominantly covalent state whose location is ideally suited for the in-situ monitoring of these species without the necessity for resorting to Laser Induced Breakdown Spectroscopy (LIBS) or photodissociation techniques.[20] As we have alluded to earlier, a major problem in these alkali systems is the formation of extensive particulate matter. This problem is particularly acute for the alkali oxide systems. Termination of a given experiment was found to result largely from particulate formation and the blockage of devices used to transport oxidant to the reaction zone. A major emphasis of our efforts has been the design of oven systems which alleviate this problem.

The Generation of Alkali Oxide Emission Spectra Under Multiple Collision Conditions - Analysis and Experimental Considerations

Two new oven designs were used to obtain chemiluminescent emission from the alkali oxides at intermediate and relatively high multiple collision pressure ranges. The purpose of these studies has been to extend previous "single collision" studies[19] through stages of pressure increase which promote changes in the chemiluminescent emission spectra resulting from relaxation and rapid energy transfer. Based on previous studies, it was felt that this combination of techniques should be conductive to the determination of molecular constants and the assessment of rapid intra- and intermolecular energy transfer.

Previously, we noted the design of a system used with moderate success to characterize the alkali oxide emission spectra for sodium and potassium oxide produced from Na,K + N_2O,O_3 reactions under multiple collision conditions (see Annual Topical Report 1[19]). With this system, we were able to produce partially resolved alkali oxide emission spectra for NaO[19]; however, there were still questions regarding long term alkali and, in the case of ozone, oxidant source stability. A further modification of the apparatus used for these multiple collision studies has now greatly improved long term stability in the intermediate multiple collision regime. This improvement is significant for it is not only important that we deduce the location of the alkali oxide emission bands but also their relative intensities. In correlation with theory, these relative intensities can allow us to assess the best regions for in-situ laser excitations of the alkali oxides. Hence they provide a means of monitoring the kinetics of these species.

A schematic of the oven system now used to produce stable alkali beams in the intermediate pressure range is shown in Figure 1. There are two important

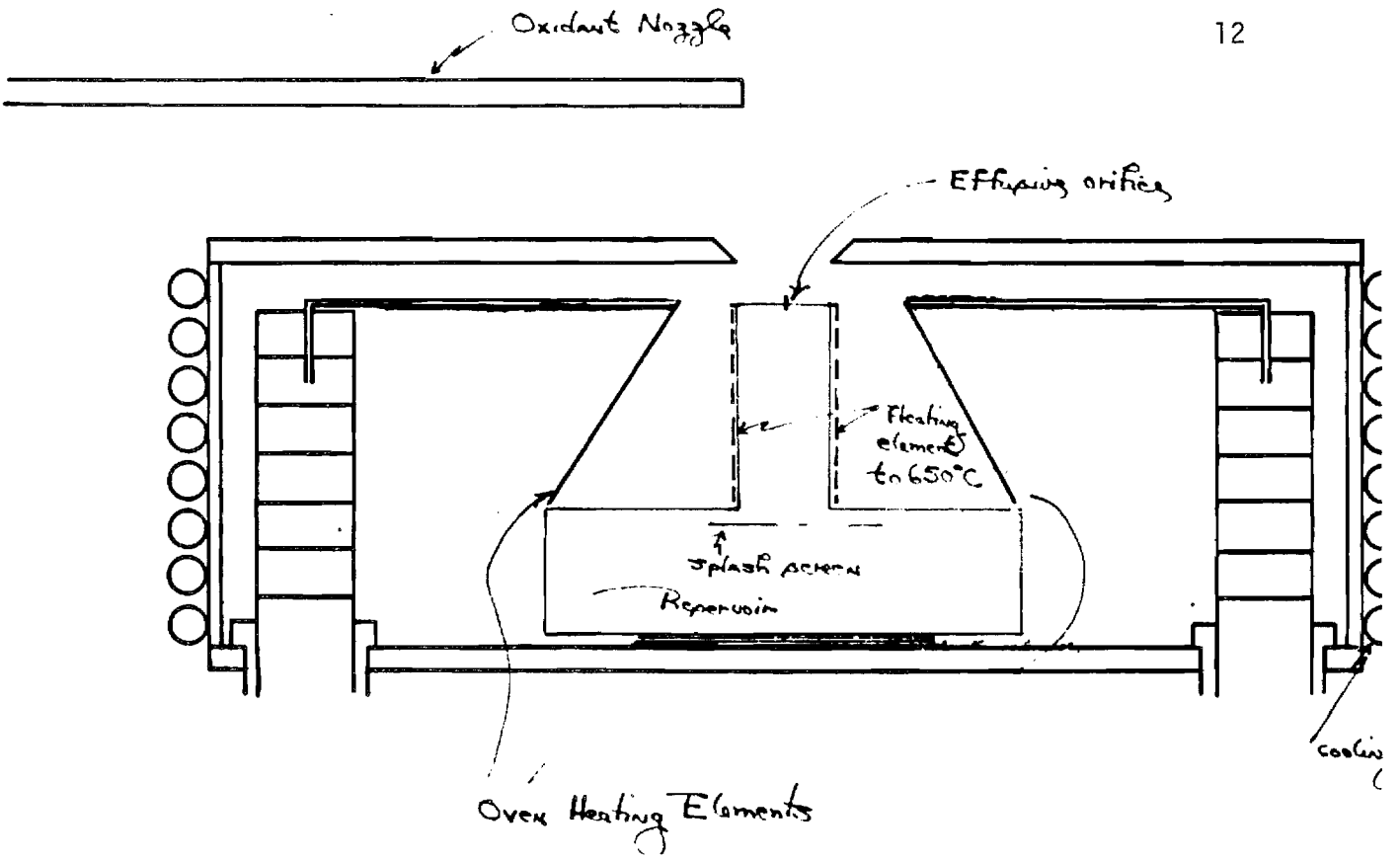

Figure 1. Schematic of Oven System for the Study of the Multiple Collision Processes $Na,K+N_2O \rightarrow NaO^*, KO^* + N_2$

features of this device. We have used a modified double oven design where alkali metal heated in a large reservoir region passes into an independently heated and more confined region and then through an effusive or near effusive orifice. As in our most recent previous design,[19] the oxidant is introduced via a nozzle offset and perpendicular to an entrained metal flow in order to prevent pronounced particulate formation. The present design involves the direct oxidation of the effusing alkali metal in a system containing, for example, 100μ Torr of N_2O. The configuration is very similar to a high pressure beam-gas system, and does not involve the entrainment of the alkali metal in argon.

Note that the design depicted in Figure 1 is in contrast to the normal multiple collision device where the entrained metal is oxidized using a tightly concentric ring injector design.[21] The injector design can quickly lead to pronounced particulate formation and hence is characterized by extremely short run times. Using the perpendicular entrained metal-oxidant flow scheme, one is able to run for a number of hours without encountering extensive particulate formation. Given long run times, there is yet another problem associated with the higher alkali metal reactant concentrations characteristic of the multiple collision system. The transition moments associated with emission from diatomic alkali metal excited electronic states are among the largest known. Therefore the collisional excitation of alkali dimer electronic emission systems (for example the Na_2 A-X system) which are located in the same region as the NaO spectrum (see Appendix B) can provide a strong if not totally eclipsing interference to the ready analysis of alkali oxide emission features. For this reason, the upper chamber from which the alkali metal effuses was heated separately to 650°C to induce dissociation of the exiting alkali metal dimers. With this precaution, the multiple collision

spectra recorded here are found to be void of the distinct alkali dimer emission systems and are characterized only by alkali atomic and alkali oxide emissions.

Using the oven system described in Figure 1, the Na-N_2O and Na-O_3 reactions have been studied in an intermediate pressure range. In addition, the device has also been used to carry out a number of preliminary studies on the emission characterizing the Li-N_2O metathesis. The sodium-N_2O, O_3 metathesis exhibit an intense red chemiluminescent flame whereas the Li-N_2O metathesis yields a lithium oxide spectrum shifted considerably to the blue and is characterized by an aqua flame. In order to carry out the ozone reactions, we entrained the ozone in argon by flowing the rare gas through a previously constructed trap in which ozone was deposited on silica gel at dry ice temperatures. The effluent argon + ozone flow was then passed through the oxidant nozzle into the reaction chamber. This procedure yielded a significant ozone flow and allowed us to produce an intense chemiluminescent flame.

The spectrum obtained for the Na-N_2O system is depicted in Figure 2. This spectrum was obtained with a cooled RCA 4840 phototube whose sensitivity drops rapidly at wavelengths longer than 7000Å. (As we will note shortly, this work has now been extended to much longer wavelength using a new detection system.) Note the three pronounced bands at approximately 7160, 7400 and 7700Å. Their correlation with the NaO^* single collision spectrum[19] was found to be excellent. The relative intensity of these bands was much more reliably and reproducibly determined and the absolute spectral intensity considerably in excess of that previously obtained;[19] however, considerable improvements have followed. The spectrum in Figure 2 was taken at considerably higher resolution (0.4 vs 5Å) than those spectra previously

Figure 2. Chemiluminescent Spectrum Resulting from the Process $Na + N_2O \rightarrow NaO^* + N_2$ Under Multiple Collision Conditions P_{N_2O} = 200μ. Spectral Resolution is 0.4Å

obtained[19] providing a clean separatioon of the Na D-line emission from that of the oxide. Similar spectra were obtained for the Na+O_3 system, however, the peaks were found to be somewhat skewed relative to those for the metathesis Na + $N_2O \rightarrow NaO^* + N_2$.

Thusfar we have described the first modification of an apparatus used for multiple collision studies which greatly improved long-term stability in the intermediate multiple collision pressure regime. We continued to improve the systems for the study of alkali metal metathesis overcoming numerous problems associated with the attainment of the NaO chemiluminescent spectrum across a wide pressure range. To more clearly define the overall impetus of study, we focused on the assessment and analysis of the chemiluminescent emission from the processes (see also Appendix B)

$$\begin{aligned} Na + N_2O &\rightarrow NaO^* + N_2 \\ + O_3 &\rightarrow NaO^* + O_2 \end{aligned} \qquad (1)$$

and

$$Na + N_2O + X \rightarrow NaO^* + N_2 + X \qquad (2)$$

where Eq. (1) denotes that the Na-N_2O and Na-O_3 reactions have been studied under low pressure single collision conditions. Temperature dependence studies have indicated that the Na-N_2O reaction is characterized by a substantial activation energy ($\geq$ 15 kcal/mole) whereas the Na-O_3 reaction proceeds more rapidly, having a much smaller barrier ($\sim$ 5-7 kcal/mole) to product formation. Eq. (2) represents the extension of the single collision studies to the multiple collision pressure regime where X = N_2O, Ar, CO, and N_2. The second group of experiments were carried out in order to relax the internal excitation characteristic of the electronic spectrum obtained under

single collision conditions. Here, as previously noted, a stream of sodium atoms was reacted with N_2O at P_{Total} (N_2O) = 50-150μ, using the configuration described in Figure 1, or sodium atoms entrained in argon ($P_{Ar} \sim$ 850-1200μ), N_2($P_{N_2} \sim$ 950-1500μ), or CO($P_{CO} \sim$ 650-850μ) were oxidized at much higher total pressure with a concentric flow of N_2O using the device depicted in Figure 3. Several problems discussed in part in the enclosed preprint (Appendix B) were overcome in order to carry out these studies. Under multiple collision conditions, for a given sodium beam flux, the alkali oxide emission spectrum was obtained over a very narrow range of oxidant and carrier gas pressure. This, in concert with the previous difficulties encountered in studying these systems, probably accounts for the inability of previous workers to observe the NaO emission spectrum.

A schematic of the apparatus used to produce stable operating conditions for the oxidation of entrained sodium atoms with N_2O (Eq. (2)) under high pressure multiple collision conditions is shown in Figure 3. This oven system incorporated many of the previous improvements made to study the Na-N_2O metathesis in the intermediate pressure range (Figure 1). We again used a modified double oven design where alkali metal heated in a large reservoir region passed into an independently heated and more confused region and then through an effusive or near effusive orifice. In order to study the Na-N_2O system for $P_{Total}(N_2O) \sim$ 50-150μ we introduced oxidant via a nozzle offset and perpendicular to the metal flow. For the higher pressure studies, the effusing sodiuum metal was entrained in Ar, N_2, or CO as depicted in Figure 3 producing, under carefully adjusted conditions, a stable intense alkali (sodium) flux at notably higher pressures. The alkali-entrainment gas mixture was oxidized by a flow of N_2O introduced concentrically from a ring injector system of a considerably more open design than used previously. In addition,

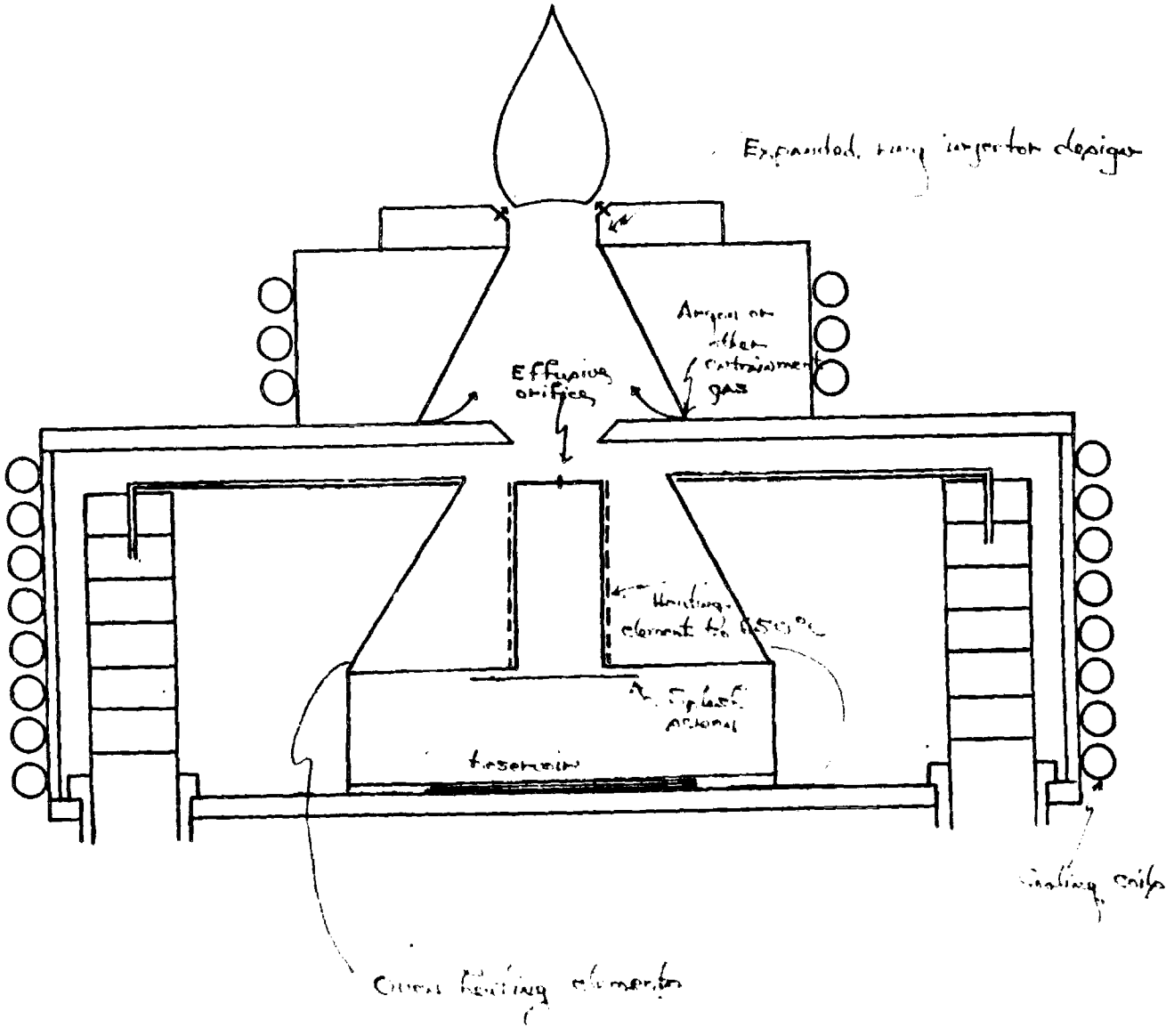

Figure 3. Schematic of Oven Systems for the Study of the Multiple Collision Processes Na + N_2O + X → NaO* + N_2 + X (X = Ar, N_2, CO, N_2O)

the oxidizing jets are placed at a much sharper angle. While particulate formation does ensue, the open design, operated with care, allowed sufficient run times for the study of NaO^* produced in the $Na-N_2O$ metathesis.

Given long run times, we again faced the problem associated with the ıigher alkali metal reactant concentrations characteristic of the multiple :ollision system. As we have noted, the transition moments associated with :he alkali metal dimer excited electronic states are among the largest known, ınd, as in the intermediate pressure range, the collisional excitation of ılkali dimer electronic emission systems can provide a strong interference to :he ready analysis of alkali oxide emission features. For this reason, the ıpper chamber from which the alkali metal effuses was heated to 750°C to nduce dissociation of the exiting alkali metal dimers. Note that somewhat ıigher temperatures are required in order to alleviate dimer formation aat .hese higher pressures. Because of (1) the increased temperature and (2) the ıigher pressure region, the power requirements for the upper oven chamber ncreased considerably as heat dissipation is more pronounced at higher ressures.

Spectra obtained for the $Na-N_2O$ system under a wide variety of conditions re depicted in Figure 4. We have been able to identify five bands ttributable to NaO whose wavelengths and intensities are listed in Table 1. he correlation of the multiple collision spectra with the NaO^* single ollision spectrum also shown in the figure is excellent. It should be pparent that the signal-to-noise in Figure 4 is considerably improved over hat in Figure 2.

The data in Table 1 may be correlated with recent extensive quantum ıemical calculations by Allison, Cave, and Goddard[22] who have studied both ıe ground $X^2\Pi$ and very low-lying $A^2\Sigma^+$ state of NaO. There are two possible

interpretations of the bands in Figure 4 and data in Table 1 one of which associates the observed features with emission from high vibrational levels of the $A^2\Sigma^+$ state to the lowest levels of the ground $X^2\Pi$ state and a second which associates these bands with emission from a higher-lying covalent state of the oxide which is bound by > 5000 cm^{-1} with respect to dissociation to ground state sodium and oxygen atoms. Allison et al. find a 2177 cm^{-1} $^2\Pi$-$^2\Sigma$ excitation energy and estimate a ground state vibrational frequency, ω_e = 464 cm^{-1} (($A^2\Sigma^+$ ≈ 493 cm^{-1}). Based on the results of their calculations on NaCl, LiO, KO, and CsO, where comparison with experiment can be made, the calculated frequency is expected to be 20-35 cm^{-1} lower than the experimental value. Energy conservation alone dictates that the spectrum which we observe in the present study may result from transitions among higher vibrational quantum levels of the $A^2\Sigma^+$ state and the lowest vibrational quantum levels of the ground $X^2\Pi$ state. The frequency separations which characterize the shorter wavelength bands catalogued in Table 1 (487 ± 20 cm^{-1}) are to be associated with a progression in the lowest vibrational quantum levels of the ground electronic state although it is not clear that the 6930Å feature should be associated with v"=0, $X^2\Pi$. It appears possible to associate the 406 ± 20 cm^{-1} frequency increment with two adjacent vibrational quantum levels in the $A^2\Sigma^+$ state.

If we take T_{oo} for the NaO $A^2\Sigma^+$ - $X^2\Pi$ transition to be 2177 cm^{-1} and assume that the 6930Å feature corresponds to v" = 0, we may estimate the upper state vibrational quantum level as v' = 26 or 27 corresponding to an anharmonicity $\omega_e x_e$ = 2 cm^{-1}. This result corresponds to $\omega_e(A^2\Sigma^+)$ ≈ 525 cm^{-1} and an expected frequency separation $\Delta\nu$ = 417 cm^{-1} for the two long wavelength bands listed in Table 1, both values being consistent with the theoretically determined vibrational frequency, ω_e, and the error bound in the observed

Figure 4. $NaO^* B^2\Pi - X^2\Pi$ chemiluminescent emission spectra for the processes (a) $Na + N_2O(P_{N_2O} \approx 125\mu) \rightarrow NaO^* + N_2$, (b) $Na + N_2O(P_{N_2O} \approx 75\mu) + Ar(P_{Ar} \sim 950\mu) \rightarrow NaO^* + N_2 + Ar$, (c) $Na + N_2O(P_{N_2O} \approx 50\mu) + CO(P_{CO} \approx 850\mu) \rightarrow NaO^* + N_2 + CO$, (d) $Na + N_2O(P_{N_2O} \approx 75\mu) + N_2(P_{N_2} \approx 1100\mu) \rightarrow NaO^* + N_2$, and (inset) single collision chemiluminescent spectrum for the metathesis $Na + N_2O(P_{N_2O} \approx 5 \times 10^{-5}$ torr$) \rightarrow NaO^* + N_2$. Spectral resolution for (a) through (d) is 1Å while the single collision spectrum was obtained at 5Å resolution. The dashed region outlined at the longest wavelengths in the single collision spectrum indicates a component of blackbody radiation. Spectra were taken with an RCA 4840 phototube.

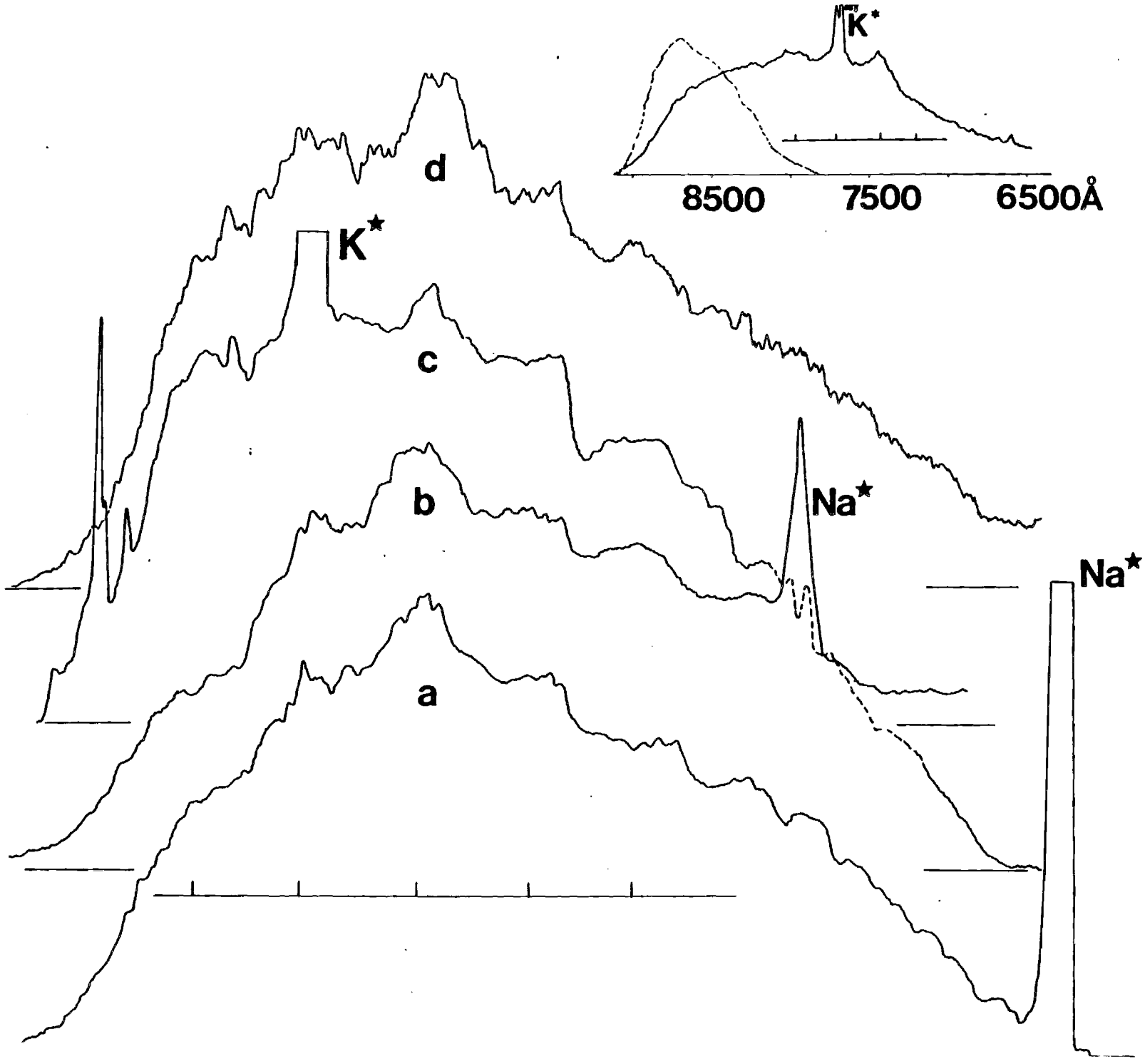
K*
8500
7500
6500Å
d
K*
c
b
Na*
a
Na*

Table 1

Observed Bands for NaO* Electronic Emission System[a]

λ (Å)[b]	(cm^{-1} vacuum)	$\Delta\nu$ (cm^{-1})
~6930	14426±20	
		502±20
~7180	13924±20	
		487±20
~7440	13437±20	
		487±20
~7720	12950±20	
		406±20
~7970	12544±20	

a. Measured with RCA 4840 Phototube.

b. Measured at the center of the observed emission feature.

frequency separation, $\Delta\nu$. If the 6930Å feature corresponds to v" > 0, the v' numbering should be increased by the corresponding increase in the v" quantum level numbering, however, based on energy conservation[23] it is highly unlikely that this band is associated with v" > 2. Thus the upper state quantum levels from which we observe emission would appear to be in the range v' = 26-29.

A problem exists with this first interpretation in that the Franck-Condon factors (vertical vibrational wavefunction overlaps) relating the high vibrational levels of the $A^2\Sigma^+$ state and the low vibrational levels of the ground $X^2\Pi$ state are extremely small. These Franck-Condon factors were obtained through an appropriate modeling of the calculated potential curves of Allison et al.[22] An RKR potential[24] was generated for both the $A^2\Sigma^+$ and $X^2\Pi$ states and these potentials were used to formulate Franck-Condon factors. Although we are operating with a system of high sensitivity, one seeks an alternate explanation for the observed features consistent with a high degree of vibrational overlap between the low-lying levels of the $X^2\Pi$ state and those excited state levels from which emission is observed. Consistent with this requirement is the observation of emission from the inner turning points of a low-lying covalent state located at much larger internuclear distance than the ground $X^2\Pi$ state. This interpretation raises some questions regarding the level spacings recorded in Table 1 and the possible influence of the sharp dropoff in spectral sensitivity at wavelengths longer than 7500Å. It soon became apparent that a strong need existed to extend the monitoring of observed chemiluminescent features further to the red, that is, to longer wavelengths. Using the described oven systems (Figures 1,3) and a new detection system, we developed the appropriate apparatus to carry out these studies extending our spectral scans to 10,500Å (Figure 5). Here we made use of an EMI 9808 selected red sensitive phototube. Through more stringent

alignment procedures, the optical system was improved to the extent that we have increased spectral sensitivity by almost two orders of magnitude. The resultant spectra obtained for both the Na-N_2O and Na-O_3 metatheses are depicted in Figure 5. Both signal-to-noise and resolution were considerably improved. Observed spectral features are tabulated in Table 2. We found that the observed spectral features at wavelengths longer than 8200Å appear very sensitive to a variety of conditions local to the flame region although those spectral features extending from 8200 to 6000Å are not nearly so strongly affected.

Consistent with the data is an interpretation which involves emission from a low-lying predominantly "covalent" state whose equilibrium internuclear distance considerably exceeds that of the $X^2\Pi$ and $A^2\Sigma^+$ states and which is bound by 6000 to 7000 cm^{-1} with respect to ground state sodium and oxygen atoms. It appears that we have monitored the emission from low vibrational quantum levels of this excited electronic state. The features marked in figure 5 appear to be dominated by a long progression in the ground state vibrational quantum levels of NaO. The frequency separations which characterize the shorter wavelength bands catalogued in Table 2 (520 $\pm$ 20 cm^{-1}) are to be associated with a progression in the lowest vibrational levels of the $X^2\Pi$ state although it is not clear that the 6740Å feature should be associated with v" = 0, $X^2\Pi$. This conclusion is based on energy conservation and on previous "limiting" independent determinations of the NaO bond energy[25] which render it highly unlikely that the 6740A band is associated with v" > 2. At the shortest wavelengths, only one progression is apparent; however, at wavelengths longer than 8500Å, additional features (alphabetic labels) are observed which are shifted by $\sim$ 265 cm^{-1} from the initial progression. This frequency separation is consistent with an anticipated vibrational level

Figure 5. NaO* Chemiluminescent Emission Spectra for the processes (a) $Na + N_2O(P_{N_2O} \approx 75\mu) + N_2(P_{N_2} \approx 950\mu) \rightarrow NaO^* + N_2$, (b) $Na + N_2O(P_{N_2O} \approx 100\mu) + N_2(P_{N_2} \approx 750\mu) \rightarrow NaO^* + N_2 + N_2$ - spectrum over the region 6500-7600Å for constrast to (b), (c) $Na + O_3(P_{O_3} \approx 5\text{-}10\mu) + He(P_{He} \approx 300\mu) \rightarrow NaO^* + O_2 + He$, and (inset) single collision chemiluminescent spectrum for the metathesis $Na + N_2O(P_{N_2} \approx 5 \times 10^{-5}$ torr$) \rightarrow NaO^* + N_2$. Spectral resolution for (a) through (c) is 3Å while the single collision spectrum was obtained at 8Å resolution. Spectra (a) through (c) were obtained with an EMI 9808 phototube whose quantum efficiency drops rapidly at wavelengths longer than 9200Å. The single collision spectrum was obtained with an RCA 4840 phototube whose quantum efficiency drops rapidly at $\lambda > 7800$Å. The dashed region outlined at the longest wavelengths in the single collision spectrum indicates a component of blackbody radiation. A small potassium impurity[16] leads to the observation of K D-line emission in the single collision spectrum.

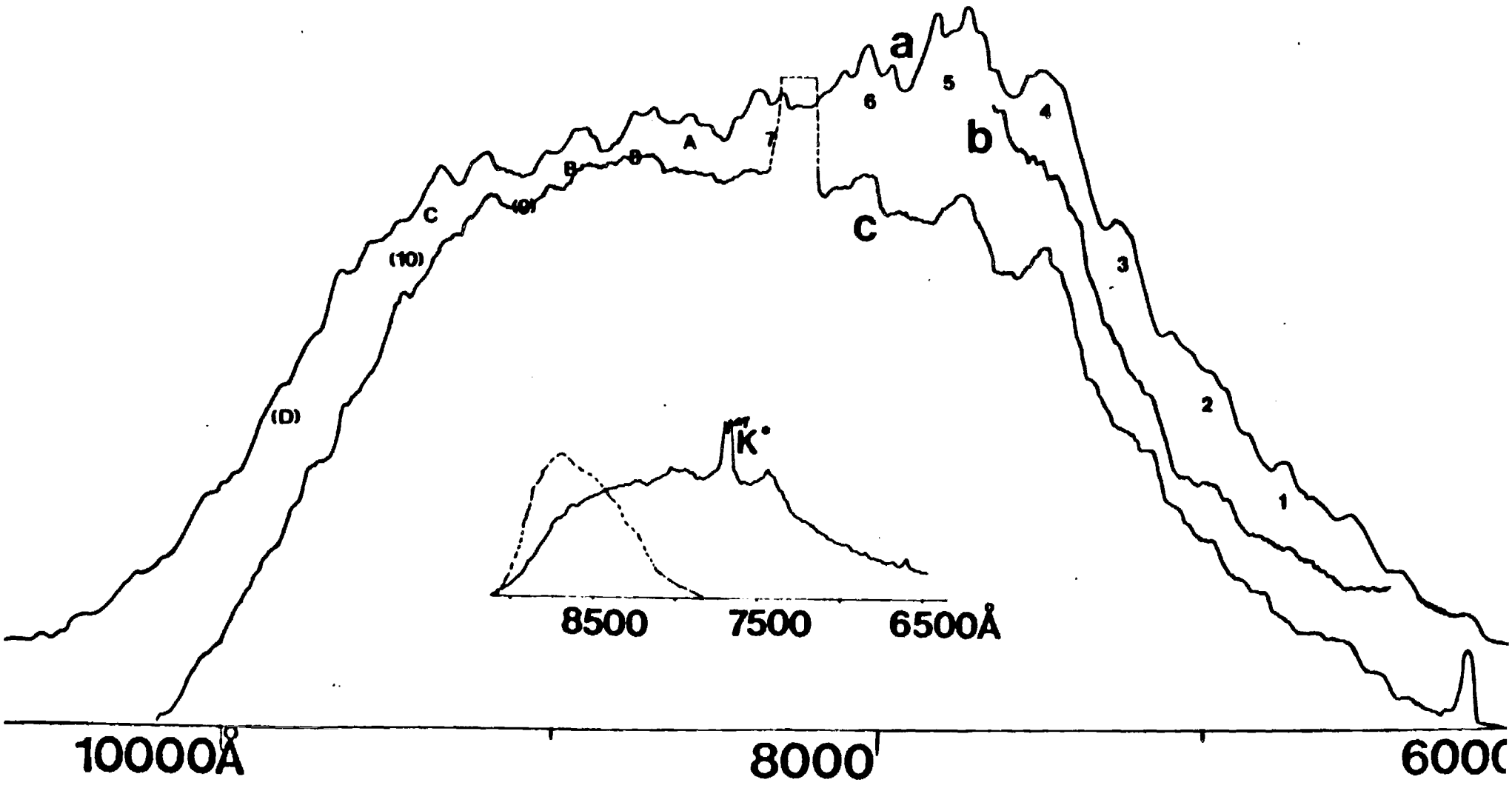
a
b
c
6
5
4
3
2
1
A
7
8
9
C
(10)
(D)
K
8500
7500
6500Å
10000Å
8000
6000

Table 2

Observed Bands for NaO* B-$X^2\Pi$

Band No.	λ(Å)	ν(cm^{-1} vacuum)	Δν(cm^{-1})
1	6740	14833 ± 20	
2	6980	14323 ± 20	510 ± 20
3	7235	13818 ± 20	505 ± 20
4	7495	13339 ± 20	479 ± 20
5	7770	12866 ± 20	473 ± 20
6	8060	12404 ± 20	462 ± 20
7	8370[a]	11944 ± 20	460 ± 20
A	8570[b]	11665 ± 20	279 ± 20
8	8710[a]	11478 ± 20	187 ± 20
B	8960[b]	11158 ± 20	320 ± 20
(9)	9078	(11016 ± 20)	
(C)	9380	(10658 ± 20)	
(10)	9460	(10568 ± 20)	
(D)	9830	(10170 ± 20)	

a. Δν (7-8) = 466 cm^{-1} b. Δν (A-B) = 507 cm^{-1}

spacing ($\omega_e \sim 283$ cm^{-1}) for a Morse Potential modeled covalent state[26] dissociating to ground state sodium and ground state oxygen atoms, however, while it is tempting to associate these additional features with excited state vibrational excitation, careful calculations demonstrate that this assignment is inconsistent with observed spectral features, relative spectral intensities, and all possible resonable Franck-Condon distributions. The dominant spectral features (numerical labels Table 2) are consistent with emission from a single vibrational level of the upper state to several lower state vibrational levels. The additional features are tentativeely associated with emission to the very low-lying $A^2\Sigma^+$ state ($\omega_e \sim 500$ cm^{-1}), this assignment being consistent with the calculated T_{oo} for the NaO $A^2\Sigma^+ - X^2\Pi$ transition.

In summary, we believe that we have observed emission from a relatively weakly bound predominantly "covalent" state of sodium oxide located ~ 15000 cm^{-1} above the ionic ground $X^2\Pi$ state. This state lies at considerably larger internuclear distance (~ 0.2Å) than the $X^2\Pi$ or very low-lying $A^2\Sigma^+$ states and it is believed that the observed emission involves primarily transitions to the outer turning points of the vibrational quantum levels associated with these two lower lying states. Based upon the present results the NaO ground state vibrational frequency is approximately 510 cm^{-1}.

After some modification and improvement of the knife edge used to seal our stainless steel oven system, we have studied the $K + N_2O \rightarrow KO^* + N_2$ reaction under conditions similar to those employed in our present studies on the analogous sodium system (see also reference 19). We extended our studies of the potassium oxide emission spectrum resulting from the $K + N_2O \rightarrow KO^* + N_2$ metathesis to the wavelength range encompassing 7500 - 10,500Å. Here, the extension to longer wavelengths reveals that the emission feature peaked at

7800Å in a previously reported emission spectrum for the potassium-N_2O system[19] actually extends from 7500 to 9800Å (Figure 6). Again, the behavior of this system is quite sensitive to flame conditions, the observed emission corresponding to either a continuous or structured feature dependent upon the nature of the flame region. The experiments carried out thusfar employ a system in virtually exact analog of that used for sodium, elevated pressures being obtained by introducing N_2 as the potassium atom entrainment gas. It is apparent that further experiments with carriers such as Ar, CO, and possibly O_2 may prove useful in analyzing the observed spectral features.

We have attempted to obtain some foothold in the analysis of the structured emission features apparent in Figure 6. The frequency separation between the individual peaks is intriguing in that it is approximately 160 cm^{-1}. This frequency may be consistent with an anticipated vibrational level spacing ($\omega_e \sim 170$ cm^{-1}) for a Morse Potential modeled covalent state[26] dissociating to ground state potassium and ground state oxygen atoms, however, a number of additional experiments and further quantum chemical calculations will be needed to establish a definitive assignment.

The observed spectra for sodium and potassium oxide appear notably different in character. Therefore, in order to establish a trend in the observed emission spectra for the oxides and thus provide another check of our work on sodium oxide, we expanded our studies to the lithium-N_2O metathesis. In order to study this reaction, a special oven system similar in design to that in Figures 1 and 3 was constructed of "low carbon" stainless steel. This approach was taken since lithium in the liquid state at elevated pressures reacts rapidly with high carbon (304) stainless steel soon leaching through the oven walls.

Using the lithium-N_2O reaction, we have been successful in exciting

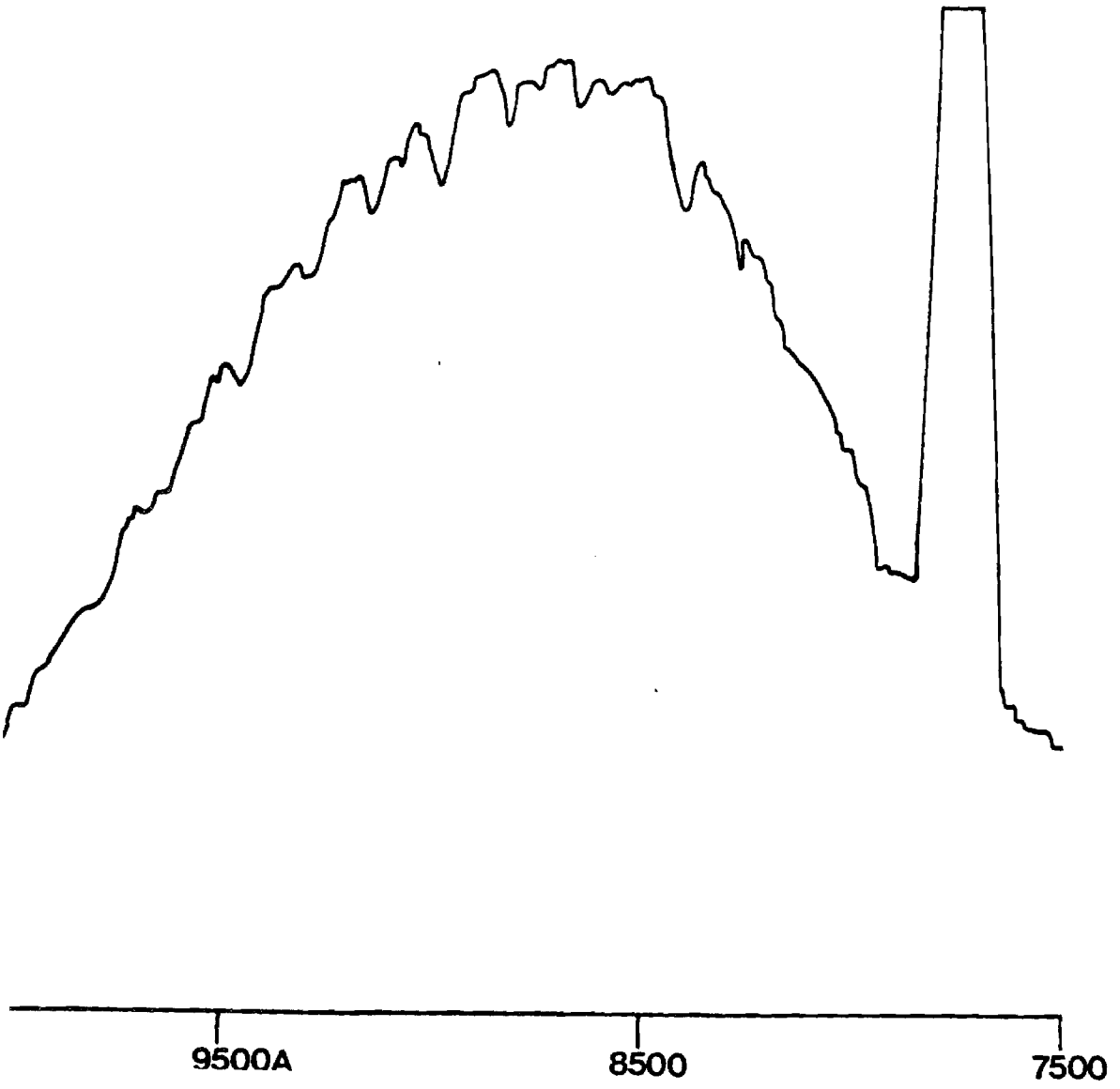

Figure 6. Chemiluminescent Spectrum Resulting from the Process $K + N_2O + N_2 \rightarrow KO^* + N_2 + N_2$

chemiluminescence from lithium oxide shifted by approximately (D_o^o(LiO) - D_o^o(NaO)) or $\sim$ 7000 cm^{-1} to the blue of the sodium oxide system. Preliminary data in the intermediate multiple collision pressure range has indicated a vibrational frequency separation of approximately 750 cm^{-1}, consistent with the expected ground state frequency of lithium oxide. Hence, the trends observed in the alkali oxide emission spectra are as expected and consistent with the observation of emission from a new predominantly covalent electronic state of the alkali oxide.

The evaluation of the NaO 6700Å system is quite significant for it provides the potential for the first straightforward in-situ route by which one can probe for sodium oxide in a combustion gas stream. Recently (see enclosed) systems have been demonstrated at the Morgantown Energy Technology Center which employ LIBS and CARS spectroscopies in a rather complicated experiment to detect the sodium and potassium content of coal gasification streams. Laser Induced Breakdown Spectroscopy generates a superhot plasma arc thermally dissociating all species within the arc by "brute force". Alkali metal compounds which are atomized can be detected by virtue of the observation of alkali atomic emissions. This process is difficult to quantify for it requires that one acquire significant and as yet only marginally available information on the very complex atomization process. In order that any quantitative information be obtained, one must reliably assess the quantum yield for excited state alkali formation verses formation of the ground electronic state. Thus the LIBS technique, which focuses on the determination of total sodium (elemental) concentration and not specific chemical speciation still requires a careful evaluation of complex branching ratios for its validity. A distinct and more advanced approach involves the direct single photon (preferably) far ultraviolet dissociation of alkali compounds promoting

subsequent atomic emission from some portion of the alkali atoms which are formed in the photodissociation process. This very promising technique, which shows the potential for distinguishing between alkali compounds as a result of a varied photodissociation dynamics, still requires as yet marginally available information on the photodissociation dynamics of the alkali compounds. With the discovery of the NaO 6700Å system, it should be possible to detect this gas stream constituent in a single step with a laser probe operating in a spectral range close to this wavelength, alleviating the need to carry out a dissociation process. Based on the information obtained, it should be possible to probe sodium oxide using laser induced fluorescence by pumping the observed band system in the region from 6600 to 7500Å. We have virtually completed a new system which can be used to study the Nd:YAG laser excitation of the NaO band systems now studied in chemiluminescence. This research effort conducted in conjunction with Professor Peter Schulz in the Georgia Tech Physics Department has required the development of a somewhat unique device to create non-equilibrium populations of sodium monoxide. We will discuss the details of this system shortly.

By combining the single and multiple collision data for the Na + N_2O and Na + O_3 reactions, we are able to make a more precise determination of the NaO bond strength. From temperature dependent studies we determine that the Na-N_2O reaction has an activation energy greater than or equal to 15 kcal/mole whereas the Na + O_3 reaction has only a 5-7 kcal/mole barrier. Both reactions yield similar chemiluminescent spectra although the O_3 metathesis is characterized by a greater NaO^* rotational excitation and a spectral intensity at least two orders of magnitude greater than that for the N_2O system. This intensity differential is consistent with the observed difference in activation barriers for the two reactions. From the short wavelength limit of the

NaO chemiluminescence which results from the Na-O_3 metathesis and the appropriate energy balance, we determine $D_0^o(NaO) \geq 65\pm2$ kcal/mole. In order to assess the KO bond strength we combine data for the K + N_2O metathesis taken under single and multiple collision conditions to determine $D_0^o(KO) \geq 73\pm2$ kcal/mole.

Laser Spectroscopy of the Alklai Oxides

In order to assess the magnitude of laser induced fluorescence from the alkali oxides and hence develop the diagnostics for an appropriate in-situ probe of sodium and potassium oxide we have constructed a device, a schematic of which is presented in Figure 7. The system consists of a cylindrical chamber in which we find an oven which can be used to heat and/or vaporize various alkali-oxygen compounds including Na_2O and NaO_2 in a non-equilibrium environment. In addition, a reactant gas inlet port passes directly into the oven which is surrounded by an appropriate cylindrical cooling jacket. The oven is held by an oven support cross directly above a port to vacuum. The system can be evacuated to 10^{-2} torr using only a forepump or 10^{-5} torr using a diffusion pump-forepump combination.

A series of four symmetrically located (90^o separation) ports are found on both the top and bottom sections of the chamber providing an ample contingent of window viewing ports, heating element inlets, phototube mounts, and laser inlet and outlet ports. The laser of choice for these experiments is a Nd:YAG pumped dye laser operating in the region 6200-7800Å. The system must contain extensive baffling in order to effectively deal with the extremely large photon fluxes emanating from a Nd:YAG pumped dye laser. There are at least three ways in which one can attenpt to generate sodium monoxide.

(1) We can pass microwave generated oxygen atoms over heated Na_2O to promote the reaction:

Figure 7

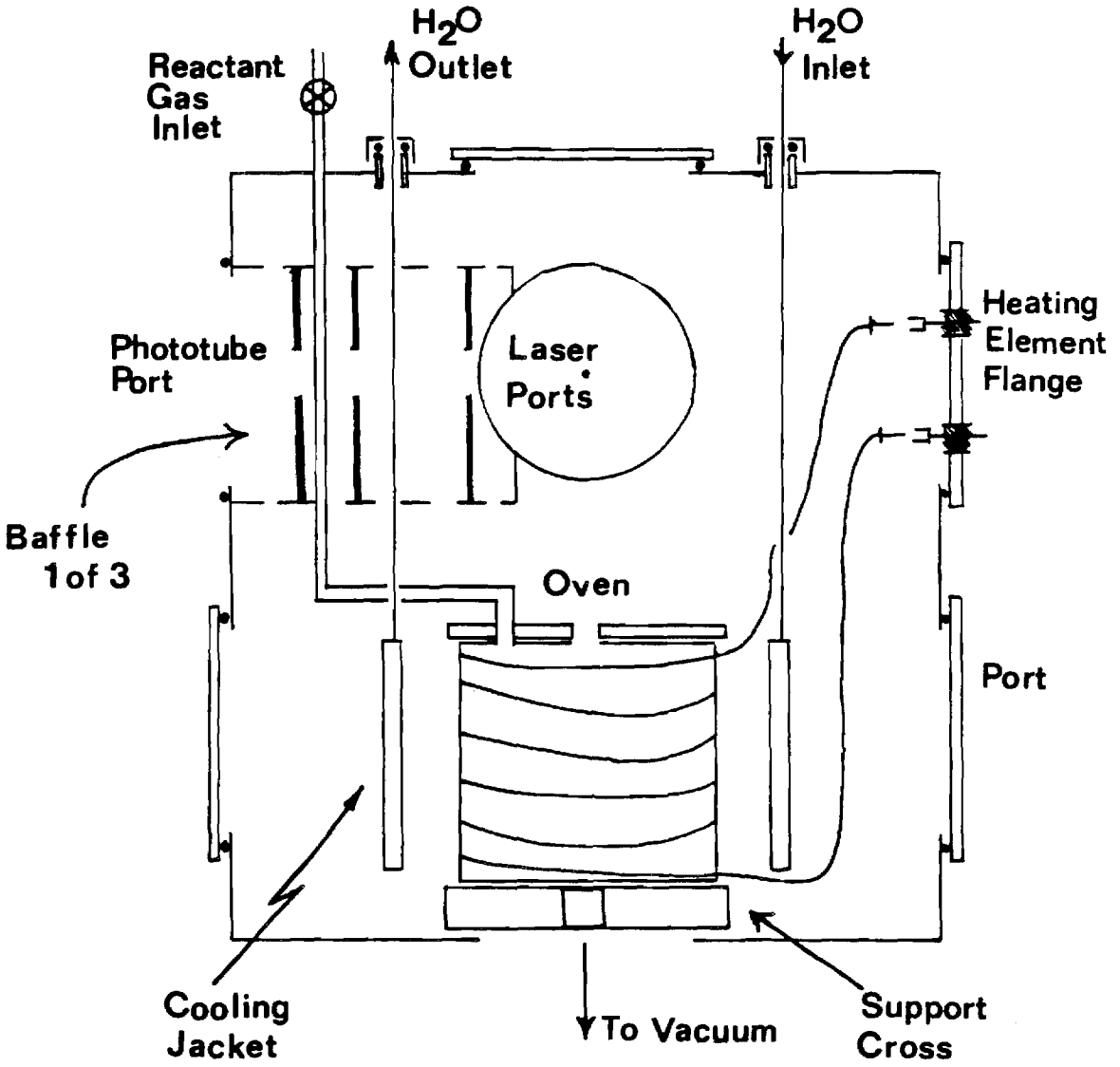

Figure 7. Schematic of Apparatus for the Study of Laser Induced Fluorescence from the Alkali Oxides

$$Na_2O + O \rightarrow 2NaO$$

(2) We can pass microwave generated oxygen atoms over NaO_2 to promote the reaction:

$$NaO_2 + O \rightarrow NaO + O_2$$

(3) We can attempt to pass sodium atoms over heated Na_2O in order to promote the in-situ synthesis:

$$Na + NaO_2 \rightarrow 2NaO$$

This experiment can be accomplished in an auxillary tube furnace, the effluents being passed into the excitation region through the port now designated for our heating element flange.

In an additional experiment it may be possible to generate sodium oxide via laser vaporization, i.e., we can allow the intense pulse from a Nd:YAG laser to impinge on either an NaO_2 or Na_2O sample producing the oxide in a non-equilibrium environment.

If the experiments which we have described above are successful, they furnish a means of detecting sodium monoxide and sodium suboxides (Na_2O) formed in the oxidation of a sodium surface.

Particulate Formation in Alkali Oxidation Environments

We have used mass spectroscopy as a means of analyzing the nature of the pronounced particulate matter formed via what appears to be the near homogeneous gas phase oxidation of alkali metals. Specifically, we have been concerned with the nature of particulate matter found in the K + N_2O reactive system. Constructing an appropriate probe and vaporizing particulate material at temperatures between 50 and 300°C, we have found (thus far) a relatively simple spectrum with major mass peaks at 90, 118, 178, and 238 amu. The possible polymeric species which correspond to these mass peaks given the presence of heated alkali (potassium with slight sodium impurity), nitrogen, and oxygen are given in Table 3. It should be apparent that polymeric alkali-oxygen-nitrogen compounds can account for the mass spectra which we observe. We have probed other regions of the particulate matter which is formed in oxidation. We find that certain samplings yield the four mass peaks (90, 118, 178 and 238 amu) discussed in Table 3 while others are characterized by a negligible vapor pressure in the temperature range 50-300°C. In other words, the particulate samples are characterized by regions of distinctly different vapor pressure. More recent extensions of the temperature range to 400°C have produced no new information.

In order to further characterize regions of lower vapor pressure associated with the particulate matter, we have prepared samples to be analyzed, at higher temperature, in the High Temperature Laboratory of Professor John Margrave at Rice University. We are still awaiting the smooth functioning of high temperature quadrupole mass spectrometers which are being brought on-line in the Margrave laboratory. Initial inlet designs, while moderately useful, have required considerable modification for proper operation. This has delayed further mass spectral analysis.

Table 3

Possible Polymeric Species Formed in Alkali Oxidation[a]

Atomic Mass Peaks[b]	Possible Compounds[c]
90	$\underline{KNaN_2}$, Na_2N_2O
118	$\underline{KNaN_4}$, Na_2N_4O
178	$KNaN_6O_2$, KNa_3, N_5
	$Na_2N_6O_3$, Na_4N_5O,
	$\underline{K_2N_6O}$
238	$KNaN_8O_4$, $KNa_3N_7O_2$, KNa_5N_6
	$Na_2N_8O_5$, $Na_4N_7O_3$
	Na_6N_5O, $Na_4N_7O_3$, $Na_2N_8O_5$
	$K_2N_8O_3$, $\underline{K_2Na_2N_7O}$, $\underline{K_3NaN_7}$

a. Potassium, Nitrogen, Oxygen, and small Sodium impurity present.

b. Relative intensities ~3(90)/5(118)/1(178)/1.5(238).

c. Favored compound is underlined.

We have been able to study the EPR spectrum of a powdered sample of the particulate matter formed in alkali oxidation. In order to carry out this effort, we constructed a special liquid nitrogen cooled EPR probe (Figure 8). In an argon atmosphere (dry-box) the hydroscopic particulate powder was placed in a pyrex capillary which was then sealed. This capillary is placed in a quartz tube (probe) which is then liquid nitrogen cooled. The spectrum depicted in Figurre 9 and centered at 3200 gauss, was obtained at liquid nitrogen temperature, 77K. It is now clear that a portion of the powdered sample contains what must be very reactive free radicals. During the course of our EPR studies, we also noticed that the powdered sample changes color reversibly. In cooling from room to liquid nitrogen temperature, the color of the sample darkens from dull orange to red and back to dull orange. Upon warming to room temperature this process repeats.

Because of the behavior of the particulate sample on cooling and its apparent coloration, we attempted to obtain a Laser Raman spectrum of several samples. These efforts have been unsuccessful, however, there are other approaches which might be used (in the future) to obtain the Raman spectrum. Finally, we should note that we have also attempted to obtain an X-ray powder pattern of the particulate matter. We feel that the combination of studies outlined here can be used to obtain a viable interpretation of the particulate matter formed in alkali oxidation. For this reason it will be worthwhile to continue to probe other regions of the particulate matter. We feel that those polymeric species which constitute the particulate can be formed with unusual efficiency in the gas phase and that they can represent the nuclei for large scale particulate formation in process streams.

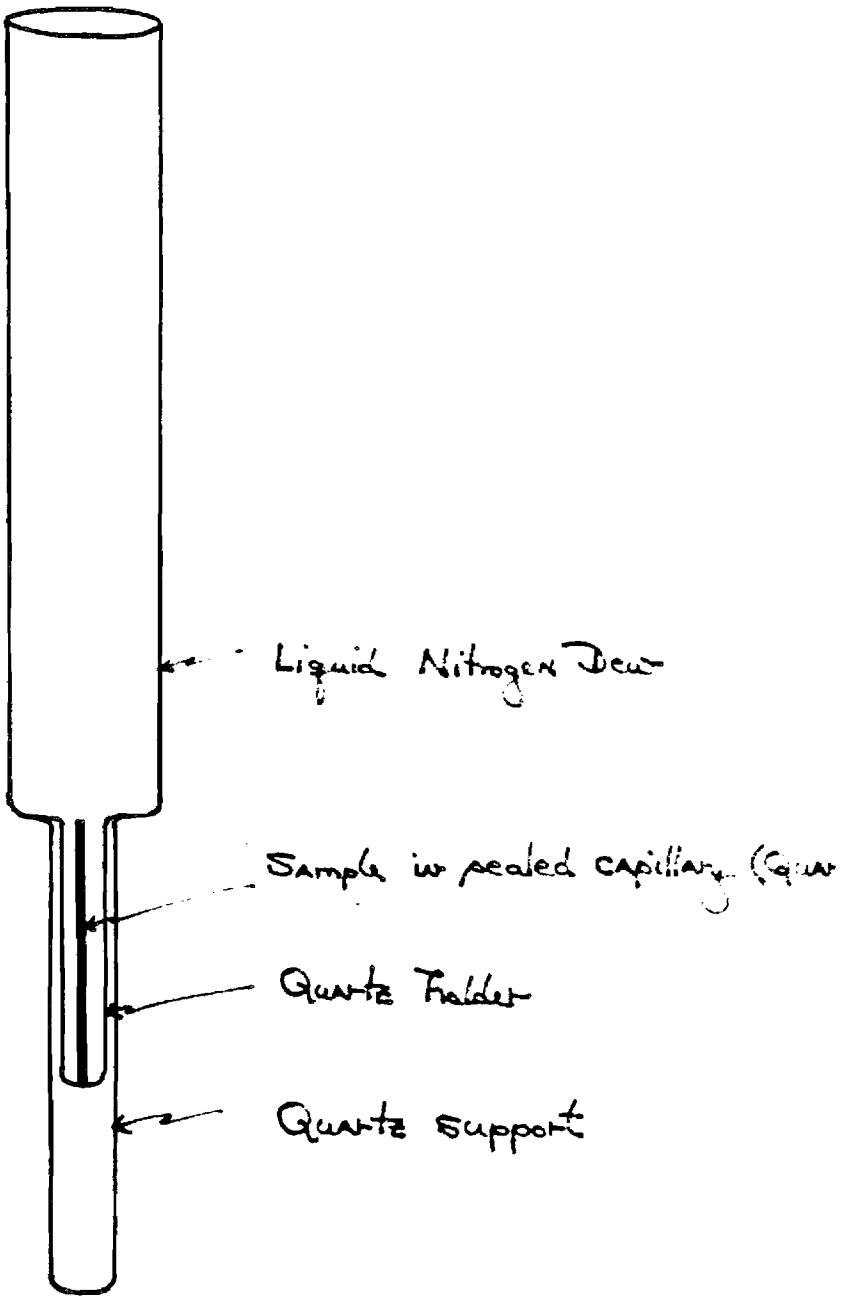

Figure 8. Schematic of Liquid Nitrogen Cooled EPR Probe

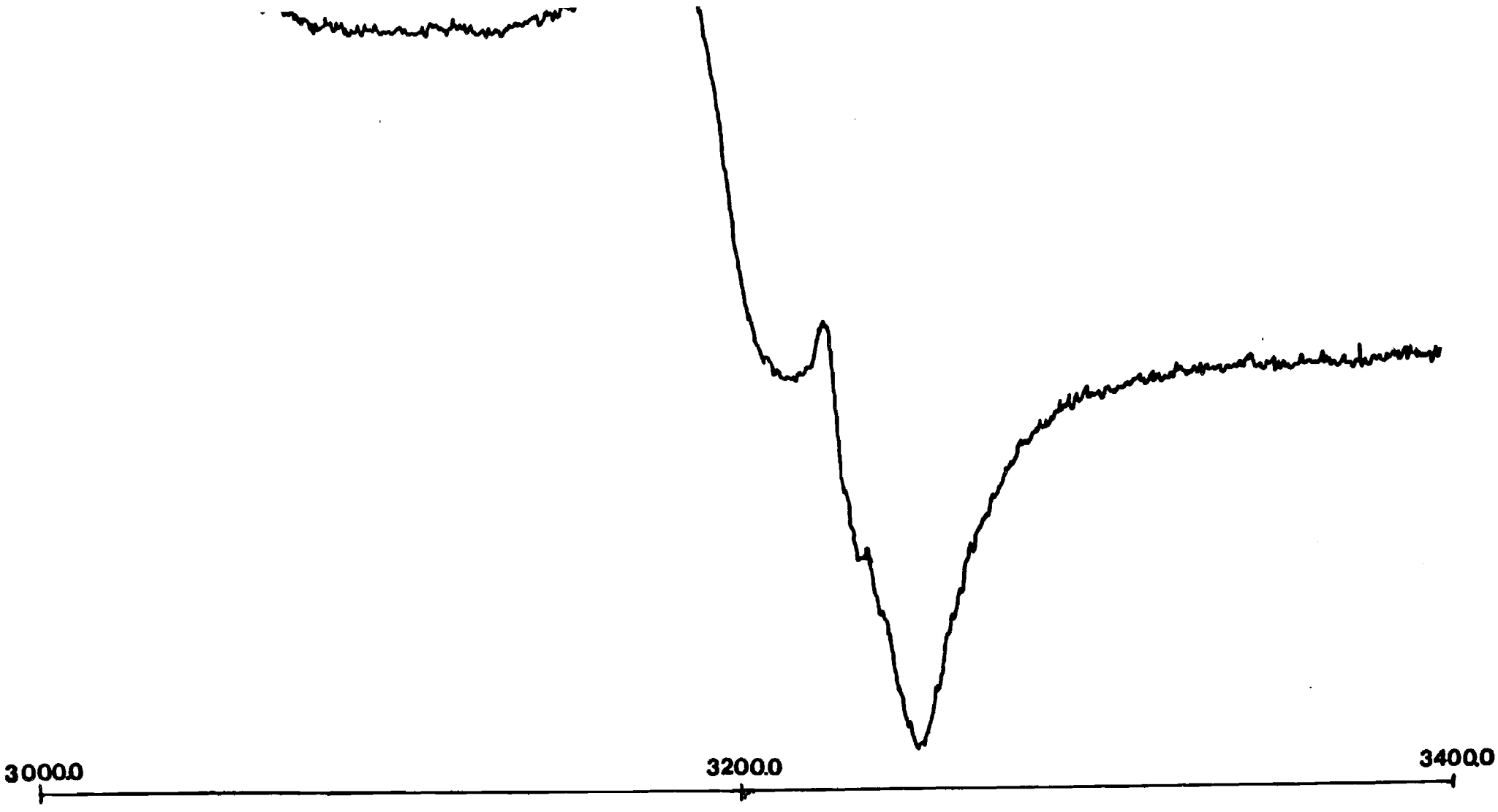

Figure 9. EPR Spectrum of Particulate Matter Formed in Oxidation (N_2O) of Potassium Metal

Silicon Oxide Electronic Emission Spectra

Previously we had carried out extensive studies of the chemiluminescent emission from two reactions producing the SiO molecule ($Si + N_2O \rightarrow SiO + N_2$ (Appendix C) $Si + O_3 \rightarrow SiO + O_2$) in order to evaluate molecular constants for the SiO ground electronic state, study ultrafast energy transfer in the SiO molecule, and deduce a lower bound for the SiO bond energy. The characterization of the $Si-N_2O$ and $Si-O_3$ reactions has allowed the determination of a lower bound for the SiO bond energy, however the dynamics of these reactions is such that further characterization of the N_2 and O_2 products will be required to obtain a sufficiently stringent measure of this quantity.

The focus of the present research effort has been to supplement our previous studies of the $Si-N_2O$ and $Si-O_3$ reactions and to determine the SiO bond energy using a direct spectroscopic approach. In studying the reaction of silicon atoms with NO_2 (Appendix D), we have determined an SiO bond energy in excellent agreement with mass spectroscopy.

The Silicon-NO_2 Metathesis - An Independent Confirmation of the SiO Bond Energy

We have studied the chemiluminescent emission from the reaction

$$Si + NO_2 \rightarrow SiO^*(a^3\Sigma^+, b^3\Pi, A^1\Pi) + NO$$

where the excited states of SiO are produced and emit a photon before undergoing subsequent collisions. In Figure 10 we depict the SiO $A^1\Pi - X^1\Sigma^+$ emission which characterize the $Si-NO_2$ reaction. We have found that the $Si-NO_2$ reaction populates the $v' = 0, 1, 2$ levels of the SiO $A^1\Pi$ state (Appendix D) in a process whose activation energy is 7.4 kcal/mole. Using the relationship[27]

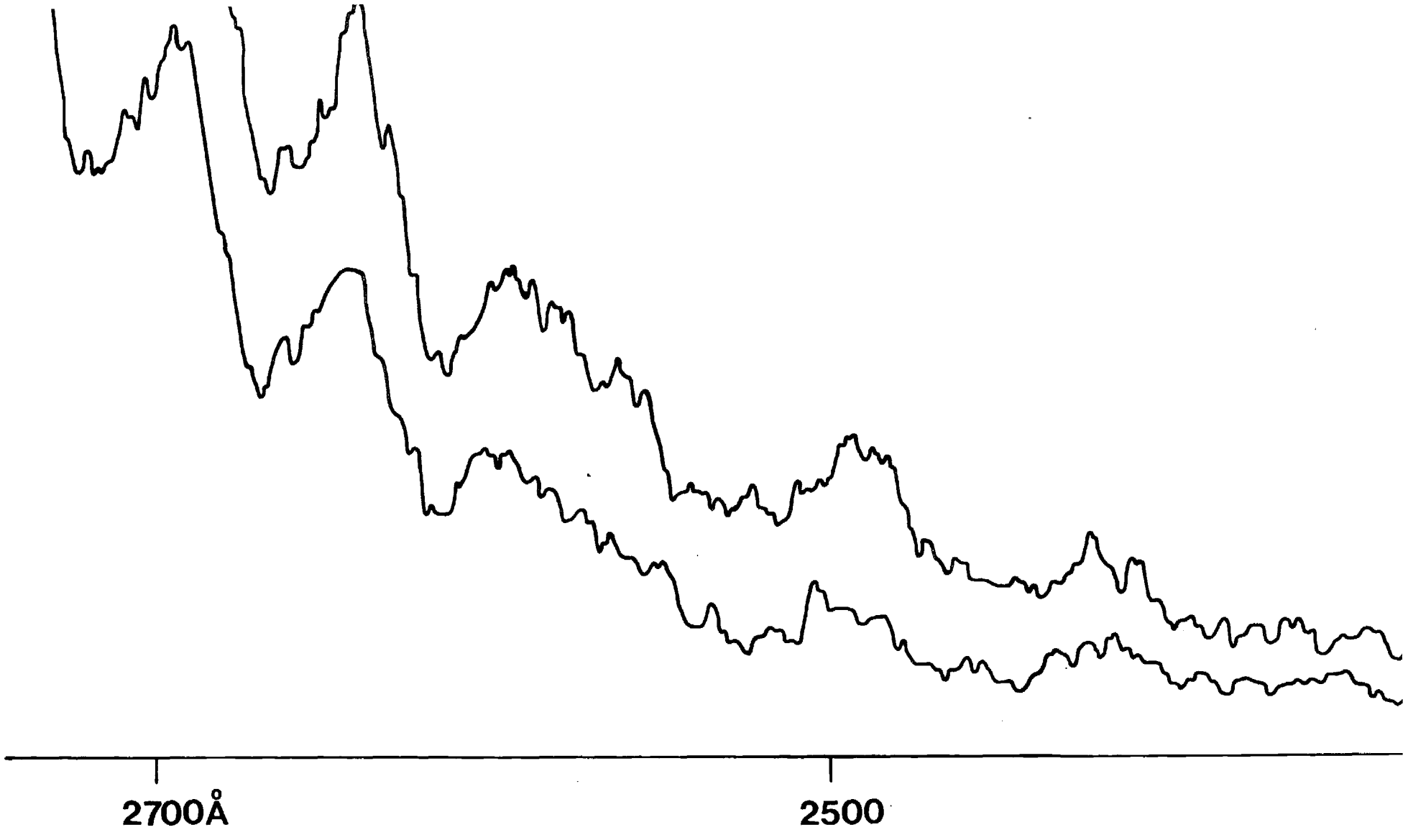

Figure 10. Chemiluminescent Spectrum for SiO* Formed in the Reaction Si + NO_2 → SiO*($A^1\Pi$) + NO

$$D_o^o(SiO) \geq D_o^o(ON\text{-}O) + E_{int}(SiO) - E_{int}(Si) - E_{int}(NO_2)$$
$$\underset{72.9}{} \qquad \underset{126.7}{} \qquad \underset{0.4}{} \qquad \underset{.85}{}$$
$$-E_T^i - E_A(Si\text{-}NO_2)$$
$$= 186.65 \pm 1 \text{ kcal/mole}$$
$$\underset{4.3 - 7.4}{}$$

where $E_{int}(Si)$, $E_{int}(NO_2)$, and $E_{int}(SiO)$ are the internal energies of the species in parentheses, E_T^i is the relative translational energy of the reactants and $E_A(Si\text{-}NO_2)$ is the measured activation energy of the metathesis considered. The evaluation of all of these quantities is discussed elsewhere.[27] The thermochemical cycle yields a lower bound to the SiO bond energy of 186±1 kcal/mole in good agreement with the mass spectrometric determination of Hildenbrand et al.[28] (188.2 kcal/mole). This determination of the SiO bond energy is the first evaluation of this quantity independent of mass spectroscopy.

Alkali Hydroxide Emission Spectra

Short Summary

The first electronic emission spectra for the alkali hydroxides have been obtained over a wide pressure range (Appendix A). The reactions of sodium and potassium dimers with hydrogen peroxide are being used to excite chemiluminescence from NaOH and KOH. The objective of this task is to determine stringent lower bounds for the K-OH and the Na-OH bond energies and molecular constants for several levels of the ground electronic state of KOH. KOH emission has been observed at low pressures under "single collision" conditions, at intermediate pressures where the effects of collisional relaxation are apparent ("multiple collision" conditions) and at higher pressures in a "diffusion flame" device, the combination of these studies leading to the evaluation of a stringent lower bound for the K-OH bond energy using a direct optical measurement (Appendix A). Similarly, a strong NaOH diffusion flame spectrum has now led to the determination of a stringent lower bound for the Na-OH bond energy by direct optical measurement (Appendix A). While constants have been determined for the lowest vibrational quantum levels of the ground electronic state of KOH (the KOH fundamental frequency in the gas phase is determined to be 423 cm^{-1}), continued improvements in the diffusion flame experiment were pursued in order to obtain higher resolution spectra to evaluate molecular constants for several ground state levels. Further, using a combination of single and multiple collision studies we hoped to extend the evaluation of ground state molecular constants. The major challenge which confronts these efforts is the generation of a long term, intense, stable flame. Flame instabilities and the possibility of multiple processes leading to KOH excited states tend to "wash out" spectral features, a factor which plagues electro-optical scans. Therefore, a spectrum must be obtained either on film

or through the use of an optical multichannel analyzer. Because the KOH emission spectrum extends across a rather wide range (3000Å), the limited range (200Å) of a given OMA scan is not conductive to ready analysis. Thus the task confronting the efficient analysis of the KOH emission spectrum has been the generation of this spectrum on film requiring a long term, intense flame. This is not a straightforward task due primarily to the extremely efficient gas phase formation of particulate matter in these systems (see previous discussion).[19]

Attempts to Extend Spectral Characterization

We constructed a revised system to study the KOH emission spectrum. This system is based on a minor modification off the diffusion flame apparatus which we have discussed previously (Appendix A) designed to facilitate the attainment of the KOH spectrum on film or using an optical multichannel analyzer. The device employs all of the improvements which we have incorporated and discussed in previous reports[19] (see also Appendix A) and considerably improves the optical system. The reconstructed optical system appears to have increased our sensitivity by close to an order of magnitude.

Using our reconstructed optical system for the study of diffusion flames we have used the most sensitive film available to study the KOH emission spectrum in the region 2800-3500Å. We have employed two spectrographs in an attempt to obtain a film of the system. These efforts have been unsuccessful and we have now ordered a new holographic spectrometer to be used in conjunction with our OMA system in order to further investigate the spectrum. It should be noted that the electro-optical traces taken of the emission spectrum during this period were found to be consistent with previous results[19] (see also Appendix A) with no marked improvement in the monitoring of observed features. In correlation with the efforts of other workers, the results

obtained thusfar indicate that the JANAF tables on the alkali hydroxides will require massive revision.

Sodium Cluster Oxidation

Short Summary

The object of this task was to evaluate the nature of sodium oxidation in the intermediate region between the gas and surface phase. The products of sodium cluster oxidation were characterized, through direct observation of the chemiluminescent emission from highly exothermic processes, through a newly developed electron impact excitation technique, and through mass spectrometric sampling of the oxidation region. Both the halogen and SO_2 oxidation of sodium clusters were studied.

Attempts to Extend Initial Oxidation Studies

In our previous discussions of sodium cluster oxidation[19] we noted that the chemiluminescent spectra which characterize the Na_x + Cl, Na_x + Br, and Na_x + SO_2 (chlorine impurity introduced) systems are characterized by a very high degree of internal excitation which renders ready resolution of spectral features difficult. To improve the resolution in the system, we constructed an entraining device placed at the point of an entrance of the supersonic Na_x beam into the reaction chamber. The ring injector device (Figure 11) was designed to increase the pressure in the reactive chamber through the introduction of a rare gas such as helium or argon. The device was designed to create a merged metal cluster-rare gas flow, in an attempt to oxidize entrained clusters under controlled conditions at elevated pressure where collisions promote rotational relaxation. In order to operate this device, the forepump system in the metal clusters apparatus was extensively modified to handle increased gas loads. The oven chamber was pumped independently of the reaction chamber by a 17 CFM forepump and the reaction chamber pumped by a 50 CFM forepump. (This should be contrasted to the previous pumping of the entire system by a 17 CFM pump.) Using this pumping configuration, we studied

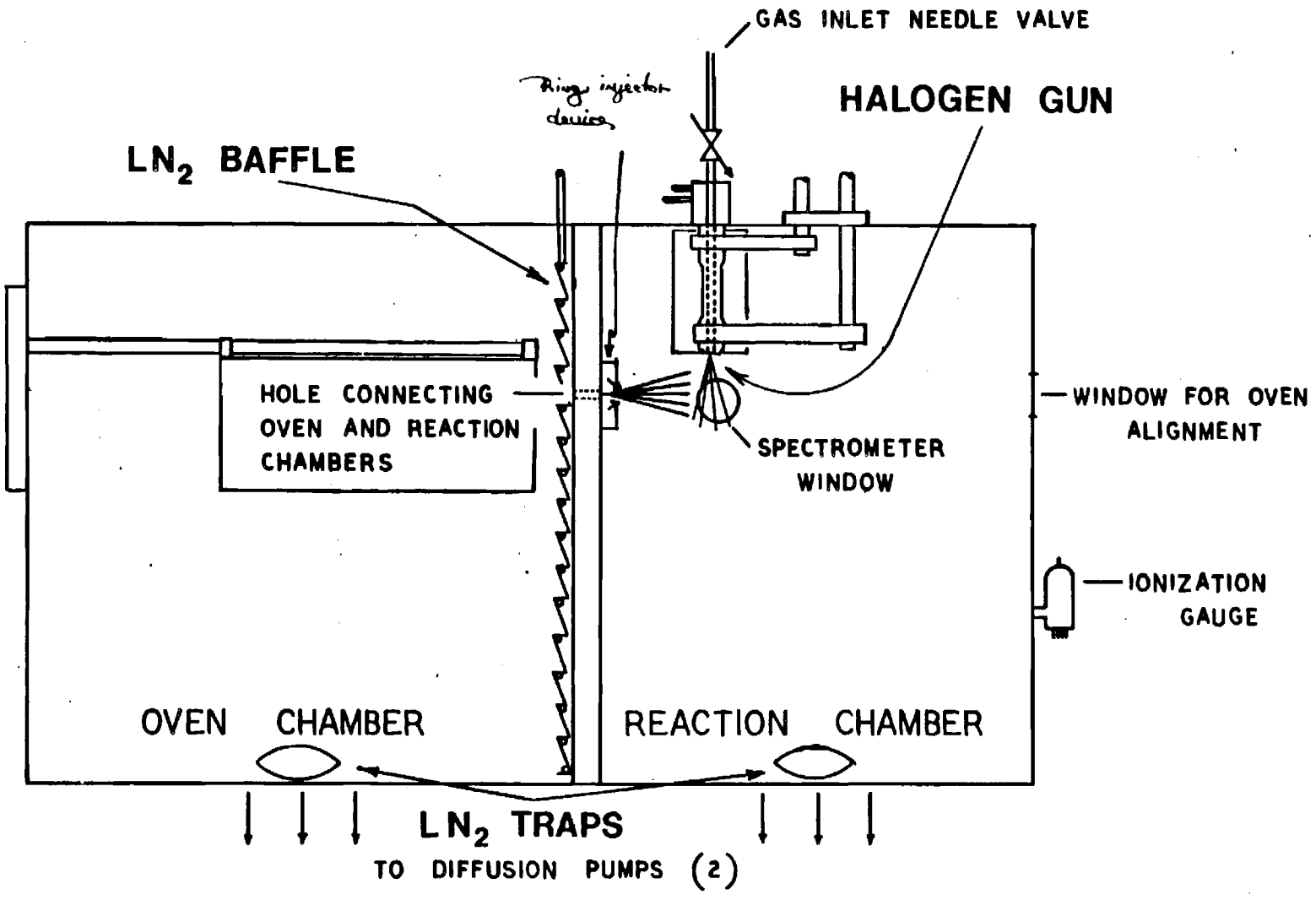

Figure 11. Schematic of Sodium Cluster Oxidation Apparatus Showing Ring Injector System

the Na_x + Br + Ar system and successfully introduced some internal relaxation in the chemiluminescent products thus increasing our ability to resolve those spectral features of interest. However, the carrier gas pressure and hence the reaction chamber pressure were somewhat oscillatory. Recently, we improved this situation with (1) a modification of the ring injector annulus so as to decrease the width of the ring orifice while increasing its convergence angle and (2) the introduction of a further needle valve into the rare gas inlet in order to control the gas pressure. This device alleviated oscillatory behavior, produced spectra which showed some relaxation, and could be operated to reaction chamber prressures of 10^{-1} torr. However, as with previous studies, the chemiluminescent flame was considerably weakened due to the rarification of alkali-halogen encounters in the viewing zone region as the result of rare gas dilution. It is also likely that the observed spectral emission emanates from excited electronic states which are sufficiently shortlived so that they do not encounter a significant number of rare gas atoms before emission. To attempt to solve this problem we began construction of a device to simultaneously supersonically expand a mixture of sodium in helium or argon creating alkali-rare gas complexes. It was felt that the clusters could then be oxidized in an insured "local" environment of helium or argon atoms.

Several experiments to study the Na_x + SO_2 + CL_2 system were initiated during this period. Here we attempted to test the catalytic activity of a slight chlorine impurity to produce a highly exothermic metathesis involving alkali clusters and SO_2 (see Annual Topical Report 1[19]). A device was constructed which allowed for the flow of SO_2 over a channel contaminated with chlorine prior to its (SO_2) introduction to the reaction chamber. In a second approach, SO_2 was mixed with slight amounts of chlorine, this mixture

interacting with the sodium cluster beam. Both the $Na_x + Cl_2$ and $Na_x + SO_2$ systems within themselves do not produce the chemiluminescent emission which has been found to characterize the mixed system (the $Na_x + Cl_2$ system does produce Na D-line and $NaCl^*$ emission (see Annual Topical Report 1), however, this emission is almost completely at wavelengths longer than that characterizing the mixed system). In all of the experimental runs conducted, initial visual observations of the anticipated weak chemiluminescence (blue-green) were encouraging, however under reaction chamber conditions, before a spectrum could be taken the oven system lost necessary power (short and oven burn out) resulting in a rapidly decreasing flame intensity.

Correlation with Surface Oxidation

We have attempted initial experiments which involve the highly exothermic oxidation of a "dirty" sodium surface with N_2O. Although oxidation was apparent and characterized by a rather evident frothing during the reactive process, only dark products were formed in the reaction. That is, only ground or very low-lying states of the reaction products were formed and they emit out of the range of either the human eye or a red sensitive visible phototube. This, of course, indicates that the oxidation of a dirty sodium surface with O_2 will produce only ground state reaction products. Therefore, it will be necessary to probe the system with an appropriate dye laser-mass spectrometer combination. For this reason, it is extremely important that we establish spectral regions where the alkali oxides NaO and Na_2O can be monitored. In these efforts, we have been quite successful.

CONCLUSIONS AND RECOMMENDATIONS

From the previous discussion, it should be clear that extensive data not previously available for the alkali hydroxides and oxides and several unusual features of alkali oxidation have been uncovered in this research effort. Although the alkali metals are more readily vaporized than the more refractory metals with which we have had considerable experience, their oxidations to produce the oxides and hydroxides are characterized by a very different and more complex gas phase chemistry than that accompanying virtually all other highly exothermic metal oxidations.

Among our most important contributions during this period (see bullet summary - Appendix C) has been the characterization of the first observed electronic emission spectra for the alkali oxides NaO, KO, and LiO and hydroxides NaOH and KOH the establishment of the potential for a direct means to detect these oxides and hydroxides either directly in process streams. Further, the girth of these studies establish bond energies and dynamic behavior to the extent that they may be helpful as a means for establishing selective photodissociation channels for the hydroxides and oxides which will be helpful in recent photodissociation studies. To this extent we have had extensive conversations with R. C. Oldenborg of the Los Alamos Scientific Laboratory.[20]

The importance of the low-lying predominantly covalent state of the alkali oxides, now identified in our laboratory, and the necessity for its characterization cannot be underestimated. Because the spectral features characterizing this state result in an electronic emission spectrum at the fringes of the visible spectral region its presence furnishes the first ready means for detecting the alkali oxide. At present, as we note in Appendix G

and previous discussion, a tauted means (LIBS) for detecting the presence of alkali compounds in process streams involves the assessment of complex multiphoton laser atomization processes and an expensive combination of laser systems. In the LIBS technique sodium compounds are atomized with an intense laser pulse and subsequent excitation of atomic sodium provides an indication of the alkali concentration which is believed to be present in a limited group of species. Though the laser techniques are eloquent, this is a somewhat tenuous back extrapolation (see previous discussions, pp. 20-30). In addition to be concentration quantitative they require considerable supplementary data on the photodissociation of alkali compounds, little of which is currently available. With the discovery of these new electronic states much of this data base may be circumvented and vastly simplified for the alkali monoxides. Further monitoring techniques can be compound specific. The new route may not only be important for the detection of sodium monoxide in the gas phase but also its detection as the product of sodium contaminated surface oxidation. In addition, the discovery of this state has important implications for the assessment of sodium chemistry in the upper atmosphere. For this reason it is important to attempt to develop new routes which take advantage of the low-lying alkali oxide state to probe for the alkali oxide. The combination of a Nd:YAG dye laser system in conjunction with several techniques for producing the ground state oxide are suggested in Section A (pp. 30-33).

It will be necessary to characterize the extremely efficient gas phase particulate formation in the alkali oxidation systems. The particulate matter studied thusfar, which consists at least in part of alkali (X_n, $n \geq 3$) - oxygen-nitrogen complexes, should be amenable to characterization via mass spectrometry (moderate temperatures $\sim$ 50-400^{o}C), EPR spectroscopy, Raman Spectroscopy, and flame spectrometry. Further experiments which involve the combina-

tion of nonequilibrium laser vaporization and quadrupole-mass spectrometry are also distinct possibilities. While initial efforts have been focused on the particulate products of the $K + N_2O$ oxidation system, this effort should be extended to the study of particulate formation in at least the $Na_x + N_2O$, $K_x + O_3$, and $K_x + H_2O_2$ ($x = 1,2$) systems.

While initial approaches have been only marginally successful, we feel that further studies of (1) sodium cluster oxidation with SO_2 and (2) the nature of the highly exothermic chlorine catalyzed SO_2 oxidation of sodium clusters are warranted. Indeed we believe that these studies can have significant import for the understanding of sodium surface oxidation.

Studies of the $Na_x + SO_2$ (neat) reaction system should be pursued using an electron impact technique[19] as a probe of possible ground state product formation. This method of excitation applied individually to SO_2, Na_x, and $Na_x + SO_2$ may demonstrate the formation of a sulfite complex. Similar experiments should be carried out on the system $Na_x + SO_x$ where a slight chlorine impurity is introduced. Lastly, we believe that a set of experiments studying the $Na_x + SO_2Cl_2$ (sulfonyl chloride) system is also appropriate. In view of our recent mass spectrometric studies of the $Na_x + Br$ system[19] we believe that mass spectrometry should be added as a probe of these three systems. A problem may exist. There is some question about the stability of those complexes whose reaction may lead to the highly exothermic process whose chemiluminescence has been observed. If these complexes are sufficiently weakly bound electron impact excitation may be blind to their presence and thus obtain an invalid mass spectrometric probe of the system. For this reason, it will be necessary to incorporate the facility for direct photoionization in the mass spectrometer system. Here ions are produced via a much milder excitation technique and the probability for the dissociative

ionization of the complexes of interest diminishes considerably.

As we have mentioned previously we have begun the construction of a device which should allow the controlled relaxation of chemiluminescing product excited electronic states in the Na_x + oxidant system. This device can be used to improve the resolution of those spectra obtained in the Na_x + halogen and Na_x + SO_2 + halogen systems thus improving product characterization. Clearly, these sodium cluster oxidation studies should be followed by the study of both contaminated and clean sodium surfaces. We anticipate that at least the study of contaminated sodium surface oxidation can be carried out in the near future. This is of course aided by our recent discovery of low-lying electronic states in the alkali monoxides and suboxides.[19] We believe that there will be important correlations between these studies and the necessity to assess the nature of gas phase particulate formaation in alklai oxidation. While it should be possible to sample these surface oxidation phenomena in-situ using optical and mass spectrometric techniques, it will probably be necessary to carry out further studies of a substantial surface residue left after oxidation. Here, it may be possible to carry out surface desorption studies, heating the sodium surfaces to remove the alkali oxidation products.

A final area warrants continued study. With the development of an intense, stable, and long-lasting alkali hydroxide diffusion flame, efforts should continue to obtain the KOH emission spectrum in 200Å sections using an optical multichannel analyzer system. The study will allow the evaluation of further molecular constants for the ground electronic state of KOH.

References

1. L. D. Landau and E. M. Lifshitz, Statistical Physics, Pergamen Press, Addison-Wesley Publishing Company, 1958.

2. G. W. Stewart, A. Chakrabasti, C. Stinespring, and K. Castleton, Western States Symposium/Combustion Institute, October, 1980.

3. a) See, for example, J. W. Hastie, "High Temperature Vapors, Science and Technology," Academic Press, New York, 1975.
   b) See also "High Temperature, High Pressure Particulate and Alkali Control in Coal Combustion Process Streams" - Proceedingsof the U.S. Department of Energy Contractor's Meeting, West Virginia, 1981.

4. "Open Cycle Magnetohydrodynamic Power Generation," J. B. Heywood and G. J. Womack, eds., Pergamon, Oxford, 1969.

5. H. C. Hottel and J. B. Howard, "New Energy Technology - Some Facts and Assessments," M.I.T. Press, Cambridge, MA (1971).

6. J. L. Gole, Optical Engineering 20, 546 (1981).

7. See for example, R. K. Sinha and P. L. Walker, Jr., Fuel 51, 329 (1972); F. S. Karn, R. A. Friedel and A. G. Sharkey, Jr., Fuel 51, 113 (1972). Note also references 2 and 3(b) also G. W. Stewart private discussions.

8. Session on High Pressure Sampling, 10th Materials Research Symposium on Characterization of High Temperature Vapors and Gases, National Bureau of Standards, Gaithersburg, MD, September 18-22, 1978.

9. F. E. Stafford and J. Berkowitz, J. Chem. Phys. 40, 2963 (1964).

10. R. Kelly and P. J. Padley, Trans, Faraday Society 67, 740 (1971).

11. L. N. Gorokhov, A. V. Gusarov and I. G. Panchenkov, Russ. J. Phys. Chem. 44, 150 (1970).

12. J. W. Hastie, E. R. Plante, D. W. Bonnell - private communication.

13. N. Acquista, S. Abramowitz and D. R. Lide, J. Chem. Phys. 49, 780 (1968).

14. N. Acquista and S. Abramowitz, J. Chem. Phys. 51, 2911 (1969).

15. A. A. Belyaeva, M. I. Dvorkin, and L. D. Sheherba, Opt. and Spectrosc. 31, 210 (1971).

16. D. R. Lide and R. L. Kuczkowski, J. Chem. Phys. 46, 4768 (1967).
    C. Matsumura and D. R. Lide, J. Chem. Phys. 50, 71 (1969).
    D. R. Lide and C. Matsumura, J. Chem. Phys. 50, 3080 (1969).
    E. F. Pearson and M. B. Trueblood, J. Chem. Phys. 58, 826 (1973), Astrophys. Journal 174, L145 (1973).
    E. F. Pearson, B. P. Winnewisser and M. B. Trueblood, Z. Naturforsch 31a, 1259 (1976).

P. Kuijpers, T. Törring and A. Dynamus, Chem. Phys. 15, 457 (1976); Z. Naturforsch 31a, 1256 (1975).

P. Kuijpers, T. Törring and A. Dynamus, Z. Naturforsch 32a, 930 (1977).

7. Of course this information will be useful for the statistical mechanical evaluation of thermodynamic properties such as the heat capacity, entropy, and free energy.

8. F. A. Cotton and G. Wilkinson, Advanced Inorganic Chemistry, Interscience John Wiley and Sons, 1974.

9. "The Characterization of High Temperature Vapor Phase Species and Vapor-Solid Interactions of Import to Combustion and Gasification Processes in the Energy Technologies," Annual Topical Report No. 1, U.S.D.O.E., Morgantown, West Virginia (Contract DE-AC21-81MC16537).

0. Note Appendix G. also R. C. Oldenborg, Los Alamos Scientific Laboratory private communication.

1. See for example J. L. Gole "The Characterization of High Temperature Vapors of Import to Combustion and Gasification Processes in the Energy Technologies," Proceedings of the Morgantown Energy Technology Center Meeting on High Temperature, High Pressure Particulate and Alkali Control in Coal Combustion Process Streams - Morgantown, West Virginia, 1981.

2. J. N. Allison, R. J. Cave, and W. A. Goddard III, J. Chem. Phys. 77, 4259 (1982) also "The Alkali Oxides. ^{2}Analysis of Bonding and Explanation of the Reversal in Ordering of the $^2\Pi$ and $^2\Sigma^+$ States" - preprint.

3. Based on energy conservation R. R. Herm and D. R. Herschbach, J. Chem. Phys. 52, 5783 (1970), D. L. Hildenbrand, and E. Murad, J. Chem. Phys. 53, 3403 (1970) it is highly unlikely that the 6740A band is associated with v">2.

4. The programs used for these computations were written by Dr. Brian Wicke. See R. N. Zare, J. Chem. Phys. 40, 1934 (1964).

5. R. R. Herm and D. R. Herschbach, J. Chem. Phys. 52, 5783 (1970), D. L. Hildenbrand, and E. Murad, J. Chem. Phys. 53, 3403 (1970) it is highly unlikely that the 6740A band is associated with v">2.

6. An estimated vibrational frequency obtained using a combination of Badger's rule and a Morse Potential fit is ~283 cm^{-1} for the covalent state of NaO and 170 cm^{-1} for the covalent state of KO.

7. See for example G. J. Green and J. L. Gole, Chem. Phys. 46, 67 (1980).

8. D. L. Hildenbrand, High Temp. Science 4, 244 (1972).

Technical Publications and Presentations

The following eight papers have been published, accepted for publication, submitted or are in the latter stages of preparation.

"Dynamic Constraints Associated with the Formation of SiS^* ($a^3\Sigma^+$) from the Chemiluminescent Si-OCS Reaction," with G. J. Green, Chemical Physics 69, 357 (1982).

"Metal Cluster Oxidation: Chemiluminescent from the Reaction of Sodium Polymers (Na_n, $n \geq 3$) with Halogen Atoms (X=Cl,Br,I)," with W. H. Crumley and D. A. Dixon, J. Chem. Phys. 76, 6439 (1982).

"Observation of Alkali Oxide Electronic Emission Spectra: Analysis of the NaO "6700Å" Band System," with Joerg Pfeifer, Jour. of Chem. Phys. 80, 565 (1984).

"The Gas Phase Characterization of the Molecular Electronic Structure of Small Metal Clusters and Cluster Oxidation," to appear in "Metal Clusters," edited by M. Moskovits, John Wiley and Sons (1986) pg. 131.

"Energetics of Silicon Oxidation Reactions - An Independent Determination off the SiO Bond Dissociation Energy," with Joerg Pfeifer and Gary Green (High Temperature Science - Brewer Issue, 17, 85 (1984).

"Energy Balance and Branching Ratios Associated with the Chemiluminescent Reaction $Si(^3P) + N_2O(^1\Sigma) \rightarrow SiO^*$ ($a^3\Sigma^+$, $b^3\Pi$, $A^1\Pi$) + $N_2(v'' \geq 5)$ - Possible Formation of Vibrationally Excited N_2 in M + N_2O Reactions," with G. J. Green, Chem. Phys. 100, 133 (1985).

"Energy Balance in the Si-NO_2 Reaction: On the Formation of SiO $a^3\Sigma^+$, $v' \geq 0$, and Ultrafast $a^3\Sigma^+$-$b^3\Pi$ E-E Energy Transfer," Chem. Phys. 100, 153 (1985).

"Formation, Electronic Spectra, and Correlation of the Alkali Halides and Hydroxides," with D. F. Dever and B. Cardelino, High Temp. Sci. 18, 159 (1984).

"The Characterization of High Temperature Vapor Phase Species and Vapor-Solid Interactions of Import to Combustion and Gasification Processes in the Energy Technologies," Annual Topical Report Nos. 1 and 2, U.S.D.O.E., Morgantown, West Virginia (Contract DE-AC21-81MC16537).

"Alkali Metal Oxide Formation - First Observed Emission from a Low-Lying Electronic State of the Alkali Monoxides LiO - CsO," with R. Woodward, R. Eades, and D. A. Dixon, in preparation.

"Electronic Emission Spectra and Bonding of the Alkali Hydroxides, NaOH CsOH," with J. S. Hayden and R. Woodward, submitted.

Presentations detailing aspects of the work discussed in this document were given at

Tulane University, Invited Talk, "Formation, Characterization, and Oxidation of Small Metal Clusters" (1982).

Oak Ridge National Laboratory, Invited Talk, "Formation, Characterization, and Oxidation of Small Metal Clusters" (1982).

The University of Alabama, Invited Talk, "Metal Cluster Formation and Oxidation" (1983).

Symposium in Honor of John Fenn, Yale University, New Haven, Connecticut, "Formation, Characterization, and Oxidation of Small Metal Clusters" (1983).

Symposium on "Spectroscopic, Photophysical and Photochemical Properties of Metal Clusters, Colloids and Rough Surfaces," A.C.S. Colloid and Surface Science Division, Invited Talk, "Formation, Characterization, and Oxidation of Small Metal Clusters" (1983).

APPENDIX A

FORMATION, ELECTRONIC SPECTRA, AND CORRELATION OF THE ALKALI HALIDES AND HYDROXIDES

D. F. Dever, B. Cardelino, and J. L. Gole

High Temperature Laboratory, Center for Atomic and Molecular Science and School of Physics

Georgia Institute of Technology

Atlanta, Georgia 30332

Abstract

The First electronic emission spectra for the alkali hydroxides have been obtained over a wide pressure range. The reactions of sodium and potassium dimers with hydrogen peroxide have been used to excite chemiluminescence from NaOH and KOH. KOH emission has been observed at low pressures under effectively "single collision" conditions, at intermediate pressures where the effects of collisional relaxation are apparent ("multiple collision" conditions) and at even higher effective pressures in a "diffusion flame" device, the combination of these studies leading to the evaluation of a lower bound for the K-OH bond energy, $D_0(K\text{-}OH) \geq 88.2$ kcal/mole, (JANAF = 85.4 $\pm$ 3 kcal/mole) using a direct optical measurement. Similarly, from the NaOH diffusion flame spectrum it has been possible to determine a lower bound for the Na-OH bond energy, $D_0(Na\text{-}OH) \geq 82.5$ kcal/mole, (JANAF = 81.5 $\pm$ 3 kcal/mole) in excellent agreement with recent photodissociation studies. The approach to bond energy determination in these systems is based on a strong correlation with the electronic spectroscopy of the isoelectronic alkali halides where the combination of single collision and diffusion flame spectroscopy leads to the prediction of bond energies for KCl, $D_0^o \geq 99.8$ kcal/mole, KBr, $D_0^o \geq 90.0$ kcal/mole, and KI, $D_0^o \geq 74.7$ kcal/mole in excellent agreement with photofragment spectroscopy. Constants are estimated for the lowest vibrational quantum levels of the ground electronic state of KOH.

Introduction

There have been relatively few gas phase studies of the metal hydroxides, and, with the exception of microwave and millimeter wave data on the alkali hydroxides, molecular parameters for the gas phase molecules are sparse if nonexistent. Abramowitz and coworkers[1(a),(b)] have obtained infrared spectra for matrix isolated NaOH, RbOH, and CsOH and their deuterated analogs. Belyaeva et al.[2] have studied the infrared spectra of matrix isolated KOH. The data from these groups is summarized in Table I and corresponds to the assignment of ν_1, the MO stretching mode and ν_2, the bending mode. It should be

TABLE I

Infrared Data for the Alkali Hydroxides

Molecules	ν_1 (cm^{-1})	ν_2 (cm^{-1})
CsOH	335.6	309.8 302.4
CsOD	330.5	226
RbOH	354.4	309.0
RbOD	345±3	229±3
KOH	408	300
KOD	399	264
NaOH	431	337
NaOD	422±3	250

emphasized that these are not necessarily the vibrational frequencies which will characterize the gas phase infrared spectra for the hydroxides.* Indeed, there is a striking similarity between the KOH, RbOH, and CsOH bending frequencies. The lack of a frequency dependence (although a deuterium isotope

*This is significant if one wishes to use a high resolution diode laser to monitor alkali hydroxide formation and reaction.

shift is clearly evident) is unusual and may be attributed to a hydroxide-matrix interaction.[3] Gas phase infrared and electronic spectra, once obtained, will allow further assessment of this phenomena. Although a detailed catalogue of infrared and electronic data is yet to be obtained, extensive microwave and millimeter wave studies have now yielded significant parameterization for the ground states of NaOH, KOH, RbOH, and CsOH,[4-9] and rotational constants have been obtained for certain excited vibrational levels.

Because potassium and its compounds are used in a wide diversity of applications involving, among others, energy generating systems[10] and the suppression of secondary muzzle flash[11(a)] and secondary rocket combustion[11(b)], KOH is among the more important constituents whose molecular electronic structure, thermodynamics, and kinetic behavior must be well understood. The gas phase spectroscopy of the KOH molecule is poorly characterized[12] and electronic and vibrational spectra should be obtained not only for molecular parameterization but also as a means of assessing regions which may be useful for the monitoring of this species in kinetic studies. Our approach to this problem is based in large part on comparison with the alkali halides.

Nature of Bonding in the Alkali Halides and Hydroxides

In Table II, we present thermochemical data on the chlorides, fluorides, and hydroxides of potassium, sodium and rubidium. Comparisons will be made be between these species because (1) they are valence isoelectronic and (2) their observed emission spectra are expected to be similar. The nature of the bonding in the alkali hydroxides should be intermediate to that in the

fluorides and chlorides. With this in mind, the trends in Table II would seem to indicate the possibility of a K-O bond strength somewhat higher than the value determined through mass spectrometry. The current chemiluminescent studies confirm this conclusion. We have found that the observed emission for KOH correlates closely with expectations based on the known chemiluminescent emission for KCl and other alkali halides.

TABLE II

Comparison of Thermochemical Data for the Alkali Fluorides, Chlorides, and Hydroxides

Molecules	D_0^o(M-X)(kcal/mole)	Comments
KF	117[a]	Thermochemical
KCl	102.6±2[b]	Thermochemical and Photofragment
KOH	84±2.5[c]	H_2-O_2-CO_2 flames 2nd law determination
80±3[d], 84.1±1[e], 84.2±0.5[f], 84.7±2[g] 85.4±2.6		Mass spectroscopy (JANAF tables estimate)
NaF	123	NaOH 79±2[c] (flame--2nd Law)
NaCl	97.6±2[b]	
RbF	115[h]	RbOH 86±3[c] (flame--2nd Law)
RbCl	101.3±2[b]	

a. E. M. Bulewicz, C. G. James, T. M. Sugden, Trans. Faraday Soc. 37, 921 (1961); A. G. Gaydon, "Dissociation Energies and Spectra of Diatomic Molecules," 3rd Edition, Chapman and Hall, 1968.

b. T-M. R. Su and S. J. Riley, J. Chem. Phys. 72, 6632 (1980).

c. R. Kelly and P. J. Padley, Trans. Faraday Society 67, 740 (1971), also the average of three other flame studies by Smith and Sugden, Proc. Roy. Soc. A219, 304 (1953) [86±1]; Jensen and Padley, Trans. Fara. Soc. 62, 2132 (1966) [82±2]; Cotton and Jenkins, Trans. Fara. Soc. 65, 1537 (1969) [86±2].

d. L. N. Gorokhov, A. V. Gusarov and I. G. Panchenkov, Russ. J. Phys. Chem. 44, 150 (1970).

e. J. W. Hastie, K. F. Zmbov, and D. W. Bonnell, "Transpiration Mass Spectrometric Analysis of Liquid KCl and KOH Vaporization," High Temp. Science, in press.

f. M. Farber, R. D. Srivastava, and J. W. Moyer, J. Chem. Thermodynamics 14, 1103 (1982).

g. A. V. Gusarov and L. N. Gorokhov, Russ. J. Phys. Chem. 42, 449 (1968).

h. See reference a and A. D. Caunt and R. F. Barrow, Nature 164, 753 (1949).

Approach to the Study of the KOH Electronic Emission Spectrum - Correlation with the Potassium Halides

In order to understand the nature of the KOH emission spectrum, it is instructive to consider the known electronic emission spectra for the alkali halides. Alkali halide spectra have been generated in three distinct experimental environments. They have been obtained under "single collision" conditions[13] where alkali dimers and halogen molecules react in a four-center process

$$M_2 + X_2 \rightarrow MX^* + MX. \qquad (1)$$

These studies have been extended to "multiple collision" conditions by entraining the alkali dimers in argon and subsequently oxidizing this mixture.[14] A much more effective collisional environment consists of a "diffusion flame" device where oxidant (Cl_2,Br_2,I_2) is passed through a nozzle into a bulb containing several torr of alkali vapor and one to twenty torr of argon.[14]

In Figure 1, we depict the emission spectrum obtained for KCl under single collision conditions.[13] The nature of the potential curves which give rise to the spectrum in Figure 1 is depicted in Figure 2. Although drawn for KBr, the general features are similar for all the alkali halides. These molecules are characterized by a relatively stable ionic ground state and a grouping of several very shallow or repulsive excited states. The emission which one observes corresponds to a transition from one of the shallow or repulsive states to levels of the ground electronic state, the spectrum corresponding to a long progression in the vibrational levels of the ground

electronic (ionic) state. The very shallow nature of the excited state potential has important consequences. One finds that the KCl spectrum changes significantly with the form of excitation and hence the experimental technique used to produce the emission system.

The "single collision" spectrum in Figure 1 onsets at 4180A (68.4 kcal/mole). A similar albeit slightly blue shifted and less clearly structured spectrum is obtained when potassium dimers are entrained in argon ($X_{K_2} \approx 10^{-2} - 10^{-4}$, $P_{Total}(Ar) \approx 0.5 - 1$ torr) and this mixture is oxidized under multiple collision conditions.[15] A significant change occurs when the reaction (1) is studied in a diffusion flame environment. Here the onset of the KCl spectrum is at 2866Å[14] some 1300A to the blue of the single and multiple collision spectrum. Similar effects, although not as pronounced, are observed in the potassium-bromine and potassium-iodine systems. The single collision KBr and KI spectra onset at 4030 and 4550Å, respectively, whereas in a diffusion flame environment the KBr and KI band systems onset at 3175 and 3826A. These large changes signal an important characteristic of the alkali halide excited state potential. Whereas emission spectra involving strongly bound excited states are not substantially altered by the nature of a changing effective potential due to rotation, the shape and nature of the potentials governing shallow or repulsive states can be quite effectively altered by rotational excitation. This is exemplified for KI in Figure 3[16] (very similar curves could be obtained for KCl). Here effective potential curves are constructed as a function of the rotational quantum number J and the relation

$$V_{effective}(J) = V_{rotationless} + h^2 \left(\frac{J(J+1)}{2\mu R^2} \right) \qquad (2)$$

It should be noted that there is a substantial change in the minima for

the effective potentials as a function of increasing rotational excitation and hence the quantum number J. The high J potentials corresponding to the single[13] collision environment where a rather high impact parameter reaction yields a high degree of rotational excitation, unrelaxed by subsequent collisions, and emission spectra onsetting at 4180Å for KCl, 4030Å for KBr, and 4550Å for KI; the low J potentials correspond to the very effectively collisionally relaxed diffusion flame emission systems onsetting at 2866, 3175, and 3826Å for KCl, KBr, and KI, respectively. As a result of the shift of the effective excited state potentials, one observes emission to differing sets of ground state levels (Figure 4). In the diffusion flame experiments emission is observed to much lower regions (Fig. 4) of the ground state potential and hence the spectra onset much further to the blue.[14]

KOH Electronic Emission Spectrum

Although we have generated the KOH emission spectrum under a variety of experimental conditions, we focus here on spectra obtained under the limits of (1) a "single collision" and (2) a "diffusion flame" environment. Depicted in Figures (5) and (6) are "single" and "multiple" collision chemiluminescent spectra for KOH generated via electrooptical scans of a very low pressure ($< 10^{-3}$ torr) system and a diffusion flame environment. At very low pressures, energy conservation dictates that the observed emission must result from the process

$$K_2 + H_2O_2 \rightarrow KOH^* + KOH \qquad (3)$$

whereas, in the "diffusion flame" environment, the three body encounter

$$K + OH + M \rightarrow KOH^{*} + M \qquad (4)$$

may also contribute to the observed emission. We have found (see also following) that moderate adjustments in the relative amounts of argon and alkali vapor in the vicinity of the flame region make it possible to significantly modify the degree of relaxation characterizing the diffusion flame spectrum.

The outlined change in the emission spectra for the alkali halides as a function of experimental conditions is also manifest in the alkali hydroxides. One anticipates that the potential function describing the K-OH stretch will be similar to that for KCl. If the potential curves for the excited states of K-OH are similar to those for KCl, they should be shallow and the KOH emission spectrum which results from reaction (3) should change significantly with excitation technique. As Figures 5 and 6 demonstrate, this is observed, although the effect is not as pronounced as that in KCl. The single collision chemiluminescent spectrum for KOH onsets at 3900Å (Figure 5) whereas the spectrum obtained in the most collisionally relaxed diffusion flame environment which we have been able to generate in the laboratory onsets at 3240Å (Figure 6). This significant change signals the presence of a shallow "effective" potential for the KOH normal mode. Of course, it is not completely correct to speak of an isolated "K-O" stretch in the KOH molecule. In reality, the potential function is more complicated and there will be some coupling with the O-H stretch and the bending mode of the triatomic. Nevertheless, the close analogy which the potassium hydroxide spectrum bears to that of KCl leads to comparisons between the two molecules which, in the final analysis, involve a direct determination of the K-OH bond energy.

Evaluation of KOH and KX (X = Cl, Br, I) Bond Energies From Direct Optical Measurement

The KCl and KOH spectra correspond to emission from shallow effective potentials close to the dissociation assymptote of the ground electronic state (Figs. 2 and 4). Given that we have strong evidence for these shallow effective potentials, we can use the onset of spectral emission to estimate the dissociation energy for the K-Cl and K-OH bonds. Because the diffusion-flame results must correspond to emission to lower levels of the ground state potential, this onset is chosen to give the best estimate of the bond dissociation energy. For K-Cl, the onset at 2866A corresponds to 99.8 kcal/mole. This should be compared to the value in Table II: D_o^o(K-Cl) = 102.6 $\pm$ 2 kcal/mole. It should be apparent that we are able to estimate a good lower bound to the K-Cl dissociation energy from the energy corresponding to the onset of the K-Cl diffusion flame spectrum. Similarly, the onsets of the KBr and KI diffusion flame spectra at 3175 and 3826A correspond to 90.05 and 74.7 kcal/mole in good agreement with the photofragment values determined by DeVries et al.[17] (D_o^o(KCl) = 89.8$\pm$1.0, 89.7 $\pm$ 0.4 kcal/mole), (D_o^o(KBr) = 76.2$\pm$0.5, 76.6 $\pm$ 0.4 kcal/mole). The onset of the KOH diffusion flame spectrum at 3240Å yields a lower bound of 88.2 kcal/mole for the K-OH bond dissociation energy which should be compared to the value 85.4 $\pm$ 3 kcal/mole recommended by JANAF.

NaOH Electronic Emission Spectrum - Evaluation of Na-OH Bond Energy

Upon extending our study of the $K_2 + H_2O_2$ diffusion flame to the corresponding sodium analog, $Na_2 + H_2O_2$, we have thusfar obtained, a virtually

unstructured yet interpretable emission spectrum. The spectrum corresponds to a continuum on which are superimposed several sharp features (see also following discussion). The NaOH emission continuum is shown in Figure (7) as it extends at long wavelengths to the intense sodium D-line. From the short-wavelength (3465Å) limit of the continuous NaOH chemiluminescent spectrum, we find a new and somewhat higher bound for the Na-OH bond dissociation energy than that suggested in the literature.[18] This value is now 82.5 kcal/mole (3465A = 28852 cm^{-1}/349.76 cm^{-1}/kcal = 82.5 kcal/mole) in good agreement with recent studies of the onset of NaOH photodissociation (82.6 kcal/mole estimated).[19] This new value should be compared with the suggested value reported in the JANAF tables, D_o(Na-OH) = 81.5 $\pm$ 3 kcal/mole. It is apparent that the current value is somewhat higher but within the bounds recommended by JANAF.

Estimation of KOH Stretching Frequency

From the short wavelength peak separations in Figure 6, it is possible to obtain an estimate of the K-OH stretch ground state vibrational frequency; we find $\omega_o \approx 412 \pm 18$ cm^{-1}. This value compares favorably with the results of Belyaeva et al. (Table 1) and the infrared study of Spinar and Margrave[20] who observed a gas phase absorption band in the vapor above KOH, determining a frequency of 408 $\pm$ 10 cm^{-1} and assigning this feature to the K-OH stretching mode.

Experimental

In contrast to all previous metal oxidation environments encountered in

our laboratory, we have found that it is substantially more difficult to formulate and maintain stable and intense alkali hydroxide or oxide chemiluminescent sources. In the case of the alkali hydroxides, efforts were hampered by the experimental difficulties entailed in handling 90+% hydrogen peroxide and the nature of extensive particulate formation in the reaction zone.

The device used to obtain the single collision spectrum depicted in Figure 5 is outlined schematically in Figure 8. It consists of a lower oven chamber and upper directing channel placed in a water cooled chamber, this combination located in a much larger vacuum chamber. The lower chamber was filled with potassium (Fisher Scientific > 99%) to two-thirds its capacity and heated to temperatures between 500 and 650 K using a concentrically wrapped thermocoax heating element (Amperex). During the heating process, which must be carried out slowly to avoid severe bumping, the potassium outgasses several contaminants including hydrogen.[21] The upper directing channel may be heated independently and, in most cases, was maintained at approximately 600 K to avoid, as well as possible, oven blockage. Potassium vapor was interacted with 90+% hydrogen peroxide which could be brought into the vacuum chamber via a concentric device, best described as a ring injector (RI), placed directly above the exit orifice of the potassium oven system. Alternately, the H_2O_2 was introduced from a weakly collimated nozzle source, perpendicular to the potassium flow, in close proximity and directly above the exit orifice of the potassium oven system. Both of these configurations proved useful in generating a single collision KOH emission spectrum, however, in many

instances, flame stability was not optimal. Much of this problem stems from the difficulties inherent in handling 90+% H_2O_2* and its flow into the reaction zone. A second and more serious problem results from the efficient formation of particulate matter in the vicinity of 1) the H_2O_2 nozzle or inlet orifice and 2) the exit orifice of the potassium oven. Both of these problems were difficult to suppress and, in general, lead to short run times. The system was operated at oven temperatures corresponding to a potassium vapor pressure between 1 and 1.5 torr. The potassium metal which exited the directing channel orifice intersected a tenuous although localized atmosphere of H_2O_2 at pressures between 1×10^{-4} and 1×10^{-3} torr.

The major experimental device which has been used thusfar to generate the KOH emission spectrum under diffusion flame conditions is shown in Figure 9. The nipple of the diffusion flame bulb was filled with potassium metal. After the system has been evacuated, the entire bulb is heated to a temperature producing approximately a 1 torr vapor pressure of potassium which can be maintained while exposing the system to vacuum. Attached to the viewing port is a self-cleaning window over which argon flows constantly to prevent potassium or potassium hydroxide condensation.[22] To obtain the spectrum depicted in Figure 6, 90+% hydrogen peroxide was introduced via the oxidant nozzle which passes through the potassium containing nipple and a flame was created in the region F. The operation of this device requires that the hydrogen peroxide not be heated to temperatures in excess of 320 K. If one attempts to increase the H_2O_2 vapor pressure and hence the oxidant flow rate by operating at temperatures in excess of 320 K, the hydrogen peroxide begins

---

*A helpful manual can be obtained from FMC corporation, 5950 Fairview Rd., 2 Fairway Plaza, Suite 712, Charlotte, N.C. 28210.

to decompose and severe pressure fluctuations are encountered followed by the quenching of KOH fluorescence and the apparent formation of what appears to be another strongly emitting species whose spectrum is shifted considerably to the red of that for KOH.[a] The gas handling system was constructed completely of stainless steel in order to avoid decomposition due to reaction with containment materials. Nevertheless, under multiple collision diffusion flame conditions, modest hydroxide decomposition is the source of a quenched KOH* emission spectrum and a dominating red shifted emission system.

The spectrum depicted in Figure 6 was obtained when the diffusion flame bulb was run at temperatures sufficient to generate two torr of potassium vapor and at the highest possible H_2O_2 flows as regulated by a needle valve. When the system was pushed to its limit in this manner, the experiment was of short duration since 1) the entrance nozzle could be rapidly blocked due to hydroxide or polymer formation at the nozzle entrance and 2) the available potassium, in many instances, was trapped on the walls of the diffusion flame bulb through the formation of an inner oxidized coating. Further, significant blockage of the port to vacuum was found to result in substantial peroxide wall decomposition and reaction causing flame quenching, as well as a severe overheating of the diffusion flame bulb.

At H_2O_2 temperatures substantially lower than 320 K, the vapor pressure of H_2O_2 was, in general, not sufficient to produce a KOH emission spectrum of the required intensity, given reasonable long term bulb operating temperatures. Hence additional methods to increase the H_2O_2 flux into the reaction were devised. The hydrogen peroxide was entrained in argon so as to

---

a. This emitter may be KO_2, however, no definitive information is yet available.

increase the relative flux of H_2O_2 into the diffusion flame bulb. This procedure was also instituted to alleviate problems with the blockage of the oxidant nozzle exit port in the direct vicinity of the flame region.[23]

Several entrainment configurations were tested in order to develop a stable, readily controllable flow, maintaining a virtually constant H_2O_2 concentration. The modifications produced a considerable increase in the potassium oxidized during reaction, leading to the substantial deposition of oxidized material. In combination with the strong flow patterns created by the entrained hydrogen peroxide (argon), the formation of condensible material often lead to a complete blockage in the exit port of the diffusion flame device, limiting run times. In order to alleviate this problem and allow extended run times and exposures, a catcher plate was incorporated into the diffusion flame bulb. As a given run progressed, a stalactite of what appears to be a potassium hydroxide oxidation product was formed on the catcher plate. This formation was found to have little effect on the KOH flame for extended periods. During this time, a stalagmite of what also appears to be a material similar to that deposited on the catcher plate fanned out and grew from the oxidant nozzle entrance port. The rate of growth of this stalagmite determined the duration of an intense, stable, and reasonably longlasting diffusion flame.

In latter diffusion flame studies a further modification was found to virtually eliminate severe particulate formation. The modification involved the transfer of the oxidant inlet tube from an entrance through the bottom of the diffusion flame device to an entrance at the point MI in Figure (9). Hence the oxidant inlet tube no longer passed through the potassium nipple and was oriented at a 45^{o} angle relative to the vertical. This design was tested for the sodium-hydrogen peroxide system. The emission generated from the Na_2

+ H_2O_2 reaction was maintained for an extended period better than doubling all previous run times. The end of the run as signaled by the almost complete oxidation of all sodium in the system. During the course of this run several electrooptical scans were taken of the chemiluminescent flame, a selection of which are indicated in Figure 7.

Spectra were taken with a 1 meter Czerny-Turner scanning spectrometer operated in first order with a Bausch and Lomb 1200 groove/mm grating blazed at 5000A. An RCA 4840 photomultiplier tube cooled to dry ice temperature was used to obtain the spectra which are uncorrected for photomultiplier response. The photomultiplier signal was detected with a Keithley 417 fast picoammeter whose output signal (partially damped) drove a Leeds and Northrup stripchart recorder. All spectra were wavelength calibrated using a low pressure mercury pen or neon lamp.

Varying Degrees of Collisional Relaxation

One of the problems inherent in the argon entrained oxidant devices is that they create a collisional environment in the flame region which is largely dominated by argon. This should be distinguished from an environment dominated by a combination of potassium, argon, and reaction products (Figure 6). In other words, the efficiency of the collisional environment is diluted by a considerably increased although transient argon population localized primarily at the frontal edge of the oxidant nozzle in the flame region. Collisional relaxation is diminished considerably relative to that inherent in the flame conditions producing the KOH spectrum in Figure 6 and a notably less structured KOH spectrum (Figure 10) is obtained. The NaOH spectrum depicted in Figure 7 was obtained using argon entrainment and hence it does not display

the structure which might be anticipated in a more efficient relaxation environment.

Discussion

Nature of KOH Electronic States and Their Relation to Bond Energy Determination

Our efforts to study the alkali hydroxides NaOH and KOH have led to the first direct observation of electronic emission spectra for these species, furnishing what is potentially a much easier means of following their behavior in the gas phase. Prior to this effort, a major component of the thermodynamic characterization of these metal hydroxides had been through indirect flame studies.[24] That is, the presence of the hydroxide has been inferred from the study of metal atom depletion. A second law analysis of this metal atom depletion has been used to deduce bond energies for primarily the alkali and alkaline earth hydroxides. Very few of the alkali and alkaline earth hydroxides have been characterized mass spectrometrically. Studies of the Group IIA hydroxides are precluded for all but the barium compounds[25] because of a very high propensity for disproportionation to the oxides and resulting loss of water. Difficulties encountered in studying the alkali hydroxides stem from their high propensity to form dimeric species on vaporization and reaction with container materials. The bond energies determined for KOH via flame and mass spectrometric studies are in reasonable agreement, yet there are several notable discrepancies in the data base. Thus, it is important that the hydroxides be characterized by another means as we have done in the present study.

The nearly repulsive nature of alkali halide excited state potential curves (Figure 2) results in large part from a playoff with the almost purely ionic ground state of the alkali halide. By virtue of the purely ionic character of the ground

state, these excited states are almost purely covalent. A decrease in the ionic character of the ground state and a subsequent increase in the ionic character of these repulsive states should result in an increased excited state stability. Although the ground electronic states of both the alkali halides and the hydroxides are possessed of rather large dipole moments (μ(KCl) = 10.269D,[26] μ(KOH) $\tilde{=}$ 8.46D[27]), the ionic character of the halides may be said to slightly exceed that of the hydroxides. If the hydroxide ground states are slightly less ionic, their excited states may possess a slightly greater ionic component. We anticipate that the excited state potential(s) corresponding to the K-OH stretch may be slightly more bound than the corresponding alkali halide state(s).

The K-OH bond energy determined in the current diffusion flame studies represents a lower bound. More refined studies may yield a slightly higher value but very little increase is anticipated. In the present study, the probable dissociation products of the KOH ground and excited states are limited. The ground electronic state is ionic, however, in direct analogy to the alkali halides (Fig. 2), we anticipate an ionic-covalent curve crossing and subsequent dissociation to ground state potassium atom and hydroxide radical. A similar analogy leads us to conclude that the KOH excited state from which we observe emission must dissociate to K (^2S) + OH($X^2\pi$). Dissociation to excited electronic states or to the ionic products $K^+ + OH^-$ is quite unlikely. The lowest lying combination of neutral species lies some 13000 cm^{-1} (K $^2P_{3/2,1/2}$)[28] above the asymptote for dissociation to ground state products whereas the ionic products, $K^+ + OH^-$ (see also Figs. 2 and 4) lie $\sim$ 19,900 cm^{-1} (4.339[28] - 1.87eV[27]) above this asymptote. If dissociation to these states occurs, the changing character of the KOH emission spectrum as a function of pressure would not be manifest; that is, the effect of changing

rotational excitation would not be clearly apparent.

If we further consider the probable dissociation products for the ground and excited states of KOH (Figure 4), it is apparent that the upper excited state potential may be bound with respect to the dissociation asymptote of the KOH ground electronic state. The much smaller change in the diffusion flame vs. single collision spectrum for KOH versus the observed changes for KCl, in correlation with our previous discussions (see also Fig. 2), indicates that this is a distinct possibility. We anticipate that the emitting excited state of KOH may be bound by as much as 5 kcal/mole relative to the dissociation asymptote of the ground state.

Although the data we have obtained in the present study in correlation with previous studies of the alkali halides indicates that we have observed emission from a weakly bound predominantly covalent excited state or states, several questions remain unanswered about the precise nature of these states in both the alkali halides and hydroxides. There is both a $^1\Sigma^+$ and $^1\Pi$ state arising from the combination $M(^2S) - X^2P_{3/2}$ (X = Cl,Br,I) and the combination $M(^2S) - X^2P_{1/2}$ for the alkali halides. Similarly, given that we are considering a linear excited state, two $^1\Sigma^+$ and two $^1\Pi$ states can be derived from $M(^2S)$ + OH ($^2\Pi_{3/2,1/2}$). Although it is probable that we have observed emission from a singlet excited state, we do not know the relative locations of the $^1\Sigma$ and $^1\Pi$ states, which of these states are bound, and which, if not a combination of the two, are responsible for the observed spectra. We can only surmise that emission from a very weakly bound halide or hydroxide excited state has been observed.

The stability of the excited state potential relative to $K(^2S)$ + $OH(X^2\Pi)$ is significant. Under diffusion flame conditions, it is likely that all emitting excited state molecules are in the lowest vibrational-rotational

states. If these levels lie below the ground state dissociation asymptote, the shortest wavelength emission which can be observed (Figure 4) is energetically smaller than the K-OH bond energy by an increment corresponding to the K-OH excited state binding. Similarly, if the excited and ground state potentials are located such that emission to the $v_1'' = 0$ level (Table I) does not occur, the limit of the diffusion flame spectrum will fall short of the correct bond energy by the increment, ΔE, corresponding to $v_1'' = n$ relative to $v_1'' = 0$. The OH $X^2\Pi$ spin-orbit splitting has been accurately measured by laser magnetic resonance and is only 126.23 cm^{-1}.[30] If we assume that there are no excited state levels below the KOH ground state dissociation asymptote and consider dissociation to OH $^2\Pi_{1/2}$ at 126.23 cm^{-1}, the determined lower bound for the KOH bond energy is 87.8 kcal/mole. All other possible corrections will yield a higher value for the K-OH bond energy. Despite these possibilities, based upon a comparison with our results for NaOH and preliminary studies of the CsOH diffusion flame spectrum, we anticipate that the K-OH bond energy does not exceed 89 kcal/mole.

Our determined lower bound for the K-OH bond energy appears to be somewhat higher than those bounds determined by other workers (Table II) although it is not inconsistent with the upper bound suggested by JANAF.[31] There are several factors which may account for the difference between the lower bound evaluated in the present study and the determinations of other workers. In their recent comprehensive study of KOH vaporization, Hastie et al.[32] have clearly and critically assessed the extremely complicated nature of the KOH system. They have challenged JANAF's critical evaluation of the available KOH vaporization data, demonstrating that their data and the second law enthalpies determined by several previous workers are consistent with a much higher dimer concentration than previously recognized. From the second

law vaporization enthalpy for monomeric KOH, Hastie et al.[32] determine a zero point dissociation energy, D_0^o = 84.1 ± 1 kcal/mole, consistent with the JANAF value of 85.4 ± 2.6 kcal/mole, Farber et al.'s value of 84.2 ± 0.5 kcal/mole,[33] and an empirical value 88.2 ± 5 kcal/mole[34] (0.86 D_0^o (KCl) from the average value of hydroxide to halide bond energies). Hastie et al. note that the agreement with Farber et al. "seems fortuitous" as the latter's partial pressure data are inconsistent with those of Hastie et al. and several previous researchers. Hastie et al. indicate that "a likely explanation for the lower pressures of Farber et al. is reaction with their alumina cell to form stable potassium aluminate" lowering the KOH(ℓ) activity. Hastie et al. reason that the conditions of Farber et al.'s experiments are not commensurate with a saturated KOH vapor. Hence, it is apparent that Farber et al.'s data and evaluations may not be reliable. Although Hastie et al. obtain a bond dissociation energy significantly lower than the lower bound obtained in the present study, it is noteworthy that their calculations of the bond energy assume that ΔH_f for KOH(ℓ) in the JANAF tables is correct. If the liquid phase data is in error, the appropriate modifications could easily bring the determined values for the bond dissociation energy into close agreement. In view of the problems noted by Hastie et al.[32] in their evaluation of the JANAF vapor data, this is not an unlikely possibility.

KOH and NaOH Emission Spectra - Tentative Assignment and Future Considerations

As should be apparent from Figures 5 and 6, both the single collision and diffusion flame KOH emission spectra are characterized by significant structure which we believe is attributable to emission to vibronic levels in

the ground electronic state of potassium hydroxide, more specifically to primarily a progression in the K-OH stretch. We base this conclusion on a direct analogy with the alkali halides. It should be noted, however, that the spectrum may be complicated by additional features due to the K-O-H bend or KO-H stretching frequencies. The ground electronic state of KOH is linear.[27] If the weakly bound excited state from which we observe emission is bent, this may result in a short progression in the ground state bending mode.[35] The ionic nature of the KOH ground state and the probable covalent nature of the excited state from which we observe emission might be deemed a reason to expect at least a short sequence in the OH stretch, however, the very similar vibrational frequencies for OH (ν = 3570 cm^{-1})[36] and OH^- ($\omega_e \approx 3680 \pm 37$ cm^{-1})[29] make this an unlikely possibility. While some considerable spectral complications are expected as one tries to unravel the KOH spectrum, the spectra should be dominated by the K-OH stretch. (Preliminary spectra now obtained for CsOH are characterized by dominant features corresponding to a long progression in the ground state Cs-OH stretch.)

As should be apparent from our previous discussion, we have not yet obtained an NaOH emission spectrum at a resolution comparable to that for KOH. A comparison of Figures 6, 7, and 10 indicates that the sodium analog of the KOH spectrum is virtually a continuum under the conditions for which the NaOH spectrum and the KOH spectrum in Figure 10 have been obtained. It is apparent that several sharp features are superimposed on the continuum. At present, a clear association of these sharp features is not possible and must await further study. Unfortunately, as has been observed in the alkali halides,[13] the NaOH emission system is much weaker and more difficult to control than that for the higher hydroxides KOH-CsOH.

There appears to be a reasonable correlation between several of the

features in the KOH diffusion flame and "single" collision spectra for $\lambda >$ 3900 Å; however, there are some differences which may be attributable to (1) significant rotational relaxation in the multiple collision "diffusion flame" environment versus the high rotational excitation expected under single collision conditions and (2) the onset of rapid energy transfer and hence collisional repopulation of KOH excited state levels from which emission is observed under single collision conditions. As a subset of the latter phenomena, collisional depopulation, should include collision induced dissociation of KOH molecules formed in the very weakly bound excited state from which emission is observed in the present study.

We have obtained an initial overall picture of the KOH and NaOH electronic emission spectra. It will now be appropriate to pursue finer details of these spectra. In addition to a refinement of the K-OH bond energy, higher resolution spectra of the K_2-H_2O_2 diffusion flame should provide very useful information on the vibrational structure of the ground state normal mode "hot" bands. It may be possible to correlate these studies with the millimeter wave results mentioned earlier to provide an extensive mapping of the vibrational structure of the ground electronic state of KOH. At present, we can only obtain an estimate of the ground state vibrational frequency, 412 ± 18 cm^{-1}, from the short wavelength peak separations measured in Figure 6; however, this should be improved with further development of the diffusion flame device.

Acknowledgements: It is a pleasure to acknowledge additional efforts on this project by Mr. Thomas Mays and Mr. David Semmes. Support of this research by the National Science Foundation and the Department of Energy is gratefully acknowledged.

Figure Captions

Figure 1. Chemiluminescent spectrum for KCl taken at a resolution of 5Å. Also present in the trace at long wavelength are small atomic emission features (Na^* etc.). Taken from reference 13. See text for discussion.

Figure 2. Schematic potential energy curves for an alkali halide molecule (drawn for KBr) showing the "zeroth order crossing" of the ionic and covalent states; I(M) = ionization potential of alkali metal, E(X) = electron affinity of halogen atom, r_c = crossing radius for ionic and covalent curves. See text for discussion.

Figure 3. Effective excited state potential curves for KI constructed from the rotationless potential of Kauffman, Kinsey, Palmer, and Tewarson (reference 16) assuming a dissociation asymptote of 27000 cm^{-1} (reference 13). See text for discussion.

Figure 4. Schematic of transition regions involving a weakly bound excited electronic state and a strongly bound ground electronic state showing the manifestation of the effective potential at high (single collision) and low (diffusion flame) rotational quantum number. See text for discussion.

Figure 5. KOH^* emission spectrum from the reaction $K_2 + H_2O_2 \rightarrow KOH^* + KOH$ taken under single collision conditions. Spectral resolution is 20Å. See text for discussion.

Figure 6. KOH^* emission spectrum taken under multiple collision conditions in a diffusion flame device. The spectrum results predominantly from the reaction $K_2 + H_2O_2 \rightarrow KOH^* + KOH$ although some contribution also obtains from the process $K + OH + M \rightarrow KOH^* + M$. Spectral resolution is 20Å. See text for discussion.

Figure 7. $NaOH^*$ emission spectra taken under multiple collision conditions in a diffusion flame device. The spectrum, which corresponds to a continuum (see also Figure 10) underlying several sharp spectral features, results predominantly from the reaction $Na_2 + H_2O_2 + Ar \rightarrow NaOH^* + NaOH + Ar$ although some contribution also obtains from the process $Na + OH + M \rightarrow NaOH^* + M$. Spectral resolution is 20Å. See text for discussion.

Figure 8. Schematic of oven system used in recording the single collision KOH^* emission spectrum. SSO = stainless steel (304) oven; TCH = thermo-coax heating element; DC = heated directing channel; OCS = surrounding chamber and oven cooling system; RI = ring injector. See text for discussion.

Figure 9. Schematic of diffusion flame reaction bulb. W = viewing port and self cleaning window; G = thermocouple gauge; F = flame region; HE = potassium (K) heating element; HM = heating mantle (2-front and back); I = typical nozzle inlet for 90+% H_2O_2; MI = modified gas inlet; P = catcher plate; C = cooling water surrounding exit port to vacuum system. See text for discussion.

Figure 10. KOH^* emission spectrum taken under multiple collision conditions in a diffusion flame device. The spectrum results predominantly from the reaction $K_2 + H_2O_2 + Ar \rightarrow KOH^* + KOH + Ar$ although some contribution also results from the process $K + OH + M \rightarrow KOH^* + M$. Spectral resolution is 20Å. See text for discussion.

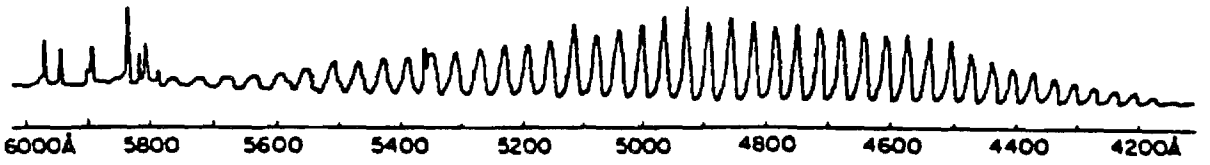

Figure 1

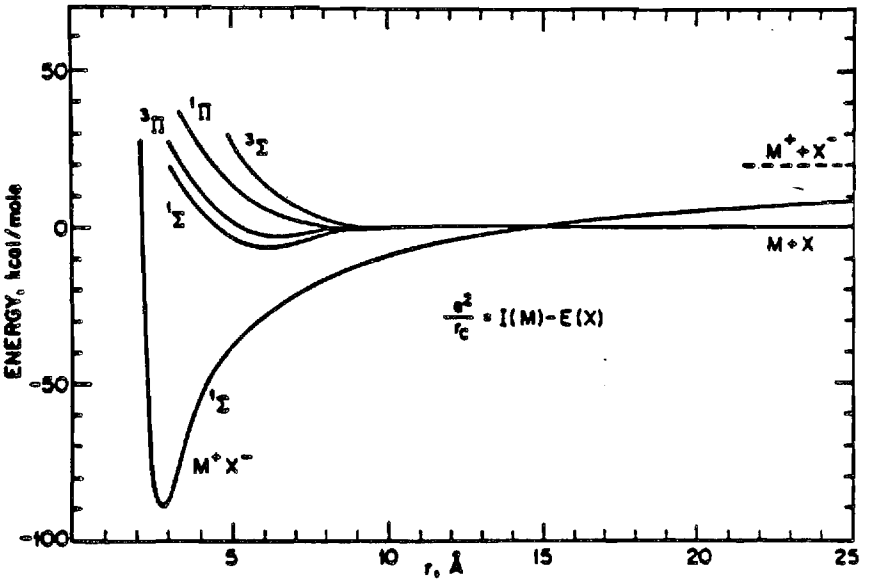
50
0
-50
-100
ENERGY, kcal/mole
5
10
15
20
25
r, Å
$^3\Pi$
$^1\Pi$
$^3\Sigma$
$^1\Sigma$
$M^+ + X^-$
M + X
$\frac{|e_e|^2}{r_c} = I(M) - E(X)$
$^1\Sigma$
M^+X^-

Figure 2

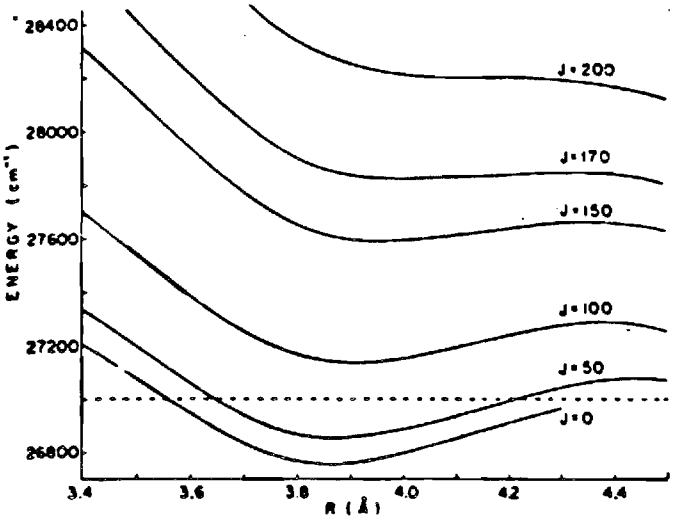
28400
28000
27600
27200
26800
ENERGY (cm⁻¹)
3.4
3.6
3.8
4.0
4.2
4.4
R (Å)
J=200
J=170
J=150
J=100
J=50
J=0

Figure 3

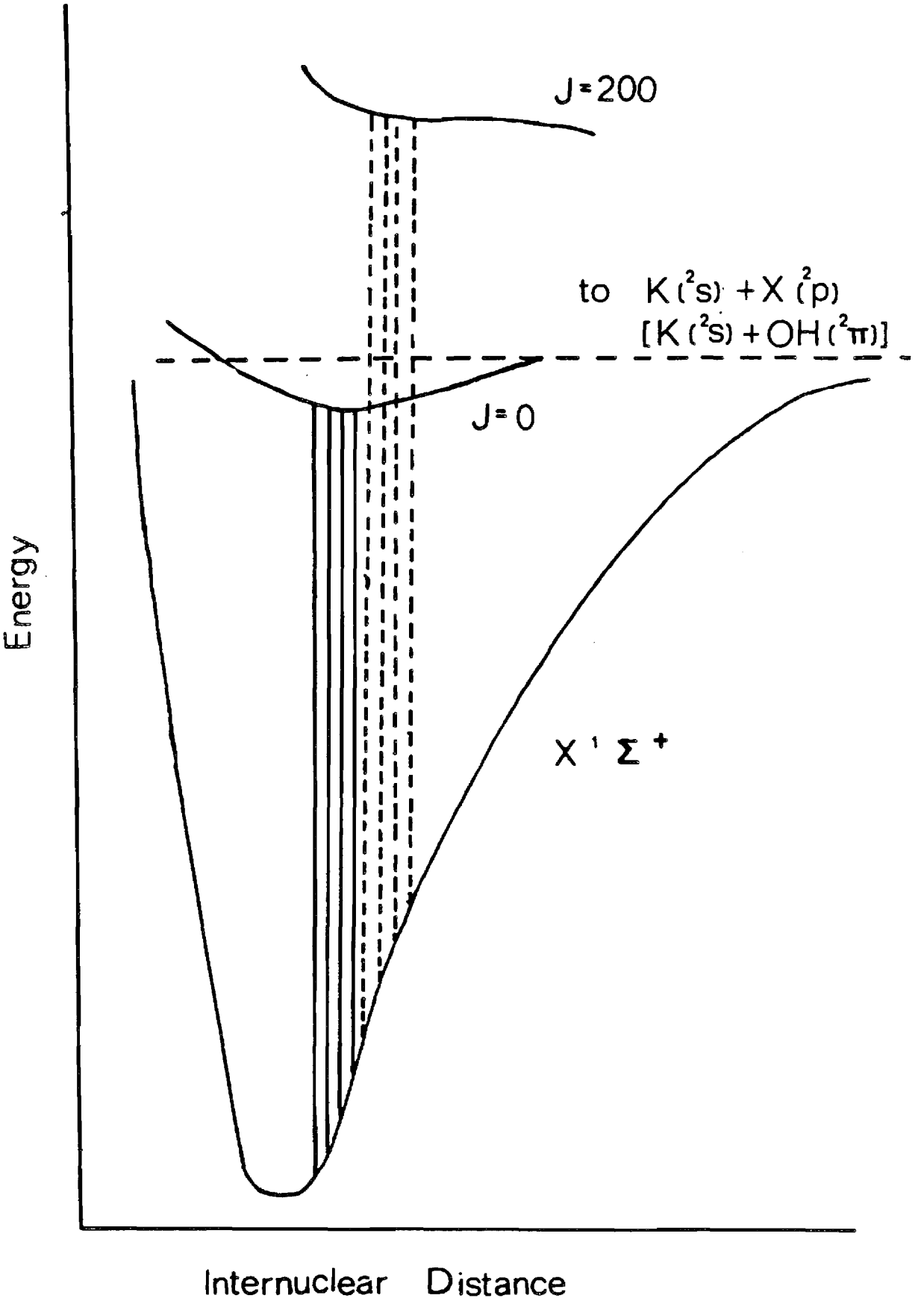
J=200
to K(²S) + X(²P)
[K(²S) + OH(²π)]
J=0
Energy
X ¹Σ⁺
Internuclear Distance

Figure 4

Figure 3

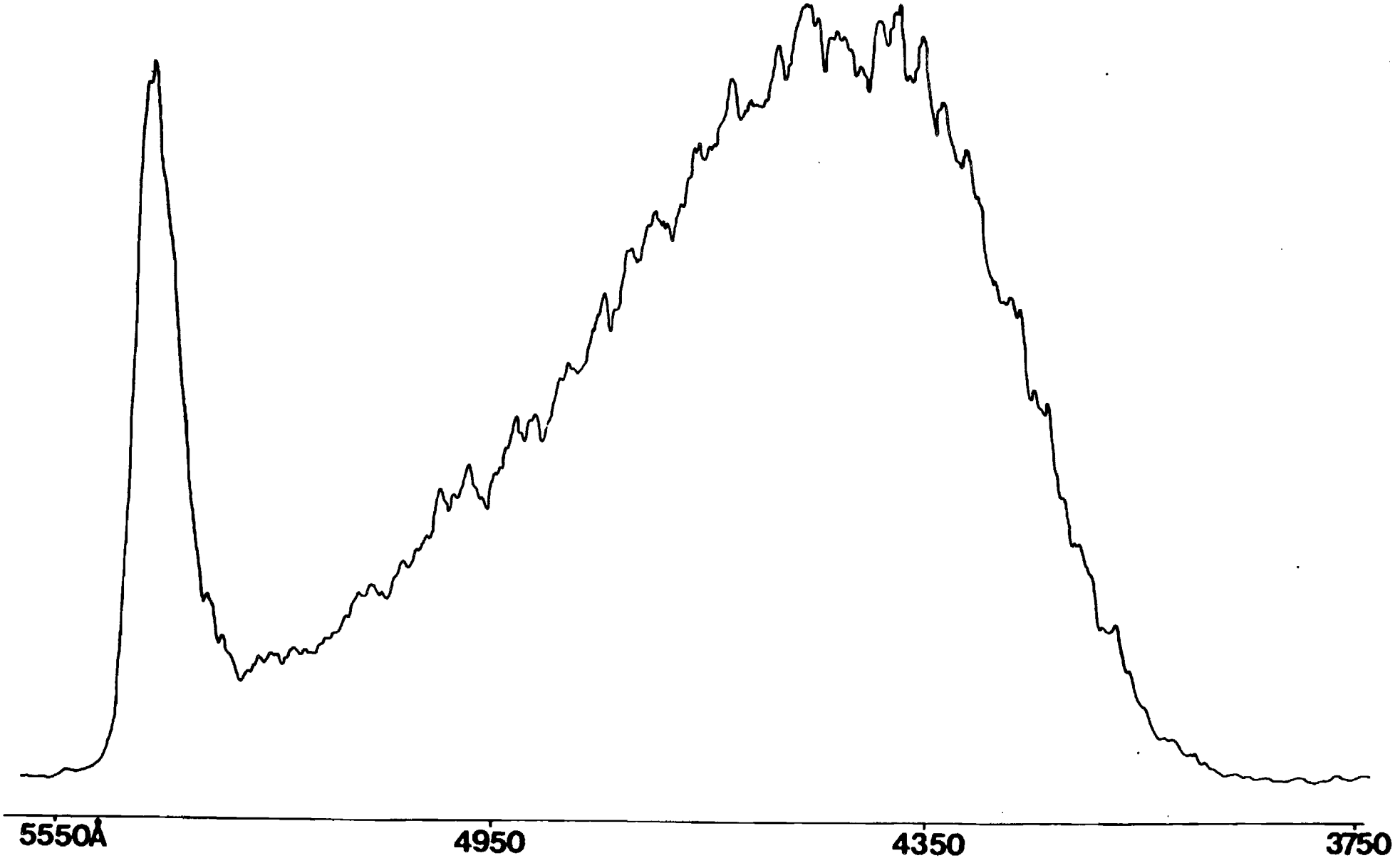

Figure 6

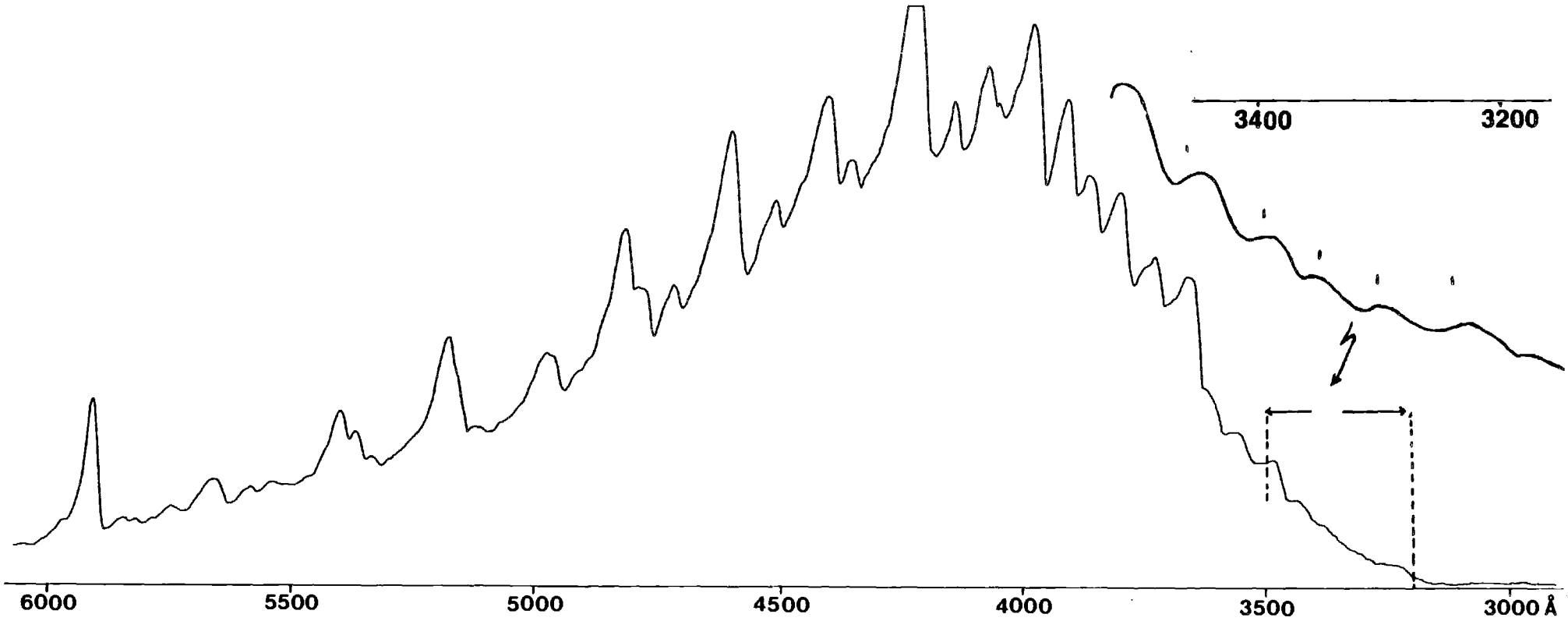


4900
3900
2900
1900

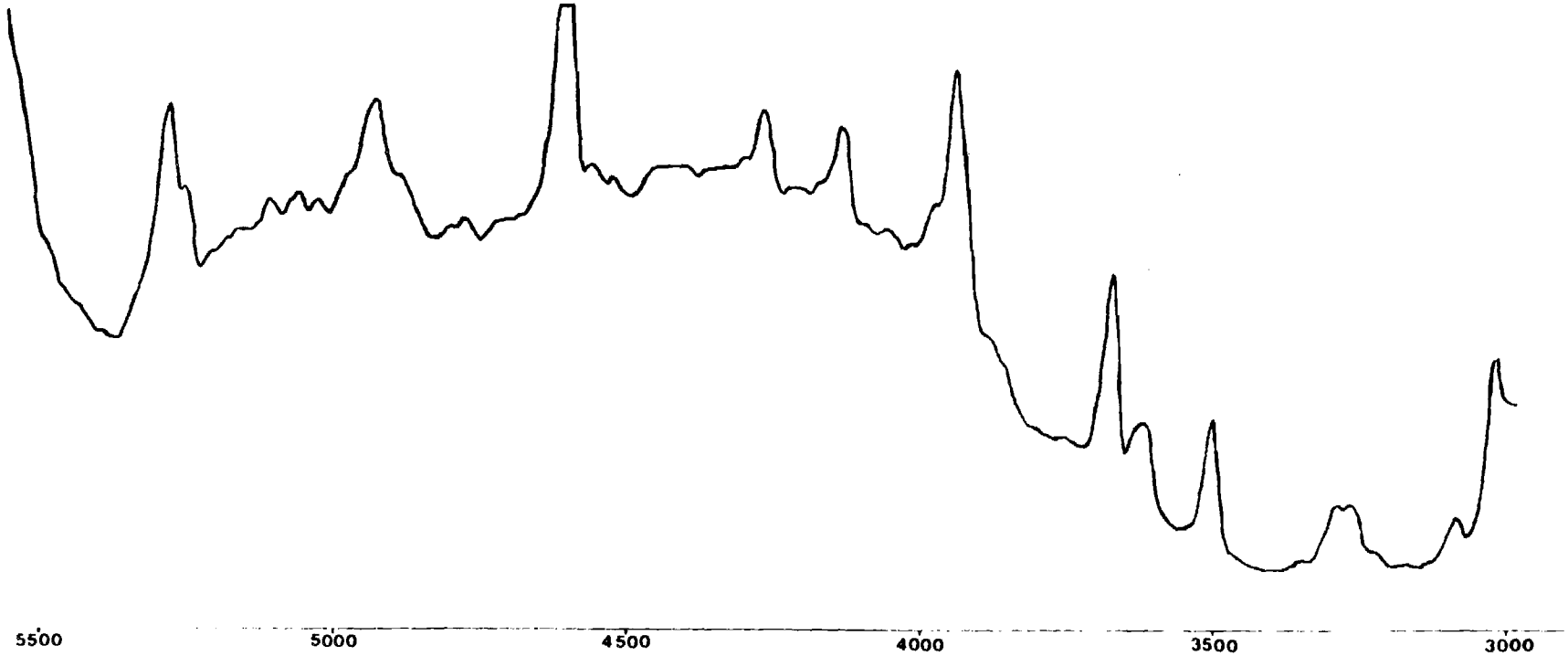
5500
5000
4500
4000
3500
3000

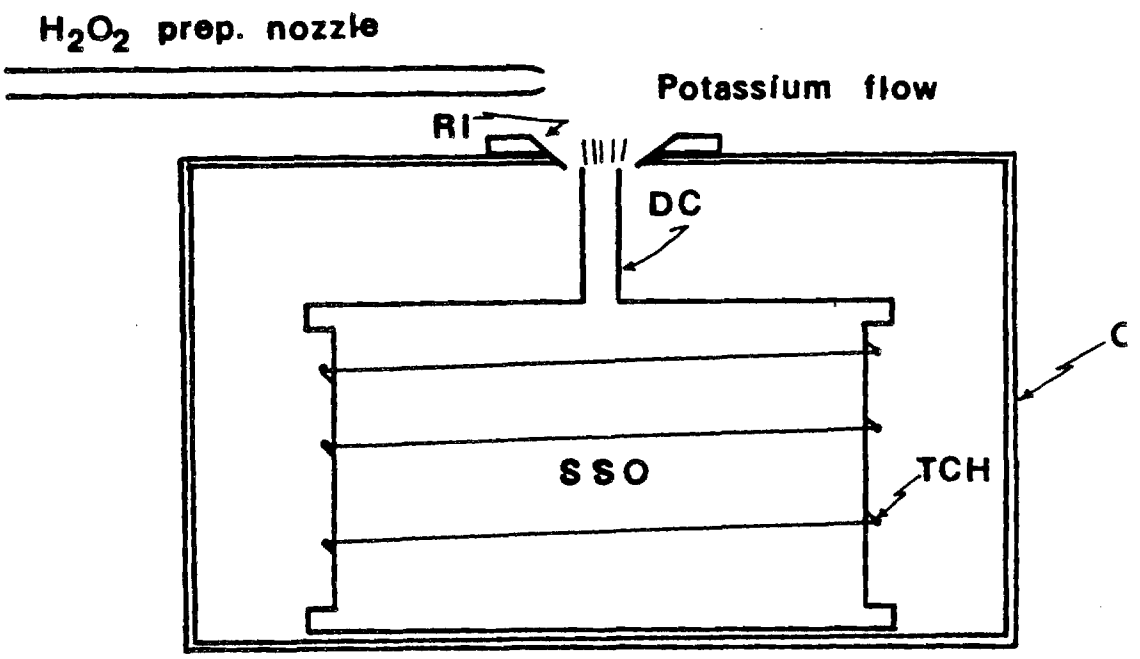

Figure 8

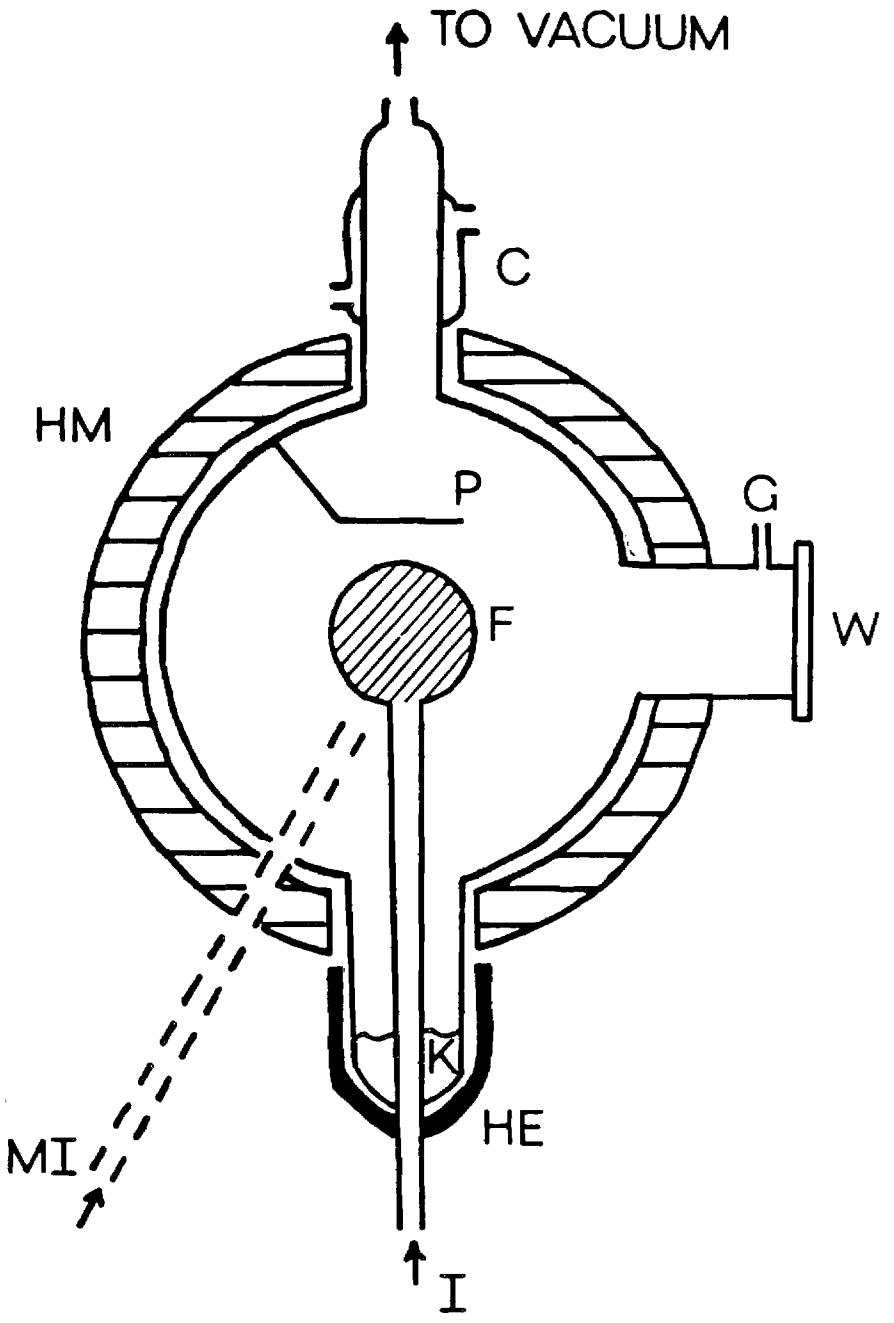

Figure 9

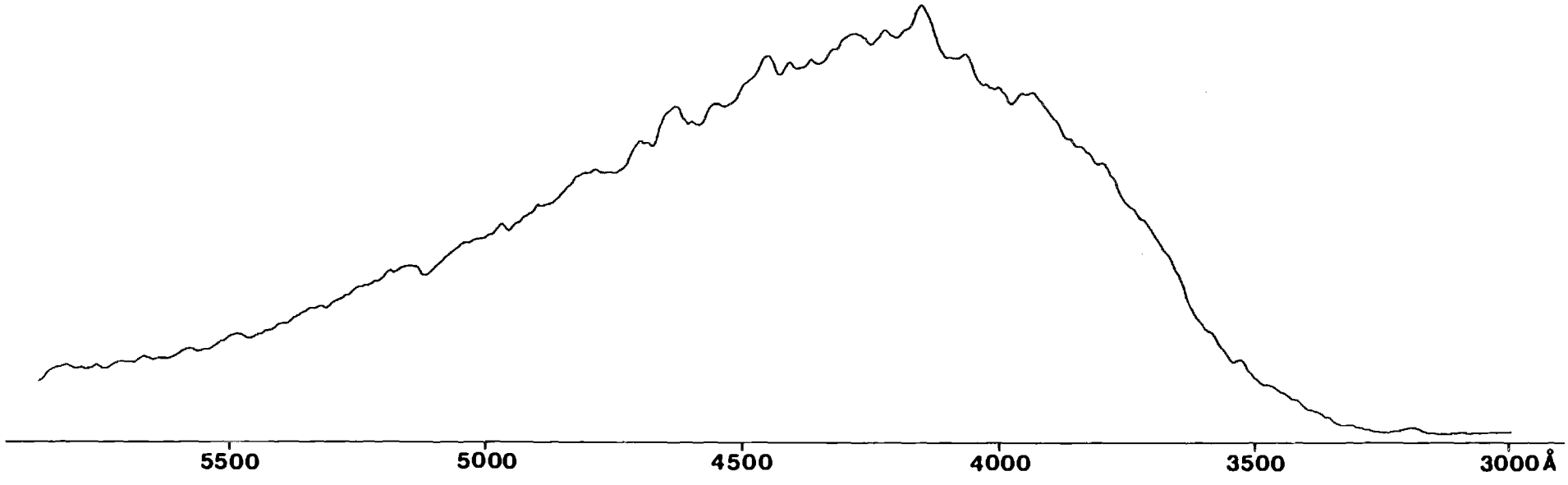

Figure 10

References

1. a) N. Acquista, S. Abramowitz and D. R. Lide, J. Chem. Phys. 49, 780 (1968).

   b) N. Acquista and S. Abramowitz, J. Chem. Phys. 51, 2911 (1969).

2. A. A. Belyaeva, M. I. Fvorkin, and L. D. Sheherba, Opt. and Spectrosc. 31, 210 (1971).

3. The damping of the bending mode frequency shift indicates a significant interaction between the ionic alkali hydroxide and the host material in which it is isolated. One expects this interaction to increase through the series KOH → CsOH as ionic character increases and the dipole-induced dipole interaction increases in magnitude (see for example J. L. Gole and E. F. Hayes, J. Chem. Phys. 55, 5132 (1971)). Indeed a matrix induced blue shift has been observed for a number of molecules (See for example: M. C. Drake and G. M. Rosenblatt in Proceedings of Symp. on Metal Halide Chemistry of the Electrochemical Society (Ed. D. L. Hildenbrand, D. D. Cubicciotti) 78, 234 (1978). Also J. W. Hastie, R. H. Hauge, and J. L. Margrave, Ann. Rev. Phys. Chem. 21, 475 (1970)). The expected decrease in the bending mode frequency for RbOH and CsOH may be counteracted by a stronger matrix interaction and an increased blue shift. There is clearly a need to obtain gas phase infrared spectra in order to assess this behavior.

4. D. R. Lide and R. L. Kuczkowski, J. Chem. Phys. 46, 4768 (1967).

5. C. Matsumura and D. R. Lide, J. Chem. Phys. 50, 71 (1969).

6. E. F. Pearson and M. B. Trueblood, J. Chem. Phys. 58, 826 (1973), Astrophys. Journal 174, L145 (1973).

7. E. F. Pearson, B. P. Winnewisser, and M. B. Trueblood, Z. Naturforsch. 31a, 1259 (1976).

8. P. Kuijpers, T. Torring, and A. Dymanus, Chem. Phys. 15, 457 (1976); Z. Naturforsch. 31a, 1256 (1975).

9. P. Kuijpers, T. Torring, and A. Dymanus, Z. Naturforsch. 32a, 930 (1977).

10. G. W. Stewart, A. Chakrabasti, C. Stinespring, and K. Castleton, Western States Symposium/Combustion Institute, October, 1980.

a) See, for example, J. W. Hastie, "High Temperature Vapors, Science and Technology," Academic Press, New York, 1975.

b) See also "High Temperature, High Pressure Particulate and Alkali Control in Coal Combustion Process Streams," - Proceedings of the U.S. Department of Energy Contractor's Meeting, West Virginia, 1981.

c) J. W. Hastie, E. R. Plante, and D. W. Bonnell, "Alkali Vapor Treatment in Coal Conversion and Combustion Systems," A.C.S. Symposium Series 179 (Editors J. L. Gole and W. C. Stwalley) pg. 543 (1982).

11. a) See for example D. E. Jensen and G. A. Jones, Combustion and Flame 41, 71-85 (1981) and references therein.

b) See for example Y. Yousefian, I. W. May, and J. A. Heimerl, "An Algebraic Criterian for the Prediction of Secondary Muzzle Flash-A Progress Report," Presented at 18th JANAF Combustion Meeting, Pasadena, California.

12. Vibrational frequencies are still estimated for higher vibrational levels. D. E. Jensen, J. Phys. Chem. 74, 207 (1970). Although matrix data is available on the fundamental vibrations, few gas phase measurements have been made and no anharmonicities are known for any of the alkali hydroxides.

13. R. C. Oldenborg, J. L. Gole, and R. N. Zare, J. Chem. Phys. 60, 4032 (1974).

14. Multiple Collision: B. Cardelino and J. L. Gole, unpublished. A.

Tewarson, "Studies of Chemiluminescent Emission in Selected Low-Pressure Diffusion Flames," Ph.D. Thesis, Penn State University, 1969.

15. B. Cardelino and J. L. Gole, unpublished.

16. Taken from Oldenborg et al. reference 13. Based on the study by K. J. Kaufmann, J. L. Kinsey, H. B. Palmer and A. Tewarson, J. Chem. Phys. 60, 4023 (1974).

17. N. J. A. Van Veen, M. S. DeVries, and A. E. DeVries, Chem. Phys. Lett. 64, 213 (1979).

18. JANAF Thermochemical Data, The Dow Chemical Company, Thermal Research Laboratory, Midland, Michigan.

19. F. S. Rowland and Y. Makide, Geophys. Res. Letts. 9, 473 (1982).

20. L. H. Spinar and J. L. Margrave, Spectrochimia Acta 12, 244 (1958).

21. J. L. Gole, G. J. Green, S. A. Pace, and D. R. Preuss, J. Chem. Phys. 76, 2247 (1982).

22. J. L. Gole, Optical Engineering 20, 546 (1981).

23. In some instances, the condensation of H_2O_2 around the outer portions of the nozzle lead to severe difficulties and short term intermitent blockage.

24. See references in Table II and references 18 and 22.

25. F. E. Stafford and J. Berkowitz, J. Chem. Phys. 40, 2963 (1964).

26. R. van Wachem and A. Dynamus, J. Chem. Phys. 46, 3749 (1967).

27. R. van Wachem and A. Dynamus, J. Chem. Phys. 46, 3749 (1967). A. J. Herbert, F. J. Lovas, C. A. Melendres, C. D. Hollowell, T. L. Story, Jr., and K. Strect, Jr., J. Chem. Phys. 48, 2824 (1968).

28. C. E. Moore, Atomic Energy Levels, National Bureau of Standards Circular 467.

29. P. A. Schultz, R. D. Mead, P. L. Jones, and W. C. Lineberger, J. Chem.

Phys. 77, 1153 (1982).

30. K. Evenson, W. Wells, and R. Radford, PRL, 25, 199 (1970).

31. JANAF Thermochemical Tables, Chase, M., Curnett, J. L., Hu, A. T., Prophet, H., Syverud, A. N., and Walker, L. C., 1974 Supplement, J. Phys. Chem. Ref. Data 3(2) (1974).

32. J. W. Hastie, K. F. Zmbov, and D. W. Bonnell, "Transpiration Mass Spectrometric Analysis of Liquid KCl and KOH Vaporization," High Temp. Sci., in press.

33. M. Farber, R. D. Srivastava, and J. W. Moyer, J. Chem. Thermodynamics 14, 1103 (1982).

34. J. W. Hastie, High Temperature Vapors: Science and Technology, Academic Press, New York (1975).

35. See for example discussions in "An Analysis of the Hydraxine-Fluorine Flame. The $A^2A' - X^2A''$ Emission Spectrum of HNF and Its Relation to Other HAB Compounds," D. M. Lindsay, J. L. Gole, and J. R. Lombardi, Chem. Phys. 37, 333 (1979).

36. A. G. Gaydon, Dissociation Energies and Spectra of Diatomic Molecules, London, Chapman and Hall Ltd., 1968. K. Huber and G. Herzberg, Constants of Diatomic Molecules, Van Nostrand-Reinhold, 1979.

APPENDIX B

OBSERVATION OF ALKALI OXIDE ELECTRONIC EMISSION SPECTRA: ANALYSIS OF THE NaO "6700 Å" BAND SYSTEM

Joerg Pfeifer and James L. Gole

High Temperature Laboratory, Center for Atomic and Molecular Science, and School of Physics
Georgia Institute of Technology
Atlanta, Georgia 30332

The alkali elements, their oxides and hydroxides are commonly found in many h temperature systems, their influence often being critical in determining per operating conditions! The sodium oxides are believed to play an important e in ionispheric sodium chemistry.[2] Unfortunately, spectroscopic data on se molecules which might well be used to probe the kinetics of their formation interaction is extremely sparse, especially for the alkali oxides. Some gas se rotational transitions have been determined and analyzed for LiO; matrix lation infrated spectra[4] have been obtained for LiO, KO, and CsO while ESR nsitions[5] have been observed for RbO and CsO and the alkali dioxides NaO_2 - $_2$.[6] Thus far, no infrared data has been obtained for NaO and RbO and no ctronic transitions have been reported for any of the alkali monoxides.[7] Elec-nic spectra, once obtained, offer not only the opportunity to understand various damental aspects of molecular electronic structure but also the potential to itor the species of interest in a spectral region where detection sensitivity siderably exceeds that at longer wavelengths.

This report outlines the initial phases of a research effort which has led to first observation of alkali monoxide and monohydroxide electronic emission ctra. Our initial studies have focused primarily on the NaO and KO emission tems because (1) the analysis of these band systems may lead to ready ection of the oxides using modern laser techniques[8] and (2) these ecules provide a test for detailed theoretical calculations.[9] Here, focus on the "6700Å" band system of NaO.

Several experimental devices, which will be described in more detail in a future ort,[10] have been used to excite and observe alkali oxide electronic emission. efly, for sodium oxide, we have focused on the chemiluminescent emission from the cesses.

$$\begin{aligned} Na + N_2O &\rightarrow NaO^* + N_2 \\ &\\ + O_3 &\rightarrow NaO^* + O_2 \end{aligned} \qquad (1)$$

and

$$\begin{aligned} Na + N_2O + X &\rightarrow NaO^* + N_2 + X \\ &\\ + O_3 + Y &\rightarrow NaO^* + O_2 + Y \end{aligned} \qquad (2)$$

where Eq. (1)[11] denotes single collision processes [12] studied in a beam-gas arrangement[11] and Eq. (2) indicates the extension of these studies to the multiple collision pressure regime[13] (X = N_2O, Ar, CO, and N_2[14]; Y = O_3 + He mixture[15]) in order to relax the internal excitation characteristic of the single collision electronic spectrum.

Figure 1 presents a selection of NaO chemiluminescent emission spectra obtained under varied experimental conditions. Although substantial internal excitation hampers the precise evaluation of band locations, a minimum of ten features associated primarily with a progression in the NaO ground state vibrational level spacing are discernable. The features are catalogued in Table 1.

The spectrum resulting from the songle collision Na-N_2O reaction is first order in both the Na and N_2O concentrations. Initial temperature dependence studies[17] indicate that the Na-N_2O reaction is characterized by a substantial activation energy ($\geq$ 15 Kcal/mole) whereas the Na-O_3 metathesis proceeds more rapidly, having a much smaller barrier to product formation. Under multiple collision conditions, for a given sodium flux, a maximized NaO emission spectrum was obtained over a very narrow range of oxidant and carrier gas pressure. The multiple collision studies were further complicated by the presence of collisionally excited sodium dimer ($NaO^+ + Na_2 \rightarrow Na_2^* + NaO. \ . \ .$), the oscillator strength of whose transitions in overlapping spectral regions considerably exceeds that for the NaO band systems. This problem was alleviated with a double oven system whereby the dimers vaporized from a first oven were thermally

sociated before carrier gas entrainment.[18] We believe that the stringent ance of energy transfer and quenching required to obtain the alkali oxide ssion spectrum accounts, in large part, for the inability of previous kers to observe the spectrum.

The data in Table 1 can be correlated with recent extensive quartrum chemical culations by Allison et al.[9] These authors determining that the separation ween the ionic $X^2\Pi$ and very low-lying $A^2\Sigma^+$ states is ~ 2177 cm^{-1} estimating a ound state vibrational frequency, ω_e = 464 cm^{-1} ($(A^2\Sigma^+)$ ≈ 493 cm^{-1}). Based on results of their calculations on NaCl, LiO, KO, and CsO, where comparison with eriment can be made, the calculated frequency is expected to be 20-35 cm^{-1} ver than the experimental value.

The observed spectra might be correlated with transitions among higher vibra- onal levels of the $A^2\Sigma^+$ state and the lowest vibrational levels of the $X^2\Pi$ state; wever, approximate Franck-Condon factors determined on the basis of the cal- lations of Allison et al.[9] make this an extremely unlikely possibility. Con- stent with the data is an interpretation which involves emission from a low-lying edominantly "covalent" state whose equilibrium internuclear distance considerably ceeds that of the $X^2\Pi$ and $A^2\Sigma^+$ states and which is bound by 6000 to 7000 cm^{-1} th respect to ground state sodium and oxygen atoms. The frequency separations ich characterize the shorter wavelength bands catalogued in Table 1 (520 ± 20 cm^{-1}) e to be associated with a progession in the lowest vibrational levels of the $X^2\Pi$ tate although it is not clear that the 6740Å features should be associated with " =0, $X^2\Pi$.[19] The dominant spectral features are consistent with emission from a ingle vibrational level of the upper state to several lower state vibrational levels.

At longer wavelengths (λ = 8200Å), the spectrum soon becomes more complicated nd additional features soon become apparent (alphabetic labels). While these

additional features might be associated with excited state vibrational excitation ($\omega_e' \approx 265$ cm^{-1})[20], this assignment is inconsistent with observed spectral features, relative spectral intensities and all possible reasonable Franck-Condon distributions. The additional features are tentatively associated with emission to the very low-lying $A^2\Sigma^+$ state (ω_e~500 cm^{-1}), this assignment being consistent with the calculated T_{oo} for the NaO $A^2\Sigma^+ - X^2\Pi$ transition.

In summary, we believe that we have observed emission from a relatively weakly bound predominantly "covalent" state of sodium oxide located ~ 15000 cm^{-1} above the ionic ground $x^2\Pi$ state. This state lies at considerably larger internuclear distance (~0.2Å) than the $X^2\Pi$ or very low-lying $A^2\Sigma^+$ states and it is believed that the observed emission involves primarily transitions to the outer turning points of the vibrational quantum levels associated with these two states.

We have outlined the results of initial efforts in our continuing study of alkali oxide electronic emission spectra. In addition, we have obtained preliminary data for LiO, KO, and RbO. We also anticipate that future detailed temperature dependent studies of both the $M+N_2O$ and $M+O_3$ metatheses analogous to Eq (1) will lead to an independent determination of alkali oxide bond energies.

Acknowledgement: It is a pleasure to acknowledge the assistance of Mr. David Semmes and most stimulating discussions with Professor Derek Lindsay.

erences

See for example J. L. Gole, Optical Engineering 20, 546 (1981); D.E. Jensen and G. A. Jones, Comb. and Flame 41, 71-85 (1981); Y. Yousefian, I. W. May, and J. A. Heimerl, "An Algebraic Criterion for the Prediction of Secondary Muzzle Flash - A Progress Report" Presented at the 18th JANAF Combustion Meeting, Pasadena, California, 1982; S. A. Medin, V. A. Ovcharenko, and E. E. Shpil'rain, High Temp. U.S.S.R. 10, 390 (1972).

See for example C. E. Kolb and J. B. Elgin, Nature, 263, 488 (1976) also E. Murad private communication.

S. M. Freund, E. Herbst, R. P. Mariella Jr., and W. Klemperer, J. Chem. Phys. 56, 1467 (1972).

a. R. C. Spiker, Jr. and Lester Andrews, J. Chem. Phys. 58, 702 (1973).
b. D. White, K. S. Seshardri, D. F. Dever, D. E. Mann and M. J. Linevsky, J. Chem. Phys. 39, 2463 (1963).
c. K. S. Seshardri, D. White and D. E. Mann, J. Chem. Phys. 45, 4697 (1966).
d. R. C. Spiker and L. Andrews, J. Chem. Phys. 58, 713 (1973).

D. M. Lindsay, D. R. Herschbach, and A. L. Kwiram, Mol. Phys. 32, 1199 (1976), D. M. Lindsay and D. R. Herschbach, J. Chem. Phys. 60, 315 (1973).

D. M. Lindsay, D. R. Herschbach, and A. L. Kwiram, Chem. Phys. Lett. 25, 175 (1974).

H. Figger, W. Schrepp, and Xu-hui Zhu, J. Chem. Phys. 79, 1320 (1983).

C. Kolb, Aerodyne Research Incorporated, private communication.

J. N. Allison, R. J. Cave, and W. A. Goddard III, J. Chem. Phys. 77, 4259 (1982) also "The Alkali Oxides. Analysis of Bonding and Explanation of the Reversal in Ordering of the $^2\Pi$ and $^2\Sigma^+$ States" - preprint.

J. Pfeifer, D. Semmes, and J. L. Gole, to be published.

See for example
C. L. Chalek and J. L. Gole, J. Chem. Phys. 65, 2845 (1976);
J. L. Gole and S. A. Pace, J. Phys. Chem. 85, 2651 (1981);
J. L. Gole, Ann. Rev. Phys. Chem. 27, 525 (1976).

12. $P_{Total} \leq 5 \times 10^{-5}$ torr, Na flux ranging to a maximum of $10^{18}/cm^2$-pac.

13. See for example
D. M. Lindsay and J. L. Gole, J. Chem. Phys. 66, 3886 (1977);
M. J. Sayers and J. L. Gole, J. Chem. Phys. 67, 5442 (1977);
J. L. Gole and S. A. Pace, J. Chem. Phys. 73, 836 (1980).

14. A stream of sodium atoms crossed by an uncollimated oxidant flow under multiple collision conditions ($P_{N_2O} \approx 50\mu$) or a mixture formed when sodium was entrained in argon ($P_{Ar} \approx 850 - 1200\mu$), N_2 ($P_{N_2} \approx 950 - 1500\mu$), or CO ($P_{CO} \approx 650 - 850\mu$) was oxidized by a concentric flow of N_2O ($P_{N_2O} \approx 50 - 95\mu$) forming a flame adjusted to obtain the maximum alkali oxide emission.

15. Uncollimated flow as in ref. 14 ($P_{O_3} \approx 5 - 10\mu$, $P_{He} \approx 20 - 80\mu$).

16. This spectrum was obtained using 99.5% purity sodium. A similar spectrum with a slightly diminished K D-line was obtained using 99.99% sodium.

17. D. R. Preuss and J. L. Gole, J. Chem. Phys. 66, 2994 (1977); J. L. Gole and D. R. Preuss, J. Chem. Phys. 66, 3000 (1977); L. H. Dubois and J. L. Gole, J. Chem. Phys. 66 779 (1977).

18. The Na D-line emission which results from primarily V-E transfer also represents a problem especially in the CO entrainment experiments where the process $NaCO + NaO\dagger \rightarrow Na^* + CO + NaO\dagger'$ can dominate the process $NaO^* + CO \rightarrow NaO^* + CO$ corresponding to internal deexcitation of the NaO^*.

19. Based on energy conservation (R. R. Herm and D. R. Herschbach, J. Chem Phys. 52, 5783 (1970), D. L. Hildenbrand, and E. Murad, J. Chem. Phys. 53, 3403 (1970) it is highly unlikely that the 6740A band is associated with v">2.

20. An estimated vibrational frequency obtained using a combination of Badger's rule and a Morse Potential fit is ~283 $cm.^{-1}$

Table 1

Observed Bands for NaO* B-$X^2\Pi$

ıd No.	λ(Å)	ν(cm^{-1} vacuum)	Δν(cm^{-1})
	6740	14833 ± 20	
	6980	14323 ± 20	510 ± 20
	7235	13818 ± 20	505 ± 20
	7495	13339 ± 20	479 ± 20
	7770	12866 ± 20	473 ± 20
	8060	12404 ± 20	462 ± 20
	8370[a]	11944 ± 20	460 ± 20
	8570[b]	11665 ± 20	279 ± 20
	8710[a]	11478 ± 20	187 ± 20
	8960[b]	11158 ± 20	320 ± 20
9)	9078	(11016 ± 20)	
:)	9380	(10658 ± 20)	
10)	9460	(10568 ± 20)	
0)	9830	(10170 ± 20)	

. Δν (7-8) = 466 cm^{-1} b. Δν (A-B) = 507 cm^{-1}

Figure Caption:

NaO* Chemiluminescent Emission Spectra for the processes (a) Na + N_2O ($P_{N_2O} \simeq 75\mu$) + N_2 ($P_{N_2} \sim 950\mu$) → NaO* + N_2 > (b) Na + N_2O ($P_{N_2O} \simeq 100\mu$) + N_2 ($P_{N_2} \simeq 750\mu$) → NaO* + N_2- spectrum over the region 6500- 7600Å for constrast to (b), (c) Na + O_3 ($P_{O_3} \simeq 5\text{-}10\mu$) + He ($P_{He} \sim 300\mu$) → NaO* + O_2 + He, and (inset) single collision chemiluminescent spectrum for the metathesis Na + N_2O ($P_{N_2} \times 5 \times 10^{-5}$ torr)→ NaO* + N_2. Spectral resolution for (a) through (c) is 3Å while the single collision spectrum was obtained at 8Å resolution. Spectra (a) through (c) were obtained with an EMI 9808 phototube whose quantum efficiency drops rapidly at wavelengths longer than 9200Å. The single collipion spectrum was obtained with an RCA 4840 phototube whose quantum efficiency drops rapidly at $\lambda >$ 7800Å. The dashed region outlined at the longest wavelengths in the single collision spectrum indicates a component of blackbody radiation. A small potassium impurity[16] leads to the observation of K D-line emission in the single collision spectrum.

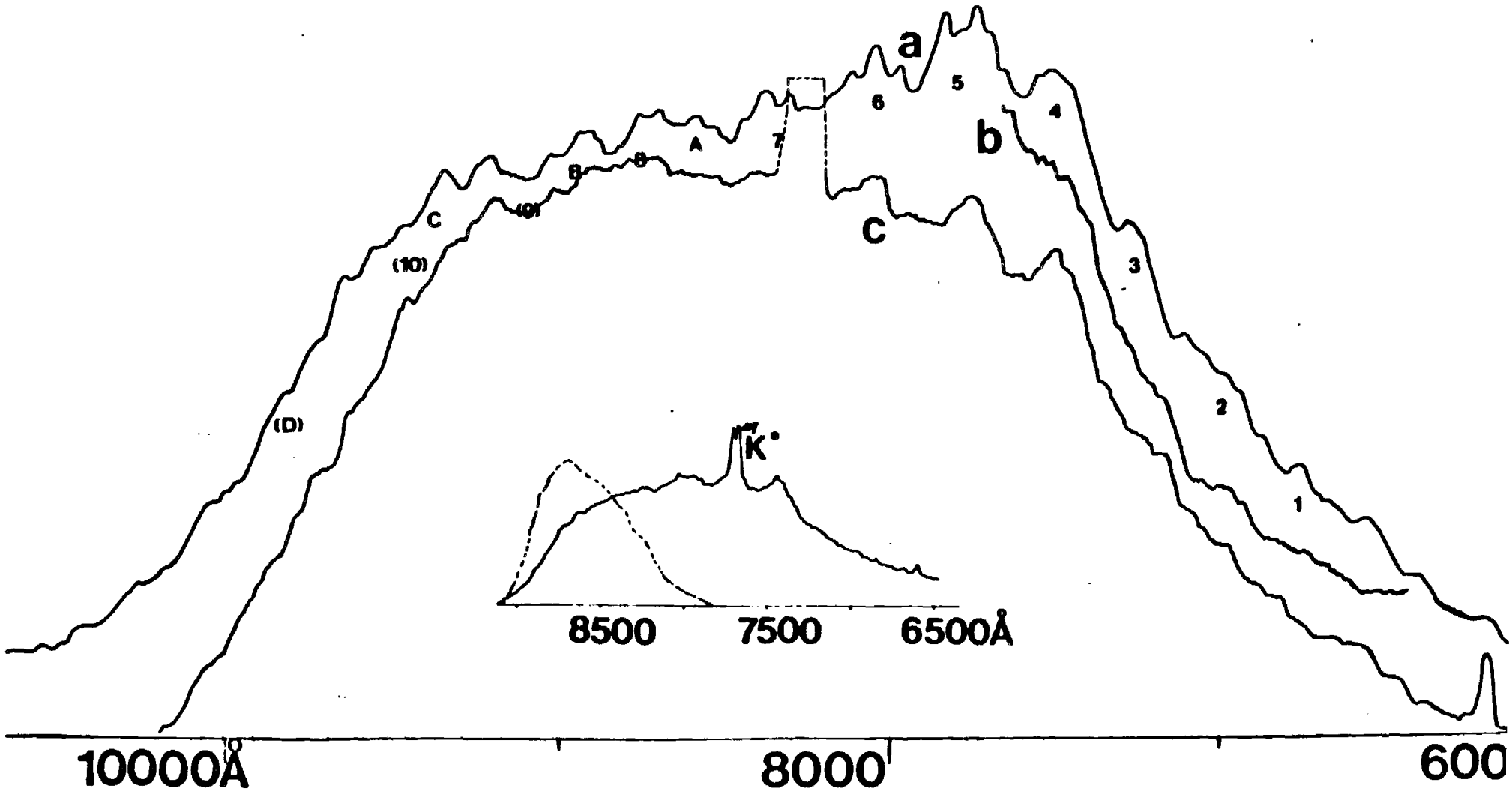
a
b
c
(D)
(10)
C
B
A
8
7
6
5
4
3
2
1
K
8500
7500
6500Å
10000Å
8000
600

APPENDIX C

ON THE NATURE OF THE ENERGY BALANCE AND BRANCHING RATIOS ASSOCIATED WITH THE CHEMILUMINESCENT REACTION $Si(^3P) + N_2O(^1\Sigma) \rightarrow SiO^*(a^3\Sigma^+, b^3\Pi, A^1\Pi) + N_2(v'' \geq 5)$ - POSSIBLE FORMATION OF VIBRATIONALLY EXCITED N_2

James L. Gole and Gary J. Green

Department of Chemistry
Georgia Institute of Technology
Atlanta, Georgia 30332

Abstract

Silicon atoms react under single collision conditions with N_2O to yield hemiluminescent emission corresponding to the SiO $a^3\Sigma^+ - X^1\Sigma^+$ and $b^3\Pi - X^1\Sigma^+$ ntercombination systems and the $A^1\Pi - X^1\Sigma^+$ band system. A most striking feaure is the energy balance associated with the formation of SiO product moleules in the $A^1\Pi$ and $b^3\Pi$ states. The analysis of the emission from these tates provides evidence for the formation of vibrationally excited N_2 in a ast Si-N_2O reactive encounter. The comparison of several M+N_2O reactions M=Si,Al,Ti,Sc,Y,La,Ca,Sr,Ba) indicates an energy discrepancy between the vailable energy to populate the highest energetically accessible excited state uantum level and the highest quantum level from which emission is observed. his difference appears to be characteristic of a vibrational excitation in N_2, he average value of the internuclear distance for which corresponds to an N-N ond length comparable to that in linear N-NO. Emission from the SiO $a^3\Sigma^+$ $A^1\Pi$) and $b^3\Pi$ ($A^1\Pi$,$E^1\Sigma_o^+$) triplet state manifold results primarily from intensity orrowing involving the indicated singlet states. Perturbation calculations ndicate the magnitude of the mixing between the $b^3\Pi$, $A^1\Pi$, and $E\ ^1\Sigma_o^+$ states anges between 0.5 and 2%. On the basis of these calculations, the branching atio (excited triplet)/(excited singlet) is found to be well in excess of 500. n approximate vibrational population distribution is deduced for those molecules ormed in the $b^3\Pi$ state. The present studies are correlated with those of preious workers in order to explain diverse relaxation effects as well as the hange in the ratio of $a^3\Sigma^+$ to $b^3\Pi$ emission as a function of pressure and xperimental environment. Some of these effects are attributable to a strong oupling between the $a^3\Sigma^+$ and $b^3\Pi$ state. Based on the current results, there ppears to be little correlation between either (1) the branching ratio for

excited state formation or (2) the total absolute cross section for excited state formation and (3) the measured quantum yield for the Si-N_2O reaction. Implications for chemical laser development are considered.

troduction

For several years, the nature of the structure, energetics, and formation the SiO molecule has been the subject of a number of experimental and theotical studies.[1] The low-lying states of SiO have recently been discussed in tail by Field et al.[2] An important contribution to our knowledge of the lowing states of SiO has come from recent studies of the chemiluminescent reaction

$$SiO(^3P) + N_2O \longrightarrow SiO^*(a^3\Sigma^+, b^3\Pi\ldots) + N_2 \qquad (1)$$

Hager et al.[3] and Linton and Capelle.[4] Much of the impetus for this effort s been the desire to exploit "spin conservation" in order to produce the low-lying Σ^+" and "$b^3\Pi$" states of SiO. These studies have offered the opportunity to characrize the "$a^3\Sigma^+$"-$X^1\Sigma^+$ and "$b^3\Pi$"-$X^1\Sigma^+$ intercombination band systems of SiO and vestigate the possibility of using spin conservation to advantage in order to eate a population inversion on the "$a^3\Sigma^+$"-$X^1\Sigma^+$ or "$b^3\Pi$"-$X^1\Sigma^+$ transitions and nce develop a medium for a visible chemical laser.

With the emphasis outlined above, previous studies have focused on the aluation of the chemiluminescent emission from reaction (1) primarily as a means determining spectroscopic constants for the $a^3\Sigma^+$ and $b^3\Pi$ states,[3,4] the lative population distributions in these states,[3] and the total quantum yield r fluorescence from those SiO excited states populated in reaction.

It is the purpose of the current effort to augment the information garnered previous studies by characterizing the Si-N_2O reaction at considerably lower essures (10^{-5}-10^{-1} torr) than those associated with the Hager et al. (2-4 torr)[3] d Linton and Capelle[4] (0.5-20 torr) studies. Based on our study of the "single llision ($P_{Tot.} \leqslant 10^{-4}$ torr) Si-N_2O reaction, we wish to suggest an explanation r the rather diverse $b^3\Pi$ excited state vibrational excitation which characterizes e spectral emissions observed by Hager et al. ($v' \leqslant 2$) and Linton and Capelle '$\leqslant 8$) in their "multiple collision" flame experiments. In addition, we have

determined that a component of the analysis of the chemiluminescence from the intercombination band systems is errant in the sense that these systems have been treated as allowed transitions when in fact the observed "$a^3\Sigma^+$" and "$b^3\Pi$" emission results primarily from intensity borrowing involving a low-lying $A^1\Pi$ state. The pursuit of the analysis of the intercombination band systems is necessary for two reasons: (1) It indicates that the chemiluminescence corresponding to the intercombination transitions ($Si + N_2O \rightarrow SiO^*(a^3\Sigma^+, b^3\Pi)$ is characterized by a much different population distribution than previously envisioned. The modified population distribution may have significant implications for the creation of a population inversion on the intercombination band transitions. (2) There is a question of the assessment of the quantum yield for these intercombination transitions in view of the fact that they are observed primarily as a result of intensity borrowing.

Previous researchers have focused primarily on SiO spectroscopy and excited state product distributions leaving apparently unnoticed an intriguing question concerning the dynamics of the $Si-N_2O$ reaction. One finds that there is a significant discrepancy between the available energy to populate SiO excited electronic states (reaction (1) exoergicity 53000 cm^{-1}) and the observed excitation which characterizes the $Si-N_2O$ system. We consider this differential and offer an explanation which appears to be consistent with observations of excited state metal oxide formation in several $M+N_2O$ reactions.

)erimental

Silicon atoms distributed thermally among the ground state $^3P_{0,1,2}$ com-
ients were reacted with N_2O in a highly exothermic process to produce an
:ense blue emission. The observed chemiluminescence was observed under both
ngle[5-7]($\leq 10^{-3}$ torr) and multiple[8] (10^{-2}-1 torr) collision conditions in
ghtly modified versions of devices described elsewhere.[5,6]

In the single collision studies, silicon was vaporized from a cylindrical
ıphite crucible (c.s. grade-Micromechanisms). This crucible was heated by a
)hite radiator substituted for the tantalum radiators (graphite inner sheath)
:viously used in our study of the Si-OCS reaction.[7,9] The graphite radiator
; surrounded by two tantalum heat shields. Maximum temperatures ranging from
)0 to 2100°C were achieved with this construction, all temperatures being mea-
·ed with a Leeds and Northrup optical pyrometer to ±10°C. The graphite crucible/
ıt shield assembly was surrounded by a water cooled copper jacket attached to a
vly designed "quick-load" bus bar/flange assembly.[10] The effusive silicon atom
ım intersected a tenuous atmosphere (10^{-5} to 10^{-3} torr) of N_2O (Matheson,
3%) and the resulting diffuse chemiluminescence resulting from the Si-N_2O reaction
; observed at right angles to the metal flow through a Suprasil quartz viewing
·t. Light baffles were placed in the reaction chamber to minimize the interference
)m blackbody radiation emanating from the oven chamber.

Multiple collision studies were carried out by vaporizing silicon at tempera-
·es between 1600 and 1800°C from a c.s. grade graphite crucible.[11] The crucible
; machined to fit inside a commercial tungsten basket heater (R. D. Mathis,
ıg Beach, CA) which was wrapped with several layers of zirconia ZrO_2 cloth
ircar Products, Florida, NY). The silicon vapor was reacted directly with N_2O
entrained in an argon buffer gas (Airco, 99.998%) and transported to the reaction
ne where the resulting mixture underwent oxidation. Typical operating pressures
re on the order of 10-100μ of oxidant and, at higher pressures, one to two torr
argon.

Spectra were taken with a 1 meter Czerny-Turner scanning spectrometer operated in first order with a Bausch and Lomb 1200 groove/mm grating blazed at 5000Å. For the study of the wavelength regions below 2500Å, the spectrometer was purged with dry N_2. Both RCA 4840 and 1P28 photomultiplier tubes were used in these experiments. In order to insure high sensitivity at wavelengths less than 2500Å, the 1P28 photomultiplier tube was coated with sodium salicylate. The sensitivity of the optical system, quartz viewing port, quartz lens system, and purged spectrometer, to short wavelength radiation was tested by monitoring the 1850Å mercury resonance line. This emission was readily detected demonstrating our ability to easily monitor chemiluminescent emission below 2000Å. The photomultiplier signal was detected with a Keithley 417 fast picoammeter whose output signal (partially damped) drove a Leeds and Northrup stripchart recorder. All spectra were wavelength calibrated using a low pressure mercury pen lamp.

:miluminescent Spectra

The Si-N_2O reaction is characterized by an intense blue chemiluminescence. : emission spectrum, which extends from 2250 to 4400Å (Figures 1-4), consists contributions from the $A^1\Pi - X^1\Sigma^+$, $b^3\Pi - X^1\Sigma^+$, and $a^3\Sigma^+ - X^1\Sigma^+$ band systems SiO and is dominated by the $b^3\Pi - X^1\Sigma^+$ band system onsetting at 2800Å. The :ctra were all taken under single collision conditions ($P_{Total} \leq 10^{-4}$ torr).

$a^3\Sigma^+ - X^1\Sigma^+$

Resolvable features for the $a^3\Sigma^+ - X^1\Sigma^+$ band system extend from 3500-4400Å jure 2). As has been observed by previous workers[3,4] under multiple collision iditions, only a single progression arising from the v' = 0 level of the $a^3\Sigma^+$ ite can definitely be identified. If emission features originating in v'=1 : present they are weak and hidden under the $b^3\Pi - X^1\Sigma^+$ features. Therefore :re has yet been no confirmation of the spectroscopic constants for the $a^3\Sigma^+$ ite predicted by Field et al.[2] and partially determined by Linton and Capelle.[4]

$b^3\Pi - X^1\Sigma^+$

Emission features corresponding to the $b^3\Pi - X^1\Sigma^+$ band system extend from)0 to 3950Å (Figures 1,2, and 3). Under single collision or near single collision iditions several new additional bandheads corresponding to vibrational levels ≤ v' ≤ 11 have been observed in the b-X system. This observation should be itrasted to the multiple collision studies of Hager et al.[3] where only emission)m v' ≤ 2 is observed and the notably different vibrational excitation, v' ≤ 8, ınd by Linton and Capelle.[4] Clearly vibrational deactivation has begun to onset the Linton and Capelle study and is quite pronounced in the experiments of ger et al. Observed bandheads and relative intensities corrected for phototube sponse are given in Table 1. Some twenty new bandheads have been observed.

$A^1\Pi - X^1\Sigma^+$

The $A^1\Pi - X^1\Sigma^+$ emission features observed in this study are depicted in gures 3 and 4. As Figure 3 demonstrates, the A-X emission which is much weaker an that from the b-X system is dominated by a progression emanating from v'=0.

While Linton and Capelle[4] have observed some A-X emission in their multiple collision study, Hager et al.[3] observed no such emission. On the basis of these results, Linton and Capelle reasoned that the A-X emission observed in their study resulted from the collisional population of the A state. Because we observe the emission system under single collision conditions and find a first order dependence of the A-X emission feature on pressure we have evidence for the direct population of the A state and the significant quenching of emission from this state in the experiments of Hager et al. In other words, our results would seem tc indicate minimal vibrational and electronic deactivation in the multiple collision studies of Linton and Capelle and complete quenching of the A-X band system, which can be populated directly, in the experiments of Hager et al. No emission from $A^1\Pi$ vibrational quantum levels greater than v'=2 (Figures 3 and 4) was found in this study. If we consider the energy available to populate excited electronic states, we might expect to observe emission from $A^1\Pi$ vibrational quantum levels $v' \leqslant 15$.

ıetics and Emission Behavior with Increasing Pressure

We find that the observed chemiluminescent emission from the $a^3\Sigma^+$, $b^3\Pi$, and I states of SiO increases linearly with oxidant pressure over the range 3 x 10^{-5} to x 10^{-4} torr indicating that these states are formed in a process first order N_2O. Although detailed temperature dependence studies to determine the :ivation energy for the Si-N_2O reaction were not performed, the chemiluminescent :ensity as a function of the Si beam source temperature was followed with :fficient accuracy so as to determine that reaction with ground state Si ^3P atoms ł occurred.

At elevated pressures the relative emission from the three excited states)ulated in the initial Si-N_2O reactive process was found to vary. Specifically : $b^3\Pi$ emission intensity was found to increase relative to the $a^3\Sigma^+$ emission such ıt the ratio I $(a^3\Sigma^+)$/I$(b^3\Pi)$ decreased to a minimum at ∿5 x 10^{-2} torr, virtually /eling off up to a pressure on the order of 2 torr. At pressures in excess of ‹ 10^{-1} torr, the $A^1\Pi$ emission intensity increased relative to that from the I and $a^3\Sigma^+$ states and some vibrational deactivation occurred in the $b^3\Pi$ state, :h of these findings being in agreement with the observations of Linton and)elle.[4]

Nature of the Intercombination Band Systems

In a strictly first order description $^3\Sigma^+ - {}^1\Sigma^+$ or $^3\Pi - {}^1\Sigma^+$ transitions are spin forbidden and should have little or no intensity. However, in the presence of perturbations the SiO $a^3\Sigma^+$ or $b^3\Pi$ states may mix with nearby $^1\Pi(A^1\Pi)$ and $^1\Sigma_o^+(E^1\Sigma_o^+)$ states, leading to nonzero "$a^3\Sigma^+$" - $X^1\Sigma^+$ or "$b^3\Pi$" - $X^1\Sigma^+$ transition moments. If the population of the "$^3\Sigma^+$" or "$^3\Pi$" states is sufficient to balance the very small "$^3\Sigma^+$" - $X^1\Sigma^+$ or "$^3\Pi$" - $X^1\Sigma^+$ oscillator strengths induced by this mixing, one can observe the corresponding band systems in emission. We are dealing with branching ratios in chemical reaction and hence the probable magnitude of the spin conservation entailed in reaction (1) leads to the strong probability that the Si-N_2O reaction forms the metal oxide largely in the "$a^3\Sigma^+$" and "$b^3\Pi$" states. This, in turn, leads to the observation of emission from these states.

We have found that a perturbation description is appropriate for the prediction of (1) the relative intensities of vibronic transitions for the "$b^3\Pi$" - $X^1\Sigma^+$ band system, (2) the relative intensities of the a"$^3\Sigma^+$" - $X^1\Sigma^+$ and "$b^3\Pi$" - $X^1\Sigma^+$ intercombination emission systems, and (3) the relative emission intensity from the $^3\Pi_{0,1,2}$ components of the $b^3\Pi$ state. In order to approach the analysis of the observed SiO* emission from the Si-N_2O reaction, we have evaluated the mixing coefficients among several of the low-lying states of SiO resulting from the following electronic configurations:

(2)...$5\sigma^2 6\sigma^2 7\sigma^2 2\pi^4$	$X^1\Sigma^+$
(3)...$5\sigma^2 6\sigma^2 7\sigma 2\pi^4 3\pi$	$b^3\Pi$, $A^1\Pi$
(4)...$5\sigma^2 6\sigma^2 7\sigma^2 2\pi^3 3\pi$	$a^3\Sigma^+$, $d^3\Delta$, $e^3\Sigma^-$, $C^1\Sigma^-$, $D^1\Delta$, $(E^1\Sigma_o^+)$.

The determinantal wavefunctions applicable to several of these states are believed to be quite analogous to those presented by Field et al.[12] for CO and will not be given in detail here. Using the appropriate parity adapted wavefunctions we have determined the interaction matrix for several

of these states employing a simplified microscopic form of the spin-orbit operator, commonly used for semiempirical calculations

$$H_{so} = \sum_i \hat{a}_i \ell_i \cdot s_i \qquad \hat{a}_i = \sum_k z_k / r_{ki}^3$$

where ℓ_i is the orbital angular momentum of electron i, s_i is the spin angular momentum of electron i, z_k is the effective charge on nucleus k, and r_{ki} is the distance between electron i and nucleus k. Spin-other-orbit interactions have been neglected and we have assumed negligible effects due to the coriolis interaction which is expected to be at least two orders of magnitude smaller than spin-orbit coupling.

In Table 2, the matrix elements in units of cm^{-1} are represented as the product of a numerical electronic factor and a vibrational overlap. In order to obtain the results presented in Table 2, the appropriate basis functions were expressed in terms of antisymmetrized products of one electron molecular orbitals in a manner similar to that described in a previous study on AlO. We assume that the 7σ and 2π orbitals correspond to $p\sigma$ and $p\pi$ orbitals respectively centered on oxygen and that the 3π orbital is derived from a $3p\pi$ orbital centered on silicon. We also assume that the electronic states with which we are concerned are well represented by the charge distribution Si^+O^-. Hence to good approximation the 7σ and 2π orbitals can be represented by atomic p orbitals $P_-(O^-)$ and $P_o(O^-)$ centered on the oxygen ion (O^-) and

$$a = 2^{\frac{1}{2}} a_o \langle v | v' \rangle \tag{5a}$$

where

$$a_o = \langle P(O^-) | \varepsilon_o(r) | P(O^-) \rangle \sim 121 \text{ cm}^{-1} \tag{5b}$$

[13]

where this equality is not exact because (1) approximate representations were assumed for 7σ and 2π, and (2) the spin orbit coupling constant, $a_o \sim 121$ cm^{-1}, is strictly appropriate to O^- and not Si^+O^-. The vibrational overlap factor (eq. 5a) is determined from RKR curves[14] which are obtained

using the molecular constants given by Field et al.[2] for the various states of interest. The parameter

$$a_z = \langle 3\pi|\hat{a}|3\pi\rangle \text{ cm}^{-1} \quad \sim 146\text{cm}^{-1} \tag{6}$$

is taken from Field et al.[2] In our calculations the $E\ ^1\Sigma_o^+$ state is assigned to configuration (4). In fact this state probably corresponds to a mixed configuration valence state with dominant contribution from configuration (4).[2] The matrix element connecting $E\ ^1\Sigma_o^+$ and $b^3\Pi_o$ will be overestimated.

In fitting the observed chemiluminescent spectra for the mixed "$b^3\Pi$" state, the wavefunctions for the components of interest may be written to reasonable approximation as

$$\psi(\text{"}b^3\Pi_1\text{"}) = c(b^3\Pi_1) + d(A^1\Pi_1) \tag{7a}$$

$$\psi(\text{"}b^3\Pi_o\text{"}) = c'(b^3\Pi_o) + d'(E^1\Sigma_o^+) \tag{7b}$$

where c>>d, c'>>d', and the $A^1\Pi$ and $E^1\Sigma_o^+$ states correspond to nearby excited states (configs. (3) and (4)) which mix significantly (Table 2) with the $^3\Pi_1$ and $^3\Pi_o$ components of the $b^3\Pi$ state and from which emission occurs in an allowed transition to the ground $^1\Sigma^+$ state. If the $^3\Pi$ components are described as in equation (7), the relative intensities $I_{v',v''}$ of vibronic transitions (v',v") in emission are related to the excited state populations $N_{v'}$ by

$$I_{em}^{v',v''} = N_{v'}\varepsilon(\nu)\nu_{v',v''}^4 \Sigma_v c^2_{v',v} q_{v,v''} \tag{8}$$

where $c_{v',v}$ is the mixing coefficient between $b^3\Pi_1$ and $A^1\Pi_1$ or $b^3\Pi_o$ and $E^1\Sigma_o^+$, $N_{v'}$ is the number of molecules in the $^3\Pi$ components, $\nu_{v',v''}$ is the frequency of the transition, and $q_{v,v''}$ is the Franck-Condon-Factor (FCF) between vibrational levels v of $A^1\Pi$ or $E^1\Sigma_o^+$ and v" of $X^1\Sigma^+$.

A similar expression can be written for the mixed "$^3\Sigma^+$" state

$$\psi(\text{"}a^3\Sigma^+\text{"}) = c''(a^3\Sigma_1^+) + d''(A^1\Pi) \qquad (9)$$

In fact, the description represented by expressions (7) and (9) is complicated further since the "$^3\Sigma^+$" and "$^3\Pi$" states can (Table 2) and apparently do couple so that the "$^3\Sigma^+$" state has some "$^3\Pi$" character and vice-versa. This point will be considered in a following section.

Upon evaluating the matrix elements in Table 2 using the molecular constants given by Field et al.[2] for the low-lying states of SiO, we find the largest mixing between $b^3\Pi_1$ and $A^1\Pi_1$. The interaction between $a^3\Sigma_1^+$ and $A^1\Pi_1$ is considerably smaller not only because of a smaller electronic factor but also because the Σ configured states (Eq. 4) are shifted relative to the Π states to considerably larger internuclear distance, thus decreasing the vibrational overlap factor. Both the $^3\Pi$ and $^1\Pi$ states derived from the same electronic configuration have similar internuclear distances and hence a significantly higher vibrational overlap. The $^3\Pi_0$ component derives its intensity from the mixed valence $E^1\Sigma_0^+$ state and therefore is characterized by a much smaller vibrational overlap than $^3\Pi_1$ - $^1\Pi_1$. Based upon these considerations and the fact that $E^1\Sigma_0^+$ is a mixed state, we anticipate that the intensity of emission from the $^3\Pi_1$ component should dominate that from the $^3\Pi_0$ component. In turn, the $^3\Pi_0$ component should dominate $^3\Pi_2$ which derives the major contribution to its intensity from a Coriolis interaction.

The predictions outlined above are born out in the spectra depicted in Figure 1(b) where the (0,0) and (0,1) bands of the "$^3\Pi$" - $X^1\Sigma^+$ band system are resolved. The "$^3\Pi_2$" emission feature should appear to the blue of the dominant "$^3\Pi_1$" feature and is barely discernable. Based on an evaluation of the matrix elements in Table 2, the intensity ratio $^3\Pi_0/^3\Pi_1$ is at a maximum for v' = 0 and tails off rapidly for levels v'>1. Therefore, the

relative intensities of the bands depicted in Figure 1(a), where the "$^3\Pi_1$" and "$^3\Pi_0$" components are unresolved, are determined primarily by the "$^3\Pi_1$" component emission, the dominance of $^3\Pi_1$ over $^3\Pi_0$ increasing with increasing v'. In addition, based on the matrix elements given in Table 2 and discussed above, we can determine that the emission corresponding to the "$b^3\Pi$" - $X^1\Sigma^+$ intercombination system should dominate that for the "$a^3\Sigma^+$" - $X^1\Sigma^+$ system. Indeed, this is observed.

Within the "$b^3\Pi$" - $X^1\Sigma^+$ band system, the relative intensity of emission from individual vibrational quantum levels v' appears to be well predicted by equation (8) where $c^2_{v',v}$ represents the mixing coefficient between the vibrational level v' of "$b^3\Pi$" and vibrational levels v of $A^1\Pi$. The population of individual vibrational levels in the "$b^3\Pi$" state rises from v' = 0 to v' = 2 tailing off for vibrational levels $v' \geq 3$.

Finally, we wish to estimate the branching ratio for population of the "$b^3\Pi$" vs. the $A^1\Pi$ state. In order to do so, we compare the intensity of certain "$b^3\Pi$" and $A^1\Pi$ emission features. This procedure is implemented by considering the "$b^3\Pi$" - $A^1\Pi$ mixing coefficients (Eq (8) and above) which are generally on the order of 0.01 or less, the largest mixing being with the v'=0 level of "$b^3\Pi$". If, correcting for phototube response, we compare the relative intensity of the (0,0) bands for the "$b^3\Pi$" - $X^1\Sigma^+$ and $A^1\Pi$ - $X^1\Sigma^+$ transitions, the relative populations of "$b^3\Pi$", v'=0, and $A^1\Pi$,v=0 are given by

$$\frac{N_o(\text{"}b^3\Pi\text{"})}{N_o(A^1\Pi)} = \frac{I(\text{"}b^3\Pi\text{"} - X^1\Sigma^+)(FCF=0.141)}{I(A^1\Pi - X^1\Sigma^+) \quad C} \left(\frac{\nu_{oo}(A^1\Pi - X^1\Sigma^+)}{\nu_{oo}(\text{"}b^3\Pi\text{"} - X^1\Sigma^+)}\right)^4 \qquad (10a)$$

$$C = (0.141 c^2_{0,0} + 0.277\ c^2_{0,1} + 0.274\ c^2_{0,2}) \qquad (10b)$$

where 0.141, 0.279, and 0.274 correspond to Franck-Condon factors for the $A^1\Pi$ - $X^1\Sigma^+$ (0,0), (1,0), and (2,0) transitions, and $c^2_{0,0}$, $c^2_{0,1}$, and $c^2_{0,2}$

correspond to the mixing coefficients for the v=0,1,2 levels of $A^1\Pi$ with v'=0, "$b^3\Pi$". The C term derives from equation 8, the dominant mixing with v'=0 $b^3\Pi$ being with the v=0,1,2 levels of $A^1\Pi$. The intensity of the "$b^3\Pi$" (0,0) band may be compared to any of the (v,v") $A^1\Pi$ emission bands simply by modifying the numerator in Eq. 10a, replacing the Franck-Condon factor and frequency for the (0,0) band with the appropriate quantities for the $A^1\Pi$ - $X^1\Sigma^+$ band of interest.

The intensities for the "$b^3\Pi$"- $X^1\Sigma^+$ and $A^1\Pi$ - $X^1\Sigma^+$ (0,0) bands are taken to be 350 and 48 respectively. These relative band intensities were determined on the basis of a conservative estimate of the relative phototube response between 2300 and 3000Å, a region in which phototube sensitivities are such that precise calibration is tenuous. In order to aid our determination of the relative phototube response in the short wavelength region, we made use of the known Franck-Condon factors for the (0,v") and (1,v") progressions of the $A^1\Pi$ - $X^1\Sigma^+$ system (Fig. 3), determining a response consistent with expected relative emission intensities. The quoted relative intensities for the (0,0) bands correspond to an upper bound estimate of the corrected relative intensity for the $A^1\Pi$ - $X^1\Sigma^+$(0,0) band (underestimate of relative phototube response) obtained on the basis of the analysis of the $A^1\Pi$ - $X^1\Sigma^+$ progressions (Fig. 3). Substituting into Eq. 10a with $\nu_{oo}(A^1\Pi)$ = 42640.9 cm^{-1}[2] and C = 0.00502 we estimate that the population of "$b^3\Pi$"(v'=0) is on the order of 500 times larger than $A^1\Pi(v=0)$. Similar results are obtained if we choose to compare the"$b^3\Pi$"- $X^1\Sigma^+$(0,0) band with other $A^1\Pi$ - $X^1\Sigma^+$(0,v") bands.

The estimated branching ratio for formation of "$b^3\Pi$" vs. $A^1\Pi$ excited state species assumes that the radiative lifetimes of the two states are comparable and that the region viewed by the spectrometer is sufficiently

large so that the relative intensity of emission from the two states is an accurate measure of the relative rates of formation in these states. However, in the present study, it is certainly the case that the two states considered have drastically different radiative lifetimes and that their relative intensities are no longer simply related to the relative rates of formation. Since the radiative lifetime of the "$b^3\Pi$" state is considerably longer than that of the $A^1\Pi$ state (see following discussion), a larger fraction of molecules formed in the "$b^3\Pi$" state will leave the viewing region before radiating and therefore will not be detected. The consideration of this fact and the nature of the estimates in our perturbation calculations leads us to the conclusion that the ratio of population which we have calculated is certainly a lower bound to the actual branching ratio.

ıergy Balance for the Si + $N_2O \rightarrow SiO^* + N_2$ Reaction

In this section, we focus on the large discrepancy between the available ıergy to populate SiO excited states, due primarily to the exoergicity of the i + N_2O reaction, and the energy for which we can account through determination f the highest excited state quantum levels populated in reaction.

From the single collision Si-N_2O reaction it is potentially possible to et a lower bound on the dissociation energy of silicon monoxide. Using eaction (1) and a previously discussed energy balance[15-17] we arrive at the nequality

$$D_o^o(SiO) \geq D_o^o(N_2O) + E_{int}(SiO) - E_{int}(Si) - E_{int}(N_2O) - E_T^i - E_A(Si\text{-}N_2O) \quad (11)$$

here the silicon atom is in the ground ^3P state and E_{int} (Si), E_{int} (N_2O), nd E_{int} (SiO) are the internal energies of the species noted in parenthesis.* ^i_T is the relative translational energy of the reactants and $E_A(Si\text{-}N_2O)$ is he measured activation energy for the metathesis considered. In considering he products of the Si-N_2O reaction, SiO and N_2, neither $E_{int}(N_2)$ nor E_T^f, he final relative translational energy of product separation can be readily etermined. Therefore these quantities are not included in Eq. (11) and he inequality applies.

If we neglect for the moment the activation energy for the Si-N_2O reaction[18] nd focus on the available energy to populate SiO excited states

$$E_{Available} = D_o^o(SiO) - D_o^o(N_2O) + E_{int}(N_2O) + E_{int}(Si) + E_T^i$$

he available energy is partitioned to

$$E_{int}(SiO) + E_{int}(N_2) + E_T^f \quad (13)$$

For the silicon reaction, we select as our reference (zero) energy the reactants and products in eq. (11) at 0°K, that is $Si(^3P_o)$, $N_2O(^1\Sigma^+, v=J=0)$, $SiO(^1\Sigma^+, v=J=0)$ and $N_2(^1\Sigma^+, v=J=0)$.

The SiO molecule is among the most widely studied high temperature molecules. Its bond energy is not only well known but represents a standard for mass spectrometry. We adopt the recent determination by Hildenbrand et al.,[19] $D_o^o(SiO) = 8.16eV = 65827\ cm^{-1}$. The N_2-O bond energy[20] is 13400 cm^{-1}.

To calculate $E_{int}(N_2O)$, we adopt a procedure similar to that described previously[21] for the determination of $E_{int}(OCS)$ and find $E_{int}(N_2O) = 298\ cm^{-1}$. To calculate $E_{int}(Si)$ we need consider only the internal energy of the ground ^3P state since it is this state which reacts to produce the observed chemiluminescence. Using standard techniques[22] we find $E_{int}(Si) = 145\ cm^{-1}$ for a beam temperature of 2170°K.

Dagdigian et al. have shown that, to good approximation[23]

$$E_T^i = 3/2kT_{eff} \qquad T_{eff} = (m_G T_B + m_B T_G)/(m_G + m_B) \tag{14}$$

where T_G is the temperature of the oxidant gas (300K), T_B is the silicon beam temperature (2170 K) and m_B and m_G are the masses of the beam atoms and gas molecules respectively. For the Si-N_2O reaction, we find $E_T^i = 1501\ cm^{-1}$.

Summing the energies considered above, we find

$$E_{Available} = 54371\ cm^{-1} \tag{12a}$$

In order to evaluate $E_{int}(SiO)$, we seek the highest quantum level populated by the Si-N_2O reaction. Here, we exclude the use of the $a^3\Sigma^+$ state since, as we have noted, (1) the emission from this state is much weaker than and obscured by that from the $b^3\Pi$ state and (2) for levels v'>0 possible strong $a^3\Sigma^+$ - $b^3\Pi$ coupling may also play a role in obscuring the $a^3\Sigma^+$ emission features.

The highest vibrational quantum level populated in the SiO $A^1\Pi$ state is v = 2. Choosing the (2,7) band in the $A^1\Pi$ - $X^1\Sigma^+$ system, we obtain

$$E_{int}(SiO) = \nu(2,7) + G''(7) - G''(0)$$
$$= 35951 \pm 30 \text{ cm}^{-1} + G''(7) - G''(0) \quad (15)$$
$$= 44314 \pm 35 \text{ cm}^{-1}$$

The highest vibrational quantum level populated in the SiO "$b^3\Pi$" state is v' = 11. Choosing the (11,16) band in the "$b^3\Pi$" - $X^1\Sigma^+$ system we obtain

$$E_{int}(SiO) = 43992 \pm 40 \text{ cm}^{-1} \quad (16)$$

The energy for which we can account using the SiO excited state emissions is some 10,000 cm^{-1} less than the potential available energy to the system! It implies that the SiO bond energy is over an electron volt less than the reliable value given in the literature, a highly unlikely possibility.

In general, single collision chemiluminescence studies yield dissociation energies that are in close agreement with careful mass spectrometric measurements. With few exceptions,[24] any discrepancies are encompassed if one takes into account the temperature dependence of the metathesis yielding chemiluminescence and the nature of the metal atom reactant. In all cases, discrepancies have resulted in the prediction of slightly higher bond energies. Therefore the result obtained here represents a significant deviation from expectation. In the present study, we have found that ground state ^3P silicon atoms react to yield the observed chemiluminescence. If, in order to provide a correction for the possible reaction of metal atoms in the high energy tail of their translational energy distribution, we determine the activation energy for the Si-N_2O reaction, this energy increment must be added to the available energy,[25] Eq. (12). Therefore the energy discrepancy is even larger than 10,000 cm^{-1}.

It is apparent that when the products SiO and N_2 are formed over an electron volt of energy must be accounted for by either the product N_2 internal

energy or the relative translational energy of product separation. In the following discussion, we document that the observed behavior in the Si-N_2O system appears to be characteristic of several M-N_2O reactions. We suggest that the most logical choice to account for the observed energy discrepancy corresponds to the internal excitation of product N_2 molecules.

Discussion

A. Energy Balance in M-N_2O Reactions

In spite of repeated efforts, we have been unable to use the Si-N_2O reaction to populate vibrational levels $v' \geq 3$ in the $A^1\Pi$ state of SiO. In addition, we have not observed fluorescence from the $E\ ^1\Sigma_o^+$ state although it should be possible to populate two vibrational levels in this state. The Si-N_2O reaction is of sufficient exothermicity to populate 15 vibrational quantum levels in the $A^1\Pi$ state. Emission from these levels can readily be observed and recently we have employed the spin conserving Si-O_3 reaction

$$Si(^3P) + O_3(^1A_1) \rightarrow SiO(A^1\Pi) + O_2(^2\Sigma_g^-) \qquad (17)$$

to populate a minimum of 12 vibrational quanta in the $A^1\Pi$ state. In short, there appears to be little reason to suspect that the lack of $A^1\Pi$ vibrational excitation which characterizes the Si-N_2O reaction can be attributed to factors associated with the intimate molecular electronic structure of the $A^1\Pi$ state. Rather it appears that the observed effects are to be associated with the dynamics of the Si-N_2O reaction. We would like to suggest a plausible explanation for the observed results based upon a comparison of the molecular N-N bond in the reactant N_2O and the product N_2 (Eq. 1).

The bond length of the N-N bond in the linear N-N-O molecule is 1.128Å.[26] The N-N bond length in molecular nitrogen is 1.0977Å.[27] We ask what vibrational excitation must be associated with the N_2 molecule in order that the corresponding bond length be 1.128Å. The vibrational excitation corresponds to $v''=5$. In other words, the average value of the internuclear distance for the fifth vibrational quantum level in the ground state of N_2 corresponds to the N-N bond distance in N_2O. The energy associated with $v''=5$ is 11350 cm^{-1}, in close agreement with the 10,000 cm^{-1} energy discrepancy which characterizes the Si-N_2O

reaction*. We suggest that this correlation may not be fortuitous and that the Si-N_2O reaction, which certainly does not proceed via an electron jump mechanism, may occur via a sufficiently fast stripping or rebound process such that the N-N bond does not have sufficient time to adjust to its equilibrium value in N_2 before the products SiO and N_2 separate. Thus, energy balance requires that the N_2 be produced in a vibrationally excited state.

The results obtained in the present study cause us to focus on the nature of the energy balance in several M + N_2O reactions where we find that the proposed explanation is consistent with observation. Consider, for example, the Ti-N_2O reaction, the chemiluminescent emission from which is depicted in Figure 5. Based on the energetics for this process, the available energy to populate excited electronic states is

$$\begin{aligned} D_o^o(TiO) &\overset{27}{=} D(N_2\text{-}O) + E_{int}(Ti) + E_{int}(N_2O) + E_T^i \\ &= 55440 - 13400 + 282 + 298 + 1384 \text{ cm}^{-1} \\ &= 44004 \text{ cm}^{-1} \end{aligned} \qquad (18)$$

where titanium atoms at 2400°K thermally distributed throughout the ground ^3F state react with N_2O to produce several TiO excited electronic states. Although the fluorescence from all of these states has not yet been analyzed, the emission corresponding to the D-$X^3\Delta$ band system of TiO (Table 3) has been analyzed and the population of vibrational levels in this state has been assessed using much higher resolution scans than that depicted in Figure 5.[28] The D state is the highest lying excited electronic state populated (and monitored) by the titanium-N_2O reaction. Based on the observed fluorescence the maximum energy associated with TiO internal excitation is

$$E_{int}(TiO) = 34840 \text{ cm}^{-1} \qquad (19)$$

---

*Note that the activation energy $E_A(Si\text{-}N_2O)$ for the silicon-N_2O reaction was not included in the evaluation of the energy discrepancy. Its inclusion would raise the calculated value by between 1000 and 2000 cm^{-1}.[18]

Here, we have an ~9000 cm^{-1} energy discrepancy between $E_{Available}$ (Eq. 18) and $E_{int}(TiO)$. We believe that this discrepancy may also be attributed to the formation of vibrationally excited N_2.

The production of vibrationally excited N_2 may also serve to explain a puzzling aspect of the chemiluminescent emission associated with highly exothermic aluminum oxidation.[29] The aluminum-ozone reaction produces extensive chemiluminescence from the $A^2\Pi$ and $B^2\Sigma^+$ states of AlO, the "single collision" process populating up to 18 vibrational quanta in the $B^2\Sigma^+$ state. Using independent measurements,[30] one finds that this is virtually the highest vibrational excitation which can be expected on the basis of the available energy ($D_o^o(AlO) - D(O-O_2) + E_{int}(Al) + E_{int}(O_3) + E_T^i$). Given the excitation which characterizes the $Al-O_3$ reaction and the relatively small energy difference, 0.63eV., between the N_2-O and O_2-O bond energies, we certainly expect to observe emission from the AlO $B^2\Sigma^+$ state if we react aluminum with N_2O. We would expect to populate 12 vibrational quanta (ω_e = 870.05 cm^{-1}, $\omega_e x_e$ = 3.5 cm^{-1}), however, no emission is observed. We feel that this result is again explained through an energy balance involving vibrationally excited N_2.

Similar and in some cases larger energy discrepancies are found to characterize several M + N_2O reactions involving the Group IIIB (Sc,Y,La) and Group IIA metals. The data is summarized in Table 4. In many of these cases further characterization of the product metal oxide chemiluminescence will be required in order to better assess the actual magnitude of the energy discrepancy.

The significant fact which emerges is that all the reactions considered display an energy balance which is consistent with the formation of a vibrationally excited N_2 product. While one might argue that the translational energy of product separation can account for a portion of these observations, it seems highly unlikely that the final relative translational energy of separation, E_T^f (Eq. 13), can account for the rather sharp energy cutoffs especially those

associated with the silicon, titanium, and aluminum reactions.

There are several experiments which might be pursued in order to obtain direct evidence for the formation of vibrationally excited N_2 produced in M = Al, Si, or Ti + N_2O reaction. The major problem confronting the experimenter is the detection of very low effective product N_2 concentrations ($\sim 10^{-7}$ torr). Promising detection techniques might involve the use of either electron bombardment excitation and ionization or multiphoton ionization. In the former studies one might attempt to use an electron gun to excite the Second Positive system of N_2 monitoring directly the N_2 $C^3\Pi_u$ - $B^3\Pi_g$ fluorescence and back extrapolating to the ground state N_2 population distribution.[31] Alternatively, we are attempting to produce N_2^+ $B^2\Sigma_u^+$, monitoring the $B^2\Sigma_u^+$ - $X^2\Sigma_g^+$ emission and again back-extrapolating to the N_2 population distribution.[31] Thusfar these studies have met with only marginal success (N_2 concentrations $\leq 10^{-5}$ torr have been detected), however the signal-to-noise in the system can be considerably improved if the reaction zone and electron gun are magnetically confined.[32] An alternate experiment might involve the elegant pulsed laser multiphoton technique which Dehmer[33], Kay[34] and coworkers have used to detect CO^+. The direct assessment of the vibrational excitat characterizing the product N_2 formed in highly exothermic M + N_2O reactions will contribute important new perspectives on the nature of reactive encounters. We encourage other workers to pursue the detection of vibrationally excited N_2 in low concentration.

B. Comparison and Correlation with Previous Studies

The present study augments and can be used to correlate the previous studies of Linton and Capelle[4] and Hager et al.[3] on the Si-N_2O reaction. Linton and Capelle studied the reaction of argon entrained silicon atoms with N_2O over the pressure range 1 to 30 torr (primarily argon >> N_2O), observing emission corresponding to the SiO $A^1\Pi - X^1\Sigma^+$, $a^3\Sigma^+ - X^1\Sigma^+$, and $b^3\Pi - X^1\Sigma^+$ band systems. The ratio of $a^3\Sigma^+$ to $b^3\Pi$ emission was unchanged with pressure and the chemiluminescence was dominated by the b-X band system. Hager et al. entrained the products of a discharge into a silane-helium mixture reacting the entrained species with N_2O at total pressures of 2 and 4 torr. These authors observed only emission from the "$a^3\Sigma^+$" (a-X) and "$b^3\Pi$" (b-X) states, finding that only levels $v' \geq 2$ were populated in the $b^3\Pi$ state in contrast to the much higher vibrational excitation ($v' \leq 8$) observed by Linton and Capelle. As the pressure was increased from 2 to 4 torr, the ratio of $a^3\Sigma^+$ to $b^3\Pi$ emission increased substantially (see also discussion of observed band systems and kinetics).

Our results obtained at low pressure ($\leq 10^{-3}$ torr) demonstrate that the "$a^3\Sigma^+$", "$b^3\Pi$", and $A^1\Pi$ states of SiO are populated directly in the Si-N_2O chemical reaction, although the branching ratio strongly favors triplet state formation in agreement with the spin conservation associated with reaction (1). Under multiple collision conditions (1-2 torr) the emission from the $A^1\Pi$ state does not increase significantly relative to that from the $b^3\Pi$ state. From these results we reach the following conclusions: (1) The population of the $A^1\Pi$ state in the Linton and Capelle study must result in large part from its direct formation in chemical reaction (in the low pressure range) and not from a collisional transfer[4] process. (2) The lack of $A^1\Pi$ emission in the Hager et al. study results from the efficient quenching of $A^1\Pi$ emitters under their experimental conditions. It is not surprising that their experimental conditions provide a

much more efficient medium for the collisional quenching of the $A^1\Pi$ state than does an argon + N_2O (argon >> N_2O) mixture at comparable pressures. (3) At higher pressures, from 4 to 30 torr, the Linton and Capelle study indicates that the $A^1\Pi$ state may also be populated by a collisional process in addition to direct $A^1\Pi$ formation. We speculate that direct $A^1\Pi$ formation, collisional population, and collisional quenching are all operative in their system, the former two processes dominating the latter.

The pressure dependent behavior of the "$a^3\Sigma^+$" and "$b^3\Pi$" emission features is distinctly different in the Linton and Capelle and Hager et al. studies. The behavior of the chemiluminescent emission in our system may serve to explain some of these differences. We believe that the present results indicate that at least 11 vibrational quanta in the "$b^3\Pi$" state are populated by the direct Si-N_2O reaction.[35] Linton and Capelle observe emission from only 8 vibrational quantum levels indicating that the argon + N_2O mixture present in their system acts as a mild vibrational quencher. In contrast, the mixture of helium, N_2O, and the discharge products of silane serves to promote significant vibrational relaxation in the experiments of Hager et al. where only emission from v'=0,1,2, "$b^3\Pi$" is observed.

Although Linton and Capelle observe no change in the relative intensities of the "$a^3\Sigma^+$" and "$b^3\Pi$" emission features as a function of pressure, Hager et al. observe a substantial increase in the $a^3\Sigma^+/b^3\Pi$ intensity ratio. This result at first appears difficult to explain in view of the location of the $a^3\Sigma^+$ and $b^3\Pi$ states (Figure 6), however, the results obtained in the present study, where the ratio of "$a^3\Sigma^+$" to "$b^3\Pi$" emission first decreases and then levels off, provide some indication of the processes involved. Consistent with observation in all three studies is the direct population of the "$a^3\Sigma^+$" state and subsequent transfer to "$b^3\Pi$". Because of its location at larger internuclear distance, the

'$a^3\Sigma^+$" state should represent the first state encountered during the SiO triplet forming process. At the very least the $a^3\Sigma^+$ and $b^3\Pi$ states should compete on equal ground for the final SiO triplet formed in reaction. Recall (Table 2) that the "$a^3\Sigma^+$" and "$b^3\Pi$" states are strongly coupled and therefore that the transfer from the mixed "$a^3\Sigma^+$" state to the mixed "$b^3\Pi$" state is readily facilitated Thus, while both the "$a^3\Sigma^+$" and "$b^3\Pi$" states may be formed in the initial stages of reaction, our results indicate that the strong coupling between these states promotes significant "$a^3\Sigma^+$" → "$b^3\Pi$" transfer with increasing pressure.

We believe that a significant coupling between the "$a^3\Sigma^+$" and "$b^3\Pi$" states also plays an important role in the pressure dependent behavior observed by Hager et al. Because vibrational deactivation is strongly manifest under their experimental conditions, one finds a substantial population buildup in the lowest vibrational levels of the "$a^3\Sigma^+$" and "$b^3\Pi$" states. That vibrational deactivation is significant in these systems is not surprising since the "$a^3\Sigma^+$" and "$b^3\Pi$" states are quite long-lived[36] (see also following discussion). An increase in the ratio of "$a^3\Sigma^+$" to "$b^3\Pi$" emission intensity results when vibrational relaxation dominates and is enhanced by all other processes in the system. Recall that we observe emission from only the v'=0 level of "$a^3\Sigma^+$." Although some emission from higher v'=1,2,... quantum levels of "$a^3\Sigma^+$" may occur, the dominance of $^3\Pi_1$ - $A^1\Pi_1$ verses $^3\Sigma_1^+$ - $A^1\Pi_1$ coupling (Table 2 and previous discussion) leads to an effective "$b^3\Pi$" - $X^1\Sigma^+$ transition moment which considerably exceeds that for "$a^3\Sigma^+$" - $X^1\Sigma^+$. Therefore the emission from vibrational levels $v' \geq 1$ in "$a^3\Sigma^+$" will underline the more dominant "$b^3\Pi$" emission system. Only the v'=0 level of "$a^3\Sigma^+$" is not overlapped by "$b^3\Pi$". As vibrational relaxation dominates to the extent that the population of the v'=0 level of "$a^3\Sigma^+$" increases significantly relative to "$b^3\Pi$," v'=0-2, the "$a^3\Sigma^+$" emission intensity can increase relative to and dominate "$b^3\Pi$." Relaxation to v'=0, "$a^3\Sigma^+$" is facilitated by the significant coupling between the a and b states. In a strong sense, one observes

relaxation to the lowest vibrational quantum level of the triplet manifold where one might envision the"$a^3\Sigma^+$"and"$b^3\Pi$"states in tandem forming a combined triplet state reservoir.

In summary, the pressure dependent effects associated with the"$a^3\Sigma^+$"and "$b^3\Pi$"states observed in the present study and in the study of Hager et al. can be attributed to a combination of (1) strong coupling between the "$a^3\Sigma^+$" and "$b^3\Pi$" states, (2) the nature of the effective transition moments for "$a^3\Sigma^+$" and "$b^3\Pi$" and (3) at higher pressures, in certain environments, pronounced vibrational relaxation. Based upon our results, the "$a^3\Sigma^+$"/"$b^3\Pi$" intensity ratio levels off when a steady-state $a^3\Sigma^+ - b^3\Pi$ transfer occurs. This is consistent with the negligible changes observed in the study of Linton and Capelle and is only modified when the extent of vibrational relaxation is such as to promote the significant population of the v'=0 level of "$a^3\Sigma^+$".

C. Branching Ratios and Quantum Yield Determinations

The results obtained in the present study in tandem with the lifetime determinations of other workers[36,37] cause us to focus on the meaning of the quantum yield determinations previously made on the Si-N_2O system. Linton and Capelle have measured a total quantum yield on the order of 0.05%. We believe that the measured quantum yield (1) does not reflect the relative populations of the $b^3\Pi$, $a^3\Sigma^+$ and $A^1\Pi$ states and (2) that the magnitude of the total quantum yield does not reflect the actual product yield in this system.

The radiative lifetime associated with the $A^1\Pi$ - $X^1\Sigma^+$ system is 9.6±1 microseconds[37] whereas the estimated radiative lifetime for the $b^3\Pi$ - $X^1\Sigma^+$ system is 48 milliseconds.[36] The ratio of these radiative lifetimes indicates that the branching ratio calculated previously represents a definite lower bound (note previous discussion). Because the radiative lifetimes differ by a factor of 5000, and the $b^3\Pi$ state is quite long-lived, the viewing zone[38] used to assess the relative excited state quantum yields will clearly prejudice measurements of the yield of the $A^1\Pi$ over the $b^3\Pi$ state. The effect will be more pronounced for the "$a^3\Sigma^+$" state whose radiative lifetime is expected to exceed that for "$b^3\Pi$" because of its smaller coupling to the $A^1\Pi$ state.

The extremely long radiative lifetimes for the "$b^3\Pi$" and "$a^3\Sigma^+$" states require that we make use of a very large viewing zone in order to correctly assess the absolute total quantum yield for the Si-N_2O reaction. From the information given in the literature, it does not appear that this requirement has yet been satisfied.[38] Therefore, the measured total quantum yield must represent a lower bound measurement of direct excited triplet state formation. This may have significant implications for the possible use of the Si-N_2O reaction as a visible chemical laser medium.

D. A Possible Chemical Laser Candidate

Much attention has focused on the Sn-N_2O reaction and the production of the low-lying "$a^3\Sigma^+$" state of tin oxide in high quantum yield (~45%). It is[39] thought that lasing action might be initiated on the SnO $a^3\Sigma^+ - X^1\Sigma^+$ band system, specifically on the (0,2), (0,3), and (0,4) transitions at ~5307, ~5532, and ~5799Å. The results obtained in this study indicate, in correlation with the efforts of other workers, that the Si-N_2O system may also represent an equally interesting candidate.

Recently, Davis and other workers[40] have determined the absolute rate coefficients for total product formation in several Group IVA metal oxidations. Their results for N_2O indicate that the rate coefficients increase in the order C > Si > Ge > Sn. The rate coefficient for $Si(^3P)$ with N_2O is $(8.2\pm4) \times 10^{-11}$ cm^3/molecule-sec whereas those for $Sn(^3P_1)$ and $Sn(^3P_2)$ with N_2O are 1.1×10^{-12} and $3.5\pm0.7 \times 10^{-11}$ respectively. This is significant, especially because the Si-N_2O reaction is expected to conserve spin more readily than Sn-N_2O which must involve the heavier intermediate complex. If spin conservation holds (Eq. (1)) and the rate coefficient measured by Davis et al. is indicative of the magnitude of triplet state formation in the Si-N_2O system, this reaction may hold possibilities for the development of a visible chemical laser.

Our interest should focus not only on the possibility of producing copious quantities of triplet state emitters in order to create a population inversion on the intercombination band system but also on the possibility of using vibrational relaxation to produce molecules in the v'=0 level of the "$a^3\Sigma^+$" state (see previous discussion). Because coupling to the ground $^1\Sigma^+$ electronic state appears to be at a minimum for the "$a^3\Sigma^+$" and "$b^3\Pi$" states, the possibility of formulating a system very much analogous to the O_2 ($^1\Delta_g$) - iodine transfer laser may well exist. In other words, one would hope to carry out an efficient energy transfer process

$$SiO(\text{"}a^3\Sigma^+\text{"}, v'=0) + X \longrightarrow SiO(X^1\Sigma^+, v''=2\text{-}7) + X^*$$

where X* preferably represents an atomic species and the energy transfer involves the formation of SiO ground state molecules in one of the vibrational levels v"=2,3,...,7.

Acknowledgement: It is a pleasure to acknowledge helpful discussions with Dr. C. D. Jonah and Professors Stewart Novick and Arthur Fontijn. This work was partly supported by the Scientific Services Program (A.R.O.) and by the Department of Energy, METC.

References

1. H. Bredohl, R. Cornet, I. Dubois, and F. Remy, J. Phys. B. 7, L66 (1974); T. G. Heil, H. F. Schaefer III, J. Chem. Phys. 56, 958 (1972); J. Drowart, A. Pattoret, and S. Smoes, Proc. Brit. Ceram. Soc. 8, 67 (1967); D. L. Hildenbrand, High Temp. Sci. 4, 244 (1972); K. F. Zmbov, L. L. Ames, and J. L. Margrave, High Temp. Sci. 5, 235 (1973); H. Kvande and P. G. Wahlbeck, High Temp.-High Press. 8, 45 (1976); D. L. Hildenbrand and E. Murad, J. Chem. Phys. 51, 807 (1969).

2. R. W. Field, A. Lagerqvist, and I. Renhorn, Phys. Scripta 14, 298 (1976).

3. G. Hager, R. Harris, and S. G. Hadley, J. Chem. Phys. 63, 2810 (1975). G. Hager, L. E. Wilson, and S. G. Hadley, Chem. Phys. Lett. 27, 439 (1974).

4. C. Linton and Gene A. Capelle, Jour. Molec. Spectros. 66, 62 (1977).

5. L. H. Dubois and J. L. Gole, J. Chem. Phys. 66, 779 (1977).

6. A. W. Hanner and J. L. Gole, J. Chem. Phys. 73, 5025 (1977). G. J. Green and J. L. Gole, Chem. Phys. Lett. 69, 45 (1980).

7. G. J. Green and J. L. Gole, Chem. Phys. 46, 67 (1980).

8. J. L. Gole and S. A. Pace, J. Chem. Phys. 73, 836 (1980).

9. J. L. Gole and G. J. Green, Chem. Phys. 69, 357 (1982).

10. S. A. Pace and J. L. Gole unpublished.

11. Silicon was also vaporized from a high purity (Union Carbide) boran nitride crucible.

12. R. W. Field, B. G. Wicke, J. D. Simmons, and S. G. Tilford, J. Molec. Spectros. 44, 383 (1972).

13. H. Hotop, T. A. Patterson, and W. C. Lineberger, Phys. Rev. A8, 762 (1973).

14. The programs used in these calculations were written by Dr. Brian Wicke. See also R. N. Zare, J. Chem. Phys. 40, 1934 (1964).

15. J. L. Gole and R. N. Zare, J. Chem. Phys. 57, 5331 (1972). R. N. Zare, Ber. Bunsenges Physik. Chem. 78, 153 (1974).

16. J. L. Gole and C. L. Chalek, J. Chem. Phys. 65, 4384 (1976).

17. C. L. Chalek and J. L. Gole, Chem. Phys. 19, 59 (1977).

18. D. R. Preuss and J. L. Gole, J. Chem. Phys. 66, 880 (1977).

19. D. L. Hildenbrand, High Temp. Sci. 4, 244 (1972).

20. D. B. Stull and H. Prophet, JANAF Thermochemical Tables, 2nd ed., Natl. Stand. Ref. Data Series, Natl. Bur. Stand. 37 (1971).

21. R. Jones and J. L. Gole, Chem. Phys. 20, 311 (1977).

22. We determine $E_{int}(Si)$ from a statistical average of the $^3P_0(0cm^{-1})$, $^3P_1$ $(77.15cm^{-1})$, and $^3P_2$ $(223.31cm^{-1})$ components of the ground ^3P state.

23. P. J. Dagdigian, H. W. Cruse, and R. N. Zare, J. Chem. Phys. 62, 1824 (1973).

24. C. R. Dickson and R. N. Zare, Chem. Phys. 7, 361 (1975).

25. See discussions in references 7 and 18.

26. K. P. Huber and G. Herzberg, Constants of Diatomic Molecules, Van Nostrand-Reinhold Company, 1979.

27. J. Pliva, J. Molec. Spectros. 12, 360 (1964).

28. L. H. Dubois and J. L. Gole unpublished.

29. Reference 15 and D. M. Lindsay and J. L. Gole, J. Chem. Phys. 66, 3886 (1977); R. C. Oldenborg and J. L. Gole unpublished data.

30. See reference 23 and E. Murad, AFGL-TR-77-0235 Environmental Research Papers. No. 610, October 1977.

31. The N_2 or N_2^+ emission spectrum obtained under reaction conditions is compared to that for room temperature N_2 at low concentrations.

32. The authors are indebted to Stewart Novick for helpful discussions on the subject of increasing the signal-to-noise from electron gun sources.

33. P. Dehmer private communication.

34. R. Kay private communication.

35. Because of the extremely long radiative lifetime of the "$b^3\Pi$" state, it is possible that a small component of "$b^3\Pi$" molecules undergo collision before entering or leaving the viewing zone. See J. L. Gole, D. R. Preuss, and C. L. Chalek, J. Chem. Phys. 66, 548 (1977).

36. B. Meyer, J. J. Smith, and K. Spitzer, J. Chem. Phys. 53, 3616 (1970).

37. W. H. Smith and H. S. Liszt, J. Quant. Spectrosc. Radiative Transfer 12, 505 (1972).

38. For an indication of the viewing zone see J. B. West, R. S. Bradford, J. D. Eversole, and C. R. Jones, Rev. Sci. Instruments 46, 164 (1975); C. R. Jones and H. P. Broida, J. Chem. Phys. 60, 4369 (1974).

39. See for example A. Fontijn, "Kinetic Spectroscopy of Metal Atom/Oxidizer Chemiluminescent Reactions for Laser Applications", Aerochem Report TP-388; W. Felder and A. Fontijn, J. Chem. Phys. 69, 1112 (1978). M. J. Linevsky and R. A. Carabetta, "Chemical Laser Potential of Selected Group IV-A Metal Oxides", AFWF-TR-77-121.

40. P. M. Swearengen, S. J. Davis, and T. M. Niemczyk, Chem. Phys. Letters 55, 274 (1978). See also references to previous work in Table 1 of this article.

Table 1

Measured SiO Bandhead Positions and Vibrational Assignments

$b^3\Pi - X^1\Sigma^+$

bandhead assignment (v',v'') [a]	bandhead origin λ_{air} (Å)	bandhead origin ν_{vacuum} (cm^{-1})	relative intensity [g]
(2,0)	2791.2	35816	---
(3,1)	2811.6	35556	45.9
(4,2)	2832.6	35293	54.0
(5,3)	2853.7	35032	35.6
(1,0) [b,c]	2869.2	34843	55.2
(2,1) [b,c]	2889.8	34594	44.6
(3,2) [b]	2911.2	34340	25.0
(4,3)	2932.4	34092	12.6
(0,0) [b,c]	2953.7	33846	100
(1,1)	2973.8	33617	33.6
(2,2)	2995.2	33377	---
[(4,4)] [d]	3038.9	32897	---
(0,1) [b,c]	3065.2	32615	90.1
(1,2) [b,c]	3085.8	32397	82.0
(2,3) [b,c]	3107.3	32172	59.8
(3,4) [b]	3129.2	31948	27.2
(4,5)	3151.3	31724	12.1
(0,2) [b,c]	3184.0	31398	18.8
(1,3) [b,c]	3205.2	31190	24.9
(2,4) [b,c]	3226.9	30981	34.4
(3,5) [b]	3249.2	30768	22.5
(4,6) [b]	3272.0	30554	25.1
(5,7) [b]	3295.8	30333	17.4
(0,3) [b]	3310.9	30195	12.6
(6,8) [b]	3320.2	30110	14.0
(1,4) [b,c]	3332.5	29999	11.5
(2,5) [b]	3354.8	29799	17.6
(3,6) [b]	3377.6	29598	11.4
(4,7) [b]	3401.0	29395	14.1
(5,8) [b]	3425.3	29186	16.3
(6,9) [b]	3450.5	28973	18.3

Measured SiO Bandhead Positions and Vibrational Assignments

$b^3\Pi - X^1\Sigma^+$ (continued)

bandhead assignment $(v',v")$ [a]	bandhead origin λ_{air} (Å)	bandhead origin ν_{vacuum} (cm^{-1})	relative intensity [g]
(7,10) [b]	3475.9	28761	13.4
(9,12) [e]	3530.6	28316	(6.4)
(4,8) [b]	3538.9	28249	6.4
(5,9) [b]	3564.1	28050	6.8
(6,10) [b]	3589.6	27850	9.5
(7,11) [b]	3616.1	27646	11.0
(8,12) [b]	3643.6	27438	(5.6)
(9,13)	3671.9	27226	5.2
(10,14)	3699.4	27024	2.9
(5,10)	3712.6	26928	2.9
(6,11)	3739.5	26734	3.4
(7,12)	3765.9	26547	4.1
(8,13) [f]	3792.2	26362	4.6
(10,15)	3849.7	25969	3.3
[(11,16)] [d]	3883.7	25741	2.0
[(7,13)] [d]	3926.8	25459	2.2
[(8,14)] [d]	3952.8	25291	2.7

a. Bandhead corresponding to $^3\Pi_1$ component

b. Previously observed by Linton and Capelle reference 4

c. Previously observed by Hager et al. reference 3

d. Weak feature - wavelength approximate

e. (8,11) band under (0,4) band of $a^3\Sigma^+ - X^1\Sigma^+$ band system

f. (9,14) band under (0,6) band of $a^3\Sigma^+ - X^1\Sigma^+$ band system

g. Corrected for phototube response

Table 2
Nonzero Matrix Elements of Spin-Orbit Operator Coupling
Low-Lying States of SiO (cm^{-1})

$\langle A^1\Pi_1, |H_{So}| a^3\Sigma_1^{+\pm}, v' \rangle = 1/4a^a \langle v|v' \rangle = 43 \langle v|v' \rangle$

$\langle A^1\Pi_1^{\pm}, v|H_{So}|b^3\Pi_1^{\pm}, v' \rangle = a_z^b \langle v|v' \rangle = 146 \langle v|v' \rangle$

$\langle E^1\Sigma_o^+, v|H_{So}|b^3\Pi_o^{\pm}, v' \rangle = -1/4(2)^{1/2}a \langle v|v' \rangle = -61\langle v|v' \rangle$

$\langle b^3\Pi_1^{\pm}, v|H_{So}|a^3\Sigma_1^{+\pm}, v' \rangle = 1/4a\langle v|v' \rangle = 43\langle v|v' \rangle$

$\langle e^3\Sigma_1^{-\pm}, v|H_{So}|b^3\Pi_1^{+\pm}, v' \rangle = -1/4a \langle v|v' \rangle = -43\langle v|v' \rangle$

$\langle e^3\Sigma_1^-, v|H_{So}|A^1\Pi_1, v' \rangle = -1/4a \langle v|v' \rangle = -43\langle v|v' \rangle$

$\langle {}^3\Pi_2^{\pm}, v|H_{So}|{}^3\Pi_2^{\pm}, v' \rangle = A({}^3\Pi) = 1/2a_z \delta_{v,v'} = 73\delta_{v,v'}$

$\langle {}^3\Pi_o^{\pm}, v|H_{So}|{}^3\Pi_o^{\pm}, v' \rangle = -A({}^3\Pi) = -1/2a_z \delta_{v,v'} = -73\delta_{v,v'}$

---

a. a defined in text.

b. a_z defined in text.

Table 3

Observed Bandheads for the

$D\text{-}X\,^3\Delta$ Bandsystem of TiO[a]

Observed Band Head (v',v")	Wavelength (Å)
(2,1)	2955
(1,0)[b]	3049
(0,0)[b]	3148
(0,1)[b]	3250
(0,2)	3359
(0,3)	3473
(0,4)	3595

a. L.H. Dubois and J.L. Gole, J. Chem. Phys. 66, 779 (1977).

b. C.M. Pathak and H.B. Palmer, J. Mol. Spectrosc. 33, 137 (1970).

Table 4

Energy Balance Discrepancies in $M+N_2O$ Reactions

Reaction	$E_{Available}$	Measured MO Excitation	$E_{int}(MO)$ (cm^{-1})	ΔE[a]
$Sc(^2D)+N_2O$[b]	45856 cm^{-1}[c]	Short Wavelength Limit ($C^2\Pi-X^2\Sigma^+$) (3000Å)	33324 cm^{-1}	12532 cm^{-1}
$Y(^2D)+N_2O$[b]	48154 cm^{-1}[c]	Short Wavelength Limit ($C^2\Pi-X^2\Sigma^+$) (3000Å)	33324 cm^{-1}	14830 cm^{-1}
$La(^2D)+N_2O$[d]	55862 cm^{-1}[c]	LaO*,$D^2\Sigma^+$,v'=17[e]	39400 cm^{-1}	16462 cm^{-1}
$Ba(^1S)+N_2O$[f]	33652 cm^{-1}	Short Wavelength Limit (4000Å)	24993 cm^{-1}	8659 cm^{-1}
$Ca(^3P)+N_2O$[g,h]	34792 cm^{-1}	Short Wavelength Limit (3850Å)	25967 cm^{-1}	9095 cm^{-1}
$Sr(^3P)+N_2O$[h]	37553 cm^{-1}	Short Wavelength Limit (3700Å)	27019 cm^{-1}	10534 cm^{-1}

a. $E_{Available} - E_{int}(MO)$

b. Reference 17.

c. $D_o^o(MO) + E_{int}(M) + E_{int}(N_2O) + E_T^i - D(N-NO)$. See text for definitions.

d. Reference 16.

e. J. L. Gole unpublished data.

f. Data from C. D. Jonah, R. N. Zare, and Ch. Ottinger, J. Chem. Phys. 56, 263(1972).

g. Data from J. A. Irwin and P. J. Dagdigian, J. Chem. Phys. 74, 6178(1981).

h. Data from B. E. Wilcomb and P. J. Dagdigian, J. Chem. Phys. 69, 1779(1978). See also P. J. Dagdigian, Chem. Phys. Lett. 55, 239(1978).

Figure Captions

Figure 1: (a) Chemiluminescent spectrum in the region 2850-3600Å resulting from the reaction $Si + N_2O \rightarrow SiO^* + N_2$ recorded under single collision conditions. The spectrum in this region corresponds to the SiO "$b^3\Pi$" - $X^1\Sigma^+$ band system. The bandheads are designated (v',v"). Spectral resolution is 10Å. (b) Higher resolution scan of (0,0) and (0,1) bands for SiO"$b^3\Pi$" - $X^1\Sigma^+$ system showing $^3\Pi_1$ and $^3\Pi_0$ component emission and dominant intensity associated with $^3\Pi_1$ component. Spectral resolution is 0.5Å. See text for discussion.

Figure 2: Chemiluminescent spectrum in the region 3550-4200Å resulting from the reaction $Si + N_2O \rightarrow SiO^* + N_2$ recorded under single collision conditions. Emission from high vibrational levels of SiO "$b^3\Pi$" and the v' = 0 level of SiO "$a^3\Sigma^+$" is monitored. The bandheads are designated (v',v"). Spectral resolution is 10Å. See text for discussion.

Figure 3: Chemiluminescent spectrum in the region 2350-2950Å resulting from the reaction $Si + N_2O \rightarrow SiO^* + N_2$ recorded under single collision conditions. The high energy end of the SiO "$b^3\Pi$ - $X^1\Sigma^+$ band system extends into the SiO $A^1\Pi$ - $X^1\Sigma^+$ emission system. The bandheads in both systems are designated (v',v"). Spectral resolution is 15Å. See text for discussion.

Figure 4: Chemiluminescent spectrum in the region ~2150-2550Å resulting from the reaction $Si + N_2O \rightarrow SiO^* + N_2$ recorded under single collision conditions. The observed spectrum corresponds to the SiO $A^1\Pi$ - $X^1\Sigma^+$ band system. Bandheads are designated (v',v"). Spectral resolution is 20Å. See text for discussion.

igure 5: Chemiluminescent spectrum in the region 2500-7500Å for the reaction Ti + $N_2O \rightarrow TiO^* + N_2$ taken under single collision conditions. The unresolved features correspond in large part to emission from the $B^3\Pi$ and $C^3\Delta$ states of TiO. Emission from the TiO D state has been resolved in this and separate scans and bands identified (Table 2). Bandheads for the D - $X^3\Delta$ system are designated (v',v"). Spectral resolution is 10Å. See text for discussion.

igure 6: Potential curves (RKR) for the ground and select low-lying states of SiO generated from spectral data given in reference 2.

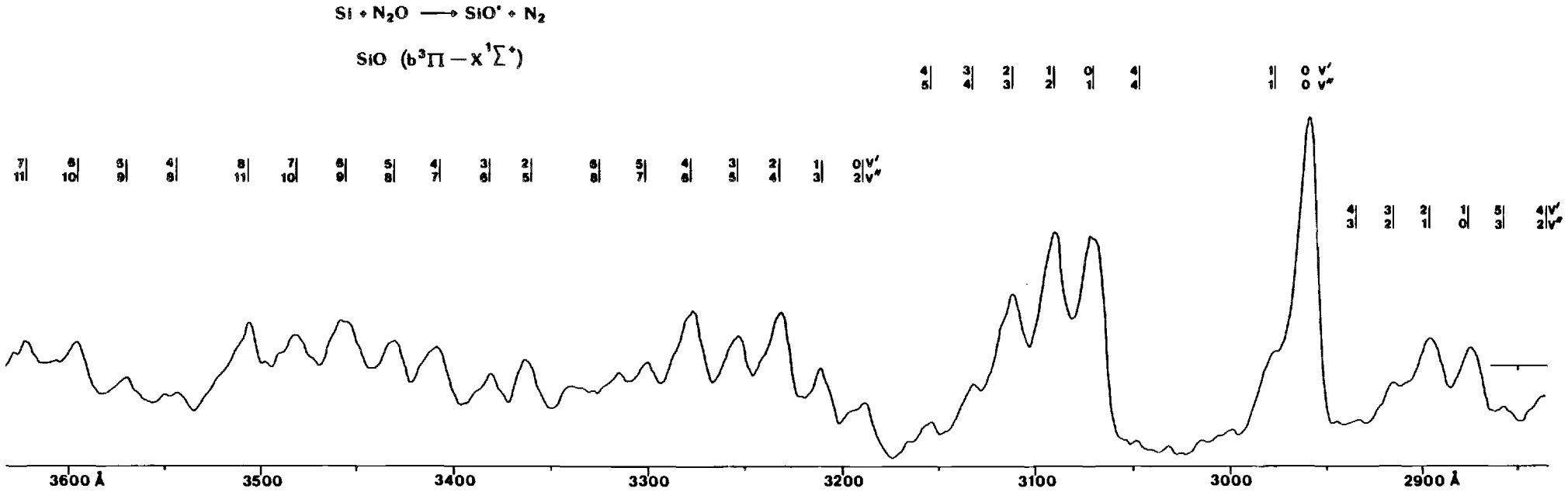
Si + N2O ⟶ SiO* + N2
SiO (b3Π − X1Σ+)
3600 Å
3500
3400
3300
3200
3100
3000
2900 Å

Figure 1(a)

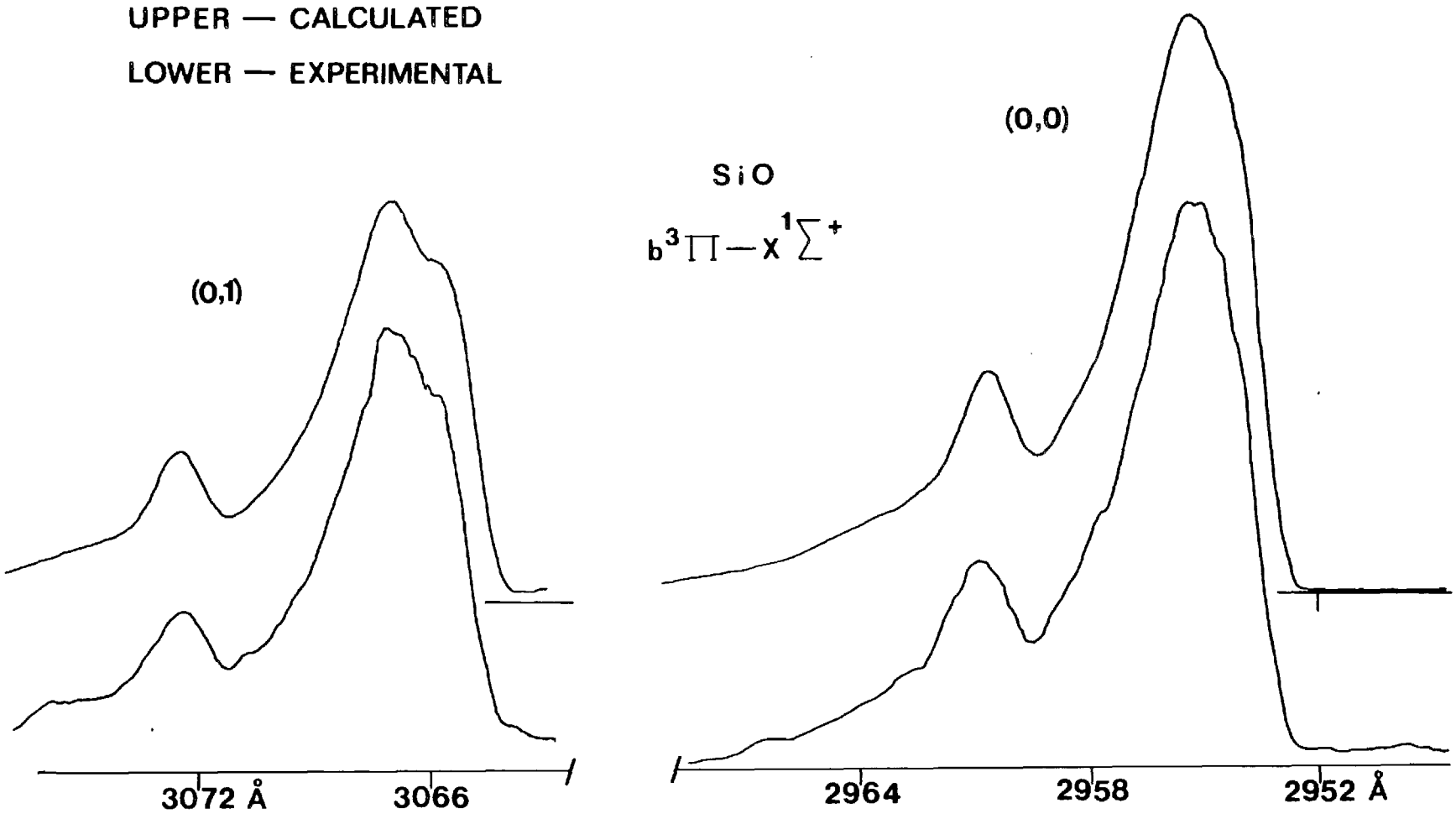
UPPER — CALCULATED
LOWER — EXPERIMENTAL
(0,1)
SiO
$b^3\Pi - X^1\Sigma^+$
(0,0)
3072 Å
3066
2964
2958
2952 Å

Figure 1(b)

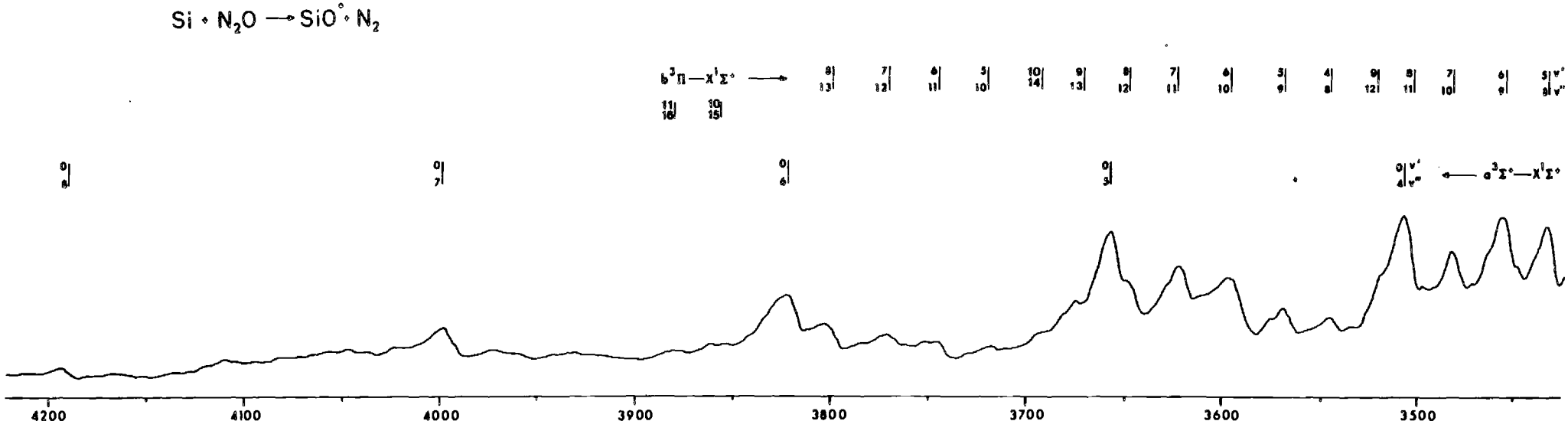
Si + N2O → SiO* + N2
b3Π—X1Σ+ →
a3Σ+—X1Σ+
4200
4100
4000
3900
3800
3700
3600
3500

Figure 2

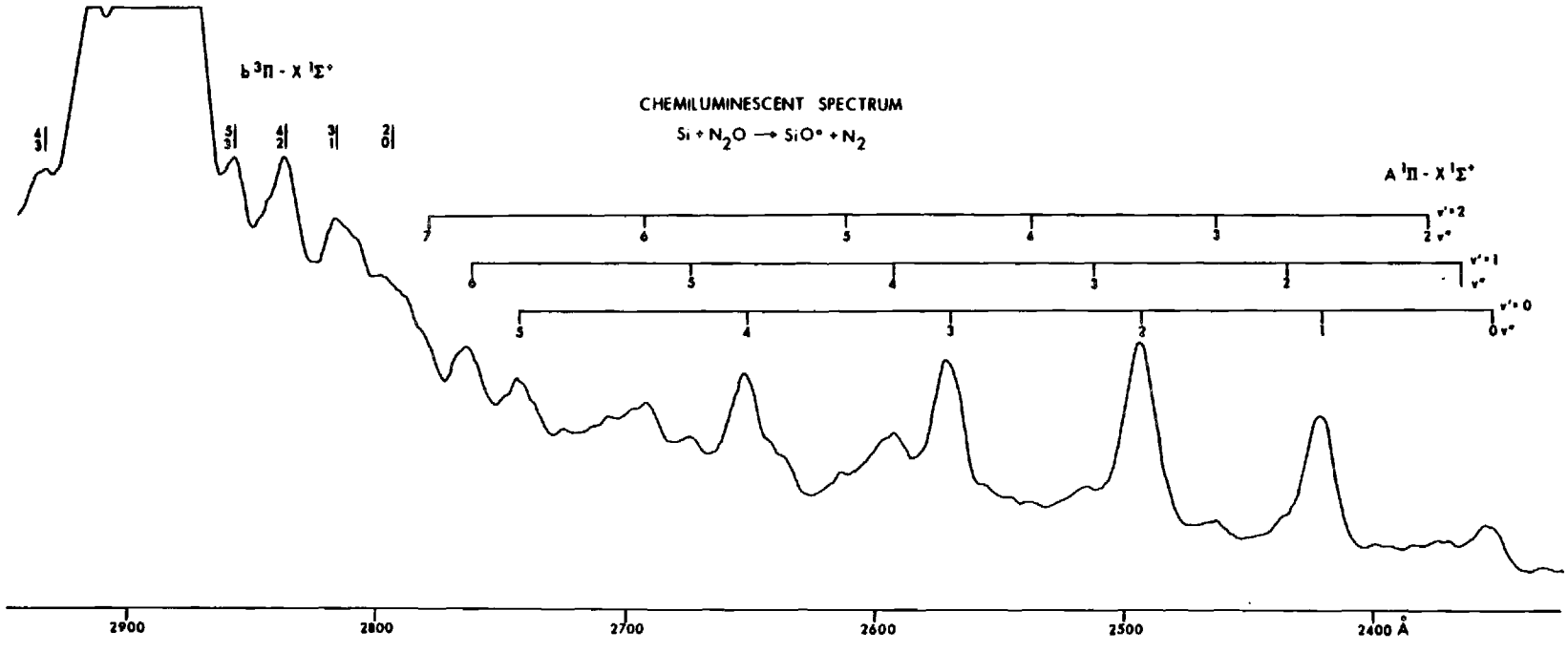
CHEMILUMINESCENT SPECTRUM
$Si + N_2O \rightarrow SiO^* + N_2$
$b\,^3\Pi - X\,^1\Sigma^+$
$A\,^1\Pi - X\,^1\Sigma^+$
v'=2
v'=1
v'=0
v"
2900
2800
2700
2600
2500
2400 Å

Figure 3

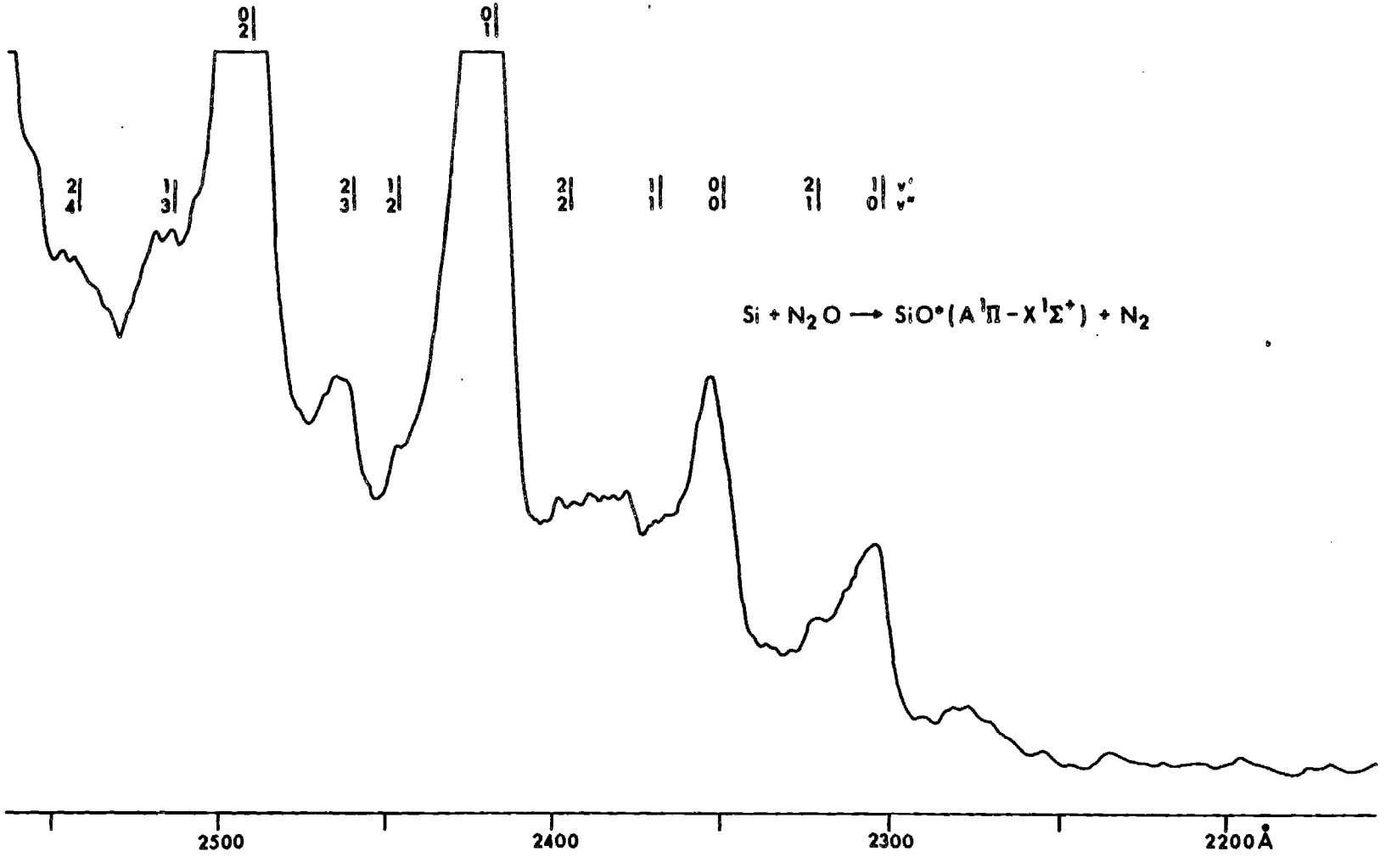
0 2
0 1
2 4
1 3
2 3
1 2
2 2
1 1
0 0
2 1
1 0
v' v''
Si + N2O → SiO*(A 1Π - X 1Σ+) + N2
2500
2400
2300
2200Å

Figure 4

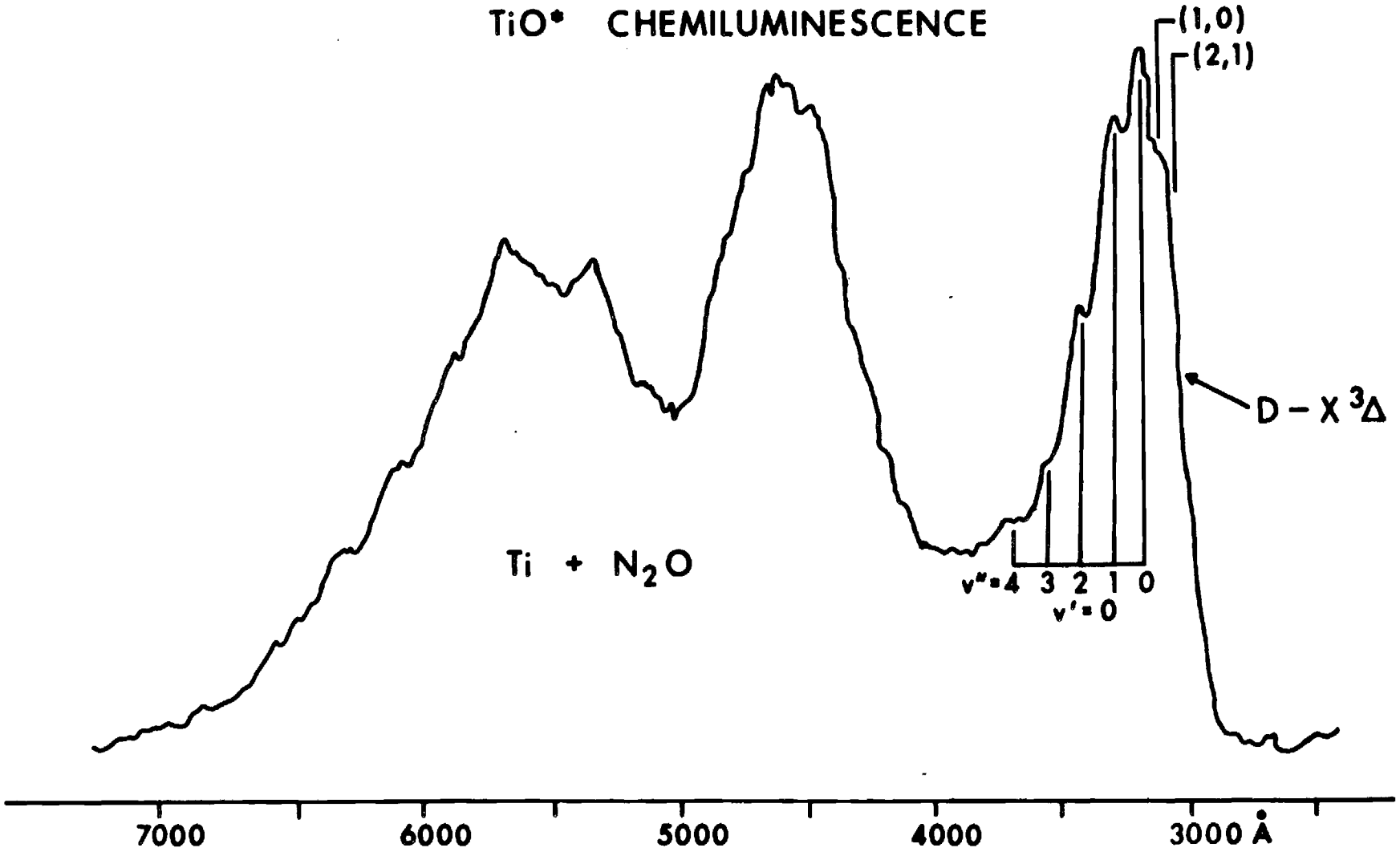
TiO* CHEMILUMINESCENCE
(1,0)
(2,1)
D – X ³Δ
Ti + N₂O
v''=4 3 2 1 0
v'=0
7000
6000
5000
4000
3000 Å

Figure 5

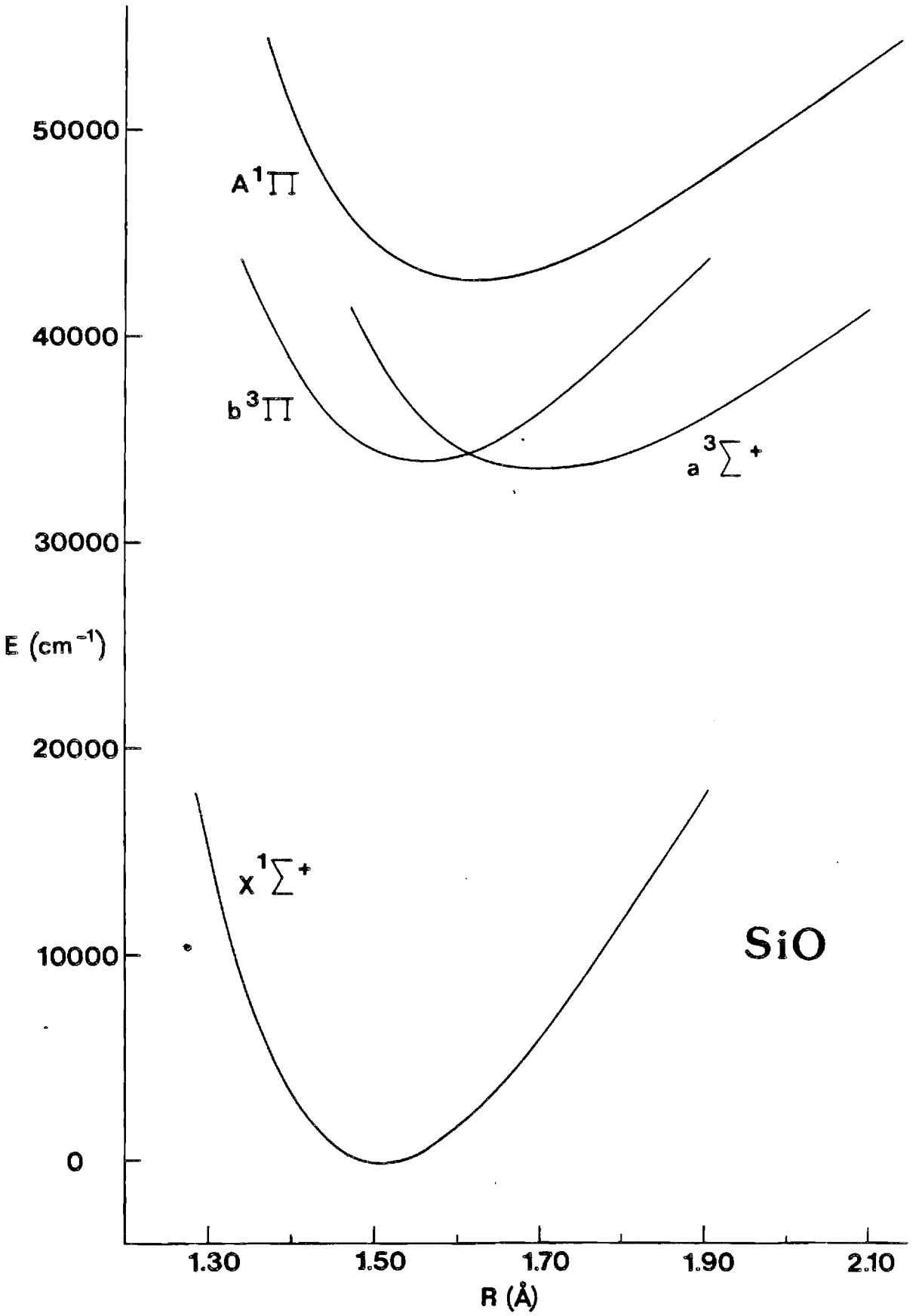
50000
40000
30000
20000
10000
0
E (cm⁻¹)
A ¹Π
b ³Π
a ³Σ⁺
X ¹Σ⁺
SiO
1.30
1.50
1.70
1.90
2.10
R (Å)

Figure 6

APPENDIX D

ENERGY BALANCE AND BRANCHING RATIOS FOR THE CHEMILUMINESCENT Si-NO_2 REACTION: FORMATION OF SiO $a^3\Sigma^+$, $v' \geq 0$, AND ULTRAFAST $a^3\Sigma^+ - b^3\Pi$ E-E ENERGY TRANSFER

R. Woodward, J. S. Hayden, and J. L. Gole

High Temperature Laboratory
Center for Atomic and Molecular Science
and School of Physics
Georgia Institute of Technology
Atlanta, Georgia 30332

Abstract

Silicon atoms react under single collision conditions with NO_2 to yield intense chemiluminescent emission from the SiO $a^3\Sigma^+ - X^1\Sigma^+$ and $b^3\Pi - X^1\Sigma^+$ intercombination band systems and weak emission from the $A^1\Pi - X^1\Sigma^+$ band system. While the cross section for formation of the SiO $a^3\Sigma^+$ and $b^3\Pi$ states appears to be notably greater than that for the far more exothermic Si + N_2O reaction, the observed intercombination emissions from the Si-NO_2 reaction involve far fewer $b^3\Pi$ vibrational quantum levels and hence considerably less spectral overlap. This facilitates the first observation of emission from SiO $a^3\Sigma^+$ vibrational quantum levels, $v' > 0$. Pressure dependent studies demonstrate that the SiO $A^1\Pi$ and $b^3\Pi$ ($P_{oxidant} < 3 \times 10^{-4}$ torr) states are formed in processes first order in oxidant while some collision induced population of the very long-lived SiO $a^3\Sigma^+$ state ($v' = 0$) may occur in combination with direct product formation even at very low pressures. Temperature dependent studies are used to indicate that reaction has occurred with ground state Si ^3P atoms and that the SiO $b^3\Pi$ ($E_A = 4.0 \pm 1.1$ kcal/mole) and $a^3\Sigma^+$ ($E_A \approx 1.8 \pm 1.2$ kcal/mole) states are formed with a considerably lower activation energy than the $A^1\Pi$ state ($E_A = 7.4 \pm 1.2$ kcal/mole). The activation energy for formation of the $a^3\Sigma^+$ state, which may be negligible, is significantly smaller than that for formation of the $b^3\Pi$ state, providing some evidence for a dynamical process involving formation of $a^3\Sigma^+$ at large internuclear distance and possible subsequent transfer to $b^3\Pi$ rovibronic levels to which the $a^3\Sigma^+$ state is strongly coupled. Higher pressure studies also provide support for this mechanism. An analysis of the weak emission from the SiO $A^1\Pi$ state leads to the determination of a lower bound ($D_0^o(SiO) \geq 186.7 \pm 1.7$ kcal/mole) for the SiO bond energy. The controlled extension of the outlined single collision studies to elevated

pressures (1) leads to a quenched SiO $A^1\Pi$ emission feature, (2) provides additional information on SiO $a^3\Sigma^+$ vibrational quantum levels, $v' > 0$ and (3) indicates, through a comparison of single and multiple collision chemiluminescent spectra, the presence of a significant ultrafast E-E transfer between the SiO $a^3\Sigma^+$ and $b^3\Pi$ states, the dominant intramolecular process corresponding to SiO $a^3\Sigma^+$, $v' = 3 + Ar \rightarrow$ SiO $b^3\Pi$, $v = 2 + Ar$.

Introduction

Because of the conception, based on reactant-product correlations, that the Si-N_2O reaction, through spin conservation, might provide a means for selectively producing excited electronic triplet states, efforts[1-3] have focused on the characterization of this metathesis. The results have not only provided a wealth of information but also raised several questions concerning the nature of (1) the SiO triplet states formed in reaction and the coupling between these states and (2) the dynamics of the Si-N_2O reaction. Silicon reacts with N_2O in a very exothermic process liberating 6.74 eV of energy of which only a maximum of 80% can be accounted in product SiO internal excitation. As we have exemplified in the previous discussion,[3] under single collision conditions, the significant energy release can result in a rather complicated and somewhat overlapped SiO spectrum. Fortunately the magnitude of the SiO bond energy provides the opportunity to study an alternate, far less exothermic, metathesis whose chemiluminescent signature is far less complicated and whose rate coefficient should exceed that for Si + N_2O.[4]

We have approached the study of the Si-NO_2 reaction with the view of both simplifying and enhancing that information garnered from the study of the Si + N_2O metathesis.[3] The Si + NO_2 reaction is expected to proceed with a higher cross section and produce SiO molecules with lower internal (rovibrational) excitation. In addition, there is reason to believe that the Si-NO_2 metathesis should also proceed readily via the triplet forming process

$$Si(^3P) + NO_2(^2A_1) \rightarrow SiO(a^3\Sigma^+, b^3\Pi, \ldots) + NO(^2\Pi), \qquad (1)$$

although the formation of ground state $X^1\Sigma^+$ SiO is not precluded by spin conservation. Questions arise regarding the relative branching ratios for formation in the $a^3\Sigma^+$ and $b^3\Pi$ states (versus Si + N_2O). Under single collision conditions, the Si-NO_2 metathesis which is $\sim$ 5.24 eV exothermic yields emission corresponding to the SiO $a^3\Sigma^+ - X^1\Sigma^+$ and $b^3\Pi - X^1\Sigma^+$ intercombination bands and very weak emission

corresponding to the $A^1\Pi$ - $X^1\Sigma^+$ band system. The combination of single and multiple collision studies demonstrates that the $A^1\Pi$ state is populated as a result of the reaction of silicon atoms in the high energy tail of the silicon beam thermal distribution. The extension of the present single collision studies to multiple collision conditions thermalizing the silicon atoms to $\sim$ 600 K results in the complete quenching of the $A^1\Pi$ - $X^1\Sigma^+$ fluorescence.[5] An analysis of the weak emission from the $A^1\Pi$ state leads to the evaluation of a lower bound for the SiO bond energy (186.7 $\pm$ 1.7 kcal/mole) in good agreement with mass spectroscopy.[6]

Measured activation energies for formation of the $a^3\Sigma^+$, $b^3\Pi$, and $A^1\Pi$ states reflect the probable validity of the spin conservation implied in reaction (1) and provide some evidence for the formation of the $a^3\Sigma^+$ state at large internuclear distance and subsequent transfer to $b^3\Pi$. Because of its higher cross section and significantly smaller reaction exoergicity, the Si-NO_2 reaction provides the first opportunity to observe $a^3\Sigma^+$ vibrational quantum levels, $v \geq 1$. Through controlled extension to multiple collision conditions we are able to further expand our knowledge of the $a^3\Sigma^+$ state and find evidence for ultrafast energy transfer among the $a^3\Sigma^+$ and $b^3\Pi$ states.

Experimental

Silicon atoms distributed thermally among the ground state $^3P_{0,1,2}$ components were reacted with NO_2 to produce an intense blue emission in a process exothermic by $\sim$ 5.25 eV. The metal beam was formed under single collision conditions in a beam-gas arrangement using two configurations, the first of which was identical to that described previously for our study of the Si-N_2O metathesis.[3] A second set of single collision experiments involved an oven configuration similar to that used previously for multiple collision studies;[7] the Si-NO_2 reaction was studied over the pressure range 10^{-5} - 10^{-3} torr. Silicon was vaporized over the range 1600 - 2050^oC from a c.s. grade graphite crucible. The capped crucible was machined to fit inside a commercial tungsten basket heater (R. D. Mathis, Long Beach, CA) which was wrapped with several layers of zirconia, ZrO_2, cloth (Zircar Products, Florida, NY). The silicon vapor was reacted directly with NO_2.

We have studied the temperature dependence of the chemiluminescence from the Si-NO_2 reaction under single collision conditions.[8] In order to carry out these careful temperature dependent studies, we have employed a two step procedure.[8] Calibrated tungsten-rhenium thermocouples (Omega Engineering, Stamford, CT) protected by a vapor deposited tungsten sheath (Ultramet, Pacoima, CA) were first used to calibrate a Leeds and Northrup optical pyrometer. All temperatures were then measured both with the pyrometer and with the calibrated thermocouple (simultaneously), the agreement of thermocouple and pyrometer measurements being required. Temperatures were measured to $\pm$ 5^oC.

Multiple collision studies were carried out with precisely that device used previously for our study of the Si-N_2O reaction. Here the metal beam was entrained in argon and this mixture subsequently oxidized. These experiments represent a direct extension of the second single collision beam-gas configuration described above in a controlled manner to multiple collision conditions.

Typical operating pressures were on the order of 10-50 μ of oxidant and 1 to 1.2 torr argon.

Again, spectra were taken with a 1 meter Czerny-Turner scanning spectrometer operated in first order with a Bausch and Lomb 1200 groove/mm grating blazed at 5000 Å. An RCA 4840 photomultiplier tube was used in these experiments. The photomultiplier signal was detected with a Keithley 417 fast picoammeter whose output signal (partially damped) drove a Leeds and Northrup stripchart recorder. All spectra were wavelength calibrated.

Chemiluminescent Spectra

The Si-NO_2 reaction is characterized by an intense blue chemiluminescence corresponding to the process

$$Si(^3P_{0,1,2}) + NO_2(^2A_1) \rightarrow SiO(a^3\Sigma^+, b^3\Pi, A^1\Pi) + NO(^2\Pi). \qquad (2)$$

The emission spectra which, under single collision conditions, extend from ~ 2400 to 4200 Å (Figs. 1,4-6) consist of contributions from the $A^1\Pi$ - $X^1\Sigma^+$, "$b^3\Pi$" - $X^1\Sigma^+$, and "$a^3\Sigma^+$" - $X^1\Sigma^+$ band systems of SiO and are dominated by the "$b^3\Pi$" - $X^1\Sigma^+$ band system onsetting at 2800 Å. The "$a^3\Sigma^+$" - $X^1\Sigma^+$ and "$b^3\Pi$" - $X^1\Sigma^+$ transitions which are nominally spin-forbidden borrow intensity through spin-orbit mixing with low-lying $A^1\Pi$ and $E\ ^1\Sigma_o^+$ states.[3] The "$a^3\Sigma^+$" and "$b^3\Pi$" states also couple to each other and hence form a partially mixed triplet manifold with neither state of pure Σ or Π character.[3] Hence they are placed in quotes.

A significant change is observed when the low pressure studies are extended to multiple collision conditions (Figs. 2-4). The $A^1\Pi$ - $X^1\Sigma^+$ band system is completely quenched and the multiple collision spectrum is dominated by the "$a^3\Sigma^+$" - $X^1\Sigma^+$ band system (Fig. 2).

a. "$a^3\Sigma^+$" - $X^1\Sigma^+$

Readily resolvable features for the "$a^3\Sigma^+$" - $X^1\Sigma^+$ band system extend from 3300 to 4200 Å. Both the low pressure (Figs. 1, 5) and multiple collision (Figs. 2,3) spectra are strongly dominated by a single progression arising from the v' = 0 level of the $a^3\Sigma^+$ state. As Figures 3 and 5 demonstrate, the Si-NO_2 reaction which is possessed of a larger cross section and smaller reaction exoergicity than the corresponding N_2O metathesis, provides the first experimental information on vibrational levels v' > 0 of the $a^3\Sigma^+$ state (considerably more intense and less overlapped spectra). Therefore, using the Si + NO_2 metathesis, it has been possible to confirm and somewhat refine the spectroscopic constants for the $a^3\Sigma^+$ state predicted by Field et al.[9] and complement the mapping partially determined by Linton and Capelle.[2]

b. $b^3\Pi$ - $X^1\Sigma^+$

Emission features corresponding to the "$b^3\Pi$" - $X^1\Sigma^+$ band system extend from ~ 2750 to 3450 Å under single collision conditions (Figs. 1,4,5). The spectra correspond to emission from $b^3\Pi$ quantum levels v' = 0 - 4. Under multiple collision conditions, the spectra are considerably modified, extending from ~ 2900 to 3350 Å (Figs. 2-4), and the spectrum is strongly dominated by emission from the v' = 0 and 2 levels although some v' = 1 emission is also evident. The dominance of the v' = 0 and 2 emission appears to result from a combination of vibrational relaxation (v' = 0) and from ultrafast energy transfer (v' = 2) among the $a^3\Sigma^+$ and $b^3\Pi$ states.

c. $A^1\Pi$ - $X^1\Sigma^+$

The $A^1\Pi$ - $X^1\Sigma^+$ emission features observed only under single collision conditions in this study are depicted in Figure 6. The A-X emission characterizing the Si-NO_2 reaction is considerably weaker than that from the $a^3\Sigma^+$ and

$b^3\Pi$ states and appears to result almost entirely from the reaction of silicon atoms in the high energy tail of their thermal distribution (T_{Si} = 2170 K). Emission from vibrational quantum levels v' = 0,1,2 is observed.

Reaction Kinetics

A. Pressure Dependences

We find that the observed chemiluminescent emission from the $A^1\Pi$ and $b^3\Pi$ states of SiO increases linearly with oxidant pressure over the range 3×10^{-5} to 6×10^{-4} torr indicating that these states are formed in a process first order in NO_2. The a-X emission features (v' = 0 emission) while dominated by direct formation in a process first order in silicon and first order in oxidant at the lowest pressures do display some nonlinear increase for pressures in excess of 1×10^{-4} torr. The radiative lifetime of the $a^3\Sigma^+$ state is probably well in excess of 10^{-2} seconds[10] while the mean time between collisions at 10^{-4} torr is on the order of 10^{-3} seconds. Therefore, a molecule in the $a^3\Sigma^+$ state should undergo several collisions before radiating. The monitored modification of the form of the pressure dependent behavior will be dependent not only on the rate of vibrational deactivation but also on the dimensions of the viewing zone[3] through which one monitors the emission from the long-lived $a^3\Sigma^+$ state.

B. Temperature Dependences - SiO ($A^1\Pi$,$a^3\Sigma^+$,$b^3\Pi$)

The results of temperature dependence studies for the Si-NO_2 reaction are shown in Figure 7. The $A^1\Pi$ emission was monitored at 2650 Å corresponding predominantly to an overlap of the (0,4) and (1,5) bands of the $A^1\Pi - X^1\Sigma^+$ band system. The $a^3\Sigma^+$ emission spectrum was monitored at 3650 Å corresponding to the (0,5) band of the "$a^3\Sigma^+$" - $X^1\Sigma^+$ band system. The $b^3\Pi$ emission system

was monitored at 3100 A corresponding to an overlap of bands in the (0,1) sequence of the "$b^3\Pi$" - $X^1\Sigma^+$ band system. In Figure 7((a),(b),(c)) we plot ℓnI vs. $1/T_B$ for the outlined selection of data. Here I is the chemiluminescent intensity and T_B is the beam (crucible) temperature. Data gathered in two runs for each band system is presented in Table I. The slope and linearity of the ℓnI vs. $1/T_B$ plots shows that the Si - NO_2 reaction is first order in metal flux.

Recently, a relation between the temperature dependence of the chemiluminescent intensity and the parameters of a beam-gas experiment has been formulated.[8(a)] It is

$$-R \frac{d(\ell nI)}{d(1/T_B)} = \Delta H_{vap} - R_{T_B} + E_A(d(1/T_{eff})/d(1/T_B)) \qquad (3)$$

where E_A is the Arrhenius activation energy for the formation of the product whose chemiluminescence is monitored, ΔH_{vap} is the enthalpy of vaporization for the metal reacting to produce the observed chemiluminescence and

$$T_{eff} = (m_B T_G + m_G T_B)/(m_G + m_B) \qquad (4)$$

where T_G is the temperature of the gas (nitrogen dioxide) and m_B and m_G are the masses of the beam atoms and gas molecules, respectively.

Equation (3) may take into account the effect of low-lying electronic states[11] and possible reactions of dimeric and trimeric species all of which must be considered in the present study. The nature of the analysis[11] depends upon which states of the metal react to produce the observed chemiluminescence.

At 2250 K (the upper limit of the temperature dependent studies - Table I) in excess of 99% of the reacting atoms are in the ground ^3P state of silicon and the single collision reaction (2) gives rise to $A^1\Pi$, $b^3\Pi$, or $a^3\Sigma^+$ chemiluminescence. The overwhelmingly probability for ^3P atom reaction as the source

of the chemiluminescence can be demonstrated directly from the plots in Figure 7. In general, we expect E_A to be positive for reactions yielding chemiluminescence. Thus from equation (3)

$$-Rd\ell nI/d(1/T_B) > \Delta H_{vap} - RT_B \qquad (5)$$

We carry out a linear least squares analysis of the ℓnI vs. $1/T_B$ data. T slope of the plot for the $A^1\Pi$ state in Figure 7(a) is -50877 $\pm$ 591K, leading to value 101.1 $\pm$ 1.2 kcal/mole for $-Rd(\ell nI)/d(1/T_B)$. Summing the slope energy and the value of RT_B over the temperature range of the experiment, we obtain a rigorous upper bound to ΔH_{vap}. Values obtained for two studies of emission from the $A^1\Pi$ state are given in column 2 of Table I.

The average T_B over the temperature range of the experiments was 2035K. At these temperatures, the heat of vaporization for the equilibrium atomic vapor is 95.1 kcal/mole, only a few kcal/mole less than the observed value of $-Rd(\ell nI)/d(1/T_B)$ for all of the slope heats presented in column 2 of Table I. The equilibrium vapor consists of silicon atoms in the ground ^3P and excited ^1D states[12] so that ΔH_{vap} for a vapor composed solely of ground state atoms will be slightly smaller. On the other hand, $\Delta H_{vaporization}$ for forming exclus ^1D atoms will be considerably higher ($\approx$ 18 kcal/mole).[12] The average value of over the range of the temperature dependence studies is $\approx$ 4.1 kcal/mole; thus the inequality (5) holds for reaction of ground state atoms but it does not hold for reaction of excited ^1D atoms.

Similar arguments can be envoked when considering possible silicon dimer and trimer reaction with heats of vaporization being 112.4[12] and 104.5[12] kcal/mole, respectively. The inequality (5) does not hold if the metathesis producing chemiluminescence results from dimer or trimer reaction. The violation of the inequality (5) is even more pronounced if we consider the possible reaction of excited state dimers and trimers. The observed chemiluminescence is due overwhelmingly to reaction of ground state ^3P silicon atoms

C. "Activation Energies" for Formation of SiO^* $A^1\Pi$, $a^3\Sigma^+$, $b^3\Pi$

In order to evaluate the activation energies for formation of SiO^* $A^1\Pi$, $a^3\Sigma^+$, and $b^3\Pi$ we rearrange the expression (3) in a manner previously described[8] to obtain

$$E_A \approx -d(R\ell n(IT_B) + \Delta H_{vap}(T_B^{mean})/T_B)/d(1/T_{eff}) \qquad (6)$$

where $\Delta H_{vap}(T_B^{mean})$ is the enthalpy of vaporization of the metal at the mean temperature over the range of the experiment. A selection of data for evaluating the activation energies is also plotted in Figure 7 with final results given in Table I.

It is likely that collision induced vibrational relaxation in the $a^3\Sigma^+$ manifold (involving levels $v' > 0$) can influence the analysis of the activation energy for formation in this state. If the $v' = 0$ level is populated not only through the direct metathesis (2) but also through relaxation from higher vibrational quantum levels, the measured temperature dependence and activation energy will be affected. The long-lived $a^3\Sigma^+$ state might undergo collisions with (1) additional NO_2 molecules, (2) product NO molecules or (3) additional silicon beam atoms. At a constant tenuous atmosphere of reactant gas, only the NO product concentration and silicon atom concentration will increase. If these increases promote an increased vibrational relaxation through subsequent collision with the long-lived $a^3\Sigma^+$ state and the concentration of $v' = 0$ emitters increases via both direct reaction and collisional transfer, the chemiluminescent intensity will increase with increasing temperature to a greater extent than it would in the absence of vibrational relaxation. This will result in a larger slope heat and hence the prediction of a larger activation energy. Therefore, we must consider the determined activation energy for formation of the $a^3\Sigma^+$ state as a tentative upper bound to the correct

activation energy. It would seem apparent that the activation energy for formation of SiO^* $a^3\Sigma^+$ from the Si - NO_2 reaction is negligible.

It is clear from the data in Table I that the $b^3\Pi$ and $a^3\Sigma^+$ states are formed with a considerably lower activation energy than the $A^1\Pi$ state. Thus there appears to be a propensity for the spin conserving process which favors formation of the $a^3\Sigma^+$ and $b^3\Pi$ states. Further, the activation energy for forma tion of the $a^3\Sigma^+$ state is significantly smaller than that for formation of the state, providing possible evidence for a dynamical process which involves forma of $a^3\Sigma^+$ at large internuclear distance and possible subsequent transfer to $b^3\Pi$ rovibronic levels to which the $a^3\Sigma^+$ state is strongly coupled (Ref. 3 - Table I). As we demonstrate shortly, the extension of our single collision studies in a controlled manner to multiple collision conditions also provides support for this mechanism.

SiO Bond Dissociation Energy - Quenching of $A^1\Pi$ Emission and Energetic Considerations

A. Bond Energy

We have found that the Si - NO_2 reaction populates the v' = 0, 1, 2 levels of the SiO $A^1\Pi$ state (Figure 6) in a process whose activation energy is 7.4 $\pm$ 1.2 kcal/mole (Table I). Using the relationship

$$D_o^o(SiO) > \underset{72.9^{15}}{D_o^o(ON\text{-}O)} + \underset{126.7}{E_{int}(SiO)} - \underset{0.4}{E_{int}(Si)^*} - \underset{.85}{E_{int}(NO_2)} \qquad (7)$$

$$- E_T^{i*} - E_A(Si\text{-}NO_2)$$

$$4.3 - 7.4 \pm 1.2 = 186.65 \pm 1.7 \text{ kcal/mole}^{14}$$

where $E_{int}(Si)$, $E_{int}(NO_2)$, and $E_{int}(SiO)$ are the internal energies of the species in parentheses,[14] E_T^i is the relative translational energy of the reactants and $E_A(Si\text{-}NO_2)$ is the measured activation energy of the metathesis

considered,[14,15] we determine a lower bound to the SiO bond energy in excellent agreement with the mass spectrometric determination of Hildenbrand et al.[6] (D_0^0 = 188.2 kcal/mole). This represents the first SiO bond energy determination independent of mass spectroscopy.

B. Quenching of $A^1\Pi$ Fluorescence under Multiple Collision Conditions

The Si-NO_2 reaction is by no means sufficiently exothermic (D_0^0(SiO) - D_0^0(ON-O)) to populate levels of the SiO $A^1\Pi$ state. The necessary energy increment comes primarily from the combination of the reactant translational energy increment, E_T^i, and the fact that we must surmount a rather significant activation barrier in order that silicon and NO_2 react to form the $^1\Pi$ state. When taking into account the determined activation energy, we provide a correction for the possible reaction of metal atoms in the high energy tail of their translational energy distribution. In this particular system, the SiO^* molecules formed must emanate from the reaction of silicon atoms in this high energy tail and the reactive channel is closed to silicon atoms which do not possess sufficient energy. Once the barrier is surmounted and product formation ensues, the required energy is returned and can be used for SiO $A^1\Pi$ product internal excitation.

The importance of the considered energy increments is vividly displayed if we extend our single collision studies (Figure 6) to the multiple collision pressure regime. Here the silicon beam is thermalized by a room temperature carrier gas to temperatures ranging between 300 and 600 K. This thermalization considerably lowers E_T^i and substantially decreases the concentration of sufficiently energetic silicon atoms. Under multiple collision conditions, no $A^1\Pi - X^1\Sigma^+$ emission is observed.

Emission Features for SiO $a^3\Sigma^+$, v > 0

As an impetus for the present studies we had hoped to obtain information on vibrational quantum levels of the SiO $a^3\Sigma^+$ state, the emission from which was obscured in the Si-N_2O system due to overlap with notably more intense "$b^3\Pi$" - $X^1\Sigma^+$ emission features.[3] Therefore we chose to study a reaction which (1) should have a larger reaction cross section, (2) produce the excited triplet states of SiO and (3) produce significantly less internal rovibrational excitatic in the $b^3\Pi$ state. Further, there is reason to believe that the Si + NO_2 metathesis (Eq. 2) might favor $a^3\Sigma^+$ over $b^3\Pi$ formation. As Figure 5 demonstrates new $a^3\Sigma^+$ v' > 0 features can be observed under single collision conditions; however, upon extension to the multiple collision pressure regime (Figure 3) we find that (1) the $a^3\Sigma^+$ emission features are not strongly quenched but dominate those associated with $b^3\Pi$ (Figs. 2 and 3) and (2) vibrational and rotational relaxation within the $b^3\Pi$ manifold further enhances spectral simplific From the combination of the spectra in Figures 3 and 5, we record the $a^3\Sigma^+$ emission features in Table II and determine ω_e = 807 cm^{-1} $\omega_e\chi_e$ = 5 cm^{-1} for the $a^3\Sigma^+$ state which represents a refinement from the estimates of Field et al.[8] The data obtained from this analysis provide a backdrop for the consideration of the ultrafast E-E energy transfer effects which manifest themselves in the observed changes in the SiO chemiluminescent spectrum as a function of increased background pressure. In Table III, we make use of our measurements of the SiO $a^3\Sigma^+$ level structure to compare the energies for several levels of the $a^3\Sigma_1^+$ and $b^3\Pi_1$ manifolds.

Significant Modifications in Observed SiO Triplet State Spectral Features as a Function of Pressure - The Results of Ultrafast Intramolecular Energy Transfer Among the Excited States of SiO

Recently, we have been concerned with the characterization of ultrafast

energy transfer in high temperature systems.[7] We believe that the effects of this rapid transfer are found in those systems in which the low-lying long-lived[16] chemiluminescing triplet states of silicon monoxide are formed in a spin conserving process.

We correlate the data obtained for the SiO $a^3\Sigma^+$ state with the information first presented by Hager et al.[2] and the information on excited state coupling discussed in reference 3. We consider the approximate SiO potential curves outlined in Figure 8. The $a^3\Sigma^+$ state lies at slightly lower energy and at considerably larger internuclear distance than the $b^3\Pi$ state. We believe that the location and coupling of the $a^3\Sigma^+$ and $b^3\Pi$ states has an important influence on the changes which accompany the observed chemiluminescent spectra for both the Si + NO_2 and Si + N_2O reactions as a function of increasing pressure. The Si + NO_2 reaction is exemplary. When this metathesis is carried out under multiple collision conditions, a major contribution to the dynamics of SiO $b^3\Pi$ formation would appear to involve the process $Si(^3P) + NO_2(^2A_1) \rightarrow SiO(a^3\Sigma_1^+) + NO(^2\Pi)$ at longer range, followed by conversion to SiO $b^3\Pi_1$ via a collision induced E-E transfer. We observe the results of a process which appears to correlate with this mechanism and the near proximity of the $a^3\Sigma^+$, v' = 3 and $b^3\Pi$, v = 2 levels (Table III).

The $b^3\Pi$ state is thought to be sufficiently long-lived ($\tau_{rad} \sim 0.5$ msec)[3,16] that significant vibrational relaxation due to collisions can be manifest at relatively low pressure and before the emission of a photon. When the $b^3\Pi$ emission spectrum is obtained at very low pressures corresponding approximately to single collision conditions, the effects of vibrational relaxation are not strongly manifest (Figs. 1,4,5); the lower spectrum in Figure 9 is taken under near "single collision" conditions and corresponds to the (0,0), (0,1) and (0,2) sequences. The bands corresponding to the (0,2) sequence are exemplary.

Under single collision conditions, we observe emission corresponding to $b^3\Pi$ vibrational levels v' = 0-4. As the pressure is raised to $P_{Total} = 1000\mu$ by entraining the silicon atoms in a carefully controlled argon pressure and subsequently oxidizing this mixture, Figure 9 demonstrates that the observed multiple collision SiO spectrum (also Figs. 3 and 4) differs markedly from the single collision spectrum. Both the (0,2) and (0,1) sequences are marked by an almost complete absence of $b^3\Pi$ emission from levels other than v = 0 and 2. The observed phenomena can be explained by envoking a combination of vibrationa energy transfer within the $b^3\Pi$ state and ultrafast E-E transfer between the $a^3\Sigma$ and $b^3\Pi$ states. Because the $b^3\Pi$ state is long-lived, collisional relaxation o its vibrational manifold can occur readily on the time scale for electronic transition. In the absence of other effects, a thermalized $b^3\Pi$ state would be characterized by an overwhelming population in the v = 0 level; however, in this case, molecules formed at longer range in the $a^3\Sigma^+$ state find a doorway to $b^3\Pi$, v = 2 at v' = 3, $a^3\Sigma^+$ (see Table III). The efficient $a^3\Sigma^+$, v' = 3 $\rightarrow$ $b^3\Pi$, v = 2, E-E transfer competes effectively with vibrational relaxation resulting in the dominance of observed emission from the v = 0 and 2 levels of the $b^3\Pi$ state.

Discussion

Spin and Angular Momentum Considerations

It is instructive to compare the chemiluminescent emission from the Si - NO_2 and Si - N_2O reactions especially (1) in the light of reactant-product correlations and (2) with respect to changes which accompany the observed chemiluminescence from these systems as a function of pressure. The reactions of interest are

$$Si(^3P_{0,1,2}) + N_2O(^1\Sigma^+) \rightarrow SiO(a^3\Sigma^+, b^3\Pi, A^1\Pi) + N_2(^1\Sigma_g^+) \quad (8a)$$

and

$$Si(^3P_{0,1,2}) + NO_2(^2A_1) \rightarrow SiO(a^3\Sigma^+, b^3\Pi, A^1\Pi) + NO(^2\Pi) \quad (8b)$$

In the first reaction a spin "1" silicon atom interacts with a spin "0" N_2O molecule forming a spin "0" N_2 product. Given that spin conservation holds, it is predictable that the Si - N_2O reaction favors formation of triplet SiO. The silicon-NO_2 reaction is not nearly as straightforward for the spin angular momenta for silicon (S_1=1) and NO_2 (S_2=1/2) can couple to yield the resultant S_{Total} = 3/2, 1/2. Angular momentum considerations for this reaction might favor formation of an SiO electronic state possessed of no orbital angular momentum. The experimental results appear to bear out this possibility suggesting that, at least in this reaction, there exists a propensity rule for product momenta. The Si + NO_2 reaction appears to favor among the energetically accessible fluorescing states, formation of SiO $a^3\Sigma^+$ over SiO $b^3\Pi$ or SiO $A^1\Pi$. Such orbital angular momentum considerations do not appear to be as straightforward for the Si - N_2O reaction. The single collision spectrum[3] would seem to indicate a dominance of $b^3\Pi$ over $a^3\Sigma^+$ fluorescence, however, the relative intensity of emission from these two states might also reflect their relative radiative lifetimes. The relative intensities of the $a^3\Sigma^+$ and $b^3\Pi$ emission features for the two metatheses considered above are exemplified in Figure 10 where we focus on multiple collision spectra. Recall also that for the Si - N_2O reaction the $a^3\Sigma^+/b^3\Pi$ intensity ratio first decreases with increasing pressure reaching a minimum for P = 5 X 10^{-2} torr and increasing for P > 5 X 10^{-1} torr. In contrast, Figures 1, 2, and 10 demonstrate that for the Si - NO_2

reaction the $a^3\Sigma^+/b^3\Pi$ intensity ratio is somewhat larger and consistently increases as a function of increasing pressure.

Differing vibrational excitation and relaxation might also account for the observed relative $a^3\Sigma^+/b^3\Pi$ ratios. Consider that the more exothermic Si + N_2O reaction might form molecules in much higher $a^3\Sigma^+$ quantum level groupings than does Si + NO_2. The emission from high $a^3\Sigma^+$ vibrational levels is likely obscured due to a significantly larger $b^3\Pi$ - $X^1\Sigma^+$ transition moment. Vibrational relaxation to v' = 0 might be more readily accomplished in the Si - NO_2 system if the distribution of (nascent product) populated $a^3\Sigma^+$ vibrational quantum levels corresponds to a much lower quantum number grouping than that for Si + N_2O. Thus, there appear to be at least two possible reasons why the emission from the "$a^3\Sigma^+$"- $X^1\Sigma^+$ band system dominates that from the "$b^3\Pi$"- $X^1\Sigma^+$ band system for the Si + NO_2 reaction.

Because of the increased dominance of the $a^3\Sigma^+$ fluorescence features relative to those for $b^3\Pi$, the Si + NO_2 + Ar system can provide a more prolific source of $a^3\Sigma^+$, v' = 0 for a chemically driven-energy transfer laser system.[3] We must note that the dominance of $a^3\Sigma^+$ over $b^3\Pi$ emission demonstrated in Figures 2 and 10 is most likely muted because of a much longer $a^3\Sigma^+$ radiative lifetime (vs. $b^3\Pi$). In fact, it is not clear that the dominance of the $b^3\Pi$ emission features in the spectra resulting from the Si-N_2O reaction indicates that the $b^3\Pi$ population exceeds that for $a^3\Sigma^+$. Since both the $a^3\Sigma^+$ and $b^3\Pi$ radiative lifetimes are long versus the time for traversal through the viewing zone, the $a^3\Sigma^+$ emission features are affected as the result of both the smaller transition moment for the $a^3\Sigma^+$ versus the $b^3\Pi$ state and because a significantly larger number of $a^3\Sigma^+$ molecules will diffuse out of the viewing zone before emission of a photon. On the other hand, the system (spectrometer + phototube + ...) has a more sensitive response in the $a^3\Sigma^+$ emission region, partially counteracting the effects of radiative lifetime.

The apparent spin and orbital angular momentum propensities which characterize the Si - NO_2 and Si - N_2O reactions are also found to be manifest in the Si - O_3 metathesis.

$$Si(^3P) + O_3(^1A_1) \rightarrow SiO^*(A^1\Pi, a^3\Sigma^+, b^3\Pi) + O_2(^3\Sigma_g^-) \qquad (9)$$

Here, we find[17] that SiO^* $A^1\Pi$ emission strongly dominates fluorescence from the $a^3\Sigma^+$ and $b^3\Pi$ states. This could be predicted on the basis of spin conservation and what are apparently similar orbital angular momentum propensities to those for the Si - NO_2 metathesis. (Here, however, we find a dominance of the $\Omega = 1$ component.) Further, we find no evidence for population of the SiO E $^1\Sigma_o^+$ state.

Activation Energy Partitioning

The measured activation energies for formation of the SiO $a^3\Sigma^+$, $b^3\Pi$, and $A^1\Pi$ states would appear to suggest (1) a set of propensity rules for product spin and orbital angular momentum and (2) in conjunction with the present multiple collision studies, the importance of the "large r" $a^3\Sigma^+$ state as an intermediate for the formation of SiO $b^3\Pi$ molecules.

The Si ^3P state is divided into three fine-structure components and there are possible questions concerning their relative contribution to the observed activation energy. If during the course of the chemiluminescence experiment, the change in the state distributions of the reactants as a function of temperature does not alter the reaction rate, and if there is no reaction selectivity with respect to a particular spin-orbit component, the experimentally measured activation energy can be expressed as

$$E_A|\ell\rangle = (\langle E_{trans}\rangle^{|\ell\rangle *} - \langle E_{trans}\rangle^{|\ell\rangle}) \qquad (10)$$

where $\langle\ \rangle^{|\ell\rangle *}$ denotes the average of all atom-molecule interactions leading to formation of product in state $|\ell\rangle$ and $\langle\ \rangle^{|\ell\rangle}$ denotes the average over all atom-molecule interactions (i.e., the thermal average). If one of the spin-

orbit components reacts more readily with the NO_2 molecule, Equation (10) must be appended and the measured activation energy, $E_A|\ell>$, must also take into account the internal energy of the beam atoms. However, the maximum correction to the partition of the measured activation energy for the Si-NO_2 interaction over the temperature range of interest is -0.60 kcal/mole for exclusive reaction with ^3P_o Si atoms and +0.30 kcal/mole for exclusive reaction $^3P_2$ Si. Thus, the activation energies presented in Table I bear primarily the significance expressed in Eq. (10) with, at best, a small adjustment for internal state corrections.[5,15]

The apparently small if not negligible activation energy for formation in the SiO $a^3\Sigma^+$ state corresponds to an activation energy for product SiO which is less than or equal to that for the formation of product molecules in any electronic states of the system. This, of course, includes the ground $X^1\Sigma^+$ state. This result thus indicates that the formation of molecules in the $a^3\Sigma^+$ state can compete effectively with ground state formation, a situation which signals the possibility of a population inversion.

Energy Balance, Population of SiO $A^1\Pi$ and $b^3\Pi$ States - Possible $b^3\Pi$ Vibrational Relaxation at Low Pressure

We have used the observed weak emission from the v' = 0, 1, 2 levels of the SiO $A^1\Pi$ state to deduce a lower bound for the SiO bond energy. As we have done previously for the Si + N_2O reaction,[3] we also consider the energy balance involving populated levels of the $b^3\Pi$ state. The highest level from which emission in the $b^3\Pi$ state is observed corresponds to v' = 4. The available energy to populate the $b^3\Pi$ state is

$$E_{Available} = D_o^o(SiO) - D_o(NO_2) + E_{int}(NO_2) + E_{int}(Si) + E_T^i + E_A(b^3\Pi)$$

$$65827\ cm^{-1} - 25498\ cm^{-1} + 298\ cm^{-1} + 145\ cm^{-1} + 1505\ cm^{-1} + 1400\ cm^{-1}$$

$$= 43672\ cm^{-1}.$$

The energy increment corresponding to v = 4, $b^3\Pi$ is 37741 cm^{-1}. The energy differential, 5931 cm^{-1}, indicates that approximately six more levels in the SiO $b^3\Pi$ state might be populated due to reaction exothermicity. This may be a real energy discrepancy or it might result in part from vibrational relaxation in the $b^3\Pi$ manifold even at very low pressure.

Ultrafast Energy Transfer - Possible Implications for Previous Studies of Silicon Oxidation

We believe that the phenomena of ultrafast energy transfer can account for Hager et al.'s[1] observation of "an anomalously high intensity for the emission from the $b^3\Pi$ v = 2 bands relative to the v = 1 bands". It is surprising that these effects do not manifest themselves strongly in the studies of Linton and Capelle,[2] however, although these authors did not observe a complete cutoff of the emission bands for the $b^3\Pi$ state at v = 2 (Hager et al.[1]), they do indicate a considerable decrease in intensity for those bands $v \geq 3$, consistent with the data obtained and conclusions drawn in the present study. Note also that Figure 10 demonstrates a significant v' = 1 $b^3\Pi$ spectral component for the Si + N_2O reaction verses its almost complete absence for Si + NO_2.

Acknowledgement: It is a pleasure to acknowledge the National Science Foundation and the Department of Energy, METC for partial support of this research.

References

1. G. Hager, R. Harris, and S. G. Hadley, J. Chem. Phys. 63, 2810 (1975). G. Hager, L. E. Wilson, and S. G. Hadley, Chem. Phys. Lett. 27, 439 (1974

2. C. Linton and Gene A. Capelle, Jour. Molec. Spectros. 66, 62 (1977).

3. J. L. Gole and G. J. Green, "The Energy Balance and Branching Ratios Associated with the Chemiluminescent Reaction $Si(^3P) + N_2O(^1\Sigma) \rightarrow SiO^* (a^3\Sigma^+, b^3\Pi, A^1\Pi) + N_2(v''\geq 5)$ - Possible Formation of Vibrationally Excited N_2," preceeding paper.

4. The Si + NO_2 reaction is far less exothermic since the O-NO bond energy exceeds that of $O-N_2$ by $\sim$ 1.5 eV. Because the NO_2 vertical electron affinity (2.36 + 0.10 eV, E. Herbst, T. A. Patterson, and W. C. Lineberger J. Chem. Phys. 61, 1300 (1974)) considerably exceeds that for N_2O (-0.15 + 0.1 eV,(J. S. Nalley, R. N. Compton, H. C. Schweinler, and V. E. Anderson, J. Chem. Phys. 59, 4125 (1973)) coulombic forces are expected to play a much larger role in this reaction.

5. G. J. Green and J. L. Gole, Chem. Phys. 46, 67 (1980).

6. D. L. Hildenbrand, High Temp. Sci. 4, 244 (1972).

7. See for example, D. M. Lindsay and J. L. Gole, J. Chem. Phys. 66, 3886 (1977). M. J. Sayers and J. L. Gole, J. Chem. Phys. 67, 5442 (1977). J. L. Gole and S. A. Pace, J. Chem. Phys. 73, 836 (1980). A. W. Hanner and J. L. Gole, J. Chem. Phys. 73, 5025 (1980).

8. D. R. Preuss and J. L. Gole, J. Chem. Phys. 66, 880, 2994 (1977). J. L. Gole and D. R. Preuss, J. Chem. Phys. 66, 3000 (1977).

9. R. W. Field, A. Lagerqvist, and I. Renhorn, Phys. Scripta 14, 298 (1976).

10. It is certainly longer than the radiative lifetime for the $b^3\Pi$ state which must have a larger effective transition moment. The radiative lifetime for the $b^3\Pi$ state is estimated to be 48 milliseconds but probably is shorter (ref. 3). (B. Meyer, J. J. Smith, and K. Spitzer, J. Chem. Phys. 53, 3616 (1970).) It is likely this represents a lower bound for the gas phase value. Thus, a radiative lifetime well in excess of 10^{-2} seconds for the $a^3\Sigma^+$ state is quite reasonable.

11. L. H. Dubois and J. L. Gole, J. Chem. Phys. 66, 779 (1977).

12. R. Hultgren, P. D. Desai, D. T. Hawkins, M. Gleiser, K. K. Kelley, and D. D. Wagman, Selected Values of the Thermodynamic Properties of the Elements (American Society for Metals, Metals Park, Ohio, 1973). Also C. E. Moore, Atomic Energy Levels, Vol. 1, Natl. Stand. Ref. Data Series, Natl. Bur. Stand. 35 (1971).

13. Joerg Pfeifer, Gary Green, and James L. Gole, "Energetics of Silicon Oxidation Reactions - An Independent Determination of the SiO Bond Dissociation Energy", High Temp. Science.

14. We determine $E_{int}(Si)$ from a statistical average of the $^3P_0(0cm^{-1})$, $^3P_1$ (77.15 cm^{-1}), and $^3P_2$ (223.31 cm^{-1}) components of the ground ^3P state. See also, P. J. Dagdigian, H. W. Cruse, and R. N. Zare, J. Chem. Phys. 62, 1824 (1973). J. L. Gole and R. N. Zare, J. Chem. Phys. 57, 5331 (1972). R. N. Zare, Ber. Bunsenges Physik. Chem. 78, 153 (1974). D. B. Stull and H. Prophet, JANAF Thermochemical Tables, 2nd ed., Natl. Stand. Ref. Data Series, Natl. Bur. Stand. 37 (1971).

15. D. R. Preuss and J. L. Gole, J. Chem. Phys. 66, 880 (1977).

16. See reference 9 and also note, W. H. Smith and H. S. Liszt, J. Quant. Spectrosc. Radiative Transfer 12, 505 (1972).

17. G. J. Green, B. Cardelino, and J. L. Gole, unpublished.

Table I

Latent heat of vaporization for silicon (^3P) and activation energy for formation of SiO^* ($A^1\Pi, a^3\Sigma^+, b^3\Pi$)[a]

Reaction Studied	$\Delta H_{vaporization}$ present study[b]	Temperature Range (^oK)	Literature[c]	E_A[d]
$Si + NO_2 \rightarrow SiO^*(A^1\Pi, v'=0,1)$	105.2 ± 1.2[e]	1850-2220	95.1	7.4 ± 1.2
$Si + NO_2 \rightarrow SiO^*(A^1\Pi, v'=0,1)$	106.8 ± 3[e]	1880-2190	95.1	8.6 ± 3
$Si + NO_2 \rightarrow SiO^*(a^3\Sigma^+, v'=0)$	97.6 ± 1.3[f]	1850-2220	95.1	1.8 ± 1.2
$Si + NO_2 \rightarrow SiO^*(a^3\Sigma^+, v'=0)$	97.1 ± 2[f]	1880-2190	95.1	1.5 ± 2
$Si + NO_2 \rightarrow SiO^*(b^3\Pi, v'=1,2)$	100.7 ± 1.5[g]	1850-2220	95.1	4.0 ± 1.1
$Si + NO_2 \rightarrow SiO^*(b^3\Pi, v'=1,2)$	102.0 ± 3[g]	1880-2190	95.1	5.0 ± 3

a) Energy in kcal/mole.

b) Values in this column obtained from the slope of $\ell n\ I$ versus $1/T_B$, where I is the chemiluminescent intensity and T_B is the beam temperature. The slope obtained through linear least-squares analysis is added to the value of RT_B over the temperature range of the experiment to yield a rigorous upper bound to $\Delta H_{vaporization}$ - see text for discussion.

c) $\Delta H_{vaporization}$ at the average temperature of the experimental runs.

d) Values in this column obtained from the slope of $[\ell n(IT_B) + \Delta H_{vap}(T_B^{mean})/RT_B]$ versus $1/T_{effective}$ - see text for discussion.

e) Spectral resolution was 30 Å - data taken at 2650 Å - see text for discussion.

f) Spectral resolution was 20 Å - data taken at 3650 Å - see text for discussion.

g) Spectral resolution was 20 Å - data taken at 3100 Å - see text for discussion.

Table II

Observed v' > 0 Bandheads for SiO $a^3\Sigma^+ - X^1\Sigma^+$

Assignment of Observed Bands	Wavelength (Å)[a]
(1,1)[b]	3032
(1,2)	3149
(1,3)	3272
(1,4)	3406
[(1,5)]	3550
(2,4)[b]	3316
(2,5)	3450
(2,6)	3597

a. Approximate wavelength of bandhead - bands well fit by expression $\nu(cm^{-1}) = 33400 + 807(v') - 5(v'^2 + v') - 1241(v'') + 6(v''^2 + v')$.

b. (1,0) band too weak to be observed.
(2,2) and (2,3) bands directly under strong $b^3\Pi - X^1\Sigma^+$ fluorescence features.
(2,1) band at frontal edge of (0,0) band $b^3\Pi - X^1\Sigma^+$.

Table III

Approximate Relative Energy Level Locations for SiO $a^3\Sigma_1^+$ and SiO $b^3\Pi_1$ Manifolds, Closest Level Separations.

Levels	Energy[a] (cm^{-1})	$\Delta(cm^{-1})$
$v = 0$, $a^3\Sigma_1^+$	33400[b]	-433
$v = 0$, $b^3\Pi_1$	33833[b]	
$v = 1$, $a^3\Sigma_1^+$	34197	+364
$v = 0$, $b^3\Pi_1$	33833[b]	
$v = 2$, $a^3\Sigma_1^+$	34984	+154
$v = 1$, $b^3\Pi_1$	34830	
$v = 3$, $a^3\Sigma_1^+$	35761	-52
$v = 2$, $b^3\Pi_1$	35813	
$v = 4$, $a^3\Sigma_1^+$	36558	-252
$v = 3$, $b^3\Pi_1$	36810	

a. For $a^3\Sigma_1^+$ $\nu = \nu_o + 807(v') - 5(v'^2 + v')$.
For $b^3\Pi_1$ $\nu = \nu_o + 1012(v') - 7.4(v'^2 + v')$.

b. Taken from references 3 and 8.

Figure Captions

Figure 1: Chemiluminescent spectra in the region 2700 - 4100 Å resulting from the reaction Si + NO_2 → SiO^* + NO recorded under "single collision" conditions as a function of increasing silicon beam temperature and metal flux. The spectrum depicts both the "$b^3\Pi$" - $X^1\Sigma^+$ and "$a^3\Sigma^+$" - $X^1\Sigma^+$ band systems. Many fewer levels of the "$b^3\Pi$" state are populated vs. the observed spectrum for the Si + N_2O reaction.[3] Bandheads are designated (v',v"). The underlying continuum towards the red end of these spectra is due to blackbody radiation from the silicon cell. Spectral resolution is 10 Å. See text for discussion.

Figure 2: Chemiluminescent spectrum in the region 2900 - 4200 Å resulting from reaction Si + NO_2 + Ar → SiO^* + NO + Ar recorded under multiple collision conditions. The spectrum depicts both the "$b^3\Pi$" - $X^1\Sigma^+$ and "$a^3\Sigma^+$" - $X^1\Sigma^+$ band systems. Many fewer levels of the "$b^3\Pi$" state are populated vs. the single collision spectrum and emission from the "$a^3\Sigma^+$" - $X^1\Sigma^+$ band system now dominates the spectral features. Bandheads are designated (v',v"). Spectral resolution is 10 Å. See text for discussion.

Figure 3: Chemiluminescent spectra in the region 2900 - 3800 Å resulting from the reaction Si + NO_2 + Ar → SiO^* + NO + Ar recorded under multiple collision conditions as a function of increasing NO_2 pressure and high silicon flux. The spectrum depicts both the "$b^3\Pi$" - $X^1\Sigma^+$ and "$a^3\Sigma^+$" - $X^1\Sigma^+$ band systems. Emission from "$a^3\Sigma^+$" vibrational quantum levels v' > 0 is noted. Bandheads are designated (v',v"). Spectral resolution is 5 Å. See also Fig. 2 and text for discussion.

Figure 4: Comparison of chemiluminescent spectra recorded under "single" and "multiple" collision conditions which correspond primarily to the (1,0) sequence of the SiO "$b^3\Pi$" - $X^1\Sigma^+$ emission system; (a) single collision spectrum in the range 2800 - 2950 Å resulting from the reaction $Si + NO_2 \rightarrow SiO^* + NO$, (b) Multiple collision spectrum in the range 2800 - 3100 Å corresponding to the process $Si + NO_2 + Ar \rightarrow SiO^* + NO + Ar$. Bandheads are designated (v',v"). Spectral resolution is 8 Å. Note the absence of the (1,0), (3,2), and (4,3) bands in the multiple collision spectrum. See text for discussion.

Figure 5: Chemiluminescent spectra resulting from the reaction $Si + NO_2 \rightarrow SiO^* + NO$ recorded under "single collision" conditions illustrating portions of the "$a^3\Sigma^+$" - $X^1\Sigma^+$ band system. (a) The spectrum depict the (0,2) and (0,3) sequences associated with the SiO "$b^3\Pi$" - $X^1\Sigma^+$ band system and the readily resolved emission from the "$a^3\Sigma^+$ - $X^1\Sigma^+$ band system including v' = 2 emission bands. (b) The spectra taker as a function of increasing beam temperature and metal flux depict primarily the "$a^3\Sigma^+$ - $X^1\Sigma^+$ emission region and demonstrate readily resolved emission from v' = 0 and v' = 2. Bandheads are designated (v',v"). Spectral resolution is 8 Å. See text for discussion.

Figure 6: Chemiluminescent spectra in the region 2300 - 2750 Å resulting from the reaction $Si + NO_2 \rightarrow SiO^* + NO$ recorded under single collision conditions as a function of increasing silicon beam temperature and metal flux. The observed spectrum corresponds primarily to the SiO $A^1\Pi$ - $X^1\Sigma^+$ band system. Spectral resolution is 20 Å. See text for discussion.

Figure 7: Natural logarithm of relative chemiluminescent intensity verses the reciprocal of the silicon beam temperature, T_B, at (a) 2650 Å (SiO $A^1\Pi - X^1\Sigma^+$), (b) 3650 Å (SiO "$a^3\Sigma^+$" - $X^1\Sigma^+$), and (c) 3100 Å (SiO ("$b^3\Pi$" - $X^1\Sigma^+$) and plot of $[\ln(IT_B) + \Delta H_{vap}(T_B^{mean})/RT_B]$ vs. 1/Teff for the Si + NO_2 reaction at (d) 2650 Å, (e) 3650 Å, and (f) 3100 Å corresponding to the formation of SiO^* $A^1\Pi$, $a^3\Sigma^+$, and $b^3\Pi$, respectively. See text for discussion.

Figure 8: Approximate Potential Energy Curves for the $X^1\Sigma^+$, $a^3\Sigma^+$, and $b^3\Pi$ states of SiO, adapted from reference 1. See text for discussion.

Figure 9: Portions of chemiluminescent spectra for the reaction Si + NO_2 → SiO^* ($b^3\Pi$) + NO obtained under (a) "single collision" ($P_T < 10^{-3}$ torr) and (b) multiple collision ($P_T \sim 1$ torr) conditions. See text for discussion.

Figure 10: Comparison of chemiluminescent spectra for the reactions (a) Si + N_2O + Ar → SiO^* + N_2 + Ar and (b) Si + NO_2 + Ar → SiO^* + NO + Ar taken under multiple collision conditions ($P_T \sim 1$ torr). See text for discussion.

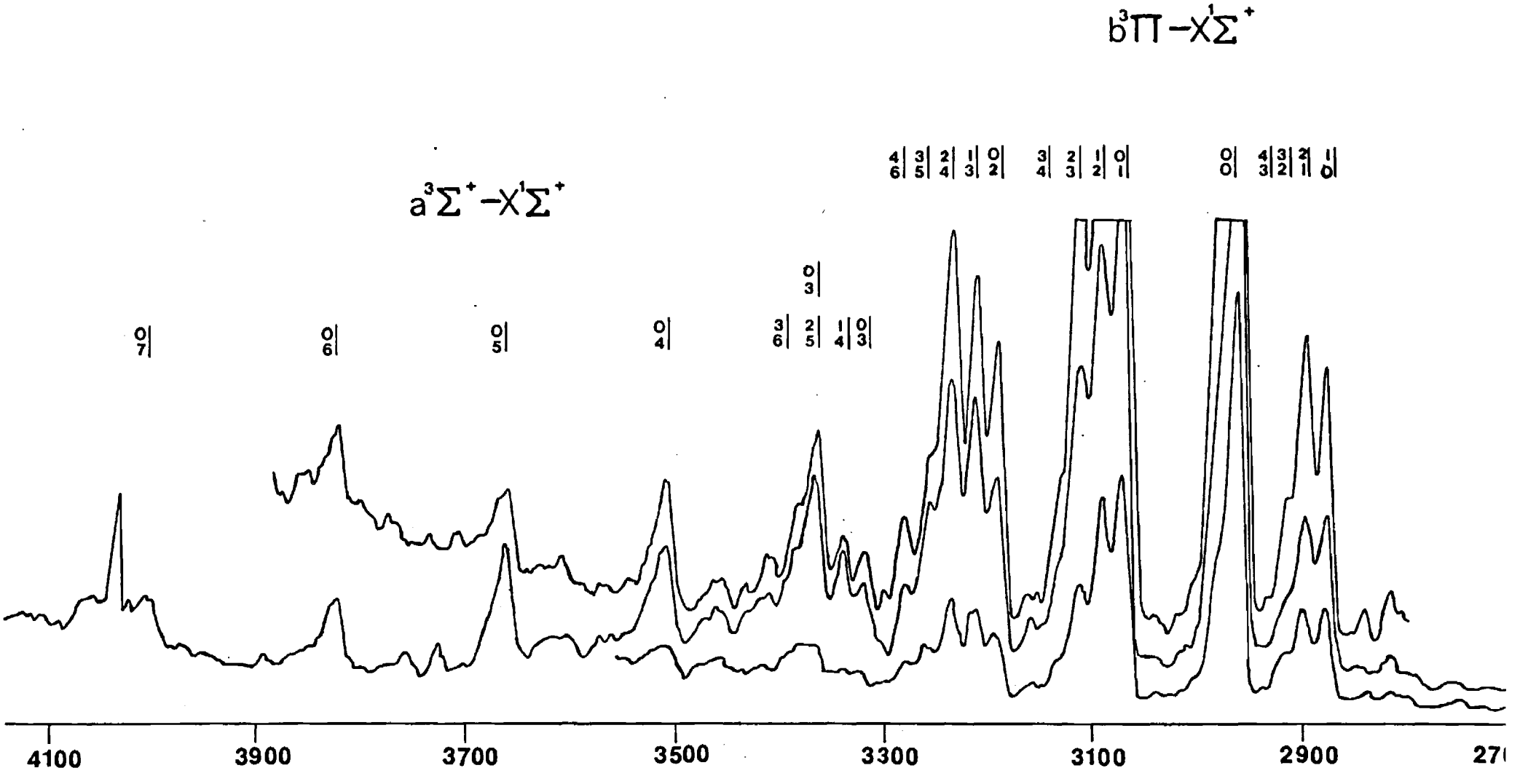
$b^3\Pi - X^1\Sigma^+$
$a^3\Sigma^+ - X^1\Sigma^+$
0|7
0|6
0|5
0|4
3|6 2|5 1|4 0|3
0|3
4|6 3|5 2|4 1|3 0|2
3|4 2|3 1|2 0|1
0|0 4|3 3|2 2|1 1|0
4100
3900
3700
3500
3300
3100
2900

Figure 1

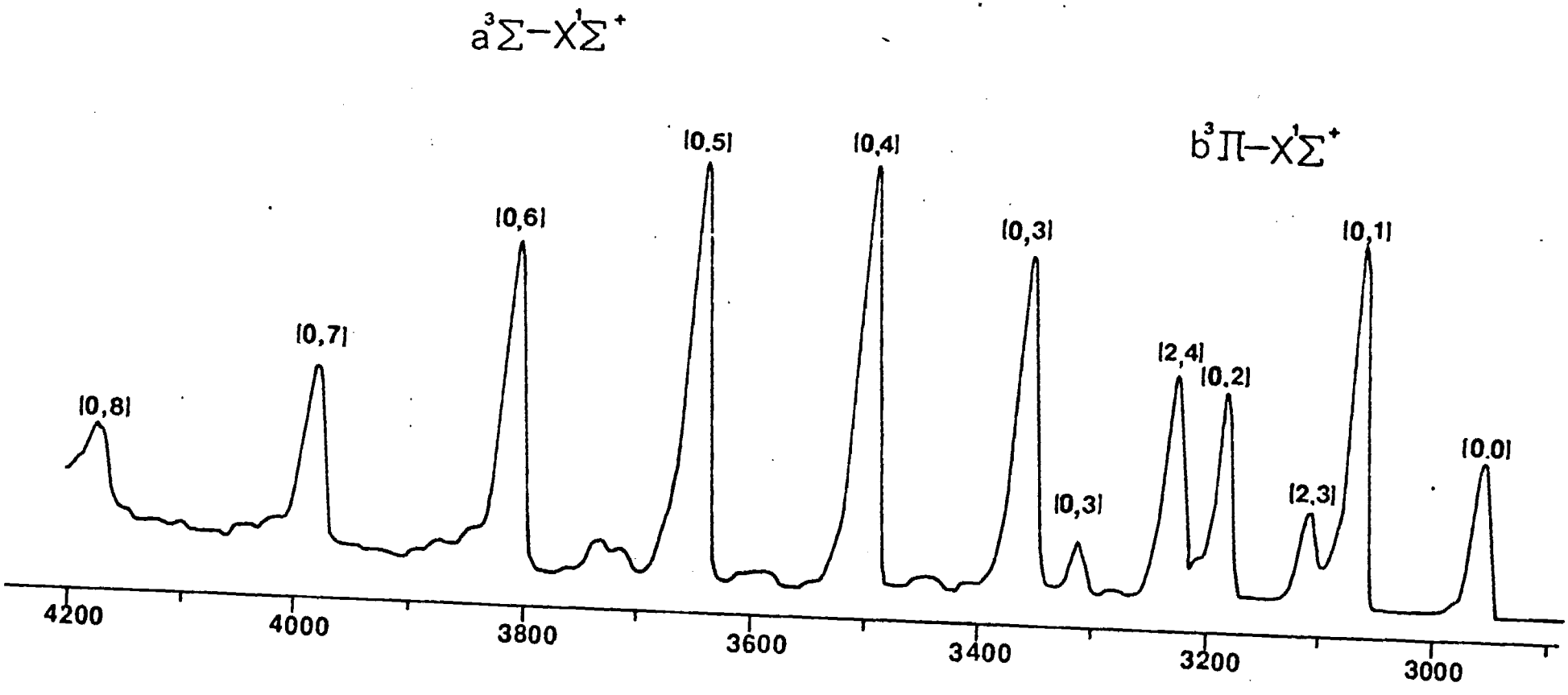
$a^3\Sigma - X^1\Sigma^+$
$b^3\Pi - X^1\Sigma^+$
(0,8)
(0,7)
(0,6)
(0,5)
(0,4)
(0,3)
(0,3)
(2,4)
(0,2)
(2,3)
(0,1)
(0,0)
4200
4000
3800
3600
3400
3200
3000

Figure 2

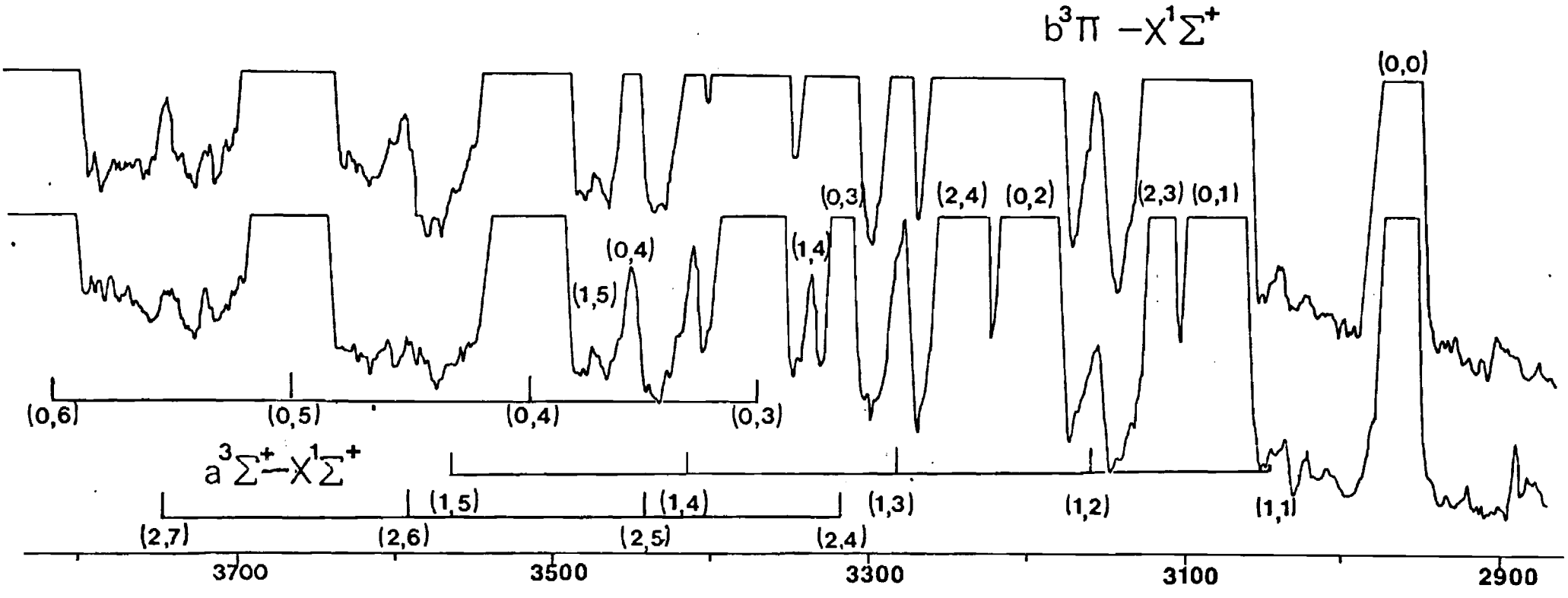
$b^3\Pi - X^1\Sigma^+$
(0,0)
(0,3)
(2,4)
(0,2)
(2,3)
(0,1)
(0,4)
(1,4)
(1,5)
(0,6)
(0,5)
(0,4)
(0,3)
$a^3\Sigma^+ - X^1\Sigma^+$
(1,5)
(1,4)
(1,3)
(1,2)
(1,1)
(2,7)
(2,6)
(2,5)
(2,4)
3700
3500
3300
3100
2900

Figure 3

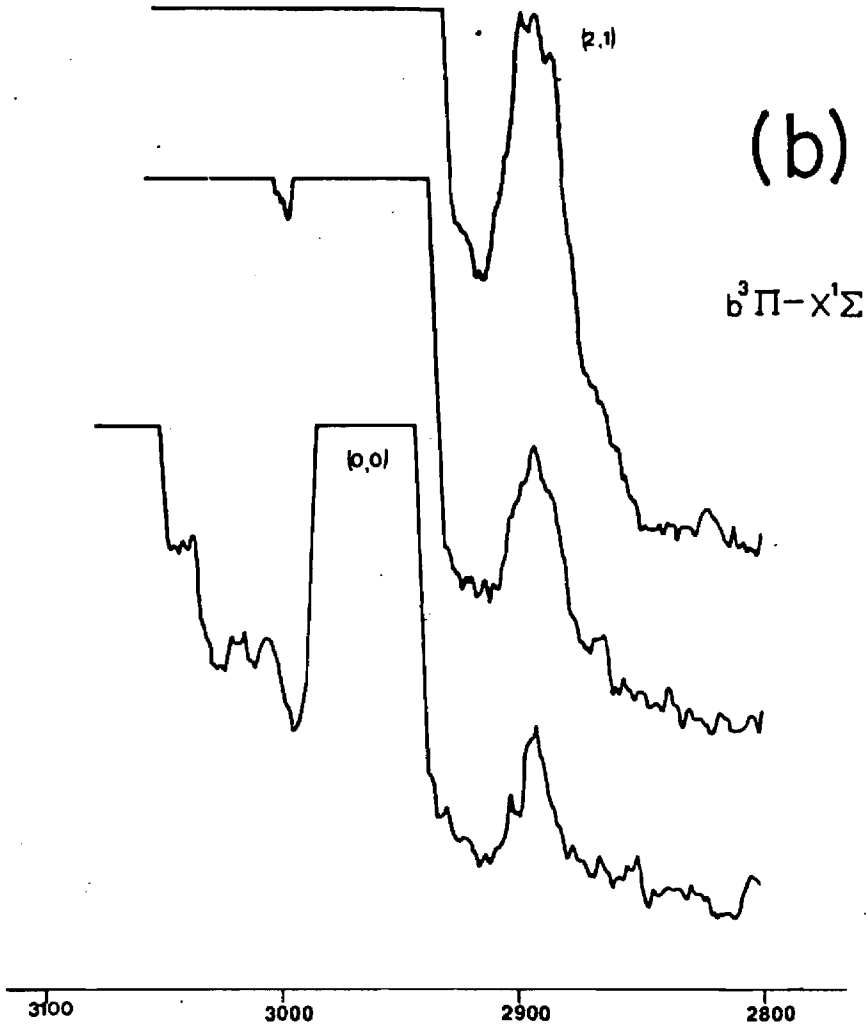
(2,1)
(b)
$b^3\Pi - X^1\Sigma^+$
(0,0)
3100
3000
2900
2800

Figure 4

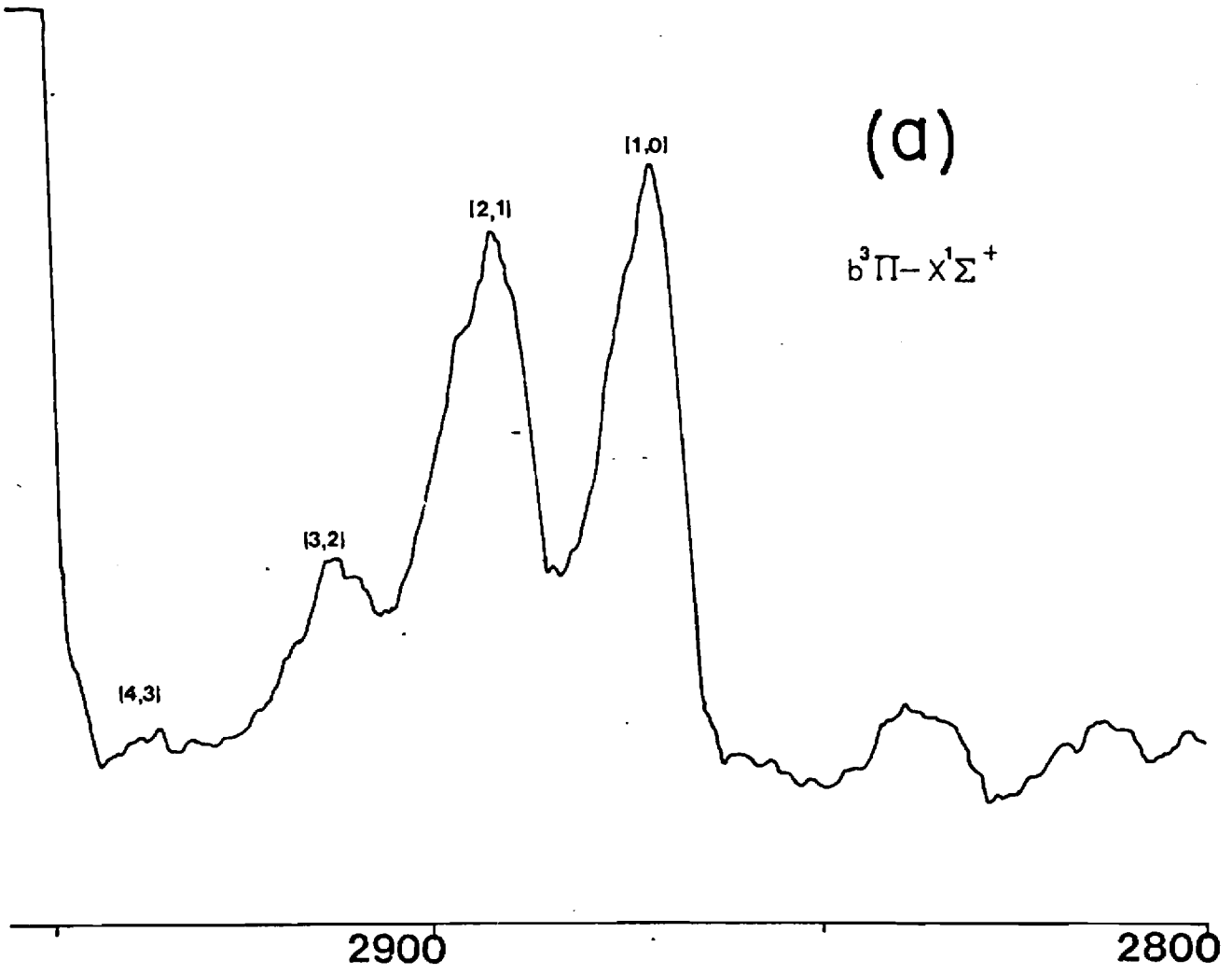
(a)
$b^3\Pi - X^1\Sigma^+$
(1,0)
(2,1)
(3,2)
(4,3)
2900
2800

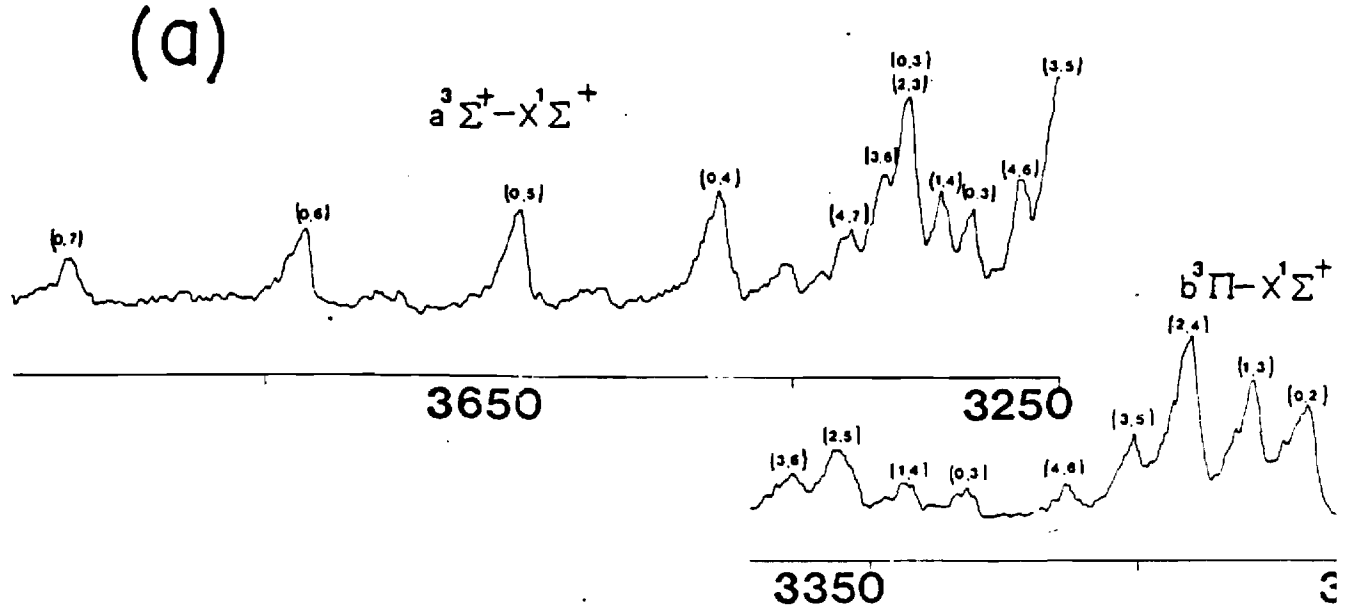
(a)
$a^3\Sigma^+ - X^1\Sigma^+$
(0,7)
(0,6)
(0,5)
(0,4)
(4,7)
(0,3)
(2,3)
(3,6)
(1,4)
(0,3)
(4,6)
(3,5)
3650
3250
$b^3\Pi - X^1\Sigma^+$
(3,6)
(2,5)
(1,4)
(0,3)
(4,6)
(3,5)
(2,4)
(1,3)
(0,2)
3350

Figure 5

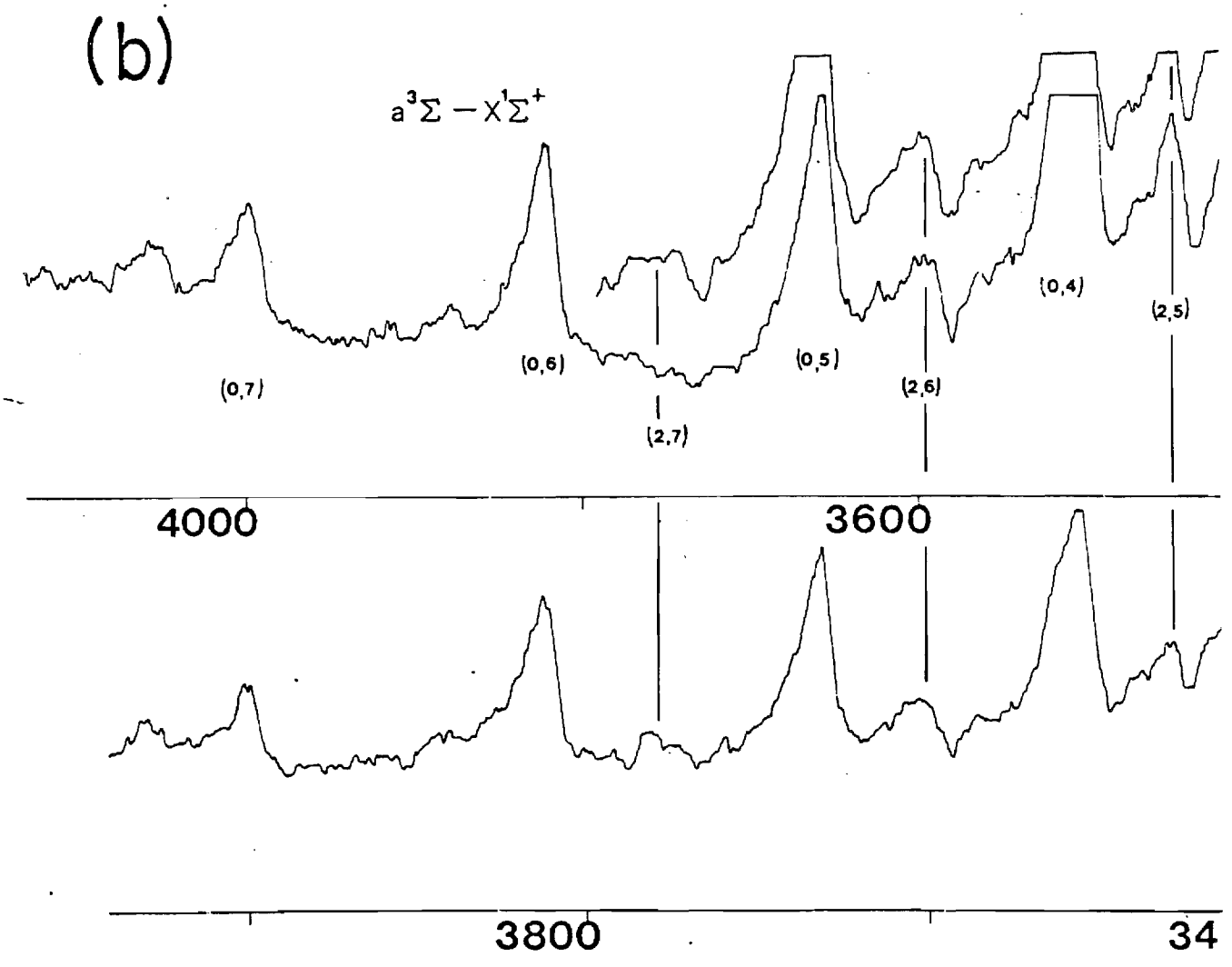
(b)
$a^3\Sigma - X^1\Sigma^+$
(0,7)
(0,6)
(2,7)
(0,5)
(2,6)
(0,4)
(2,5)
4000
3600
3800
34

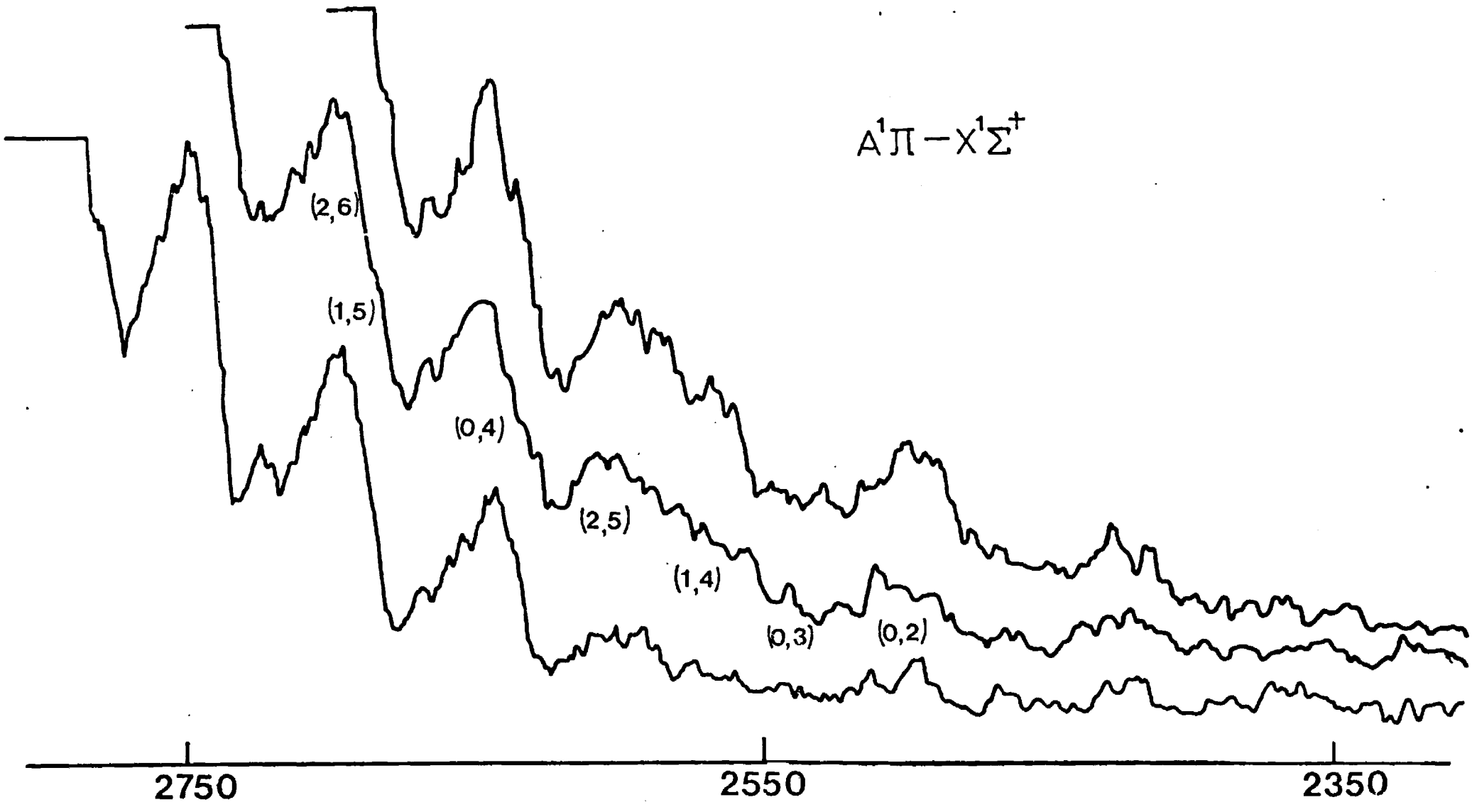

Figure 6

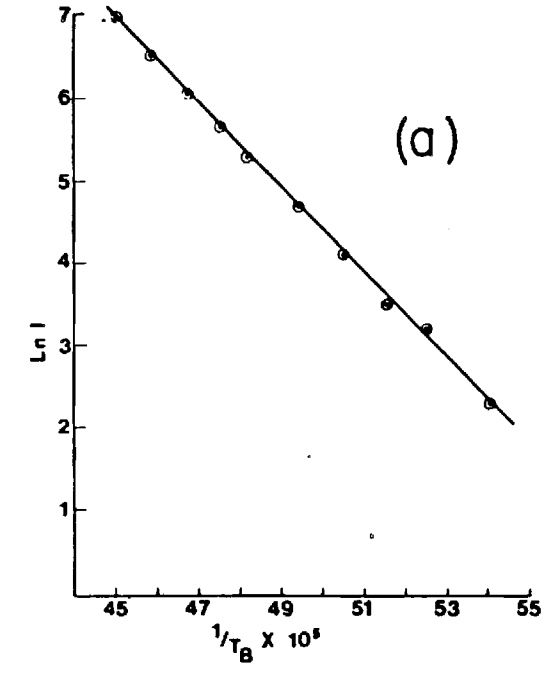
(a)
Ln I
7
6
5
4
3
2
1
45
47
49
51
53
55
1/T_B X 10^5

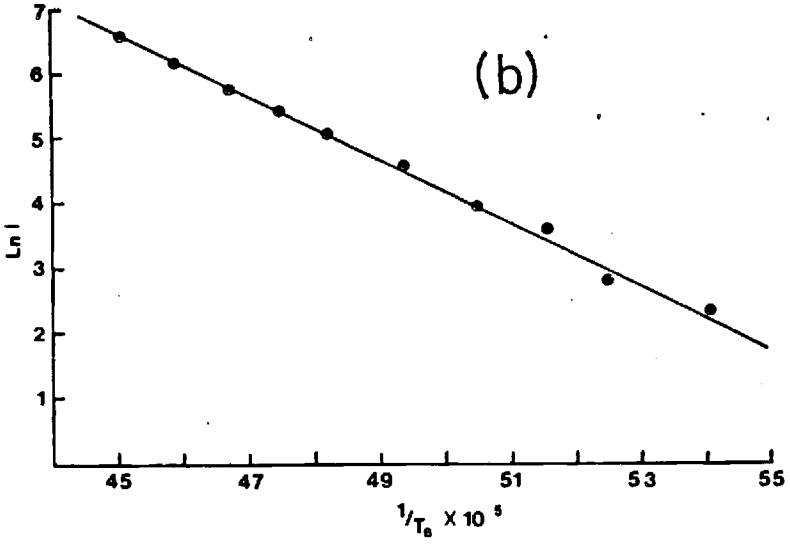
(b)
Ln I
7
6
5
4
3
2
1
45
47
49
51
53
55
1/T_B X 10^5

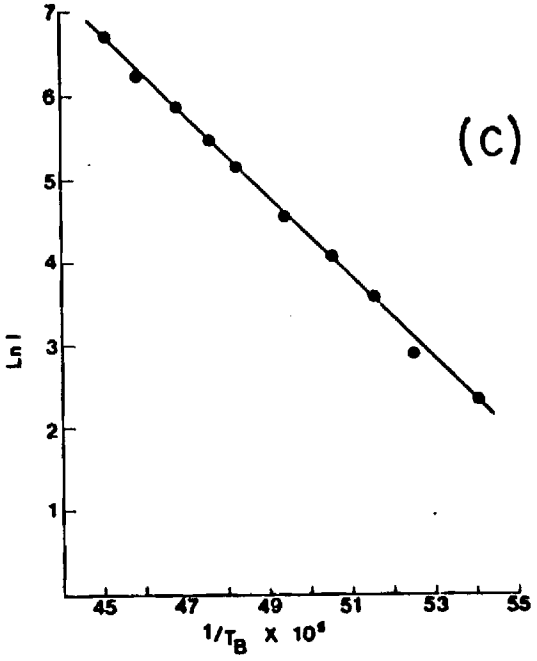
(c)
Ln I
7
6
5
4
3
2
1
45
47
49
51
53
55
1/T_B X 10^5

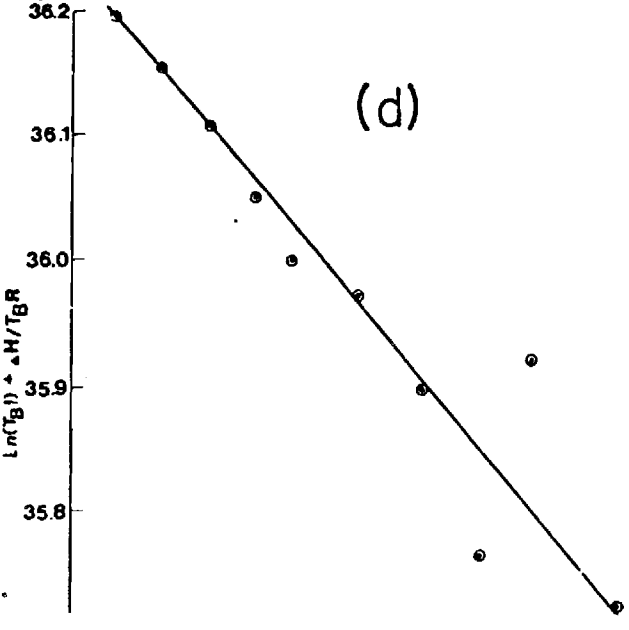
(d)
Ln(T_B I) + ΔH/T_B R
36.2
36.1
36.0
35.9
35.8

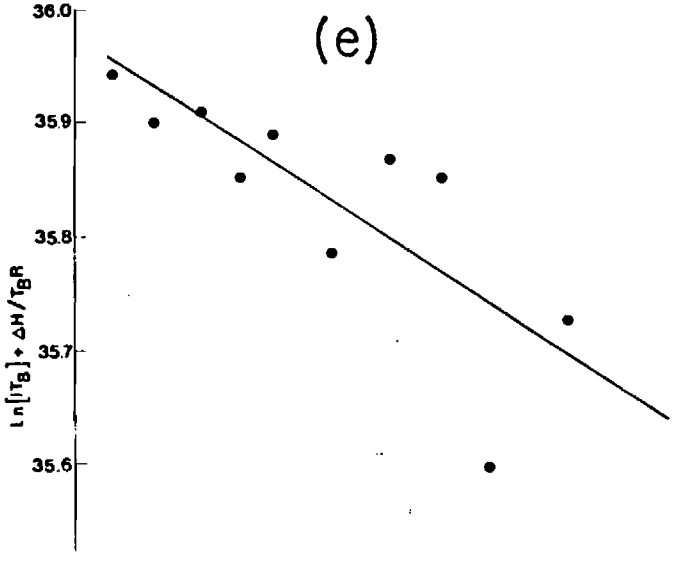
(e)
Ln[I T_B] + ΔH/T_B R
36.0
35.9
35.8
35.7
35.6

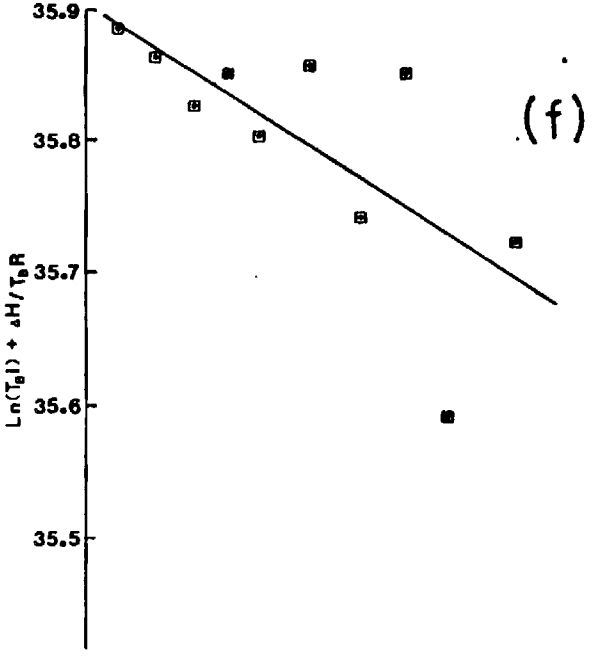
(f)
Ln(T_B I) + ΔH/T_B R
35.9
35.8
35.7
35.6
35.5

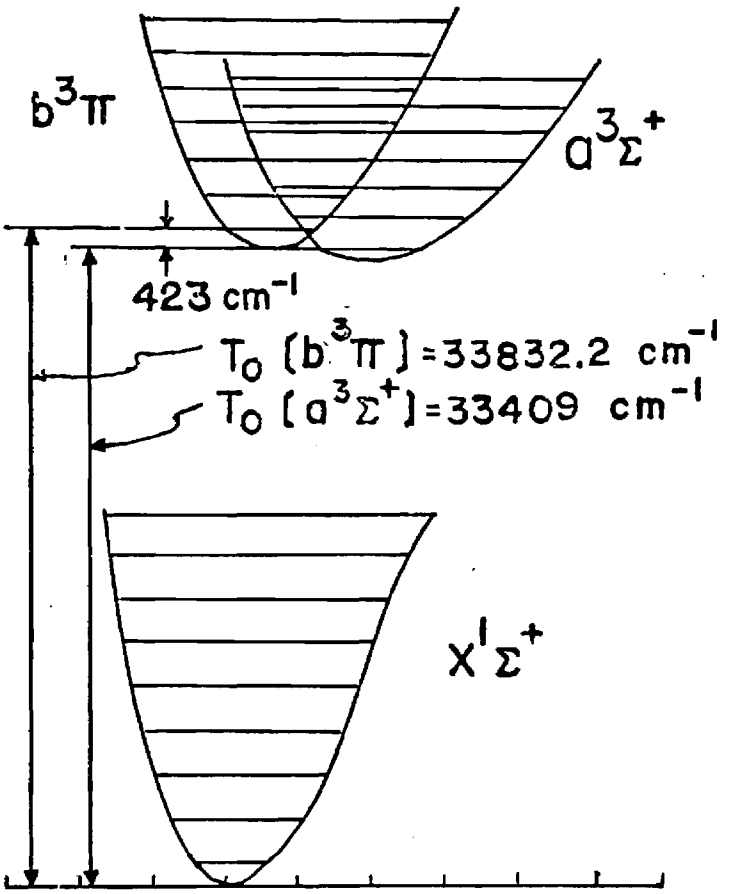
$b^3\pi$
$a^3\Sigma^+$
423 cm^{-1}
T_0 [$b^3\pi$] = 33832.2 cm^{-1}
T_0 [$a^3\Sigma^+$] = 33409 cm^{-1}
$X^1\Sigma^+$

Figure 8

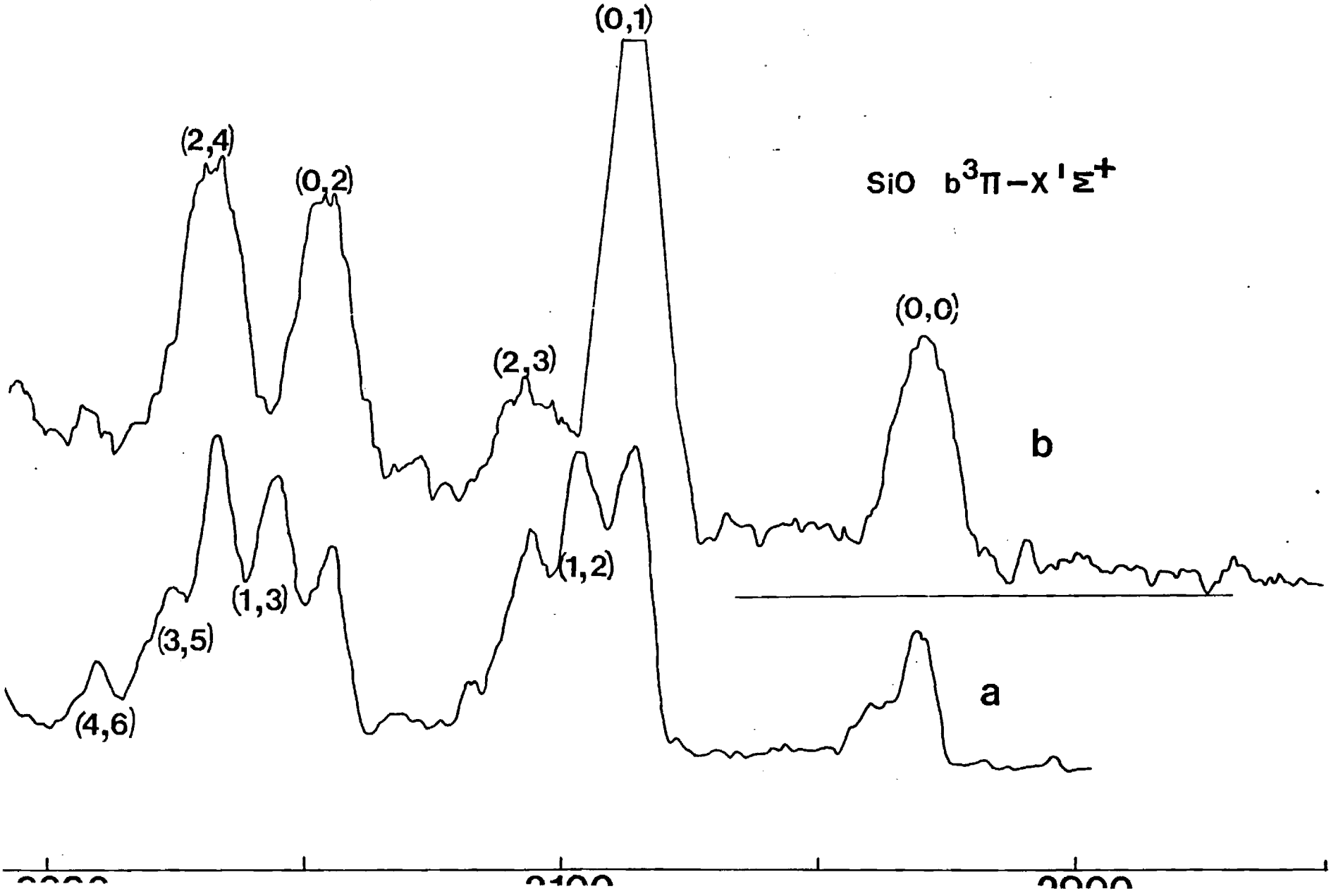
(0,1)
(2,4)
(0,2)
SiO b³Π–X¹Σ⁺
(0,0)
(2,3)
b
(1,2)
(1,3)
(3,5)
(4,6)
a

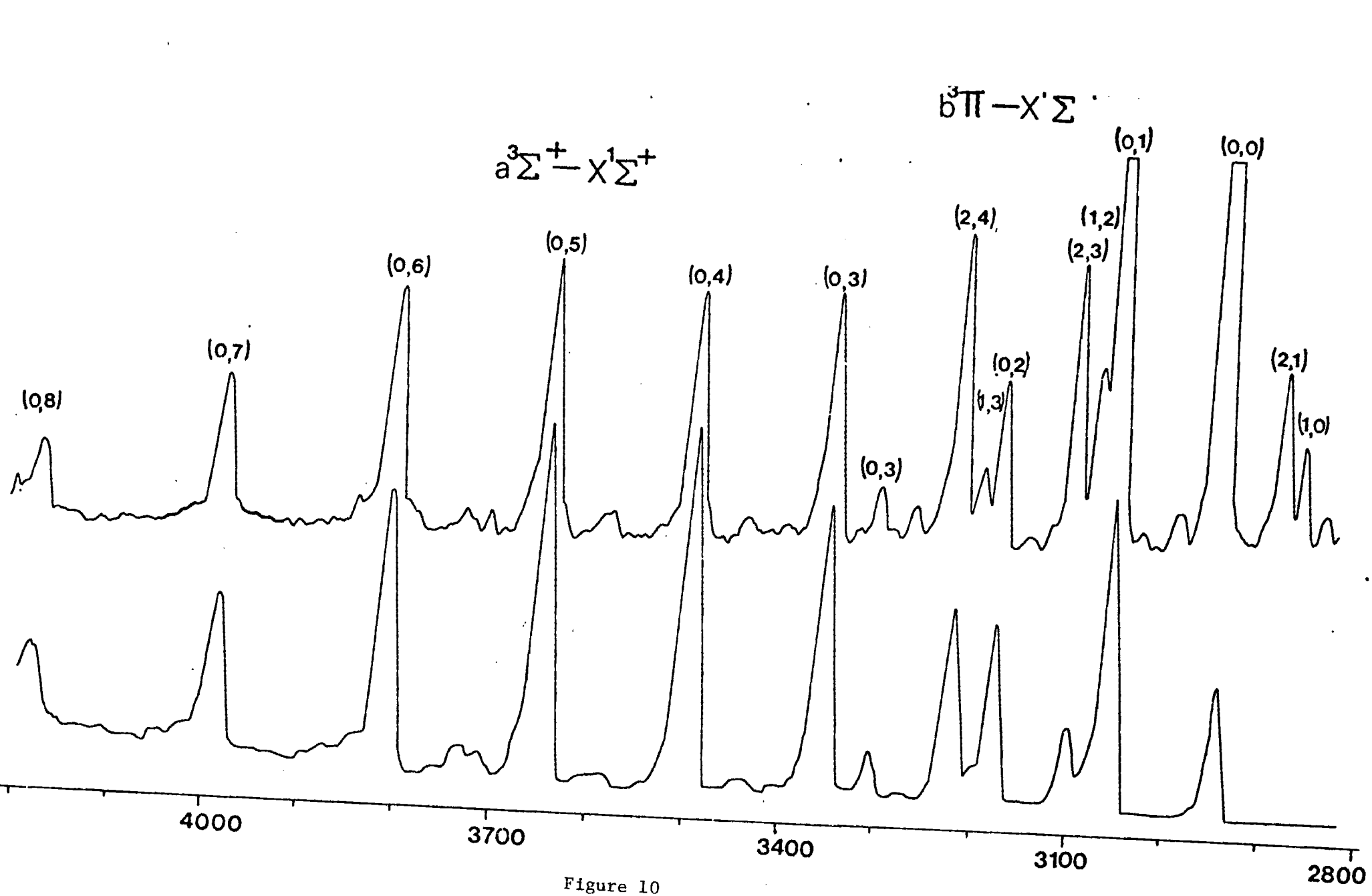
$b^3\Pi - X^1\Sigma$
$a^3\Sigma^+ - X^1\Sigma^+$
(0,8)
(0,7)
(0,6)
(0,5)
(0,4)
(0,3)
(0,3)
(2,4)
(1,3)
(0,2)
(2,3)
(1,2)
(0,1)
(0,0)
(2,1)
(1,0)
4000
3700
3400
3100
2800

Figure 10

APPENDIX E

ENERGETICS OF SILICON OXIDATION REACTIONS - AN INDEPENDENT DETERMINATION OF THE SiO BOND DISSOCIATION ENERGY

Joerg Pfeifer, Gary Green, and James L. Gole

High Temperature Laboratory, Center for Atomic and Molecular Science and School of Physics
Georgia Institute of Technology
Atlanta, Georgia 30332

Abstract

Silicon atoms react under single collison conditions with N_2O and NO_2 to yield chemiluminescent emission corresponding to the SiO $a^3\Sigma^+ - X^1\Sigma^+$ and $b^3\Pi - X^1\Sigma^+$ intercombination systems and the $A^1\Pi - X^1\Sigma^+$ band system. From the Si-NO_2 reaction, it has been possible to obtain a lower bound to the SiO bond energy, the first such determination independent of mass spectrometry. The result obtained, $D_0^0(SiO) > 186.7 \pm 1.7$ kcal/mole, is in good agreement with mass spectrometry ($D_0^0 = 188.2$ kcal/mole). To facilitate this determination, the temperature dependence of the $A^1\Pi - X^1\Sigma^+$ spectrum has been analyzed to deduce the nature of the metal reactant beam and to determine the activation energy for formation of SiO* $A^1\Pi$ ($E_A = 7.4 \pm 1.2$ kcal/mole). A most striking feature of the Si-N_2O reaction is the energy balance associated with the formation of SiO product molecules in the $A^1\Pi$ and $b^3\Pi$ states. A significant energy discrepancy ($\approx 10{,}000$ cm^{-1} = 1.24eV.) is found between the available energy to populate the highest energetically accessible excited state quantum levels and the highest quantum level from which emission is observed. It is suggested that this discrepancy may result from the formation of vibrationally excited N_2 in a concerted fast Si-N_2O reactive encounter.

Introduction

It is a pleasure to contribute this paper to the Brewer Symposium Issue of High Temperature Science. Leo Brewer has had a strong influence on the manner in which our research group approaches what might be called high temperature quantum chemistry. It has always been a pleasure to discuss our experimental results with Leo and, as all of us have found, there usually is an added important insight and suggestion which places the work in even clearer perspective. This paper discusses the SiO molecule and specifically focuses on a topic over which John Chipman, Leo Brewer, John Elliott, and myself have had several discussions. Although the SiO molecule is well studied and its bond dissociation energy represents and important standard in mass spectrometry on which several other measurements are based, a confirmation of this important quantity, independent of mass spectrometry, has not yet been presented. As we all know, these confirmations have been of particular interest to Leo Brewer.

For several years, the nature of the structure,[1] energetics,[2] and formation[3,4] of the SiO molecule has been the subject of a number of experimental and theoretical studies. The low-lying states of SiO have recently been discussed in detail by Field et al.[5] An important contribution to our knowledge of the low-lying states of SiO has come from recent studies of the chemiluminescent reaction

$$Si(^3P) + N_2O \rightarrow SiO^*(a^3\Sigma^+, b^3\Pi \ldots) + N_2 \qquad (1)$$

by Hager et al.[3] and Linton and Capelle.[4] Much of the impetus for this effort has been the desire to exploit "spin conservation" in order to produce the

low-lying "$a^3\Sigma^+$" and "$b^3\Pi$" states of SiO. Although reaction (1) is believed to strongly favor spin conservation, Linton and Capelle[4] have also observed some considerable emission corresponding to the $A^1\Pi - X^1\Sigma^+$ band system. These studies have offered the opportunity to characterize the "$a^3\Sigma^+$"-$X^1\Sigma^+$ and "$b^3\Pi$"-$X^1\Sigma^+$ intercombination band systems of SiO and investigate the possibility of using spin conservation to advantage in order to create a population inversion on the "$a^3\Sigma^+$"-$X^1\Sigma^+$ or "$b^3\Pi$"-$X^1\Sigma^+$ transitions and hence develop a medium for a visible chemical laser.

With the emphasis outlined above, previous studies have focused on the evaluation of the chemiluminescent emission from reaction (1) primarily as a means of determining spectroscopic constants for the $a^3\Sigma^+$ and $b^3\Pi$ states,[3,4] the relative population distributions in these states,[3] and the total quantum yield for fluorescence from those SiO excited states populated in reaction.

It has been the purpose of our current effort, focusing both on reaction dynamics and energetics, to augment the information garnered in previous studies by characterizing the chemiluminescent emission from both the Si-N_2O and Si-NO_2 reactions at considerably lower pressures (10^{-5} - 10^{-1} torr) than those associated with the studies of Hager et al. (2-4 torr) and Linton and Capelle (0.5-20 torr). As a result of our study of the "single collision" ($P_{Tot} \lesssim 10^{-4}$ torr) Si-N_2O and Si-NO_2 metatheses, it appears possible to provide explanations for the rather diverse $b^3\Pi$ excited state vibrational excitation which characterizes the spectral emissions observed by Hager et al. ($v' \lesssim 2$) and Linton and Capelle ($v' \lesssim 8$) in their "multiple collision" flame experiments. There are also subtleties in the evaluation of excited state population distributions, branching ratios for excited state formation, and quantum yields for these systems.[6] However, in the present manuscript, we limit ourselves to the discussion of the energetics of these processes. We

will use an analysis of the chemiluminescent emission from the Si-NO_2 metathesis to deduce a lower bound for the SiO bond energy.

Previous researchers have focused primarily on SiO spectroscopy and excited state product distributions leaving apparently unnoticed an intriguing question concerning the dynamics of the Si-N_2O reaction. One finds that there is a significant discrepancy between the available energy to populate SiO excited electronic states (reaction (1) exoergicity $\approx$ 53000 cm^{-1}) and the observed excitation which characterizes the Si-N_2O system. We consider this differential and offer an explanation which appears to be consistent with observations of excited state metal oxide formation in several M + N_2O reactions.

Experimental

Silicon atoms distributed thermally among the ground state $^3P_{0,1,2}$ components were reacted with NO_2 and N_2O in a highly exothermic process to produce an intense blue emission. The metal beam was formed from two sources: (1) Silicon was vaporized from a cylindrical graphite crucible (c.s. grade-Micromechanisms). This crucible was heated by a graphite radiator substituted for the tantalum radiators (graphite inner sheath) previously used in our study of the Si-OCS reaction.[7,8] The graphite radiator was surrounded by two tantalum heat shields. Maximum temperatures ranging from 1900 to 2100°C were achieved with this construction, all temperatures being measured with a Leeds and Northrup optical pyrometer to ±10°C. The graphite crucible/heat shield assembly was surrounded by a water cooled copper jacket attached to a newly designed "quick-load" bus bar/flange assembly.[9] The effusive silicon atom beam intersected a tenuous atmosphere (10^{-5} to 10^{-3} torr) of N_2O (Matheson, >98%) and the resulting diffuse chemiluminescence resulting from the Si-N_2O reaction was observed at right angles to the metal flow through a Suprasil quartz viewing port. Light baffles were placed in the reaction chamber to minimize the interference from blackbody radiation emanating from the oven chamber. (2) Using an oven configuration similar to that used previously for multiple collision studies,[10] the Si-NO_2 reaction was studied over the pressure range 10^{-5} to 10^{-3} torr. Silicon was vaporized over the temperature range 1600-2050°C from a c.s. grade graphite crucible. The crucible was machined to fit inside a commercial tungsten basket heater (R. D. Mathis, Long Beach, CA) which was wrapped with several layers of zirconia ZrO_2 cloth (Zircar Products, Florida, NY). The silicon vapor was reacted directly with NO_2.

Spectra were taken with a 1 meter Czerny-Turner scanning spectrometer operated in first order with a Bausch and Lomb 1200 groove/mm grating blazed at 5000Å. For the study of the wavelength regions below 2500Å, the spectrometer was purged with dry N_2. Both RCA 4840 and 1P28 photomultiplier tubes were used in these experiments. In order to insure high sensitivity at wavelengths less than 2500Å, the 1P28 photomultiplier tube was coated with sodium salicylate. The sensitivity of the optical system, quartz viewing port, quartz lens system, and purged spectrometer, to short wavelength radiation was tested by monitoring the 1850Å mercury resonance line. This emission was readily detected demonstrating our ability to easily monitor chemiluminescent emission below 2000Å. The photomultiplier signal was detected with a Keithley 417 fast picoammeter whose output signal (partially damped) drove a Leeds and Northrup stripchart recorder. All spectra were wavelength calibrated using a low pressure mercury pen lamp.

Chemiluminescent Spectra

Both the Si-N_2O and Si-NO_2 reactions are characterized by an intense blue chemiluminescence. The reactions of interest are

$$Si(^3P_{0,1,2}) + N_2O(^1\Sigma^+) \rightarrow SiO(a^3\Sigma^+, b^3\Pi, A^1\Pi) + N_2(^1\Sigma^+) \quad (1a)$$

and

$$Si(^3P_{0,1,2}) + NO_2(^2B_1) \rightarrow SiO(a^3\Sigma^+, b^3\Pi, A^1\Pi) + NO(^2\Pi) \quad (2)$$

The emission spectra, which extend from ~2250 to 4400Å (Figures 1-6), consist of contributions from the $A^1\Pi - X^1\Sigma^+$, $b^3\Pi - X^1\Sigma^+$, and $a^3\Sigma^+ - X^1\Sigma^+$ band systems of SiO and are dominated by the $b^3\Pi - X^1\Sigma^+$ band system onsetting at 2800Å.

a. $a^3\Sigma^+ - X^1\Sigma^+$

Readily resolvable features for the $a^3\Sigma^+ - X^1\Sigma^+$ band system extend from 3500-4400Å (Si-N_2O, Fig. 2; Si-NO_2, Fig. 5). As has been observed by previous workers[3,4] under multiple collision conditions, the spectrum is strongly dominated by a single progression arising from the v' = 0 level of the $a^3\Sigma^+$ state. If emission features originating in v' = 1 are present in the Si-N_2O system they are weak and hidden under the $b^3\Pi - X^1\Sigma^+$ features. In contrast, the silicon-NO_2 reaction, possessed of both a much larger cross section and a smaller reaction exothermicity does yield some information on v' = 1,2 $a^3\Sigma^+$, [6] by virtue of considerably more intense and less overlapped spectra.

b. $b^3\Pi - X^1\Sigma^+$

Emission features corresponding to the $b^3\Pi - X^1\Sigma^+$ band system extend from 2800 to 3950Å (Figures 1-3) for the Si-N_2O reaction and from 2750 to 3450Å (Figure 5) for the Si-NO_2 metathesis. Under single collision or near single collision conditions the emission from the Si-N_2O metathesis is characterized by several new additional bandheads corresponding to vibrational levels $9 \leq v' \leq 11$ in the b-X system. This observation should be contrasted to the multiple collision studies of Hager et al.[3] where only emission from $v' \leq 2$ is observed and the notably different vibrational excitation, $v' \leq 8$, found by Linton and Capelle.[4] Vibrational deactivation[6] has begun to onset in the Linton and Capelle study and is quite pronounced in the experiments of Hager et al. Observed bandheads and relative intensities corrected for phototube response are given in Table 1. Some twenty new bandheads have been observed.

c. $A^1\Pi - X^1\Sigma^+$

The $A^1\Pi - X^1\Sigma^+$ emission features observed in this study are depicted in Figures 3, 4 and 6. As Figure 3 demonstrates, the A-X emission characterizing the Si-N_2O reaction, is much weaker than that from the b-X system and is dominated by a progression emanating from $v' = 0$. The much less exothermic Si-NO_2 reaction ($D_o^o(ON-O) - D_o^o(N_2-O) \approx 1.5$eV) is characterized by an even weaker A-X emission feature (relative to the b-X and a-X emission features). No emission from $A^1\Pi$ vibrational quantum levels greater than $v' = 2$ (Figures 3 and 4) results from the Si-N_2O metathesis. If we consider the energy available to populate excited electronic states, we might expect to observe emission from $A^1\Pi$ vibrational quantum levels $v' \leq 15$.

Reaction Kinetics

A. Pressure dependences

We find that the observed chemiluminescent emission from the $A^1\Pi$ amd $b^3\Pi$ states of SiO increases linearly with oxidant pressure over the range 3×10^{-5} to 6×10^{-4} torr indicating that these states are formed in a proces: first order in N_2O and NO_2. The a-X emission features (v' = 0 emission) whil dominated by direct formation in a process first order in silicon and first order in oxidant at the lowest pressures do display some nonlinear increase for pressures in excess of 1×10^{-4} torr. Although detailed temperature dependence studies to determine the activation energy for the Si-N_2O reaction were not performed, the chemiluminescent intensity as a function of the Si beam source temperature was followed with sufficient accuracy so as to determine that reaction with ground state Si ^3P atoms had occurred.

B. Temperature Dependences - Si - $NO_2 \rightarrow SiO^*(A^1\Pi)$ + NO

The results of temperature dependence studies for the Si-NO_2 reaction are shown in Figures 7 and 8. The $A^1\Pi$ emission was monitored at 2650Å corresponding predominantly to an overlap of the (0,4) and (1,5) bands of the $A^1\Pi - X^1\Sigma^+$ band system. In Figure 7, we plot ℓnI vs. $1/T_B$ for a selection of the data obtained. Here I is the chemiluminescent intensity and T_B is the beam (crucible) temperature. Data gathered for two runs is presented in Table 2. The slope and linearity of the plot in Fig. 7 shows that the Si-NO_2 reaction is first order in metal flux.

Recently, a relation between the temperature dependence of the chemiluminescence intensity and the parameters of a beam-gas experiment has been formulated.[11] It is

$$-R\frac{d(\ell nI)}{d(1/T_B)} = \Delta H_{vap} - R_{T_B} + E_A(d(1/T_{eff})/d(1/T_B)) \qquad (3)$$

where E_A is the Arrhenius activation energy for the formation of the product whose chemiluminescence is monitored, ΔH_{vap} is the enthalpy of vaporization for the metal reacting to produce the observed chemiluminescence and

$$T_{eff} = (m_B T_G + m_G T_B)/(m_G + m_B) \qquad (4)$$

where T_G is the temperature of the gas (nitrogen dioxide) and m_B and m_G are the masses of the beam atoms and gas molecules respectively.

Equation (3) may take into account the effect of low-lying electronic states[12] but generally considers the reaction of only ground state metal atoms. It may also take into account possible reactions of dimeric and trimeric species which must be considered in the present study. The nature of the analysis[12] depends upon which states of the metal react to produce the observed chemiluminescence.

At 2250K (the upper limit of the temperature dependence studies) in excess of 99% of the reacting atoms are in the ground ^3P state of silicon and the single collision reaction (2) gives rise to the $A^1\Pi$ chemiluminescence. The overwhelming probability for ^3P atom reaction as the source of the chemiluminescence can be demonstrated directly from the plot in Figure 7. In general, we expect E_A to be positive for reactions yielding chemiluminescence. Thus from equation (3)

$$-Rd\ell nI/d(1/T_B) > \Delta H_{vap} - RT_B \qquad (5)$$

Figure 7 denotes one of the least squares fits to obtained data points, the

slope of the plot being -50877 ± 591K, leading to the value 101.1 ± 1.2 kcal/mole for $-Rd(\ell nI)/d(1/T_B)$. Summing the slope energy and the value of RT_B over the temperature range of the experiment, we obtain a rigorous upper bound to ΔH_{vap}. These values are given in column 2 of Table 2.

The average T_B over the temperature range of the experiment was 2035K. At these temperatures, the heat of vaporization for the equilibrium atomic vapor is 95.1 kcal/mole, only a few kcal/mole less than the observed value of $-Rd(\ell nI)/d(1/T_B)$. The equilibrium vapor consists of silicon atoms in the ground ^3P and excited ^1D states[13] so that ΔH_{vap} for a vapor composed solely of ground state atoms will be slightly smaller. $\Delta H_{vaporization}$ for forming ^1D atoms will be considerably higher (≈ 18 kcal/mole).[13] The average value of RT_B over the range of the temperature dependence studies is ≈ 4.1 kcal/mole; thus the inequality (5) holds for reaction of ground state atoms but it does not hold for reaction of excited ^1D atoms.

Similar arguments can be envoked when considering possible silicon dimer and trimer reaction with heats of vaporization being 112.4[13] and 104.5[13] kcal/mole, respectively. The inequality (5) does not hold if the metathesis producing chemiluminescence results from dimer or trimer reaction. The violation of the inequality (5) is even more pronounced if we consider the possible reaction of excited state dimers and trimers. The observed chemiluminescence is due overwhelmingly to reaction of ground state silicon atoms.

"Activation Energy" for Formation of SiO* $A^1\Pi$

In order to evaluate the activation energy for formation of SiO* $A^1\Pi$, we rearrange the expression (3) in a manner previously described[11] to obtain

$$E_A \approx -d(R\ell n(IT_B) + \Delta H_{vap}(T_B^{mean})/T_B)/d(1/T_{eff})$$

where $\Delta H_{vap}(T_B^{mean})$ is the enthalpy of vaporization of the metal at the mean temperature over the range of the experiment. A selection of the data for evaluating the activation energy is plotted in Figure 8 and final results are given in Table 2.

Energy Balance for the Si + N_2O → SiO* + N_2 Reaction

In this section, we focus on the large discrepancy between the available energy to populate SiO excited states, due primarily to the exoergicity of the Si + N_2O reaction, and the energy for which we can account through determination of the highest excited state quantum levels populated in reaction.

From the single collision Si-N_2O reaction it is potentially possible to set a lower bound on the dissociation energy of silicon monoxide. Using reaction (1) and a previously discussed energy balance[14-16] we arrive at the inequality

$$D_o^o(SiO) > D_o^o(N_2O) + E_{int}(SiO) - E_{int}(Si) - E_{int}(N_2O) - E_T^i - E_A(Si\text{-}N_2O) \qquad (6)$$

where the silicon atom is in the ground ^3P state and $E_{int}(Si)$, $E_{int}[N_2O)$ and $E_{int}(SiO)$ are the internal energies of the species noted in parenthesis.* E_T^i is the relative translational energy of the reactants and $E_A(Si\text{-}N_2O)$ is the measured activation energy for the metathesis considered. In considering the products of the Si-N_2O reaction, SiO and N_2, neither $E_{int}(N_2)$ nor E_T^f, the final relative translational energy of product separation can be readily determined. Therefore these quantities are not included in Eq. (6) and the inequality applies

If we neglect for the moment the activation energy for the Si-N_2O reaction[17] and focus on the available energy to populate SiO excited states

$$E_{Available} = D_o^o(SiO) - D_o^o(N_2O) + E_{int}(N_2O) + E_{int}(Si) + E_T^i \qquad (7)$$

---

*For the silicon reaction, we select as our reference (zero) energy the reactants and products in eq. (6) at 0°, that is $Si(^3P_o)$, $N_2O(^1\Sigma^+,v=J=0)$, $SiO(^1\Sigma^+,v=J=0)$ and $N_2(^1\Sigma^+,v=J=0)$.

The available energy is partitioned to

$$E_{int}(SiO) + E_{int}(N_2) + E_T^f \qquad (8)$$

As we have noted, the SiO molecule is among the most widely studied high temperature molecules. Its bond energy represents a standard for mass spectrometry. We adopt the recent determination by Hildenbrand et al.,[18] $D_0^o(SiO) = 8.16eV = 65827\ cm^{-1}$. The N_2-O bond energy[19] is 13400 cm^{-1}.

To calculate $E_{int}(N_2O)$, we adopt a procedure similar to that described previosuly[20] for the determination of $E_{int}(OCS)$ and find $E_{int}(N_2O) = 298\ cm^{-1}$. To calculate $E_{int}(Si)$ we need consider only the internal energy of the ground ^3P state since it is this state which reacts to produce the observed chemiluminescence. Using standard techniques[21] we found $E_{int}(Si) = 145\ cm^{-1}$ for a beam temperature of 2170°K.

Dagdigian et al. have shown that, to good approximation[22]

$$E_T^i = 3/2kT_{eff} \quad T_{eff} = (m_G T_G + m_B T_G)/(m_G + m_B) \qquad (9)$$

where T_G is the temperature of the oxidant gas (300K), T_B is the silicon beam temperature (2170 K) and m_B and m_G are the masses of the beam atoms and gas molecules respectively. For the Si-N_2O reaction, we find $E_T^i = 1501\ cm^{-1}$.

Summing the energies considered above, we find

$$E_{Available} = 54371\ cm^{-1} \qquad (8a)$$

In order to evaluate $E_{int}(SiO)$, we seek the highest quantum level populated by the Si-N_2O reaction. Here, we exclude the use of the $a^3\Sigma^+$ state

since, as we have noted,[6] (1) the emission from this state is much weaker than and obscured by that from the $b^3\Pi$ state and (2) for levels $v' > 0$ possible strong $a^3\Sigma^+ - b^3\Pi$ coupling may also play a role in obscuring the $a^3\Sigma^+$ emission features.

The highest vibrational quantum level populated in the SiO $A^1\Pi$ state is $v = 2$. Choosing the (2,7) band in the $A^1\Pi - X^1\Sigma^+$ system, we obtain

$$\begin{aligned} E_{int}(SiO) &= \nu(2,7) + G''(0) \\ &= 35951 \pm 30\ cm^{-1} + G''(7) - G''(0) \\ &= 44314 \pm 35\ cm^{-1} \end{aligned} \qquad (10)$$

The highest vibrational quantum level populated in the SiO "$b^3\Pi$" state is $v' = 11$. Choosing the (11,16) band in the "$b^3\Pi$" - $X^1\Sigma^+$ system we obtain

$$E_{int}(SiO) = 43992 \pm 40\ cm^{-1} \qquad (11)$$

The energy for which we can account using the SiO excited state emissions is some 10,000 cm^{-1} less than the potential available energy to the system! It implies that the SiO bond energy is over an electron volt less than the reliable value given in the literature, a highly unlikely possibility.

In general, single collision chemiluminescence studies yield dissociation energies that are in close agreement with careful mass spectrometric measurements. With few exceptions,[23] any discrepancies are encompassed if one takes into account the temperature dependence of the metathesis yielding chemiluminescence and the nature of the metal atom reactant. In all cases, discrepancies have resulted in the prediction of slightly higher bond energies. Therefore the result obtained here represents a significant deviation from

expectation. In the present study, we have found that ground state ^3P silicon atoms react to yield the observed chemiluminescence. If, in order to provide a correction for the possible reaction of metal atoms in the high energy tail of their translational energy distribution, we determine the activation energy for the Si-N_2O reaction, this energy increment must be added to the available energy,[24] Eq. (8). Therefore the energy discrepancy is even larger than 10,000 cm^{-1}.

It is apparent that when the products SiO and N_2 are formed over an electron volt of energy must be accounted for by either the product N_2 internal energy or the relative translational energy of product separation.

Energy Balance for the Si - NO_2 → SiO* ($A^1\Pi$) + NO Reaction

In Figure 6 we depict the SiO $A^1\Pi$ - $X^1\Sigma^+$ emission which characterizes the Si-NO_2 reaction. We have found that this reaction populates the v' = 0, 1, 2 levels of the SiO $A^1\Pi$ state in a process whose activation energy is 7.4 ± 1.2 kcal/mole. Using the relationship

$$D_o^o(SiO) > D_o^o(ON-O) + E_{int}(SiO) - E_{int}(Si)^* - E_{int}(NO_2)$$
$$\underset{}{\quad 72.9 \quad 126.7 \quad 0.4 \quad .85}$$
$$-E_T^{i*} - E_A(Si-NO_2) \qquad (12)$$
$$4.3 - 7.4 \pm 1.2 = 186.65 \pm 1.7 \text{ kcal/mole}$$

where $E_{int}(Si)$, $E_{int}(NO_2)$, and $E_{int}(SiO)$ are the internal energies of the species in parentheses, E_T^i is the relative translational energy of the reactants and $E_A(Si-NO_2)$ is the measured activation energy of the metathesis considered, we find $D_o^o(SiO) > 186.65 \pm 1.7$ kcal/mole. All energies are given in kcal/mole below the respective quantities evaluated as outlined in the previous section. The lower bound dissociation energy is in excellent agreement with the mass spectrometric determination of Hildenbrand et al.[18] (D_o^o = 188.2 kcal/mole). This evaluation of the SiO bond dissociation energy is the first such determination independent of mass spectrometry.

It should be emphasized that the silicon-NO_2 reaction is by no means sufficiently exothermic ($D_o^o(SiO) - D_o^o(ON-O)$) to populate levels of the SiO $A^1\Pi$ state. The necessary energy increment comes primarily from the combination of the reactant translational energy increment, E_T^i, and the fact that we must surmount a rather significant activation barrier in order that silicon and NO_2 interact. When taking into account the determined activation energy for excited state formation, we provide a correction for the possible reaction of

metal atoms in the high energy tail of their translational energy distribution. In this particular system, the SiO* $A^1\Pi$ molecules formed must emanate from the reaction of silicon atoms in this high energy tail. In effect, this reactive channel is closed to silicon atoms which do not possess sufficient energy. Once the barrier is surmounted and product formation ensues, the required energy is returned and can be used for product internal excitation.

The importance of these considered energy increments is vividly displayed if we extend the single collision studies described here to the multiple collision pressure regime. Here, the silicon beam is thermalized by a room temperature carrier gas to temperatures ranging between 300 and 600 K. This thermalization considerably lowers E_T^i and substantially decreases the concentration of sufficiently energic silicon atoms. Under multiple collision conditions, no $A^1\Pi - X^1\Sigma^+$ emission is observed.[6]

*Evaluated for a silicon beam temperature of 2170°K.

Discussion

It is satisfying that one can use chemiluminescent studies to confirm, independently, one of the benchmark bond energies upon which mass spectrometry relies. At the same time, it is quite intriguing that the silicon-N_2O reaction leads to the population of far fewer excited state levels than are energetically accessible. In spite of repeated efforts, we have been unable to use the Si-N_2O reaction to populate vibrational levels $v' > 3$ in the $A^1\Pi$ state of SiO. In addition, we have not observed fluorescence from the $E\ ^1\Sigma_o^+$ state although it should be possible to populate two vibrational levels in this state. The Si-N_2O reaction is of sufficient exothermicity to populate 15 vibrational quantum levels in the $A^1\Pi$ state. Emission from these levels can readily be observed and recently we have employed the spin conserving Si-O_3 reaction

$$Si(^3P) + O_3(^1A_1) \rightarrow SiO(A^1\Pi) + O_2(^2\Sigma_g^-) \qquad (13)$$

to populate a minimum of 12 vibrational quanta in the $A^1\Pi$ state. In short, there appears to be little reason to suspect that the lack of $A^1\Pi$ vibrational excitation which characterizes the Si-N_2O reaction can be attributed to factors associated with the intimate molecular electronic structure of the $A^1\Pi$ state. Rather it appears that the observed effects are to be associated with the dynamics of the Si-N_2O reaction.

One can envision two possibilities; (1) a fast reactive silicon-N_2O encounter leading to the formation of SiO* $A^1\Pi$ or SiO* $b^3\Pi$ also produces ground state N_2 in a concerted process with a minimum of five vibrational quanta of excitation ($N_2\ ^1\Sigma_g^+$, $v'' > 5$) or (2) the $Si + N_2O \rightarrow SiO + N_2$ surface

is characterized by an extremely large translational energy barrier in the product exit channel. We favor the former possibility based on (1) preliminary quantum chemical calculations of the Si-N_2O surface which demonstrate that the N-N bond in N_2O lengthens upon approach of a silicon atom and (2) a comparison of the N-N bond length in N-NO (1.128Å)[25] and that for ground state N_2, v = 0 (1.0977Å).[26] Although, in the final analysis, we must be concerned with the bond lengths corresponding to the turning points of the potentials describing the N-N bond in N_2O and N_2, it is intriguing that the vibrational excitation which must be associated with the N_2 molecule in order that the corresponding bond length be 1.128Å is v" = 5. In other words, the average value of the internuclear distance for the fifth vibrational quantum level in the ground state of N_2 corresponds to the N-N bond distance in N_2O.

The results obtained in the present study cause us to focus on the nature of the energy balance in several M + N_2O reactions where we find similar behavior. In some cases larger energy discrepancies are found to characterize several M + N_2O reactions involving the Group IIIB (Sc,Y,La) and Group IIA metals. The data is summarized in Table 3. In many of these cases further characterization of the product metal oxide chemiluminescence will be required in order to better assess the actual magnitude of the energy discrepancy.

The significant fact which emerges is that the reactions outlined display an energy balance which is consistent with the formation of a vibrationally excited N_2 product. While one might argue that the translational energy of product separation can account for a portion of these observations, it would seem somewhat surprising that a final relative translational energy of separation, E_T^f (Eq. 8), can account for the rather sharp energy cutoffs especially those associated with the silicon and titanium reactions.

There are several experiments which might be pursued in order to obtain direct evidence for the formation of vibrationally excited N_2 produced in M = Si, or Ti + N_2O reaction. The major problem confronting the experimenter is the detection of very low effective product N_2 concentrations ($\sim 10^{-7}$ torr). Promising detection techniques might involve the use of either electron bombardment excitation and ionization or multiphoton ionization. In the former studies one might attempt to use an electron gun to excite the Second Positive system of N_2 monitoring directly the N_2 $C^3\Pi_u$ - $B^3\Pi_g$ fluorescence and back extrapolating to the ground state N_2 population distribution.[27] Alternatively, we are attempting to produce N_2^+ $B^2\Sigma_u^+$, monitoring the $B^2\Sigma_u^+$ - $X^2\Sigma_g^+$ emission and again back-extrapolating to the N_2 population distribution.[27] Thusfar these studies have met with only marginal success (N_2 concentrations $\leq 10^{-5}$ torr have been detected), however the signal-to-noise in the system can be considerably improved if the reaction zone and electron gun are magnetically confined.[28] An alternate experiment might involve the elegant pulsed laser multiphoton technique which Dehmer,[29] Kay[30] and coworkers have used to detect CO^+. The direct assessment of the vibrational excitation characterizing the product N_2 formed in highly exothermic M + N_2O reactions will contribute important new perspectives on the nature of reactive encounters. We encourage other workers to pursue the detection of vibrationally excited N_2 in low concentration.

References

1. H. Bredohl, R. Cornet, I. Dubois, and F. Remy, J. Phys. B. 7, L66 (1974); T.G. Heil, H. F. Schaefer III, J. Chem, Phys. 56, 958 (1972) see also reference 5.
2. J. Drowart, A. Pattoret, and S. Smoes, Proc. Brit. Ceram. Soc. 8, 67 (1967); D. L. Hildenbrand, High Temp. Sci. 4, 244 (1972); K. F. Zmbov, L. L. Ames, and J. L. Margrave, High Temp. Sci. 5, 235 (1973); H. Kvande and P. G. Wahlbeck, High Temp. High Press. 8, 45 (1976); D. L. Hildenbrand and E. Murad, J. Chem. Phys. 51, 807 (1969).
3. G. Hager, R. Harris, and S. G. Hadley, J. Chem. Phys. 63, 2810 (1975). G. Hager, L. E. Wilson, and S. G. Hadley, Chem. Phys. Lett. 27, 439 (1974).
4. C. Linton and Gene A, Capelle, Jour. Molec. Spectros. 66, 62 (1977).
5. R. W. Field, A. Lagerqvist, and I. Renhorn, Phys. Scripta 14, 298 (1976).
6. a. "On the Nature of the Energy Balance and Branching Ratios Associated with the Chemiluminescent Reaction $Si(^3P) + N_2O(^1\Sigma) \rightarrow SiO^*(a^3\Sigma^+, b^3\Pi, A^1\Pi) + N_2(v''\geq 5)$ - Possible Formation of Vibrationally Excited N_2 in M + N_2O Reactions," with G. J. Green, K. D. Jordan and J. Yates, work in progress.
   b. "Energy Balance in the Si-NO_2 Reaction: On the Formation of SiO $a^3\Sigma^+$, $v'>0$," and Ultrafast $a^3\Sigma^+ - b^3\Pi$ E-E Energy Transfer.
7. G. J. Green and J. L. Gole, Chem. Phys. 46, 67 (1980).
8. J. L. Gole and G. J. Green, Chem. Phys. 69, 357 (1982).
9. S. A. Pace and J. L. Gole unpublished.
10. See for example
    D. M. Lindsay and J. L. Gole, J. Chem. Phys. 66, 3886 (1977).
    M. J. Sayers and J. L. Gole, J. Chem. Phys. 67, 5442 (1977).
    J. L. Gole and S. A. Pace, J. Chem. Phys. 73, 836 (1980).
    A. Hanner and J. L. Gole, J. Chem. Phys. 73, 5025 (1980).
11. D. R. Preuss and J. L. Gole, J. Chem. Phys. 66, 880, 2994 (1977).
    J. L. Gole and D. R. Preuss, J. Chem. Phys. 66, 3000 (1977).
12. L. H. Dubois and J. L. Gole, J. Chem. Phys. 66, 779 (1977).

13. R. Hultgren, P. D. Desai, D. T. Hawkins, M. Gleiser, K. K. Kelley, and D. D. Wagman, Selected Values of the Thermodynamic Properties of the Elements (American Society for Metals, Metals Park, Ohio, 1973). Also C.E. Moore.
14. J. L. Gole and R. N. Zare, J. Chem. Phys. 57, 5331 (1972). R. N. Zare, Ber. Bunsenges Physik. Chem. 78, 153 (1974).
15. J. L. Gole and C. L. Chalek, J. Chem. Phys. 65, 4384 (1976).
16. C. L. Chalek and J. L. Gole, Chem. Phys. 19, 59 (1977).
17. D. R. Preuss and J. L. Gole, J. Chem. Phys. 66, 880 (1977).
18. D. L. Hildenbrand, High Temp. Sci. 4, 244 (1972).
19. D. B. Stull and H. Prophet, JANAF Thermochemical Tables, 2nd ed., Natl. Stand. Ref. Data Series, Natl. Bur. Stand. 37 (1971).
20. R. Jones and J. L. Gole, Chem. Phys. 20, 311 (1977).
21. We determine $E_{int}(Si)$ from a statistical average of the $^3P_0(0\ cm^{-1})$, $^3P_1$ $(77.15\ cm^{-1})$, and $^3P_2$ $(233.31\ cm^{-1})$ components of the ground ^3P state.
22. P. J. Dagdigian, H. W. Cruse, and R. N. Zare, J. Chem. Phys. 62, 1824 (1973).
23. C. R. Dickson and R. N. Zare, Chem. Phys. 7, 361 (1975).
24. See discussions in references 7 and 17.
25. K. P. Huber and G. Herzberg, Constants of Diatomic Molecules, Van Nostrand-Reinhold Company, 1979.
26. J. Pliva, J. Molec. Spectros. 12, 360 (1964).
27. The N_2 or N_2^+ emission spectrum obtained under reaction conditions is compared to that for room temperature N_2 at low concentrations.
28. The authors are indebted to Stewart Novick for helpful discussions on the subject of increasing the signal-to-noise from electron gun sources.
29. J. Dehmer, private communication.
30. B. Kay, private communication.

Table 1

Measured SiO Bandhead Positions and Vibrational Assignments

$b^3\Pi - X^1\Sigma^+$

bandhead assignment (v',v")[a]	bandhead origin λ_{air} (Å)	bandhead origin ν_{vacuum} (cm^{-1})	relative intensity[g]
(2,0)	2791.2	35816	---
(3,1)	2811.6	35556	45.9
(4,2)	2832.6	35293	54.0
(5,3)	2853.7	35032	35.6
(1,0)[b,c]	2869.2	34843	55.2
(2,1)[b,c]	2889.8	34594	44.6
(3,2)[b]	2911.2	34340	25.0
(4,3)	2932.4	34092	12.6
(0,0)[b,c]	2953.7	33846	100
(1,1)	2973.8	33617	33.6
(2,2)	2995.2	33377	---
[(4,4)][d]	3038.9	32897	---
(0,1)[b,c]	3065.2	32615	90.1
(1,2)[b,c]	3085.8	32397	82.0
(2,3)[b,c]	3107.3	32172	59.8
(3,4)[b]	3129.2	31948	27.2
(4,5)	3151.3	31724	12.1
(0,2)[b,c]	3184.0	31398	18.8
(1,3)[b,c]	3205.2	31190	24.9
(2,4)[b,c]	3226.9	30981	34.4
(3,5)[b]	3249.2	30768	22.5
(4,6)[b]	3272.0	30554	25.1
(5,7)[b]	3295.8	30333	17.4
(0,3)[b]	3310.9	30195	12.6
(6,8)[b]	3320.2	30110	14.0
(1,4)[b,c]	3332.5	29999	11.5
(2,5)[b]	3354.8	29799	17.6
(3,6)[b]	3377.6	29598	11.4
(4,7)[b]	3401.0	29395	14.1
(5,8)[b]	3425.3	29186	16.3
(6,9)[b]	3450.5	28973	18.3

Measured SiO Bandhead Positions and Vibrational Assignments

$b^3\Pi - X^1\Sigma^+$ (continued)

bandhead assignment (v',v'') [a]	bandhead origin λ_{air} (Å)	bandhead origin ν_{vacuum} (cm^{-1})	relative intensity [g]
(7,10) [b]	3475.9	28761	13.4
(9,12) [e]	3530.6	28316	(6.4)
(4,8) [b]	3538.9	28249	6.4
(5,9) [b]	3564.1	28050	6.8
(6,10) [b]	3589.6	27850	9.5
(7,11) [b]	3616.1	27646	11.0
(8,12) [b]	3643.6	27438	(5.6)
(9,13)	3671.9	27226	5.2
(10,14)	3699.4	27024	2.9
(5,10)	3712.6	26928	2.9
(6,11)	3739.5	26734	3.4
(7,12)	3765.9	26547	4.1
(8,13) [f]	3792.2	26362	4.6
(10,15)	3849.7	25969	3.3
[(11,16)] [d]	3883.7	25741	2.0
[(7,13)] [d]	3926.8	25459	2.2
[(8,14)] [d]	3952.8	25291	2.7

a. Bandhead corresponding to $^3\Pi_1$ component

b. Previously observed by Linton and Capelle reference 4

c. Previously observed by Hager et al. reference 3

d. Weak feature - wavelength approximate

e. (8,11) band under (0,4) band of $a^3\Sigma^+ - X^1\Sigma^+$ band system

f. (9,14) band under (0,6) band of $a^3\Sigma^+ - X^1\Sigma^+$ band system

g. Corrected for phototube response

Table 2

Latent heat of vaporization for silicon (^3P) and activation energy for formation of $SiO^*(A^1\Pi)$[a]

Reaction Studied	$\Delta H_{vaporization}$ present study[b]	Temperature Range (°K)	Literature[c]	E_A[d]
$Si + NO_2 \rightarrow SiO^*(A^1\Pi, v'=0,1)$	105.2 ± 1.2[e]	1850-2220	95.1	7.4 ± 1.2
$Si + NO_2 \rightarrow SiO^*(A^1\Pi, v'=0,1)$	106.8 ± 3[e]	1880-2190	95.1	8.6 ± 3

a) Energy in kcal/mole.

b) Values in this column obtained from the slope of $\ell n\ I$ versus $1/T_B$, where I is the chemiluminescent intensity and T_B is the beam temperature. The slope obtained through linear least-squares analysis is added to the value of RT_B over the temperature range of the experiment to yield a rigorous upper bound to $\Delta H_{vaporization}$ - see text for discussion.

c) $\Delta H_{vaporization}$ at the average temperature of the experimental runs.

d) Values in this column obtained from the slope of $[\ell n(IT_B) + \Delta H_{vap}(T_B^{mean})/RT_B]$ versus $1/T_{effective}$ - see text for discussion.

e) Spectral resolution was 30Å.

Table 3

Energy Balance Discrepancies in $M+N_2O$ Reactions

Reaction	$E_{Available}$	Measured MO Excitation	$E_{int}(MO)$ (cm^{-1})	ΔE[a]
$Sc(^2D)+N_2O$[b]	45856 cm^{-1}[c]	Short Wavelength Limit ($C^2\Pi-X^2\Sigma^+$) (3000Å)	33324 cm^{-1}	12532 cm^{-1}
$Y(^2D)+N_2O$[b]	48154 cm^{-1}[c]	Short Wavelength Limit ($C^2\Pi-X^2\Sigma^+$) (3000Å)	33324 cm^{-1}	14830 cm^{-1}
$La(^2D)+N_2O$[d]	55862 cm^{-1}[c]	$LaO^*, D^2\Sigma^+, v'=17$[e]	39400 cm^{-1}	16462 cm^{-1}
$Ba(^1S)+N_2O$[f]	33652 cm^{-1}	Short Wavelength Limit (4000Å)	24993 cm^{-1}	8659 cm^{-1}
$Ca(^3P)+N_2O$[g,h]	34792 cm^{-1}	Short Wavelength Limit (3850Å)	25967 cm^{-1}	9095 cm^{-1}
$Sr(^3P)+N_2O$[h]	37553 cm^{-1}	Short Wavelength Limit (3700Å)	27019 cm^{-1}	10534 cm^{-1}
$Ti(^3F) + N_2O$	44004 cm^{-1}	$D-X^3\Delta(2,1)$ band	34840 cm^{-1}	9060 cm^{-1}

a. $E_{Available} - E_{int}(MO)$

b. J. L. Gole and C. L. Chalek, J. Chem. Phys. 65, 4384 (1976).

c. $D_o^o(MO) + E_{int}(M) + E_{int}(N_2O) + E_T^i - D(N-NO)$. See text for definitions.

d. C. L. Chalek and J. L. Gole, Chem. Phys. 19, 59 (1977).

e. J. L. Gole unpublished data.

f. Data from C. D. Jonah, R. N. Zare, and Ch. Ottinger, J. Chem. Phys. 56, 263(19

g. Data from J. A. Irwin and P. J. Dagdigian, J. Chem. Phys. 74, 6178(1981).

h. Data from B. E. Wilcomb and P. J. Dagdigian, J. Chem. Phys. 69, 1779(1978). See also P. J. Dagdigian, Chem. Phys. Lett. 55, 239(1978).

Figure Captions

Figure 1: (a) Chemiluminescent spectrum in the region 2850-3600Å resulting from the reaction Si + N_2O → SiO* + N_2 recorded under single collision conditions. The spectrum in this region corresponds to the SiO "$b^3\Pi$" - $X^1\Sigma^+$ band system. The bandheads are designated (v',v"). Spectral resolution is 10Å.

Figure 2. Chemiluminescent spectrum in the region 3550-4200Å resulting from the reaction Si + N_2O → SiO* + N_2 recorded under single collision conditions. Emission from high vibrational levels of SiO "$b^3\Pi$" and the v' = 0 level of SiO "$a^3\Sigma^+$" is monitored. The bandheads are designated (v',v"). Spectral resolution is 10Å. See text for discussion.

Figure 3. Chemiluminescent spectrum in the region 2350-2950Å resulting from the reaction Si + N_2 → SiO* + N_2 recorded under single collision conditions. The high energy end of the SiO "$b^3\Pi$" - $X^1\Sigma^+$ band system extends into the SiO $A^1\Pi$ - $X^1\Sigma^+$ emission system. The bandheads in both systems are designated (v',v"). Spectral resolution is 15Å. See text for discussion.

Figure 4. Chemiluminescent spectrum in the ~2150-2550Å resulting from the reaction Si + N_2O → SiO* + N_2 recorded under single collision conditions. The observed spectrum corresponds to the SiO $A^1\Pi$ - $X^1\Sigma^+$ band system. Bandheads are designated (v',v"). Spectral resolution is 20Å. See text for discussion.

Figure 5. Chemiluminescent spectrum in the region 2700-4100Å resulting from the reaction Si + NO_2 → SiO* + NO recorded under single collision conditions as a function of increasing silicon beam temperature and metal flux. The spectrum depicts both the "$b^3\Pi$" - $X^1\Sigma^+$ and "$a^3\Sigma^+$" - $X^1\Sigma$ band systems. Many fewer levels of the "$b^3\Pi$" state are populated vs. the observed spectrum for the Si + N_2O reaction. Bandheads are designated (v',v"). Spectral resolution is 10Å.

Figure 6. Chemiluminescent spectrum in the region 2300-2750Å resulting from the reaction Si + NO_2 → SiO* + NO recorded under single collision conditions as a function of increasing silicon beam temperature and metal flux. The observed spectrum corresponds primarily to the SiO $A^1\Pi$ - $X^1\Sigma^+$ band system. Spectral resolution is 20Å. See text for discussion.

Figure 7. Natural logarithm of relative chemiluminescent intensity verses the reciprocal of the silicon metal beam temperature at 2650Å corresponding to the SiO $A^1\Pi - X^1\Sigma^+$ band system. See text for discussion.

Figure 8. Plot of $[\ell n(IT_B) + \Delta H_{vap}(T_B^{mean})/RT_B]$ vs. $1/T_{eff}$ for the Si + NO_2 reaction at 2650Å. The slope of the plot yields the activation energy for formation of SiO* $A^1\Pi$ product molecules. See text for discussion.

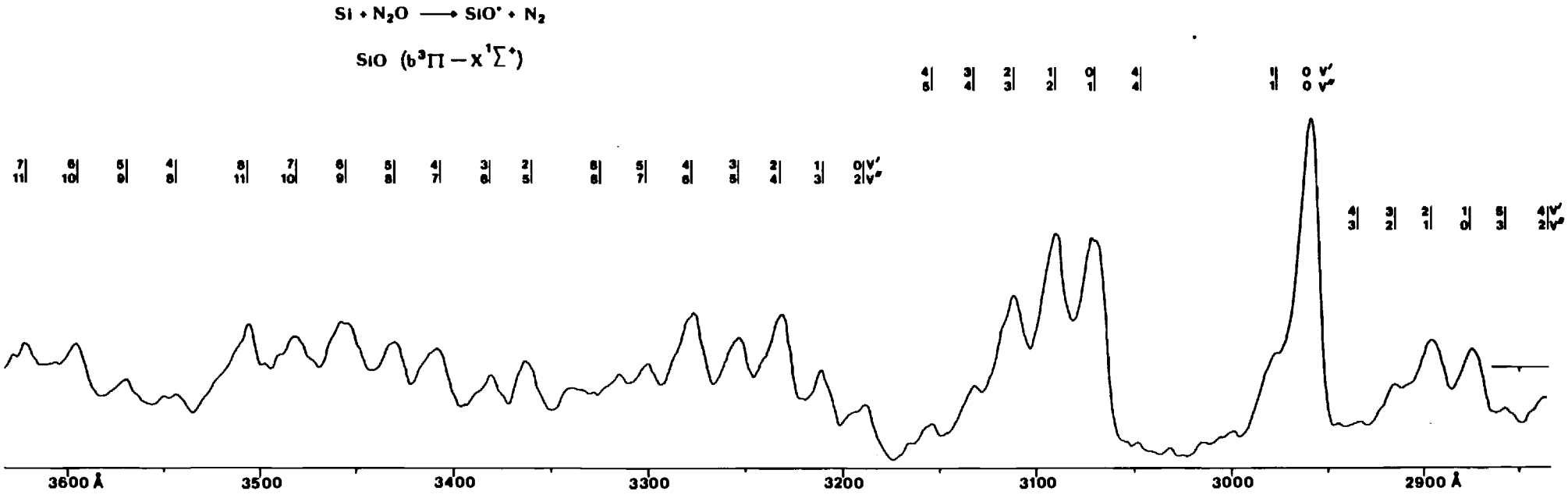
Si + N2O ⟶ SiO* + N2
SiO (b3Π − X1Σ+)
7|11 6|10 5|9 4|8 8|11 7|10 6|9 5|8 4|7 3|6 2|5 6|8 5|7 4|6 3|5 2|4 1|3 0|2 v'v''
4|5 3|4 2|3 1|2 0|1 4|4 1|1 0 v' 0 v''
4|3 3|2 2|1 1|0 5|3 4|2 v'v''
3600 Å
3500
3400
3300
3200
3100
3000
2900 Å

Figure 1

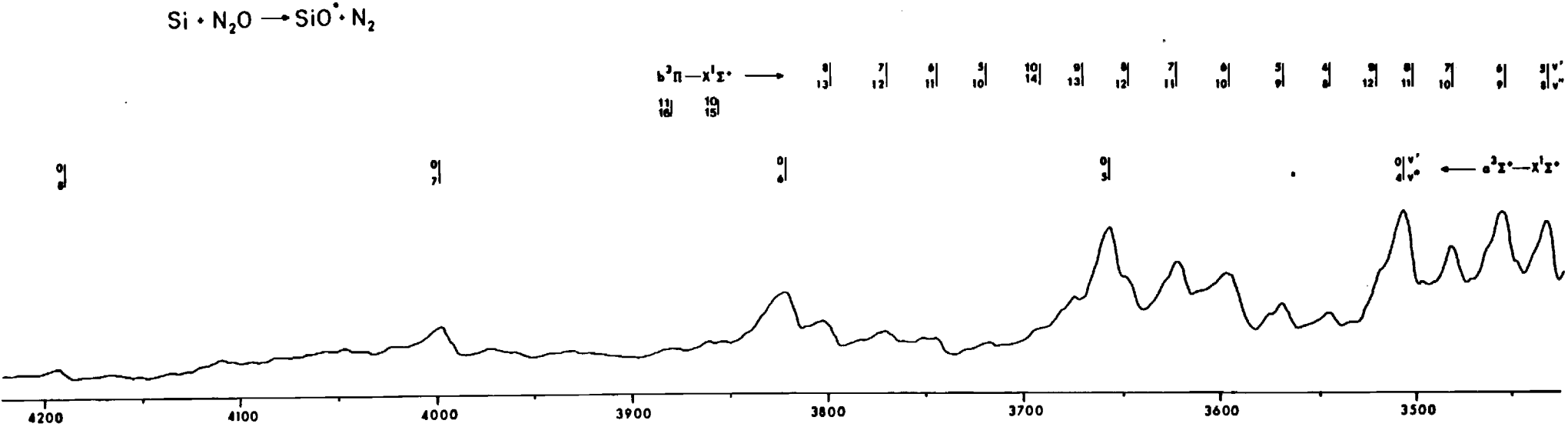
Si + N2O → SiO* + N2
b3Π—X1Σ+ →
a3Σ+—X1Σ+
4200
4100
4000
3900
3800
3700
3600
3500

Figure 2

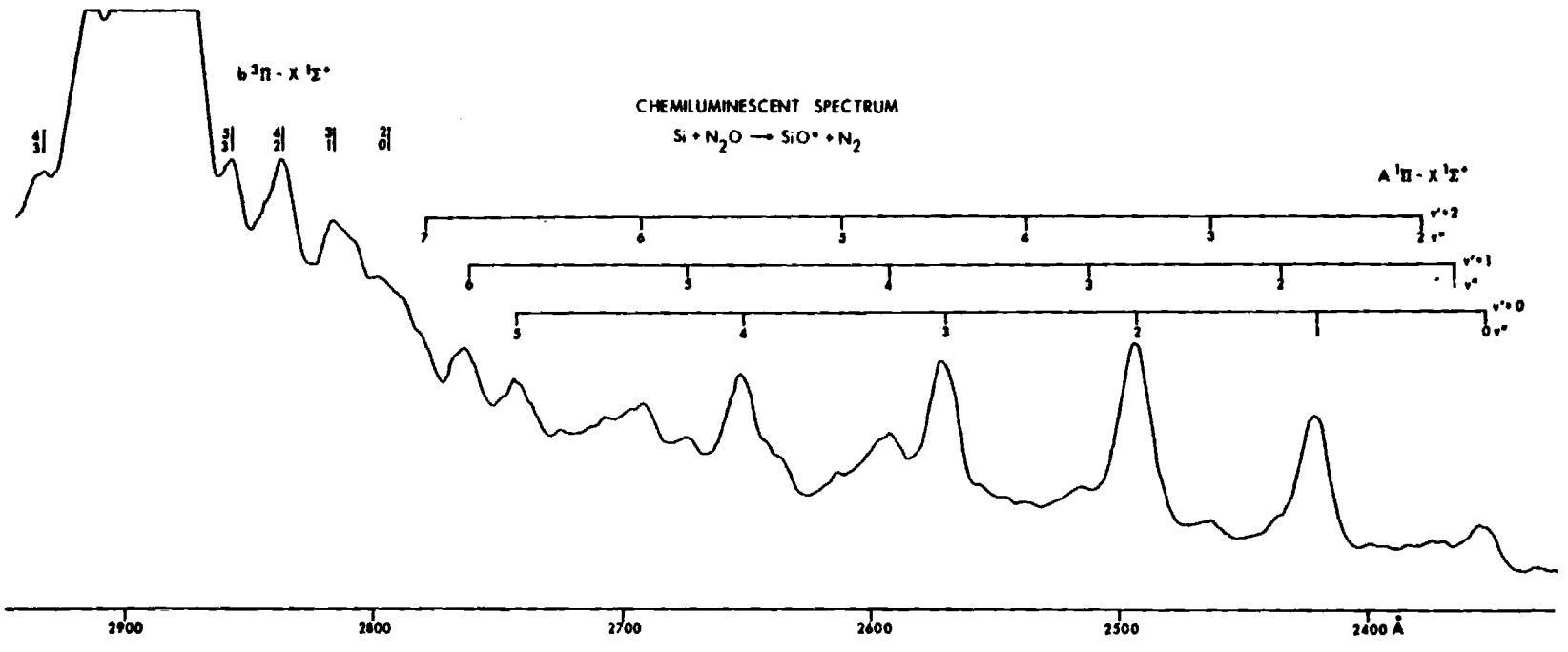
CHEMILUMINESCENT SPECTRUM
$Si + N_2O \rightarrow SiO^* + N_2$
$b\,^3\Pi - X\,^1\Sigma^+$
$A\,^1\Pi - X\,^1\Sigma^+$
4|3|
3|3|
4|2|
3|1|
2|0|
v'=2
v'=1
v'=0
v''
2900
2800
2700
2600
2500
2400 Å

Figure 3

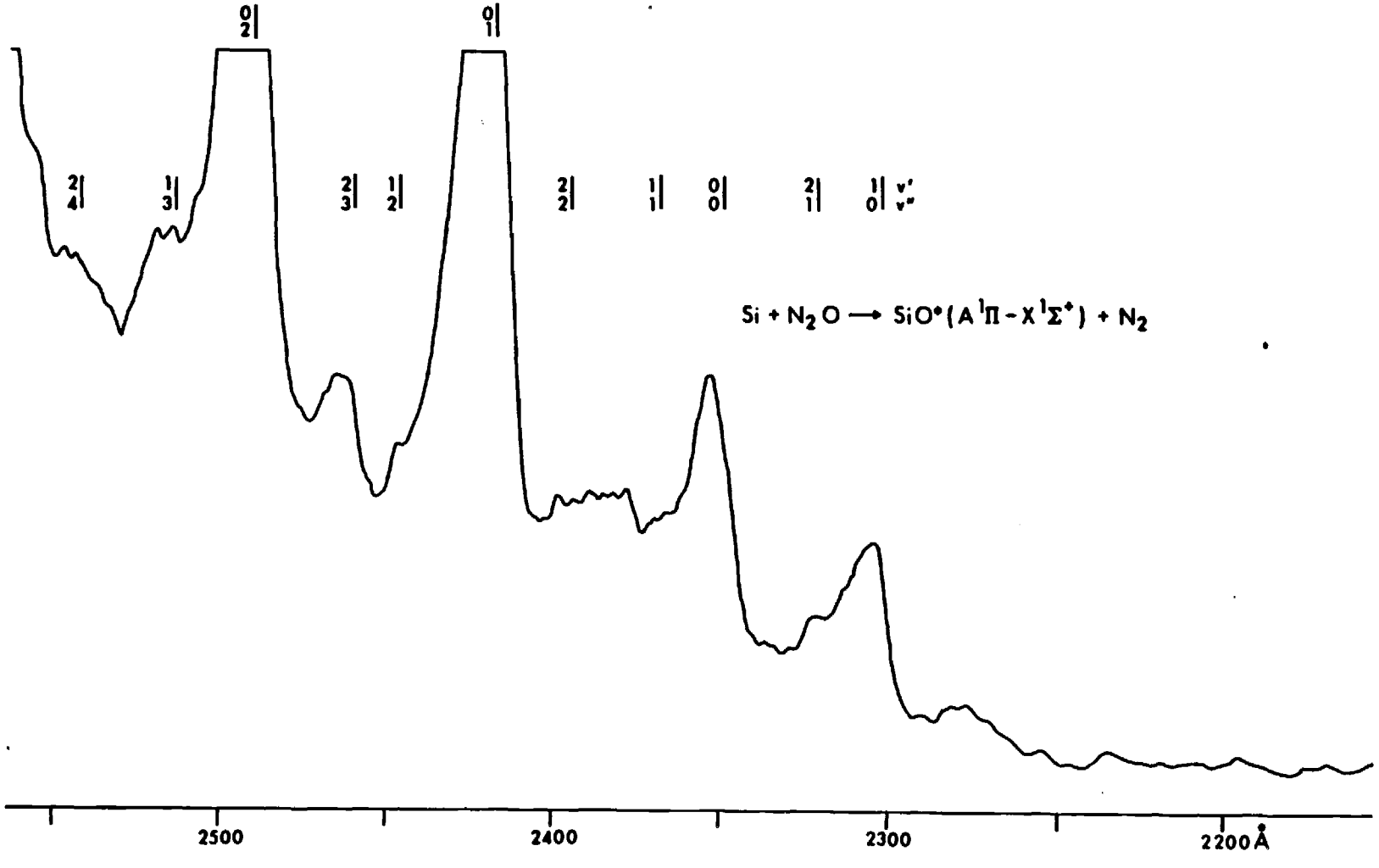
0 2
0 1
2 4
1 3
2 3
1 2
2 2
1 1
0 0
2 1
1 0
v' v''
Si + N2O → SiO*(A1Π - X1Σ+) + N2
2500
2400
2300
2200 Å

Figure 4

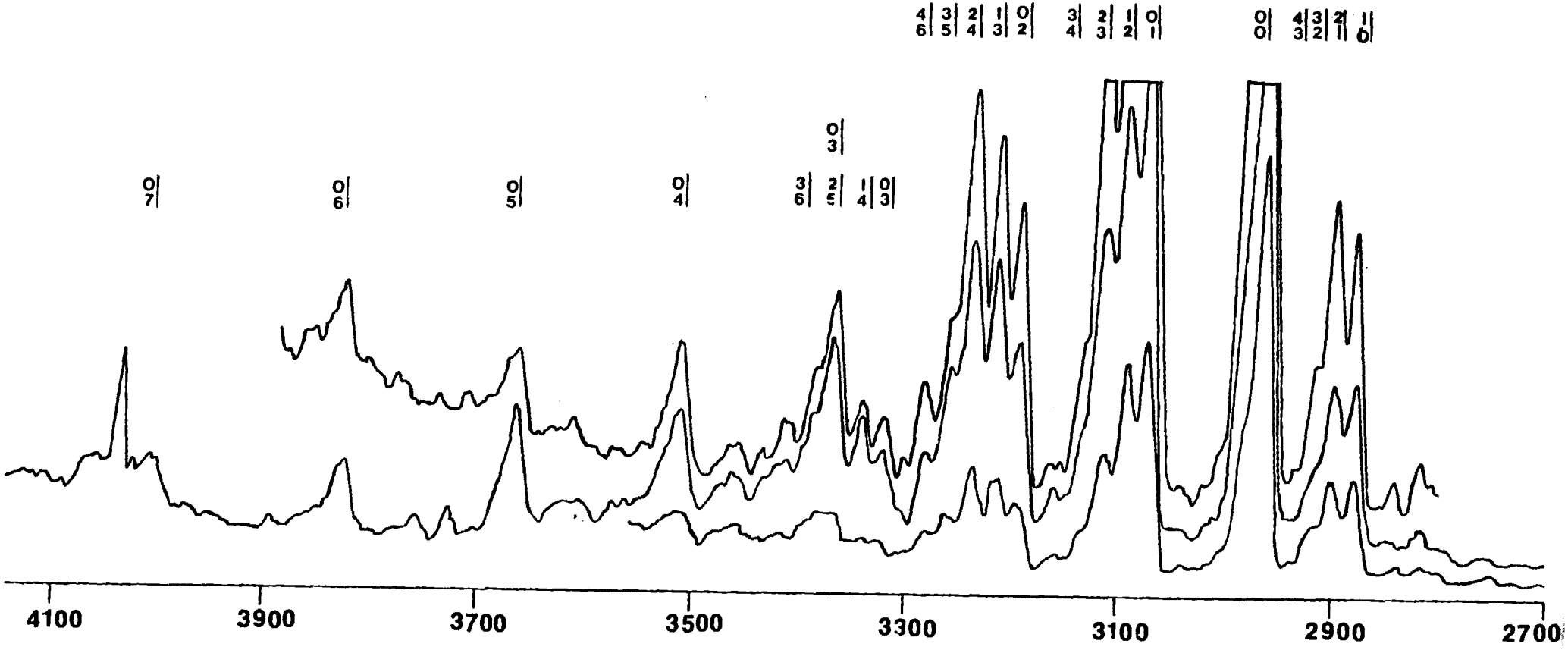

Figure 5

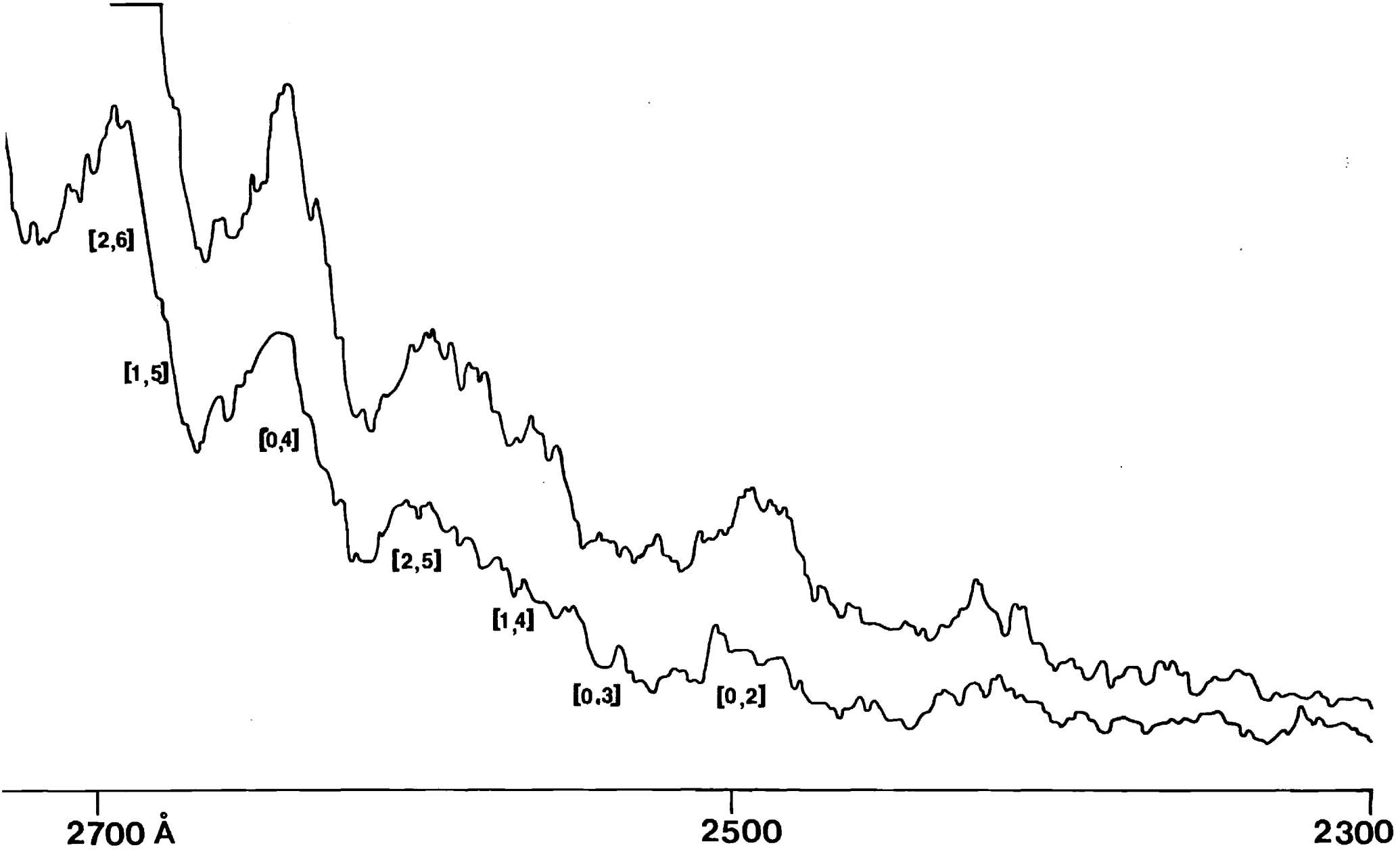

Figure 6

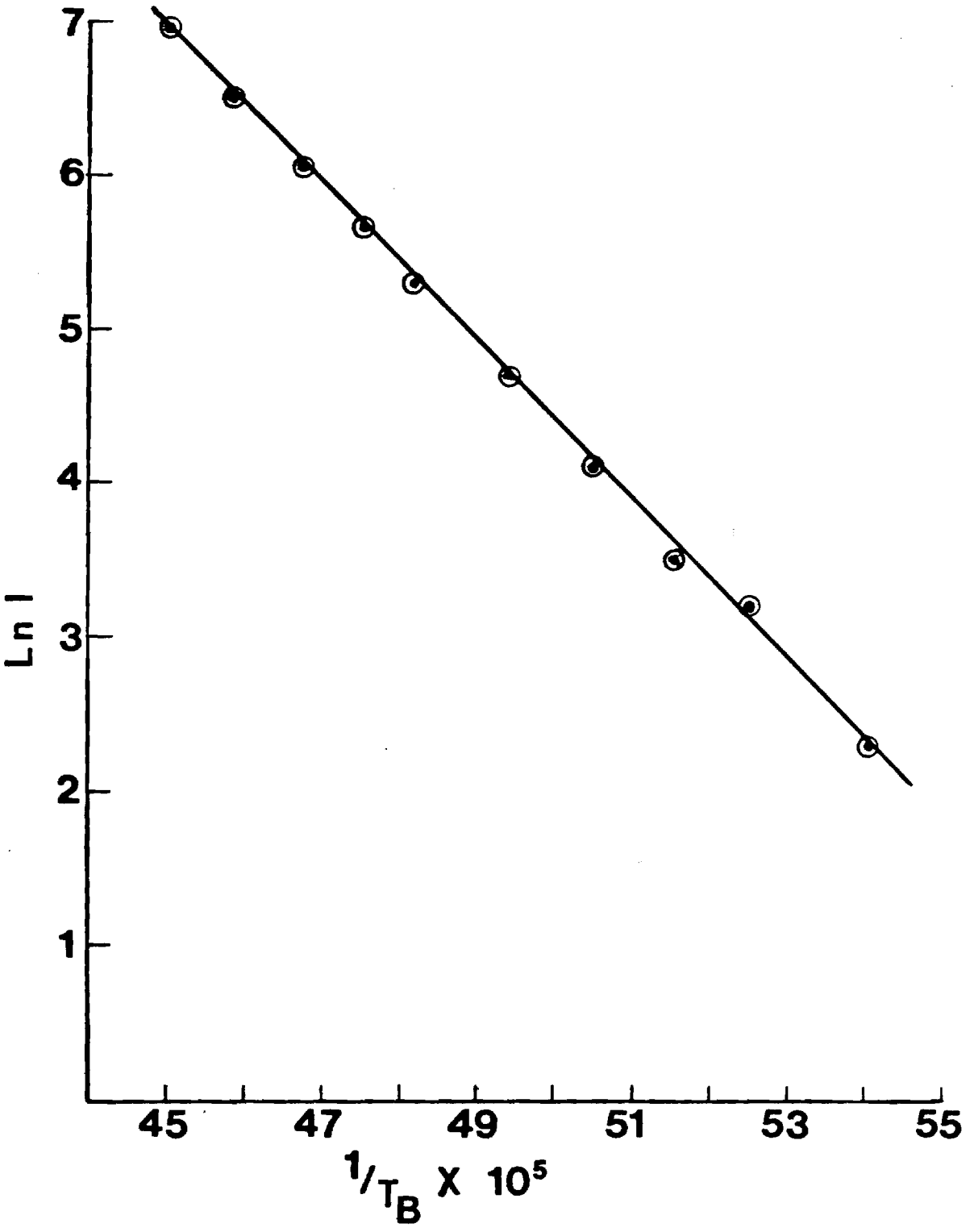

Figure 7

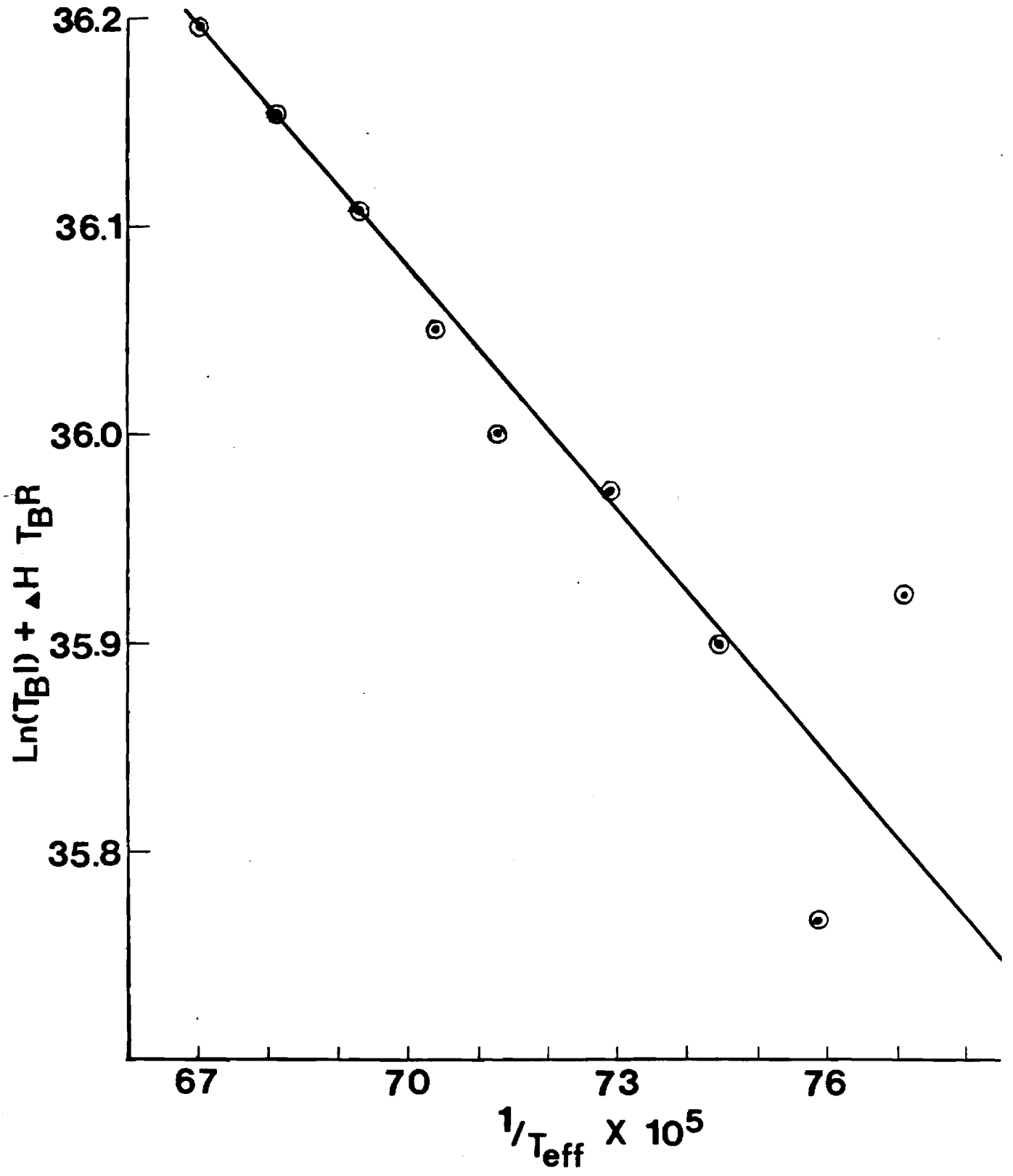

Figure 8

APPENDIX F

. Accomplishments and Publications for the Period 3/1/80-8/30/81

1. A lower bound was determined for the SiS dissociation energy which has been compared with previous mass spectrometric results. This work has been published (Chem. Phys. 46, 67 (1980)).[1] The work also involved the characterization of several quantum levels and hence molecular constants for the ground and low-lying electronic states of SiS. Finally the dynamics of the reactions leading to SiS formation has been characterized (Chem. Phys. 69, 357 (1982).[2]

2. The chemiluminescent emission from two reactions producing the SiO molecule ($Si + N_2O \rightarrow SiO + N_2$ and $Si + O_3 \rightarrow SiO + O_2$) was extensively studied. Molecular constants have been evaluated for the ground electronic state. This work involved the development of techniques which allow the study of chemiluminescent processes across a wide pressure range. This work lead not only to the improved evaluation of molecular constants but also to the discovery of "ultafast" (see below) energy transfer in high temperature systems. The characterization of the $Si-N_2O$ and $Si-O_3$ reactions has allowed the determination of a lower bound for the SiO bond energy, however the dynamics of these reactions is such that further characterization of the N_2 and O_2 products will be required to obtain a sufficiently stringent measure of this quantity.

3. The first electronic emission spectra for the alkali hydroxides were obtained over a wide pressure range. The reactions of sodium and potassium with hydrogen peroxide have been used to excite chemiluminescence from KOH and NaOH. This work led to the direct determination (later refined) of stringent lower bounds for the K-OH and Na-OH bond energies. For KOH, we found $D_0^o \geq 88.2$ kcal/mole, notably higher than the bond energy previously accepted and commonly used in modeling energy generating systems. This result indicated that concentrations determined previously for KOH in combustion systems were

too low. The K-OH fundamental frequency in the gas phase was determined to be ~423 cm^{-1}. For NaOH our initial studies indicated $D_0^o \geq 75.2$ kcal/mole in good agreement with the JANAF tables value. These are important results for they represent a direct spectroscopic confirmation of a quantity previously determined by indirect methods. We noted at this time that it was surprising that the Na-OH bond energy was found to be significantly less than that of K-OH. The measured Na-OH bond strength has now been revised upward. (Optical Engineerin 20, 546 (1981)).[3]

4. An apparatus was constructed for the characterization of Na_2O, an important contaminant in combustion systems, using laser fluorescence spectroscopy. A significant component of spectra were obtained using argon-ion laser induced fluorescence. This work, which is summarized elsewhere (Optical Eng. 20, 546 (1981)),[3] has led to the tentative determination of ground state molecular constants.

5. The first electronic emission spectra for NaO and KO were obtained. From initial studies of the single collision chemiluminescence resulting from the Na-N_2O and K-N_2O reactions, tentative values for the dissociation energies of NaO (70 $\pm$ 5 kcal/mole) and KO (75 $\pm$ 5 kcal/mole) were determined.

6. The phenomena of ultrafast energy transfer, both intra- and intermolecular, among the electronic states of small high temperature molecules was observed and characterized. These studies indicated that energy transfer could occur at rates which may approach 1000 times the calculated gas kinetic rate. These surprising results demonstrated that vibrationally and/or electronically excited high temperature molecules act as if they were "large" and "diffuse" entities capable of significant interaction at very long range. The rapid energy transfer was found to be a general phenomenon and effects have been observed in several molecules including SiO and KOH. The observation of such rapid energy transfer has significant implications for the

odeling of energy generating systems and the characterization of heat flow in hese systems. The nature of the rapid energy transfer means that both kinetic eaction rate data and energy transfer data must be included in order to obtain realistic modeling of an energy generating system. Portions of this work ave been published (J. Chem. Phys. 73, 836 (1980);[4] 73, 5025 (1980);[5] J. Phys. hem. 85, 2651 (1981)).[6]

7. In conjunction with the Morgantown Energy Technology Center, the ethane-fluorine combustion system has been characterized. This work has been ublished (Chem. Phys. 52, 461 (1980)).[7]

8. As an intermediate step to the study of sodium surface oxidation with SO_2, the highly exothermic channels for the oxidation of sodium clusters with SO_2 and the halogens have been characterized.[1] This work is continuing.

9. Extensive computer programs were written for the calculation of Molecular Electronic Spectra for the diatomic and small polyatomic species of interest in combustion environments. These programs were made available to the Morgantown Energy Technology Center and the scientific community.

10. A user's manual was prepared for the calibration and operation of an Optical Multichannel Analyzer system. This user's manual was made available to the Morgantown Energy Technology Center.

11. Extensive computer programs for the Normal Coordinate Analysis of Polyatomic Molecules were prepared and supplied to METC.

1. "Single and Multiple Collision Chemiluminescent Studies of the Si-OCS and Ge-OCS Reactions--A Study of the SiS and GeS $a^3\Sigma^+ - X^1\Sigma^+$ and SiS $b^3\Pi - X^1\Sigma^+$ Intercombination Systems and the Nature of SiS Collisional Quenching," with G. J. Green, Chem. Phys. 46, 67 (1980).

2. "Dynamic Constraints Associated with the Formation of SiS* ($a^3\Sigma^+$) from the Chemiluminescent Si-OCS Reaction," with G. J. Green, Chemical Physics 69, 357 (1982).

3. "Aspects of Sparsely Studied Gas Phase Chemistry of Import to the Energy Technologies," Optical Engineering 20, 546 (1981).

4. "Nonequilibrium Product Distributions Observed in the Multiple Collision Chemiluminescent Reaction of Sc with NO_2. Perturbations, Rapid Energy Transfer Routes and Evidence for a Low-Lying Reservoir State," with S. A. Pace, J. Chem. Phys. 73, 836 (1980).

5. "Evidence for Ultrafast V-E Transfer in Boron Oxide (BO)," with A. Hanner, J. Chem. Phys. 73, 5025 (1980).

6. "Chemiluminescence from the Interaction of Boron Atoms and Water Vapor," with S. A. Pace, J. Phys. Chem. 85, 2651 (1981).

7. "A Study of the Methane-Fluorine Flame Including an Analysis of the A^1A'' - X^1A' Emission Spectrum of HCF," with R. I. Patel, G. W. Stewart, K. Castleton, and J. R. Lombardi, Chem. Phys. 52, 461 (1980).

Other publications for this period presenting DOE sponsored work

1. "Laser Spectroscopy of Refractory Compounds," presented as an invited contribution to Electro-Optics Laser 80, Proceedings of the Electro-Optics/Laser 80 Conference and Exhibition, pp. 127-140.

2. "The Characterization of High Temperature Vapors of Import to Combustion and Gasification Processes in the Energy Technologies," Proceedings of the Morgantown Energy Technology Center Meeting on High Temperature, High Pressure Particulate and Alkali Control in Coal Combustion Process Streams - Morgantown, West Virginia, 1981, pg. 245.

B. Accomplishments and Publications for the period 8/30/81-2/8/83

During this period we improved our direct spectroscopic measurements of the M-O bond dissociation energies of the alkali hydroxides, NaOH and KOH (D_0^0(K-OH) $\geqslant$ 88.6 kcal/mole, D_0^0(Na-OH) $\geqslant$ 82.5 kcal/mole). The determined values have indicated that the concentration of these species in process streams exceeds previous expectations. Also in a direct measurement we redetermined the NaO and KO bond energies (D_0^0(NaO) = 70 $\pm$ 5 kcal/mole, D_0^0(KO) = 75 $\pm$ 5 kcal/mole). In the course of our studies, allowing these bond energy determinations, we obtained the more definitive information on first electronic emission spectra for these oxides and hydroxides. This data, which has subsequently

been refined in our laboratory, has provided the first gas phase information which can be used to develop techniques for the direct monitoring of these species in process streams or in experiments which are being used to obtain kinetic data to model the process stream.

Experiments carried out in our laboratory revealed that the oxidations producing the alkali oxides and hydroxides are characterized by a very different gas phase chemistry than that accompanying virtually all other highly exothermic metal oxidations with which we have had considerable experience. Most pronounced in this chemistry is an extremely efficient gas phase particulate formation especially in the alkali oxide systems. This particulate matter, which consists of alkali (X_n, $n \geq 3$)-oxygen-nitrogen complexes, has been analyzed in our laboratory using a combination of mass spectrometry (moderate temperatures 50-350°C) and EPR spectroscopy. Further studies employing High Temperature mass spectroscopy and laser Raman spectroscopy were undertaken in order to continue to characterize the nature of those polymers which make up the observed particulate matter which we believe can serve as a seed for the formation of larger alkali containing ash components in the process stream.

As an intermediate step to the study of sodium surface oxidation with SO_2, we continued studies of the reaction channels for the oxidation of sodium clusters with SO_2 and the halogens. It is known that alkali sulfates represent a portion of the deliterious material formed in process streams. It is necessary that we gain some understanding of how the alkali present in the stream leads to this alkali sulfate formation. SO_2 is known to be an important gas stream species and it is thought that alkali enriched-surface-SO_2 interactions lead eventually to the formation of the sulfate. It is apparent that one need ascertain the nature of the alkali-SO_2 interaction. With this impetus, we attempted to observe the products of oxidation of various

sized sodium clusters. Although the Na-SO_2 and probably Na_2-SO_2 reactions are slow and endothermic, it is not obvious that this kinetic and thermodynamic behavior will hold for multicenter processes involving $n \geq 3$ atoms. Here it is possible that NaO, NaS, and Na_2O may represent the products of cluster oxidation. Other workers have suggested that chlorine interacts with the alkali impurities in a combustion stream, resulting in the formation of alkali chloride complexes which then repartition with O,S,H,C,Al, or Si ash particulates. As an outgrowth of this suggestion we were concerned with the influence of chlorine and other halogens on the formation of alkali clusters and the subsequent reaction of these clusters with the sulfur oxides. We carried out several studies of sodium cluster-halogen atom interactions discerning that small chlorine impurities catalyze the reaction of sodium clusters with SO_2 in a very exothermic process.

Publications

"Metal Cluster Oxidation: Chemiluminescence from the Reaction of Sodium Polymers (Na_n, $n \geq 3$) with Halogen Atoms (X=Cl,Br,I)," with W. H. Crumley and D. A. Dixon, J. Chem. Phys. 76, 6439 (1982).

C. Accomplishments and Publications for the period 2/8/83-10/31/83

Major accomplishments for this period involved two main focuses, (1) the detailed characterization of the alkali oxides LiO, NaO, and KO and the establishment of a new direct means to detect these oxides directly in process streams and (2) the continued characterization of extremely efficient gas phase particulate formation in alkali oxidation systems. Further projects involved improvement of our direct determination of the bond energies for SiO, NaO, and KO and the characterization of their molecular parameters.

Experiments carried out in our laboratory definitively revealed the existence of a low-lying predominantly covalent state of the alkali oxides. The importance of this state and the necessity for its characterization

:annot be underestimated. Its presence furnishes the first ready means for detecting the alkali oxide. At present, one of the major techniques for detecting alkali and specifically sodium compounds in process streams involves a complex and expensive combination of laser systems. Sodium compounds are photodissociated with an initial laser pulse and subsequent excitation of atomic sodium provides an indication of the alkali concentration which is believed to be present in a limited group of species. Even though the laser techniques are eloquent, this is a somewhat tenuous back extrapolation. This can now be circumvented and vastly simplified for the alkali monoxide. The new route is not only important for the detection of sodium monoxide in the gas phase but also its detection as the product of sodium contaminated surface oxidation. In addition, the discovery of this state has important implications for the assessment of sodium chemistry in the upper atmosphere.

Using the SiO* chemiluminescence from the Si-NO_2 reaction we carried out a spectroscopic and independent determination of the SiO bond strength. This determination confirmed, for the first time, the mass spectrometric determination of the bond strength for a compound which represents the standard for mass spectroscopy. In addition, several new molecular constants were evaluated for SiO.

In addition to SiO, several new molecular parameters have also been determined for the alkali oxides LiO, NaO, and KO.

Publications

1. "Observation of Alkali Oxide Electronic Emission Spectra: Analysis of the NaO "6700A" Band System," with Joerg Pfeifer, Jour. of Chem. Phys. 80, 565 (1984).

2. "The Gas Phase Characterization of the Molecular Electronic Structure of Small Metal Clusters and Cluster Oxidation," to appear in "Metal Clusters," edited by M. Moskovits, John Wiley and Sons (1986) pg. 131.

3. "Energy Balance and Branching Ratios Associated with the Chemiluminescent Reaction $Si(^3P) + N_2O(^1\Sigma) \rightarrow SiO^*(a^3\Sigma^+, b^3\Pi, A^1\Pi) + N_2(v'' \geq 5)$ - Possible Formation of Vibrationally Excited N_2 in M + N_2O Reactions," with G. J. Green, Chemical Physics 100, 133 (1985).

4. "Energy Balance in the Si-NO_2 Reaction: On the Formation of AiO $a^3\Sigma^+$, v' " $\geq$ 0, and Ultrafast $a^3\Sigma^+ - b^3\Pi$ E-E Energy Transfer," Chemical Physics 100, 153 (1985).

5. "Formation, Electronic Spectra, and Correlation of the Alkali Halides and Hydroxides," with D. F. Dever and B. Cardelino, High Temp. Sci. 18, 159 (1984).

6. "Energetics of Silicon Oxidation Reactions - An Independent Determination of the SiO Bond Dissociation Energy," with Joerg Pfeifer and Gary Green (High Temperature Science - Brewer Issue 17, 85 (1984).

7. "The Characterization of High Temperature Vapor Phase Species and Vapor-Solid Interactions of Import to Combustion and Gasification Processes in the Energy Technologies," Annual Topical Report Nos. 1 and 2, U.S.D.O.E., Morgantown, West Virginia (Contract DE-AC21-81MC16537).

8. "Electronic Emission Spectra and Bonding of the Alkali Hydroxides, NaOH CsOH," with J. S. Hayden and R. Woodward, submitted.

9. "Alkali Metal Oxide Formation - First Observed Emission from a Low-Lying Electronic State of the Alkali Monoxides LiO - CsO," with R. Woodward, R. Eades, and D. A. Dixon, in preparation.

APPENDIX G

A CLEAN-UP JOB FOR LASERS

Coal gas, which is produced by reacting coal with steam, has a long if dirty history. It illuminated the original London Bridge in the days of George the Third. By the mid-19th century it had become the fuel of choice in big cities everywhere, reigning supreme until it was knocked out of the box by the advent of cheap oil.

Now that oil is no longer cheap, coal gas is well positioned to make a strong comeback as a leading fuel technology of the future — if it can clean up its act. Coal is abundant, and the gasification process is relatively inexpensive. But the environmental problems, which no one thought much about in the gaslight era, are a very big worry today. Coal gas won't win widespread public acceptance until it can be efficiently laundered.

That's where lasers come in. At the US Department of Energy's experimental coal gasifier in Morgantown, W. Va., researchers from the Los Alamos National Laboratory have been demonstrating a continuous-monitoring laser technique for determining process pollutants and increasing process efficiency. The success of their work to date strongly suggests that coal gasification plants of the future will come equipped with laser systems to keep real-time tabs on pollutant levels in the gas stream and make sure that scrubber systems are preventing noxious material from escaping into the air we breathe.

Two laser systems are being used in the Morgantown experiments, and like just about everything else these days, they're known by their acronyms. LIBS (for Laser-Induced Breakdown Spectroscopy) is used primarily for determining sodium and potassium contents of coal gasification streams, which is important in controlling costly corrosion of equipment exposed to hot combustion products. CARS (for Coherent Anti-Stokes Raman Scattering) is a more complex system for determining the presence and temperature of a variety of air-polluting molecules. Both use readily available lasers.

A tricky aspect of CARS is that it employs two lasers to produce a third laser beam. By mixing two beams of different frequencies, researchers can tune to the vibrational frequency of the molecule they want to examine. The intensity of the third beam, generated by the interaction of the two initial beams with the molecule, yields the molecule's concentration. This technique has enabled CARS to measure concentrations of nitrogen, carbon monoxide and hydrogen sulfide in the dirtiest parts of the gas stream where temperatures run to 1000°F and pressures are 200 pounds per square inch, with high particle and tar-vapor loadings.

LIBS and CARS are complementary systems. "Together," says Los Alamos scientist David Taylor, "they can tell you everything you ever wanted to know about what is happening in the gasification system and what is coming out of it." Armed with that kind of information, the producers of coal gas should be able to give us a fuel we can live with, while making a significant contribution to the nation's eventual energy self-sufficiency. □